

**STRUCTURAL ACTIVITY AND MECHANISTIC STUDIES
ON GLYCOSYLATED ANTITUMOR ETHER LIPIDS (GAELS)**

By Makanjuola Ogunsina

A thesis submitted to the Faculty of Graduate Studies of the University of Manitoba

in partial fulfillment of the degree of

Doctor of philosophy

Department of Chemistry, University of Manitoba

Winnipeg, Manitoba, Canada

Copyright© 2016 by Makanjuola Ogunsina

For 'Kemi and Timon who made the needed sacrifice

Abstract:

A major impediment to successful treatment of cancer is the inability of clinically available drugs to kill cancer stem cells (CSCs), a subset of tumor cells that mediate progression, resistance and relapse of cancer. Glycosylated Antitumor Ether Lipids (GAELs), a class of amphiphilic antitumor agents such as *1-O-Hexadecyl-2-O-methyl-3-O-(2'-amino-2'-deoxy-β-D-glucopyranosyl)-sn-glycerol* (GLN), represent a new class of anticancer agents that kill cancer cells by a non-apoptotic pathway, an attractive approach to overcome resistance to many pro-apoptotic anticancer agent, in addition to potent cytotoxicity against CSCs. Previous studies show that GLN displayed potent cytotoxic effects against breast cancer stem cells, inhibited the formation of tumor spheres and caused the disintegration of preformed tumorspheres from BT474 CSCs. A major challenge to clinical development of GAELs such as GLN is lack of activity in xenograft model. This has been associated to metabolic degradation in animal, a problem common to *O*-glycosides. To take advantage of interesting pharmacological features of GAELs, we here explore structural features that are pivotal to activity in order to optimize anticancer activity after which various strategies were employed to enhance metabolic stability. This thesis presents the outcome of structural activity studies on GLN and strategies used to overcome metabolic degradation in GAELs. Our result showed that unsubstituted amines, *O*-glycosidic linkage, and glycerolipids are very crucial to activity. Metabolic stability can be achieved by using an L-enantiomer of the sugar without sacrificing potency. Mechanistic studies showed that the potent GAELs analogs discovered in this study kill cancer cells by non-apoptotic mode of action. Also the GAELs enter into the cells but do not lyse or disrupt the cell membrane. Moreover, the cytotoxicity of potent analogs of GAELs discovered is better than that of clinical anticancer drugs

like cisplatin, chlorambucil and the experimental anti-CSCs agent salinomycin. These analogs are potential anticancer drug candidates for clinical development.

Acknowledgements

This thesis would not have been possible without the guidance and help of several individuals who in one way or another contributed and extended their valuable assistance in the preparation and completion of this study.

First and foremost, my gratitude goes to my supervisor Dr. Frank Schweizer for given me the uncommon privilege to study for my Ph.D. in his lab. Your constructive criticism and guidance will be forever appreciated.

I would like to thank my co-supervisor and the main collaborator for this project Dr. Gilbert Arthur. I will never forget your fatherly advice and sacrifice towards the success of this study. I will always remember you coming to lab on holidays even during Christmas. The priceless contribution of Dr. Pranati Sammader toward the success worth been mentioned

To the entire committee members, Dr. Frank Schweizer, Dr. Gilbert Arthur, Dr. Philip Hultin and Dr. Sean McKenna, I am very grateful for your invaluable contribution and sacrifices you made toward the success of this work.

To the members of “Schweizer International Research Group”, both former and present, without you, this study would have been very boring. Also it has been a great experience working in a group with members from five different continents, I will always remember you guys.

I am very grateful to my parents, siblings, nieces, nephews, friends and in-laws for their support and encouragement during this training. My special thanks goes to my wife ‘Kemi and son Timon, this would have been impossible without you.

Thanks to John Wiley and Sons for given me the copyright permission (License Number 3893200903204) to include the article: “Structure–Activity Relationships of Glucosamine-Derived Glycerolipids: the Role of the Anomeric Linkage, the Cationic Charge and the Glycero Moiety on the Antitumor Activity” originally published in ChemMedChem, 2013, 8(3), 511-520 in this thesis.

I am also grateful to University of Manitoba and Government of Manitoba for University of Manitoba Graduate Fellowship (UMGF) and Manitoba Graduate Scholarship (MGS). Without these funds it would have been impossible for me to finish this PhD. I also appreciate various financial awards from Department of Chemistry during this PhD training.

My utmost gratitude goes to my creator, Jehovah, for your answer to my cries for help and preservation of life during this study. I will always meditate on all your activities and ponder over your dealings, for you are the true God who does marvelous things.

Table of Contents	
Abstract	iii
Acknowledgements	iv
List of Figures	xiii
List of Tables	xvii
Abbreviations	xviii
Table of Contents	v
Chapter 1 – Introduction and Background	1
1.1. Challenges in Cancer Treatment	1
1.2. Current Drugs Used in the Treatment of Cancer and Their Mechanism of Actions	5
1.3. Drugs that Kill Cancer Stem Cells and Their Possible Mechanisms of Action	10
1.4. Antitumor Ether Lipids	14
1.5. Development of GAELs as Anticancer Agents	20
1.5.1. Mechanism of GAEL-Induced Cell Death	23
1.5.2. Anti-Cancer Stem Cells’ Properties of GAELs	23
1.6. Methodologies for Evaluation of Cytotoxicity	24

1.7. Assessment of Apoptosis and Apoptosis-independent Mechanisms	26
1.8. Identification and Isolation of CSCs	28
1.9. References	31
Chapter 2 - Thesis Objectives	57
Chapter 3 - Structure Activity Relationships of Glucosamine-Derived Glycerolipids:	
 The Role of the Anomeric Linkage, the Cationic Charge and the	
 Glycero Moiety on the Antitumor Activity	61
3.1. Authorship considerations	61
3.2. Abstract	61
3.3. Introduction	62
3.4. Results and Discussion	63
3.4.1. Chemistry	63
3.4.2. Biology	69
3.5. Conclusion	77
3.6. Experimental Section	78
3.6.1. Chemistry	78
3.6.2. Biological methods	90
3.7. Acknowledgements	91

3.9. References	92
Chapter 4 - Structure Activity Relationships of N-linked and Diglycosylated	
 Glucosamine-based Antitumor Glycerolipids	97
4.1. Authorship considerations	97
4.2. Abstract	97
4.3. Introduction	98
4.4. Results and Discussion	100
4.4.1. Chemistry	100
4.4.2. Cytotoxicity	105
4.5. Experimental	109
4.5.1. General Methods	109
4.5.2. General Procedure for the Synthesis of N-Linked Compounds 2–5	110
4.5.3. General Procedure for the Synthesis of Diglycosylated	
 Compounds 6 and 7	118
4.6. Biological Activity	120
4.6.1. Cell Culture	120
4.6.2. Cytotoxicity Assay	120

4.7.	Conclusions	121
4.8.	Acknowledgements	121
4.9.	References	122
Chapter 5 - Design, Synthesis and Evaluation of Glucosylated Antitumor Ether		
Lipids Bearing Two Amino Groups as Cytotoxic Agents Against		
Epithelial Cancer Cells, Breast and Prostate Cancer Stem Cell		
		126
5.1.	Authorship considerations	126
5.2.	Abstract	126
5.3.	Introduction	127
5.4.	Results	130
5.4.1	Chemistry	130
5.4.2.	Biological Studies	140
5.5.	Discussion and Conclusions	152
5.6.	Experimental section	155
5.6.1.	Materials and methods: Synthesis of GAELs	155
5.6.2.	Chemistry: general methods	155
5.6.3.	Biological methods	180
5.7.	Acknowledgements	182
5.8.	References	183

Chapter 6 - Replacing D-glucosamine with its L-enantiomer in glycosylated antitumor ether lipids (GAELs) retains cytotoxic effects against epithelial cancer cells and cancer stem cells	188
6.1. Authorship considerations	188
6.2. Abstract	188
6.3. Introduction	189
6.4. Results and discussion	191
6.5. Conclusions	201
6.6. Acknowledgements	201
6.7. Supplementary information	201
6.7.1. Results – Biology and Chemistry	204
6.7.2. Experimental section	209
6.8. References	234
Chapter 7 - Cytotoxic Properties of L-Sugar Linked Amino Lipids in Cancer Cells and Stem Cells	240
7.1. Authorship considerations	240
7.2. Abstract	240
7.3. Introduction	241
7.4. Results	244
7.4.1. Synthesis of L-Sugar Derived Glycolipids 3 -7	245

7.4.2. Biological and biochemical studies	249
7.5. Discussion and Conclusion	267
7.6. Experimental section	271
7.6.1. Chemistry	271
7.6.2. Biological techniques	286
7.7. Acknowledgements	292
7.8. References	293
Chapter 8: Summary and future works	303
8.1. Summary	303
8.2. Future works	310
8.3. References	312
Appendix	316

List of Figures

Figure 1.1. General classification of antitumor ether lipids (AELs)	15
Figure 1.2. Examples of antitumor ether lipids	16
Figure 1.3. Structural activity map of GAELs	18
Figure 1.4. Conversion of MTT to formazan	24
Figure 1.5. Conversion of MTS to formazan	25
Figure 2.1. Proposed chemical modifications for structural activity relationship studies in this project	58
Figure 3.1. Structures of D-glucosamine-based glycerolipids used in this study	64
Figure 3.2. Effects of compounds 1-10 on the viability of epithelial cancer cell lines	71
Figure 3.3. Effects of 1-10 on formation of LAVs	75
Figure 4.1. Structures of the synthesized glycolipids used in the study	102
Figure 4.2. Effects of compounds 2-4 on the viability of epithelial cancer cell lines: breast (BT474, JIMT1), prostate (DU 145), pancreas (MiaPaCa2)	109
Figure 4.3. Effects of compounds 5-7 on the viability of epithelial cancer cell lines: breast (BT474, JIMT1, MDA-MB-231), prostate (DU145, PC3), pancreas (MiaPaCa2)	111
Figure 5.1. Structures of various glycosylated antitumor ether lipids (GAELs) and edelfosine, an antitumor ether lipid (AEL) of the ALP subclass	132

Figure 5.2. Structures of diamine-based and <i>N</i> -substituted glucosylated antitumor ether lipids (GAELs) used in this study	133
Figure 5.3. Effects of compounds 1 – 10 , β -GLN, cisplatin and salinomycin on the viability of MDA-MB-231, JIMT-1, BT-474, DU-145, PC3, and MiaPaCa2 cell lines	147
Figure 5.4. Effects of compounds 1, 2, 4, 8, α-GLN on the viability of cancer stems cells isolated form BT-474 breast cancer (A), DU-145 cell lines (B) and comparison of 1 with salinomycin, cisplatin and myristylamine (C)	150
Figure 5.5. Effect of compounds 1, 2, 4, 8 , cisplatin, salinomycin and myristylamine on the integrity of prostate and breast cancer stem spheroids	153
Figure 6.1. Structures of D- and L-glucosamine-based glycosylated antitumor ether lipids (GAELs) 1-5	190
Figure 6.2. Effects of compounds 1-5 , cisplatin and salinomycin on the viability of MiaPaCa-2, DU-145 BT-474 and MDA-MB-231 cell lines assessed by using the MTS assay	194
Figure 6.3. Effect of GAEL compounds 2-5 , myristylamine, cisplatin and salinomycin on the integrity of BT474 breast cancer stem cell spheroids	196
Figure 6.4. Effects of compounds 2-5 , myristylamine (C ₁₄ H ₂₉ NH ₂), cisplatin, adriamycin	

and salinomycin (0-20 μ M) on the viability of cancer stems cells isolated	
form BT-474 breast cancer cell line, assessed by MTS assay	197
Figure 6.5. Evaluation of effect of pan-caspases inhibitor, QVD-OPh (40 μ m) on	
cytotoxicity of L-GAELs 3 and 4 against DU-145 and L-GAEL 4 against	
JIMT-1 cells. Cancer cell lines were treated with drugs in the presence or	
absence of QVD-OPh	198
Figure 6.6. Evaluation of membrane effect of compounds 4 and 5 on DU-145 cell lines	
using cell impermeant ethidium homodimer-1 (EthD-1) dye that	
emits red fluorescence upon binding to DNA	199
Figure 6.7. Formation of large vacuoles by 5 μ M of 4 in BxPC-3 cells after 4 hrs of	
incubation observed on an Olympus IX70 microscope and the images	
recorded with an LCD camera	200
Figure 7.1. List of compounds tested in this study. L- mannose 1 and L-glucose 2 were	
included to determine if they are independently cytotoxic	244
Figure 7.2. Effects of compounds 1 – 9 , cisplatin and salinomycin on the viability of	
MiaPaCa-2, DU-145, PC3, JIMT-1, MDA-MB-231 and BT-474 cell lines	251
Figure 7.3. Cytotoxic Effect of compound 4 on triple negative breast cancer cell lines:	
BT549, MDA-MB-453, MDA-MB-468, Hs578t and MDA-MB-231	254

Figure 7.4. Cytotoxic Effect of compound 4 on glioblastoma cell lines - U-87 and U-251	256
Figure 7.5. Effect of compound 4 , 8 , salinomycin, cisplatin and myristylamine on viability of DU-145 and BT-474 CSCs and integrity of BT474 breast CSCs spheroids	259
Figure 7.6. Demonstration of caspase/apoptosis independent cell death	261
Figure 7.7. Evaluation of effect of compound 4 on cell membrane of DU-145 and JIMT-1 cell lines using cell impermeant ethidium homodimer-1 (EthD-1) dye that emits red fluorescence upon binding to DNA	264
Figure 7.8. Hemolytic properties of GAEL 4 using freshly isolated ovine erythrocytes. 1% ammonium hydroxide was used for 100% hemolysis, the control. The values were determined as % of control	265
Figure 7.9. Tolerability study, effect of compound 4 on weight of animal	267
Figure 8.1. List of some important GAELs synthesised and evaluated for anticancer activity in this thesis	309

List of Tables

Table 1.1. Chemical structure of some anticancer agents and their mechanism of actions	8
Table 1.2. Chemical structure of some anti-CSCs agents and their mechanisms of action	13
Table 3.1. Cytotoxicity of compounds 1-10 in μM to induce 50% killing against a panel of human cancer cell lines	69
Table 4.1. Cytotoxicity of compounds 1–7 on a panel of human epithelial cancer cell lines	108
Table 5.1. CC_{50} and CC_{90} values of compounds 1-10 and $\beta\text{-GLN}$ on a panel of human epithelial cancer cell lines: breast (BT474, JIMT1, MDA-MB-231), pancreas (MiaPaCa2) and prostate (DU145, PC3)	148
Table 7.1. CC_{50} values of compounds 1 - 10 , Chlorambucil, salinomycin, and cisplatin on a panel of human epithelial cancer cell lines: breast (BT474, JIMT1, MDA-MB-231), pancreas (MiaPaCa2) and prostate (DU145, PC3)	261
Table 7.2. CC_{50} and CC_{90} values of compounds 4 on a panel of human triple negative Breast cancer cell lines: MDA-MB-231, BT549, MDA-MB-453, MDA-MB-468 and Hs578t.	263
Table 7.3. CC_{50} and CC_{90} values of compounds 4 on glioblastoma U-87 and U-251 cell lines	265

Abbreviations

AELs	Antitumor ether lipids
AgOTf	Silver trifluoromethanesulfonate
ALDH1	Aldehyde dehydrogenase
ALP	Alkyl lysophosphocholine
APC	Alkylphosphocholine
BF ₃ .Et ₂ O	Borontrifluoride diethyl etherate
CC ₅₀	Cytotoxic concentration that kill 50% of cells
CC ₉₀	Cytotoxic concentration that kill 90% of cells
CSCs	Cancer stem cells
DCM	Dichloromethane
DMAP	4-Dimethylaminopyridine
DMF	<i>N,N</i> -Dimethylformamide
EthD-1	Ethidium homodimer-1
GLN	1-O-Hexadecyl-2-O-methyl-3-O-(2'-amino-2'-deoxy-β-D-glucopyranosyl)-sn-glycerol
HER2	Human epidermal growth factor receptor 2
NaOMe	Sodium methoxide
NIS	<i>N</i> -iodosuccinimide

PhSH	Thiophenol
QVD-OPh	(3S)-5-(2,6-difluorophenoxy)-3-[[[(2S)-3-methyl-2-(quinoline-2-carboxylamino)butanoyl]amino]-4-oxopentanoic acid
rt	room temperature
TBTU	O-(Benzotriazol-1-yl)-N,N,N',N'-tetramethyluronium tetrafluoroborate
THF	Tetrahydrofuran
TNBC	Triple negative breast cancer cell lines
TsCl	4-Toluenesulfonyl chloride
MTS	3-(4,5-dimethylthiazol-2-yl)-5-(3-carboxymethoxyphenyl)-2-(4-sulfophenyl)-2H-tetrazolium
MTT	3-(4,5-dimethylthiazol-2-yl)-2,5-diphenyltetrazolium bromide

Chapter 1

Introduction and Background

By Makanjuola Ogunsina

1.1. Challenges in Cancer Treatment

Cancer is a group of diseases that can affect any part of the body. It involves aberrant cell growth with a propensity to migrate to other parts of the body. The cause of cell proliferation in cancer is usually due to changes, mostly mutations, in genes responsible for cell growth and division.¹ Death associated with cancer is primarily due to the effect of the cancer cells, which form lumps in the case of solid tumor, on functioning of vital organs.² These lumps can block vital processes and change the tumor microenvironment. For instance, cancer in the digestive systems can significantly affect food absorption in the intestine by blocking the movement of food down the digestive system. Another example is lung cancer which interferes with the capacity of lung tissue to deliver the oxygen needed for body metabolism. Bone and brain tumors can affect blood chemistry and mental functioning adversely.² Cancer is one of the leading killer diseases worldwide affecting both the poor and the rich, male and female equally.³ The damage caused by cancer is enormous and extends beyond morbidity and the number of lives lost (mortality) each year. It includes physical, emotional, social, and spiritual challenges experienced by cancer patients, as well as their family members, friends, and caregivers.⁴ The financial costs of cancer are also mind-boggling. According to the National Institutes of Health, cancer cost the United States an estimated \$263.8 billion in medical costs and lost productivity in 2010.⁴ Also, approximately 14 million new cases and 8.2 million cancer related deaths were reported in 2012 worldwide and the numbers are expected to increase by nearly 70% in the next

two decades.³ These statistics are really astounding taking into consideration the magnitude of investment into cancer research and treatment. Some researchers have described the cost of cancer as economically unsustainable.⁵⁻⁹ In fact, the yearly cost of some cancer treatments is multiple times the annual wages of many people. Despite increasing approval of many new chemical entities for cancer treatment by the US Food and Drug Administration (FDA), death resulting from cancer is not abating but increasing. Clinical trials of these newly approved drugs usually demonstrate that they can only delay disease progression time from a few months and in extreme cases to a few years. A good example is Alectinib (marketed as Alecensa), an oral drug that blocks the activity of anaplastic lymphoma kinase approved by the FDA in 2015 to treat non-small cell lung cancer (NSCLC).¹⁰ This drug was able to achieve a partial shrinkage of NSCLC tumors in 38 – 44 % of treated patients, an effect that lasted for an average of 7.5 to 11.2 months.¹⁰ Darzalex (daratumumab), a human CD38-directed monoclonal antibody, was approved by FDA in November 2015 for the treatment of refractory multiple myeloma. Clinical trials show 29.2% response rate out of which 26.4 was partial.¹¹ The median time to response was one month and the median duration of response was 7.4 months.¹¹ Other examples include: Cabometyx (cabozantinib) a kinase inhibitor approved in April 2016 with overall survival of 21.4 months and 17% response rate in advance renal, carcinomas¹²; Lenvima (lenvatinib) a receptor tyrosine kinase (RTK) inhibitor approved in May 2016 prolong disease progression free period by 10.1 months and objective response rate of 37%, greater than 90% of which is partial.¹³ If these latest inventions in combating cancer is not really helping in the prevention of relapse, hope is not on the horizon for prevention of tumor relapse and reduction of associated death, hence need for further research.

There are several reasons for the current state of affairs. One reason is our inability to detect cancers in their early stages, especially tumor in the peritoneal region.¹⁴ Another reason is that cancer cells have devised various methods of avoiding death including escaping the ability of the immune system to get rid of them.¹⁵ Another hypothesis to explain the lack of progress against the disease that is currently gaining lot of attention is the cancer stem cell (CSC) hypothesis. According to this hypothesis, a limited number of stem cells within the tumor are responsible for its progression, homeostasis, metastasis and relapse.¹⁶⁻²⁶ The CSCs hypothesis asserts that current chemotherapeutic drugs only kill the non-CSCs in the tumor and leave behind a small set of CSCs which are resistant to drugs. This small population of CSCs have the capacity to self-renew and differentiate into cells that form the bulk of the recurred tumor. These tumors usually have a different phenotype from the original tumor and are very resistant to drugs that were initially used for treatment. Also, relapsed tumors are usually aggressive and highly metastasizing and patients with such tumors have a very poor prognosis. Currently there are no drugs clinically indicated for eradication of CSCs in tumors, though a few chemical entities have been reported with the capacity to kill CSCs.^{24,27} These drugs will be discussed in more details in the later part of this Chapter.

Another challenge facing cancer treatment is that it is heterogeneous, it differs from person to person. Therefore, the current treatment approach of 'one size fit all' may not work for every patient. There are currently increasing investigations on how cancer therapy can be individualized but this area of research is still in its infancy.²⁸⁻³⁰ The goal of this approach is to be able to predict the right drug to be given at the right time to the right patient using predictive biomarkers by practitioners based on genetic differences.³⁰⁻³²

Toxicity and serious side effects that can negatively impact on quality of life are also problems associated with available cancer treatment be surgery, radio- or chemo-therapy.^{33,34} These effects can be physiological, physical, emotional, social and even spiritual.³⁵ They are usually divided into two groups, short and long term effects. The short term effects include fatigue, nausea and vomiting, pain, hair loss, anemia, infection, blood clotting problems, mouth, gum and throat problems. These side effects can seriously impact one's quality of life. One of the major long term drawbacks of cancer drugs is the fear of relapse after treatment. Moreover, cancer treatments can cause major chronic diseases including infertility, cardiac disorders, diabetes, memory problems, hypothyroidism, incontinence, osteoporosis, sexual dysfunction and others, to mention just a few.^{36,37} An unfortunate side effect of some treatment is the development of secondary cancers which have been associated with some class of anticancer compounds including alkylating agents and topoisomerase II inhibitors.³⁸

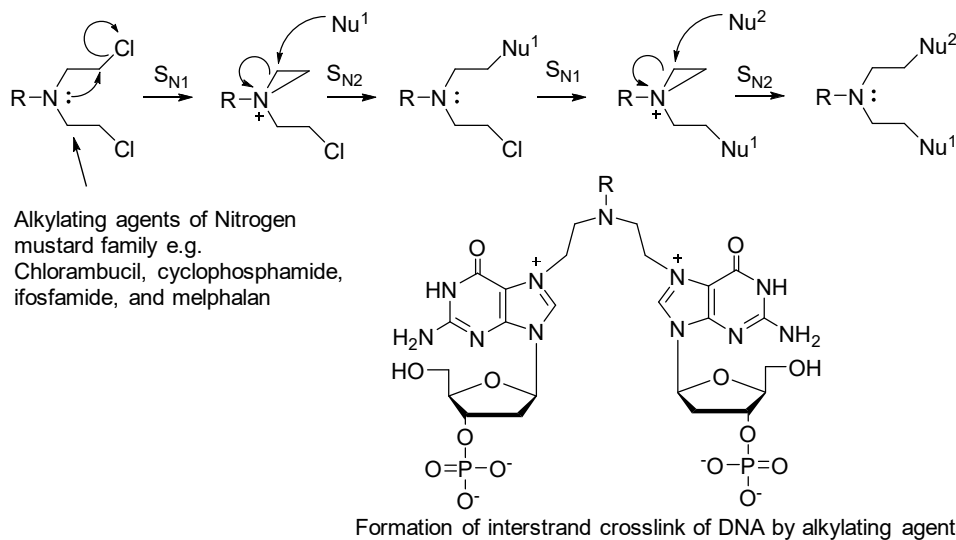
Another important issue in cancer management is the resistance of the tumor to available chemotherapeutic drugs. Resistance can be either acquired³⁹ or intrinsic.⁴⁰ It can significantly reduce or totally abolish the expected therapeutic effect of a drug leading to treatment failure in a large number of cases.³⁹ Based on the literature, cancers have developed resistance against virtually all chemotherapeutic and molecularly targeted agents in clinical use.⁴⁰ There are various propositions on possible mechanisms responsible for chemo resistance. They include alterations in the drug target, activation of pro-survival pathways, drug metabolism and ineffective induction of cell death.^{41,42} Increased drug efflux, mutations of the drug target, enhanced DNA damage repair, activation of alternative signaling pathways and evasion of cell death are other mechanism of drug resistance.^{40,43-45} Resistance to cancer drugs has also been a major challenge to the research community, because new effective agents must be discovered and developed.

1.2. Current Drugs Used in the Treatment of Cancer and Their Mechanism of Actions

There are different types of treatments for cancer patients. They include surgery, radiotherapy, chemotherapy, immunotherapy, targeted therapy, hormone therapy, and precision medicine, which was mentioned earlier.⁴⁶ Available modalities used in the clinic may involve combinations of the aforementioned treatments depending on the stage and nature of the cancer. There are over 400 drugs currently in clinical use for the treatment of cancer.⁴⁷ Here, I will focus mainly on chemotherapy. Generally chemotherapeutic agents can be classified on the basis of their mechanism of action. Thus, we have the following: alkylating agents, antimetabolites, antitumor antibiotics including anthracyclines, topoisomerases inhibitors, mitotic inhibitors, corticosteroids, and others including some enzyme inhibitors (Table 1.1).⁴⁸

The alkylating agents were the first chemotherapeutic agents used for treating cancer and comprise a number of subclasses.^{49,50} The nitrogen mustards comprise one subclass and include compounds like chlorambucil, cyclophosphamide, ifosfamide, and melphalan.⁵¹ Another subclass of the alkylating agents are the nitrosoureas which encompass drugs like streptozocin, carmustine and lomustine.⁵² The alkyl sulfonates like busulfan, the triazines such as dacarbazine and temozolomide, and ethylenimines like thiotepa and altretamine are also alkylating agents. The platinum based drugs including cisplatin, carboplatin, and oxaplatin are sometimes grouped with alkylating agents because they kill cells in a similar way.⁵³ Alkylating agents directly damage DNA by forming an interstrand cross-link, usually between two guanines, this produces double strand breaks in DNA, which prevents cells from replicating (Scheme 1.1).⁵⁴⁻⁵⁶ These drugs work in all phases of the cell cycle and are used to treat many different cancers, including leukemia, lymphoma, hodgkin disease, multiple myeloma, and sarcoma, as well as cancers of the lung, breast, and ovary.⁵⁷⁻⁵⁹ These drugs are DNA damaging agents, they can cause leukemia

because of damage to the bone marrow. The platinum based drugs are less likely to cause leukemia.⁵⁸ The chances of having leukemia after treatment with alkylating agents is directly proportional to the dose received and the risk is highest about 5 – 10 years post treatment.⁵⁷⁻⁶⁰



Scheme 1.1. Mechanism of action of alkylating agents. Alkylating agents of the Nitrogen mustard family formed interstrand crosslink by substitution reaction with N-7 of the guanine of DNA. This crosslink produces double strand break in DNA, which subsequently prevents replication of cancer cells.⁶¹

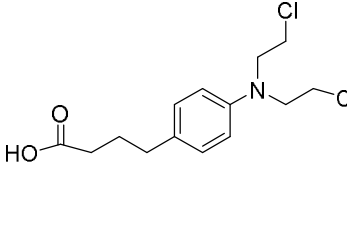
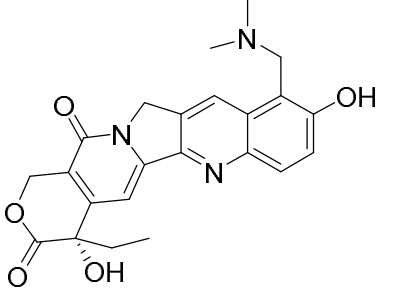
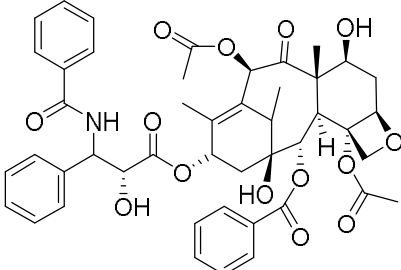
Antimetabolites are another class of cancer chemotherapy. They interfere with DNA and RNA synthesis by exchanging for the normal building blocks of nucleic acids. The damage induced by these agents occurs during the process of copying the cell's chromosome, during the S-phase of the cell's cycle.^{62,63} They are commonly used to treat leukemia, breast, ovarian, and intestinal tract cancer, as well as other types of cancer.^{48,64} Examples of antimetabolites include 5-fluorouracil, 6-mercaptopurine, capecitabine, cytarabine, floxuridine, fludarabine, gemcitabine, hydroxyurea, methotrexate, pemetrexed.^{48,62-66}

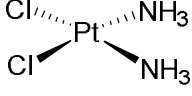
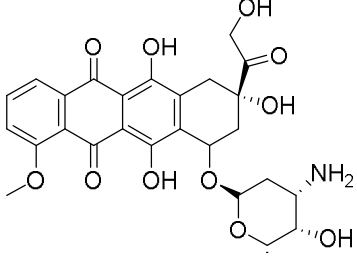
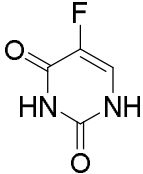
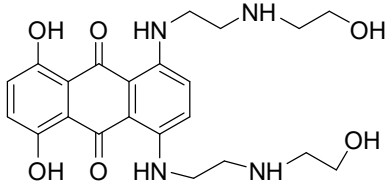
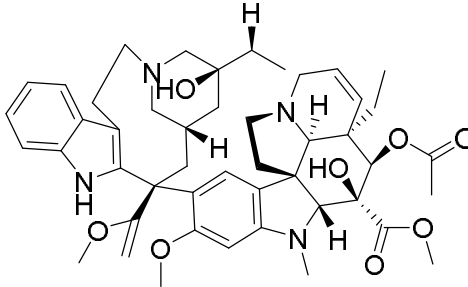
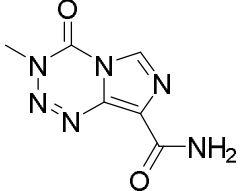
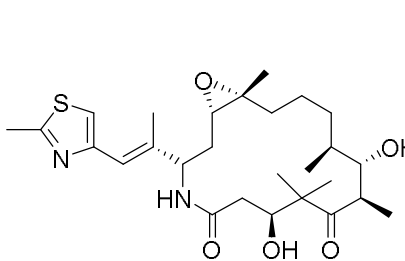
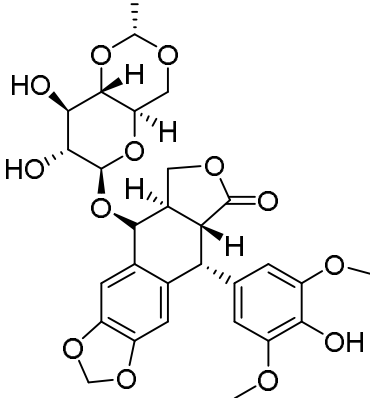
Antitumor antibiotics are another category of chemotherapy.⁶⁷ The anthracyclines including daunorubicin, doxorubicin, epirubicin and idarubicin are very prominent members of this group.⁶⁸ Other drugs in this group include actinomycin-D, bleomycin, mitomycin-C and mitoxantrone which also inhibit topoisomerases II.⁶⁹ Antitumor antibiotics generally execute their tumoricidal effect by numerous mechanisms including interfering with enzymes involved in DNA replication like the topoisomerases, they are also DNA intercalating agents.⁷⁰ These drugs work in all phases of the cell cycle and are widely used for a variety of cancers. A major concern with the use of anthracycline is the possibility of permanent damage to the heart. This effect is dependent on cumulative dose.⁷¹⁻⁷³

Topoisomerases and mitotic inhibitors are two other groups of cancer chemotherapeutic agents. The topoisomerases inhibitors are sub classified as topoisomerase I inhibitors which include topotecan and irinotecan⁷⁴ or topoisomerase II inhibitor represented by etoposide, teniposide and the antitumor antibiotic mitoxantrone. Topoisomerase II inhibitors induce double DNA strand break and this can occur at any stage of cell division while topoisomerase I inhibitor only induces single DNA strands break and affects mainly the S-phase or DNA synthesis of the cell cycle. These drugs execute their effects by inhibiting topoisomerases, important enzymes involved in regulation of winding or coiling of DNA, they act to maintain DNA topology and are essential for the integrity of the genetic material during transcription, replication and recombination processes.^{75,76} Drugs like etoposide, mitoxantrone increase the amount of topoisomerase II - DNA covalent complexes. This practically blocks DNA transcription and replication which results in DNA break and subsequent induction of apoptosis by the cells.⁷⁶ Topoisomerase II inhibitors can lead to secondary cancers like acute myelogenous leukemia as early as two years after the initial treatment.⁷⁷

The mitotic inhibitors are often plant alkaloids and other derivatives of natural products.⁷⁸ Their mechanism of action is usually through arresting mitosis in the M phase of the cell cycle, though damage of cells in all phases cannot be ruled out.⁷⁸ Examples of mitotic inhibitors include the taxanes such as paclitaxel and docetaxel, the epothilones including ixabepilone and vinca alkaloids like vinblastine, vincristine, and vinorelbine.⁷⁸ Also, estramustine has been reported to inhibit mitosis. Most of these drugs impair the normal function of mitotic spindles by targeting tubulins, the basic building blocks of microtubules.⁷⁹ Because these agents affect mitosis of normal cells, they cause a lot of side effects including myelosuppression and neurotoxicity. Myelosuppression is reversible and can be well managed, but the neurotoxicity can be very disabling.^{78,79}

Table 1.1. Chemical structure of some anticancer agents and their mechanism of action.

 <p>Chlorambucil- an alkylating agents, kills cancer cells by DNA cleavage as a result of interstrand cross-link to ganine bases.^{51,54,61}</p>	 <p>Topotecan - A topoisomerase inhibitor which stabilize DNA-topoisomerase 1 complex and prevent the DNA replication⁸⁰</p>	 <p>Paclitaxel – A mitotic inhibitor inhibits mitosis by stabilizing microtubules⁸¹</p>
---	---	--

 <p>Cisplatin – Platinum based anticancer agent, forms crosslink with the purine bases on the DNA.^{82,83}</p>	 <p>Doxorubicin – Belongs to anthracycline, mode of action includes inhibition of DNA-topoisomerases II and DNA intercalation.⁷⁰</p>	 <p>Methotrexate – An antimetabolite anticancer agents, inhibits dihydrofolate reductase which result in reduced synthesis of purines and pyrimidines.⁶⁴</p>
 <p>5-Fluorouracil – Antimetabolite anticancer agent which is converted intracellularly to several active metabolites which disrupt RNA synthesis.⁶²</p>	 <p>Mitoxantrone – An antitumor antibiotic and topoisomerase II inhibitor, works by increasing the amount of topoisomerase II - DNA covalent complexes.⁷⁶</p>	 <p>Vinblastine – A mitotic inhibitor that alter the microtubule dynamics of the cells which in turn leads to arrest of mitosis.⁸⁴</p>
 <p>Temozolomide - an alkylating agent prodrug, delivering a methyl group to purine bases of DNA (O6-guanine; N7-guanine and N3-adenine).⁸⁵</p>	 <p>Ixabepilone – is a mitotic inhibitor which exert its effect by binding to and subsequently polymerizing and stabilizing microtubules, thus preventing mitosis and resulting in apoptosis.⁸⁶</p>	 <p>Etoposide – A topoisomerase II inhibitor which works by increasing the amount of topoisomerase II-DNA covalent complexes.⁷⁶</p>

1.3. Drugs that Kill Cancer Stem Cells and Their Possible Mechanisms of Action

As discussed earlier, two major factors contributing to the high mortality of cancer are tumor relapse and drug resistance. CSCs have been implicated as the cause of tumor relapse, drug resistance and metastases.^{21,87-92} The CSC theory, like other theories such as clonal evolution,^{93,94} serves as a framework to guide the development of strategies to successfully eliminate tumors.^{22,95} The theory sees CSCs as the driving force behind the growth and progression of the tumor and the theory is being supported by increasing experimental data.^{88,90,96-99} The origin of CSCs in tumor is not fully known, but it may either be as a result of mutation to normal totipotent stem cells, which may lead to abnormal self-renewal and differentiation or as a result of cancer cell plasticity, that is, de-differentiation of cancer cells to CSCs.^{93,94}

CSCs have now been reported in virtually all solid and hematopoietic tumors.^{20,90,91,96,98-102} Aggressive cancers that are refractory to treatment contain more CSCs and there is correlation between the presence of CSC markers with clinical progression and clinical outcome.^{20,21,89,98} Elimination of CSCs is therefore crucial to successful cancer therapy according to the CSC theory.^{19,100} This may be achieved by directly killing the CSCs, inducing their differentiation with loss of CSC characteristics, or disrupting the niche signals they require for maintenance.

Taking into consideration the central role played by CSCs in cancer pathogenesis and progression, development of novel anticancer agents that kill the cells of the bulk of a tumor as well as the CSCs are important biomedical needs. There is currently no drug that is clinically indicated for use alone, or as part of combination therapy to eradicate CSCs, although few drugs have been reported to show activity against CSCs in *in vitro* (Table 1.2).

Various molecular complexes and pathways that confer drug resistance and survival of CSCs in presence of current anticancer agents have been elucidated. These include expression of ATP-binding cassette (ABC) drug transporters, activation of the Wnt/ β -catenin, Hedgehog, Notch and PI3K/Akt/mTOR signaling pathways, and acquisition of epithelial-mesenchymal transition (EMT).^{103,104} Also aldehyde dehydrogenase (ALDH) activity and pro-survival B-cell lymphoma-2 (BCL-2) protein family members in CSCs have been linked to their chemoresistance.¹⁰⁵ ALDH is associated with chemical modification of drug while BCL-2 binds to the pro-apoptotic proteins BCL2-associated-X-protein (BAX) and BCL-2 homologous antagonist killer (BAK) this binding impairs the ability of mitochondria to release apoptogenic proteins such as cytochrome c.¹⁰⁵ Another mechanism by which CSCs become resistant to chemotherapy is via their advanced anti-oxidative properties which include expression of reactive oxygen/nitrogen species scavengers and apoptosis inhibitor proteins.¹⁰⁶

Among the reported anti-CSC agents are some drugs currently used clinically in the treatment of cancer. However, considerably higher doses would be required than the current prescribed dosage to kill CSCs. One example of an anticancer agent that reportedly possesses anti-CSC property is temozolomide, a drug commonly used in the treatment of glioblastoma, a brain tumor.¹⁰⁷ The concentration of temozolomide required to kill CSCs is 10x the concentration needed to kill cells that are negative for CSC markers *in vitro*.¹⁰⁷ Other chemical agents that kill CSCs include salinomycin, metformin, parthenolide, lapatinib, mitochondrial targeted vitamin E succinate (mitoVES), thiodarizine and tranilast.^{27,92,101,108-113} Recently some antimicrobial agents including doxycycline, azithromycin, tigecycline and pyrvinium pamoate have been reported to inhibit CSCs spheroid formation *in vitro*.²⁴ Another group of compounds with potent ability to eradicate CSCs in addition to their broad spectrum of activity against cell

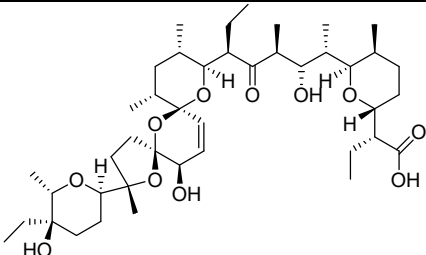
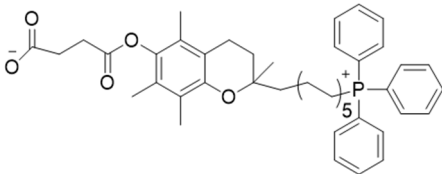
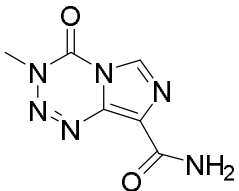
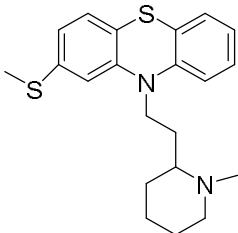
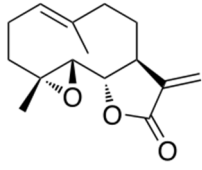
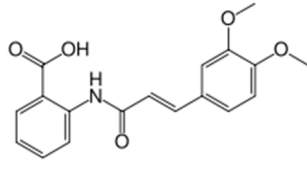
lines from multiple tumor types are some analogs of glycosylated antitumor ether lipids (GAELs), a class of antitumor ether lipids which is the focus of this thesis.¹¹⁴

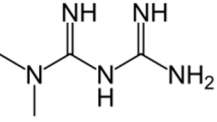
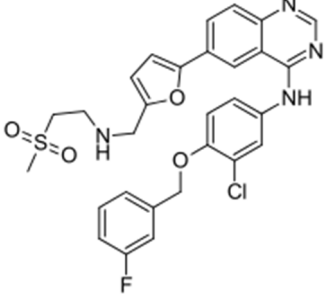
Among the drugs with anti-CSC effect, none has received as much attention as salinomycin. This may be because its discovery as an anti-CSC agent renewed interest in CSCs as a target for cancer chemotherapy and salinomycin is also commercially available and can be easily acquired. Salinomycin executes its CSCs' death induction activity via many mechanisms which are not yet fully understood. Induction of apoptosis is one of the mechanisms of cell death by salinomycin,¹¹⁵ but the pathway depends on the origin of the cells. For example, salinomycin induced apoptosis is caspase dependent in CSCs isolated from prostate PC-3 cancer cells, through generation of reactive oxygen species while salinomycin induced apoptosis in human leukemic stem cells are caspase independent and also independent of the p53 status of the cell.^{116,117} Also expression of ABC transporter protein by these cells has no effect on the activity of salinomycin.¹¹⁷ Modulation of Hedgehog signaling, especially via down regulation of Smo and Gli1 is another mechanism by which salinomycin exerts its anti-CSC properties in breast cancer.¹⁰⁴ A recent study also showed that salinomycin exhibited its CSCs' death via decreased ALDH1 activity and Nanog, Oct4 and Sox2 downregulation.¹¹⁸

Another drug that has been frequently investigated for killing CSCs is the antidiabetic drug metformin that was discovered in the 1950s. Interestingly metformin selectively kills CSCs with minimal or no effect on non-stem cancer cells.^{24,27,92,108,109,119} This should not be surprising because its phenylethyl analog phenformin was previously reported to enhance activity of other anticancer agents about 40 years ago.¹²⁰ Anti-CSC property of metformin has been associated with various mechanisms including activation of Liver Kinase B1/ AMP-activated protein kinase (LKB1/AMPK) pathway, induction of cell cycle arrest and/or apoptosis, inhibition of protein

synthesis, reduction in circulating insulin levels, inhibition of the unfolded protein response (UPR), activation of the immune system, and eradication of CSCs.^{108,109,119,121,122} Also, increasing evidence from retrospective clinical studies suggest that metformin may be associated with a decreased risk of developing cancer and with a better response to chemotherapy.¹²² AMP-activated protein kinase (AMPK) plays a major role in in the regulation of metabolism and growth of normal or cancerous cells.¹¹⁹

Table 1.2. Chemical structure of some anti-CSC agents and their mechanisms of action^b

Anti-CSC agents	
 <p>Salinomycin^{88,103,104,115,116} - Caspase dependent apoptosis,¹¹⁵ modulation of Hedgehog signaling.¹⁰⁴</p>	 <p>mitoVES¹²³ - targets mitochondrial complex and inhibition of oxygen consumption.¹²³</p>
 <p>Temozolomide¹⁰⁷</p>	 <p>Thioridazine¹²⁴ - Kills CSCs by autophagy.¹²⁴</p>
	

<p>Parthenolide^{27,125} - Suppression of the NF-κB/COX-2 Pathway¹²⁵</p>	<p>Tranilast¹²⁶ - induction of translocation of the aromatic hydrocarbon receptor (AHR), a transcription factor, to the nucleus. This prevent binding of the AHR to CDK4, which has been linked to cell-cycle arrest</p>
<p></p> <p>Metformin^{27,92,108,109,119,122} modulation of energy metabolism: inhibition of mTORC1 signaling and glycosis.^{121,127}</p>	<p></p> <p>Lapatinib¹²⁸</p>

1.4. Antitumor Ether Lipids

Antitumor ether lipids (AELs) are a group of disparate synthetic compounds that share the characteristic structural feature of being ether lipids capable of killing cancer cell lines. They are unnatural synthetic compounds and primarily classified into 3 groups: alkyllysophospholids (ALPs), alkylphospholipids (APLs) and glycosylated antitumor ether lipids, GAELs (Figure 1.1). The first AEL developed belong to the group of ALPs. ALPs are phosphoglycerolipids with a long alkyl chain at the *sn*-1 position of the glycerol moiety, a short-chain ether group at the *sn*-2 position, and a phosphocholine at the *sn*-3 position of glycerol. The ALPs were initially developed as stable analogs of lysophosphatidylcholine (LPC), by the insertion of the two ether bonds, for studies on the immunomodulatory properties of LPC in animals.¹²⁹ They are represented by edelfosine, 2-methoxy-3-(octadecyloxy) propyl 2-(trimethylammonio)-ethyl phosphate (Figure 1.2). ALPs were subsequently discovered to possess antiproliferative and cytotoxic activity *in vitro* and *in vivo*.¹³⁰ Structural activity relationship studies of edelfosine

have been extensively investigated.^{131–135} Edelfosine has many features desired of any anticancer agents including non mutagenicity, lack of interaction with DNA and relative selectivity for cancer cells compared to normal cells.^{130,135,136}

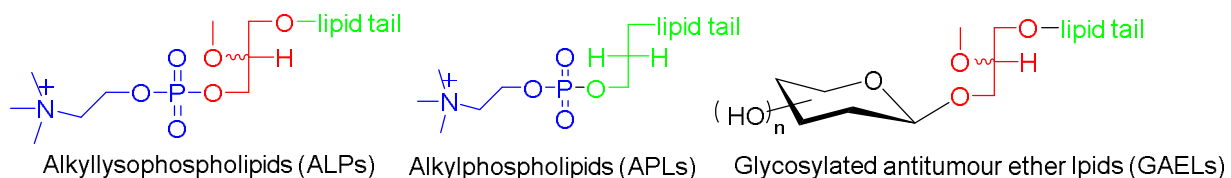


Figure 1.1. General classification of antitumor ether lipids (AELs)

Edelfosine kills cancer cells independent of the p53 status of the cell via caspase-dependent apoptosis²² and can be administered both intravenously and orally.^{137,138} Phase II clinical trials with edelfosine, the gold standard of ALPs in acute leukemia and non-small-cell bronchogenic carcinoma, did not result in objective remission but there was significant reduction in disease progression.^{129,139,140} Another drawback to clinical development of edelfosine is gastrointestinal toxicity which can be improved by using lipid nanoparticle formulation.¹⁴¹

Alkylphospholipids (APLs), the second subgroup of AELs lack a glycerol backbone and the alkyl group is directly esterified to the phosphobase, generally phosphocholine. APLs are technically not ether lipids because of the lack of ether linkages, but they have been consistently and historically classified as AEL in the literature. This may be because of structural features, long lipid tail and phosphocholine moiety, it shares with ALPs. The prototype of this subclass is miltefosine, hexadecyloxyl-2-(trimethylammonio)ethyl phosphate (Figure 1.2), which has undergone clinical trials and is in use as a topical treatment for skin metastases in breast cancer.^{142–144} Novel analogues of miltefosine with longer alkyl chains (C_{22:1}),

erycylphosphocholine (Figure 1.2), and an analogue where the phosphocholine moiety was replaced with a heterocyclic piperidine group, perifosine, have been synthesized and shown to possess promising anticancer activity *in vitro* and *in vivo*.¹⁴⁵ In fact perifosine showed very promising results in phase II clinical trials in multiple myeloma in patient previously treated with bortezomib¹⁴⁶ but the outcome of phase III clinical trials in colorectal cancer and multiple myeloma by Aeterna Zentaris Inc. was impressive. Like ALPs, APLs kill cancer cell via apoptosis mediated cell death.¹⁴²

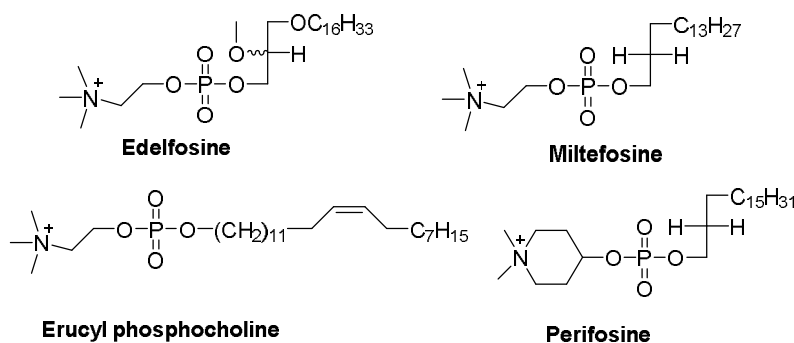


Figure 1.2. Examples of antitumor ether lipids

Glycosylated antitumor ether lipids (GAELs), the AEL class of focus in this thesis, represent the third subclass of AELs. GAELs differ from the other two subclasses of AELs by the replacement of the phosphocholine portion found in ALPs or APLs by a sugar moiety which is attached to the glycerol at the *sn*-3 position. The reason for focusing on developing GAELs as clinical anticancer drugs is because their mode of cell death is independent of apoptosis, and is thus, different from the mechanism of action of ALPs and APLs as well as many conventional chemotherapeutic agents.^{147,148} As alluded to above, cancer cells, including CSCs, have developed several strategies to escape cell death by apoptosis. Consequently, they survive exposure to apoptosis-inducing drugs and subsequently repopulate the tumor. Because GAELs

do not kill cancer cells by apoptosis, they have the potential of by-passing the mechanisms utilized by cancer cells to avoid death by apoptosis and could conceivably kill cancer CSCs which are usually resistant to apoptosis. They could therefore potentially be used in combination therapy with apoptosis inducing compounds to completely eliminate all the cells in a tumor.

1.5. Development of GAELs as Anticancer Agents

The development of GAELs as anticancer agents can be traced back to 1986, but its progress has trailed that of ALPs.¹⁴⁸ This maybe due to inferior potency of the early GAELs analogues, relative to the ALPs, and edelfosine in particular.¹³³ Also with the assumption that the mechanisms of action of all AELs were similar, it was logical to focus developmental efforts on the more active compounds like edelfosine. The motivation to develop GAELs as clinically useful agents gained momentum after the discovery of, 1-O-hexadecyl-2-O-methyl-3-O-(2'-amino-2'-deoxy- β -D-glucopyranosyl)-*sn*-glycerol, **GLN** (Figure 1.3, compound **4**) as potent cytotoxic agent followed by the discovery of its apoptosis-independent mechanism of cell death.^{149,150} Ultimately, for GAELs to be useful clinical drugs they would have to deliver anticancer activity *in vivo*. This would require metabolically stable analogs. The analogs of GAELs that demonstrated potent activity in *in vitro* experiments were *O*-glycosides. Such compounds may be very sensitive to hydrolases, especially the glycosidases in human and animals. This necessitated the development of metabolically stable GAELs with potent activity against drug sensitive and drug resistant cancer cells including CSCs. Until recently, very limited structural activity studies had been conducted with these compounds to determine the structural features pivotal to their activity and identify changes that would improve on their anticancer properties. Figure 1.3 shows the structural activity map of GAELs based on literature. Some of the compounds presented were previously published^{147,148,150-155} prior to the

commencement of this project while some were synthesized in the course of this project by different investigators in our lab.¹¹⁴ The map was used as a guide during this project.

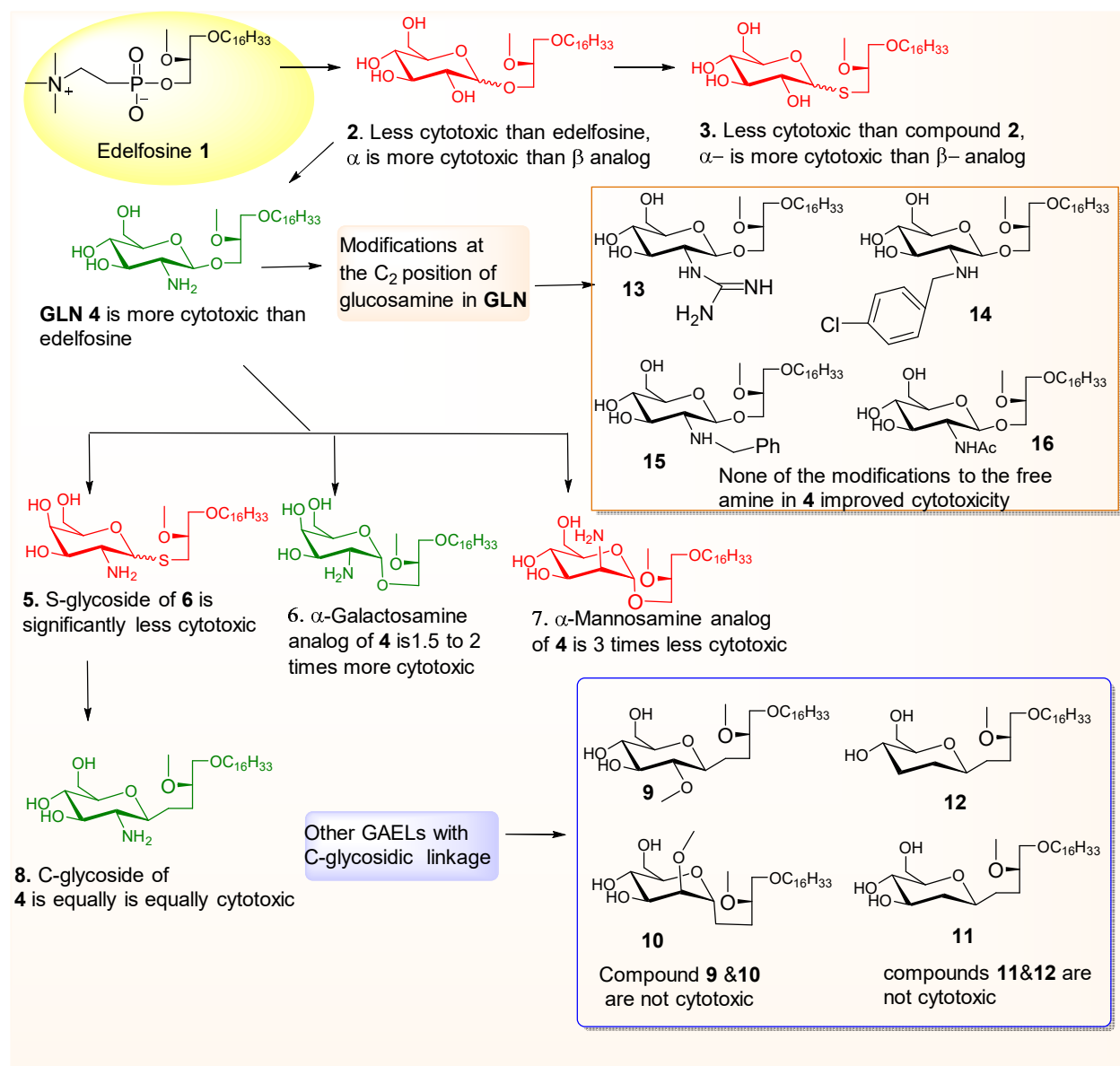


Figure 1.3. Structural activity map of GAELs.

Edelfosine 1, the most studied AEL was more potent than the *O*-glucoside 2 which in turn was more potent than the *S*-glucoside 3.¹⁴⁸ The analog 3 was initially synthesized because of the stability of thioglycosidic linkages, but it was significantly less potent than the *O*-glycoside. Unlike edelfosine which has both positive and negative charges on choline and phosphate moiety

respectively, compound **2** and **3** are without any charge. This may account for differences in activity in addition to other structural modifications. Compound **4**, **GLN**, an analog of **2** with amino substituents at position C-2 of the glucose moiety in lieu of hydroxyl moiety was more potent than edelfosine.¹⁴⁸ It was the discovery of compound **4** and its apoptosis-independent mechanism of cell death that renewed the enthusiasm to further develop GAELs as potential useful anticancer drugs. *In vivo* studies in mice revealed that toxic levels were not attained and **GLN** had no effect on breast cancer xenografts in mice. This was attributed to metabolic degradation as a result of glycosidases-catalysed hydrolysis of the glycosidic linkage. This was not surprising because glycosidases are ubiquitously expressed in animals^{156–158} Further modifications were made in an attempt to enhance the activity. The glucosamine in **4** was replaced with galactosamine in compound **6** and mannosamine in compound **7**. Compound **6** was significantly better than **4** while **7** was inactive at highest concentration tested, 30 μM . This indicated that the sugar type and configuration have a significant effect on activity. The α -anomer, **6** was > 3 times more potent than its β -anomer. The glycosidase stable thiogalactoside analogs of **6** were not cytotoxic at the highest concentration tested, 30 μM .¹¹⁴ This indicated that the *O*-glycosidic linkage in GAELs is pivotal to their cytotoxic effect.

GLN analogs with a *C*-glycosidic linkage were synthesized to afford resistance to glycosidases.¹⁵⁴ The *C*-glycoside **8** had similar activity as **GLN 4**,¹⁵⁴ but due to the cumbersome synthesis, scale-up synthesis for animal and possibly clinical studies may not be viable. *C*-glycoside analogs **9 - 12** without an amino substituent at C-2 position were significantly less active.¹⁴⁸ Analogs **13 - 16** with various modifications on the amino substituent of **GLN 4** were significantly less cytotoxic than **4**. This observation emphasized the significance of free amino substituent at the C-2 position of sugar to activity of GAELs.^{114,159}

1.5.1. Mechanism of GAEL-induced Cell Death

As pointed out earlier, the attractive feature of GAELs that distinguishes it from other AEL classes and many conventional anticancer agents is their ability to kill cancer cells via an apoptosis-independent mechanism, with similar characteristics to methuosis.^{160–162} Methuosis is a non-apoptotic cell death pathway characterized by an accumulation of large vacuoles derived from macropinocytosis.¹⁶² Macropinocytosis is a clathrin-independent form of endocytosis whereby cells internalize extracellular fluid inside vesicles formed by closure of actin-rich plasma membrane.¹⁶⁰ The build-up of the macropinosome-derived vacuoles may lead to decreased ATP generation, rupture of cell membrane and subsequently cell death.¹⁶⁰ This cell death is independent of caspase activation or apoptosis.^{161,162}

That the mechanism used by GAELs to kill cells is distinct from the apoptotic mechanisms used by ALPs or APLs was evident from the differential cytotoxic effects the different classes had on several cell lines.¹⁴⁸ A comparison of the cytotoxic effects of the GAEL subclasses against the drug resistant ovarian cancer cell line, OVCAR 3, showed that GAELs were the only class that significantly inhibited the proliferation of the cells or killed them.¹⁴⁸ In studies with NIH 3T3 cells transformed with oncogenic protein kinases (mos, fes, raf and src), edelfosine was unable to kill the transformed cell lines at concentrations that killed the wild-type NIH 3T3 cells, in contrast, GAEL 4 killed both the wild-type and transformed cells at similar concentrations.¹⁶³ More direct evidence of the fundamental differences between the mode of action of GAELs and ALPs was the demonstration that GAELs were able to kill mouse embryonic fibroblasts (MEFs) devoid of key apoptotic components like caspase 3, 9 and Apaf-1, which made them apoptosis-incompetent, edelfosine was unable to kill these cells.¹⁴⁹ These studies showed that an active apoptosis pathway was required for manifestation of the

cytotoxicity of ALPs but was not required for GAELs to kill the cells. Studies have also demonstrated that incubation of cells with GAELs did not result in the loss of mitochondria membrane permeability, release of cytochrome c to the cytosol, activation of caspase 9 or 3 or cleavage of t-Bid which are requirements for apoptosis.^{137,149,150,164,165}

The molecular mechanisms by which GAELs kill cells is not completely understood, but available studies have yielded insight on some events that may be involved. A striking observation of cells incubated with cytotoxic GAELs is the presence of large acidic vacuoles (LAV) that literally fill the cells. These vacuoles are morphologically similar to those described in methuosis induced by vacquinols,^{166,167} and indolyl-pyridinyl-propenones.^{161,162} The vacuoles stain red with acridine orange, an indication of their acidic nature. Studies with fluorescent markers including lysotracker red, LAMP1 and Igp120, the rat homologue of LAMP1, indicate that the vacuoles have some lysosomal characteristics.¹⁴⁹ In addition to the lysosomal molecules, LC3-II, a key protein marker of autophagy was observed, associated with the vacuoles. But the vacuoles are unlikely to be autophagosomes because there was no distinction between the vacuoles formed in wild type and autophagy incapable MEFs¹⁶⁸ The formation of the vacuoles was also observed in both wild type and Bif^{-/-} cells which are also autophagy incompetent.¹⁶⁹ These vacuoles may be derived from perturbation of endocytic pathways by cytotoxic GAELs, because when cells were incubated with GAEL in the presence or absence of beta-methyl cyclodextrin which inhibits endocytosis,¹⁷⁰ no vacuoles were observed in the cells pretreated with beta-methyl cyclodextrin for 1h before incubated with **GLN 4** and the GAEL did not kill the cells.^{147,148,153} To ensure that the lack of vacuole formation was not due to possible binding between the glycolipid **GLN 4** and beta-methyl cyclodextrin, the experiment was also carried out at 20°C, a temperature that prevent formation of endosomes, there was no formation of

vacuoles.¹⁴⁷ In contrast, in control cells with only **GLN**, the vacuoles were formed and the cells were killed. The lack of LAV formation in beta-methyl cyclodextrin (MCD) treated cells at temperature that prevent formation of endosomes indicates that an active endocytic pathway is required for manifestation of GAEL toxicity.¹⁴⁷ Because of the large size of these vacuoles, they are likely derived from macropinosomes which are usually 2-5 μm in diameter.¹⁷¹ Other endocytic pathways form significantly smaller vacuoles.¹⁷¹ Evaluating cytotoxicity of GAELs in presence of inhibitor of macropinocytosis, such as amiloride, sangliferin A or rapamycin will help to confirm that the mechanism of cell death of GAELs is methuosis.¹⁷¹

The current working hypothesis is that cells take up GAEL by a yet to be established mechanism, resulting in accumulation of macropinosomes-derived vacuoles. The excessive cytoplasmic vacuolization then leads to a form of cytolytic non-apoptotic cell death.¹⁶⁰ Available studies on GAELs activity have clearly linked the vacuolisation in cells with cell death.¹⁴⁸ Thus, only compounds that generate vacuoles kill the cells, while those that do not are unable to kill the cells. The molecular events linking GAEL-induced vacuole generation and accumulation to cell death have yet to be elucidated, but there is evidence it may involve lysosomal hydrolases such as cathepsins. The acidic and lysosomal-like nature of the vacuoles makes this feasible. It has been demonstrated that incubation of cells with **GLN 4**, results in the release of cathepsins B, D, and L into the cytosol of the cells.¹⁵² This was assessed by extracting the cytosol of the cells under conditions that do not cause rupture of the lysosomes. The level of cathepsins B, D, and L in the cytosolic fraction as measured by the enzyme activity and Western blotting for the proteins were greatly elevated in the cytosol of GAEL-treated cells.¹⁵² These observations suggest that **GLN 4** induces lysosomal membrane permeability in cells. When the cells were incubated with **GLN 4** in the presence of pepstatin A, a cathepsin D inhibitor, **GLN 4** induced cell death was

reduced by 40% relative to the controls with the GAEL alone.¹⁵² The lack of complete protection may be a function of the involvement of other cathepsins in the death process. To confirm this, an attempt to use other cathepsin inhibitor including E64, a cathepsin B inhibitor did not work because of its toxicity to the cells.¹⁵² Cathepsins-mediated apoptosis has been previously reported but this occurs via conversion of Bid to t-Bid.¹⁷² Cathepsins released in response to GAEL do not generate t-Bid or induce apoptosis as there was no loss of mitochondria membrane potential, cytochrome c release or activation of caspases.^{148–150,152} So the current working hypothesis is that cathepsins and perhaps other lysosomal hydrolases may contribute to effecting cell death subsequent to the generation of the vacuoles by GAELs.

1.5.2. Anti-Cancer Stem Cells Properties of GAELs

Since CSCs appear to be intrinsically resistant to apoptosis and radiotherapy, it is not surprising that current chemotherapeutic agents and radiotherapy which kill cells by inducing apoptosis are unable to prevent relapse. Agents that kill cells by apoptosis-independent mechanism could be effective in killing CSCs and thus prevent recurrence of the tumor. As discussed above, GAELs kill cells via an apoptosis-independent mechanism and would be expected to be effective against CSCs. The hypothesis was tested by isolating breast CSCs and comparing the effects of the apoptosis-inducing edelfosine with GAELs. Breast CSCs were isolated from BT474 and JIMT1 breast cancer cell lines by sorting for cells that highly express aldehyde dehydrogenase-1 (ALDH1), a stem cell marker for breast CSCs.¹⁷³ The sorted cells were grown as spheroids in suspension in ultra-low adhesion tissue culture ware in mammo cult medium.¹¹⁴ Large tumorspheres were formed within 7 days. The GAELs **4** and **6** were able to disintegrate and kill CSCs spheroid. They also prevent formation of spheroids whereas the controls formed spheroids.¹¹⁴ In contrast when the cells were incubated with edelfosine,

spheroids growth was observed. These observations showed that GAELs, unlike ALP, are cytotoxic to CSCs.

1.6. Methodologies for Evaluation of Cytotoxicity

Various methods have been used for evaluation of cytotoxicity. They include tetrazolium reduction assays, resazurin reduction assay, protease viability marker assay, a procedure in which cell permeable glycyphenylalanyl-aminofluoroumarin (GF-AFC) substrate is converted by cytoplasmic aminopeptidase activity to generate fluorescent aminofluorocoumarin (AFC)¹⁷⁴ and ATP assay.¹⁷⁴ Other procedures for evaluation of cytotoxicity includes lactose dehydrogenase (LDH) leakage assay,¹⁷⁵ and adenylate kinase assay.¹⁷⁶ These assays are more of cell viability assays rather than cell proliferation assays, but inferences on proliferation may be gleaned from the assays' results because of direct relationship between proliferation and viability. Most reports on cytotoxicity of GAELs have employed the tetrazolium reduction assays. The focus of the remaining part of this section will be on tetrazolium reduction assays.

Tetrazolium reduction assays employ various tetrazolium compounds to measure cell viability. These compounds can be classified into two classes, the positively charged and membrane permeable, type and the negatively charged and membrane impermeable type. The positively charged and membrane permeable MTT (3-(4,5-dimethylthiazol-2-yl)-2,5-diphenyltetrazolium bromide) enters the cell and is reduced to an insoluble purple formazan by electrons from mitochondrial activity of viable cells (Figure 1.4). Dead cells do not have the ability to convert MTT to formazan. This formazan accumulates as insoluble solids in the cells and the culture medium. The formazan is then solubilised using a variety of solvents including isopropanol, DMSO or dimethylformamide before the absorbance can be read.

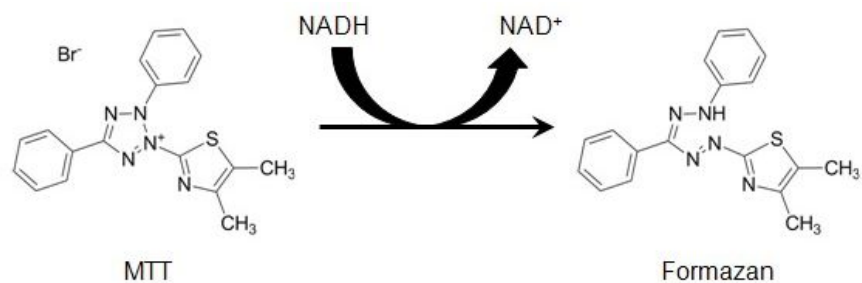


Figure 1.4. Conversion of MTT to formazan

Cell viability is directly proportional to absorbance. The second class of tetrazolium compounds used in assessment of cytotoxicity are the negatively charged and membrane impermeable type which includes MTS, XTT, and WST-1. These compounds are typically used with an intermediate electron acceptor like phenazine ethosulfate (PES) that can transfer electrons from the cytoplasm or plasma membrane to facilitate the reduction of the tetrazolium into the colored formazan product (Figure 1.5).

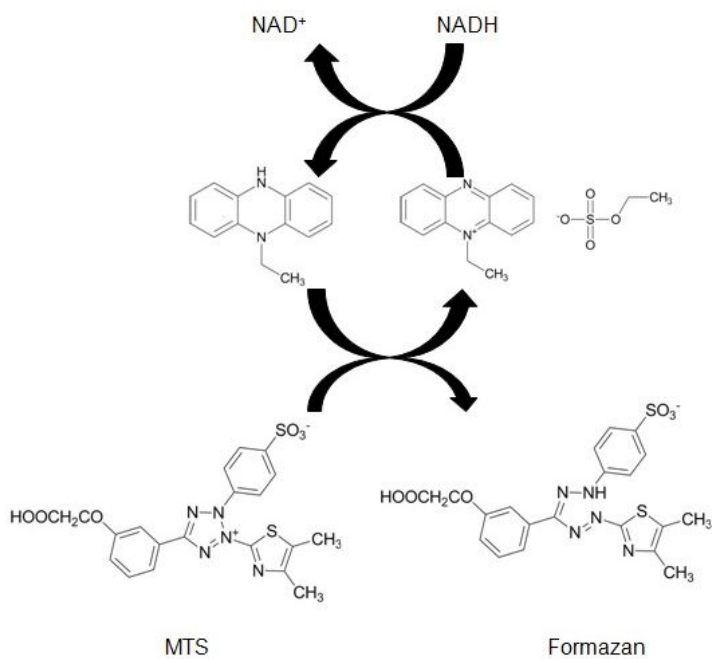


Figure 1.5. Conversion of MTS to formazan.

The advantage of MTS assay is that it does not require the solubilisation of the formazan before reading the absorbance.

1.7. Assessment of Apoptosis and Apoptosis-independent Mechanisms

Apoptosis is a very important physiological process critical for growth control and tissue homeostasis. It is characterised by the following features: activation of caspases, condensation of chromatin, activation of endonucleases leading to DNA fragmentation, preservation of organelles within cells, cell dehydration leading to its shrinkage, plasma membrane blebbing and formation of apoptotic bodies.¹⁷⁷ Apoptotic cell death can be caspase dependent or independent. Caspase activation is pivotal to most of the apoptotic events. Because most apoptotic events require activation of caspases, assessment of cell death (in)dependent of apoptosis usually focus on activation of caspases. There are two pathways involved in caspase dependent cell death: extrinsic and intrinsic pathways.¹⁷⁸

The extrinsic or death receptor pathway is activated when extracellular signals of tumor necrosis factor (TNF) family such as TNF or FAS ligands engage death receptors which include a subset of the TNF receptor family, including TNFR1, Fas/CD95, the TRAIL receptors-1 and death receptor 3.¹⁷⁷ This leads to activation of these receptors through trimerization and assembly of a large death-inducing signalling complex (DISC) on the cytoplasmic side of the plasma membrane.¹⁷⁸ DISC then recruits and mediates the auto-activation of the initiator caspase, procaspase 8 (and possibly of caspase10). Active caspase 8 then proteolytically cleaves and activates caspases 3, 6 and 7 leading to further caspase activation events that culminate in substrate proteolysis and cell death.¹⁷⁸

The intrinsic pathway, also known as the mitochondrial pathway, depends on permeabilization of the mitochondrial membrane. This leads to release of pro-apoptotic factors like cytochrome *c* from the intermembrane space of cells' mitochondria. For instance, during conditions of cell stress, antiapoptotic members of the Bcl-2 family of proteins (e.g., Bcl-2 and Bcl-xL), residing in the outer mitochondrial membrane, can be destabilized through decreased expression, or by the induction of pro-apoptotic Bcl-2 family members (e.g. Bax, Bad, and Bak). The ratio of pro-apoptotic to anti-apoptotic family members becomes greater. This promotes the assembly of Bax-Bak oligomers within the mitochondrial outer membranes. These oligomers compromise the permeability of this membrane, allowing the formation of proteinaceous outer membrane channels.¹⁷⁸ As a consequence, pro-apoptotic factors from the inter-membrane space of mitochondria are released into the cytoplasm. Among these, cytochrome *c* (Cyt *c*) directly activates the apoptosis protease-activating factor (Apaf-1) and, in the presence of dATP or ATP, seeds the formation of a large multimeric complex, the “apoptosome”. The apoptosome recruits and mediates the auto-activation of the initiator caspase, procaspase 9, which goes on to activate caspases 3, 6 and 7.¹⁷⁸

Assays for determining apoptosis (in)dependent cell death involve detecting various features of apoptosis mentioned above including, activation of caspases, condensation of chromatin, DNA fragmentation, preservation of organelles within cells, cell dehydration leading to its shrinkage, plasma membrane blebbing and formation of apoptotic bodies.¹⁷⁹ For high throughput screening, many studies have employed the use of pan-caspase inhibitors and compare cell death in the absence of the caspase inhibitor with cell death in presence of the inhibitor to assess for significance difference.¹⁸⁰ Any significant decrease in cell death in the presence of caspase inhibitor is evidence of caspase dependent apoptosis and vice versa.¹⁸⁰ Various pan-caspase

inhibitors have been employed in determining caspase-mediated apoptosis cell death. The most commonly used caspase inhibitors are Q-VD-OPH ((3S)-5-(2,6-Difluorophenoxy)-3-[[[(2S)-3-methyl-1-oxo-2-[(2-quinolinylcarbonyl)amino]butyl]amino]-4-oxo-pentanoic acid hydrate), ZVAD-FMK (N-Benzyloxycarbonyl-Val-Ala-Asp(O-Me) fluoromethyl ketone) and Boc-D-FMK (Boc-D-fluoromethyl ketone).¹⁸¹ Of these caspases inhibitors, Q-VD-OPH has been reported to be the most active with broader spectrum of caspases inhibition. In addition, Q-VD-OPH is not toxic to cells at high concentrations unlike ZVAD-fmk.¹⁸²⁻¹⁸⁵ Another important method of evaluating apoptosis (in)dependence in cell death is by using cell deficient of mediators that are critical to various pathways of apoptosis, these cells are usually resistant to pro-apoptotic agents.^{149,186}

In addition to apoptosis, other forms of programmed cell death include autophagy,¹⁷⁹ a process characterized by sequestration of bulk cytoplasm and organelles in double or multimembrane autophagic vesicles and their delivery to and subsequent degradation by the cell's own lysosomal system.¹⁸⁷ Another form of programmed cells death is paraptosis. It is characterized by cytoplasmic vacuolization that begins with progressive swelling of mitochondria, the endoplasmic reticulum (ER) and mitotic catastrophe which is usually triggered by mitotic failure caused by defective cell cycle checkpoints.¹⁷⁹

1.8. Identification and Isolation of CSCs

CSCs constitute a very small proportion of the cells in a tumor and as a consequence their identification and isolation presents challenges. The gold standard of CSCs identification is evaluation of self-renewing capacity and lineage differentiation potential after serial transplantation in animal models.¹⁸⁸ If after transplantation, a tumor is not formed, the transplanted subset of cells is deficient of CSCs. Because this *in vivo* approach does not lend

itself to routine use, Therefore, in *in vitro* experiments, the hallmark for identification of CSCs following their isolation is their ability to form spheroids/aggregates in ultra-low adhesion cell culture ware that precludes the growth of differentiated cells.¹⁸⁸

The commonly used approach for the isolation of CSCs is to sort cells based on the expression of various cell surface biomarkers either alone or in combination^{188,189} using magnetic activated cell sorting (MACS) which is based on super-paramagnetic and biodegradable microbeads linked to a specific monoclonal antibody (mAb) that allows the enrichment of cells that express the desired antigen or fluorescent-activated cell sorting (FACS). These biomarkers are specific cell surface proteins particularly expressed by CSCs in a tissue specific manner.^{190,191} This method of CSCs' identification is becoming more difficult as a result of frequent phenotypic transitions.¹⁹⁰⁻¹⁹² Various surface biomarkers expressed by CSCs include CD44, CD29, CD133, CD24, CD166, CD66, CD117, CD13, CD15, CD20, EpCAM and many others which are either overexpressed, under expressed or not expressed at all.^{188,191} The expression of cell surface biomarkers differs with the origin of the CSCs. For instance, while CD133 and CD44 are used in determining the identity of many types of CSCs, CD13, CD15 and CD20 have only been reported for identification of liver, glioma and melanoma CSCs respectively.¹⁸⁸ Aldehyde dehydrogenase 1 (ALDH1) activity is another means of identifying CSCs. ALDH1 is usually overexpressed in stem cells.^{173,193} This method was used in identification of CSCs used in evaluation of anti-CSC properties of GAELs.¹¹⁴ Another important fact is that the CSC population within a tumor are heterogeneous depending on their stage of self-renewal or differentiation. Some cells initially formed during the process of CSCs' self-renewal/differentiation which are described as transit-amplifying or progenitor cells also express some biomarkers particular to CSCs population.¹⁸⁹ This cell population significantly contributes

to heterogeneity of CSCs, which has posed a challenges to isolation and identification of pure CSCs using surface biomarkers.¹⁸⁹ The side population analysis has also been used in identifying and sorting of CSCs based on their ability to efflux out Hoechst 33,342 dye,¹⁹⁴ but it may not be the most effective identification technique.¹⁹⁵ Also, CSCs could be simply enriched by growing cancer cells in serum free media under non-adherent conditions.^{24,191} This method has also been used as an isolation technique. Furthermore, another way of enriching CSCs population is via intermittent drug treatment using incremental doses.¹⁹⁶ In addition, activation of the endothelia-mesenchymal transition (EMT) programme has increasingly been shown to generate CSCs.^{111,191} Genetic analysis has also been reported as a means of identifying CSCs.¹⁹⁷

To address one of the challenges facing cancer management, lack of clinically effective agents for killing CSCs, I hereby present my results on establishing structural features of GAELs crucial to their antitumor properties. This knowledge was used in optimization of GAELs to improve potency of GAELs' cytotoxicity against both CSCs and cancer cells. Also presented are various strategies to enhance metabolic stability while retaining the potency and non-apoptotic mechanism of cell death. I know that the information presented in this thesis will be an important part of expanding knowledge required to combat cancer.

1.3. References

- (1) Bukhtoyarov, O. V; Samarin, D. M.; Bukhtoyarov, O. V; Samarin, D. M. Pathogenesis of Cancer: Cancer Reparative Trap. *J. Cancer Ther.* **2015**, *6* (6), 399–412.
- (2) Cancer Research UK. How Can Cancer Kill You?
[Http://www.cancerresearchuk.org/about-Cancer/cancers-in-General/cancer-Questions/how-Can-Cancer-Kill-You](http://www.cancerresearchuk.org/about-Cancer/cancers-in-General/cancer-Questions/how-Can-Cancer-Kill-You). Cancer Research UK February 9, 2014.
- (3) WHO | Cancer <http://www.who.int/mediacentre/factsheets/fs297/en/> (accessed Dec 18, 2015).
- (4) The Global Burden of Cancer 2013 | Institute for Health Metrics and Evaluation
<http://www.healthdata.org/research-article/global-burden-cancer-2013> (accessed Aug 13, 2015).
- (5) Montero, A. J.; Avancha, K.; Glück, S.; Lopes, G. A Cost-Benefit Analysis of Bevacizumab in Combination with Paclitaxel in the First-Line Treatment of Patients with Metastatic Breast Cancer. *Breast Cancer Res. Treat.* **2012**, *132* (2), 747–751.
- (6) Leukemia, E. in C. M. The Price of Drugs for Chronic Myeloid Leukemia (CML) Is a Reflection of the Unsustainable Prices of Cancer Drugs: From the Perspective of a Large Group of CML Experts. *Blood* **2013**, *121* (22), 4439–4442.
- (7) American Society of Clinical Oncology. The State of Cancer Care in America, 2014: A Report by the American Society of Clinical Oncology. *J. Oncol. Pract.* **2014**, *10* (2), 119–142.
- (8) Kantarjian, H.; Steensma, D.; Rius Sanjuan, J.; Elshaug, A.; Light, D. High Cancer Drug

- Prices in the United States: Reasons and Proposed Solutions. *J. Oncol. Pract.* **2014**, *10* (4), e208-11.
- (9) McFarlane, J.; Riggins, J.; Smith, T. J. SPIKE\$: A Six-Step Protocol for Delivering Bad News about the Cost of Medical Care. *J. Clin. Oncol.* **2008**, *26* (25), 4200–4204.
- (10) Alecensa New FDA Drug Approval | CenterWatch <http://www.centerwatch.com/drug-information/fda-approved-drugs/drug/100124/alecensa-alectinib> (accessed Mar 22, 2016).
- (11) Darzalex New FDA Drug Approval | CenterWatch <http://www.centerwatch.com/drug-information/fda-approved-drugs/drug/100115/darzalex-daratumumab> (accessed Mar 22, 2016).
- (12) Cabometyx New FDA Drug Approval | CenterWatch <https://www.centerwatch.com/drug-information/fda-approved-drugs/drug/100141/cabometyx-cabozantinib> (accessed Jun 20, 2016).
- (13) Lenvima New FDA Drug Approval | CenterWatch <https://www.centerwatch.com/drug-information/fda-approved-drugs/drug/100148/lenvima-lenvatinib> (accessed Jun 20, 2016).
- (14) Kim, V. M.; Ahuja, N. Early Detection of Pancreatic Cancer. *Chin. J. Cancer Res.* **2015**, *27* (4), 321–331.
- (15) Vinay, D. S.; Ryan, E. P.; Pawelec, G.; Talib, W. H.; Stagg, J.; Elkord, E.; Lichtor, T.; Decker, W. K.; Whelan, R. L.; Kumara, H. M. C. S.; Signori, E.; Honoki, K.; Georgakilas, A. G.; Amin, A.; Helferich, W. G.; Boosani, C. S.; Guha, G.; Ciriolo, M. R.; Chen, S.; Mohammed, S. I.; Azmi, A. S.; Keith, W. N.; Bilsland, A.; Bhakta, D.; Halicka, D.; Fujii, H.; Aquilano, K.; Ashraf, S. S.; Newsheer, S.; Yang, X.; Choi, B. K.; Kwon, B. S.

- Immune Evasion in Cancer: Mechanistic Basis and Therapeutic Strategies. *Semin. Cancer Biol.* **2015**, *35 Suppl*, S185-98.
- (16) Hermann, P. C.; Huber, S. L.; Herrler, T.; Aicher, A.; Ellwart, J. W.; Guba, M.; Bruns, C. J.; Heeschen, C. Distinct Populations of Cancer Stem Cells Determine Tumor Growth and Metastatic Activity in Human Pancreatic Cancer. *Cell Stem Cell* **2007**, *1* (3), 313–323.
- (17) Kreso, A.; Dick, J. E. Evolution of the Cancer Stem Cell Model. *Cell Stem Cell* **2014**, *14* (3), 275–291.
- (18) Wicha, M. S. Cancer Stem Cells and Metastasis: Lethal Seeds. *Clin. Cancer Res.* **2006**, *12* (19), 5606–5607.
- (19) Boman, B. M.; Wicha, M. S. Cancer Stem Cells: A Step toward the Cure. *J. Clin. Oncol.* **2008**, *26* (17), 2795–2799.
- (20) Charafe-Jauffret, E.; Ginestier, C.; Iovino, F.; Wicinski, J.; Cervera, N.; Finetti, P.; Hur, M.-H.; Diebel, M. E.; Monville, F.; Dutcher, J.; Brown, M.; Viens, P.; Xerri, L.; Bertucci, F.; Stassi, G.; Dontu, G.; Birnbaum, D.; Wicha, M. S. Breast Cancer Cell Lines Contain Functional Cancer Stem Cells with Metastatic Capacity and a Distinct Molecular Signature. *Cancer Res.* **2009**, *69* (4), 1302–1313.
- (21) Li, F.; Tiede, B.; Massagué, J.; Kang, Y. Beyond Tumorigenesis: Cancer Stem Cells in Metastasis. *Cell Res.* **2007**, *17* (1), 3–14.
- (22) Al-Hajj, M.; Becker, M. W.; Wicha, M.; Weissman, I.; Clarke, M. F. Therapeutic Implications of Cancer Stem Cells. *Curr. Opin. Genet. Dev.* **2004**, *14* (1), 43–47.
- (23) Zhang, Y.; Wu, M.; Han, X.; Wang, P.; Qin, L. High-Throughput, Label-Free Isolation of

- Cancer Stem Cells on the Basis of Cell Adhesion Capacity. *Angew. Chem. Int. Ed. Engl.* **2015**, *54* (37), 10838–10842.
- (24) Lamb, R.; Ozsvari, B.; Lisanti, C. L.; Tanowitz, H. B.; Howell, A.; Martinez-Outschoorn, U. E.; Sotgia, F.; Lisanti, M. P. Antibiotics That Target Mitochondria Effectively Eradicate Cancer Stem Cells, across Multiple Tumor Types: Treating Cancer like an Infectious Disease. *Oncotarget* **2015**, *6* (7).
- (25) Zhao, J. Cancer Stem Cells and Chemoresistance: The Smartest Survives the Raid. *Pharmacol. Ther.* **2016**, *160*, 145–158. doi: 10.1016/j.pharmthera.2016.02.008.
- (26) Skvortsova, I.; Debbage, P.; Kumar, V.; Skvortsov, S. Radiation Resistance: Cancer Stem Cells (CSCs) and Their Enigmatic pro-Survival Signaling. *Semin. Cancer Biol.* **2015**, *35*, 39–44.
- (27) Zabalova, R. .; Stantic, M. .; Stapelberg, M. .; Prokopova, K. .; Dong, J. .; Truksa, J. et al. Drugs That Kill Cancer Stem-like Cells. In *Cancer Stem Cells Theories and Practice*; Shosta, S., Ed.; InTech, 2011; pp 361–378.
- (28) Forum discusses challenges facing cancer research, prevention and therapy in Europe. EurocanPlatform - News <http://eurocanplatform.eu/news/3848-forum-discusses-challenges-facing-cancer-research--prevention-and-therapy-in-europe.php> (accessed Dec 23, 2015).
- (29) Hayden, E. C. Personalized Cancer Therapy Gets Closer. *Nature* **2009**, *458* (7235), 131–132.
- (30) Villarroel, M. C.; Rajeshkumar, N. V; Garrido-Laguna, I.; De Jesus-Acosta, A.; Jones, S.;

- Maitra, A.; Hruban, R. H.; Eshleman, J. R.; Klein, A.; Laheru, D.; Donehower, R.; Hidalgo, M. Personalizing Cancer Treatment in the Age of Global Genomic Analyses: PALB2 Gene Mutations and the Response to DNA Damaging Agents in Pancreatic Cancer. *Mol. Cancer Ther.* **2011**, *10* (1), 3–8.
- (31) Dancey, J. E.; Bedard, P. L.; Onetto, N.; Hudson, T. J. The Genetic Basis for Cancer Treatment Decisions. *Cell* **2012**, *148* (3), 409–420.
- (32) Duffy, M. J.; Crown, J. A Personalized Approach to Cancer Treatment: How Biomarkers Can Help. *Clin. Chem.* **2008**, *54* (11), 1770–1779.
- (33) Cancer Research UK. Cancer Treatments. [Http://www.cancerresearchuk.org/about-Cancer/cancers-in-General/treatment/](http://www.cancerresearchuk.org/about-Cancer/cancers-in-General/treatment/). Cancer Research UK.
- (34) Treatments and Side Effects | American Cancer Society
<http://www.cancer.org/treatment/treatmentsandsideeffects/> (accessed Dec 23, 2015).
- (35) Social and Emotional Impacts of Cancer and Cancer Treatment
<http://www.ohsu.edu/xd/health/services/cancer/getting-treatment/services/cancer-survivorship/information-for-survivors/social-emotional-impact-cancer.cfm> (accessed Jul 16, 2016).
- (36) Side Effects of Chemotherapy & Cancer Treatment | MD Anderson Cancer Center
<http://www.mdanderson.org/patient-and-cancer-information/cancer-information/cancer-topics/survivorship/side-effects-of-cancer-treatment/index.html> (accessed Dec 23, 2015).
- (37) Cancer survivors: Late effects of cancer treatment - Mayo Clinic
<http://www.mayoclinic.org/diseases-conditions/cancer/in-depth/cancer-survivor/art->

20045524 (accessed Dec 23, 2015).

- (38) Ezoe, S. Secondary Leukemia Associated with the Anti-Cancer Agent, Etoposide, a Topoisomerase II Inhibitor. *Int. J. Environ. Res. Public Health* **2012**, *9* (7), 2444–2453.
- (39) Lu, H.-P.; Chao, C. C. K. Cancer Cells Acquire Resistance to Anticancer Drugs: An Update. *Biomed. J.* *35* (6), 464–472.
- (40) Holohan, C.; Van Schaeybroeck, S.; Longley, D. B.; Johnston, P. G. Cancer Drug Resistance: An Evolving Paradigm. *Nat. Rev. Cancer* **2013**, *13* (10), 714–726.
- (41) Holohan, C.; Van Schaeybroeck, S.; Longley, D. B.; Johnston, P. G. Cancer Drug Resistance: An Evolving Paradigm. *Nat. Rev. Cancer* **2013**, *13* (10), 714–726.
- (42) Hanane Akhdar, C. L. C. A. and F. M. *Topics on Drug Metabolism*; Paxton, J., Ed.; InTech, 2012.
- (43) Denisenko, T. V; Sorokina, I. V; Gogvadze, V.; Zhivotovsky, B. Mitotic Catastrophe and Cancer Drug Resistance: A Link That Must to Be Broken. *Drug Resist. Updat.* **2016**, *24*, 1–12.
- (44) Huijbers, E. J. M.; van Beijnum, J. R.; Thijssen, V. L.; Sabrkhany, S.; Nowak-Sliwinska, P.; Griffioen, A. W. Role of the Tumor Stroma in Resistance to Anti-Angiogenic Therapy. *Drug Resist. Updat.* **2016**, *25*, 26–37.
- (45) Persidis, A. Cancer Multidrug Resistance. *Nat. Biotechnol.* **1999**, *17* (1), 94–95.
- (46) Types of Cancer Treatment - National Cancer Institute <http://www.cancer.gov/about-cancer/treatment/types> (accessed Dec 23, 2015).
- (47) Cancer Research UK. Cancer Drugs. <Http://www.cancerresearchuk.org/about->

Cancer/cancers-in-General/treatment/cancer-Drugs/ ?openFull=1#list. Cancer Research UK March 2, 2014.

- (48) Types of chemotherapy drugs | American Cancer Society
<http://www.cancer.org/treatment/treatmentsandsideeffects/treatmenttypes/chemotherapy/chemotherapyprinciplesanin-depthdiscussionofthetechniquesanditsroleintreatment/chemotherapy-principles-types-of-chemo-drugs> (accessed Dec 24, 2015).
- (49) Goodman, L. S. Nitrogen Mustard Therapy. *J. Am. Med. Assoc.* **1946**, *132* (3), 126.
- (50) Gilman, A. The Initial Clinical Trial of Nitrogen Mustard. *Am. J. Surg.* **1963**, *105* (5), 574–578.
- (51) Masta, A.; Gray, P. J.; Phillips, D. R. Nitrogen Mustard Inhibits Transcription and Translation in a Cell Free System. *Nucleic Acids Res.* **1995**, *23* (17), 3508–3515.
- (52) Colvin, M. Alkylating Agents. BC Decker 2003.
- (53) AlkylatingAgents <http://livertox.nih.gov/AlkylatingAgents.htm> (accessed Jun 20, 2016).
- (54) Trams, E. G.; Nadkarni, M. V.; Smith, P. K. On the Mechanism of Action of the Alkylating Agents. I. Interaction of Alkylating Agents with Nucleic Acids. *Cancer Res.* **1961**, *21* (4), 560–566.
- (55) Beranek, D. T. Distribution of Methyl and Ethyl Adducts Following Alkylation with Monofunctional Alkylating Agents. *Mutat. Res. Mol. Mech. Mutagen.* **1990**, *231* (1), 11–30.
- (56) Warwick, G. P. The Mechanism of Action of Alkylating Agents. *Cancer Res.* **1963**, *23*

- (8_Part_1), 1315–1333.
- (57) Reimer, R. R.; Hoover, R.; Fraumeni, J. F.; Young, R. C. Acute Leukemia after Alkylating-Agent Therapy of Ovarian Cancer. *N. Engl. J. Med.* **1977**, *297* (4), 177–181.
- (58) Pedersen-Bjergaard, J.; Daugaard, G.; Hansen, S. W.; Roth, M.; Philip, P.; Larsen, S. O. Increased Risk of Myelodysplasia and Leukaemia after Etoposide, Cisplatin, and Bleomycin for Germ-Cell Tumours. *Lancet* **1991**, *338* (8763), 359–363.
- (59) Tucker, M. A.; Meadows, A. T.; Boice, J. D. . J.; Stovall, M.; Oberlin, O.; Stone, B. J.; Birch, J.; Voute, P. A.; Hoover, R. N.; Fraumeni, J. F. . J.; Late Effects Study Group. Leukemia After Therapy With Alkylating Agents for Childhood Cancer. *J Natl Cancer Inst* **1987**, *78* (3), 459–464.
- (60) Pedersen-Bjergaard, J.; Olesen Larsen, S.; Struck, J.; Hansen, H.; Specht, L.; Ersbll, J.; Hansen, M.; Nissen, N. Risk of Therapy-Related Leukemia and Preleukemia after Hodgkin’s Disease. *Lancet* **1987**, *330* (8550), 83–88.
- (61) Hall, A. G.; Tilby, M. J. Mechanisms of Action Of, and Modes of Resistance To, Alkylating Agents Used in the Treatment of Haematological Malignancies. *Blood Rev.* **1992**, *6* (3), 163–173.
- (62) Longley, D. B.; Harkin, D. P.; Johnston, P. G. 5-Fluorouracil: Mechanisms of Action and Clinical Strategies. *Nat. Rev. Cancer* **2003**, *3* (5), 330–338.
- (63) Burchenal, J. H.; Murphy, M. L.; Ellison, R. R.; Sykes, M. P.; Tan, T. C.; Leone, L. A.; Karnofsky, D. A.; Craver, L. F.; Dargeon, H. W.; Rhoads, C. P. Clinical Evaluation of a New Antimetabolite, 6-Mercaptopurine, in the Treatment of Leukemia and Allied

- Diseases. *Blood* **1953**, 8 (11), 965–999.
- (64) Kaye, S. B. New Antimetabolites in Cancer Chemotherapy and Their Clinical Impact. *Br. J. Cancer* **1998**, 78 Suppl 3, 1–7.
- (65) Longley, D. B.; Johnston, P. G. Molecular Mechanisms of Drug Resistance. *J. Pathol.* **2005**, 205 (2), 275–292.
- (66) Plunkett, W.; Huang, P.; Gandhi, V. Preclinical Characteristics of Gemcitabine. *Anticancer. Drugs* **1995**, 6 Suppl 6, 7–13.
- (67) Gewirtz, D. A Critical Evaluation of the Mechanisms of Action Proposed for the Antitumor Effects of the Anthracycline Antibiotics Adriamycin and Daunorubicin. *Biochem. Pharmacol.* **1999**, 57 (7), 727–741.
- (68) Sparreboom, A.; Nooter, K.; Verweij, J. *The Cancer Handbook*; Alison, M. R., Ed.; John Wiley & Sons, Ltd: Chichester, UK, 2005.
- (69) Harker, W. G.; Slade, D. L.; Dalton, W. S.; Meltzer, P. S.; Trent, J. M. Multidrug Resistance in Mitoxantrone-Selected HL-60 Leukemia Cells in the Absence of P-Glycoprotein Overexpression. *Cancer Res.* **1989**, 49 (16), 4542–4549.
- (70) Beretta, G. L.; Zunino, F. Molecular Mechanisms of Anthracycline Activity. *Top. Curr. Chem.* **2008**, 283, 1–19.
- (71) Volkova, M.; Russell, R. Anthracycline Cardiotoxicity: Prevalence, Pathogenesis and Treatment. *Curr. Cardiol. Rev.* **2011**, 7 (4), 214–220.
- (72) Rahman, A. M.; Yusuf, S. W.; Ewer, M. S. Anthracycline-Induced Cardiotoxicity and the Cardiac-Sparing Effect of Liposomal Formulation. *Int. J. Nanomedicine* **2007**, 2 (4), 567–

- 583.
- (73) Scott, J. M.; Khakoo, A.; Mackey, J. R.; Haykowsky, M. J.; Douglas, P. S.; Jones, L. W. Modulation of Anthracycline-Induced Cardiotoxicity by Aerobic Exercise in Breast Cancer: Current Evidence and Underlying Mechanisms. *Circulation* **2011**, *124* (5), 642–650.
- (74) Ewesuedo, R.; Ratain, M. Topoisomerase I Inhibitors. *Oncologist* **1997**, *2* (6), 359–364.
- (75) Binaschi, M.; Zunino, F.; Capranico, G. Mechanism of Action of DNA Topoisomerase Inhibitors. *Stem Cells* **1995**, *13* (4), 369–379.
- (76) Nitiss, J. L. Targeting DNA Topoisomerase II in Cancer Chemotherapy. *Nat. Rev. Cancer* **2009**, *9* (5), 338–350.
- (77) Seiter, K. Toxicity of the Topoisomerase II Inhibitors. *Expert Opin. Drug Saf.* **2005**, *4* (2), 219–234.
- (78) Gascoigne, K. E.; Taylor, S. S. How Do Anti-Mitotic Drugs Kill Cancer Cells? *J. Cell Sci.* **2009**, *122* (Pt 15), 2579–2585.
- (79) Jiang, N.; Wang, X.; Yang, Y.; Dai, W. Advances in Mitotic Inhibitors for Cancer Treatment. *Mini Rev. Med. Chem.* **2006**, *6* (8), 885–895.
- (80) Lorusso, D.; Pietragalla, A.; Mainenti, S.; Masciullo, V.; Di Vagno, G.; Scambia, G. Review Role of Topotecan in Gynaecological Cancers: Current Indications and Perspectives. *Crit. Rev. Oncol. Hematol.* **2010**, *74* (3), 163–174.
- (81) Horwitz, S. B. Taxol (Paclitaxel): Mechanisms of Action. *Ann. Oncol.* **1994**, *5 Suppl 6*, S3-6.

- (82) Dasari, S.; Bernard Tchounwou, P. Cisplatin in Cancer Therapy: Molecular Mechanisms of Action. *Eur. J. Pharmacol.* **2014**, *740*, 364–378.
- (83) Siddik, Z. H. Cisplatin: Mode of Cytotoxic Action and Molecular Basis of Resistance. *Oncogene* **2003**, *22* (47), 7265–7279.
- (84) Panda, D.; Jordan, M. A.; Chu, K. C.; Wilson, L. Differential Effects of Vinblastine on Polymerization and Dynamics at Opposite Microtubule Ends. *J. Biol. Chem.* **1996**, *271* (47), 29807–29812.
- (85) Zhang, J.; Stevens, M. F. G.; Bradshaw, T. D. Temozolomide: Mechanisms of Action, Repair and Resistance. *Curr. Mol. Pharmacol.* **2012**, *5* (1), 102–114.
- (86) Puhalla, S.; Brufsky, A. Ixabepilone: A New Chemotherapeutic Option for Refractory Metastatic Breast Cancer. *Biologics* **2008**, *2* (3), 505–515.
- (87) Kucia, M.; Reza, R.; Miekus, K.; Wanzeck, J.; Wojakowski, W.; Janowska-Wieczorek, A.; Ratajczak, J.; Ratajczak, M. Z. Trafficking of Normal Stem Cells and Metastasis of Cancer Stem Cells Involve Similar Mechanisms: Pivotal Role of the SDF-1-CXCR4 Axis. *Stem Cells* **2005**, *23* (7), 879–894.
- (88) Vinogradov, S.; Wei, X. Cancer Stem Cells and Drug Resistance: The Potential of Nanomedicine. *Nanomedicine (Lond)*. **2012**, *7* (4), 597–615.
- (89) Dean, M.; Fojo, T.; Bates, S. Tumour Stem Cells and Drug Resistance. *Nat. Rev. Cancer* **2005**, *5* (4), 275–284.
- (90) Yu, Z.; Pestell, T. G.; Lisanti, M. P.; Pestell, R. G. Cancer Stem Cells. *Int. J. Biochem. Cell Biol.* **2012**, *44* (12), 2144–2151.

- (91) Reya, T.; Morrison, S. J.; Clarke, M. F.; Weissman, I. L. Stem Cells, Cancer, and Cancer Stem Cells. *Nature* **2001**, *414* (6859), 105–111.
- (92) He, Y.-C.; Zhou, F.-L.; Shen, Y.; Liao, D.-F.; Cao, D. Apoptotic Death of Cancer Stem Cells for Cancer Therapy. *Int. J. Mol. Sci.* **2014**, *15* (5), 8335–8351.
- (93) de Souza, V. B.; Schenka, A. A. Cancer Stem and Progenitor-Like Cells as Pharmacological Targets in Breast Cancer Treatment. *Breast Cancer (Auckl)*. **2015**, *9* (Suppl 2), 45–55.
- (94) Iseghohi, S. O. Cancer Stem Cells May Contribute to the Difficulty in Treating Cancer. *Genes Dis.* **2016**, *3* (1), 7–10.
- (95) Medema, J. P. Cancer Stem Cells: The Challenges Ahead. *Nat. Cell Biol.* **2013**, *15* (4), 338–344.
- (96) Clarke, M. F.; Dick, J. E.; Dirks, P. B.; Eaves, C. J.; Jamieson, C. H. M.; Jones, D. L.; Visvader, J.; Weissman, I. L.; Wahl, G. M. Cancer Stem Cells--Perspectives on Current Status and Future Directions: AACR Workshop on Cancer Stem Cells. *Cancer Res.* **2006**, *66* (19), 9339–9344.
- (97) Fulda, S. Regulation of Apoptosis Pathways in Cancer Stem Cells. *Cancer Lett.* **2013**, *338* (1), 168–173.
- (98) Karnoub, A. E.; Dash, A. B.; Vo, A. P.; Sullivan, A.; Brooks, M. W.; Bell, G. W.; Richardson, A. L.; Polyak, K.; Tubo, R.; Weinberg, R. A. Mesenchymal Stem Cells within Tumour Stroma Promote Breast Cancer Metastasis. *Nature* **2007**, *449* (7162), 557–563.

- (99) Li, C.; Heidt, D. G.; Dalerba, P.; Burant, C. F.; Zhang, L.; Adsay, V.; Wicha, M.; Clarke, M. F.; Simeone, D. M. Identification of Pancreatic Cancer Stem Cells. *Cancer Res.* **2007**, *67* (3), 1030–1037.
- (100) Dingli, D.; Michor, F. Successful Therapy Must Eradicate Cancer Stem Cells. *Stem Cells* **2006**, *24* (12), 2603–2610.
- (101) Beier, D.; Röhrli, S.; Pillai, D. R.; Schwarz, S.; Kunz-Schughart, L. A.; Leukel, P.; Proescholdt, M.; Brawanski, A.; Bogdahn, U.; Trampe-Kieslich, A.; Giebel, B.; Wischhusen, J.; Reifenberger, G.; Hau, P.; Beier, C. P. Temozolomide Preferentially Depletes Cancer Stem Cells in Glioblastoma. *Cancer Res.* **2008**, *68* (14), 5706–5715.
- (102) Wang, J. C. Y.; Dick, J. E. Cancer Stem Cells: Lessons from Leukemia. *Trends Cell Biol.* **2005**, *15* (9), 494–501.
- (103) Naujokat, C.; Steinhart, R. Salinomycin as a Drug for Targeting Human Cancer Stem Cells. *J. Biomed. Biotechnol.* **2012**, *2012*, 1–17.
- (104) Lu, Y.; Ma, W.; Mao, J.; Yu, X.; Hou, Z.; Fan, S.; Song, B.; Wang, H.; Li, J.; Kang, L.; Liu, P.; Liu, Q.; Li, L. Salinomycin Exerts Anticancer Effects on Human Breast Carcinoma MCF-7 Cancer Stem Cells via Modulation of Hedgehog Signaling. *Chem. Biol. Interact.* **2015**, *228*, 100–107.
- (105) Abdullah, L. N.; Chow, E. K.-H. Mechanisms of Chemoresistance in Cancer Stem Cells. *Clin. Transl. Med.* **2013**, *2* (1), 3.
- (106) Lyakhovich, A.; Leonart, M. E. Bypassing Mechanisms of Mitochondria-Mediated Cancer Stem Cells Resistance to Chemo- and Radiotherapy. *Oxid. Med. Cell. Longev.*

2016, 2016.

- (107) Beier, D.; Rohrl, S.; Pillai, D. R.; Schwarz, S.; Kunz-Schughart, L. A.; Leukel, P.; Proescholdt, M.; Brawanski, A.; Bogdahn, U.; Trampe-Kieslich, A.; Giebel, B.; Wischhusen, J.; Reifenberger, G.; Hau, P.; Beier, C. P. Temozolomide Preferentially Depletes Cancer Stem Cells in Glioblastoma. *Cancer Res.* **2008**, *68* (14), 5706–5715.
- (108) Hirsch, H. A.; Iliopoulos, D.; Tsihchlis, P. N.; Struhl, K. Metformin Selectively Targets Cancer Stem Cells, and Acts Together with Chemotherapy to Block Tumor Growth and Prolong Remission. *Cancer Res.* **2009**, *69* (19), 7507–7511.
- (109) Vazquez-Martin, A.; Oliveras-Ferraros, C.; Del Barco, S.; Martin-Castillo, B.; Menendez, J. A. The Anti-Diabetic Drug Metformin Suppresses Self-Renewal and Proliferation of Trastuzumab-Resistant Tumor-Initiating Breast Cancer Stem Cells. *Breast Cancer Res. Treat.* **2011**, *126* (2), 355–364.
- (110) Chavez, K. J.; Garimella, S. V; Lipkowitz, S. Triple Negative Breast Cancer Cell Lines: One Tool in the Search for Better Treatment of Triple Negative Breast Cancer. *Breast Dis.* **2010**, *32* (1–2), 35–48.
- (111) Gupta, P. B.; Onder, T. T.; Jiang, G.; Tao, K.; Kuperwasser, C.; Weinberg, R. A.; Lander, E. S. Identification of Selective Inhibitors of Cancer Stem Cells by High-Throughput Screening. *Cell* **2009**, *138* (4), 645–659.
- (112) Sachlos, E.; Risueño, R. M.; Laronde, S.; Shapovalova, Z.; Lee, J.-H.; Russell, J.; Malig, M.; McNicol, J. D.; Fiebig-Comyn, A.; Graham, M.; Levadoux-Martin, M.; Lee, J. B.; Giacomelli, A. O.; Hassell, J. A.; Fischer-Russell, D.; Trus, M. R.; Foley, R.; Leber, B.; Xenocostas, A.; Brown, E. D.; Collins, T. J.; Bhatia, M. Identification of Drugs Including

- a Dopamine Receptor Antagonist That Selectively Target Cancer Stem Cells. *Cell* **2012**, *149* (6), 1284–1297.
- (113) Prud'homme, G. J.; Glinka, Y.; Toulina, A.; Ace, O.; Subramaniam, V.; Jothy, S. Breast Cancer Stem-like Cells Are Inhibited by a Non-Toxic Aryl Hydrocarbon Receptor Agonist. *PLoS One* **2010**, *5* (11), e13831.
- (114) Samadder, P.; Xu, Y.; Schweizer, F.; Arthur, G. Cytotoxic Properties of D-Gluco-, D-Galacto- and D-Manno-Configured 2-Amino-2-Deoxy-Glycerolipids against Epithelial Cancer Cell Lines and BT-474 Breast Cancer Stem Cells. *Eur. J. Med. Chem.* **2014**, *78* (78), 225–235.
- (115) Zhang, C.; Tian, Y.; Song, F.; Fu, C.; Han, B.; Wang, Y. Salinomycin Inhibits the Growth of Colorectal Carcinoma by Targeting Tumor Stem Cells. *Oncol. Rep.* **2015**, *34* (5), 2469–2476.
- (116) Fuchs, D.; Heinold, A.; Opelz, G.; Daniel, V.; Naujokat, C. Salinomycin Induces Apoptosis and Overcomes Apoptosis Resistance in Human Cancer Cells. *Biochem. Biophys. Res. Commun.* **2009**, *390* (3), 743–749.
- (117) Fuchs, D.; Daniel, V.; Sadeghi, M.; Opelz, G.; Naujokat, C. Salinomycin Overcomes ABC Transporter-Mediated Multidrug and Apoptosis Resistance in Human Leukemia Stem Cell-like KG-1a Cells. *Biochem. Biophys. Res. Commun.* **2010**, *394* (4), 1098–1104.
- (118) An, H.; Kim, J. Y.; Lee, N.; Cho, Y.; Oh, E.; Seo, J. H. Salinomycin Possesses Anti-Tumor Activity and Inhibits Breast Cancer Stem-like Cells via an Apoptosis-Independent Pathway. *Biochem. Biophys. Res. Commun.* **2015**, *466* (4), 696–703.

- (119) Kourelis, T. V.; Siegel, R. D. Metformin and Cancer: New Applications for an Old Drug. *Med. Oncol.* **2012**, *29* (2), 1314–1327.
- (120) Cohen, M. H.; Strauss, B. L. Enhancement of the Antitumor Effect of 1,3-bis(2-Chloroethyl)-L-Nitrosourea (BCNU) by Phenylethylbiguanide (Phenformin). *Oncology* **1976**, *33* (5–6), 257–259.
- (121) Kim, T. H.; Suh, D. H.; Kim, M.-K.; Song, Y. S. Metformin against Cancer Stem Cells through the Modulation of Energy Metabolism: Special Considerations on Ovarian Cancer. *Biomed Res. Int.* **2014**, *2014*, 132702.
- (122) Seppa, N. Old Drug, New Tricks: Metformin, Cheap and Widely Used for Diabetes, Takes a Swipe at Cancer. *Sci. News* **2013**, *184* (11), 18–21.
- (123) Yan, B.; Stantic, M.; Zobalova, R.; Bezawork-Geleta, A.; Stapelberg, M.; Stursa, J.; Prokopova, K.; Dong, L.; Neuzil, J. Mitochondrially Targeted Vitamin E Succinate Efficiently Kills Breast Tumour-Initiating Cells in a Complex II-Dependent Manner. *BMC Cancer* **2015**, *15*, 401.
- (124) Cheng, H.-W.; Liang, Y.-H.; Kuo, Y.-L.; Chuu, C.-P.; Lin, C.-Y.; Lee, M.-H.; Wu, A. T. H.; Yeh, C.-T.; Chen, E. I.-T.; Whang-Peng, J.; Su, C.-L.; Huang, C.-Y. F. Identification of Thioridazine, an Antipsychotic Drug, as an Antiglioblastoma and Anticancer Stem Cell Agent Using Public Gene Expression Data. *Cell Death Dis.* **2015**, *6*, e1753.
- (125) Liao, K.; Xia, B.; Zhuang, Q.-Y.; Hou, M.-J.; Zhang, Y.-J.; Luo, B.; Qiu, Y.; Gao, Y.-F.; Li, X.-J.; Chen, H.-F.; Ling, W.-H.; He, C.-Y.; Huang, Y.-J.; Lin, Y.-C.; Lin, Z.-N. Parthenolide Inhibits Cancer Stem-like Side Population of Nasopharyngeal Carcinoma Cells via Suppression of the NF- κ B/COX-2 Pathway. *Theranostics* **2015**, *5* (3), 302–321.

- (126) Prud'homme, G. J.; Glinka, Y.; Toulina, A.; Ace, O.; Subramaniam, V.; Jothy, S. Breast Cancer Stem-like Cells Are Inhibited by a Non-Toxic Aryl Hydrocarbon Receptor Agonist. *PLoS One* **2010**, *5* (11), e13831.
- (127) Mayer, M. J.; Klotz, L. H.; Venkateswaran, V. Metformin and Prostate Cancer Stem Cells: A Novel Therapeutic Target. *Prostate Cancer Prostatic Dis.* **2015**, *18* (4), 303–309.
- (128) Urtasun, N.; Vidal-Pla, A.; Pérez-Torras, S.; Mazo, A. Human Pancreatic Cancer Stem Cells Are Sensitive to Dual Inhibition of IGF-IR and ErbB Receptors. *BMC Cancer* **2015**, *15*, 223.
- (129) Gajate, C.; Mollinedo, F. Biological Activities, Mechanisms of Action and Biomedical Prospect of the Antitumor Ether Phospholipid ET-18-OCH(3) (Edelfosine), a Proapoptotic Agent in Tumor Cells. *Curr. Drug Metab.* **2002**, *3* (5), 491–525.
- (130) Berdel, W. E. Membrane-Interactive Lipids as Experimental Anticancer Drugs. *Br. J. Cancer* **1991**, *64* (2), 208–211.
- (131) Cailleau, R.; Young, R.; Olive, M.; Reeves, W. J. . J. Breast Tumor Cell Lines From Pleural Effusions. *J Natl Cancer Inst* **1974**, *53* (3), 661–674.
- (132) Danhauser, S.; Berdel, W. E.; Schick, H. D.; Fromm, M.; Reichert, A.; Fink, U.; Busch, R.; Eibl, H.; Rastetter, J. Structure-Cytotoxicity Studies on Alkyl Lysophospholipids and Some Analogs in Leukemic Blasts of Human Origin in Vitro. *Lipids* **1987**, *22* (11), 911–915.
- (133) Nosedá, A.; Berens, M. E.; Piantadosi, C.; Modest, E. J. Neoplastic Cell Inhibition with New Ether Lipid Analogs. *Lipids* **1987**, *22* (11), 878–883.

- (134) Berdel, W. E. Ether Lipids and Analogs in Experimental Cancer Therapy. A Brief Review of the Munich Experience. *Lipids* **1987**, *22* (11), 970–973.
- (135) Gajate, C.; Santos-Beneit, A.; Modolell, M.; Mollinedo, F. Involvement of c-Jun NH2-Terminal Kinase Activation and c-Jun in the Induction of Apoptosis by the Ether Phospholipid 1-O-Octadecyl-2-O-Methyl-Rac-Glycero-3-Phosphocholine. *Mol. Pharmacol.* **1998**, *53* (4), 602–612.
- (136) Berdel, W. E.; Bausert, W. R.; Fink, U.; Rastetter, J.; Munder, P. G. Anti-Tumor Action of Alkyl-Lysophospholipids (Review). *Anticancer Res.* **1981**, *1* (6), 345–352.
- (137) Smets, L. A.; Rooij, H. Van; Salomons, G. S. Signalling Steps in Apoptosis by Ether Lipids. *Apoptosis* *4* (6), 419–427.
- (138) Jackson, J. K.; Burt, H. M.; Oktaba, A. M.; Hunter, W.; Scheid, M. P.; Mouhajir, F.; Lauener, R. W.; Shen, Y.; Salari, H.; Duronio, V. The Antineoplastic Ether Lipid, S-Phosphonate, Selectively Induces Apoptosis in Human Leukemic Cells and Exhibits Antiangiogenic and Apoptotic Activity on the Chorioallantoic Membrane of the Chick Embryo. *Cancer Chemother. Pharmacol.* **1998**, *41* (4), 326–332.
- (139) Drings, P.; Günther, I.; Gatzemeier, U.; Ulbrich, F.; Khanavkar, B.; Schreml, W.; Lorenz, J.; Brugger, W.; Schick, H. D.; Pawel, J. v.; Nordström, R. Final Evaluation of a Phase II Study on the Effect of Edelfosine (an Ether Lipid) in Advanced Non-Small-Cell Bronchogenic Carcinoma. *Onkologie* **1992**, *15* (5), 375–382.
- (140) Vogler, W. R.; Berdel, W. E.; Geller, R. B.; Brochstein, J. A.; Beveridge, R. A.; Dalton, W. S.; Miller, K. B.; Lazarus, H. M. A Phase II Trial of Autologous Bone Marrow Transplantation (ABMT) in Acute Leukemia with Edelfosine Purged Bone Marrow. *Adv.*

- Exp. Med. Biol.* **1996**, *416*, 389–396.
- (141) Lasa-Saracíbar, B.; Aznar, M. Á.; Lana, H.; Aizpún, I.; Gil, A. G.; Blanco-Prieto, M. J. Lipid Nanoparticles Protect from Edelfosine Toxicity in Vivo. *Int. J. Pharm.* **2014**, *474* (1–2), 1–5.
- (142) van Blitterswijk, W. J.; Verheij, M. Anticancer Mechanisms and Clinical Application of Alkylphospholipids. *Biochim. Biophys. Acta* **2013**, *1831* (3), 663–674.
- (143) Barratt, M. J.; Frail, D. E. *Drug Repositioning: Bringing New Life to Shelved Assets and Existing Drugs*; John Wiley & Sons, 2012.
- (144) Dorlo, T. P. C.; Balasegaram, M.; Beijnen, J. H.; de Vries, P. J. Miltefosine: A Review of Its Pharmacology and Therapeutic Efficacy in the Treatment of Leishmaniasis. *J. Antimicrob. Chemother.* **2012**, *67* (11), 2576–2597.
- (145) Gills, J. J.; Dennis, P. A. Perifosine: Update on a Novel Akt Inhibitor. *Curr. Oncol. Rep.* **2009**, *11* (2), 102–110.
- (146) Richardson, P. G.; Wolf, J.; Jakubowiak, A.; Zonder, J.; Lonial, S.; Irwin, D.; Densmore, J.; Krishnan, A.; Raje, N.; Bar, M.; Martin, T.; Schlossman, R.; Ghobrial, I. M.; Munshi, N.; Laubach, J.; Allerton, J.; Hideshima, T.; Colson, K.; Poradosu, E.; Gardner, L.; Sportelli, P.; Anderson, K. C. Perifosine plus Bortezomib and Dexamethasone in Patients with Relapsed/refractory Multiple Myeloma Previously Treated with Bortezomib: Results of a Multicenter Phase I/II Trial. *J. Clin. Oncol.* **2011**, *29* (32), 4243–4249.
- (147) Samadder, P.; Byun, H.-S.; Bittman, R.; Arthur, G. An Active Endocytosis Pathway Is Required for the Cytotoxic Effects of Glycosylated Antitumor Ether Lipids. *Anticancer*

- Res* **2011**, *31* (11), 3809–3818.
- (148) Arthur, G.; Bittman, R. Glycosylated Antitumor Ether Lipids: Activity and Mechanism of Action. *Anticancer. Agents Med. Chem.* **2014**, *14* (4), 592–606.
- (149) Samadder, P.; Bittman, R.; Byun, H.-S.; Arthur, G. A Glycosylated Antitumor Ether Lipid Kills Cells via Paraptosis-like Cell Death. *Biochem. Cell Biol.* **2009**, *87* (2), 401–414.
- (150) Jahreiss, L.; Renna, M.; Bittman, R.; Arthur, G.; Rubinsztein, D. C. 1-O-Hexadecyl-2-O-Methyl-3-O-(2'-acetamido-2'-deoxy-Beta-D-Glucopyranosyl)-Sn-Glycerol (Gln) Induces Cell Death with More Autophagosomes Which Is Autophagy-Independent. *Autophagy* **2009**, *5* (6), 835–846.
- (151) Samadder, P.; Arthur, G. Decreased Sensitivity to 1-O-Octadecyl-2-O-Methyl-Glycerophosphocholine in MCF-7 Cells Adapted for Serum-Free Growth Correlates with Constitutive Association of Raf-1 with Cellular Membranes. *Cancer Res.* **1999**, *59* (19), 4808–4815.
- (152) Jahreiss, L.; Renna, M.; Bittman, R.; Arthur, G.; Rubinsztein, D. C. 1- O -Hexadecyl-2- O -Methyl-3- O -(2'-acetamido-2'-deoxy- β -D-Glucopyranosyl)- Sn -Glycerol (Gln) Induces Cell Death with More Autophagosomes Which Is Autophagy-Independent. *Autophagy* **2009**, *5* (6), 835–846.
- (153) Samadder, P.; Byun, H.-S.; Bittman, R.; Arthur, G. An Active Endocytosis Pathway Is Required for the Cytotoxic Effects of Glycosylated Antitumor Ether Lipids.
- (154) Yang, G.; Franck, R. W.; Bittman, R.; Samadder, P.; Arthur, G. Synthesis and Growth Inhibitory Properties of Glucosamine-Derived Glycerolipids. *Org. Lett.* **2001**, *3* (2), 197–

200.

- (155) Byun, H.-S.; Bittman, R.; Samadder, P.; Arthur, G. Synthesis and Antitumor Activity of Ether Glycerophospholipids Bearing a Carbamate Moiety at the Sn-2 Position: Selective Sensitivity against Prostate Cancer Cell Lines. *ChemMedChem* **2010**, *5* (7), 1045–1052.
- (156) Collin, W. F.; Fleet, G. W.; Haraldsson, M.; Cenci di Bello, I.; Winchester, B. Effect on Human Liver Glycosidases and Short Syntheses of 1 alpha,2 alpha,6 alpha,7 alpha,7a Beta-1,2,6,7-Tetrahydroxypyrrolizidine from D-Glycero-D-Gulo-Heptono-1,4-Lactone. *Carbohydr. Res.* **1990**, *202*, 105–116.
- (157) Ernst, B.; Magnani, J. L. From Carbohydrate Leads to Glycomimetic Drugs. *Nat. Rev. Drug Discov.* **2009**, *8* (8), 661–677.
- (158) McCarter, J. D.; Withers, S. G. Mechanisms of Enzymatic Glycoside Hydrolysis. *Curr. Opin. Struct. Biol.* **1994**, *4* (6), 885–892.
- (159) Erukulla, R. K.; Zhou, X.; Samadder, P.; Arthur, G.; Bittman, R. Synthesis and Evaluation of the Antiproliferative Effects of 1-O-Hexadecyl-2-O-Methyl-3-O-(2'-acetamido-2'-deoxy-Beta-D- Glucopyranosyl)-Sn-Glycerol and 1-O-Hexadecyl-2-O-Methyl-3-O- (2'-amino-2'-deoxy-Beta-D-Glucopyranosyl)-Sn-Glycerol on Epithelial Canc. *J. Med. Chem.* **1996**, *39* (7), 1545–1548.
- (160) Maltese, W. A.; Overmeyer, J. H. Non-Apoptotic Cell Death Associated with Perturbations of Macropinocytosis. *Front. Physiol.* **2015**, *6* (FEB), 1–10.
- (161) Trabbic, C. J.; Overmeyer, J. H.; Alexander, E. M.; Crissman, E. J.; Kvale, H. M.; Smith, M. A.; Erhardt, P. W.; Maltese, W. A. Synthesis and Biological Evaluation of Indolyl-

- Pyridinyl-Propenones Having Either Methuosis or Microtubule Disruption Activity. *J. Med. Chem.* **2015**, *58* (5), 2489–2512.
- (162) Maltese, W. A.; Overmeyer, J. H. Methuosis: Nonapoptotic Cell Death Associated with Vacuolization of Macropinosome and Endosome Compartments. *Am. J. Pathol.* **2014**, *184* (6), 1630–1642.
- (163) Samadder, P.; Byun, H. S.; Bittman, R.; Arthur, G. Glycosylated Antitumor Ether Lipids Are More Effective against Oncogene-Transformed Fibroblasts than Alkyllysophospholipids. *Anticancer Res.* *18* (1A), 465–470.
- (164) Susin, S. A.; Zamzami, N.; Castedo, M.; Hirsch, T.; Marchetti, P.; Macho, A.; Daugas, E.; Geuskens, M.; Kroemer, G. Bcl-2 Inhibits the Mitochondrial Release of an Apoptogenic Protease. *J. Exp. Med.* **1996**, *184* (4), 1331–1341.
- (165) *Apoptosis: Involvement of Oxidative Stress and Intracellular Ca²⁺ Homeostasis*; Salido, G. M., Rosado, J. A., Eds.; Springer Netherlands: Dordrecht, 2009.
- (166) Cully, M. Cancer: Turning Glioblastoma Cells Vacuous. *Nat. Rev. Drug Discov.* **2014**, *13* (6), 417.
- (167) Kitambi, S. S.; Toledo, E. M.; Usoskin, D.; Wee, S.; Harisankar, A.; Svensson, R.; Sigmundsson, K.; Kalderén, C.; Niklasson, M.; Kundu, S.; Aranda, S.; Westermark, B.; Uhrbom, L.; Andäng, M.; Damberg, P.; Nelander, S.; Arenas, E.; Artursson, P.; Walfridsson, J.; Forsberg Nilsson, K.; Hammarström, L. G. J.; Ernfors, P. Vulnerability of Glioblastoma Cells to Catastrophic Vacuolization and Death Induced by a Small Molecule. *Cell* **2014**, *157* (2), 313–328.

- (168) Mizushima, N.; Yamamoto, A.; Hatano, M.; Kobayashi, Y.; Kabeya, Y.; Suzuki, K.; Tokuhisa, T.; Ohsumi, Y.; Yoshimori, T. Dissection of Autophagosome Formation Using Apg5-Deficient Mouse Embryonic Stem Cells. *J. Cell Biol.* **2001**, *152* (4), 657–668.
- (169) Takahashi, Y.; Coppola, D.; Matsushita, N.; Cuaing, H. D.; Sun, M.; Sato, Y.; Liang, C.; Jung, J. U.; Cheng, J. Q.; Mulé, J. J.; Pledger, W. J.; Wang, H.-G. Bif-1 Interacts with Beclin 1 through UVRAG and Regulates Autophagy and Tumorigenesis. *Nat. Cell Biol.* **2007**, *9* (10), 1142–1151.
- (170) Ivanov, A. I. Pharmacological Inhibition of Endocytic Pathways: Is It Specific Enough to Be Useful? *Methods Mol. Biol.* **2008**, *440*, 15–33.
- (171) Lim, J. P.; Gleeson, P. A. Macropinocytosis: An Endocytic Pathway for Internalising Large Gulp. *Immunol. Cell Biol.* **2011**, *89* (8), 836–843.
- (172) Appelqvist, H.; Johansson, A.-C.; Linderöth, E.; Johansson, U.; Antonsson, B.; Steinfeld, R.; Kågedal, K.; Ollinger, K. Lysosome-Mediated Apoptosis Is Associated with Cathepsin D-Specific Processing of Bid at Phe24, Trp48, and Phe183. *Ann. Clin. Lab. Sci.* **2012**, *42* (3), 231–242.
- (173) Nakahata, K.; Uehara, S.; Nishikawa, S.; Kawatsu, M.; Zenitani, M.; Oue, T.; Okuyama, H. Aldehyde Dehydrogenase 1 (ALDH1) Is a Potential Marker for Cancer Stem Cells in Embryonal Rhabdomyosarcoma. *PLoS One* **2015**, *10* (4), e0125454.
- (174) Riss, T. L.; Moravec, R. A.; Niles, A. L.; Benink, H. A.; Worzella, T. J.; Minor, L. Cell Viability Assays. Eli Lilly & Company and the National Center for Advancing Translational Sciences. <http://www.ncbi.nlm.nih.gov/books/NBK144065/> June 29, 2015.

- (175) Fotakis, G.; Timbrell, J. A. In Vitro Cytotoxicity Assays: Comparison of LDH, Neutral Red, MTT and Protein Assay in Hepatoma Cell Lines Following Exposure to Cadmium Chloride. *Toxicol. Lett.* **2006**, *160* (2), 171–177.
- (176) Cho, M.-H.; Niles, A.; Huang, R.; Inglese, J.; Austin, C. P.; Riss, T.; Xia, M. A Bioluminescent Cytotoxicity Assay for Assessment of Membrane Integrity Using a Proteolytic Biomarker. *Toxicol. In Vitro* **2008**, *22* (4), 1099–1106.
- (177) Czabotar, P. E.; Lessene, G.; Strasser, A.; Adams, J. M. Control of Apoptosis by the BCL-2 Protein Family: Implications for Physiology and Therapy. *Nat. Rev. Mol. Cell Biol.* **2014**, *15* (1), 49–63.
- (178) Fulda, S.; Debatin, K.-M. Extrinsic versus Intrinsic Apoptosis Pathways in Anticancer Chemotherapy. *Oncogene* **2006**, *25* (34), 4798–4811.
- (179) Elmore, S. Apoptosis: A Review of Programmed Cell Death. *Toxicol. Pathol.* **2007**, *35* (4), 495–516.
- (180) Han, B. S.; Hong, H.-S.; Choi, W.-S.; Markelonis, G. J.; Oh, T. H.; Oh, Y. J. Caspase-Dependent and -Independent Cell Death Pathways in Primary Cultures of Mesencephalic Dopaminergic Neurons after Neurotoxin Treatment. *J. Neurosci.* **2003**, *23* (12), 5069–5078.
- (181) Chauvier, D.; Ankri, S.; Charriaut-Marlangue, C.; Casimir, R.; Jacotot, E. Broad-Spectrum Caspase Inhibitors: From Myth to Reality? *Cell Death Differ.* **2007**, *14* (2), 387–391.
- (182) Caserta, T. M.; Smith, A. N.; Gultice, A. D.; Reedy, M. A.; Brown, T. L. Q-VD-OPh, a

- Broad Spectrum Caspase Inhibitor with Potent Antiapoptotic Properties. *Apoptosis* **2003**, 8 (4), 345–352.
- (183) Keoni, C. L.; Brown, T. L. Inhibition of Apoptosis and Efficacy of Pan Caspase Inhibitor, Q-VD-OPh, in Models of Human Disease. *J. Cell Death* **2015**, 8, 1–7.
- (184) Callus, B. A.; Vaux, D. L. Caspase Inhibitors: Viral, Cellular and Chemical. *Cell Death Differ.* **2007**, 14 (1), 73–78.
- (185) Kuželová, K.; Grebeňová, D.; Brodská, B. Dose-Dependent Effects of the Caspase Inhibitor Q-VD-OPh on Different Apoptosis-Related Processes. *J. Cell. Biochem.* **2011**, 112 (11), 3334–3342.
- (186) Ullman, E.; Fan, Y.; Stawowczyk, M.; Chen, H.-M.; Yue, Z.; Zong, W.-X. Autophagy Promotes Necrosis in Apoptosis-Deficient Cells in Response to ER Stress. *Cell Death Differ.* **2008**, 15 (2), 422–425.
- (187) Bröker, L. E.; Kruyt, F. A. E.; Giaccone, G. Cell Death Independent of Caspases: A Review. *Clin. Cancer Res.* **2005**, 11 (9), 3155–3162.
- (188) Akbari-Birgani, S.; Paranjothy, T.; Zuse, A.; Janikowski, T.; Ciešlar-Pobuda, A.; Likus, W.; Uraśńska, E.; Schweizer, F.; Ghavami, S.; Klonisch, T.; Łos, M. J. Cancer Stem Cells, Cancer-Initiating Cells and Methods for Their Detection. *Drug Discov. Today* **2016**, No. March.
- (189) Pattabiraman, D. R.; Weinberg, R. A. Tackling the Cancer Stem Cells - What Challenges Do They Pose? *Nat. Rev. Drug Discov.* **2014**, 13 (7), 497–512.
- (190) Abdulmajeed, A. A.; Dalley, A. J.; Farah, C. S. Putative Cancer Stem Cell Marker

- Expression in Oral Epithelial Dysplasia and Squamous Cell Carcinoma. *J. Oral Pathol. Med.* **2013**, *42* (10), 755–760.
- (191) Ghuwalewala, S.; Ghatak, D.; Das, P.; Dey, S.; Sarkar, S.; Alam, N.; Panda, C. K.; Roychoudhury, S. CD44(high)CD24(low) Molecular Signature Determines the Cancer Stem Cell and EMT Phenotype in Oral Squamous Cell Carcinoma. *Stem Cell Res.* **2016**, *16* (2), 405–417.
- (192) Smith, N. R.; Gallagher, A. C.; Wong, M. H. Defining a Stem Cell Hierarchy in the Intestine: Markers, Caveats and Controversies. *J. Physiol.* **2016**.
- (193) Liu, S.-Y.; Zheng, P.-S. High Aldehyde Dehydrogenase Activity Identifies Cancer Stem Cells in Human Cervical Cancer. *Oncotarget* **2013**, *4* (12), 2462–2475.
- (194) Liu, P.-P.; Liao, J.; Tang, Z.-J.; Wu, W.-J.; Yang, J.; Zeng, Z.-L.; Hu, Y.; Wang, P.; Ju, H.-Q.; Xu, R.-H.; Huang, P. Metabolic Regulation of Cancer Cell Side Population by Glucose through Activation of the Akt Pathway. *Cell Death Differ.* **2014**, *21* (1), 124–135.
- (195) Yasuda, K.; Torigoe, T.; Morita, R.; Kuroda, T.; Takahashi, A.; Matsuzaki, J.; Kochin, V.; Asanuma, H.; Hasegawa, T.; Saito, T.; Hirohashi, Y.; Sato, N. Ovarian Cancer Stem Cells Are Enriched in Side Population and Aldehyde Dehydrogenase Bright Overlapping Population. *PLoS One* **2013**, *8* (8), e68187.
- (196) Xu, Z.-Y.; Tang, J.-N.; Xie, H.-X.; Du, Y.-A.; Huang, L.; Yu, P.-F.; Cheng, X.-D. 5-Fluorouracil Chemotherapy of Gastric Cancer Generates Residual Cells with Properties of Cancer Stem Cells. *Int. J. Biol. Sci.* **2015**, *11* (3), 284–294.
- (197) Lee, W. J.; Kim, S. C.; Yoon, J.-H.; Yoon, S. J.; Lim, J.; Kim, Y.-S.; Kwon, S. W.; Park,

J. H. Meta-Analysis of Tumor Stem-Like Breast Cancer Cells Using Gene Set and Network Analysis. *PLoS One* **2016**, *11* (2), e0148818. doi:10.1371/journal.pone.0148818

Chapter 2

Thesis Objectives

The compilation of this thesis is based on “Sandwich Thesis” format. It includes published results from my graduate studies edited from their original form for consistency. The edits include reformatting of the references to a uniform style, modifications of the text to correct errors and other appropriate alteration required for clearer presentation of my results.

Having summarised the trend of investigations on the development of GAELs, it is obvious that studies on structural activity relationship of GAELs have not been extensively explored, the potency of existing analogs can still be improved. Metabolically stable and non toxic or tolerable GAEL analog(s) have not been identified for either animal based *in vivo* or clinical studies. Additionally, the mechanisms of action of GAELs are yet to be fully explored. The objectives of this thesis are:

1. To synthesize structurally-diverse and conceptually similar analogues of GAELs with a goal of determining the structural features crucial to activity and non-apoptotic mode of action of GAELs in order to improve or optimise the biological activity of the lead compound **GLN**. Another goal here is to synthesize GAEL molecules that are metabolically stable without sacrificing the biological properties especially potency and mechanism of action, by taking into consideration important structural features required for anticancer properties. Figure 2.1 highlights various sites on the lead compounds for modifications to explore the SAR. Though some of the sites highlighted in Figure 2.1 have been previously modified, new form of chemical modifications will be explored.

- To evaluate anticancer properties of the newly-synthesized compounds using aggressively-growing cancer cell lines from multiple tumor types and cells in the G0/G1 phase of the cell cycles. The rationale for using many cell lines from multiple tumor type is to investigate the effect of tumor genotype and phenotype on the cytotoxicity and other anticancer properties of the new compounds. Promising compounds will be evaluated for their ability to destroy and disintegrate CSCs spheroids.

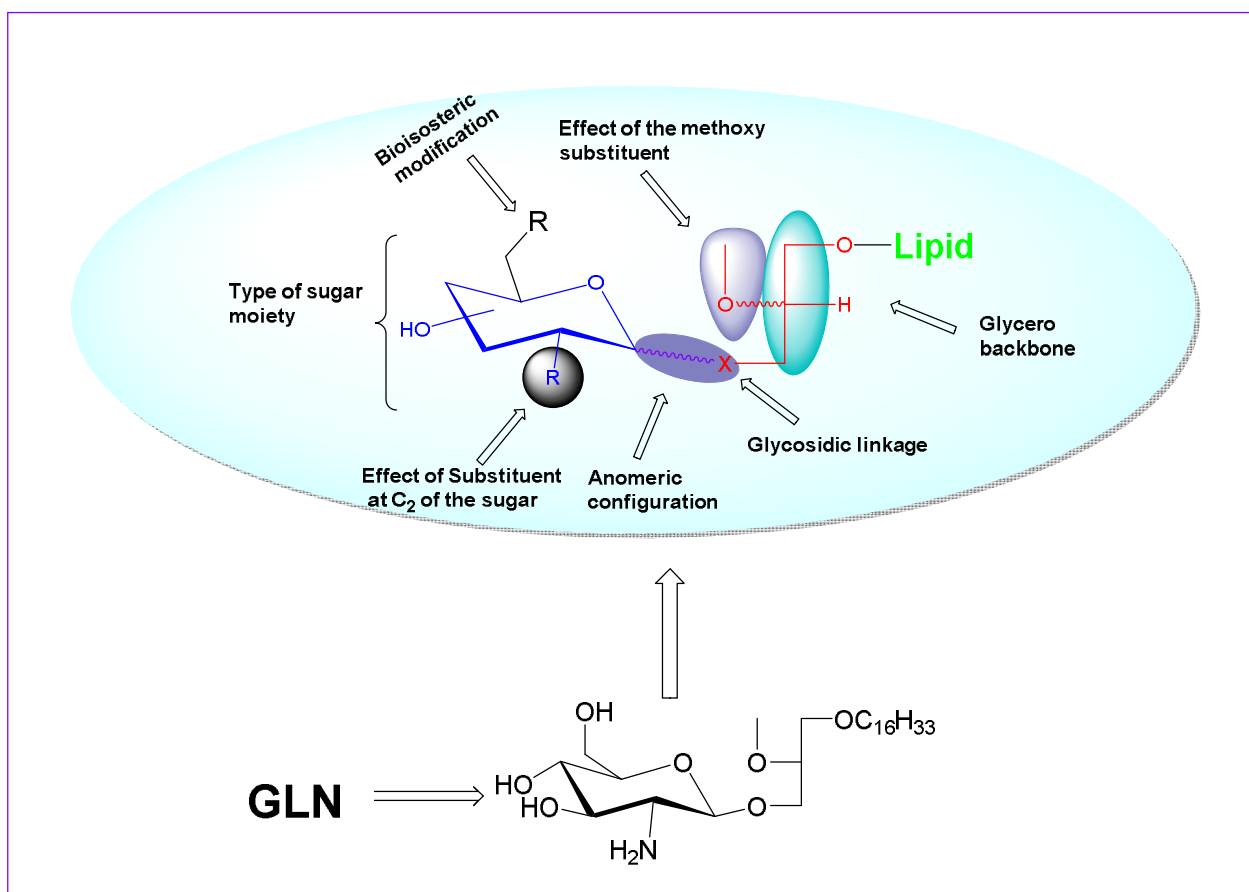


Figure 2.1. Proposed chemical modifications for structural activity relationship studies in this project.

3. To carry out mechanistic studies to determine if the new molecules exhibit same mode of action as the lead GAEL, **GLN**. The mode of action studies includes investigation of the role of caspases mediated apoptosis on cell death and formation of large acidic vacuole in cells after treatment with GAELs. Also the effect of the new compounds on membrane disruption will be evaluated to determine if the activity of the compounds is basically membrane effect, due to the amphiphilic nature of the compounds.

The outcome of the proposed structural activity studies described in Figure 2.1 are presented in details in Chapters 3-7. The focus of Chapters 3 and 4 is the elucidation of structural features that are critical to anticancer effects of GAELs. In Chapter 3 I will explore the importance of methoxy group of the glycerol backbone and the glycerol moiety of **GLN** on its cytotoxicity. For this purpose, analogs without the glycerol moiety and the methoxy group were synthesized and they were evaluated for their cytotoxic activity. Chapter 4 focuses on outcome of replacing the methoxy group with another sugar moiety and the role of stereochemistry at the *sn*-2 position of glycerol backbone on activity. Additionally, the glycerol moiety was completely substituted with a glycosidic triazole group to enhance stability to glycosidases and to further expand on the importance of the glycerol backbone.

In Chapter 5, I present the outcome of structural optimization of **GLN** to improve its potency by introducing another amino group. The rationale behind this was the discovery that **GLN** which has a single amino substituent was more potent than the neutral glucose analog. To achieve this, the hydroxyl group at the C-6 of the glucosamine was substituted with a primary amino group. In this Chapter further structural activity studies were reported on optimization of the position of the second amino moiety. Also the effect of various substitution on the second

amino group was presented. One more structural feature that was reported in this Chapter is the effect of anomeric configuration on cytotoxicity.

Chapters 6 and 7 focus on effects of new different types sugar configuration and their chirality on cytotoxicity, metabolic stability and mechanism of GAELs. These two Chapters describe our work on L-sugar derived GAELs. The rationale for introducing L-sugar instead of the usual D-sugars is because unnatural L-sugars are metabolically inert to human metabolic pathways. So with this concept, a major challenge impeding clinical development of GAELs, metabolic degradation could be overcome.

Chapter 8 summarises the overall outcome of this research with emphasis on compounds that are promising for further preclinical evaluation and clinical development. The body of work presented in this thesis has greatly advanced the development of GAELs as promising anticancer agent, but more work may still be needed especially in the area of advanced preclinical studies to determine the molecular basis of ability of GAELs to induce cell death especially in stem cells originating from tumor. Currently we have limited information on toxicological properties of GAELs, a detailed investigation should be initiated in this area. Though in this study potent and metabolically stable analogs of GAELs have been identified, scale up synthesis and optimization is still required for advance preclinical and clinical studies.

Chapter 3

Structure Activity Relationships of Glucosamine-Derived Glycerolipids: The Role of the Anomeric Linkage, the Cationic Charge and the Glycero Moiety on the Antitumor Activity

By Yaozu Xu, Makanjuola Ogunsina, Pranati Samadder, Gilbert Arthur, and Frank Schweizer

Originally published in ChemMedChem, 2013, 8(3), 511-520.

3.1. Authorship considerations

Makanjuola Ogunsina was responsible for synthesis, purification and characterization of glycolipids **6** and **7** on the advice of Frank Schweizer. Yaozu Xu was responsible for the synthesis of and purification of the remaining compounds on advice of Frank Schweizer. The biochemical studies were carried out by Pranati Samadder on the advice of Gilbert Arthur. The manuscript was jointly written by all the authors and then rendered into its final form by Frank Schweizer who is the corresponding author.

3.2. Abstract

Previously, we reported on the potent antitumor activity of 1-O-hexadecyl-2-O-methyl-3-O-(2'-amino-2'-deoxy- β -D-glucopyranosyl)-sn-glycerol **1** (Figure 3.1) which kills cancer cells by an apoptosis-independent pathway. In this paper we describe a systematic structure activity study in which we explore how the anomeric linkage, the cationic charge and the glycero moiety affects its antitumor activity. Eight analogs of **1** were synthesized and their antitumor activity against breast (JIMT1 and BT549), pancreas (MiaPaCa2) and prostate cancer (DU145, PC3) was determined. Our results demonstrate that 1-O-hexadecyl-2-O-methyl-3-O-(2'-amino-2'-deoxy- β -D-glucopyranosyl)-sn-glycerol (**2**) consistently, displays the most potent activity against all five cell lines with a CC50 at 6-10 μ M. However, replacement of the O-glycosidic linkage by a

thioglycosidic linkage or replacement of the amino group by azide or guanidino group leads to a 3-fold or higher reduction in potency. The glycerol moiety also contributes to the overall activity of **1** and **2** but its effect is of lesser importance.

3.3. Introduction

Cancer is a devastating disease with significant mortality and morbidity worldwide. It is one of the leading causes of death worldwide and results in about 7 million deaths every year. With an aging population, there are more than 11 million newly diagnosed cancer cases annually and by the year 2020, there will be 16 million new cases every year.¹ The major classes of anticancer drugs include antimetabolites, anthracyclines, taxanes and alkylating agents.² They disrupt cell DNA, prevent DNA synthesis or target microtubules to stop cancer cells from dividing. These disruptions induce apoptosis to kill the cells.³ The resistance of tumors to chemo and radiotherapy⁴⁻⁷ lies at the heart of our inability to cure cancer. Even targeted antibody based therapies such as trastuzumab (herceptin), are also affected by the phenomenon of drug resistance.^{8,9} Several mechanisms are responsible for resistance to drugs or ionizing radiation. Molecularly they include enhanced recognition and repair of DNA damage, impairment of apoptotic pathways, changes to cell cycle check points, and the ability to extrude drugs out of the cells.^{10,11} Defects in apoptosis are common in cancer and makes it difficult to kill the cells by the very pathways activated by most chemotherapeutic agents.^{12,13} One approach to overcome these problems is to develop novel compounds that kill cells by pathways other than apoptosis.

Antitumor ether lipids (AELs) were developed as long-lived analogs of lysophosphatidylcholine, a naturally occurring phospholipid, through the insertion of two ether bonds at the C-1 and C-2 positions. They are small, amphiphilic stable compounds that can be administered intravenously or orally. Their action is independent of the p53 status of the cell¹⁴

and they do not interact with cellular DNA.¹⁵ They have also demonstrated selective toxic effects against cancer cells relative to normal cells both *in vitro* and *in vivo*.^{15,16} Two of the AEL subclasses alkyllysophospholipids (ALP), alkylphosphocholines (APC) kill cells by apoptosis.^{14,17}

Recently, we reported that the cationic glucosamine-derived glycerolipid **1**, a member of the glycosylated AEL (GAEL) subclass which have a sugar moiety in place of the phosphorylcholine found in the antitumor agent edelfosine, kills cancer cells by an apoptosis-independent pathway.^{18,19} A hallmark of this pathway is the formation of large acidic vacuoles (LAVs) in the cells as a consequence of perturbation of the endocytic pathway leading to death via release of cathepsins.^{19,20} Inspired by this novel mode of action we initiated a program to explore the structure activity relationships of **1**. In particular, we were interested to study (a) how the nature of the anomeric linkage (b) the nature of the cationic charge and (c) the nature of glycerol moiety affects its antitumor activity against a selection of cancer cell lines.

3.4. Results and Discussion

3.4.1. Chemistry

In order to get insight into the pharmacophore responsible for the antitumor effect we decided to prepare a variety of structural analogs of **1** (Figure 3.1). Initially, we were interested to study how the nature of the anomeric O-glycosidic linkage affects its antitumor effect. Compound **2** containing an α -glucosidic linkage instead of β -glucosidic linkage was prepared. Anomeric glycolipids **3** and **4** bearing a neutral azido function instead of a positively charged amino group were selected to explore how the cationic charge at the 2-position of glucose influences the antitumor activity. Similarly, guanidinylated glycolipid **5** was selected to explore how steric

changes in size and basicity affects the anticancer activity. To explore how the nature of the glycerol moiety influences the antitumor activity the β -glucosidic glycolipid **6** devoid of the glycerol-based methoxy substituent and the β -glucosidic glycolipid **7** which lacks the glycerol group were prepared. In anticipation of potential problems associated with the use of O-glycosidic linkages in future *in vivo* studies we prepared thioglycolipids **8** and **9** as thioglycosidic linkages are known to resist hydrolysis by glycosidases.²¹ Finally, in order to explore how the cationic amphiphilic nature of the glycolipids affect their biological activity the cationic lipid myristylamine **10** devoid of a carbohydrate moiety was selected as a noncarbohydrate-based cationic amphiphile.

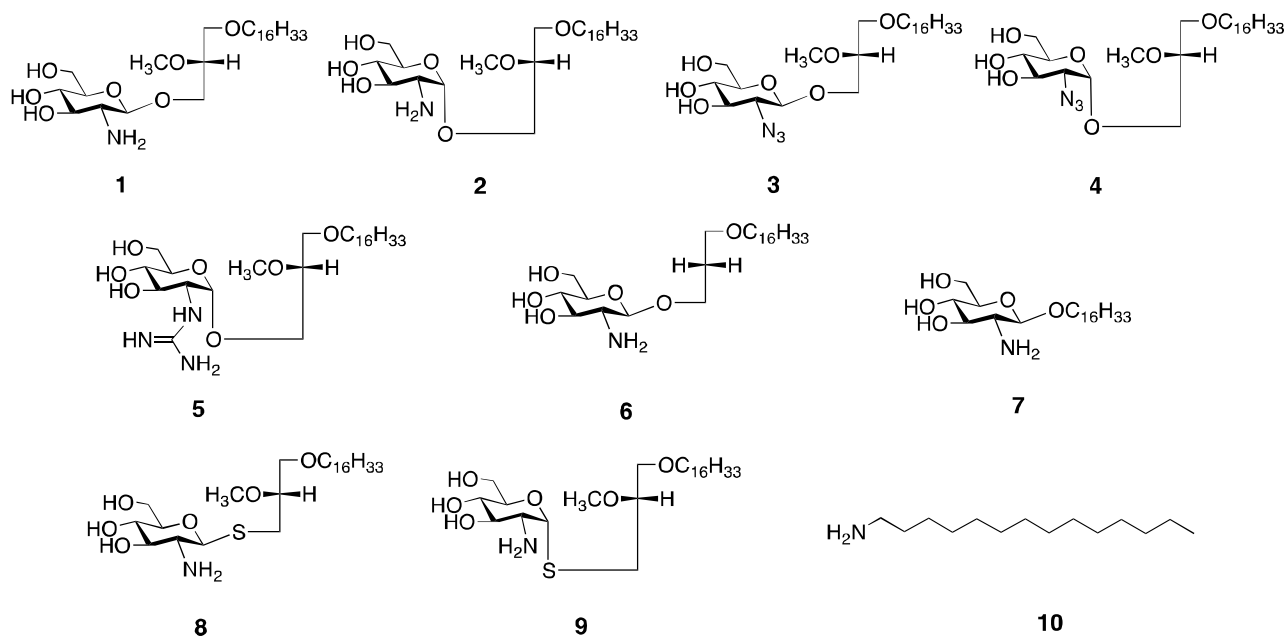
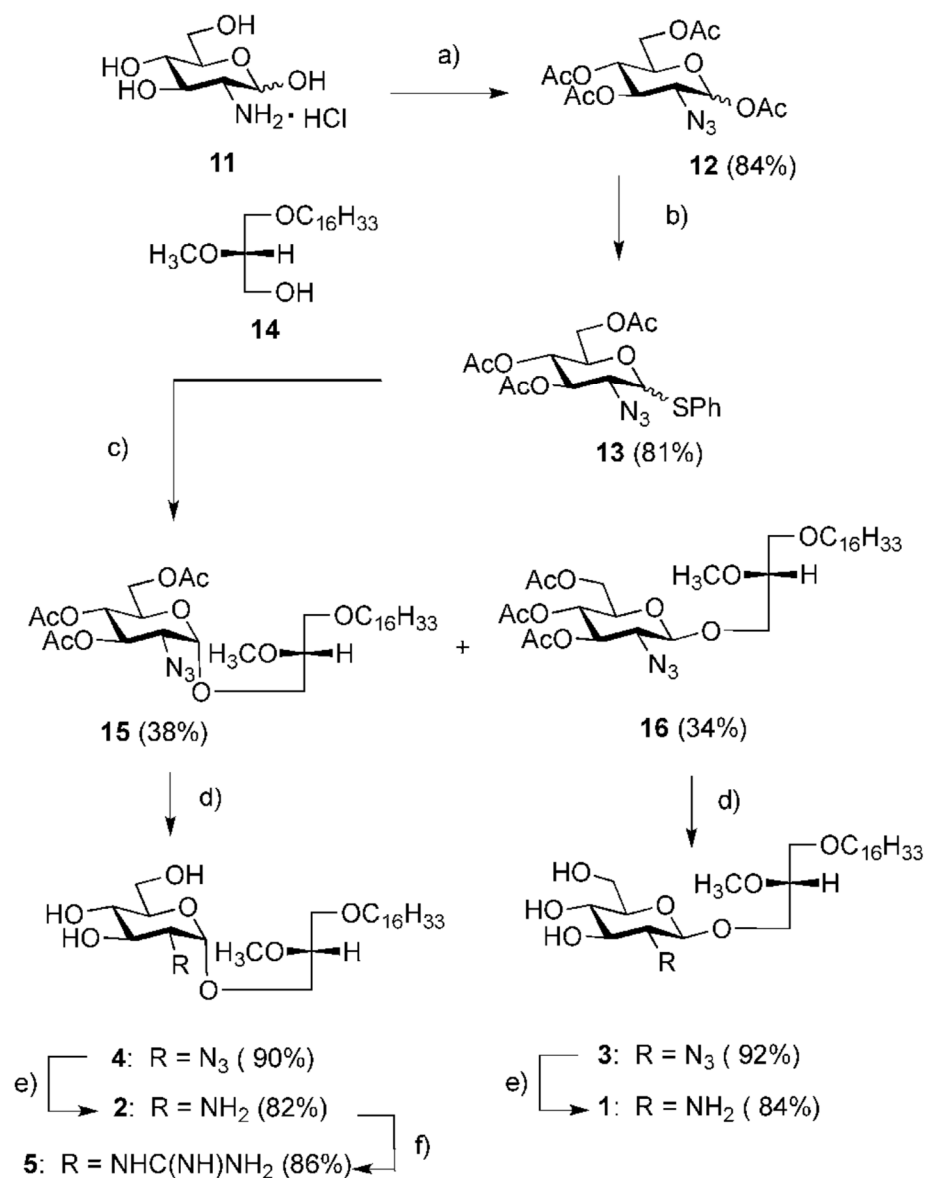


Figure 3.1. Structures of D-glucosamine-based glycerolipids used in this study.

The synthesis of glycolipids **1-5**, **8** and **9** commenced from acetate protected 2-azido-2-deoxy glucose **12** prepared from commercially available glucosamine **11** as previously described.²² Conversion of the anomeric acetate **12** into thioglycoside donor **13** was achieved by boron

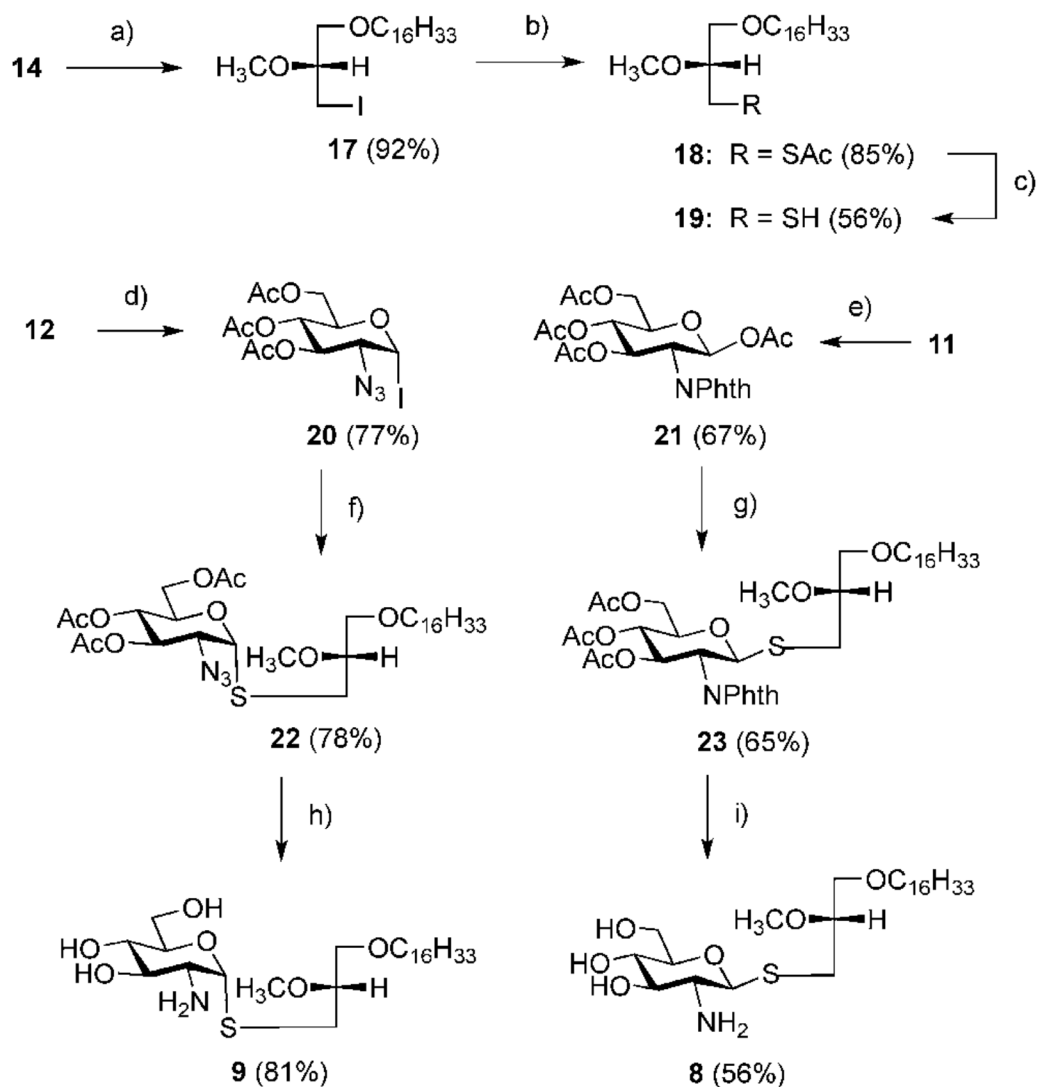
trifluoride diethyl etherate promoted thioglycosylation with thiophenol to afford thiophenyl glycoside **13** as an anomeric mixture (1:3 α/β) in 81% yield. Thioglycoside donor **13** was glycosylated with commercially available lipid alcohol **14** via N-iodosuccinimide/silver triflate promoted conditions to afford both glycolipid anomers **15** and **16** in 38% and 34% yield, respectively. Deacetylation using sodium methoxide in methanol produced azido-modified glycolipids **3** and **4** in high yield while reduction of the azido function by catalytic hydrogenolysis with palladium afforded the cationic glycolipids **1** and **2**. Guanidinylated glycolipid **5** was prepared from amine **2** by exposure to N,N'-DiBoc-N''triflylguanidine²³ followed by removal of the t-butoxycarbonyl group (Scheme 3.1).



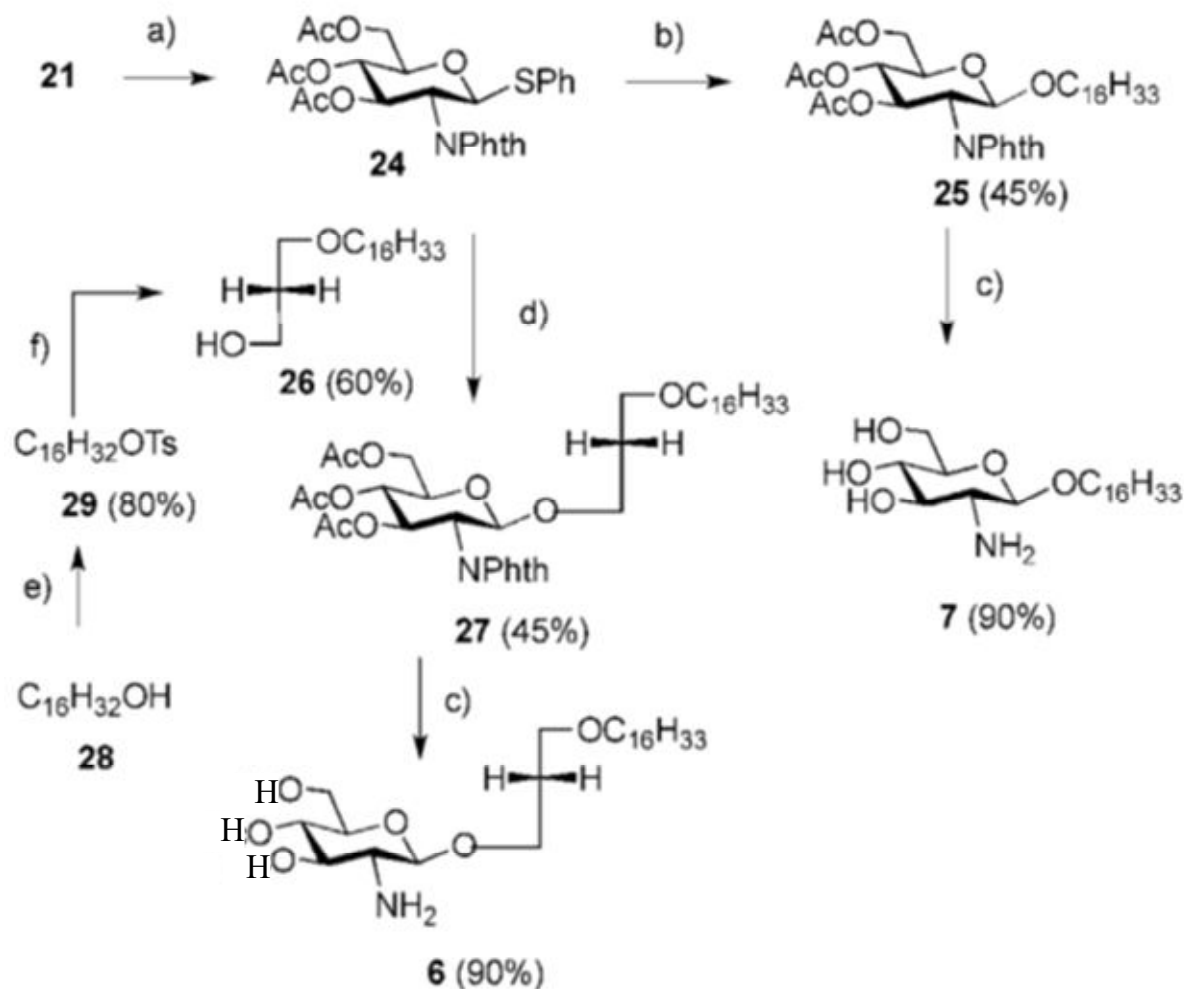
Scheme 3.1. Synthesis of compounds **1-5**. *Reagents and conditions*; a) (1) TfN₃, CuSO₄, Et₃N, H₂O, RT; (2) Ac₂O, DMAP, pyridine, RT; b) PhSH, BF₃·Et₂O, DCM, rt.; c) AgOTf, NIS, DCM, RT; d) NaOMe, MeOH, RT; e) Pd/C, H₂, MeOH, RT; f) (1) N, N'-diBoc-N''-triflylguanidine, Et₃N, H₂O, 1,4-dioxane, RT; (2) TFA, DCM, RT.

The anomeric thioglycolipids **8** and **9** were prepared from known glycosyliodide donor **20**²⁴ and phthalimido-protected donor **21**²⁵ by reaction with thiolipid acceptor **19** (Scheme 3.2). Acceptor **19** was prepared from lipid alcohol **14** in a three-step reaction sequence. At first the primary alcohol was converted into glycerol iodide **17** by reaction with triphenylphosphine, imidazole and iodine to yield **17** in 92% yield. Nucleophilic displacement with thioacetate in acetone produced thioacetate **18** in 85% yield which was deblocked to afford desired thiolipid acceptor **19** in 56% yield. With acceptor **19** in hand we now focused on the preparation of the glycosyl donor. Initially, we envisaged that reaction of acceptor **19** with glycosyliodide donor **20** bearing a non-participating group at C-2 would provide access to both anomeric thioglycolipids. However, activation of **20** with silver triflate in dichloromethane exclusively afforded α -anomer **22**. In order to prepare the desired β -anomer **23** we employed phthalimido-protected β -acetate donor **21** which was activated with boron trifluoride diethyl etherate in dichloromethane to give exclusively protected glycolipid **23** in 65% yield. Deblocking of **22** using sodium methoxide in methanol followed by reduction of the azido function produced target α -thioglycolipid **9** in 81% yield. Similarly, deblocking of the phthalimido and acetate protecting groups using methylamine in methanol afforded desired β -thioglycolipid **8** in 56% yield (Scheme 3.2).

To explore the importance of the glycerol moiety in lead structure **1**, we also prepared β -thio-glycolipids **6** and **7**. In both cases known thioglycoside donor **24**²⁶ was used for glycosylation with commercially available acceptor **28** or analog **26**. Compound **26** was prepared by activation of alcohol **28** as sulfonate ester **29** which by exposure to deprotonated 1,3-propanediol produced acceptor **26** in 60% yield (Scheme 3.3). Finally, deblocking of the sugar moiety using methylamine in methanol afforded desired β -glycolipids **6** and **7**.



Scheme 3.2. Synthesis of compounds **8** and **9**. *Reagents and conditions:* a) PPh_3 , I_2 , imidazole, toluene, reflux; b) AcSK , acetone, RT; c) NaOMe , MeOH , RT; d) aluminium metal, I_2 , DCM , RT; e) (1) 1 M NaOH , phthalic anhydride, rt; (2) Ac_2O , DMAP , pyridine, RT; f) AgOTf , DCM , RT; g) $\text{BF}_3 \cdot \text{Et}_2\text{O}$, DCM , RT; h) (1) NaOMe , MeOH , RT; (2) Pd/C , H_2 , MeOH , RT; i) $\text{MeNH}_2/\text{EtOH}$, reflux.



Scheme 3.3. Synthesis of compounds **6** and **7**. Reagents and conditions: a) PhSH, $\text{BF}_3 \cdot \text{Et}_2\text{O}$, DCM, RT; b) AgOTf, NIS, DCM, RT; c) $\text{MeNH}_2/\text{EtOH}$, reflux; d) AgOTf, NIS, DCM, RT; e) TsCl, pyridine, RT; f) NaH, DMF, 80 °C.

3.4.2. Biology

3.4.2.1. Cytotoxicity

The ability of compounds **1-9** to kill a number of epithelial cancer cell lines was assessed using the MTS assay.²⁷ The cell lines were derived from breast (JIMT1, BT549), pancreas (MiaPaCa2) and prostate (DU145, PC3). Myristylamine, **10**, a cationic lipid devoid of the

glucosamine moiety was selected as a nonspecific cytotoxic agent for comparison with the glycolipids. The compounds were added to exponentially growing cells, and the cells were incubated with the drugs for 48 h.

The results for the glucose-based glycolipids **1**, **2** and **6** to **9** are shown in Figure 3.2a, while the results for compounds **3**, **4** and **5** were shown in the Figure 3.2b. The concentrations of all the compounds (**1** to **10**) that reduce viability of the cells by 50% (CC₅₀) are listed in Table 3.1. The most potent compound against all five cell lines is the α -glucosidic lipid **2** with a CC₅₀ between 6- to 10 μ M followed by β -glucosidic lipid **1**, then compound **6** which is devoid of the methoxy substituent at the glycerol-based aglycon and compound **7** which lacked the glycerol moiety. Replacement of the O-glucosidic linkage in **1** and **2** by a glycosidase-resistant S-glucosidic linkage to form compounds **8** or **9** led to a 2-3-fold reduction in activity. The least active compound was the guanidinylated glycolipid **5** with an CC₅₀ of 30 μ M or higher against all the cell lines. Thus, surprisingly, conversion of the amino function into a guanidino group leads at least to an approximately 3-fold loss in activity indicating that the amino group is the best of the three different groups that were examined at that position. By comparison, the neutral azido-based glycolipids **3** and **4** showed very moderate activity. At concentrations of 20 μ M of **3** or **4**, viability of all the cell lines with the exception of PC3 cells were affected by 0 - 20 % (data not shown) while the viability of PC3 cells was reduced by 30%. In comparison, non-carbohydrate-based cationic lipid **10** displays reduced CC₅₀ values when compared to the more active glycolipids **1**, **2** and **6** indicating that the cationic amphiphilic nature contributes to the overall cytotoxicity. Our results show that the cytotoxicity of compounds **1-10** is affected by the nature of cationic charge, the nature of the anomeric linkage and the nature of the glycerol moiety. In general, the most potent compounds do not discriminate between the various cell types.

Figure 3.2a. Effects of compounds **1**, **2** and **6-10** on the viability of epithelial cancer cell lines

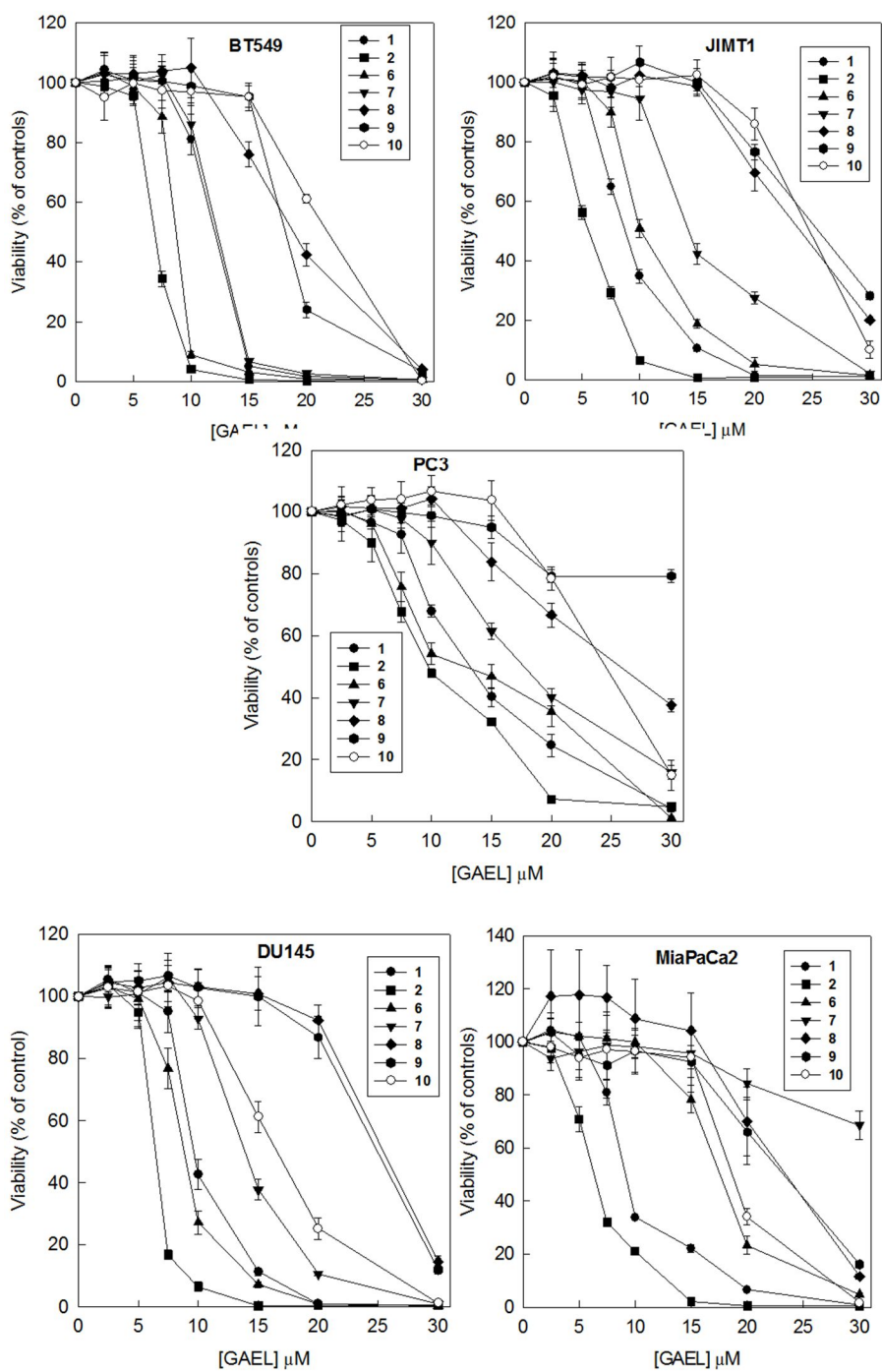


Figure 3.2b Effects of compounds 3-5 on the viability epithelial cancer cell lines derived from breast (JIMT1, BT549), pancreas (MiaPaCa2) and prostate (DU145, PC3).

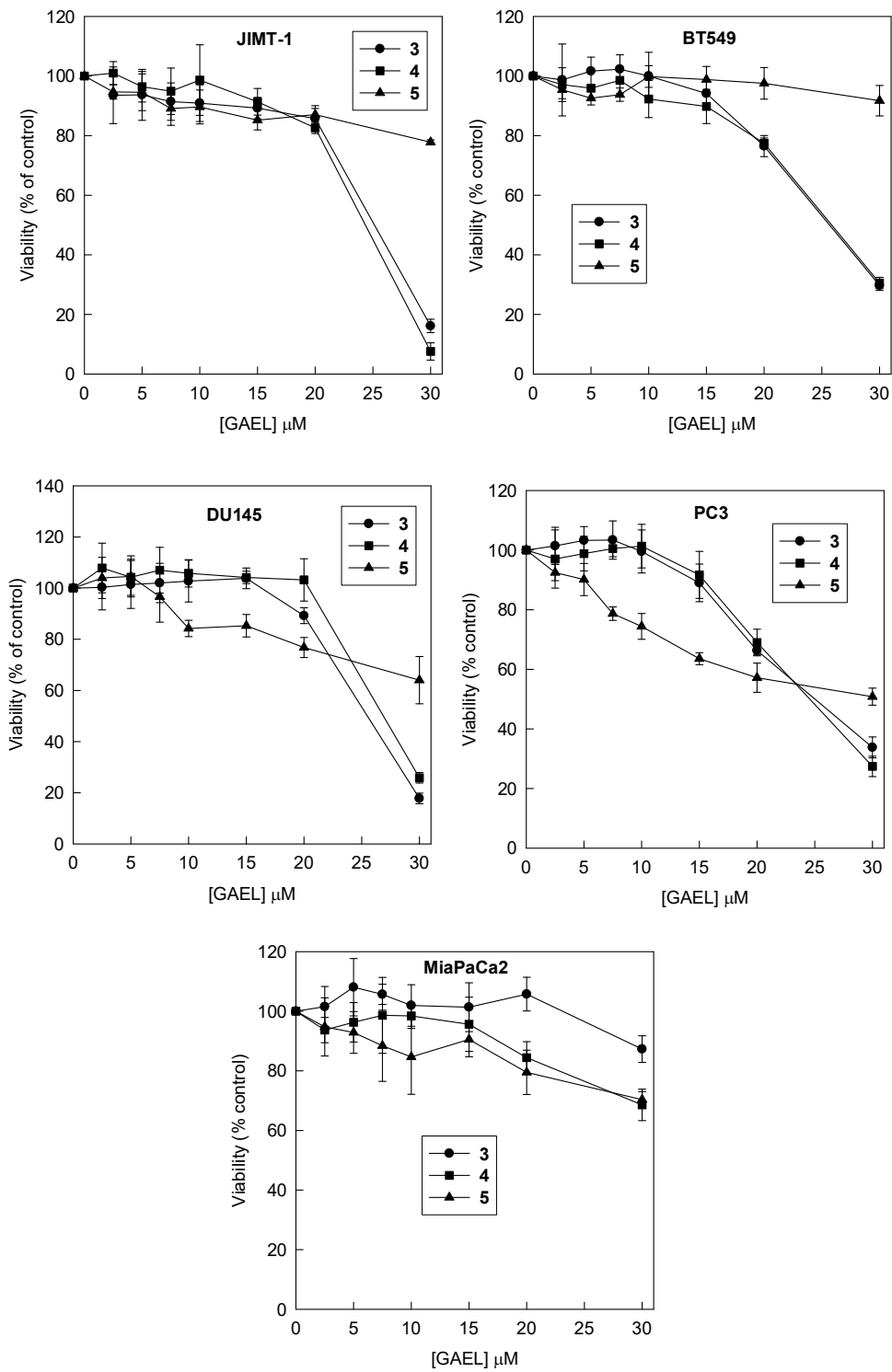


Table 3.1. Cytotoxicity of compounds **1-10** in μM to induce 50% killing against a panel of human cancer cell lines.

Compound	JIMT-1	BT549	MiaPaCa2	DU145	PC3
1	9	13	9	10	13.5
2	6	7	7	7	10.5
3	26	27	>30	26.5	26
4	25	27	>30	27.5	25
5	>30	>30	>30	>30	>30
6	10	9	17.5	9	12.5
7	15	13	>30	13.5	17.5
8	24	20	23.5	25	25.5
9	25	18	23	26	>30
10	27	26	18	16.5	24

3.4.2.2 Mode of action studies (LAV formation)

We have previously demonstrated that glycolipid **1** kills cells by an apoptosis-independent mechanism^{18,19} that involves uptake of the compound by endocytosis²⁸ which leads to the formation of LAVs that are a hallmark of active glycolipids of this kind. To investigate whether compounds **2-10** share the same mechanism of action as **1**, we investigated the ability of the

compounds to induce LAV formation in ATG5 ^{-/-} mouse embryonic fibroblasts.¹⁸ These cells were used because they eliminate any contribution by autophagy to the formation of the vacuoles and secondly, the cells are very sensitive to **1** and generate the LAVs in a very short period.¹⁸ The results of the studies are shown in Figure 3.3A-C. Compounds **1**, **2** which were the most active against the cancer cell lines formed LAVs within 4-5 h at concentrations of 5 μ M. At a concentration of 7.5 μ M rounded dead cells are prominent (Fig 3.3A). Compounds **6** and **7** showed prominent LAVs within 5 h at 7.5 μ M but at 10 μ M they were quite prominent (Fig 3.3A). Incubation of the ATG5 ^{-/-} cells with 20 μ M of compounds **3**, **4** and **5** for 12 h did not induce LAV formation in the cells (Fig 3.3B). This was not surprising because as discussed above, these compounds showed little activity against the cancer cell lines at this concentration. The alpha- and beta-thioglycosidic GAELs **8** and **9** which were not as active as their O-glycosidic analogs against the cancer cell lines formed LAVs at much higher concentrations. Prominent LAVs were observed with **8** or **9** at concentrations of 15 μ M or greater after 6 h incubation. The images obtained with 20 μ M **8** or **9** are shown in Fig 3.3C. Under similar incubation conditions of 20 μ M for 6 h with the reference compound **10**, a few of the cells had LAVs (Fig 3.3C) but these were not prominent or as numerous as those found in cells incubated with the active GAELs. Overall the degree with which the compounds formed LAVs correlates with their activity against the cancer cell lines.

Figure 3.3. Effects of compounds **1-10** on formation of large acidic vacuoles (LAV). Ability to form LAVs by compounds is directly related to their ability to kill cancer cells. Magnification X20

Figure 3.3A. Effect of **1**, **2**, **6** and **7**

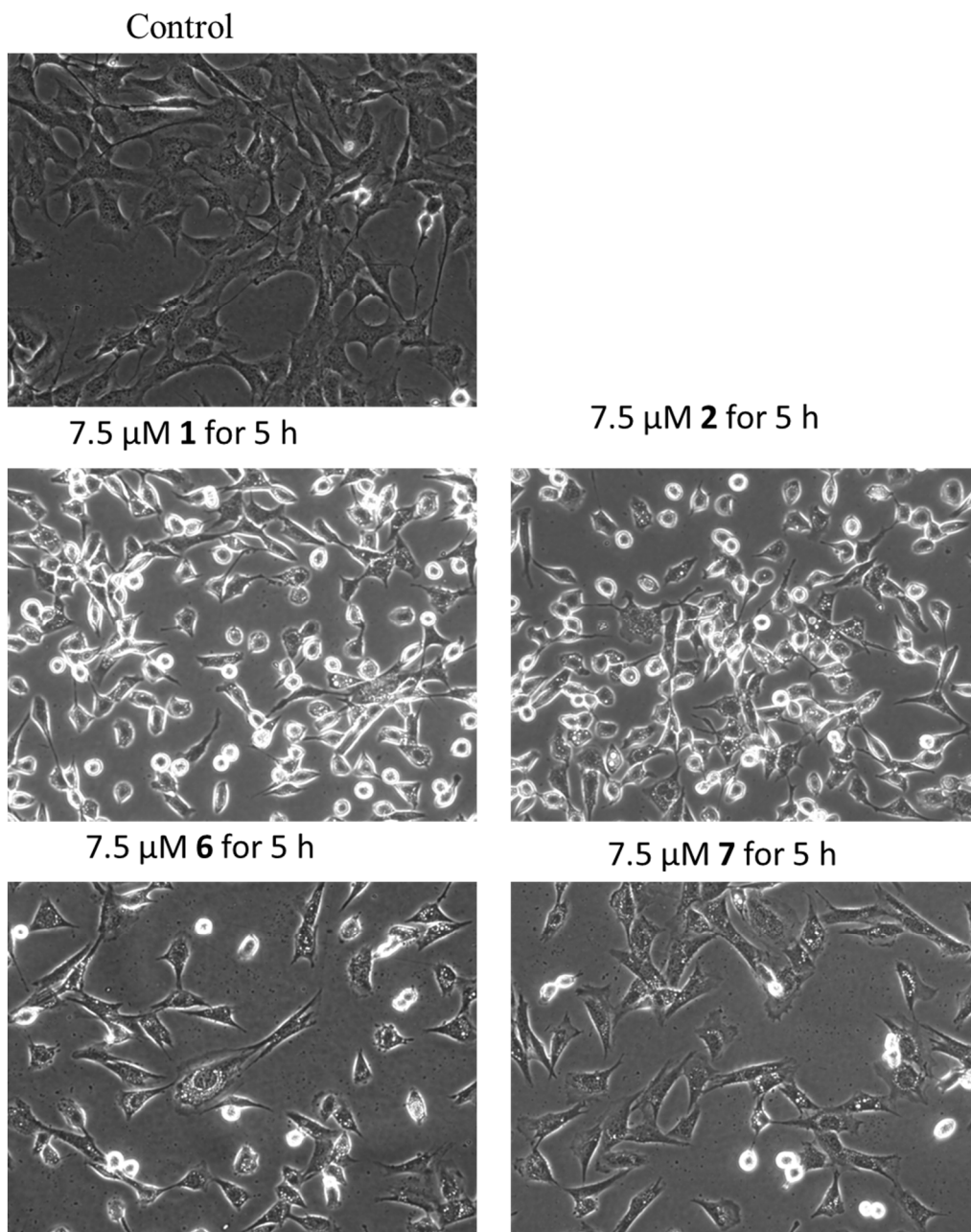
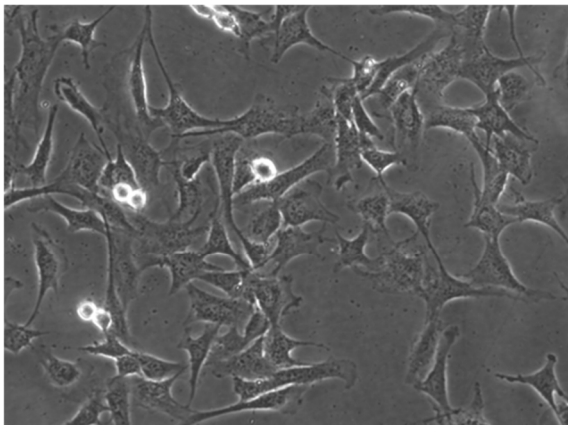
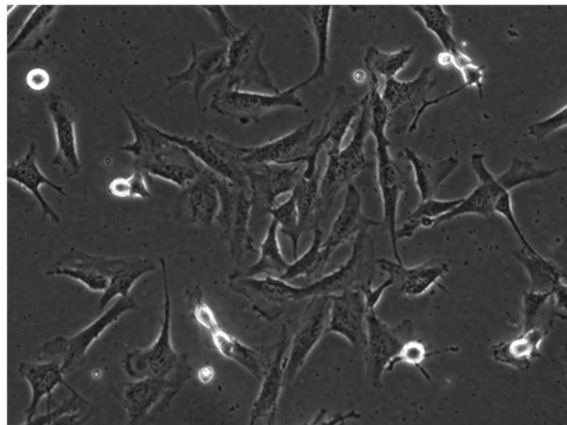


Figure 3.3B. Effect of **3**, **4** and **5**

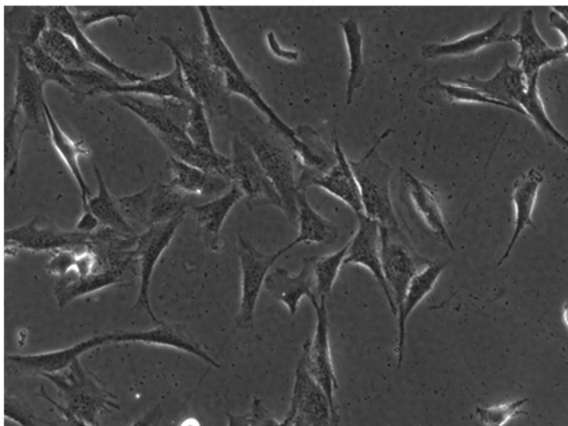
Control



7.5 μ M **3** for 12 h



7.5 μ M **4** for 12 h



7.5 μ M **5** for 12 h

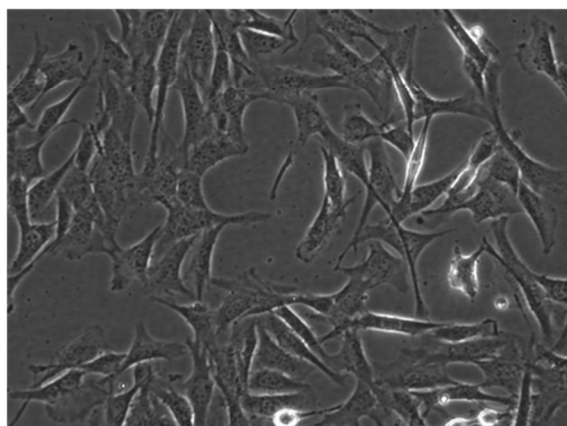
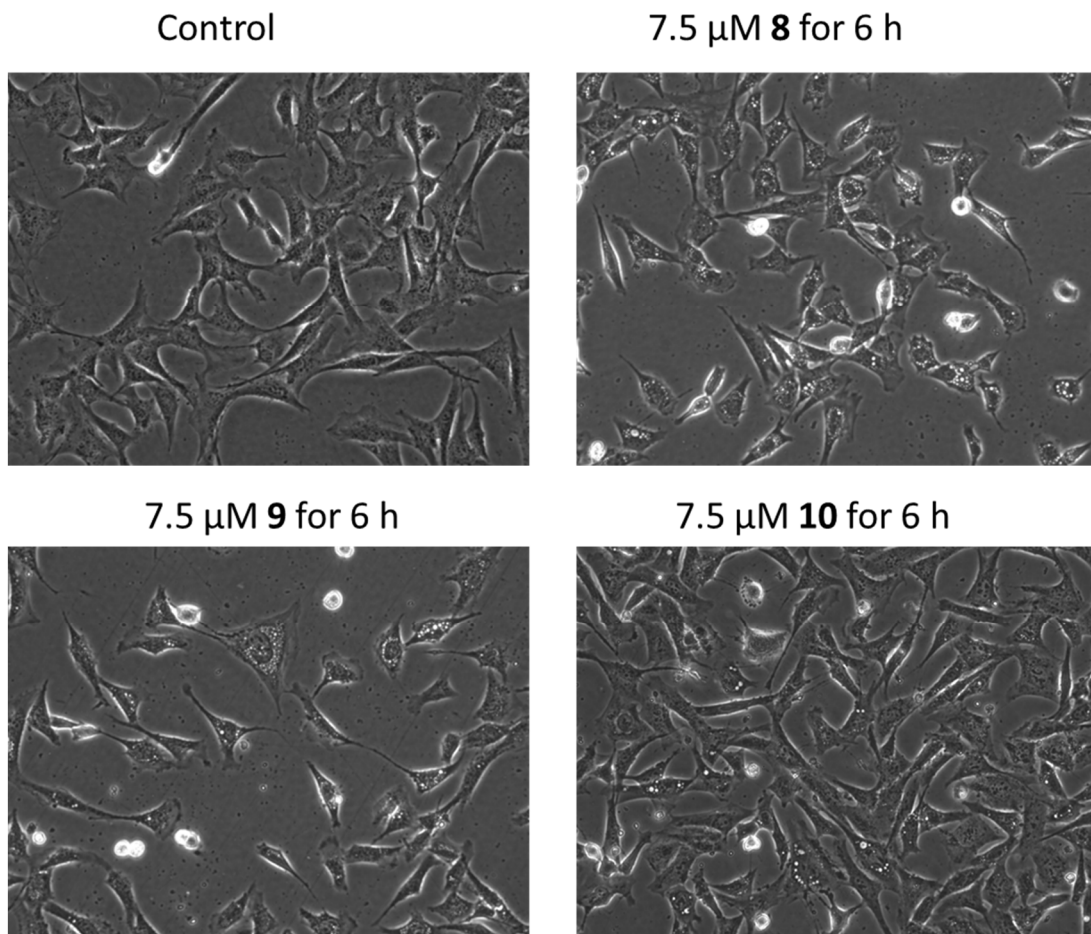


Fig 3.3C. Effect of **8**, **9** and **10**



3.5 Conclusions

In summary, we discovered that α -linked glucosamine-derived glycerolipid **2** consistently displays enhanced antitumor activity against five different cancer cell lines when compared to the β -anomer **1**. Both anomers induce the formation of intracellular large acidic vacuoles that appears to be responsible for their cytotoxicity. Replacement of the O-glycosidic linkage by a S-glycosidic linkage and loss of the cationic charge significantly reduces the antitumor activity in the analogs.

In comparison, changes in the nature of the hydrophobic glycerol moiety result in reduced antitumor activity but the effect is less pronounced. Overall our results demonstrate that an O-glycosidic glucosamine-based cationic head group is optimal for antitumor activity. By comparison, non-glucosamine-derived cationic amphiphiles such as myristylamine **10** display significantly reduced antitumor activity with little or no formation of LAVs at even four-fold higher concentration. Previously, several classes of cationic amphiphiles have been shown to display potent antitumor activities including short cationic amphiphilic peptides,²⁹ but also chlorhexidine,³⁰ benzethonium chloride³¹ and cetrimonium bromide.³² In many cases the mode of action of these cationic amphiphiles resulted in a membranolytic mode of action. Our results show that compounds **1** and **2** belong to a different class of cationic amphiphiles that display a different mode of action.

3.6 Experimental Section

3.6.1 Chemistry

Solvents were dried over CaH₂. ¹H, ¹³C spectra were recorded at 500 or 100 MHz, respectively and were referenced to the residual CHCl₃ at δ = 7.24 (¹H) and 77.00 ppm (¹³C). TLC was carried out on Al-backed silica gel GF plates (250 μ m thickness) and the compounds were visualized by charring with 10% H₂SO₄ in EtOH and /or short wavelength UV light. The products were purified by flash chromatography on silica gel 60 (230-400 ASTM mesh) or by reverse phase C₁₈ silica gel. HRMS and LRMS data were obtained by electrospray ionization.

Preparation of triflic azide stock solution

Sodium azide (436 mg, 6.70 mmol) was dissolved in pyridine (8.0 mL). The reaction mixture was cooled to 0 °C with vigorously stirring. Triflic anhydride (1.57 g, 5.56 mmol) was added dropwise to the mixture. The mixture was left to stir for 2 h at 0 °C to give a stock solution of triflic azide.

1,3,4,6-Tetra-O-acetyl-2-azido-2-deoxy- α/β -D-glucopyranose (12).

D-Glucosamine hydrochloride (1.00 g, 4.64 mmol) was dissolved in water (5.0 mL). Triethylamine (937 mg, 9.27 mmol) was added, along with copper sulphate pentahydrate (12 mg, 0.05 mmol). Triflic azide stock solution was then added. The blue mixture was stirred rapidly overnight, and then reduced in vacuo (water bath temperature kept below 20 °C). The resultant green syrup was dissolved in pyridine (10.0 mL), and acetic anhydride (3.0 mL) and DMAP (50 mg) were added slowly. After stirring overnight, the reaction mixture was evaporated to dryness, and the resulting residue was purified by flash chromatography (hexane/EtOAc, 3:2) to yield **12** as a yellow solid (1.44 g, 84%, predominately β - anomer); Rf 0.13 (hexane/EtOAc, 4:1); ¹H NMR data were in agreement with those reported earlier.²²

Phenyl 3,4,6-Tri-O-acetyl-2-azido-2-deoxy-1-thio-D-glucopyranoside (13).

To a solution of **12** (373 mg, 1.00 mmol) in CH₂Cl₂ (10 mL) at room temperature was added thiophenol (0.2 mL, 2.00 mmol) and boron trifluoride–diethyl ether (0.5 mL, 4.00 mmol). After stirring overnight, the reaction mixture was washed with saturated NaCl solution, dried with Na₂SO₄, and evaporated to dryness. The resulting residue was purified by flash chromatography (hexane/EtOAc, 3:1) afforded **13** (343 mg, 81%), as a 1:3 α/β mixture; Rf 0.27 (hexane/EtOAc, 3:1); ¹H NMR data were in agreement with those reported earlier.³³

1-O-Hexadecyl-2-O-methyl-3-O-(2'-azido-2'-deoxy-3',4',6'-tri-O-acetyl-D-glucopyranosyl)-sn-glycerol (α anomer: **15**; β anomer: **16**).

To a solution of **13** (300 mg, 0.71 mmol), **14** (100 mg, 0.30 mmol), and NIS (136 mg, 0.60 mmol) in dry dichloromethane (10 mL) was added silver triflate (16 mg, 0.06 mmol). After stirring overnight, the reaction mixture was washed with saturated NaHCO₃ solution and water, dried over Na₂SO₄, and evaporated to dryness. The residue was purified by flash chromatography (hexane/EtOAc, 6:1), giving both 74 mg of **15** (38%) and 66 mg of **16** (34%) as a yellow solid.

15: Rf 0.21 (hexane/EtOAc, 4:1); ¹H NMR (300 MHz, CDCl₃): δ = 5.49 (dd, J = 10.6, 9.3, 1H), 5.07 (dd, J = 11.5, 7.9, 2H), 4.32 (dd, J = 12.3, 4.3, 1H), 4.17 – 4.04 (m, 2H), 3.88 (d, J = 6.8, 1H), 3.67 – 3.53 (m, 4H), 3.52 – 3.40 (m, 5H), 3.30 (dd, J = 10.6, 3.5, 1H), 2.16 – 2.01 (m, 9H), 1.59 (s, 2H), 1.27 (s, 27H), 0.90 (t, J = 6.7, 3H); ¹³C NMR (75 MHz, CDCl₃): δ = 170.53, 170.14, 169.58, 98.21, 79.08, 71.92, 70.27, 69.49, 68.50, 67.77, 67.57, 61.72, 60.89, 57.94, 31.79, 29.57, 29.24, 25.93, 22.55, 20.57, 14.09; EIMS: calcd for C₃₂H₅₇N₃NaO₁₀⁺ 666.8, Found 666.8 [M + Na]⁺.

16: Rf 0.18 (hexane/EtOAc, 4:1); ¹H NMR (500 MHz, CDCl₃): δ = 5.00 – 4.90 (m, 2H), 4.40 (d, J = 8.1, 1H), 4.22 (dd, J = 12.3, 4.8, 1H), 4.07 (dd, J = 12.3, 2.1, 1H), 3.96 – 3.89 (m, 1H), 3.73 – 3.66 (m, 1H), 3.66 – 3.58 (m, 1H), 3.56 – 3.36 (m, 9H), 2.05 (t, J = 8.0, 6H), 1.98 (d, J = 12.3, 3H), 1.55 – 1.48 (m, 5H), 1.21 (s, 27H), 0.84 (t, J = 6.9, 3H); ¹³C NMR (126 MHz, CDCl₃): δ = 170.59, 169.95, 169.59, 102.19, 79.01, 72.42, 71.82, 69.63, 69.36, 68.43, 63.80, 61.91, 57.98, 31.91, 29.69, 29.64, 29.61, 29.48, 29.35, 26.10, 22.68, 20.70, 20.67, 20.57, 14.10; EIMS: calcd for C₃₂H₅₇N₃NaO₁₀⁺ 666.8, Found 666.8 [M + Na]⁺.

1-O-Hexadecyl-2-O-methyl-3-O-(2'-azido-2'-deoxy-D-glucopyranosyl)-sn-glycerol (α anomer: **4**; β anomer: **3**).

To a solution of **15** (74 mg, 0.11 mmol) in MeOH (5 mL) at room temperature was added NaOMe until pH came up to 9. The reaction mixture was stirred overnight, neutralized with Amberlite IR120 H⁺ exchange resin, filtered, and evaporated under vacuum to afford a yellow solid. The residue was purified by flash chromatography (DCM/MeOH, 10:1) to afford **4** (52 mg, 90%) as a yellow solid; R_f 0.26 (DCM/MeOH, 10:1); ¹H NMR (300 MHz, CD₃OD): δ = 4.97 (d, J = 3.4, 1H), 4.09 – 3.97 (m, 1H), 3.91 – 3.80 (m, 3H), 3.77 – 3.68 (m, 1H), 3.68 – 3.52 (m, 5H), 3.51 – 3.42 (m, 5H), 3.19 (dd, J = 10.3, 3.4, 1H), 1.64 – 1.52 (m, 2H), 1.27 (s, 28H), 0.90 (t, J = 6.7, 3H); ¹³C NMR (75 MHz, CDCl₃): δ = 98.5, 79.3, 71.9, 71.5, 71.3, 70.5, 69.7, 67.3, 62.8, 61.4, 57.9, 31.9, 29.7, 29.7, 29.6, 29.5, 29.4, 26.1, 22.7, 14.1; ESI-HRMS: calcd for C₂₆H₅₁N₃O₇Na⁺ 540.3625, Found 540.3602 [M + Na]⁺.

49 mg of **3** (92%) was obtained from 66 mg of **16** (0.10 mmol) according to above procedure; R_f 0.23 (DCM/MeOH, 10:1); ¹H NMR (500 MHz, CD₃OD): δ = 4.40 (d, J = 7.5, 1H), 4.24 (s, 1H), 4.11 (s, 1H), 3.97 (dd, J = 10.4, 5.7, 1H), 3.88 (s, 2H), 3.71 (dd, J = 10.4, 4.3, 1H), 3.64 – 3.52 (m, 4H), 3.51 – 3.41 (m, 6H), 1.64 – 1.53 (m, 2H), 1.27 (s, 29H), 0.89 (t, J = 6.7, 3H); ¹³C NMR (75 MHz, CDCl₃): δ = 102.4, 79.2, 77.5, 77.0, 76.6, 75.4, 74.8, 71.9, 70.0, 69.7, 69.6, 65.9, 61.7, 58.1, 31.9, 29.7, 29.7, 29.6, 29.5, 29.4, 26.1, 22.7, 14.1; ESI-HRMS: calcd for C₂₆H₅₁N₃O₇Na⁺ 540.3625, Found 540.3634 [M + Na]⁺.

1-O-Hexadecyl-2-O-methyl-3-O-(2'-amino-2'-deoxy-D-glucopyranosyl)-sn-glycerol (α anomer: **2**; β anomer: **1**). To a solution of **3** (49 mg, 0.09 mmol) in MeOH (5 mL) at room temperature was

added 10wt% of Pd/C (10 mg). The mixture was stirred under the atmosphere of hydrogen for 2 h, filtered, and then evaporated to dryness. The resulting residue was purified by flash chromatography (DCM/MeOH, 6:1) to afford **1** as a white solid (39 mg, 84%); Rf 0.15 (DCM/MeOH, 6:1); ¹H NMR (300 MHz, CD₃OD): δ = 3.93 – 3.78 (m, 2H), 3.72 (dd, J = 11.7, 5.2, 1H), 3.64 – 3.43 (m, 11H), 3.38 (s, 1H), 2.64 (dd, J = 9.9, 3.4, 1H), 1.58 (d, J = 6.4, 2H), 1.43 – 1.23 (m, 27H), 0.97 – 0.85 (m, 3H); ¹³C NMR (75 MHz, CD₃OD): δ = 100.56, 80.59, 75.99, 74.25, 72.72, 71.89, 71.23, 68.10, 62.66, 58.08, 57.18, 33.09, 30.80, 30.62, 30.49, 27.27, 23.75, 14.45; ESI-HRMS: calcd for C₂₆H₅₃NO₇Na⁺ 514.3720, Found 514.3706 [M + Na]⁺.

40 mg of **2** (82%) was obtained from 52 mg of **4** (0.10 mmol) according to above procedure; Rf 0.13 (DCM/MeOH, 6:1); ¹H NMR (500 MHz, CD₃OD): δ = 4.25 (d, J = 8.0, 1H), 3.93 (dd, J = 10.7, 4.6, 1H), 3.85 (d, J = 11.8, 1H), 3.66 (dd, J = 10.6, 3.9, 2H), 3.60 – 3.53 (m, 2H), 3.53 – 3.41 (m, 7H), 3.26 – 3.21 (m, 2H), 2.59 (t, J = 15.1, 1H), 1.54 (dd, J = 13.7, 6.7, 2H), 1.27 (s, 29H), 0.88 (t, J = 6.9, 3H); ¹³C NMR (126 MHz, CD₃OD): δ = 104.31, 80.56, 78.27, 77.20, 72.66, 71.81, 71.42, 69.66, 62.73, 58.24, 58.13, 33.07, 30.77, 30.73, 30.59, 30.47, 27.23, 23.73, 14.43; ESI-HRMS: calcd for C₂₆H₅₃NO₇Na⁺ 514.3720, Found 514.3741 [M + Na]⁺.

1-O-Hexadecyl-2-O-methyl-3-O-guanidino-2'-amino-2'-deoxy-α-D-glucopyranosyl)-sn-glycerol
(5).

To a solution of **2** (20 mg, 0.04 mmol) in H₂O (0.5 mL) was added 1,4-dioxane (2.5 mL) and N,N'-diBoc-N''-triflylguanidine (80 mg, 0.21 mmol). After 5 min, Et₃N (0.82 mmol) was added at room temperature. After 3-4 days, the reaction mixture was evaporated to dryness. The resulting residue was purified by flash chromatography (DCM/MeOH, 10:1) to afford a yellow solid, which was

dissolved in TFA/CH₂Cl₂ (1:1, 2 mL). After approximately 4 h, the mixture was evaporated to dryness. The resulting residue was purified by flash chromatography (DCM/MeOH, 4:1) to afford **5** as a white solid (17 mg, 86%); R_f 0.25 (DCM/MeOH, 4:1); ¹H NMR (500 MHz, CD₃OD): δ = 4.89 (d, J = 3.5, 1H), 3.86 – 3.77 (m, 2H), 3.72 (dd, J = 11.8, 5.0, 1H), 3.68 – 3.36 (m, 13H), 3.33 (s, 2H), 3.20 (q, J = 7.3, 1H), 1.54 (dd, J = 13.7, 6.7, 2H), 1.36 – 1.22 (m, 26H), 0.88 (t, J = 6.9, 3H); ¹³C NMR (126 MHz, CD₃OD): δ = 159.41, 98.67, 80.59, 74.04, 73.96, 72.74, 71.67, 70.76, 68.05, 62.27, 57.99, 57.70, 47.91, 33.06, 30.77, 30.74, 30.60, 30.46, 27.26, 23.72, 14.42, 9.20; ESI-HRMS: calcd for C₂₇H₅₆N₃O₇⁺ 534.4040, Found 534.4063 [M + H]⁺.

1-O-Hexadecyl-2-O-methyl-3-iodide-sn-glycerol (17).

To a solution of **14** (660 mg, 2.00 mmol) in toluene (10 mL) at room temperature was added PPh₃ (524 mg, 2.00 mmol), **12** (508 mg, 2.00 mmol) and imizadole (272 mg, 4.00 mmol). The reaction mixture was heated to reflux and stirred overnight, and then evaporated to dryness. The resulting residue was purified by flash chromatography (hexane/EtOAc, 6:1) to afford **17** as a yellow solid (810 mg, 92%); R_f 0.28 (hexane/EtOAc, 6:1); ¹H NMR (300 MHz, CDCl₃): δ = 3.58 (dd, J = 10.0, 4.8, 1H), 3.54 – 3.43 (m, 6H), 3.42 – 3.32 (m, 2H), 3.31 – 3.24 (m, 1H), 1.57 (dd, J = 14.0, 7.2, 2H), 1.27 (s, 27H), 0.90 (t, J = 6.7, 3H).

1-O-Hexadecyl-2-O-methyl-3-S-acetyl-sn-glycerol (18).

To a solution of **17** (660 mg, 1.50 mmol) in acetone (10 mL) at room temperature was added AcSK (343 mg, 3.00 mmol). After stirring overnight, the mixture was evaporated to dryness. The resulting residue was purified by flash chromatography (hexane/EtOAc, 5:1) to afford **18** as a yellow solid (496 mg, 85%); R_f 0.26 (hexane/EtOAc, 5:1); ¹H NMR (300 MHz, CDCl₃): δ = 3.51

– 3.42 (m, 8H), 3.17 – 3.08 (m, 2H), 2.36 (s, 3H), 1.65 – 1.52 (m, 2H), 1.27 (s, 28H), 0.89 (t, J = 6.7, 3H).

1-O-Hexadecyl-2-O-methyl-3-thiol-sn-glycerol (19).

To a solution of **18** (480 mg, 1.23 mmol) in MeOH (10 mL) at room temperature was added NaOMe until pH came up to 9. The mixture was stirred overnight, neutralized with Amberlite IR120 H⁺ exchange resin, filtered, and evaporated to dryness. The resulting residue was purified by flash chromatography (hexane/EtOAc, 6:1) to afford **19** as a yellow solid (239 mg, 56%); R_f 0.24 (hexane/EtOAc, 6:1); ¹H NMR (300 MHz, CDCl₃): δ = 3.63 – 3.28 (m, 8H), 2.85 – 2.59 (m, 2H), 1.86 – 1.47 (m, 2H), 1.27 (s, 26H), 0.97 (dt, J = 13.4, 6.7, 3H).

3,4,6-Tri-O-acetyl-2-azido-2-deoxy-α-D-glucopyranosyl iodide (20).

To a solution of **12** (200 mg, 0.54 mmol) in DCM (10 mL) at room temperature was added Aluminum metal (10 mg) and iodide (40 mg). The mixture was stirred overnight, and evaporated to dryness. The resulting residue was purified by flash chromatography (hexane/EtOAc, 4:1) to afford **20** as a yellow solid (182 mg, 77%); R_f 0.22 (hexane/EtOAc, 4:1); ¹H NMR data were in agreement with those reported earlier.²⁴

1-O-Hexadecyl-2-O-methyl-3-S-(2'-azido-2'-deoxy-3',4',6'-tri-O-acetyl-α-D-glucopyranosyl)-sn-glycerol (22).

To a solution of **19** (100 mg, 0.29 mmol) and **20** (127 mg, 0.29 mmol) was added a suspension of silver triflate (34 mg, 0.14 mmol) in dry dichloromethane (10 mL). After stirring overnight, the reaction mixture was washed with saturated NaHCO₃ solution and water, dried over Na₂SO₄, and

concentrated under reduced pressure. The residue was purified by flash chromatography (hexane/EtOAc, 6:1) to afford **22** (149 mg, 78%) of as a yellow solid; Rf 0.21 (hexane/EtOAc, 6:1); ¹H NMR (300 MHz, CDCl₃): δ = 5.56 (d, J = 5.6, 1H), 5.30 (dd, J = 10.3, 9.4, 1H), 5.10 – 4.98 (m, 1H), 4.46 (ddd, J = 10.1, 4.5, 2.1, 1H), 4.33 (dd, J = 12.3, 4.6, 1H), 4.05 (ddd, J = 16.1, 11.4, 3.9, 2H), 3.60 – 3.38 (m, 8H), 2.82 – 2.72 (m, 2H), 2.12 – 2.02 (m, 9H), 1.62 – 1.52 (m, 2H), 1.27 (s, 30H), 0.89 (t, J = 6.7, 3H); ¹³C NMR (75 MHz, CDCl₃): δ = 170.53, 169.79, 83.47, 80.17, 71.97, 71.85, 71.06, 68.73, 68.01, 61.93, 61.57, 57.93, 31.93, 31.09, 29.71, 29.67, 29.65, 29.62, 29.49, 29.37, 26.11, 22.70, 20.69, 20.66, 20.60, 14.12; EIMS: calcd for C₃₂H₅₇N₃O₉SNa⁺ 682.9, Found 682.5 [M + Na]⁺.

1-O-Hexadecyl-2-O-methyl-3-S-(2'-amino-2'-deoxy-α-D-glucopyranosyl)-sn-glycerol (9).

To a solution of **22** (100 mg, 0.15 mmol) in MeOH (5 mL) at room temperature was added NaOMe until pH came up to 9. The mixture was stirred overnight, neutralized with Amberlite IR120 H⁺ exchange resin, filtered, and evaporated under vacuum to afford a white solid, which was directly dissolved in MeOH (5 mL) and to the solution was added dropwise 10wt% of Pd/C (20 mg). After stirring under the atmosphere of hydrogen for 2 h, the mixture was filtered and then evaporated to dryness. The resulting residue was purified by flash chromatography (DCM/MeOH, 5:1) to afford **9** as a white solid (62 mg, 81%); Rf 0.18 (DCM/MeOH, 5:1); ¹H NMR (500 MHz, CD₃OD): δ = 5.36 (d, J = 5.1, 1H), 3.95 (ddd, J = 11.0, 5.5, 3.2, 1H), 3.81 (dd, J = 12.0, 2.3, 1H), 3.72 (dd, J = 12.0, 5.4, 1H), 3.54 (ddd, J = 15.4, 8.4, 4.8, 3H), 3.47 – 3.41 (m, 6H), 3.34 – 3.31 (m, 1H), 3.07 (dd, J = 10.4, 5.1, 1H), 2.84 – 2.76 (m, 2H), 1.58 – 1.52 (m, 2H), 1.29 (d, J = 17.5, 31H), 0.88 (t, J = 7.0, 3H); ¹³C NMR (126 MHz, CD₃OD): δ = 87.17, 81.30, 74.89, 72.66, 72.29, 72.18, 62.46, 57.99, 56.67, 33.28, 33.07, 30.77, 30.73, 30.58, 30.46, 27.24, 23.73, 14.42; HRMS: calcd for C₂₆H₅₃NO₆SNa⁺ 530.3491, Found 530.3510 [M + Na]⁺.

2-Phthalimido-2-deoxy-β-D-glucopyranoside tetraacetate (21).

To a solution of D-Glucosamine hydrochloride (1.00 g, 4.64 mmol) in 1 M NaOH solution (10.0 mL) was added phthalic anhydride (2.96 g, 20.00 mmol). After stirring overnight, the mixture was evaporated to dryness. The resultant syrup was dissolved in pyridine (10.0 mL), and acetic anhydride (3.0 mL) and DMAP (50 mg) were added slowly. After stirring overnight, the reaction mixture was evaporated to dryness, and the resulting residue was purified by flash chromatography (hexane/EtOAc, 1:1) to yield **21** as a yellow solid (1.48 g, 67%); R_f 0.37 (hexane/EtOAc, 1:1); ¹H NMR data were in agreement with those reported earlier.²⁵

1-O-Hexadecyl-2-O-methyl-3-S-(2'-phthalimido-2'-deoxy-3',4',6'-tri-O-acetyl-β-D-glucopyranosyl)-sn-glycerol (23).

To a solution of **19** (100 mg, 0.29 mmol) and **21** (230 mg, 0.48 mmol) in dry dichloromethane (10 mL) was added boron trifluoride–diethyl ether (0.25 mL, 2.00 mmol). After stirring overnight, the reaction mixture was washed with saturated NaHCO₃ solution and water, dried over Na₂SO₄, and concentrated under reduced pressure. The residue was purified by flash chromatography (hexane/EtOAc, 4:1) to afford **23** (144 mg, 65%) as a yellow solid; R_f 0.17 (hexane/EtOAc, 4:1); ¹H NMR (300 MHz, CDCl₃): δ = 7.94 – 7.83 (m, 2H), 7.81 – 7.72 (m, 2H), 5.85 (dd, J = 10.1, 9.2, 1H), 5.55 (d, J = 10.6, 1H), 5.21 (dd, J = 23.3, 13.3, 1H), 4.38 (dd, J = 16.6, 6.1, 1H), 4.34 – 4.25 (m, 1H), 4.19 (dd, J = 12.3, 2.2, 1H), 3.90 (ddd, J = 10.1, 4.8, 2.3, 1H), 3.52 – 3.44 (m, 3H), 3.37 (d, J = 5.6, 5H), 2.93 (dd, J = 13.7, 5.5, 1H), 2.74 (dd, J = 13.7, 5.6, 1H), 2.16 – 2.08 (m, 3H), 2.03 (d, J = 9.4, 3H), 1.88 (s, 3H), 1.60 – 1.48 (m, 2H), 1.26 (s, 29H), 0.89 (t, J = 6.7, 3H); ¹³C NMR (75 MHz, CDCl₃): δ = 170.65, 170.09, 169.50, 134.42, 123.52, 81.71, 79.64, 75.96, 71.73, 71.51, 70.83, 68.91, 62.38, 62.16, 57.69, 53.85, 31.93, 31.15, 29.71, 29.49, 29.37, 26.08, 22.70, 20.76, 20.64, 20.46, 14.13; EIMS: calcd for C₄₀H₆₁NO₁₁SNa⁺ 787.0, Found 786.5 [M + Na]⁺.

1-O-Hexadecyl-2-O-methyl-3-S-(2'-amino-2'-deoxy-β-D-glucopyranosyl)-sn-glycerol (8).

100 mg of **23** (0.13 mmol) was directly dissolved in 33wt% of MeNH₂/EtOH (5 mL), and the resulting mixture was heated to reflux and stirred overnight, and then evaporated to dryness. The resulting residue was purified by flash chromatography (DCM/MeOH, 3:1) to afford **8** as a white solid (37 mg, 56%); R_f 0.27 (DCM/MeOH, 3:1); ¹H NMR (300 MHz, CD₃OD): δ = 4.41 (d, J = 9.8, 1H), 3.88 (d, J = 12.0, 1H), 3.73 – 3.55 (m, 5H), 3.53 – 3.44 (m, 6H), 3.36 (d, J = 8.4, 1H), 2.97 (dd, J = 13.7, 5.4, 1H), 2.85 (dd, J = 13.8, 5.4, 1H), 2.70 (d, J = 18.3, 1H), 1.58 (d, J = 6.6, 2H), 1.32 (s, 33H), 0.93 (t, J = 6.7, 3H); ¹³C NMR (75 MHz, CD₃OD): δ = 87.82, 82.33, 81.38, 78.92, 72.65, 72.12, 71.66, 62.98, 58.00, 57.74, 49.87, 49.58, 49.30, 49.02, 48.73, 48.45, 48.17, 33.09, 31.85, 30.79, 30.59, 30.48, 27.26, 23.75, 14.45; ESI-HRMS: calcd for C₂₆H₅₃NO₆SNa⁺ 530.3491, Found 530.3487 [M + Na]⁺.

Phenyl 3,4,6-Tri-O-acetyl-2-phthalimido-2-deoxy-1-thio-β-D-glucopyranoside (24).

To a solution of **21** (477 mg, 1.00 mmol) in CH₂Cl₂ (10 mL) at room temperature was added thiophenol (0.2 mL, 2.00 mmol) and boron trifluoride–diethyl ether (0.5 mL, 4.00 mmol). After stirring overnight, the reaction mixture was washed with saturated NaCl solution, dried with Na₂SO₄, and evaporated to dryness. The resulting residue was purified by flash chromatography (hexane/EtOAc, 3:1) afforded **24** (390 mg, 74%); R_f 0.24 (hexane/EtOAc, 3:1); ¹H NMR data were in agreement with those reported earlier.²⁶

Hexadecyl p-toluenesulfonate (29).

To a solution of **28** (500 mg, 2.06 mmol) in dry pyridine (20 mL) was added p-toluenesulfonylchloride (2.0 g, 10.31 mmol) at 0 °C. After stirring overnight, the reaction mixture was evaporated to dryness. The resulting residue was purified by flash chromatography (hexane/EtOAc, 10:1) to afford **29** as a white solid (653 mg, 89%); Rf 0.23 (hexane/EtOAc, 10:1); ¹H NMR (300 MHz, CDCl₃): δ = 7.79 (d, J = 8.3, 2H), 7.34 (d, J = 8.0, 2H), 4.02 (t, J = 6.5, 2H), 2.44 (s, 3H), 1.68 – 1.55 (m, 2H), 1.34 – 1.15 (m, 26H), 0.88 (t, J = 6.7, 3H).

3-(Hexadecyloxy)-propan-1-ol (26).

To a solution of 1,3-propanediol (192 mg, 2.52 mmol) in dry DMF (10 mL) was added NaH (14 mg, 0.60 mmol) and the mixture was stirred for 30 min. To this solution was added **29** (200 mg, 0.50 mmol) all at once. The reaction mixture was heated to 80 °C and stirred overnight. After quenching the reaction with 1 ml of MeOH, the mixture was evaporated to dryness. The resulting residue was purified by flash chromatography (hexane/EtOAc, 8:1) to afford **26** as a waxy solid (89 mg, 60%); Rf 0.19 (hexane/EtOAc, 8:1); ¹H NMR (300 MHz, CDCl₃): δ = 3.79 (dd, J = 10.7, 5.3, 2H), 3.62 (t, J = 5.7, 2H), 3.44 (t, J = 6.6, 2H), 1.89 – 1.79 (m, 2H), 1.65 – 1.51 (m, 2H), 1.27 (s, 26H), 0.89 (t, J = 6.7, 3H).

3-(Hexadecyloxy)propan-1-O-(2'-phthalimido-2'-deoxy-3',4',6'-tri-O-acetyl-β-D-glucopyranosyl)-sn-glycerol (27).

To a solution of **24** (56 mg, 0.17 mmol), **26** (89 mg, 0.17 mmol) and NIS (69 mg, 0.30 mmol) in dry dichloromethane (10 mL) was added silver triflate (8 mg, 0.03 mmol). After stirring overnight, the reaction mixture was washed with saturated NaHCO₃ solution and water, dried over Na₂SO₄, and evaporated to dryness. The residue was purified by flash chromatography (hexane/ EtOAc, 4:1) to afford **27** (53 mg, 45%) as a yellow solid; Rf 0.18 (hexane/EtOAc, 4:1); ¹H NMR (300

MHz, CDCl₃): δ = 7.94 – 7.65 (m, 4H), 5.81 (dd, J = 10.7, 9.1, 1H), 5.36 (d, J = 8.5, 1H), 5.27 – 5.05 (m, 1H), 4.41 – 4.25 (m, 2H), 4.22 – 4.11 (m, 1H), 3.96 – 3.81 (m, 2H), 3.69 – 3.47 (m, 1H), 3.27 – 3.15 (m, 2H), 3.13 – 2.94 (m, 2H), 2.18 – 2.06 (m, 3H), 2.04 (d, J = 3.0, 3H), 1.91 – 1.79 (m, 3H), 1.77 – 1.61 (m, 2H), 1.38 (dt, J = 13.4, 6.9, 2H), 1.26 (brs, 26H), 0.95 – 0.77 (m, 3H);

3-(Hexadecyloxy)propan-1-O-(2'-amion-2'-deoxy- β -D-glucopyranosyl)-sn-glycerol (6).

53 mg of **27** (0.08 mmol) was directly dissolved in 33wt% of MeNH₂/EtOH (5 mL), and the resulting mixture was heated to reflux and stirred overnight, and then evaporated to dryness. The resulting residue was purified by flash chromatography (DCM/MeOH, 5:1) to afford **6** as a white solid (32 mg, 90%); R_f 0.21 (DCM/MeOH, 5:1); ¹H NMR (300 MHz, CD₃OD): δ = 4.26 (d, J = 8.0, 1H), 4.00 (dt, J = 9.7, 6.4, 1H), 3.89 (d, J = 11.1, 1H), 3.67 (ddd, J = 13.0, 11.7, 5.4, 2H), 3.56 (t, J = 6.3, 2H), 3.45 (t, J = 6.6, 2H), 3.38 – 3.25 (m, 5H), 2.61 (dd, J = 11.3, 5.8, 1H), 1.98 – 1.81 (m, 2H), 1.67 – 1.50 (m, 2H), 1.32 (brs, 26H), 0.93 (t, J = 6.5, 3H); ¹³C NMR (75 MHz, CD₃OD): δ = 103.5, 75.7, 67.5, 61.9, 57.1, 30.0, 29.7, 29.5, 29.3, 26.2, 22.6, 14.0; ESI-HRMS: calcd for C₂₅H₅₁NO₆Na⁺ 484.3614, Found 484.3633 [M + Na]⁺.

Hexadecan-1-O-(2'-phthalimido-2'-deoxy-3',4',6'-tri-O-acetyl- β -D-glucopyranosyl)-sn-glycerol (25).

To a solution of **24** (116 mg, 0.22 mmol), hexadecane-1-ol (53 mg, 0.22 mmol) and NIS (69 mg, 0.30 mmol) in dry dichloromethane (10 mL) was added silver triflate (8 mg, 0.03 mmol). After stirring overnight, the reaction mixture was washed with saturated NaHCO₃ solution and water, dried over Na₂SO₄, and evaporated to dryness. The residue was purified by flash chromatography (hexane/ EtOAc, 4:1) to afford **25** (65 mg, 45%) as a yellow solid; R_f 0.21 (hexane/EtOAc, 4:1); ¹H NMR (300 MHz, CDCl₃): δ = 7.96 – 7.69 (m, 4H), 5.81 (dd, J = 10.8, 9.1, 1H), 5.37 (d, J =

8.5, 1H), 5.25 – 5.11 (m, 1H), 4.33 (dd, J = 7.4, 4.9, 2H), 4.18 – 4.09 (m, 2H), 3.95 – 3.77 (m, 2H), 3.46 (t, 1H), 2.13 (s, 3H), 1.87 (s, 3H), 1.87 (s, 3H), 1.43 (m, 2H), 1.29 (brs, 26H), 0.93 – 0.85 (t, 3H); ¹³C NMR (75 MHz, CDCl₃): δ = 198.7, 134.0, 123.7, 123.1, 122.8, 122.8, 97.9, 29.7, 13.7;

Hexadecan-1-O-(2'-amino-2'-deoxy-β-D-glucopyranosyl)-sn-glycerol (7).

65 mg of **25** (0.10 mmol) was directly dissolved in 33wt% of MeNH₂/EtOH (5 mL), and the resulting mixture was heated to reflux and stirred overnight, and then evaporated to dryness. The resulting residue was purified by flash chromatography (DCM/MeOH, 5:1) to afford **7** (36 mg, 90%) as a white solid; R_f 0.22 (DCM/MeOH, 5:1); ¹H NMR (300 MHz, CD₃OD): δ = 4.25 (d, J = 8.0, 1H), 4.00 – 3.84 (m, 2H), 3.71 (dd, J = 11.1, 3.6, 1H), 3.54 (dt, J = 9.5, 6.7, 1H), 3.40 – 3.21 (m, 8H), 2.61 (dd, J = 11.2, 6.1, 1H), 1.72 – 1.53 (m, 2H), 1.32 (brs, 26H), 1.01 – 0.85 (m, 3H); ¹³C NMR (75 MHz, CDCl₃): δ = 104.0, 103.8, 78.0, 77.0, 71.7, 70.5, 62.4, 58.4, 30.8, 30.3, 30.0, 27.0, 23.0, 14.2; ES-HRMS: calcd for C₂₂H₄₅NO₅Na⁺ 426.3195, Found 426.3208 [M + Na]⁺.

3.6.2 Biological methods

Cell culture: BT549, DU145, PC3 and MiaPaCa2 cell lines were grown from frozen stocks of cell lines that were originally obtained from ATCC (Manassas, VA, USA). JIMT-1 cells were originally obtained from DSMZ (Braunschweig, Germany). ATG5 ^{-/-} mouse embryonic fibroblasts were obtained from Dr Ichijo (University of Tokyo, Japan). JIMT1, DU145, and ATG5 ^{-/-} cells were grown in Dulbecco's modified Eagle's medium, BT549 was grown in RPMI medium and PC3 cells were grown in F12K medium. The cells were grown in media supplemented with 10% FBS, penicillin (100 U/ml) and 0.1 mg/ml streptomycin.

Toxicity assay: Cell viability was determined with the Cell Titre 96 Aqueous One solution (MTS assay; Promega). Equal numbers of the cancer cell lines were dispersed into 96-well plates in 100

µL. 100 µl of medium without cells were also placed in some wells which were treated similarly to the cell-containing wells. The values obtained from these wells were used as blanks. 24-48 h after the cells were dispersed, 100 µl of each compound dissolved in medium at twice the desired concentration was added to the wells. Incubation was for 48 h after which the MTS reagent (40 µl) was added to each well. The plates were incubated for 1-4 h on a Nutating mixer in a CO₂ incubator. The OD was read at 490 nm in a plate reader.

LAV formation: ATG5 ^{-/-} mouse embryonic fibroblasts were grown in 6-well plates and incubated with varying concentrations of the GAELs for up to 12 h. The generation of LAVs with time was observed on an Olympus IX70 microscope and the images recorded with an LCD camera.

3.7. Acknowledgements

This study was supported by the Natural Science and Engineering Council of Canada (NSERC) and the Canadian Breast Cancer Foundation Prairie/NWT.

3.8. References

- (1) Worldwide data | World Cancer Research Fund International
<http://www.wcrf.org/int/cancer-facts-figures/worldwide-data> (accessed Dec 26, 2015).
- (2) Ferguson, L. R.; Pearson, A. E. The Clinical Use of Mutagenic Anticancer Drugs. *Mutat. Res.* **1996**, *355* (1-2), 1–12.
- (3) MacFarlane, M. Cell Death Pathways – Potential Therapeutic Targets. *Xenobiotica* **2009**.
- (4) Wong, S. T.; Goodin, S. Overcoming Drug Resistance in Patients with Metastatic Breast Cancer. *Pharmacotherapy* **2009**, *29* (8), 954–965.
- (5) Fulda, S.; Pervaiz, S. Apoptosis Signaling in Cancer Stem Cells. *Int. J. Biochem. Cell Biol.* **2010**, *42* (1), 31–38.
- (6) Kruh, G. D. Introduction to Resistance to Anticancer Agents. *Oncogene* **2003**, *22* (47), 7262–7264.
- (7) Dai, Y.; Lawrence, T. S.; Xu, L. Overcoming Cancer Therapy Resistance by Targeting Inhibitors of Apoptosis Proteins and Nuclear Factor-Kappa B. *Am. J. Transl. Res.* **2009**, *1* (1), 1–15.
- (8) Slamon, D. J.; Leyland-Jones, B.; Shak, S.; Fuchs, H.; Paton, V.; Bajamonde, A.; Fleming, T.; Eiermann, W.; Wolter, J.; Pegram, M.; Baselga, J.; Norton, L. Use of Chemotherapy plus a Monoclonal Antibody against HER2 for Metastatic Breast Cancer That Overexpresses HER2. *N. Engl. J. Med.* **2001**, *344* (11), 783–792.
- (9) Bedard, P. L.; Cardoso, F.; Piccart-Gebhart, M. J. Stemming Resistance to HER-2 Targeted Therapy. *J. Mammary Gland Biol. Neoplasia* **2009**, *14* (1), 55–66.

- (10) Longley, D. B.; Johnston, P. G. Molecular Mechanisms of Drug Resistance. *J. Pathol.* **2005**, *205* (2), 275–292.
- (11) Hamza, E.; Gerber, V.; Steinbach, F.; Marti, E. Equine CD4(+) CD25(high) T Cells Exhibit Regulatory Activity by Close Contact and Cytokine-Dependent Mechanisms in Vitro. *Immunology* **2011**, *134* (3), 292–304.
- (12) Deming, P. B.; Schafer, Z. T.; Tashker, J. S.; Potts, M. B.; Deshmukh, M.; Kornbluth, S. Bcr-Abl-Mediated Protection from Apoptosis Downstream of Mitochondrial Cytochrome c Release. *Mol. Cell. Biol.* **2004**, *24* (23), 10289–10299.
- (13) Soengas, M. S.; Capodici, P.; Polsky, D.; Mora, J.; Esteller, M.; Opitz-Araya, X.; McCombie, R.; Herman, J. G.; Gerald, W. L.; Lazebnik, Y. A.; Cordón-Cardó, C.; Lowe, S. W. Inactivation of the Apoptosis Effector Apaf-1 in Malignant Melanoma. *Nature* **2001**, *409* (6817), 207–211.
- (14) Smets, L. A.; Rooij, H. Van; Salomons, G. S. Signalling Steps in Apoptosis by Ether Lipids. *Apoptosis* **4** (6), 419–427.
- (15) Berdel, W. E. Membrane-Interactive Lipids as Experimental Anticancer Drugs. *Br. J. Cancer* **1991**, *64* (2), 208–211.
- (16) Samadder, P.; Arthur, G. Decreased Sensitivity to 1-O-Octadecyl-2-O-Methyl-Glycerophosphocholine in MCF-7 Cells Adapted for Serum-Free Growth Correlates with Constitutive Association of Raf-1 with Cellular Membranes. *Cancer Res.* **1999**, *59* (19), 4808–4815.
- (17) Gajate, C.; Santos-Beneit, A.; Modolell, M.; Mollinedo, F. Involvement of c-Jun NH2-

- Terminal Kinase Activation and c-Jun in the Induction of Apoptosis by the Ether Phospholipid 1-O-Octadecyl-2-O-Methyl-Rac-Glycerol-3-Phosphocholine. *Mol. Pharmacol.* **1998**, *53* (4), 602–612.
- (18) Samadder, P.; Bittman, R.; Byun, H.-S.; Arthur, G. A Glycosylated Antitumor Ether Lipid Kills Cells via Paraptosis-like Cell Death. *Biochem. Cell Biol.* **2009**, *87* (2), 401–414.
- (19) Jahreiss, L.; Renna, M.; Bittman, R.; Arthur, G.; Rubinsztein, D. C. 1- O -Hexadecyl-2- O -Methyl-3- O -(2'-acetamido-2'-deoxy- β -D-Glucopyranosyl)- Sn -Glycerol (Gln) Induces Cell Death with More Autophagosomes Which Is Autophagy-Independent. *Autophagy* **2009**, *5* (6), 835–846.
- (20) Samadder, P.; Byun, H.-S.; Bittman, R.; Arthur, G. An Active Endocytosis Pathway Is Required for the Cytotoxic Effects of Glycosylated Antitumor Ether Lipids.
- (21) Auzanneau, F.-I.; Bennis, K.; Fanton, E.; Promé, D.; Defaye, J.; Gelas, J. Synthesis of S-Linked Thiooligosaccharide Analogues of Nod Factors. Part 1: Selectively N-Protected 4-Thiochitobiose Precursors. *J. Chem. Soc. Perkin Trans. 1* **1998**, No. 21, 3629–3636.
- (22) Allman, S. A.; Jensen, H. H.; Vijayakrishnan, B.; Garnett, J. A.; Leon, E.; Liu, Y.; Anthony, D. C.; Sibson, N. R.; Feizi, T.; Matthews, S.; Davis, B. G. Potent Fluoro-Oligosaccharide Probes of Adhesion in Toxoplasmosis. *Chembiochem* **2009**, *10* (15), 2522–2529.
- (23) Baker, T. J.; Luedtke, N. W.; Tor, Y.; Goodman, M. Synthesis and Anti-HIV Activity of Guanidinoglycosides. *J. Org. Chem.* **2000**, *65* (26), 9054–9058.
- (24) Weng, S.-S.; Li, C.-L.; Liao, C.-S.; Chen, T.-A.; Huang, C.-C.; Hung, K.-T. Facile

- Preparation of α -Glycosyl Iodides by In Situ Generated Aluminum Iodide:
Straightforward Synthesis of Thio-, Seleno-, and O -Glycosides from Unprotected
Reducing Sugars. *J. Carbohydr. Chem.* **2010**, *29* (8-9), 429–440.
- (25) McGearry, R. P.; Wright, K.; Toth, I. Conversion of Glucosamine to Galactosamine and Allosamine Derivatives: Control of Inversions of Stereochemistry at C-3 and C-4. *J. Org. Chem.* **2001**, *66* (15), 5102–5105.
- (26) Sau, A.; Misra, A. Odorless Eco-Friendly Synthesis of Thio- and Selenoglycosides in Ionic Liquid. *Synlett* **2011**, *2011* (13), 1905–1911.
- (27) Daker, M.; Ahmad, M.; Khoo, A. S. Quercetin-Induced Inhibition and Synergistic Activity with Cisplatin - a Chemotherapeutic Strategy for Nasopharyngeal Carcinoma Cells. *Cancer Cell Int.* **2012**, *12* (1), 34.
- (28) Samadder, P.; Byun, H.-S.; Bittman, R.; Arthur, G. An Active Endocytosis Pathway Is Required for the Cytotoxic Effects of Glycosylated Antitumor Ether Lipids. *Anticancer Res* **2011**, *31* (11), 3809–3818.
- (29) Schweizer, F. Cationic Amphiphilic Peptides with Cancer-Selective Toxicity. *Eur. J. Pharmacol.* **2009**, *625* (1-3), 190–194.
- (30) Park, K. G.; Chetty, U.; Scott, W.; Miller, W. The Activity of Locally Applied Cytotoxics to Breast Cancer Cells in Vitro. *Ann. R. Coll. Surg. Engl.* **1991**, *73* (2), 96–99.
- (31) Yip, K. W.; Mao, X.; Au, P. Y. B.; Hedley, D. W.; Chow, S.; Dalili, S.; Mocanu, J. D.; Bastianutto, C.; Schimmer, A.; Liu, F.-F. Benzethonium Chloride: A Novel Anticancer Agent Identified by Using a Cell-Based Small-Molecule Screen. *Clin. Cancer Res.* **2006**,

12 (18), 5557–5569.

- (32) Ito, E.; Yip, K. W.; Katz, D.; Fonseca, S. B.; Hedley, D. W.; Chow, S.; Xu, G. W.; Wood, T. E.; Bastianutto, C.; Schimmer, A. D.; Kelley, S. O.; Liu, F.-F. Potential Use of Cetrimonium Bromide as an Apoptosis-Promoting Anticancer Agent for Head and Neck Cancer. *Mol. Pharmacol.* **2009**, 76 (5), 969–983.
- (33) Martín-Lomas, M.; Flores-Mosquera, M.; Chiara, J. Attempted Synthesis of Type-A Inositolphosphoglycan Mediators – Synthesis of a Pseudo-hexasaccharide Precursor. *European J. Org. Chem.* **2000**, 2000 (8), 1547–1562.

Chapter 4

Structure Activity Relationships of N-linked and Diglycosylated Glucosamine-based Antitumor Glycerolipids

By Makanjuola Ogunsina, Hangyi Pan, Pranati Samadder, Gilbert Arthur and Frank Schweizer

First published in *Molecules*, 2013, 18(12), 15288-15304

4.1 Authorship considerations

Hangyi Pan synthesized and purified compound **2-4** on the advice of Makanjuola Ogunsina. Makanjuola was responsible for designing, synthesis, purification and characterization of the glycolipids **5-7** on the advice of Frank Schweizer. Biological activity was investigated by Makanjuola Ogunsina and Pranati Samadder on the advice of Gilbert Arthur. The preliminary draft of the paper was written by Makanjuola Ogunsina reviewed by Frank Schweizer and Gilbert Arthur, and then rendered into its final form by Makanjuola Ogunsina. Frank Schweizer is the corresponding author.

4.2 Abstract

1-*O*-Hexadecyl-2-*O*-methyl-3-*O*-(2'-amino-2'-deoxy- β -D-glucopyranosyl)-*sn*-glycerol (**1**) was previously reported to show potent *in vitro* antitumor activity on a range of cancer cell lines derived from breast, pancreas and prostate cancer. This compound was not toxic to mice and was inactive against breast tumor xenografts in mice. This inactivity was attributed to hydrolysis of the glycosidic linkage by glycosidases. Here three *N*-linked (glycosylamide)

analogs **2–4**, one triazole-linked analog **5** of **1** as well as two diglycosylated analogs **6** and **7** with different stereochemistry at the *sn*-2-position of the glycerol moiety were synthesized and their antitumor activity against breast (JIMT-1, BT-474, MDA-MB-231), pancreas (MiaPaCa2) and prostate (DU145, PC3) cancer cell lines was determined. The diglycosylated analogs 1-*O*-hexadecyl-2(*R*)-, 3-*O*-di-(2'-amino-2'-deoxy- β -D-glucopyranosyl)-*sn*-glycerol (**7**) and the 1:1 diastereomeric mixture of 1-*O*-hexadecyl-2(*R/S*), 3-*O*-di-(2'-amino-2'-deoxy- β -D-glucopyranosyl)-*sn*-glycerol (**6**) showed the most potent cytotoxic activity at CC₅₀ values of 17.5 μ M against PC3 cell lines. The replacement of the *O*-glycosidic linkage by a glycosylamide or a glycosyltriazole linkage showed little or no activity at highest concentration tested (30 μ M), whereas the replacement of the glycerol moiety by triazole resulted in CC₅₀ values in the range of 20 to 30 μ M. In conclusion, the replacement of the *O*-glycosidic linkage by an *N*-glycosidic linkage or triazole-linkage resulted in about a two to three-fold loss in activity, whereas the replacement of the methoxy group on the glycerol backbone by a second glucosamine moiety did not improve the activity. The stereochemistry at the C2-position of the glycerol backbone has minimal effect on the anticancer activities of these diglycosylated analogs.

4.3 Introduction

Cancer is a devastating disease with significant mortality and morbidity in both developed and developing countries.^{1,2} Acquired and intrinsic resistance to major classes of anticancer agents: antimetabolites, anthracyclines, taxanes and alkylating agents which are mostly pro-apoptotic present a serious challenge to management of cancer.³ Even targeted antibody based therapies such as trastuzumab (Herceptin) are also affected by the problem of drug resistance.^{3,4} So there is need for new anticancer agents with new mechanisms of action that are apoptosis independent.

Glycosylated antitumor ether lipids (GAELs), represent a subclass of antitumor ether lipids (AELs) in which the phosphocholine moiety of the prototypic compound, edelfosine is replaced by a sugar moiety.⁵ The antitumor activity of these compounds has been well established.⁶ Edelfosine is an investigational drug that has undergone phase II clinical trials. The best studied GAEL analog, glucosamine-based glycerolipid **1** (Figure 4.1) has potent antitumor effects against a range of cancer cell lines derived from breast, pancreas and prostate cancer with CC₅₀ values in the range of 9–15 μ M. This compound has been reported to kill cancer cells via an apoptosis independent pathway and is more active than the prototypic AELs, edelfosine, which kills cell via an apoptosis dependent pathway.^{6–8}

A major drawback for compound **1** is the lack of antitumor activity in *in vivo* studies using mice. A maximum tolerability dose could not be attained at concentrations of 500 mg/kg oral dosage or 4 mg/kg given intraperitoneally in Rag2M mice and there was no effect on the body weight of the animals.⁹ Furthermore, at a dose of 100 mg/kg given orally and 4 mg/kg given intraperitoneally, it had no effect on the growth of JIMT-1 or MDA-MB231 xenografts growing in female Rag2M mice.⁹ These observations are consistent with the hypothesis that the likely cause of the *in vivo* inactivity is due to cleavage of the β -*O*-glycosidic linkage by glucosidases. A *C*-glycosidic analogue of **1** has been synthesized to enhance the metabolic stability of the compound.¹⁰ However, the synthesis is very involved and alternative facile approaches have to be considered to generate metabolically stable analogues. Based on the rationale that both glycosylamide- and glycosyltriazole linkages will be resistant towards glycosidic cleavage,^{11–13} we synthesized compounds **2–4** where the β -*O*-glycosidic linkage was replaced by a glycosylamide or a triazole-linkage as in compound **5**. In addition, we synthesized compounds **6** and **7** to study the effects of: (a) diglycosylation and (b) stereochemistry of the glycerol moiety on antitumor activity

in a cell based assay. The rationale behind the synthesis of compounds **6** and **7** is to test our hypothesis that an additional glucosamine moiety on the molecule will increase the anticancer activity because glucosamine is cytotoxic against human epidermoid carcinoma cells in tissue culture¹⁴ and YD-8 human oral cancer cells.¹⁵ Here we report on the *in vitro* antitumor activity of compounds **2–7**.

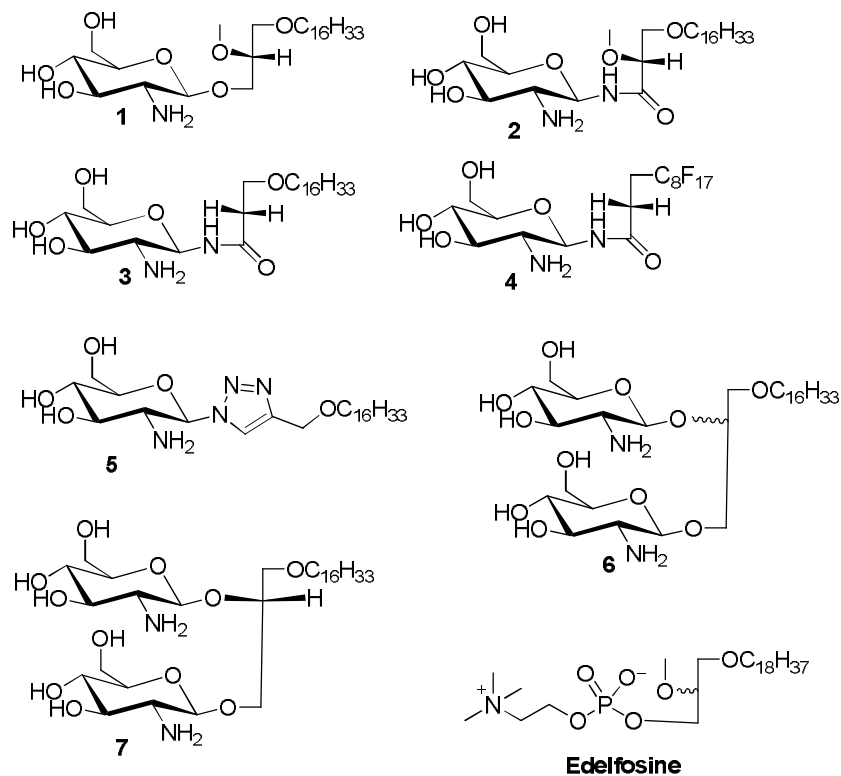


Figure 4.1. Structures of the synthesized glycolipids used in the study. Compound **1** is the reference GAEL while compounds **2–5** are glycolipid analogs differing in the nature of the glycosidic linkage and glycerol moiety. Compounds **6** and **7** are glycolipid analogs where the glycerolipid moiety contains two glycosidic linkages. Edelfosine is shown as a prototypic AEL analog.

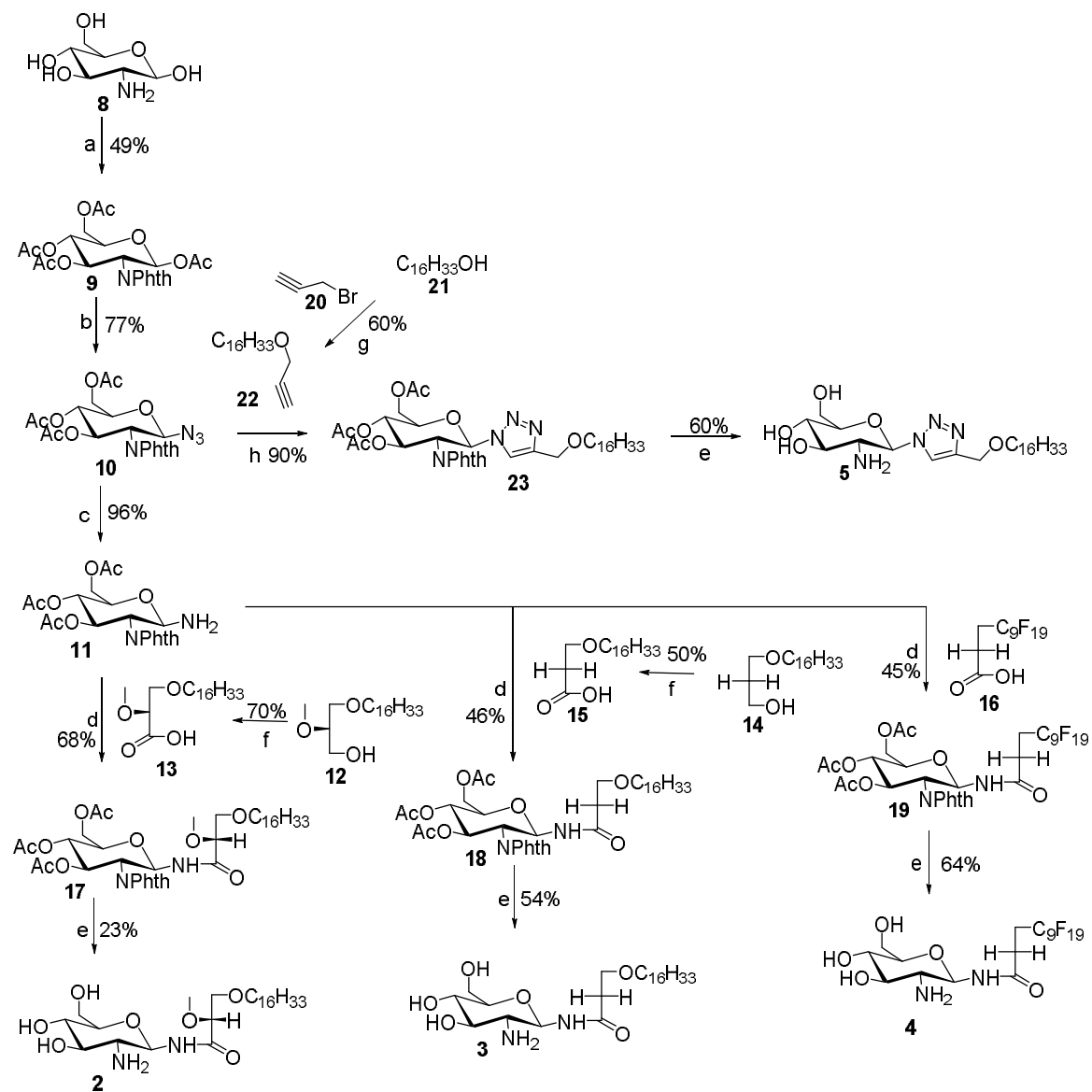
4.4 Results and Discussion

4.4.1. Chemistry

In order to prepare easily accessible analogs with improved metabolic stability towards glycosidases we initially were interested in analogs that contain a glycosylamide linkage. Glycosylamides **2–4** were synthesized to evaluate the effect of amide linkage and nature of the lipid moiety on the antitumor properties. Compound **3** which lacks the methoxy substituent was prepared to explore how the methoxy group affects the antitumor properties. Compound **4** that contains a lipophobic polyfluorinated lipid tail instead of a lipophilic carbon chain was prepared to explore how modifications in the lipid tail affect the antitumor activity. Compound **5** was synthesized to evaluate the effect of a triazole linkage at the anomeric position. Both linkages, the glycosylamide and glycosyltriazole linkages are expected to be metabolically stable to hydrolysis by glycosidases in *in vivo* studies.^{11–13} In addition, the glycosyltriazole linkage will be inert towards peptidases and proteases which may provide additional benefits for future *in vivo* studies.¹⁶

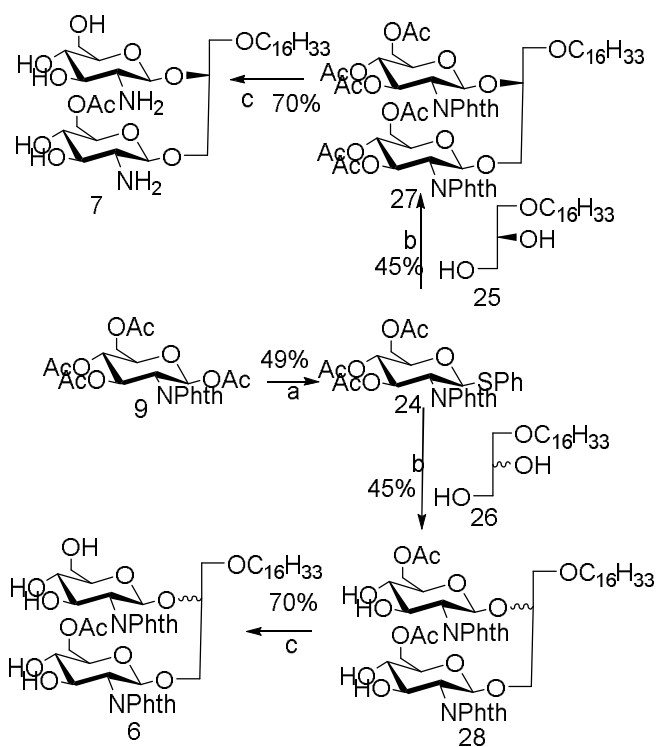
GAEL mimetics **2–4** were prepared by coupling of glycosylamine **11** to carboxylic acids **13**, **15** and **16** (Scheme 4.1). Glycosylamine **11** was synthesized in three steps from glucosamine hydrochloride (**8**) in 49% yield.¹⁷ The amino substituent at C₂ position of glucosamine hydrochloride group was protected with phthalic anhydride followed by protection of the hydroxyl groups as acetate esters by reaction with acetic anhydride in pyridine to afford compound **9**. The anomeric amino group in **11** was installed through conversion of **9** into the corresponding anomeric azide **10**. Originally, we planned to introduce the anomeric azido group by nucleophilic

displacement of the α -anomeric chloride. However conversion of the anomeric acetate into the chloride by reaction with PCl_5 did not afford the corresponding glucosylhalides.¹⁸ However, the anomeric azide **10** was prepared by Fe(III) chloride- promoted reaction of **9** with trimethylsilyl azide to afford azide **10** in 75% yield. The anomeric azide was reduced to the amine by catalytic hydrogenation to provide glucosylamine **11** in 96% yield. Synthesis of the fatty acid compounds **13** and **15** was achieved by Jones oxidation of the corresponding commercially available alcohol **12** or known alcohol **14**.¹⁹ The polyfluorinated fatty acid **16** was purchased from commercial source. Coupling of fatty acids **13**, **15** and **16** to the glucosylamine **11** was achieved by using TBTU²⁰ as coupling agent to afford the protected glycolipids **17**, **18** and **19**, respectively. The acetate and phthalimido protecting groups were removed using an ethylenediamine-butanol mixture (1:1) at 90 °C for 3 h to afford desired target compounds **2**, **3** and **4** respectively. The triazole analog **5** was synthesized by Cu(I)-promoted click chemistry²¹ using azide **10** and 3-hexadecyloxyprop-1-yne (**22**) to produce glycosyltriazole **23**. Deblocking using the same method as described above gave compound **5**.



Scheme 4.1. Synthesis of compounds 2–5. *Reagents and conditions:* (a) (i) phthalic anhydride, NaOH, H₂O, 16 h, rt; (ii) pyridine, DMAP, Ac₂O, 16 h, rt; (b) TMSN₃, FeCl₃ as catalyst, DCM, rt; (c) Pd/C, MeOH, H₂, 2 h, rt; (d) TBTU, DIPEA. DMF 3 h, rt; (e) ethylenediamine/butanol (1:1), 90 °C, 2 h; (f) Jones reagent, acetone, 0 °C, 20 min; (g) NaH, DMF, 80 °C; (h) CuI, acetic acid, DIPEA.

Compounds **6** and **7** were synthesized to study the effects of diglycosylation and stereochemistry of the glycerol moiety on the antitumor properties. Glycolipids **6** and **7** were prepared from known thioglycoside donor **24**²² by glycosylation with commercially available lipid alcohol **25** or racemic alcohol **26** using silver triflate as catalyst and *N*-iodosuccinimide as promoter to afford protected glycolipids **27** or **28**, respectively (Scheme 4.2). The acetate and phthalimido protective groups were removed using ethylenediamine:butanol mixture (1:1) at 90 °C for 3 h to provide compounds **6** and **7**, respectively.



Scheme 4.2. Synthesis of compounds **6** and **7**. *Reactions and conditions:* (a) $\text{BF}_3 \cdot \text{Et}_2\text{O}$, DCM, thiophenol, reflux 16 h; (b) AgOTf , *N*-iodosuccinimide, DCM, rt, 5 h; (c) ethylenediamine/butanol (1:1), 90 °C, 4 h.

4.4.2 Cytotoxicity

The cytotoxicity of compounds **1–7** was evaluated against a number of epithelial cancer cell lines using the MTS assay²². The cells were derived from cancers of the breast (JIMT-1, BT-474, MDA-MB-231), pancreas (MiaPaCa2), and prostate (DU145, PC3). The cytotoxic effect of compounds **2–6** were compared with that of **1** the most studied glycosylated antitumor ether lipid (see Table 4.1).^{5–7} Exponentially growing cells were treated with test compound and then incubated for 48 h. The result for compounds **2–4** are shown in Figure 4.2, while that of compounds **5–7** are shown in Figure 4.3. The CC_{50} values that lead to a reduction of cell viability by 50% relative to untreated control are reported in Table 4.1. At the highest concentration tested none of the *N*-linked glycolipids **2–4** was able to achieve 50% reduction in viability against all the four cell lines tested (see Figure 4.2). It is noteworthy that compound **2** with similar glycerolipid moiety as reference compound **1**, is consistently more active than compounds **3** and **4**, leading to a 19%–29% reduction in viability relative to untreated control at the highest dose tested (30 μ M). At this dose and lower concentration, compound **4** with polyfluorinated lipid moiety is consistently the least active analogue among these *N*-linked (amide) glycolipids. This relative difference in activity is an indication that the nature of the lipids of this class of compounds plays an important role on their cytotoxicity against human cancer cell lines. The triazole-linked glycolipid compound **5** at concentration of 30 μ M or below was unable to achieve CC_{50} values against prostate and pancreas cell lines used in this experiment, indicating that both the nature of the glycosidic linkage and the glycerol moiety influences the antitumor properties. It is noteworthy that compound **5** was able to achieve more than 80% reduction in viability of JIMT1, a trastuzumab resistant cell line²³ at the dose of 30 μ M, (CC_{50} : 23 μ M) and more than 60% reduction in viability of BT474, a trastuzumab sensitive cell lines (see Figure 4.3). *In vivo*, triazole-linked glycolipid **5** is expected to be

metabolically stable relative to lead compound **1**, however the loss of activity does not make it a worthwhile compound for further development.

Table 4.1. Cytotoxicity of compounds **1–7** on a panel of human epithelial cancer cell lines.^e

Compd	CC ₅₀ (μM)					
	JIMT1	MiaPaCa2	DU145	PC3	BT474	MDA-MB-231
1	9	9	10	13.5	6.5	NT
2	>30	>30	>30	NT	>30	NT
3	>30	>30	>30	NT	>30	NT
4	>30	>30	>30	NT	>30	NT
5	23	>30	>30	>30	28	>30
6	27	>30	20	17.5	>30	>30
7	29	>30	25	17.5	>30	>30

^eBreast (BT474, JIMT1, MDA-MB-231), prostate (DU145, PC3), pancreas (MiaPaCa2). The CC₅₀ value is defined as the concentration required to decrease cell viability by 50% relative to the untreated control. Values were determined by MTS assay. The CC₅₀ values were obtained by estimating the drug concentration at 50% viability on the y axis using line plots (graph not shown); NT = not tested. Please note that CC₅₀ values for compound **1** were obtained from our previously published work.²²

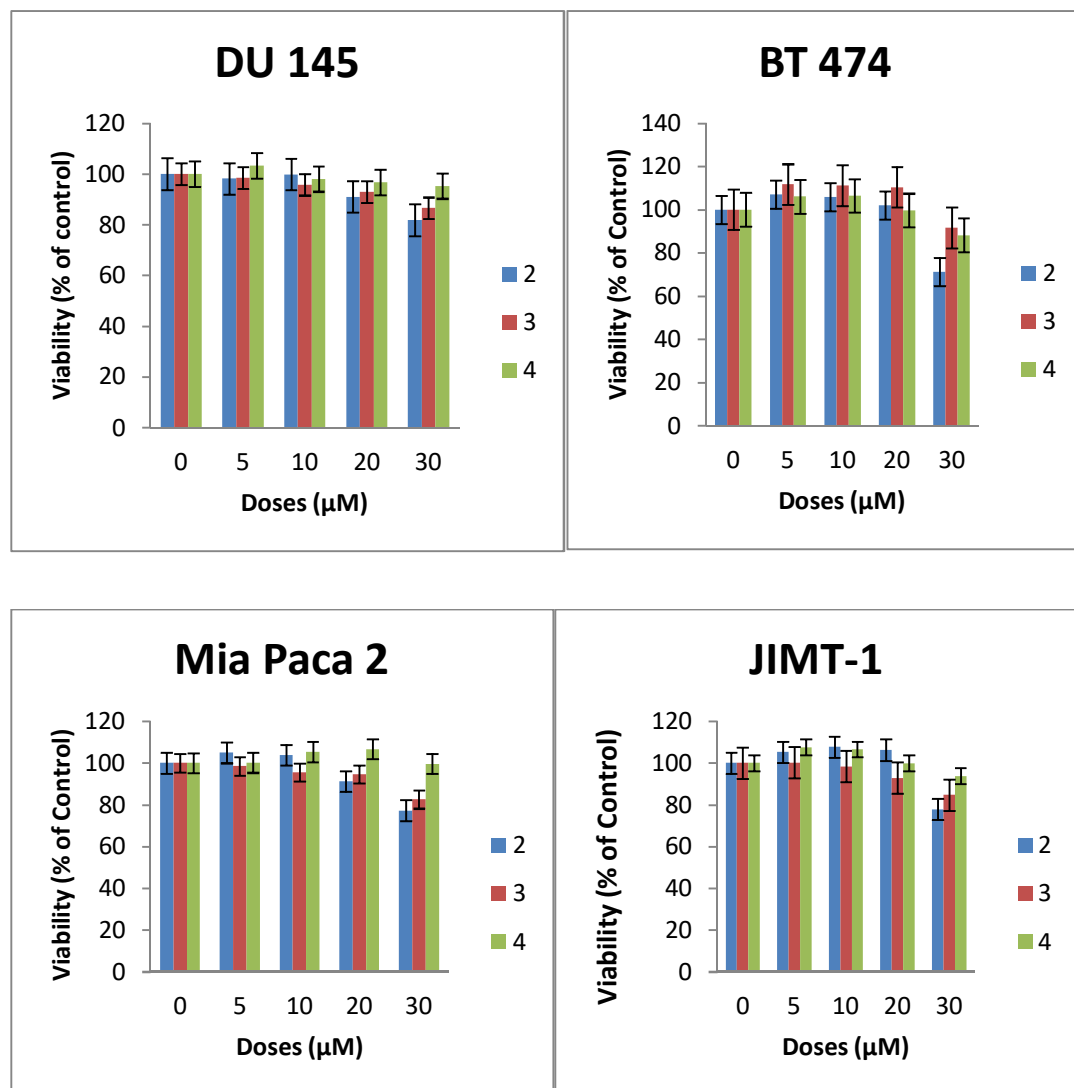
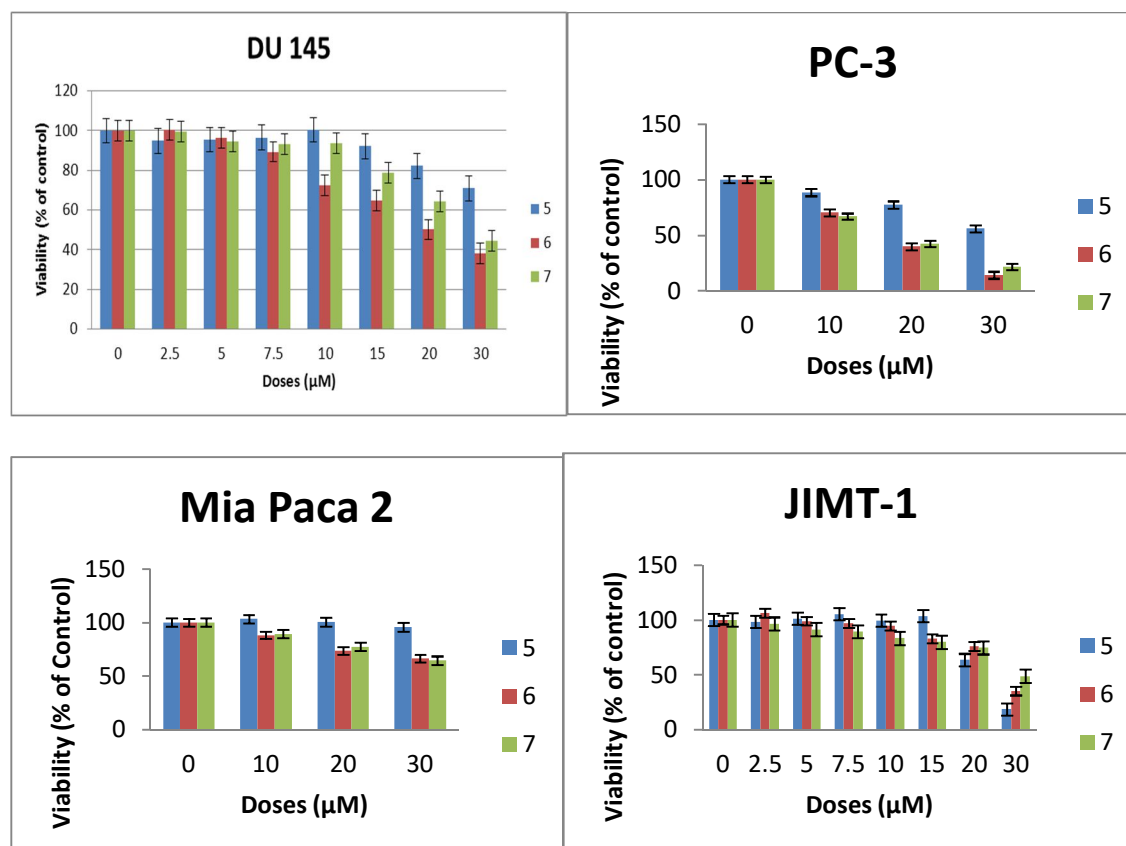


Figure 4.2. Effects of compounds 2–4 on the viability of epithelial cancer cell lines: breast (BT474, JIMT1), prostate (DU 145), pancreas (MiaPaCa2). The results represent the means \pm standard deviations of six independent determinations (compound 1 is not included in this chart because we have previously published the data.²²)

The diglycosylated analogues, compounds **6** and **7** with different stereochemistry at position *sn*-2 of the glycerol backbone have very similar activity but are significantly less active than GAEL-based reference compound **1** (Figure 4.3 and Table 4.1) indicating that additional glucosamine moieties on the glycerol backbone reduce the cytotoxic effect of the compounds. This reduction in activity may be due to increased polarity of the compound which in turn can affect the absorption of the drug across cell membrane, and subsequent decreased drug concentration in the cell. The fact that both compounds despite the difference in stereochemistry at the C-2 position of the glycerol backbone have similar activity especially in the more sensitive prostrate cell lines (Figure 4.3) is an indication that stereochemistry at this position has minimal to no effect on the anticancer activity.



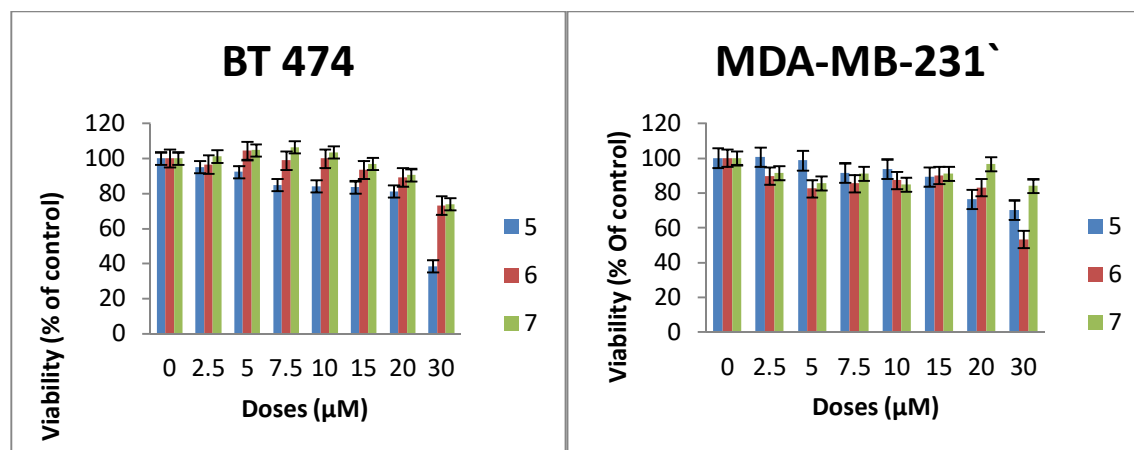


Figure 4.3. Effects of compounds 5–7 on the viability of epithelial cancer cell lines: breast (BT474, JIMT1, MDA-MB-231), prostate (DU145, PC3), pancreas (MiaPaCa2). The results represent the means \pm standard deviations of six independent determinations.

4.5. Experimental

4.5.1 General Methods

All fine chemicals such as glucosamine hydrochloride, phthalic anhydride, pyridine, 1-hexadecanol, 4-toluenesulfonyl chloride, 60% sodium hydride, dimethylformamide (DMF), 1,3-dihydroxypropane, sodium methoxide, concentrated sulfuric acid, palladium on carbon, trimethylsilyl azide, toluene, phosphorus pentachloride, boron trifluoride, *N,N*-diisopropylethylamine, ethylenediamine and iron (III) chloride butanol were purchased from Sigma-Aldrich (Oakville, ON, Canada). All solvents such as dichloromethane (DCM), hexane, acetone, methanol, ethyl acetate, butanol were purchased from Sigma-Aldrich (Oakville, ON, Canada). Carboxylic acid **16** (2*H*,2*H*,3*H*,3*H*-perfluoroundecanoic acid) were purchased from Fluorous Technologies now available through Sigma-Aldrich. The lipid alcohol, 1-*O*-hexadecyl-2-*O*-methyl-*sn*-glycerol, was purchased from Chem-Implex (Wood Dale, IL, USA). 5 $\frac{3}{4}$ and 9 inch pipets used in lab were

obtained from Fisher Scientific (Ottawa, ON, Canada. TLC plates (CCM Gel silica 60 F254) were visualized by ultraviolet light or by charring (9:1 methanol and sulfuric acid). All chromatography solvents were prepared by mixing hexane and ethyl acetate in various ratios based on the polarity of the compound. Column chromatography was performed by using silica gel p60 (40–63 μm) or reverse-phase C18 silica gel. Solutions were concentrated on reduced pressure rotary evaporator (IKA RV 10 Basic, that was connected to building vacuum and high vacuum pump (Welch 8907). $^1\text{H-NMR}$ and $^{13}\text{C-NMR}$ spectra were recorded on a 300 MHz (Bruker Avance-300 spectrometer. Low-resolution mass spectrometry (MS) data were obtained on a Varian 500-MS IT Mass spectrometer using electrospray ionization (ESI).

4.5.2 General Procedure for the Synthesis of N-Linked Compounds 2–5

1,3,4,6-Tetra-O-acetyl-2-deoxy-2-N-phthalimido- β -D-glucopyranoside (9).

Glucosamine hydro-chloride **8** (3.016 g, 14 mmol) and NaOH (28 mmol) were dissolved in water (50 mL). The resulting mixture was stirred at room temperature for 30 min. Phthalic anhydride (2.34 g, 0.0157 mol) was added to the solution. The mixture was stirred vigorously at room temperature for 16 h. The mixture was concentrated and dried using rotary evaporator. The residue was dissolved in pyridine (30 mL), and then Ac_2O (19.8 mL) was added to the solution. The resulting solution was allowed to stir vigorously overnight. The reaction was checked by the TLC. Methanol (6 mL) was used to quench the excess of Ac_2O , and then excess pyridine was removed under high vacuum. The remaining solid was dissolved in CH_2Cl_2 (40 mL), and then the solution was washed with 10% HCl (40 mL \times 1), Saturated NaHCO_3 solution (40 mL \times 3), H_2O (40 mL \times 1) and brine (40 mL \times 1) and dried over anhydrous MgSO_4 . The final solution was concentrated under reduced pressure, and the obtained product **9** (3.3g, 49.4%) was dried overnight. NMR data were consistent with data in the literature.²²

3,4,6-tri-O-Acetyl-2-deoxy-2-N-phthalimido-β-D-glucopyranosyl azide (10).

Compound **9** (1.8 g, 8 mmol) and trimethylsilyl azide (1.7 g, 148 mmol) were both dissolved in CH₂Cl₂ (20 mL) in a 100 mL-round bottom flask with vigorous stirring. Then FeCl₃ (1.77 g) was added to the reacting mixture. The reaction was allowed to stir for 24 h and then progress was checked by TLC. The dispersion solution was made by mixing hexane and ethyl acetate in 1:1 ratio. The solution was concentrated under reduced pressure by rotary evaporator. The product **10** was isolated and purified by column chromatography (1:2 ethyl acetate/hexane). The obtained product **10** (1.3 g, 76.53%) was a light yellow solid. NMR data were consistent with previously published data.¹⁶

3,4,6-tri-O-Acetyl-1-amino-2-deoxy-2-N-phthalimido-β-D-glucopyranose (11).

Compound **10** (0.11 g, 0.24 mmol) was dissolved in methanol (2 mL) in a 25 mL-round bottom flask with vigorous stirring, and then Pd/C (0.29 g) was added. After that, round bottom flask was connected to a hydrogen balloon. The reaction was allowed to take place for half hour, and checked by TLC. The reaction was stopped when all starting material has disappeared, and the solution was concentrated to provide compound **11** (100 mg, 96%). This compound was not characterised by ¹H-NMR, because it is chemically unstable. Therefore it was directly used for the next step, *i.e.*, coupling of carboxylic acids using TBTU as coupling reagent.

3-(Hexadecyloxy)-2-methoxypropanoic acid (13).

A 2.7 M solution of Jones reagent (0.5 mL) was added dropwise into a stirred solution of commercially available 3-*O*-hexadecyloxy-2-*O*-methyl-*sn*-glycerol **12** (23 mg) in acetone (5 mL) at 0 °C. The reaction was monitored by TLC and was completed after 1 h. Isopropyl alcohol was

added dropwise until a green color remained, to remove excess of CrO₃ totally. The organic solvent was removed under reduced pressure. The solid was dissolved in water, and then 3-(hexadecyloxy)-2-methoxypropanoic acid was extracted using ethyl acetate. The combined organic layers were washed with brine, dried using MgSO₄ and concentrated under vacuum. The 3-(hexadecyloxy)-2-methoxypropanoic acid (**13**) was purified by silica gel column flash chromatography (4:1 hexane/ethyl acetate) to yield white solid (16 mg, 70%). ¹H-NMR (CDCl₃): δ = 4.00–3.75 (m, 3H), 3.55 (s, 3H, –OCH₃), 2.66 (t, *J* = 6.4 Hz, 2H, –OCH₂–CH₂–(CH₂)₁₃), 1.59 (m, 2H, –CH₂–(CH₂)₁₃), 1.23–1.34 (brs, 26H, –(CH₂)₁₃), 0.90 (t, *J* = 6.9 Hz, 3H, –CH₃). ESMS: calcd for C₂₀H₄₀O₄Na⁺ *m/z* 367.3; found: *m/z* [M+Na]⁺ 367.3.

3-(Hexadecyloxy)-propanoic acid (15).

A 2.7 M solution of Jones reagent (2.0 mL) was added dropwise into a stirred solution of compound **14** (0.124 g, 0.4 mmol) in acetone (20 mL) at 0 °C. The reaction was monitored by TLC and was completed after 1 h. Isopropyl alcohol was added dropwise until a stable green color appeared, to remove the excess of CrO₃. The organic solvent was removed under reduced pressure. The solid was dissolved in water, and then compound **15** was extracted using ethyl acetate. The combined organic layers were washed by brine, dried using MgSO₄ and concentrated under reduced pressure. The compound **15** was purified by silica gel column flash chromatography (4:1 hexane/ethyl acetate) to yield white solid (63 mg, 50.1%). ¹H-NMR (CDCl₃): δ = 3.72 (t, *J* = 6.3 Hz, 2H, –CH₂–COOH), 3.48 (t, *J* = 6.7 Hz, 2H, –OCH₂–CH₂–COOH), 2.65 (t, *J* = 6.3 Hz, 2H, –OCH₂–CH₂–(CH₂)₁₃), 1.59 (m, 2H, –CH₂–(CH₂)₁₃), 1.23–1.34 (brs, 26H, –(CH₂)₁₃), 0.90 (t, *J* = 6.9 Hz, 3H, CH₃). ESMS: calcd for C₁₉H₃₈O₃Na⁺ *m/z* 337.3; found: *m/z* [M+Na]⁺ 337.4

3-Hexadecyloxy-2-methoxyl-1-N-(3,4,6-tri-O-acetyl-2-deoxy-2-N-phthalimido-β-D-glucopyranosyl)-propanamide (17).

Glucosylamine **11** (110 mg, 0.25 mmol), carboxylic acid **13** (110 mg, 0.32 mmol), DIPEA (0.40 mL) and TBTU (0.245 g) were dissolved in DMF (10 mL) in a round bottom flask with vigorous stirring overnight and was monitored by TLC. At the completion of the reaction DMF was removed under reduced pressure to obtain a solid residue. The solid residue was dissolved in water, and the product was extracted by ethyl acetate. The combined organic layers were concentrated under reduced pressure to yield a light yellow compound **17** (130 mg, 68%). ¹H-NMR (CDCl₃): δ = 8.84 (s, br, 1H), 7.93–7.67 (m, 4H, phthalimido), 7.11(d, *J* = 9.0 Hz, 1H, H-1), 6.14–5.96 (m, 2H, H-2, H-3), 5.19 (dd, *J*₁ = *J*₂ = 12 Hz, 1H, H-4), 4.44–3.54 (m, 8H), 3.26 (s, 3H, –OCH₃), 2.12(s, 3H, acetate–CH₃), 2.06 (s, 3H, acetate–CH₃), 1.89 (s, 3H, acetate–CH₃), 1.53 (m, 2H–CH₂–(CH₂)₁₃), 1.39–1.15 (brs, 26H, (CH₂)₁₃), 0.90 (t, *J* = 6.0 Hz, 3H, CH₃). ES-MS: calcd for C₄₀H₆₀N₂O₁₂Na⁺ *m/z* 783.4: found: *m/z* [M+Na]⁺ 783.6.

3-Hexadecyloxy-1-N-(3,4,6-tri-O-acetyl-2-deoxy-2-N-phthalimido-β-D-glucopyranosyl)-propanamide (18).

Glucosylamine **11** (100 mg, 0.23 mmol) and carboxylic acid **15** (43.7 mg, 0.15 mmol) and DIPEA (0.04 g) and TBTU (0.04 g) and DMF (4 mL) were added into a 25-mL round bottom flask with vigorous stirring. The reaction allowed to stir for overnight and was monitored by TLC. DMF was removed under reduced pressure to obtain solid. The solid was dissolved in water, and the product was extracted by ethyl acetate. The combined organic layers were concentrated by reduced pressure rotary evaporator to yield a light yellow compound **18** (50 mg, 45.5%). ¹H-NMR (CDCl₃): δ = 8.84 (s, br, 1H), 7.89–7.76 (m, 4H, phthalimido), 7.03 (d, *J* = 9.0 Hz, 1H, H-1), 6.08 (dd, *J*₁

= $J_2 = 9.8$ Hz, 1H, H-3), 6.02 (dd, $J_1 = J_2 = 9.6$ Hz, 1H, H-2), 5.18 (dd, $J_1 = J_2 = 9.8$ Hz, 1H, H-4), 4.36 (m, 1H, H-5), 4.28 (dd, $J_1 = J_2 = 10.2$ Hz, 2H,), 4.09 (dd, $J_1 = J_2 = 10.0$ Hz, 2H, H-6), 3.51 (m, 1H), 3.34 (m, 2H), 2.26 (m, 2H), 2.12 (s, 3H, acetate-CH₃), 2.05 (s, 3H, acetate-CH₃), 1.88 (s, 3H, acetate-CH₃), 1.53 (m, 2H, CH₂-(CH₂)₁₃), 1.31–1.28 (brs, 26H, -(CH₂)₁₃), 0.90 (t, $J = 6.9$ Hz, 3H, -CH₃). ES-MS: calcd for C₃₉H₅₈N₂O₁₁Na⁺ m/z 753.4: found: m/z [M+Na]⁺ 753.8.

Heptadecylfluoro-1-N-(3,4,6-tri-O-acetyl-2-deoxy-2-N-phthalimido-β-D-glucopyranosyl)-undecanamide (19).

Glucosylamine **11** (110 mg, 0.25 mmol), fluorinated carboxylic acid (250 mg, 0.51 mmol), DIPEA (0.04 g), TBTU (0.245 g) and DMF (10 mL) were added into a 25-mL round bottom flask with vigorous stirring. The reaction allowed to stir for overnight and was monitored by TLC. DMF was removed under reduced pressure to obtain solid. The solid was dissolved in water, and the product was extracted by ethyl acetate. The combined organic layers were concentrated by reduced pressure rotary evaporator to yield a light yellow compound **19** (105 mg, 45%). ¹H-NMR (CDCl₃): δ = 8.93 (s, br. 1H), 7.93–7.69 (m, 4H, phthalimido), 7.05 (d, $J = 9.0$ Hz, 1H, H-1), 6.15–5.99 (m, 2H, H-2, H-3), 5.17 (dd, $J_1 = J_2 = 9.0$ Hz, 1H, H-4), 4.45–3.98 (m, 5H), 2.38 (m, 2H), 2.13 (s, 3H, acetate-CH₃), 2.06 (s, 3H, acetate-CH₃), 1.89 (s, 3H, acetate-CH₃). ES-MS: calcd for C₃₁H₂₅F₁₇N₂O₁₀Na⁺ m/z 931.1: found: m/z [M+Na]⁺ 931.5.

3-Hexadecyloxy-2-methoxy-1-N-(2-deoxy-2-amino-β-D-glucopyranosyl)-propanamide (2).

Compound **17** (130 mg, 0.17 mmol) was dissolved in mixture of butanol (2 mL) and ethylenediamine (2 mL). The resulting mixture was heated to 90 °C and stirred for 3 h. The reaction was monitored by TLC plate. The solution was concentrated to dryness. The resulting residue was purified by flash chromatography (reverse-phase C18 silica gel). The collected product was 20 mg

(yield 23%). The compound was acidified with TFA to convert it into the TFA salt. ¹H-NMR (CD₃OD): δ = 5.14 (d, *J* = 9.6 Hz, 1H, H-1), 3.87–3.52 (m, 6H), 3.50–3.24 (m, 7H, H-3), 3.08 (dd, *J* = 9.6 Hz, 10 Hz, 1H, H-2), 1.56–1.36 (m, 2H, CH₂-(CH₂)₁₃), 1.25–1.13 (brs, 26H, -(CH₂)₁₃), 0.80 (t, *J* = 6.9 Hz, 3H, -CH₃). ¹³C-NMR (75 MHz, CD₃OD) characteristic data: 174.03 (C-1), 82.50, 80.41, 78.00, 74.87, 72.88, 71.49, 71.25, 62.11, 58.94 56.46, + multiple methylene carbons, 14.40 (CH₃). ES-HRMS: calcd for C₂₆H₅₂N₂O₇Na⁺ *m/z* 527.3667, found: *m/z* [M+Na]⁺ 527.3677.

3-Hexadecyloxy-1-N-(-2-deoxy-2-amino-β-D-glucopyranosyl)-propanamide (3).

Compound **8** (50 mg, 0.07 mmol) was dissolved in mixture of butanol (2 mL) and ethylenediamine (2 mL). The resulting mixture was heated to 90 °C and stirred for 3 h. The reaction was monitored by TLC. The solution was concentrated to dryness. The resulting residue was purified by flash chromatography (reverse-phase C18 silica gel). The collected product was 18 mg (yield 54%). The compound **3** was acidified with TFA to enhance solubility in methanol. ¹H-NMR (CD₃OD): δ = 5.14 (d, *J* = 10 Hz, 1H, H-1), 3.74–3.56 (m, 4H), 3.48–3.42 (m, 1H), 3.40–3.32 (m, 2H), 3.30–3.25 (m, 2H), 2.89 (dd, *J*₁ = *J*₂ = 10.0 Hz, 1H, H-2), 2.44 (t, *J* = 6 Hz, 2H), 1.51–1.42 (m, 2H, CH₂-(CH₂)₁₃), 1.25–1.18 (brs, 26 H, -(CH₂)₁₃), 0.81 (t, *J* = 7 Hz, 3H, -CH₃). ¹³C-NMR (CD₃OD) characteristic data: 174.50 (amide), 80.30 77.83, 74.87, 72.43, 71.43, 67.11, 62.18, 56.90, 37.54, (multiple methylene carbons), 14.43 (CH₃). ES-HRMS: calcd for C₂₅H₅₀N₂O₆Na⁺ *m/z* 497.3567: found: *m/z* [M+Na]⁺ 497.3554.

Heptadecylfluoro-1-N-(-2-deoxy-2-amino-β-D-glucopyranosyl)-dodecanamide (4).

Compound **19** (105 mg, 0.11 mmol) was dissolved in mixture of butanol (2 mL) and ethylenediamine (2 mL). The resulting mixture was heated to 90 °C and stirred for 3 h. The reaction was monitored by TLC plate. The solution was concentrated to dryness. The resulting residue was

purified by flash chromatography (reverse-phase C18 silica gel using water - methanol gradient elution) to yield product **4** (50 mg, 64% yield). The compound **3** was acidified with TFA to enhance solubility in methanol. ¹H-NMR (CD₃OD): δ = 5.16 (d, *J* = 9.9 Hz, 1H, H-1), 3.80–3.73 (m, 1H, H-6a), 3.65–3.55 (m, 1H, H-6b), 3.52–3.43 (m, 1H, H-5), 3.34–3.17 (m, 4H), 2.91 (dd, *J*₁ = 9.9 Hz, *J*₂ = 9.9 Hz, 1H, H-2), 2.59–2.33 (m, 2H). ¹³C-NMR (CD₃OD) for sugar carbons 173.32 (amide), 80.33, 77.96, 74.88, 71.45, 62.21, 56.87. ES-HRMS: calcd for C₁₇H₁₇F₁₇N₂O₅Na⁺ *m/z* 675.0758: found: *m/z* [M+Na]⁺ 675.0786.

3-Hexadecyloxy-propyl-1-ene (**22**).

Compound **20** (8.25 mmol, 2.0 g) and **21** (9.9 mmol, 0.884 mL) were dissolved in dry DMF (20 mL) under nitrogen atmosphere, then NaH (9.9 mmol, 237 mg) was added and the reaction mixture was heated to 90 °C overnight. The reaction was stopped by addition of water (8 mL). The mixture was concentrated under high vacuum and the residue was purified by flash chromatography using hexane/ethyl acetate mixture (9.5:0.5) to give compound **22** as a white sticky solid yield 60%. The NMR data correspond to the previously reported data [24].

4-(Hexadecyloxy)methyl-1-(3,4,6-tri-O-acetyl-2'-deoxy-2'-N-phthalimido-β-D-glucopyranosyl)-1,2,3-triazole (**23**).

Compound **10** (0.09 mmol, 40 mg) and compound **22** (0.1 mmol, 29 mg) were dissolved in DCM (5 mL), CuI (0.009 mmol, 1.65 mg), acetic acid (0.17 mmol, 12.88 mg), and diisopropylethylamine (0.17 mmol, 22.48 mg) were added at the same time and the reaction mixture were left stirring for 6 h. At the end of the reaction (TLC monitoring), the reaction mixture was concentrated under vacuum and purified by flash chromatography using a hexane/ethyl acetate mixture (6:4) to give compound **23** as a white solid. Yield 58 mg (90%). ¹H-NMR (CDCl₃): δ = 7.81–7.71 (m, 5H,

phthalimido and triazole), 6.79 (d, $J = 9.9$ Hz, 1H, H-1), 6.03 (dd, $J_1 = 10.2$ Hz, $J_2 = 9.6$ Hz, 1H, H-3), 5.34 (dd, $J_1 = J_2 = 9.6$ Hz, 1H, H-4), 4.85 (dd, $J_1 = 9.9$ Hz, $J_2 = 10.2$ Hz, 1H, H-2), 4.55 (s, 2H, $-\underline{\text{CH}_2}-\text{O}-\text{CH}_2$), 4.37 (m, 1H, H-5), 4.26–4.05 (m, 2H, H-6), 3.42 (t, $J = 6.7$ Hz, 2H), 2.14 (s, 3H, acetate- CH_3), 2.05 (s, 3H, acetate- CH_3), 2.01 (s, 3H, acetate- CH_3), 1.45–1.55 (m, 2H, $\text{CH}_2-(\text{CH}_2)_{13}$), 1.25 (brs, 26 H, $-(\text{CH}_2)_{13}$), 0.88 (t, $J = 6.6$ Hz, 3H, $-(\text{CH}_2)_{13}-\text{CH}_3$). $^{13}\text{C-NMR}$ (CDCl_3) δ 171.18, 170.59, 169.91, 169.43, 146.16, 134.56, 123.90, 120.75, 83.03, 77.50, 77.28, 77.08, 76.65, 75.05, 73.58, 70.96, 70.47, 68.24, 64.05, 61.69, 60.40, 54.03, 31.92, 29.69, 29.65, 29.59, 29.49, 29.35, 26.07, 22.68, 21.03, 20.71, 20.66, 20.58, 20.34, 14.19, 14.11. ESMS: calcd for $\text{C}_{39}\text{H}_{56}\text{N}_4\text{O}_{10}\text{Na}^+$ m/z : 763.4, found m/z $[\text{M}+\text{Na}]^+$ 763.7.

4-(Hexadecyloxy)methyl-1-(2'-deoxy-2'-amino- β -D-glucopyranosyl)-1,2,3-triazole (5).

Compound **23** (58 mg) was dissolved in mixture of butanol (2 mL) and ethylenediamine (2 mL). The resulting mixture was heated to 90 °C and stirred for 3 h. The reaction was monitored by TLC. The solution was concentrated to dryness. The resulting residue was purified by flash gradient chromatography (reverse-phase C18 silica gel, 100 water to 100 methanol) to give compound **5** as a white solid in a yield 22 mg (60%). $^1\text{H-NMR}$ (CD_3OD) δ = 8.21 (s, 1H, triazole H), 5.60 (d, $J = 9.2$ Hz, 1H, H-1), 3.91 (dd, $J = 12.2, 12.1$ Hz, 1H H-3), 3.74 (dd, $J = 12.2, 5.0$ Hz, 1H, H-4), 3.67–3.25 (m, 8H), 1.69–1.53 (m, 2H, $-\text{CH}_2-(\text{CH}_2)_{13}$), 1.32 (brs, 26H, $-(\text{CH}_2)_{13}$), 0.93 (t, $J = 6.9$ Hz, 3H, $-\text{CH}_3$). $^{13}\text{C-NMR}$ (CD_3OD) δ = 124.58 (triazole-CH), 81.27 ($-\text{C}1$), 71.85, 64.63, 62.43, 49.89, 49.60, 49.32, 49.04, 48.75, 48.47, 48.19, 33.09, 30.79, 30.75, 30.62, 30.48, 27.24, 23.75, 14.47. ES-HRMS: calcd for $\text{C}_{25}\text{H}_{48}\text{N}_4\text{O}_5\text{Na}^+$ m/z 507.3517: found: m/z $[\text{M}+\text{Na}]^+$ 507.3532.

4.5.3 General Procedure for the Synthesis of Diglycosylated Compounds 6 and 7

Compounds **6** and **7** were synthesized by diglycosylation of commercially available lipids **25** and racemic alcohol **26**, respectively. The previously reported thioglycoside donor **24** was synthesized from compound **9** and thiophenol using $\text{BF}_3 \cdot \text{Et}_2\text{O}$ as promoter in DCM at 60 °C for 16 h. The glycosylation reaction was carried out using silver triflate and *N*-Iodosuccinimide in anhydrous DCM under argon atmosphere for 5 h. The reaction was stopped by addition of saturated sodium thiosulphate solution followed by washing with saturated NaHCO_3 solution ($\times 3$). The organic layer was concentrated under vacuum to give a brownish residue which was purified with flash chromatography using hexane/ethyl acetate mixture (6:4) to give protected diglycosylated glycolipids **27** and **28** as a white foam (yield 45%). Compounds **27** and **28** were subsequently deprotected using a 1:1 mixture of ethylenediamine and butanol for 4 h, followed by removal of solvent under vacuum and purified with Ethyl acetate/methanol mixture (7:3) to give compounds **6** and **7**, respectively (yield 70%).

3-Hexadecyloxy-1,2R-di(3,4,6-tri-O-acetyl-2'-deoxy-2'-N-phthalimido- β -D-glucopyranosyl)-sn-glycerol (27).

$^1\text{H-NMR}$ (CDCl_3) δ = 7.93–7.71 (m, 8H, phthalimido), 5.75–5.62 (m, 2H), 5.53 (d, J = 8.5 Hz, 1H), 5.17 (d, J = 8.7 Hz, 1H), 5.14–5.00 (m, 2H), 4.41–4.38 (m, 2H), 4.26–4.09 (m, 3H), 3.91–3.83 (m, 1H), 3.82–3.66 (m, 4H), 3.50–3.33 (m, 2H), 3.09–3.15 (m, 3H), 2.17 (s, 3H), 2.12 (s, 3H), 1.95 (d, J = 2.8 Hz, 6H, acetate- CH_3), 1.91 (d, J = 2.8 Hz, 6H, acetate- CH_3), 1.64 (m, 2H), 1.43–1.05 (brs, 26H, $-(\text{CH}_2)_{13}$), 0.88 (t, J = 6.6 Hz, 3H). $^{13}\text{C-NMR}$ (CDCl_3) δ = 171.22, 170.27, 169.74, 168.66, 165.86, 134.16, 123.51, 123.49, 98.76, 96.97, 77.56, 76.71, 71.64, 71.61, 70.66,

70.47, 69.89, 69.16, 68.91, 62.18, 54.61, 54.40, 37.02, 31.94, 29.72, 29.51, 29.38, 25.98, 22.70, 22.70, 20.80, 14.13. ESMS: Calcd for $C_{59}H_{78}N_2O_{21}Na^+$ m/z 1173.5, found m/z $[M+Na]^+$ 1173.6.

3-Hexadecyloxy-1,2S/R-di(3,4,6-triacetyl-2'-deoxy-2'-N-phthalimido-β-D-glucopyranosyl)-sn-glycerol (28).

The NMR data of compound **28** shown here are for the 2R and 2S 1:1 diastereomeric mixture and the four anomeric protons were identified and labeled accordingly. 1H -NMR ($CDCl_3$) characteristic data: δ = 7.90–7.68 (m, 16H aromatic protons), 5.76–5.63 (m, 2H, H-3 (sugar 1), H-3 (sugar 2), 5.53 (d, J = 8.5 Hz, 1H, H-1 (sugar 1-2R-isomer), 5.39 (d, J = 8.5 Hz, 1H, H-1 (sugar 1 2S isomer), 5.33 (d, J = 8.3 Hz, 1H, H-1 (sugar 2-2S isomer), 5.17 (d, J = 8.7 Hz, 1H, H-1 (sugar 2-2R-isomer), 1.43–1.05 (brs, 52H, $-(CH_2)_{13}$), 0.85 (t, J = 6.6 Hz, 6H). ^{13}C -NMR ($CDCl_3$) characteristic data: δ = 170.72, 170.05, 169.55, 167.80, 134.25, 131.47, 123.70, 123.41, 98.77, 98.36, 78.65, 71.76, 71.64, 71.37, 70.76, 70.71, 69.90, 69.17, 69.00, 68.91, 62.19, 62.02, 54.63, 54.42, 31.95, 29.63, 29.38, 28.94, 22.71, 20.80, 14.13. ESMS: Calcd for $C_{59}H_{78}N_2O_{21}Na^+$ m/z 1173.5, found m/z $[M+Na]^+$ 1173.5.

3-Hexadecyloxy-1,2S/R-di(-2'-deoxy-2'-amino-β-D-glucopyranosyl)-glycerol (6).

1H -NMR (CD_3OD) characteristic data for the diastereomeric mixture: δ 4.83–4.73 (m, 2H, H-1 (sugar 1, 2R/2S), 4.71–4.57 (m, 2H, H-1 (sugar 2, 2R/2S), 1.59 (m, 4H, $-CH_2-(CH)_{13}$), 1.32 (brs, 52H, $(CH_2)_{13}$), 0.93 (2xt, 6H, $-CH_3$). ^{13}C -NMR (MeOD) δ 102.75, 102.01, 101.47, 100.89 (anomeric carbons) 78.82, 78.75, 78.69, 78.53, 78.12, 75.45, 75.16, 74.95, 73.18, 72.18, 72.14, 71.85, 69.97, 62.80, 62.71, 62.12, 61.93, 58.33, 58.16, 50.24, 49.67, 34.98, 34.86, 33.45, 31.16, 31.14, 31.06, 31.02, 30.84, 27.57, 24.65, 24.11, 19.13, 14.82. ES-HRMS: calcd for $C_{31}H_{62}N_2O_{11}Na^+$ m/z 661.4246, found: m/z $[M+Na]^+$ 661.4241.

3-Hexadecyloxy-1,2R-di(-2'-deoxy-2'-amino-β-D-glucopyranosyl)-sn-glycerol (7).

¹H-NMR (methanol-*d*₄) δ = 4.78 (dd, *J* = 8.3, 7.9 Hz, 1H, H-1a), 4.68 (dd, *J* = 8.3 Hz, 7.8 Hz, 1H, H-1b) 4.27–4.19 (m, 1H), 4.09–3.90 (m, 4H), 3.85–3.62 (m, 4H), 3.62–3.45 (m, 4H), 3.45–3.25 (m, 4H), 2.98–2.79 (m, 2H, H-2a, H-2b), 1.66–1.53 (m, 2H, –CH₂–CH₂–(CH₂)₁₃), 1.32 (brs, 26H, –(CH₂)₁₃–), 0.93 (t, *J* = 6.8 Hz, 3H, –CH₃). ¹³C-NMR (CD₃OD) δ = 101.92, 100.38, 78.17, 77.74, 74.40, 71.83, 71.69, 71.35, 71.24, 69.52, 67.17, 62.37, 57.95, 57.71, 35.99, 33.08, 30.80, 27.19, 23.74, 14.44. ES-HRMS: calcd for C₃₁H₆₂N₂O₁₁Na⁺ *m/z* 661.4246, found: *m/z* [M+Na]⁺ 661.4222.

4.6 Biological Activity

4.6.1 Cell Culture

Breast (BT474, MDA-MB-231), prostate (DU 145, PC3), pancreas (MiaPaCa2) cell lines were grown from frozen stocks of cells that were originally obtained from ATCC (Manassas, VA, USA). JIMT-1 breast cancer cells were originally obtained from DSMZ (Braunschweig, Germany). JIMT1, DU145 cells were grown in Dulbecco's modified Eagle's medium (DMEM), PC3 cells were grown in F12K medium. The cells were grown in media supplemented with 10% fetal bovine serum (FBS), penicillin (100 U/mL) and streptomycin (0.1 mg/mL)

4.6.2 Cytotoxicity Assay

The cytotoxicity assay was carried out using a previously reported method [22]. Cell viability was determined with the cell Titre 96 AQueous One Solution (MTS assay, Promega, Madison, WI. Equal numbers of cancer cells (7500–9500) in media (100 μL) were dispersed into 96-well plates. As blanks, media without cells (100 μL) were also placed in some wells and treated similarly to the cell containing wells. After an incubation period of 24 h, a solution of test

compound ((100 μ L) in medium at twice the desired concentration was added to each well. The treated cells were incubated for a further 48 h, after which time methanethiosulfonate (MTS) reagent (20%^V/_V) was added to each well. The plates were incubated for 1–4 h on a Nutating mixer in a 5% CO₂ incubator, and then the optical density (OD) was read at 490 nm by using a SpectraMax M2 plate reader (Molecular Devices Corp., Sunnyvale, CA, USA). The blank values were subtracted from each value, and the viability values of the treated samples relative to controls with vehicle were calculated. The values for the plots are the means \pm standard deviation of six different wells.

4.7 Conclusions

Six novel cationic GAEL analogs were synthesized to explore novel SAR in this class of compounds. We were especially interested to explore how changes in the nature of the anomeric linkage, the nature of the hydrophobic lipid tail and the stereochemistry of the glycerol moiety affects the cytotoxic properties against breast, pancreas and prostate cancer cell lines. During our study, we discovered that replacement of the *O*-glycosidic linkage of lead compound **1** with an *N*-glycosidic linkage or a triazole linkage resulted in significant loss of anticancer activity against all six cancer cell lines tested. Moreover, replacement of the hydrophobic lipid tail by a fluorinated tail as well as replacement of the methoxy substituent by a second glucosamine moiety resulted in decreased cytotoxic activity.

4.8 Acknowledgements

This study was supported by the Natural Science and Engineering Research Council of Canada (NSERC) to FS and the Canadian Breast Cancer Foundation Prairie/Northwest Territories (NMT) to GA. Makanjuola Ogunsina is grateful to University of Manitoba and Manitoba Provincial

Government for graduate scholarships, UMGF (University of Manitoba Graduate Fellowship) and MGS (Manitoba Graduate Scholarship), respectively.

4.9 References

- (1) Canadian-Cancer-Statistics-2015-EN.pdf
[https://www.cancer.ca/~media/cancer.ca/CW/cancer information/cancer 101/Canadian cancer statistics/Canadian-Cancer-Statistics-2015-EN.pdf](https://www.cancer.ca/~media/cancer.ca/CW/cancer%20information/cancer%20101/Canadian%20cancer%20statistics/Canadian-Cancer-Statistics-2015-EN.pdf) (accessed Jan 2, 2016).
- (2) World Health Organization. Fact Sheet 2007, N° 310; WHO Media Centre, 2007
<http://www.who.int/mediacentre/factsheets/fs310.pdf> (accessed Jan 2, 2016).
- (3) Tan, D. S.-W.; Gerlinger, M.; Teh, B.-T.; Swanton, C. Anti-Cancer Drug Resistance: Understanding the Mechanisms through the Use of Integrative Genomics and Functional RNA Interference. *Eur. J. Cancer* **2010**, *46* (12), 2166–2177.
- (4) Tanner, M.; Kapanen, A. I.; Junttila, T.; Raheem, O.; Grenman, S.; Elo, J.; Elenius, K.; Isola, J. Characterization of a Novel Cell Line Established from a Patient with Herceptin-Resistant Breast Cancer. *Mol. Cancer Ther.* **2004**, *3* (12), 1585–1592.
- (5) Erukulla, R. K.; Zhou, X.; Samadder, P.; Arthur, G.; Bittman, R. Synthesis and Evaluation of the Antiproliferative Effects of 1-O-Hexadecyl-2-O-Methyl-3-O-(2'-acetamido-2'-deoxy-Beta-D- Glucopyranosyl)-*Sn*-Glycerol and 1-O-Hexadecyl-2-O-Methyl-3-O- (2'-amino-2'-deoxy-Beta-D-Glucopyranosyl)-*Sn*-Glycerol on Epithelial Canc. *J. Med. Chem.* **1996**, *39* (7), 1545–1548.
- (6) Samadder, P.; Bittman, R.; Byun, H.-S.; Arthur, G. A Glycosylated Antitumor Ether Lipid

- Kills Cells via Paraptosis-like Cell Death. *Biochem. Cell Biol.* **2009**, *87* (2), 401–414.
- (7) Samadder, P.; Byun, H.-S.; Bittman, R.; Arthur, G. An Active Endocytosis Pathway Is Required for the Cytotoxic Effects of Glycosylated Antitumor Ether Lipids. *Anticancer Res* **2011**, *31* (11), 3809–3818.
- (8) Samadder, P.; Byun, H.-S.; Bittman, R.; Arthur, G. An Active Endocytosis Pathway Is Required for the Cytotoxic Effects of Glycosylated Antitumor Ether Lipids.
- (9) Arthur, Gilbert; Samadder, P. *Tolerability of Rag2M Mice to 1-O-Hexadecyl-2-O-Methyl-3-O-(2'-amino-2'-deoxy- β -D-Glucopyranosyl)-Sn-Glycerol (Unpublished)*; Winnipeg, 2012.
- (10) Yang, G.; Franck, R. W.; Bittman, R.; Samadder, P.; Arthur, G. Synthesis and Growth Inhibitory Properties of Glucosamine-Derived Glycerolipids. *Org. Lett.* **2001**, *3* (2), 197–200.
- (11) Rempel, B. P.; Withers, S. G. Covalent Inhibitors of Glycosidases and Their Applications in Biochemistry and Biology. *Glycobiology* **2008**, *18* (8), 570–586.
- (12) Guo, W.; Hiratake, J.; Ogawa, K.; Yamamoto, M.; Ma, S. J.; Sakata, K. Beta-D-Glycosylamidines: Potent, Selective, and Easily Accessible 1-Glycosidase Inhibitors. *Bioorg. Med. Chem. Lett.* **2001**, *11* (4), 467–470.
- (13) Spevak, W.; Tropper, F. D. β -Glycosylamide Glycopolymers: Synthesis, Physical Properties, Chemical and Enzymatic Stability. *MRS Proc.* **2011**, *394*, 187.
- (14) Fjelde, A.; Sorkin, E.; Rhodes, J. M. The Effect of Glucosamine on Human Epidermoid

- Carcinoma Cells in Tissue Culture. *Exp. Cell Res.* **1956**, *10* (1), 88–98.
- (15) Jung, C.-W.; Jo, J.-R.; Lee, S.-H.; Park, Y.-K.; Jung, N.-K.; Song, D.-K.; Bae, J.; Nam, K.-Y.; Ha, J.-S.; Park, I.-S.; Park, G.-Y.; Jang, B.-C.; Park, J.-W. Anti-Cancer Properties of Glucosamine-Hydrochloride in YD-8 Human Oral Cancer Cells: Induction of the Caspase-Dependent Apoptosis and down-Regulation of HIF-1 α . *Toxicol. In Vitro* **2012**, *26* (1), 42–50.
- (16) Adibekian, A.; Martin, B. R.; Wang, C.; Hsu, K.-L.; Bachovchin, D. A.; Niessen, S.; Hoover, H.; Cravatt, B. F. Click-Generated Triazole Ureas as Ultrapotent in Vivo-Active Serine Hydrolase Inhibitors. *Nat. Chem. Biol.* **2011**, *7* (7), 469–478.
- (17) Salunke, S. B.; Babu, N. S.; Chen, C.-T. Iron(III) Chloride as an Efficient Catalyst for Stereoselective Synthesis of Glycosyl Azides and a Cocatalyst with Cu(0) for the Subsequent Click Chemistry. *Chem. Commun. (Camb)*. **2011**, *47* (37), 10440–10442.
- (18) Ibatullin, F. M.; Selivanov, S. I. Reaction of 1,2-Trans-Glycosyl Acetates with Phosphorus Pentachloride: New Efficient Approach to 1,2-Trans-Glycosyl Chlorides. *Tetrahedron Lett.* **2002**, *43* (52), 9577–9580.
- (19) Bowden, K.; Heilbron, I. M.; Jones, E. R. H.; Weedon, B. C. L. 13. Researches on Acetylenic Compounds. Part I. The Preparation of Acetylenic Ketones by Oxidation of Acetylenic Carbinols and Glycols. *J. Chem. Soc.* **1946**, 39.
- (20) Bera, S.; Dhondikubeer, R.; Findlay, B.; Zhanel, G. G.; Schweizer, F. Synthesis and Antibacterial Activities of Amphiphilic Neomycin B-Based Bilipid Conjugates and Fluorinated Neomycin B-Based Lipids. *Molecules* **2012**, *17* (8), 9129–9141.

- (21) Paul, K. J. V.; Loganathan, D. Synthesis of Novel Glycolipids Derived from Glycopyranosyl Azides and N-(β -Glycopyranosyl)azidoacetamides. *Tetrahedron Lett.* **2008**, 49 (44), 6356–6359.
- (22) Xu, Y.; Ogunsina, M.; Samadder, P.; Arthur, G.; Schweizer, F. Structure-Activity Relationships of Glucosamine-Derived Glycerolipids: The Role of the Anomeric Linkage, the Cationic Charge and the Glycero Moiety on the Antitumor Activity. *ChemMedChem* **2013**, 8 (3), 511–520.
- (23) Tanner, M.; Kapanen, A. I.; Junttila, T.; Raheem, O.; Grenman, S.; Elo, J.; Elenius, K.; Isola, J. Characterization of a Novel Cell Line Established from a Patient with Herceptin-Resistant Breast Cancer. *Mol. Cancer Ther.* **2004**, 3 (12), 1585–1592.

Chapter 5

Design, Synthesis and Evaluation of Glucosylated Antitumor Ether Lipids Bearing Two Amino Groups as Cytotoxic Agents Against Epithelial Cancer Cells, Breast and Prostate Cancer Stem Cells

By Makanjuola Ogunsina, Pranati Samadder, Gilbert Arthur and Frank Schweizer

Submitted to MedChemComm

5.1. Authorship considerations

Makanjuola Ogunsina was responsible for design, synthesis, purification and characterization of all glycolipids on the advice of Frank Schweizer. Biological activity was investigated by Makanjuola Ogunsina and Pranati Samadder on the advice of Gilbert Arthur. The preliminary draft of the paper was written by Makanjuola Ogunsina reviewed by Frank Schweizer and Gilbert Arthur, and then rendered into its final form by Makanjuola Ogunsina. Frank Schweizer and Gilbert Arthur are corresponding authors.

5.2. Abstract

Glycosylated Antitumor Ether Lipids (GAELs) are a class of amphiphilic antitumor agents that kill cancer cells by a non-apoptotic pathway. Previous studies have shown that 2-amino-2-deoxy-D-*gluco*-based GAELs such as α -GLN and β -GLN show greatly improved antitumor activity against epithelial cancer cells when compared to GAELs devoid of an amino group. Moreover, α -GLN and β -GLN displayed potent cytotoxic effects against breast cancer stem cells, inhibited the formation of tumorspheres and caused the disintegration of preformed tumorspheres from BT474

cancer stem cell lines. To further optimize the bioactivity, we prepared a series of diamino-D-*gluco*-based GAELs and their analogs and screened them against a panel of human epithelial cancer cell lines and cancer stem cells. Most of the new GAEL analogs are more potent than chlorambucil, cisplatin and salinomycin. The most potent bisamine-based GAEL analogs **1**, **2**, **4** and **8** analogs showed 2- to 3-fold enhanced cytotoxicity against various cancer cell lines when compared to β -GLN indicating that the addition of a second amino group enhances the cytotoxic effect. The effect of the most active dicationic GAELs **1** and **4** on cancer stem cell isolated from breast (BT474) and prostate (DU145) revealed that the two GAELs inhibited the formation of tumorspheres and resulted in > 95% loss of viability of the cancer stem cells at 5 μ M. Activity of GAEL **1** against BT-474 cancer stem cells is superior to that of salinomycin. Compound **1** is currently the most potent GAEL against epithelial cancer cell lines and their respective cancer stem cells.

5.3. Introduction

Cancer remains a major health problem worldwide despite the huge investment to find effective treatments for the disease. A recent UN report projects that global cancer cases will rise from 14 million to 22 million per year within the next two decades, with annual cancer deaths rising from 8.2 million to 13 million.¹ The major problems impeding the development of cures for cancer are resistance to drugs, resistance to radiotherapy and metastasis. Many of the existing anticancer drugs act by disrupting cell DNA, preventing DNA synthesis and/or targeting microtubules, while radiotherapy kills cells by damaging DNA. The cellular perturbation caused by these treatments induces apoptosis which kills the cancer cells. While many drugs are initially successful in killing the cancer cells resulting in tumor shrinkage, there is invariably a relapse and the tumor reappears with cells that resist existing chemotherapeutic agents,^{2,3,4,5} so the tumors are

refractory to treatment leading to metastases and death. There are also very few drugs, if any, for treatment of metastasized cancer.

There is increasing evidence that the relapse of tumors and development of drug and radiation resistant tumors as well as progression to metastases may be due to the presence of a small population of cells in the tumor called cancer stem cells (CSCs) or tumor initiating cells. CSCs are distinct from the cells of the bulk tumor in having the capacity for self-renewal, asymmetric division and differentiation. CSCs have been identified and isolated from virtually all solid and hematological tumors.^{6,7} These cells resist apoptotic cell death induced by chemotherapy and radiotherapy, and may ultimately generate drug resistant differentiated cells of the recurrent bulk tumor.^{6,7} In light of the potential role these cells play in tumor relapse, drug resistance and metastases, effective cancer treatment will require targeting the CSCs along with the bulk differentiated cells of the tumor.

Only a few compounds that kill CSCs have been identified. They include parthenolide, salinomycin, metformin, lapatinib, and mitoVES.⁷ The mechanisms via which they achieve this are not known but salinomycin, parthenolide and the biguanide metformin, induce apoptosis in various human cancer cells.⁸⁻¹² The potential of the ionophore antibiotic salinomycin is reinforced by its ability to kill highly multidrug- and apoptosis-resistant cancer cells¹¹⁻¹³ and CSCs.^{11,15-17}

Antitumor ether lipids (AELs) are synthetic lipids that possess anticancer activity and comprise three subclasses; the alkyllysophospholipid (ALP), alkylphosphocholine (APC) and the non-phosphorylated glycosylated antitumor ether lipids (GAELs). The cytotoxic properties of GAELs, prototypified by α -GLN and β -GLN, have been established to be superior to the most studied AEL, edelfosine (Figure 5.1). Unlike ALPs and APCs, which kill cells by apoptosis, GAELs kill cells by an apoptotic independent mechanism.¹⁸⁻²¹ Though the mechanism of action of

GAELs is yet to be fully understood, it appears to involve the perturbation of the endocytosis pathway to generate large acidic vacuoles that ultimately leads to the release of acid hydrolases to induce cell death.¹⁹⁻²¹ This ability to kill cells by an apoptosis-independent pathway led to the postulation that GAELs could kill CSCs because their mode of action will not be impacted by the strategies cells use to prevent death by apoptosis. Recently this hypothesis was validated by the demonstration that a number of GAELs were cytotoxic against CSCs isolated from BT-474 cell lines.²²

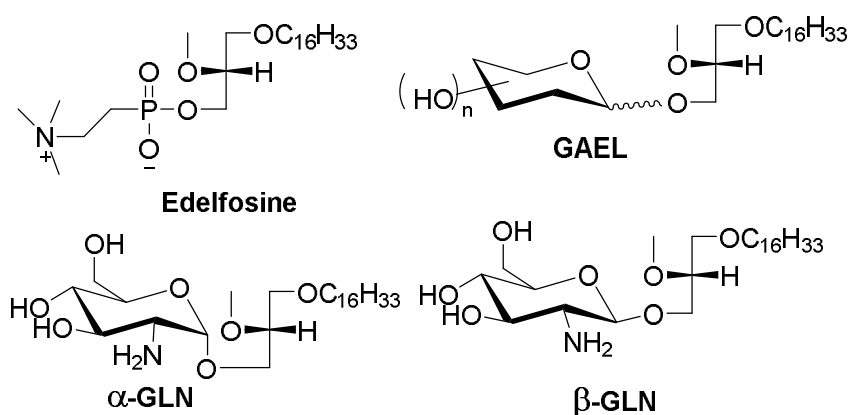


Figure 5.1. Structures of various glycosylated antitumor ether lipids (GAELs) and edelfosine, an antitumor ether lipid (AEL) of the ALP subclass.

Our ongoing structure activity studies on GAELs have led to the observation that the anticancer potency of GAELs is intimately linked to their cationic nature. Our previously identified leads α -GLN and β -GLN contain a 2-amino group in the *gluco*-portion of the glycolipid (Figure 5.1). Replacement of the 2-amino substituent by a neutral hydroxyl- or azido group as well as replacement by a guanidino, and secondary amine-based substituents including benzyl amine-substituted groups resulted in more than 3-fold reduced activity against various cancer cell lines.^{23,24} The observation that primary amine-based GAELs are significantly more potent than

their nonamine-based counterparts raised the question whether introduction of a second primary amino group in GAELs could further enhance the antitumor properties. We disclose here our structure activity study on diamine-based as well as *N*-substituted *gluco*-based GAEL analogs **1-10** (Figure 5.2).

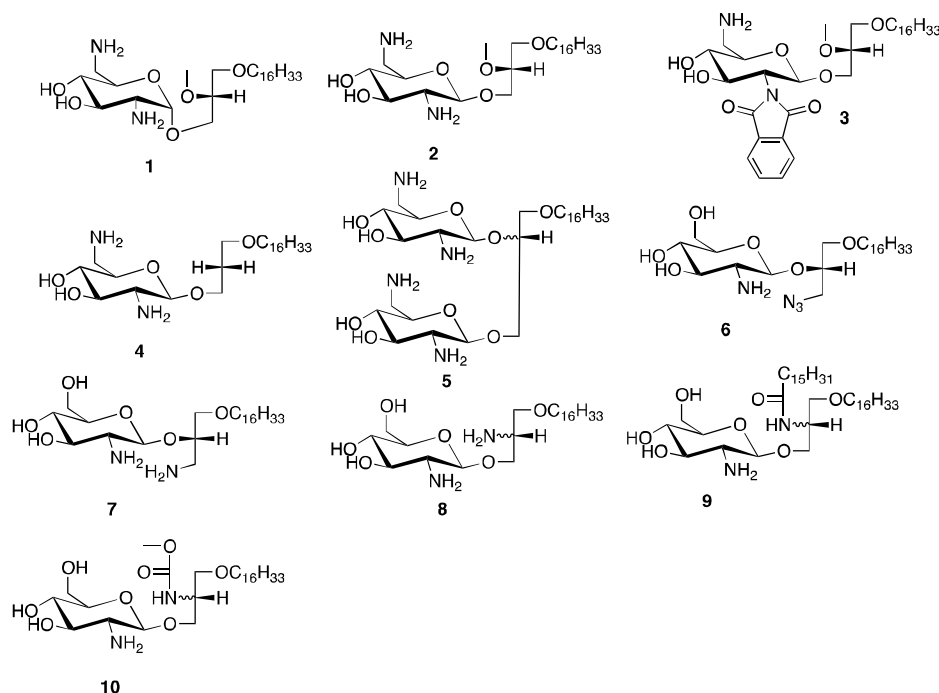


Figure 5.2. Structures of diamine-based and *N*-substituted glucosylated antitumor ether lipids (GAELs) used in this study.

5.4. Results

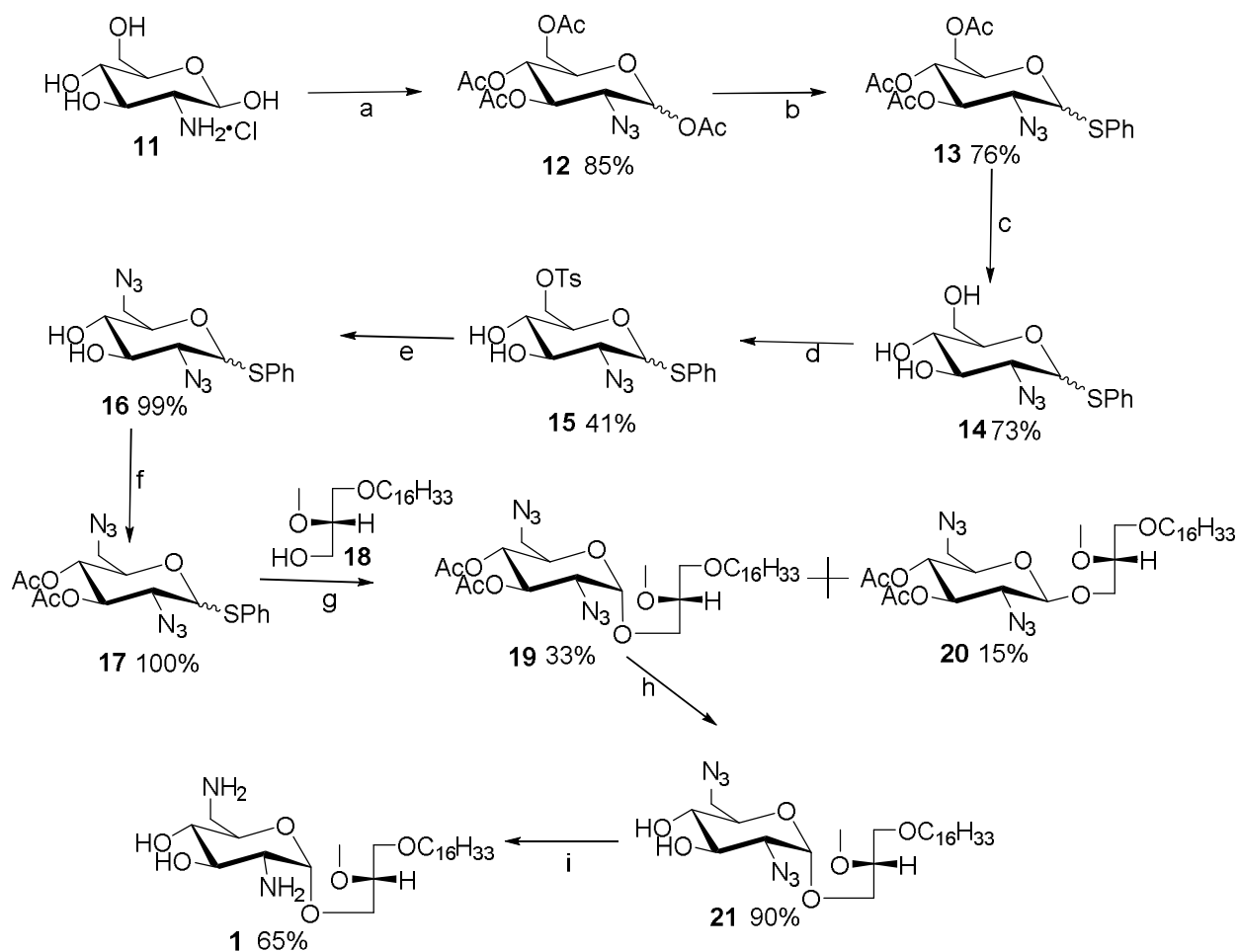
5.4.1 Chemistry

To study the effects of diamino and *N*-substituted GAELs, a second amino substituent was introduced at the C-6 position of glucose as shown in compounds **1** and **2** (Figure 5.2). Besides the presence of a second amino substituent, glycolipids **1** and **2** were also selected to study the nature of the glycosidic linkage on antitumor activity as previous reports had indicated that the anomeric

configuration can influence the antitumor potency in mono-amino GAELs.^{18,21,23} Compound **3** with a phthalimido group at the C-2 position of glucose was synthesized to study how the absence of a cationic charge at that position affects cytotoxicity. In addition, the phthalimido group was selected as some compounds bearing this group exhibits significant cytotoxicity against both human and murine cancer cell lines.^{25,26} Compounds **4** and **5** were synthesized to explore the effect of the methoxy substituent at the *sn*-2 position of the glycerol moiety. Previous studies on *gluco*-based GAELs had shown that the nature of the methoxy substituent is not critical for antitumor activity and can be replaced by hydrogen.²³ Another reason for synthesizing tetraamine-containing bisglycolipid **5** was based on the hypothesis that replacement of the methoxy substituent by an additional 2,6-diamino- β -D-glucose moiety may lead to enhanced antitumor activity as seen for other polyamine structures.²⁷ Diamino glycolipids **7-8** were synthesized to explore how the positioning of a second amino substituent on the glycerol moiety affects the antitumor properties. Azido compound **6** was also prepared to study how the position of amino substituent of a in **7** affects cytotoxicity. Compound **9** was synthesized to explore how the presence of two lipid tails and modification of the free amino substituent at the *sn*-2 position affect the biological properties of compound **8**. We also synthesized carbamate **10** to explore whether the presence of a methoxy carbamate substituent at the *sn*-2 position of the glycerolipid will induce prostate cancer selectivity based on previous findings.²⁸

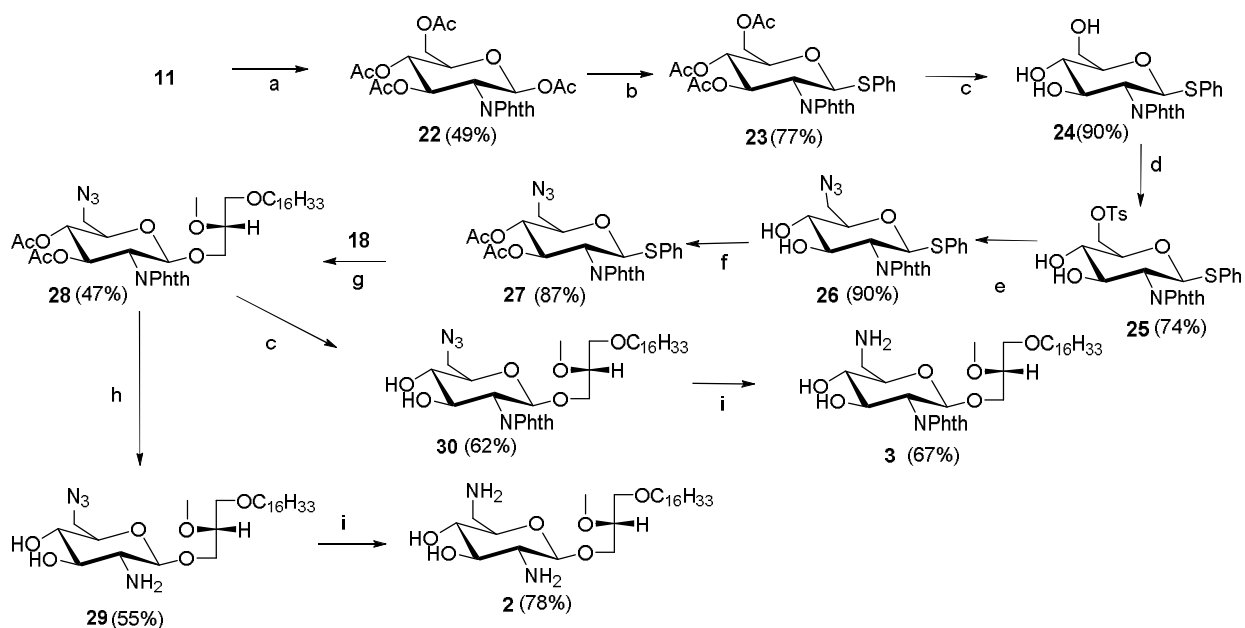
Compounds **5**, **8**, **9**, and **10** were studied as diastereomeric 1:1 mixture based on the stereochemistry at *sn*-2 position of the glycerolipid. We have previously reported that the stereochemistry at this position has little or no effect on anticancer activity.²⁴ Moreover, edelfosine (Figure 5.1) the most studied AEL is used as a racemic mixture.²⁹

Compound **1** was synthesized by coupling of glycoside donor **17** to the commercially available lipid alcohol **18** to afford a mixture of α - and β -glycolipid **19** and **20** in a 4:1 ratio, respectively (Scheme 5.1). The glycoside donor **17** was synthesized from glucosamine hydrochloride **11** in seven steps. At first, the amino substituent of glucosamine **11** was converted to azide **12** as previously reported.²³ Compound **12** was converted into thiophenyl glycoside **13** by borontrifluoride diethyl etherate-promoted glycosylation with thiophenol.²³ The azido function at the C-6-position was installed by selective activation of the C-6 hydroxyl group in **14** as sulphonate ester **15**, followed by nucleophilic displacement of the sulphonate group by sodium azide in DMF to afford the 2,6-diazido analog **16**. Protection of the remaining hydroxyl groups using acetic anhydride in pyridine produced the glycoside donor **17**. Donor **17** was used in glycosylation reaction with commercially available lipid alcohol **18** to produce a mixture of the glycolipids **19** and **20** in ratio 7:3. The α -glycolipid **19** was isolated in pure form and the ester groups were deprotected to afford the 2,6-diazido compound **21** which was subsequently subjected to azide reduction using trimethyl-phosphine in THF to produce the desired α -anomeric glycolipid **1** (Scheme 5.1).



Scheme 5.1. Synthesis of compound **1**. *Reagents and conditions:* (a) 1. TfN_3 , CuSO_4 , ETN_3 , H_2O , rt; 2 h 2. Ac_2O , DMAP, Pyridine, 18 h, rt (b) PhSH , $\text{BF}_3 \cdot \text{Et}_2\text{O}$, DMAP, DCM, 18, h, rt (c) MeONa , MeOH , 1 hr (d) TsCl , Pyridine, DMAP, 0°C - rt, 18 h (e) DMF , NaN_3 , 70°C 24 h (f) Ac_2O , DMAP, Pyridine, 18 h, rt (g) AgOTf , NIS, DCM, 3 h, rt (h) MeONa , MeOH , 30 minutes (i) $\text{P}(\text{CH}_3)_3$, THF, H_2O , 2 h, rt. Abbreviations: 4-Dimethylaminopyridine (DMAP), Dichloromethane (DCM), 2,2,*N,N*-dimethylformamide (DMF), room temperature 23°C (rt), *N*-iodosuccinimide (NIS), Triisopropyl benzyl sulphonate ester (OTIBs).

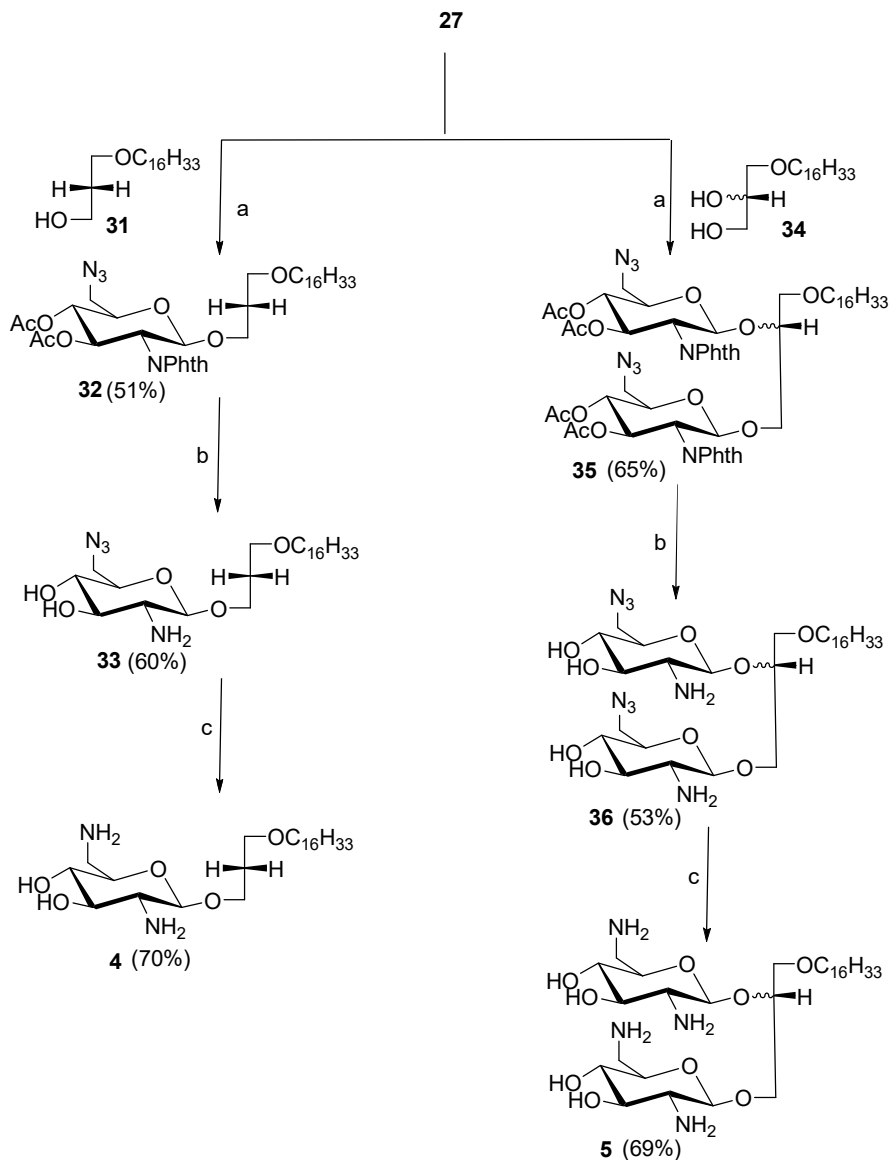
Glycolipids **2** and **3**, were prepared by coupling of lipid alcohol **18** to thioglycoside donor **27** (Scheme 5.2). Donor **27** was prepared from glucosamine hydrochloride **11** in seven steps. Compound **11** was initially converted into anomeric acetate **22** by exposure to phthalic anhydride followed by acylation with acetic anhydride in pyridine. Acetate **22** was converted into donor **27** using established methodologies. At first, acetate **22** was converted into protected thioglycoside donor **23**. Deblocking of the remaining acetate groups produced unprotected thioglycoside **24**. The azido group at C-6 was installed by selective activation of the 6-hydroxy group as sulphonate ester **25** followed by nucleophilic displacement with sodium azide in DMF to produce azido analog **26** which was acylated to afford the desired thioglycoside donor **27**. Donor **27** was coupled to lipid alcohol **18** to produce glycolipid **28**. Removal of the acetate- and phthalimido-based protecting groups was achieved by exposure to ethylenediamine in butanol (1:1) at elevated temperature to yield azide **29** which was reduced to the desired dicationic glycolipid **2**. To synthesize the target compound **3** the acetate protecting groups of compound **28** were selectively removed using catalytic amount of sodium methoxide in methanol to give 6-azido-2-phthalimido analog **30**. Reduction of the azido group using trimethylphosphine in THF and water (9:1) produced glycolipid **3** (Scheme 5.2).



Scheme 5.2. Synthesis of compounds **2** and **3**. *Reagents and conditions:* (a) 1. Phthalic anhydride, NaOH, H₂O, 18 h, rt; 2. Ac₂O, DMAP, Pyridine, 18 h, rt (b) PhSH, BF₃·Et₂O, DMAP, DCM, 18 h, rt (c) MeONa, MeOH, 20 minutes (d) TsCl, Pyridine, DMAP, 0°C - rt, 18 h (e) DMF, NaN₃, 70°C 24 h (f) Ac₂O, DMAP, Pyridine, 18 h, rt (g) AgOTf, NIS, DCM, 3 h, rt (h) Ethylenediamine/butanol (1:1), 90°C 2 h, rt (i) P(CH₃)₃, THF, H₂O, 2 h, rt. Abbreviations: 4-Dimethylaminopyridine (DMAP), Dichloromethane (DCM), 2,2, *N,N*-dimethylformamide (DMF), room temperature 23°C (rt), *N*-iodosuccinimide (NIS).

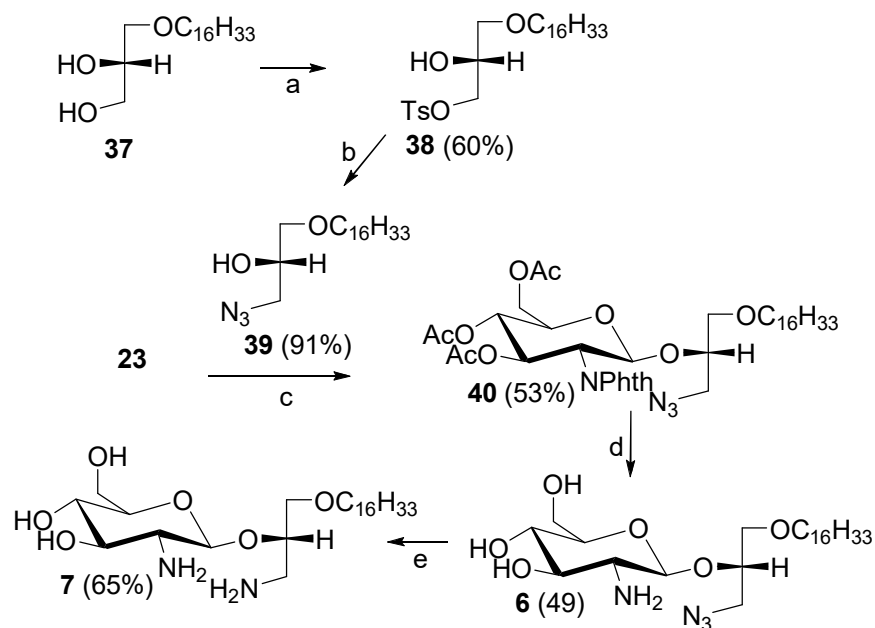
To synthesize compound **4**, the glycoside donor **27** was glycosylated to the known lipid alcohol **31**²³ to produce glycolipid **32** (Scheme 5.3). Deblocking of the acetate and phthalimido protecting groups produced azide **33** which was reduced to the desired diamine-based glycolipid **4**. Target molecule **5** was synthesized by glycosylating commercially available lipophilic diol **34** to thioglycoside donor **27** to afford protected diglycosylated lipid **35**. Deblocking of diglycosylated

lipid produced bisazido compound **36** which was subsequently reduced to produce tetraamine-based glycolipid **5** (Scheme 5.3).



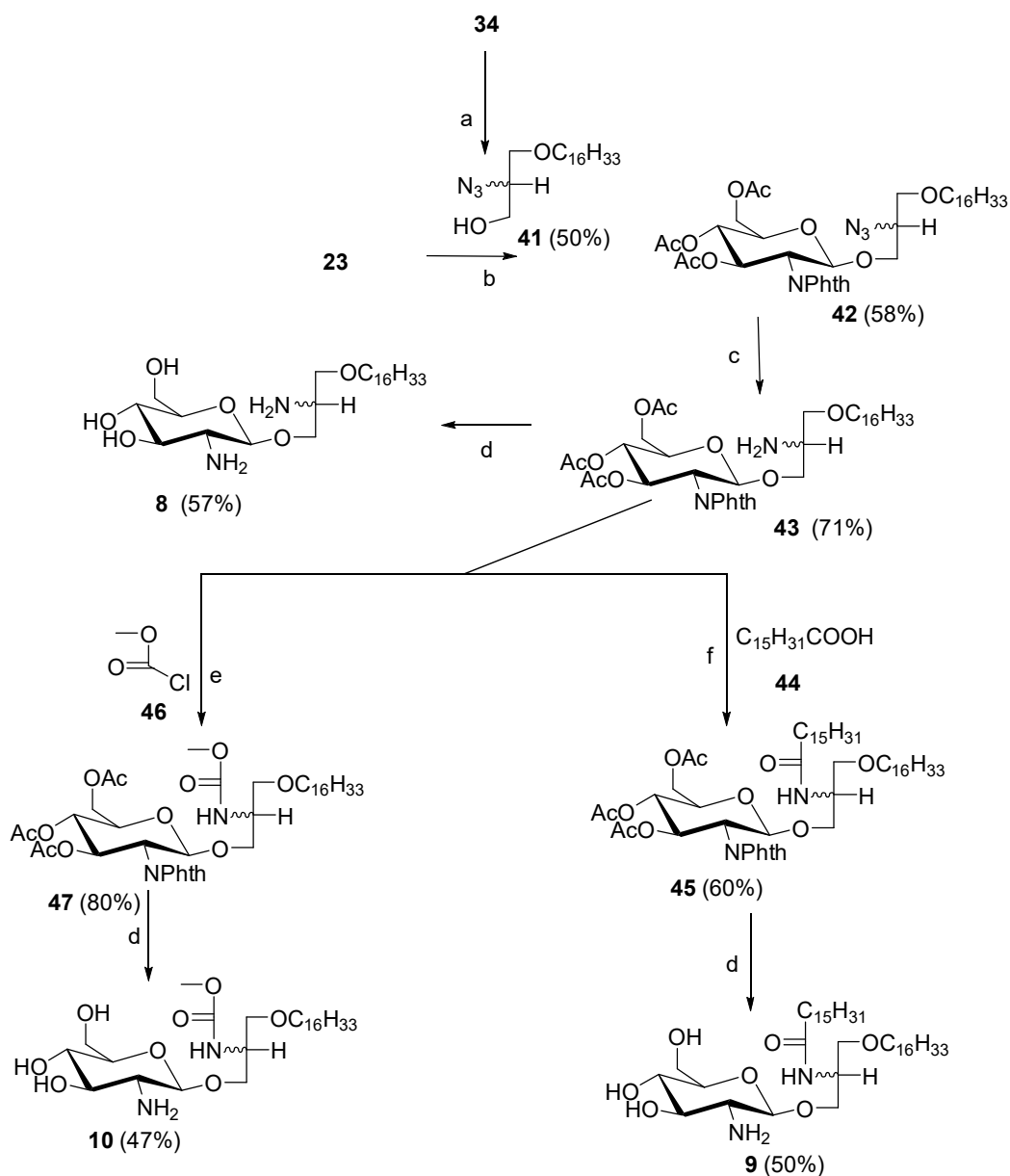
Scheme 5.3. Synthesis of compounds **4** and **5**. *Reagents and conditions:* (a) AgOTf, NIS, DCM, 3 h, rt (b) Ethylenediamine/butanol (1:1), 90°C 2 h, rt (c) P(CH₃)₃, THF, H₂O, 2 h, rt. Abbreviations: 4-Dimethylaminopyridine (DMAP), Dichloromethane (DCM), 2,2,*N,N*-dimethylformamide (DMF), room temperature 23°C (rt), *N*-iodosuccinimide (NIS)

Compounds **6** and **7** were synthesized as outlined in Scheme 5.4. Azido lipid alcohol **39** was synthesized from commercially available lipophilic diol **37** in two synthetic steps. At first the primary hydroxyl group in diol **37** was selectively activated as sulphonate ester **38** followed by nucleophilic displacement using sodium azide in DMF to produce azido acceptor **39**. The glycoside donor **23** was glycosylated with acceptor **39** to afford the protected glycolipid **40**. The acetate and phthalimido protective groups of **40** were removed with ethylenediamine in butanol (1:1) at 90°C for 2 h to give the desired compound **6**. The azido substituent of **6** was reduced as described above to afford the diamino analog **7** (Scheme 5.4).



Scheme 5.4. Synthesis of compounds **6** and **7**. *Reagents and conditions:* (a) TsCl, Pyridine, DMAP, 0°C - rt, 18 h (b) DMF, NaN₃, 70°C, 24 h (c) AgOTf, NIS, DCM, 3 h, rt (d) Ethylenediamine/butanol (1:1), 90°C 2 h, rt (e) P(CH₃)₃, THF, H₂O, 2 h, rt. Abbreviations: 4-Dimethylaminopyridine (DMAP), Dichloromethane (DCM), 2,2,*N,N*-dimethylformamide (DMF), room temperature (rt), *N*-iodosuccinimide (NIS)

Bisamino glycolipid **8**, was synthesized according to Scheme 5.5. The lipid alcohol **41**, was synthesized from the commercially available lipid alcohol as previously reported¹⁶ and coupled to the glycoside donor **23** to afford the protected glycolipid **42** (Scheme 5.5). Reduction of the azido substituent in **42** gave compound **43** which was subsequently de-protected using ethylenediamine in butanol (1:1) at elevated temperature to yield dicationic glycolipid **8**. To synthesize glycolipid **9**, the amine **43** was coupled to palmitic acid **44** by condensation with TBTU³⁰ to give compound **45** which was de-protected to produce target glycolipid **9** (Scheme 5.5). Finally, compound **10** was synthesized by reaction of amine **43** with methyl chloroformate **46** to produce carbamate **47** which was subsequently deblocked to afford the desired carbamate-based glycolipid **10** (Scheme 5.5).¹⁸



Scheme 5.5. Synthesis of compounds **8-10**. *Reagents and conditions:* (a) DIAD, Ph_3P , Me_3SiN_3 , DCM, 8 h (b) AgOTf , NIS, DCM, 3 h, rt (c) $\text{P}(\text{CH}_3)_3$, THF, H_2O , 2 h, rt (d) Ethylenediamine/butanol (1:1), 90°C 2 h, rt. (e) Et_3N , ClCO_2Me , DCM, (f) TBTU, DIPEA, DMF, 3 h, rt. Abbreviations: 4-Dimethylaminopyridine (DMAP), Dichloromethane (DCM), 2,2,*N,N*-dimethylformamide (DMF), room temperature 23°C (rt), *N*-iodosuccinimide (NIS), Diisopropylethylamine (DIPEA), Diisopropylazodicarboxylate (DIAD).

5.4.2. Biological Studies

5.4.2.1. *In vitro* screening of GAEL activity against epithelial cancer cell lines

The cytotoxicity of compounds **1-10** was evaluated against exponentially growing epithelial cancer cell lines including BT-474, JIMT-1, MDA-MB-231 (breast), DU145, PC3 (prostate) and MiaPaCa2 (pancreas). Compounds were incubated with varying concentrations of **1-10** (0-30 μM) for 48 h followed by determination of cell viability using an MTS assay.²² The results of the viability studies are shown in Figure 5.2. Lead compound **β -GLN** the most studied GAEL to date, was selected as the reference compound for comparison. The CC_{50} values for all the compounds and the CC_{90} values for the most active analogs are summarized in Table 5.1. The most potent GAEL among the compounds tested against all six cell lines is dicationic glycolipid **1** with CC_{50} values of 3.0 to 7.5 μM while 90% loss of cell viability was observed at a concentration range 4.5-9.5 μM depending on cell lines. This compound bears two primary amino groups at positions 2 and 6 of the glucose moiety and contains an α -glucosidic linkage to the glycerolipid. The next most potent analog was the GAEL **2** which in contrast to GAEL **1** contains a β -glucosidic linkage. This compound was typically 1.5- to 3-fold less active than glycolipid **1** with CC_{50} values in the range of 4.2-11.5 μM (Table 5.1). This is consistent with our previous results in the monocationic GAEL series, which showed that **α -GLN** is consistently more active than its anomer **β -GLN**.^{22,23} Comparison of the β -dicationic analog **2** with β -monocationic analog **β -GLN** indicates that the dicationic GAEL is consistently more potent than its monocationic analog except against BT 474 cell lines. Compound **3** containing an uncharged phthalimido substituent at the C₂-position showed weak antitumor activity against all six cell lines ($\text{CC}_{50} \geq 15 \mu\text{M}$) indicating that

the primary amino group at the C₂ position is crucial for optimal antitumor activity. GAEL **4**, an analog of **2** without a methoxy substituent at the glycerol moiety displayed comparable activity to **2**. Statistical analysis indicated that there was no significant difference between the activity of **2** and **4** across all cell lines except for BT 474 cells. This suggested that the methoxy substituent is not essential for manifestation of antitumor activity in the β -anomeric dicationic glycolipids. This is consistent with previous SAR studies on monocationic, 2-amino-D-gluco-based GAEL which have demonstrated that the methoxy group is not crucial for antitumor activity.²² However, tetracationic glycolipid **5** which was generated by replacement of the methoxy substituent at the *sn*-2 position by a second 2,6-diamino- β -D-gluco residue had greatly reduced antitumor activity and was unable to achieve 50% loss of cell viability at the highest dose (30 μ M) tested. This may be the result of increased hydrophilicity leading to reduced cellular absorption.

Compounds **6-8** were synthesized primarily to determine the effect of the position of the sugar on the glycerolipid. The azido compound **6** has its CC₅₀ values in the range of 6 - 22 μ M. It was significantly more active against PC-3 cell lines than β -GLN; CC₅₀ of 6.0 μ M compared to 13.5 μ M but was less against BT 474 cell lines when compared to β -GLN, 22 μ M compared to 8 μ M. For other cell lines the activities are comparable. The diamino GAEL **7** with a primary amino group at the *sn*-3 position of the glycerolipid is significantly less active than mono-cationic **6** across all cell lines. This indicates that the positioning of the second amino group on the glycerol moiety is not optimal. Compound **8** with the sugar moiety on *sn*-3 position of the glycerolipid, was significantly more active compared to compound **7** with the aminosugar on *sn*-2 position of glycerol. GAEL **8** was also more active than β -GLN against all the cell lines with the exception of the BT 474 cell line. This result indicates that activity of this class of compounds is better when the sugar moiety is on *sn*-3 position of the glycerolipid.

The increased potency of compound **8** compared to β -GLN against most of the cell lines also shows that replacement of the methoxy group at *sn*-2 position of the glycerolipid with amino substituent significantly increased the activity.

Comparison of the activity of compounds **7** and **8** with that of **1**, **2**, and **4** demonstrates that better activities can be achieved when both amino groups are placed on the sugar as compared to a combination where one amino group is present at the sugar and the other one is attached to the glycerol portion of the lipid.

Compound **9** with a second hydrophobic C16-moiety attached to the *sn*-2 position of the glycerolipid via an amide linkage was not cytotoxic at the highest concentration tested, 30 μ M. At this dose there was no significant difference in viability of cells incubated with **9** compared to vehicle treated cells (controls). The lack of activity might be caused by increased lipophilicity which could decrease cellular absorption of the drug.

Compound **10** with a methyl-carbamate substituent at the *sn*-2-position of the glycerolipid, was synthesized to potentially promote selectivity for prostate cancer cell lines. The rationale behind this idea was based on previous report where edelfosine analog bearing carbamate at *sn*-2 position of the glycerolipid was more selective against prostate cancer cell lines.²⁸ The CC₅₀ values of compound **10** which is in the range of 14 – 23 μ M is significantly less active than that of β -GLN indicating that the carbamate substituent neither increase activity nor promoted selectivity for prostate cell line in GAEL series compared to edelfosine.

It is noteworthy that the most active analogs **1**, **2**, **4** and **8** were 2- to 3-fold more toxic toward the drug resistant cancer cell lines, JIMT-1, MB-MDA-231, DU-145 and PC3 relative to

β-GLN (Tables 5.1 A and 5.1 B). The reason why there was no significant difference between the activity of **1** and **β-GLN** against BT474 cells is unclear.

To compare the cytotoxic activity of our synthesized compounds with that of drugs in clinical use or development, we tested chlorambucil, cisplatin and salinomycin against all the six cell lines used in this study (Table 5.1A). Chlorambucil, an alkylating clinical anticancer agent did not kill up to 50% of all the six cell lines at the highest dose (150 μM) tested. Moreover, we were unable to reach CC₅₀ values for cisplatin against BT-474, MDA-MB-231 and MiaPaCa2 cell lines at the highest dose (20 μM) tested. In the case of salinomycin, an experimental drug with CSCs killing properties we were able to demonstrate that the most potent GAEL **1** displayed > 6-fold activity against MDA-MB-231, >4-fold activity against DU-145, 2-fold higher activity against MiaPaCa2 and BT-474. Improved activity was also seen with GAELs **2**, **4** and **8** when compared to salinomycin.

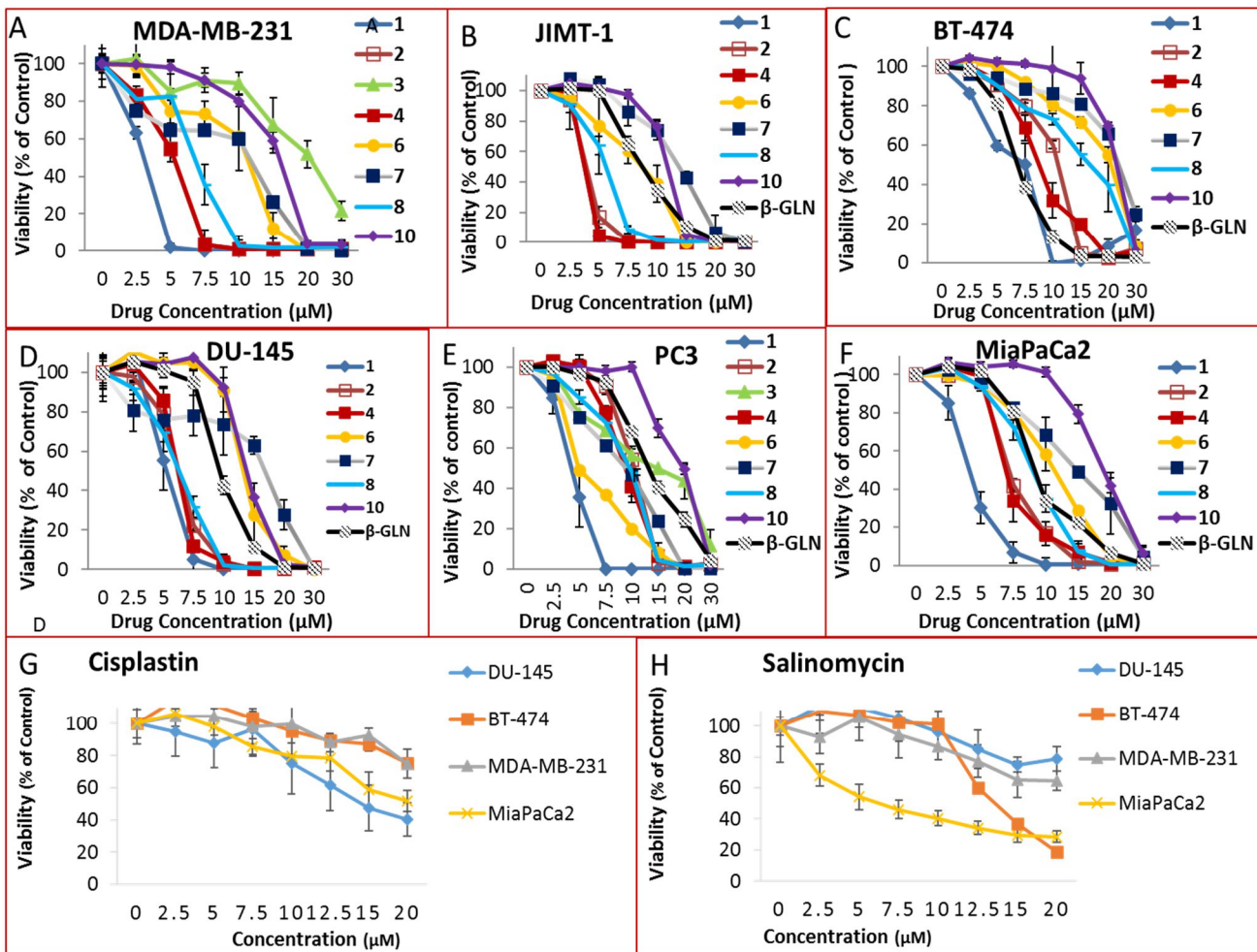


Figure 5.3. Effects of compounds **1** – **10**, β -GLN, on the viability of MDA-MB-231 (**A**), JIMT-1 (**B**), BT-474 (**C**), DU-145 (**D**), PC3 (**E**) and MiaPaCa2 (**F**) cell lines. Effect of cisplatin (**G**) and salinomycin (**H**) on viability of DU-145, BT-474, MDA-MB-231 and MiaPaCa2 were included for comparison purpose. MDA-MB-231, JIMT-1, DU-145 and MiaPaCa2 cells were cultured in DMEM medium supplemented with 10% FBS, BT-474 cells were cultured in DMEM/F12 medium supplemented with 10% FBS and PC3 cells were cultured in F12K medium supplemented with 10% FBS. Equal numbers were dispersed into 96-well plates. After 24 h, the cells were incubated with compounds **1-11** (0-30 μM) for 48 h. At the end of the incubation, MTS reagent (20% vol/vol) was added and the plates were incubated for 1-4 h. The OD₄₉₀ was read with a plate reader. Wells

with media but no cells were treated in similar fashion and the values utilized as blank. The results represent the mean \pm standard deviation of 6 independent determinations. Compounds **5**, **8**, **9**, and **10** were studied as diastereomeric 1:1 mixture based on the stereochemistry at *sn*-2 position of the glycerolipid.

Table 5.1. CC₅₀ (A) and CC₉₀ (B) values of compounds **1-10** and β -GLN on a panel of human epithelial cancer cell lines: breast (BT474, JIMT1, MDA-MB-231), pancreas (MiaPaCa2) and prostate (DU145, PC3).^e

A

Drugs	CC ₅₀ values (μ M)					
	MDA-MB-231	DU-145	JIMT-1	MiaPaCa2	PC3	BT-474
1	3.0	5.2	3.5	3.5	3.5	7.5
2	5.5	6.0	4.2	7.0	11.0	11.5
3	20.0	>30	>30	>30	15.0	NT
4	4.5	6.0	4.0	6.5	8.0	8.5
5	>30	>30	>30	>30	>30	>30
6	11.0	12.5	9.5	11.5	6.0	22.0
7	12.0	17.5	14.0	15.0	9.5	25.0
8	6.0	6.0	5.5	8.5	9.0	15.5
9	>30	>30	>30	>30	>30	>30
10	16.0	14.0	12.5	18.0	20.0	23.0
β -GLN	NT	10.0	9.0	9.0	13.5	8.0
cisplatin	>20	14.8	NT	>20	NT	>20
salinomycin	>20	>20	NT	6.5	NT	14.0
chlorambucil	>150	>150	>150	>150	>150	>150

B

	CC ₉₀ values (μM)					
Drugs	MDA-MB- 231	DU-145	JIMT-1	MiaPaCa2	PC3	BT-474
1	4.5	7.4	4.9	6.5	6.0	9.5
2	7.0	8.5	6.5	12.0	14.0	14.0
4	7.0	8.5	6.0	13.0	14.0	17.5
6	15.0	18.0	13.5	18.5	15.0	28.0
7	17.5	25.0	19.0	28.0	17.0	>30
8	9.0	9.0	7.5	14.0	14.0	28.0
10	19.0	19.0	15.0	29.0	29.0	29.0
β-GLN	NT	15.0	16.0	18.0	28.0	13.0

^eThe CC₅₀ value is defined as the concentration required to decrease cell viability by 50% relative to the untreated control, while the CC₉₀ value is defined as the concentration required to decrease cell viability by 90% relative to untreated control. The values were obtained by estimating the drug concentration at 50% and 10% viability on the y-axis using line plots. Compounds **5**, **8**, **9**, and **10** were studied as diastereomeric 1:1 mixture based on the stereochemistry at *sn*-2 position of the glycerolipid. NT – Not tested.

5.4.2.2. Effect of dicationic GAELs 1, 2, 4, or 8 on the integrity and viability of BT-474 and DU-145 cancer stem cells (CSCs)

To assess the effect of the most potent GAELs on cancer stem cells (CSCs), high expressing ALDH cells were sorted from BT474 and DU145 cells and the sorted cells were cultured in low-adhesion culture plates in stem cell growth media. The spheroids were isolated by cell sieving,

trypsinised and counted. Equal numbers were dispersed in wells and allowed to form spheroids. The active dicationic GAELs, **1**, **2**, **4**, or **8** were added to the spheroids.

The viability of the cells at the end of the 6-day incubation were assessed with the MTS assay and the results are displayed in Figure 5.4A for BT474 CSCs and Figure 5.4B for DU145 CSCs. The GAELs were able to completely inhibit the viability of the CSCs at concentrations ranging from 5-10 μM depending on the compound. The most active compounds were **1**, **4** and **2** for BT474 CSCs and **1**, **4** and β -GLN for DU145 CSCs. The activity of the most active analog **1** was compared to that of salinomycin the most studied anti-CSCs agent till date, cisplatin, a clinical anticancer agent and myristylamine a known surfactant using CSCs isolated for BT-474 after 3 days of incubation (Figure 5.4C). Compound **1** demonstrated a better anti-CSCs activity than salinomycin. Cisplatin did not show any significant reduction in viability at highest dose tested (20 μM). Myristylamine, a classical amphiphile did not show any activity at the highest dose tested (20 μM) indicating that the disruption of mammosphere formed by BT-474 CSCs is not the result of a detergent effect.

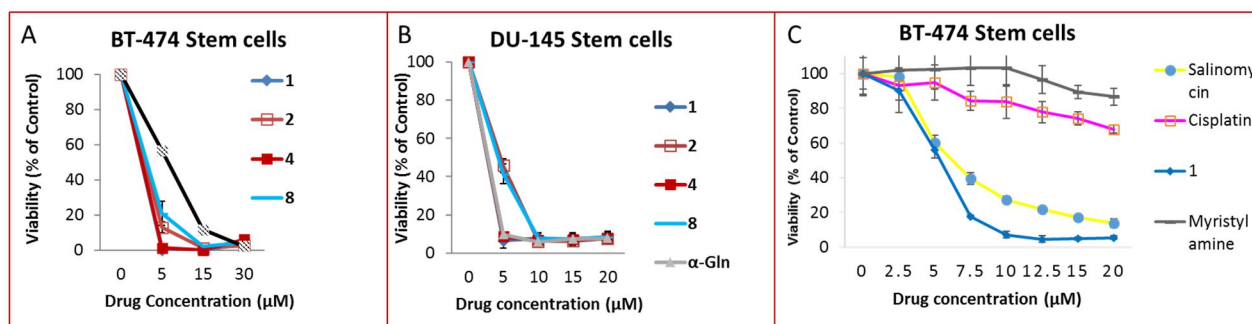


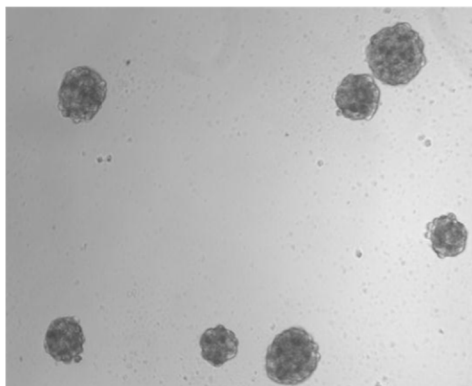
Figure 5.4. Effects of compounds **1**, **2**, **4**, **8**, α -GLN on the viability of cancer stem cells isolated from BT-474 breast cancer (A), DU-145 cell lines (B) and comparison of **1** with salinomycin, cisplatin, myristylamine (C). α -GLN has been previously reported to be more active than our reference β -GLN against cancer cell lines^{22, 23} and CSCs obtained from BT-474 cell line.²² Also it

is being tested on CSCs from DU-145 for the first time. BT-474 and DU-145 cancer stem cells were obtained by staining for ALDH1 and sorting the cells by flow cytometry. The spheroids from BT-474 stem cells were grown in ultra-low adhesion plates in mammo-cult medium for 6 days, while the spheroids from DU-145 stem cells were grown in ultra-low adhesion plates in prostatosphere growth medium for 6 days. The spheroids formed were harvested, trypsinised and equal numbers were seeded in 48-well low adhesion plates for 5-6 days to allow formation of spheroids. The spheroids were incubated with varying concentrations of compounds **1**, **2**, **4**, **8** (0 - 30 μ M) for 6 days (**A** and **B**) and 3 days (**C**). At the end of the incubation the MTS reagent was added to each well and the plates were incubated in a 5% CO₂ incubator for 4 h. The absorbance was read at 470 nm in a plate reader. The results are the means \pm standard deviation for 4 independent determinations (**A** and **B**) and 6 independent determinations (**C**).

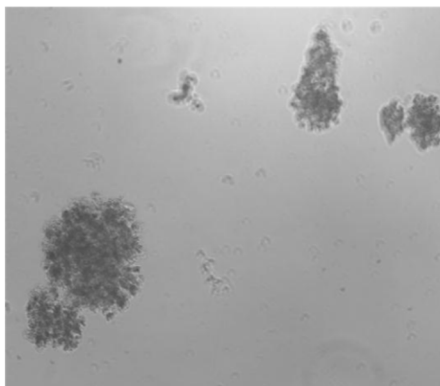
Figure 5.5A show the results of the effects of GAELs on the integrity of BT474 CSC spheroids. Incubations with the vehicle revealed the spheroids grew larger and more compact. In contrast, incubations with the GAELs resulted in disintegration of the spheroids. Similar results were obtained with CSCs derived from DU145 prostate cancer cell lines (Figure 5.5B).

A.1

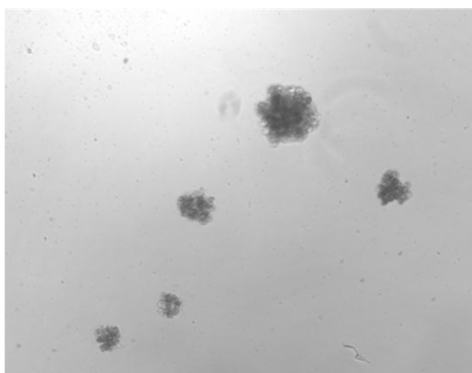
Control



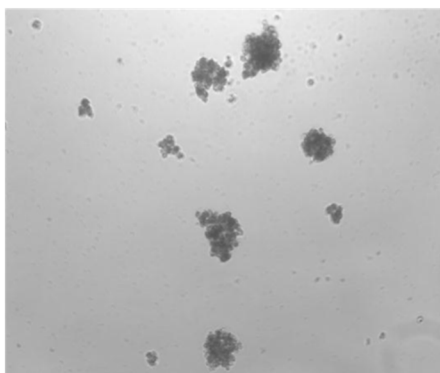
GAEL 1 – 10 μ M



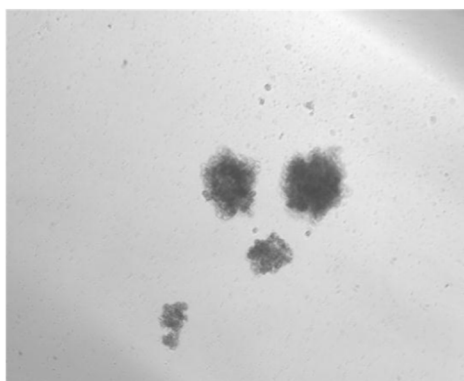
GAEL 2 – 10 μ M



GAEL 4 – 10 μ M

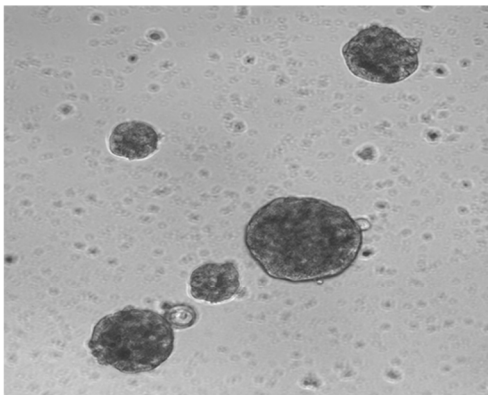


GAEL 8 – 10 μ M

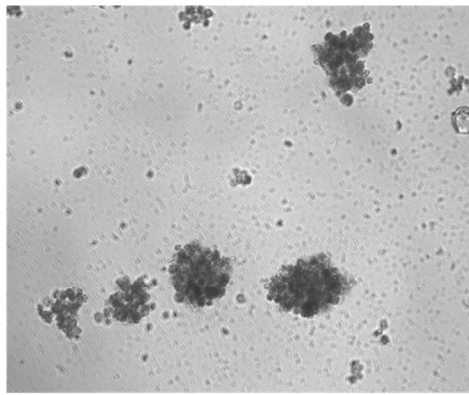


A.2

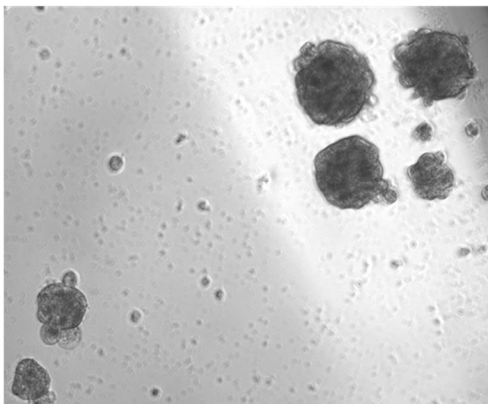
Control



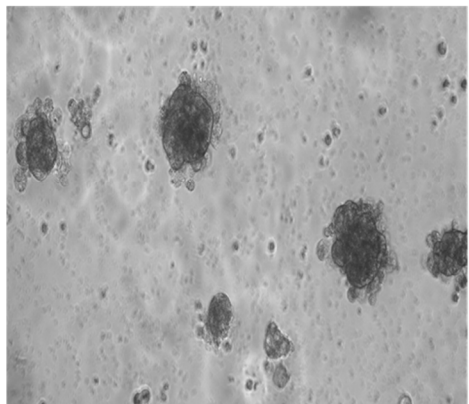
GAEL 1 – 7.5 μ M



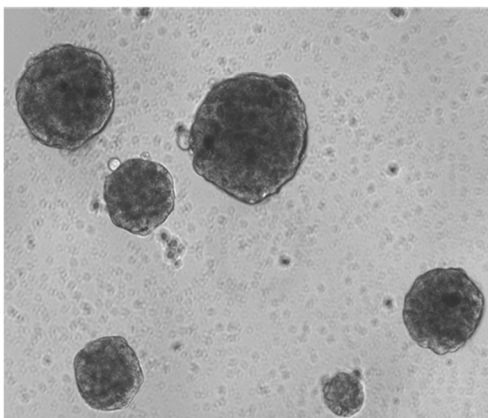
Salinomycin – 7.5 μ M



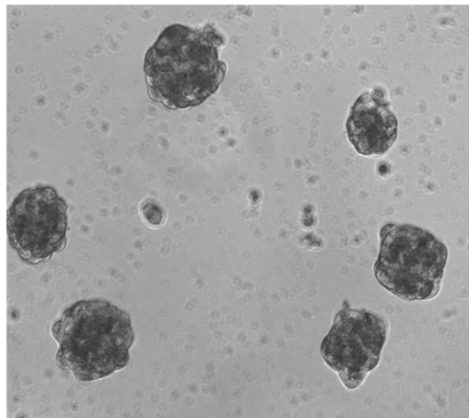
Salinomycin – 20 μ M



Myristylamine – 10 μ M



Cisplatin – 20 μ M



B

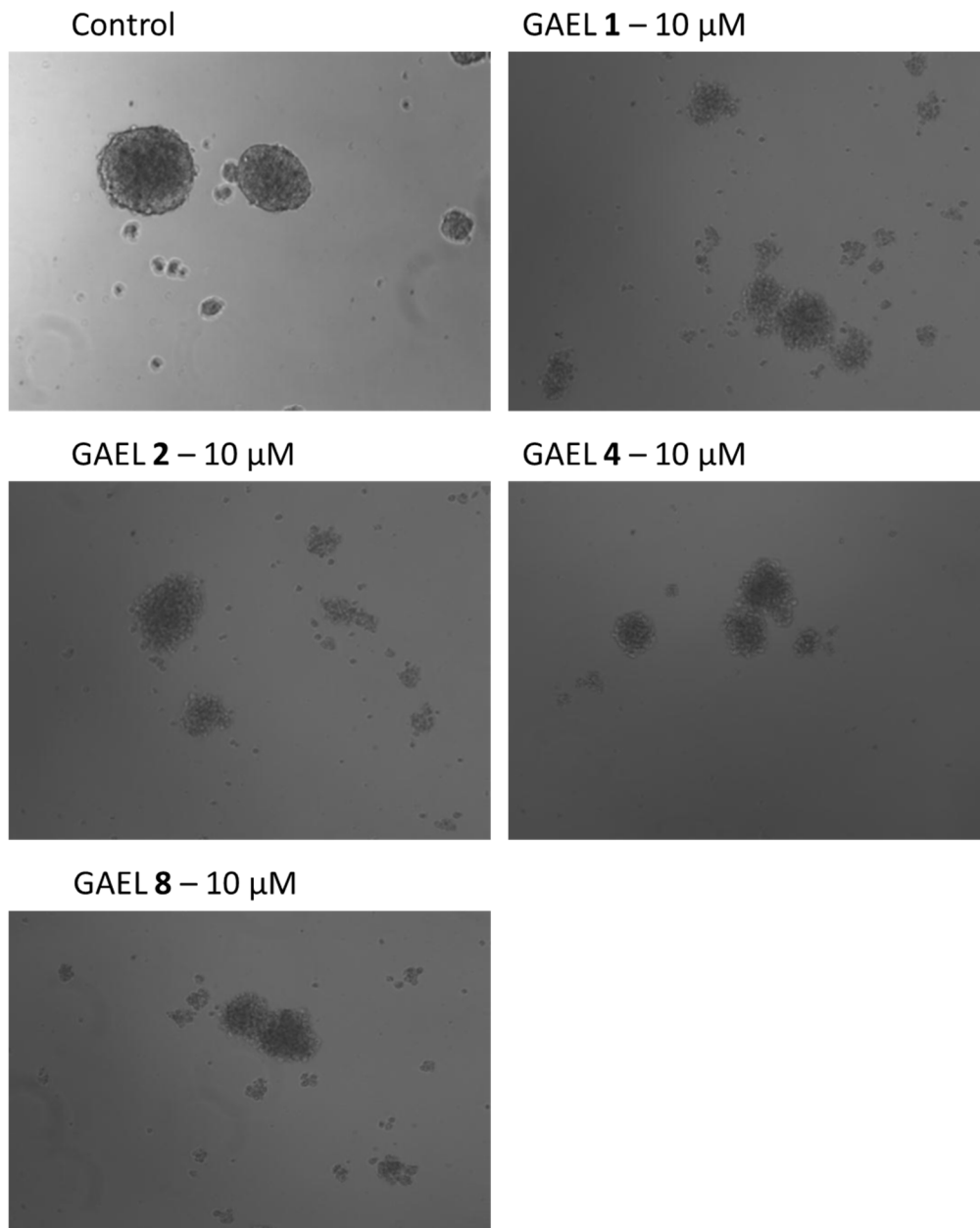


Figure 5.5. Effect of compounds **1**, **2**, **4**, **8**, cisplatin, salinomycin and myrtilamine on the integrity of prostate and breast cancer stem spheroids. (A.1) Effect of GAEL compounds **1**, **2**, **4**, and **8** on the integrity of BT474 breast cancer stem cell spheroids. Equal numbers of BT-474 cancer stem cells were seeded into ultra-low adhesion 48-well plates and grown for 5 days to allow for

spheroid formation. The spheroids were incubated with or without 10 μ M GAELs for up to 6 days. The images were taken after 4 days of incubation with an Olympus IX70 microscope at a magnification of x10. (A.2) The anti CSCs activity of GAEL **1** was compared to that of salinomycin, cisplatin and the classical amphiphile myristylamine after 3 days of incubation of spheroids with or without the drugs. The images were taken after 3 days of incubation with an Olympus IX70 microscope at a magnification of x10. (B) Effect of GAEL compounds **1**, **2**, **4**, and **8** on the integrity of DU145 prostate cancer stem cell spheroids. Equal numbers of DU-145 cancer stem cells were seeded into ultra-low adhesion 48-well plates and grown for 5 days to allow for spheroid formation. The spheroids were incubated with or without 10 μ M GAELs for up to 6 days. The images were taken after 4 days of incubation with an Olympus IX70 microscope at a magnification of x10.

5.5. Discussion and Conclusions

GAELs represent a novel class of potential anticancer agents. The most active compounds reported herein display CC_{50} values in the range of 3.0 to 7.5 μ M. Since GAELs with a primary amino substituent at the C₂-position of the sugar moiety show higher toxicity against cancer cells compared to analogs without amino function¹⁸, we explored the possibility that increasing the number of cationic charges would lead to enhanced cytotoxic activity. Our results demonstrated that this was indeed the case. Diamino GAELs **1**, **2**, **4** and **8** but not bisamino GAEL **7** were 2-3-fold more active than our previous monobasic lead structure β -GLN. The fact that GAEL **7** which has the carbohydrate moiety linked at the *sn*-2 position shows reduced antitumor activity when compared to other dicationic GAELs may indicate that the carbohydrate moiety should be linked to the *sn*-3 position of the glycerolipid for optimal antitumor activity. Within the class of diamine-

based GAELs, glycolipid **1**, containing an α -glucosidic-2,6-diamino head group, consistently showed the highest activity against all 6 cancer cell lines indicating that the α -glucosidic linkage and positioning of the two cationic charges in the glucose moiety are optimal for anticancer activity. The lack of activity of compound **3** in comparison to β -GLN despite the free amino group at the C-6 position of glucose indicates that the amino group at C-2 remains critical for anticancer activity. Comparison of the activity of GAELs **6** and **7** with that of compound **8** showed that glycosylation of the hydroxyl group at the *sn*-3 position of the glycerol moiety appears to be optimal for antitumor activity. The significantly higher activity of compound **2** when compared to that of compound **8** indicates that the presence of both amino substituents on the glucose moiety is optimal for anticancer activity. Similar to previous findings in the monocationic GAEL series,^{22,23} replacements of the methoxy substituent in the glycerol portion by a H-atom had little effect on the cytotoxicity against most cancer cell lines except the PC3 and BT474 cell lines where a slight improvement was observed. On the other hand, replacement of the methoxy substituent by a second β -glycosidic 2,6-amino-D-glucosyl moiety as in compound **5** or acylation of GAEL **8** by palmitic acid to afford **9**, caused a loss of antitumor activity. While the reasons for the loss in activity are not known, the substitutions could affect the physical properties of the compound which could impact the absorption and thus the activity. Unlike edelfosine replacement of the methoxy group at *sn*-2 position of the glycerolipid with methyl carbamate as in GAEL **10** significantly reduced anticancer activity and it did not enhance selectivity toward prostate cancer.

Juxtaposition of cytotoxicity of **1**, cisplatin and salinomycin, the most researched anti-CSCs agent,³¹ against BT474, DU145 and MDAMB231 cancer cell lines and CSCs isolated from BT474 cell lines revealed that GAELs could be superior anticancer agents. GAEL **1** displayed significantly more potent activity than the clinical anticancer drug, cisplatin, which showed little

activity against cancer lines and minimalistic effect against CSCs. Salinomycin activity against both CSCs and cancer cell lines are less than that of GAEL 1 (Figure 5.3G, 5.3H and 5.4C) The fact that the classical amphiphile myristyl amine is unable to decrease the viability and disintegrate the CSCs spheroid indicates that the anti CSCs properties of GAELs is not the result of a detergent effect.

While there has been great progress in the diagnosis and treatment of several forms of cancers in the last 40 years, it remains true that certain cancers have very poor prognoses and remain intractable to current treatments. Accumulating evidence suggests that a major impediment to effective treatment that prevents the relapse of cancer may be the inability to eradicate CSCs which have been implicated in tumor progression, drug resistance and metastases.^{6,7, 22} A major goal of current cancer research is to elucidate means to kill or inactivate CSCs .⁷ Several approaches to curtail the activity of CSCs in tumors have been suggested^{7,32-35} but as CSCs resist apoptotic cell death it has been challenging to kill them with current anticancer agents. One approach that might eliminate CSCs is to develop compounds that kill cells by non-apoptotic mechanisms. Such compounds would by-pass the variety of strategies used by CSCs to evade apoptotic cell death. Because GAELs kill cells by a non-apoptotic mechanism,^{19-21,23,24,29,32} it was postulated that they would be effective in killing CSCs. This postulate was validated by demonstration that monobasic GAELs cause the disintegration of BT474 breast CSC spheroids and kill the CSCs²². In this study we have demonstrated that glucose-configured diamine-based GAELs also cause the disintegration of BT474 and DU145 CSC spheroids and kill CSCs with enhanced activity. We can infer from this that the structural modifications made to generate the diamine-based glycolipids have not fundamentally altered their mechanism of action. Thus, the

ability to disrupt the integrity of CSC growing under 3D conditions and kill the cells is not restricted to one cell type and may be a general characteristic of GAELs.

5.6 Experimental section

5.6.1. Materials and methods: Synthesis of GAELs

Solvents were dried over CaH₂. ¹H, ¹³C NMR spectra were recorded with a JMN A500 FT NMR spectrometer at 500 and Avance 300 MHz at 126 and 75 MHz respectively, and chemical shifts were reported in parts per million (ppm). Thin-layer chromatography (TLC) was carried out on aluminum-backed silica gel GF plates (250 μm thickness) and plates were visualized by charring with 5% H₂SO₄ in MeOH and or short wavelength UV light. Compounds were purified by flash chromatography on silica gel 60 (230-400 ASTM mesh). Matrix assisted laser desorption/ionization-time of flight (MALDI-TOF)-MS was recorded on a Voyager RP mass spectrometer. High-resolution (HR) mass spectra were recorded on a JEOL JMS700 under FAB conditions. Purity of compounds **1-10** were assessed by elemental analysis of C, H, N and were within ± 0.5 % of the theoretical values.

5.6.2. Chemistry: general methods

5.6.2.1 General method for acetylation

Acetylation reactions were carried out in pyridine with dimethyl amino pyridine (DMAP, 0.2 molar equivalent) as the catalyst using acetic anhydride (2 molar equivalents) After stirring for 18 h at room temperature, the reaction was stopped by addition of methanol (10 ml), and then concentrated to dryness. The resulting residue was dissolved in ethyl acetate and washed with saturated sodium bicarbonate (3 times) and distilled water (2 times). The resulting organic layer

was dried over Na₂SO₄ and concentrated to dryness. The residue was purified by flash chromatography. Generally the yield was 40-80%

5.6.2.2. General method for glycosylation reaction

The glycoside donor and 1.1 molar equivalent of the lipid alcohol, the glycoside acceptor, were dissolved in anhydrous dichloromethane (DCM) under argon atmosphere. N-Iodosuccinimide (NIS, 1.5 molar equivalents of the glycoside donor) and silver triflate (AgOTf, 0.2 molar equivalent of the glycoside donor) were simultaneously added. The reaction mixture was left under vigorous stirring for 3 h. At the completion of reaction (TLC monitoring), the reaction mixture was diluted with DCM and then filtered over Celite. The resulting organic layer was washed with saturated sodium thiosulphate solution (2 times), saturated sodium bicarbonate (3 times) and water (2 times). The organic layer was dried over anhydrous Na₂SO₄ and then concentrated under vacuum to give a residue which was purified by flash chromatography (Hexane/Ethyl acetate, 4:6)

5.6.2.3. General method for conversion of primary hydroxyl group to azide

Triisopropylbenzylsulphonylchloride (TIBS) (1.5 molar equivalent) or p-toluenesulphonylchloride (1.1 molar equivalent) were used to activate the primary hydroxyl group at the C₆ position of the sugar or primary hydroxyl group of the glycerolipid-based diol, using DMAP (0.2 molar equivalent) as catalyst in anhydrous pyridine under argon or nitrogen atmosphere. The reaction was stirred vigorously at room temperature for 12 - 24 h after which it was stopped by addition of methanol (10 ml) and then stirred vigorously for 10 minutes. The methanol and pyridine were removed under high vacuum. The crude mixture was dissolved in EtOAc and washed with 5% HCl (2 times,) then saturated sodium bicarbonate solution (2 times) and water (once) to give usually a dark brown organic layer. The organic solvent was removed

under vacuum and crude residue was purified by flash chromatography EtOAc/Hexane, (4:6) or 100% ethyl acetate depending on the compound. The sulphonate ester was displaced with azide in a nucleophilic substitution reaction using sodium azide (10 molar equivalents) in anhydrous DMF at 70 – 90°C under argon or nitrogen atmosphere for 12 – 24 h. At the end of the reaction, the solvent DMF was removed under high vacuum. The residue was resuspended in ethyl acetate and then filtered to remove excess sodium azide. The solvent was removed under vacuum and the residue was purified using flash chromatography.

5.6.2.4. General method for deprotection of acetate group

The acetate protected compounds were dispersed in methanol followed by addition of NaOMe (0.5 molar equivalent). The mixture was vigorously stirred for 1 h and at the completion of the reaction ion exchange resin (H^+) was added. When the reaction mixture was clear, the resin was removed by filtration, the filtrate was then concentrated under vacuum. The residue was purified by flash chromatography (100% EtOAc). For selective deprotection of acetate in the presence of phthalimido protective group, only a catalytic amount of sodium methoxide (0.1 molar equivalent) was used and the solution was stirred for 20-40 min.

5.6.2.5. General method for simultaneous deprotection of acetate and phthalimido group

To simultaneously remove acetate and phthalimido protecting group, the protected compound was dissolved in a mixture of ethylenediamine/n-butanol (1:1), the solution was heated to 90°C, under vigorous stirring for 2 h. Then the reaction mixture was concentrated under high vacuum and the residue was purified using reverse phase C_{18} -silica gel column by gradient elution (100% water/0% methanol to 0% water/100% methanol).

5.6.2.6. General method for reduction of azide

To reduce the azido protecting group to free amine, the azido compounds were suspended in a mixture of THF/water (9:1), then trimethyl phosphine in THF (1M) (5 to 10 molar equivalent of trimethyl phosphine) was added. The reaction mixture was stirred at room temperature for 2 h, then it was concentrated under vacuum. The residues especially in case of final compounds were purified using C₁₈ coated silica gel column chromatography by gradient elution (100% water/0% methanol to 0% water/100% methanol). For lipid molecules with azido groups, the purifications were carried using normal phase flash chromatography by hexane/EtOAc mixture (9:1) and 100% EtOAc was used in purification of protected glycolipid.

5.6.2.7 Synthetic procedures for the synthesis of intermediates and final compounds

1,3,4,6-Tetra-O-acetyl-2-azido-2-deoxy- α/β -D-glucoopyranoside (12)

D-glucosamine hydrochloride **11** (3.0 g, 13.92 mmol) was dissolved in water (15.0 ml). To the solution was added Et₃N (2.8 g, 27.80 mmol) and CuSO₄ x 5H₂O (0.036 g, 0.015 mmol). Triflic azide (16.00 mmol), prepared as previously reported,²³ was then added to the reaction mixture. The resulting blue mixture was stirred vigorously for 18 h and then concentrated under vacuum at room temperature. The residue was dissolved in pyridine (30.0 ml) and DMAP (0.15 g, 1.20 mmol) was added followed by addition of acetic anhydride (9.0 ml, 96.00 mmol). After stirring for 18 h at room temperature, the reaction was stopped with methanol (10.0 ml), and concentrated to dryness. The resulting residue was dissolved in ethyl acetate (120.0 ml) and washed with saturated sodium bicarbonate (×3) and distilled water (×2). The organic layer was dried over anhydrous sodium sulphate, concentrated to dryness, and purified by flash chromatography (Hexanes:EtOAc, 3:2) to

yield **12** as an off white solid (4.5 g, 85 %). The NMR data was in agreement with previously reported data.²³ ES-MS: m/z [M + Na]⁺ calc'd for C₁₄H₁₉N₃O₉Na⁺: 396.1, found: 396.2.

Phenyl 3,4,6-tri-O-acetyl-2-azido-2-deoxy-1-thio- α/β -D-glucopyranoside (13)

To a solution of **12** (4.5 g, 12.10 mmol) in DCM (60.0 ml) at room temperature was added thiophenol (2.4 ml, 24.00 mmol) and BF₃·Et₂O (3.0 ml, 24.00 mmol). After stirring overnight at room temperature, the reaction was stopped with saturated sodium bicarbonate solution and the organic layer washed with same solution (×3) and distilled water (×2). This was then dried over anhydrous sodium sulphate and concentrated to dryness. The residue was purified by flash chromatography (Hexanes:EtOAc, 3:2) to afford **13** as a α/β (4:1) mixture in the form of a brownish white solid (3.9 g, 76 %). The NMR data was in agreement with previously reported data.²³ ES-MS: m/z [M + Na]⁺ calc'd for C₁₈H₂₁N₃O₇SNa⁺: 446.1, found: 446.3

Phenyl -2-azido-2-deoxy-1-thio- α/β -D-glucopyranoside (14)

To a dispersion of **13** (3.9 g, 9.21 mmol) in methanol was added NaOMe (1.0 g). The mixture was stirred for 1 h and stopped with 1.0 g of ion exchange resin (H⁺). When the reaction mixture became clear, the resin was filtered and the mixture was concentrated under vacuum. The residue was purified by flash chromatography (100 % ethyl acetate) to give **14** as an off-white solid. α/β (3/1) mixture (2.0 g, 73 %). Characteristic ¹H NMR (300 MHz, CDCl₃) δ 5.53 (d, *J* = 4.4 Hz, 0.75H, α H-1), 4.54 (d, *J* = 10.2 Hz, 0.25H, β H-1). ES-MS: m/z [M + Na]⁺ calc'd for C₁₂H₁₅N₃O₄SNa⁺: 320.1, found: 320.3.

Phenyl-2-azido-2-deoxy-1-thio-6-O-(-2,4,6-triisopropylbenzylsulphonyl- α/β -D-glucopyranoside
(15)

Compound **14** (3.2 g, 10.76 mmol), catalytic DMAP, and triisopropylbenzylsulphonylchloride (TIBS) were added together in a flask and cooled to 0 °C under vacuum for 20-30 mins, after which it was connected to a nitrogen atmosphere. 50.0 ml of dry pyridine was added and the reaction was stirred for 24 h at room temperature, after which it was stopped by addition of methanol (10.0 ml). The methanol and pyridine were removed under high vacuum. The crude mixture was dissolved in EtOAc and washed with 5 % HCl ($\times 2$), saturated sodium bicarbonate solution ($\times 2$), and water ($\times 1$), to give a dark brown organic layer. The organic solvent was removed under vacuum and crude residue was purified by flash chromatography (Hexanes/EtOAc, 3:2) to give **15** as a brown solid (2.5 g, 4.43 mmol). Yield 41 % (4.8:5.2, $\alpha:\beta$). Characteristic ^1H NMR (300 MHz, CDCl_3) δ 7.60 – 7.37 (m, 2H, TIBS aromatic proton), 7.32 – 7.16 (m, 5H, thiophenyl proton), 5.53 (d, $J = 4.3$ Hz, 0.48H, α H-1), 4.44 (d, $J = 9.1$ Hz, 0.52H, β H-1), 1.37 – 1.14 (m, 18H, TIBS isopropyl $-\text{CH}_3$). ES-MS: m/z $[\text{M} + \text{Na}]^+$ calc'd for $\text{C}_{27}\text{H}_{37}\text{N}_3\text{O}_6\text{S}_2\text{Na}^+$: 586.2, found: 586.4.

Phenyl -2, 6-diazido-2, 6-dideoxy-1-thio- α/β -D-glucopyranoside **(16)**

Compound **15** (2.5 g, 4.43 mmol) was dissolved in anhydrous DMF (25.0 ml) under dry conditions, followed by the addition of NaN_3 (2.3 g, 35.44 mmol). The reaction stirred overnight at 70 °C. The DMF was removed under high vacuum and the residue was suspended in ethyl acetate and filtered to remove excess sodium azide. The organic layer was then concentrated under vacuum and purified by flash chromatography (100 % EtOAc) to give **16** as a brownish gel (1.36 g, 4.40 mmol). Yield 99 % (5.5:4.5, $\alpha:\beta$). Characteristic ^1H NMR (300 MHz, CDCl_3) δ 7.67 – 7.19 (m, 5H,

thiophenyl aromatic protons), 5.64 (d, $J = 4.8$ Hz, 0.55H, α H-1), 4.51 (d, $J = 9.9$ Hz, 0.45H, β H-1). ES-MS: m/z $[M + Na]^+$ calc'd for $C_{12}H_{14}N_6O_3SNa^+$: 345.1, found: 345.5.

Phenyl – 3,4-diacetyl-2, 6-diazido-2, 6-dideoxy-1-thio- α/β - D-glucoopyranoside (17)

To a solution of compound **16** (1.4 g, 4.40 mmol) in pyridine (25.0 ml) was added DMAP (0.1 g) and acetic anhydride (5.0 ml). The solution was stirred overnight at room temperature and upon completion, excess acetic anhydride was quenched with methanol (5.0 ml). The solvents were removed under high vacuum to give a brownish residue, and dissolved in DCM, washed with 5 % HCl solution ($\times 2$), saturated sodium bicarbonate ($\times 3$) and distilled water ($\times 2$). The organic layer was dried over anhydrous sodium sulphate and concentrated under vacuum to give a brown gel residue. The residue was then purified by flash chromatography (Hexane:EtOAc, 2:3) to give compound **17** as a brown gel (1.5 g, 4.40 mmol), yield 98% (4.6:5.4, $\alpha:\beta$). Characteristic proton NMR data: 1H NMR (300 MHz, $CDCl_3$) δ 7.65 – 7.24 (m, 15H, thiophenyl aromatic protons), 5.66 (d, $J = 5.6$ Hz, 0.46H, α H-1), 4.51 (d, $J = 10.2$ Hz, 0.54H), 2.13 – 1.99 (m, 6H, acetate $-CH_3$). ES-MS: calcd $C_{16}H_{18}N_6O_5SNa^+$ m/z : 429.10 found $[M+Na]^+$ m/z : 429.1

1-O-Hexadecyl-2-O-methyl-3-O-(3',4'-O-diacetyl-2', 2',6'-diazido-, 6',2'-dideoxy- α -D-glucoopyranosyl)-sn-glycerol (19)

Compound **17** (0.16 g, 0.40 mmol) and compound **18** (0.17 g, 0.48 mmol) were dissolved in anhydrous DCM (10.0 ml) under argon atmosphere. NIS (0.18 g, 0.80 mmol) and silver triflate (0.02 g, 0.08 mmol) were added. The reaction mixture was stirred for 3 h. Upon completion, the reaction mixture was diluted with DCM (20.0 ml) and filtered over celite. The resulting organic layer was washed with saturated sodium thiosulphate solution ($\times 2$), saturated sodium bicarbonate ($\times 3$), and water ($\times 2$). The organic layer was then dried over anhydrous sodium sulphate and then

concentrated under vacuum to give a brownish gel residue. The residue was purified by flash chromatography (Hexanes/EtOAc, 2:3) to isolate compound **19** as a brown gel from a mixture of **19** and **20**. Yield 33 % (0.082 g, 0.13 mmol). ¹H NMR (300 MHz, CDCl₃) δ 5.52 – 5.43 (m, 1H, H-3), 5.06 (d, *J* = 3.5 Hz, 1H, α H-1), 5.00 (dd, *J* = 10.2, 9.1 Hz, 1H, H-4), 4.07 (dt, *J* = 10.2, 4.4 Hz, 1H), 3.91 (dd, *J* = 9.7, 2.5 Hz, 1H), 3.69 – 3.51 (m, 5H), 3.48 (s, 3H, -OCH₃), 3.47 – 3.35 (m, 1H), 3.29 (m, 3H, H-2, H-6), 2.09 (s, 3H, acetate CH₃), 2.05 (s, 3H, acetate CH₃), 1.58 (m, 2H), 1.26 (s, 26H, lipid tail), 0.89 (t, *J* = 6.6 Hz, 3H, lipid terminal -CH₃). ¹³C NMR (75 MHz, CDCl₃) δ 170.13, 170.01, 98.04, 79.11, 71.86, 70.10, 69.72, 69.46, 68.90, 67.91, 60.90, 57.96, 50.96, 31.93, 29.70, 29.36, 26.11, 22.69, 20.62, 14.11. ES-MS: *m/z* [M + Na]⁺ calc'd for C₃₀H₅₄N₆O₈Na⁺ *m/z*: 649.4, found: 649.4

1-O-Hexadecyl-2-O-methyl-3-O-(2',6'-diazido-2',6'-dideoxy-α-D-glucopyranosyl)-sn-glycerol
(21)

Compound **19** was treated according to the general method of acetate deprotection to give **21** as a brown gel. Yield 90 % (0.063 g, 0.12 mmol) ¹H NMR (300 MHz, CDCl₃) δ 4.98 (d, *J* = 3.5 Hz, 1H, H-1), 4.00 (dd, *J* = 10.4, 8.6 Hz, 1H, H-3), 3.94 – 3.78 (m, 3H), 3.64 – 3.53 (m, 5H), 3.52 – 3.41 (m, 8H), 3.18 (dd, *J* = 10.3, 3.5 Hz, 1H, H-2), 1.58 (m, 2H), 1.27 (s, 26H, lipid tail), 0.89 (t, *J* = 6.6 Hz, 3H, lipid terminal -CH₃). ¹³C NMR (75 MHz, CDCl₃) δ 98.21, 79.24, 71.90, 71.72, 71.39, 70.90, 69.67, 67.18, 62.82, 57.91, 51.36, 31.94, 29.72, 29.67, 29.64, 29.62, 29.52, 29.37, 26.10, 22.70, 14.12. ES-MS: *m/z* [M + Na]⁺ calc'd for C₂₆H₅₀N₆O₆Na⁺: 565.4, found: 565.3.

1-O-Hexadecyl-2-O-methyl-3-O-(2',6'-diamino-2',6'-dideoxy-α-D-glucopyranosyl)-sn-glycerol
(1)

Compound **21** was deprotected as described under general method for azide reduction to give **1** as yellowish white solid. Yield 65 % (0.04 g, 0.08 mmol). ¹H NMR (300 MHz, MeOD) δ 4.8 (d, *J* = 3.6 Hz, 1H, H-1), 3.85 (m, 1H), 3.66 – 3.40 (m, 11H), 3.18 (dd, *J* = 9.3 Hz, 1H, H-4), 3.07 – 2.95 (m, 1H, H-6a), 2.77 (dd, *J* = 13.4, 6.9 Hz, 1H, H-6b) 2.60 (dd, *J* = 10.0, 3.6 Hz, 1H, H-2), 1.62 – 1.56 (m, 2H), 1.32 (s, 26H), 0.93 (t, *J* = 6.5 Hz, 3H). ¹³C NMR (75 MHz, MeOD) δ 100.82, 80.67, 76.13, 73.90, 73.50, 72.73, 71.24, 68.25, 58.21, 57.36, 43.78, 33.12, 30.83, 30.80, 30.64, 30.52, 27.30, 23.78, 14.50. HRMS: *m/z* [M + Na]⁺ calc'd for C₂₆H₅₄N₂O₆Na⁺: 513.3880, found: 513.3956. Elemental Analysis: calc'd: C, 63.64; H, 11.09; N, 5.71, found: C, 63.41; H, 10.83; N 5.38.

1, 3, 4, 6-tetra-O-acetyl-2-deoxy-2-N-phthalimido-D-glucopyranoside (22)

Glucosamine hydrochloride **11** (3.0 g, 14.00 mmol) and NaOH (1.1 g, 28.00 mmol) were dissolved in 50.0 ml of water. The resulting mixture was stirred at room temperature for 30 mins. Phthalic anhydride (2.4 g, 157.0 mmol) was added to the solution. The mixture was stirred at room temperature for 18 h and concentrated. The residue was dissolved in pyridine (30.0 mL), and 19.8 ml acetic added. The resulting solution was stirred overnight at room temperature, quenched with 6.0ml methanol, and concentrated under high vacuum. The remaining solid was dissolved in CH₂Cl₂ (40.0 mL), and washed each with 40.0 ml 10 % HCl (×1), saturated NaHCO₃ solution (×3), H₂O (×1), and brine (×1) successively. The organic layer was dried over anhydrous MgSO₄., concentrated under reduced pressure, and purified to give **22** (3.3 g, 49 %). NMR data were consistent with literature.³³

Phenyl 3,4,6-tri-O-acetyl-2-N-phthalimido-2-deoxy-1-thio-β-D-glucopyranose (23)

To a solution of **22** (1.5 g, 3.16 mmol) in DCM (20.0 ml) was added thiophenol (1.2 ml, 9.48 mmol) and $\text{BF}_3 \cdot \text{Et}_2\text{O}$ (1.0 ml, 9.48 mmol). After stirring overnight at room temperature, the reaction was stopped and washed with saturated sodium bicarbonate solution ($\times 3$), water ($\times 2$), and was dried over anhydrous sodium sulphate. The organic layer was concentrated and purified by flash chromatography (Hexanes:EtOAc, 3:2) to afford **23** as a brownish white solid (1.3 g yield 77 %). The NMR data was in agreement with previously reported data.²³

Phenyl-2-phthalimido-2-deoxy-1-thio- β -D-glucofuranose (24)

To a dispersion of **23** (1.3 g, 2.85 mmol) in methanol was added NaOMe (0.15 g). The mixture was stirred until complete dissolution of **23** (15 mins) and 1.0 g of ion exchange resin (H^+) was added. When the reaction mixture was clear, the resin was filtered, concentrated, and purified by flash chromatography (100 % ethyl acetate) to give **24** as a white solid. Yield 80 %. NMR data for compound **24**: ^1H NMR (300 MHz, MeOD) $\delta = 8.04 - 7.74$ (m, 4H, phthalimido aromatic protons), 7.49 – 7.17 (m, 5H, thiophenyl aromatic protons), 5.61 (d, $J=10.4$, 1H, H-1), 4.28 (dd, $J=10.2$, 7.8, 1H, H-3), 4.08 (dd, $J=10.4$, 1H), 3.97 (dd, $J=12.0$, 2.0, 1H), 3.78 (dd, $J=12.1$, 5.1, 1H), 3.59 – 3.41 (m, 2H). ^{13}C NMR (75 MHz, MeOD) $\delta = 135.67, 134.47, 132.84, 130.00, 128.71, 124.49, 124.20, 85.49, 82.69, 73.87, 72.28, 62.86, 57.82$. ES-MS: m/z $[\text{M} + \text{Na}]^+$ calc'd for $\text{C}_{20}\text{H}_{19}\text{NO}_6\text{SNa}^+$: 424.1, found: 424.1.

Phenyl-2-N-phthalimido-2-deoxy-6-(O-toluenesulphonyl)-1-thio- β -D-glucofuranose (25)

To a solution of compound **24** (0.7 g, 1.74 mmol) in anhydrous pyridine (15.0 ml) at 0 °C was added *p*-toluenesulphonyl chloride (0.4 g, 2.09 mmol) and DMAP (0.05 g) under nitrogen atmosphere. The reaction was warmed up to room temperature and stirred overnight, after which it was stopped with 5.0 ml methanol. The mixture was concentrated under high vacuum and

purified by flash chromatography (Hexanes/EtOAc, 9:1) to give **25** as a white foam (0.7 g, 1.3 mmol). Yield 74 %. ¹H NMR (300 MHz, CDCl₃) δ = 7.93 – 7.68 (m, 6H, aromatic protons), 7.44 – 7.13 (m, 7H, aromatic protons), 5.53 (d, *J* = 10.3, 1H, H-1), 4.45 – 4.25 (m, 3H, H-3), 4.19 – 4.02 (m, 2H, H-2), 3.78 – 3.46 (m, 2H), 3.31 (br s, 1H, OH), 3.05 (br s, 1H, OH), 2.45 (s, 3H, toluene CH₃). ¹³C NMR (75 MHz, CDCl₃) δ = 134.32, 132.61, 129.96, 128.87, 128.07, 83.51, 77.24, 72.62, 70.95, 68.58, 55.23, 21.69. ES-MS: *m/z* [M + Na]⁺ calc'd for C₂₇H₂₅NO₈S₂Na⁺: 578.1, found: 578.2.

Phenyl -2-N-phthalimido-2-deoxy-6-azido-6-deoxy-1-thio-β-D-glucopyranose (26)

Compound **25** (2.8 g, 5.19 mmol) was dissolved in anhydrous DMF (25.0 ml) under nitrogen gas atmosphere, then NaN₃ (2.7 g, 41.53 mmol) was added and stirred at 70 °C overnight. The DMF was removed under high vacuum and the residue suspended in ethyl acetate, filtered to remove excess sodium azide, re-concentrated, and partially purified by flash chromatography using Ethylacetate to give **26** as a brownish gel (1.99 g, 4.67 mmol) Yield 90 %. Compound **26** was not characterized by NMR before it was used for next reaction. ES-MS: *m/z* [M + Na]⁺ calc'd for C₂₀H₁₈N₄O₅SNa⁺: 449.1, found: 449.1.

Phenyl 3,4-diacetyl-2-N-phthalimido-2-deoxy-6-azido-6-deoxy-1-thio-β-D-glucopyranose (27)

To a solution of compound **26** (1.5 g, 3.66 mmol) in pyridine (25.0 ml) was added a catalytic amount of DMAP, and acetic anhydride (3.0 ml). The solution was stirred overnight at room temperature. Upon completion of reaction, excess acetic anhydride was quenched with methanol (5.0 ml), and solvents removed under high vacuum to give a brownish residue. The residue was dissolved in DCM, washed with 5 % HCl solution (×2), saturated sodium bicarbonate (×3) and distilled water (×2). The organic layer was dried over anhydrous Na₂SO₄, concentrated, and

purified by flash chromatography (Hexanes/EtOAc, 2:3) to give **27** as a light yellow solid. Yield 87 % (1.6 g, 3.20 mmol). Characteristic ^1H NMR (300 MHz, CDCl_3) δ = 7.80 (m, 4H, phthalimido aromatic protons), 7.49 – 7.18 (m, 5H, thiophenyl aromatic protons), 5.57 (d, J = 10.2, 1H, H-1), 4.29 - 4.25 (m, 1H), 4.14 (dd, J = 10.2, 1H, H-2), 3.66 – 3.55 (m, 2H, H-6a), 3.55 – 3.42 (m, 2H, H-6b), 3.37 (d, J = 4.0, 1H), 3.30 (d, J = 5.9, 1H). ^{13}C NMR (75 MHz, CDCl_3) δ = 170.13, 170.01, 134.41, 133.28, 128.95, 128.31, 123.54, 83.67, 78.59, 73.04, 72.23, 55.57, 51.59, 21.46, 20.87. ES-MS: m/z $[\text{M} + \text{Na}]^+$ calc'd for $\text{C}_{24}\text{H}_{22}\text{N}_4\text{O}_7\text{SNa}^+$: 533.1, found: 533.1.

1-O-Hexadecyl-2-O-methyl-3-O-(3',4'-O-diacetyl-2'-N-phthalimido-6'-azido-2',6'-dideoxy- β -D-glucopyranosyl)-sn-glycerol (28)

Compound **27** (0.2 g, 0.39 mmol) was glycosylated with lipid alcohol **21** (0.13 g, 0.43 mmol) according to the general method of glycosylation, to give glycolipid **28** as a yellowish white solid. Yield 47 % (0.13 g, 0.18 mmol). ^1H NMR (300 MHz, CDCl_3) δ = 7.81 (m, 4H, phthalimido aromatic protons), 5.86 (dd, J = 10.8, 9.0, 1H, H-3), 5.40 (d, J = 8.5 Hz, 1H, H-1), 5.06 (dd, J = 10., 9.0, 1H, H-4), 4.33 (dd, J = 10.8, 8.4, 1H, H-2), 3.98 – 3.83 (m, 2H), 3.63 (dd, J = 10.7, 4.9, 1H), 3.52 – 3.41 (m, 2H), 3.38 – 3.08 (m, 8H), 2.06 (s, 3H, acetate CH_3), 1.88 (s, 3H, acetate CH_3), 1.66 – 1.58 (m, 2H), 1.27 (s, 26H, lipid tail), 0.89 (t, J = 6.6 Hz, 3H, lipid terminal $-\text{CH}_3$). ^{13}C NMR (75 MHz, CDCl_3) δ = 170.11, 169.63, 134.25, 123.54, 98.47, 78.60, 73.61, 71.66, 70.41, 70.38, 69.82, 68.71, 57.59, 54.64, 51.23, 31.94, 29.71, 29.67, 29.61, 29.48, 29.37, 26.01, 22.70, 20.66, 20.48, 14.12. ES-MS: m/z $[\text{M} + \text{Na}]^+$ calc'd for $\text{C}_{38}\text{H}_{58}\text{N}_4\text{O}_{10}\text{Na}^+$: 753.4, found: 753.5.

1-O-Hexadecyl-2-O-methyl-3-O-(-2'-amino-6'-azido-2',6'-dideoxy-β-D-glucopyranosyl)-sn-glycerol (29)

Compound **31** (0.1 g, 0.14 mmol) was deprotected using the general method of simultaneous deprotection of acetate and phthalimido group to give **32** as a yellowish white solid. Yield 55 % (0.04 g, 0.08 mmol). ¹H NMR (300 MHz, MeOD) δ = 4.29 (d, *J* = 8.1, 1H, H-1), 3.95 (dd, *J* = 10.5, 4.3, 1H), 3.71 (dd, *J* = 10.5, 4.2, 1H), 3.64 – 3.51 (m, 4H), 3.51 – 3.38 (m, 7H), 3.29 – 3.20 (m, 2H, H-3), 2.70 – 2.55 (dd, *J* = 8.1, 1H, H-2), 1.59-1.52 (m 2H), 1.32 (s, 26H, lipid tail), 0.88 (t, *J* = 6.6 Hz, 3H, lipid terminal –CH₃). ¹³C NMR (75 MHz, MeOD) δ = 104.73, 80.48, 79.10, 77.41, 77.31, 72.65, 71.46, 69.44, 58.33, 58.04, 52.79, 33.10, 30.80, 30.61, 30.50, 27.25, 23.76, 14.47. ES-MS: *m/z* [M + Na]⁺ calc'd for C₂₆H₅₂N₄O₆Na: 539.4, found: 539.4.

1-O-Hexadecyl-2-O-methyl-3-O-(-2',6'-diamino-2',6'-dideoxy-β-D-glucopyranosyl)-sn-glycerol (2)

Compound **29** (0.04 g, 0.08 mmol) was treated according to the general method for azide reduction to give compound **2** as an off white solid. Yield 78 % (0.03 g, 0.06 mmol). ¹H NMR (300 MHz, MeOD) δ = 4.26 (d, *J* = 8.0, 1H, H-1), 3.95 (dd, *J* = 10.8, 4.6, 1H), 3.70 (dd, *J* = 10.6, 4.2, 1H), 3.66 – 3.45 (m, 8H), 3.33 – 3.14 (m, 3H), 3.06 (dd, *J* = 13.4, 2.7, 1H), 2.61 (dd, *J* = 9.6, 8.0, 1H, H-2), 1.66 -1.54 (m, 2H), 1.32 (s, 26H, lipid tail), 0.87 (t, *J* = 6.6 Hz, lipid terminal –CH₃). ¹³C NMR (75 MHz, MeOD) δ = 104.98, 80.58, 78.08, 77.51, 73.51, 72.68, 71.41, 69.74, 58.45, 58.17, 43.99, 33.12, 30.83, 30.79, 30.64, 30.52, 27.28, 23.78. HRMS: *m/z* [M + Na]⁺ calc'd for C₂₆H₅₄N₂O₆Na⁺: 513.3612, found: 513.3612. Elemental Analysis: calc'd: C, 63.64; H, 11.09; N, 5.71, found: C, 63.39; H, 10.88; N, 5.98.

1-O-Hexadecyl-2-O-methyl-3-O-(2'-N-phthalimido-6'-azido-2',6'-dideoxy-β-D-glucopyranosyl)-sn-glycerol (30)

Compound **28** (0.05 g, 0.07 mmol) was dissolved in methanol followed by the addition of catalytic NaOMe (0.1 equiv) and stirred for 20 mins. The reaction was stopped by with ion exchange resin (H⁺), filtered, concentrated, and purified by flash chromatography using 100 % ethyl acetate to give **30** as a yellowish white solid. Yield 62 % (0.025 g, 0.04 mmol) ¹H NMR (300 MHz, CDCl₃) δ 7.89 – 7.77 (m, 4H, phthalimido aromatic protons), 5.20 (d, *J* = 8.3 Hz, 1H, H-1), 4.34 (dd, *J* = 10.9, 8.5 Hz, 1H, H-3), 4.13 (dd, *J* = 10.9, 8.3 Hz, 1H, H-2), 3.87 (dd, *J* = 10.7, 4.6 Hz, 1H, H-6a), 3.76 - 3.66 (m, 1H), 3.62 – 3.49 (m, 4H, H-4, H-5, H-6b), 3.49 – 3.39 (m, 2H), 3.35 -3.28 (m, 2H), 3.26 (d, *J* = 4.0 Hz, 1H), 3.23 – 3.07 (m, 5H), 1.45 – 1.36 (m, 2H), 1.26 (s, 26H, lipid tail), 0.90 (t, *J* = 6.6 Hz, 3H lipid terminal –CH₃). ¹³C NMR (75 MHz, CDCl₃) δ 168.40, 134.18, 131.70, 123.42, 98.68, 78.67, 77.46, 75.23, 72.78, 71.69, 69.95, 68.32, 57.56, 56.56, 51.48, 31.94, 29.72, 29.67, 29.62, 29.47, 29.38, 26.00, 22.70, 14.13. ES-MS: *m/z* [M + Na]⁺ calc'd for C₃₄H₅₄N₄O₈Na⁺: 669.4, found: 669.4

1-O-Hexadecyl-2-O-methyl-3-O-(2'-N-phthalimido-6'-amino-2',6'-dideoxy-β-D-glucopyranosyl)-sn-glycerol (3)

Compound **30** (0.025 g, 0.04 mmol) was subjected to the general method for azide reduction to give compound **3** (0.017 g, 0.03 mmol) as light yellow solid. Yield 67 %. ¹H NMR (300 MHz, MeOD) δ 8.03 – 7.61 (m, 4H), 5.20 (d, *J* = 8.5 Hz, 1H, H-1), 4.33 (dd, *J* = 10.7, 8.6 Hz, 1H, H-3), 4.00 (dd, *J* = 10.7, 8.5 Hz, 1H, H-2), 3.87 (dd, *J* = 11.0, 4.2 Hz, 1H), 3.72 – 3.55 (m, 2H), 3.43 – 3.26 (m, 17H), 3.26 – 3.07 (m, 6H, H-6a), 2.88 (dd, *J* = 13.5, 7.5 Hz, 1H, H-6b),), 1.58 – 1.46 (m,

2H), 1.32 (s, 26H), 0.83 (t, $J = 6.8$ Hz, 3H). ^{13}C NMR (75 MHz, MeOD) δ 168.40, 134.18, 131.70, 123.42, 98.68, 78.67, 77.46, 75.23, 72.78, 71.69, 69.95, 57.56, 56.56, 52.45, 51.48, 31.94, 29.72, 29.67, 29.62, 29.47, 29.38, 26.00, 22.70, 14.13. HRMS: m/z $[\text{M} + \text{Na}]^+$ calc'd for $\text{C}_{34}\text{H}_{56}\text{N}_2\text{O}_8\text{Na}^+$: 643.3934, found: 643.3857. Elemental Analysis: calc'd: C, 65.78; H, 9.09; N, 4.51, found: C, 65.69; H, 8.99; N, 4.61.

1-O-Hexadecyl-2-deoxy-3-O-(3',4'-O-diacetyl-2'-N-phthalimido-6'-azido-2',6'-dideoxy- β -D-glucopyranosyl)-sn-glycerol (32)

Compound **27** (0.2 g, 0.39 mmol) and the previously reported lipid compound **31** (0.17 g, 0.48 mmol) were dissolved in anhydrous DCM (10.0 ml) under argon atmosphere. NIS (0.18 g, 0.80 mmol) and silver triflate (0.02 g, 0.08 mmol) were added and stirring at room temperature for 3 h. Upon completion, the reaction mixture was diluted with DCM (20.0 ml), filtered over celite, washed with saturated sodium thiosulphate solution ($\times 2$), saturated sodium bicarbonate ($\times 3$), and water ($\times 2$) successively. The organic layer was then dried over anhydrous sodium sulphate, concentrated, and purified by flash chromatography (Hexanes/EtOAc, 2:3) to give **32** (0.14 g, 0.2 mmol) as a white solid. Yield 51 %. ^1H NMR (300 MHz, CDCl_3) $\delta = 7.85$ (dd, $J = 5.5, 3.1$, 2H, phthalimido aromatic protons), 7.73 (dd, $J = 5.5, 3.1$, 2H, phthalimido aromatic protons), 5.79 (dd, $J = 10.8, 9.0$, 1H, H-3), 5.38 (d, $J = 8.5$, 1H, H-1), 5.05 (dd, $J = 10.1, 9.0$, 1H, H-4), 4.30 (dd, $J = 10.8, 8.5$, 1H, H-2), 3.96 – 3.81 (m, 2H), 3.63 – 3.52 (m, 1H), 3.43 (d, $J = 13.6, 6.9$, 1H), 3.28 – 3.16 (m, 3H), 3.15 – 2.99 (m, 2H), 2.03 (s, 3H, acetate CH_3), 1.85 (s, 3H, acetate CH_3), 1.76 – 1.58 (m, 2H), 1.26 (s, 26H, lipid tail), 0.89 (t, $J = 6.6$ Hz, 3H, lipid terminal $-\text{CH}_3$). ^{13}C NMR (75 MHz, CDCl_3) $\delta = 170.12, 169.62, 134.27, 123.57, 97.99, 73.60, 71.82, 71.00, 70.53, 70.37, 67.04, 66.96, 54.68, 51.24, 31.91, 29.73, 29.68, 29.59, 29.48, 29.34, 26.07, 22.67, 14.10$. ES-MS: m/z $[\text{M} + \text{Na}]^+$ calc'd for $\text{C}_{37}\text{H}_{56}\text{N}_4\text{O}_9\text{Na}^+$: 723.4, found: 723.5.

1-O-Hexadecyl-2-deoxy-3-O-(2'-amino-6'-azido-2',6'-dideoxy-β-D-glucopyranosyl)-sn-glycerol

(33)

Compound **32** (0.14 g, 0.20 mmol) was subjected to general method for simultaneous deprotection of acetate and phthalimido group to give **33** (0.074 g, 0.12 mmol). Yield 60 %. ¹H NMR (300 MHz, MeOD) δ = 4.28 (d, *J* = 7.9, 1H, H-1), 3.98 (dd, *J* = 9.6, 6.3, 1H), 3.69 – 3.61 (m, 1H), 3.57 – 3.53 (m, 2H), 3.51 – 3.41 (m, 5H, H-6), 3.30 – 3.21 (m, 2H, H-3), 2.63 (dd, *J* = 9.8, 7.9, 1H), 1.96 – 1.82 (m, 2H, -OCH₂-CH₂-CH₂O-), 1.66 - 1.57 (m, 2H), 1.32 (s, 26H, lipid tail), 0.86 (t, *J* = 6.7 Hz, 3H, lipid terminal -CH₃). ¹³C NMR (75 MHz, MeOD) δ = 104.54, 77.34, 72.72, 72.10, 68.77, 67.91, 58.37, 52.81, 33.12, 31.16, 30.82, 30.65, 30.52, 27.31, 23.78, 14.50. ES-MS: *m/z* [M + Na]⁺ calc'd for C₃₃H₅₂N₄O₇Na⁺: 639.4, found: 639.4.

1-O-Hexadecyl-2-deoxy-3-O-(2'6'-diamino-2',6'-dideoxy-β-D-glucopyranosyl)-sn-glycerol (**4**)

Compound **33** (0.074 g, 0.12 mmol) was subjected to the general method for azide reduction to give compound **4** (0.039 g, 0.08 mmol) as a white solid. Yield 70 %. ¹H NMR (300 MHz, MeOD) δ = 4.25 (d, *J* = 8.0, 1H, H-1), 3.99 – 3.61 (m, 2H), 3.50-3.60 (m, *J* = 6.3, 3.8, 3H), 3.45 (t, *J* = 6.5, 3H), 3.31 – 3.14 (m, 2H, H-3), 3.06 (dd, *J* = 13.4, 2.8, 1H, H-6a), 2.76 (dd, *J* = 13.4, 7.0, 1H, H-6b), 2.59 (dd, *J* = 9.5, 8.0, 1H, H-2), 1.96 – 1.82 (m, 2H, -OCH₂-CH₂-CH₂O-), 1.64 - 1.55 (m, 2H), 1.32 (s, 26H, lipid tail), 0.85 (t, *J* = 6.7 Hz, 3H, lipid terminal -CH₃). ¹³C NMR (75 MHz, MeOD) δ = 104.78, 78.00, 77.55, 73.57, 72.10, 68.70, 67.89, 58.50, 44.00, 33.11, 31.21, 30.82, 30.66, 30.51, 27.32, 23.77, 14.50. HRMS: *m/z* [M + Na]⁺ calc'd for C₂₅H₅₂N₂O₅Na⁺: 483.3774, found: 483.3781. Elemental Analysis: calc'd: C, 65.18; H, 11.38; N, 6.08, found: C, 65.43; H, 11.21; N, 5.79.

1-O-Hexadecyloxy-2S/R, 3-di (-3,4-diacetyl-6'azido-2-N-phthalimido-2',6'-dideoxy-β-D-glucopyranosyl)-glycerol (35)

Compound **27** (0.300 g, 0.59 mmol) and lipid diol **37** (0.063 g, 0.20 mmol) were subjected to the general procedure for the glycosylation reaction to give the diglycosylated glycolipid **35** (0.15 g, 0.13 mmol) as a brownish white solid. Yield 65 % (S:R, 1:1). ¹H NMR (300 MHz, CDCl₃) δ 7.95 – 7.65 (m, 8H, phthalimido aromatic protons), 5.71 (td, *J* = 10.4, 9.1 Hz, 2H, H-3a, H-3b), 5.53 (d, *J* = 8.5 Hz, 1H, H-1a), 5.20 (d, *J* = 8.4 Hz, 1H, H-1b), 5.02 (dd, *J* = 10.1, 8.9 Hz, 1H), 4.94 – 4.81 (m, 1H), 4.28-4.15 (m, 2H, H-2a), 3.97 – 3.67 (m, 4H), 3.67 – 3.28 (m, 6H, H-2b), 3.26 – 2.98 (m, 3H), 2.06 (s, 6H, acetate CH₃), 1.86 (s, 3H, acetate CH₃), 1.64 (s, 3H, acetate CH₃), 1.66 – 1.57 (m, 2H), 1.28 (s, 26H, lipid tail), 0.89 (t, *J* = 6.7 Hz, 3H, lipid terminal –CH₃). ¹³C NMR (75 MHz, CDCl₃) δ 134.30, 134.19, 123.81, 123.52, 96.74, 96.69, 76.57, 73.25, 72.90, , 71.53, 70.40, 70.39, 70.36, 70.15, 70.14, 70.12, 69.77, 69.76, 54.68, 54.41, 51.22, 51.23, 51.09, 31.89, 31.85, 29.65, 25.97, 25.87, 21.71, 22.65, 21.47, 20.68, 20.43, 14.13. ES-MS: *m/z* [M + Na]⁺ calc'd for C₅₅H₇₂N₈O₁₇Na⁺: 1139.5, found: 1139.4.

1-O-Hexadecyloxy-2S/R, 3-di(-2'-amino-6'azido-2',6'-dideoxy-β-D-glucopyranosyl)-glycerol (36)

Compound **35** (0.15 g, 0.13 mmol) was subjected to the general method for simultaneous deprotection of acetate and phthalimido protective group to give **36** (0.048 g, 0.07 mmol) as a white solid. Yield 53 % (S:R, 1:1). ¹H NMR (300 MHz, MeOD) δ 4.49 (d, *J* = 8.0 Hz, 1H, H-1a), 4.33 (dd, *J* = 8.4, 1H, H-1b), 4.16 – 3.97 (m, 2H), 3.78 (dd, *J* = 10.7, 5.5 Hz, 1H), 3.67 (dd, *J* = 5.1, 2.7 Hz, 2H), 3.59 – 3.39 (m, 2H), 3.36 – 3.22 (m, 7H, H-3a, H-3b), 2.75 – 2.54 (m, 2H, H-2a, H-2b), 1.60 (m, 2H), 1.31 (s, 26H, lipid tail), 0.93 (t, *J* = 4.5 Hz, 3H, lipid terminal –CH₃). ¹³C NMR

(75 MHz, MeOD) δ 104.87, 104.28, 78.63, 77.23, 77.05, 72.64, 72.60, 72.52, 71.57, 70.72, 58.48, 58.35, 52.79, 33.10, 30.81, 30.65, 30.49, 27.31, 23.76, 14.47. ES-MS m/z $[M + Na]^+$ calc'd for $C_{31}H_{60}N_8O_9Na^+$: 711.4, found: 711.4

1-O-Hexadecyloxy-2S/R, 3-di(-2',6'-diamino-2',6'-dideoxy- β -D-glucopyranosyl)-glycerol (5)

Compound **36** (0.048 g, 0.07 mmol) was subjected to general method for azide reduction to give compound **5** (0.032 g, 0.05 mmol) as a white solid. Yield 69 % (S:R, 1:1). 1H NMR (300 MHz, MeOD) δ 4.44 (d, $J = 8.3$ Hz, 1H, H-1a), 4.29 (d, $J = 8.4$ Hz, 1H, H-1b), 4.03 (d, $J = 14.5$ Hz, 2H), 3.8 - 3.59 (m, 3H), 3.56 - 3.35 (m, 5H), 3.28 - 3.17 (m, 4H, H-3a, H-3b), 3.15 - 3.01 (m, 2H, H-6a'', H-6b''), 2.81 - 2.69 (m, 2H, H-6a', H-6b'), 2.64 - 2.58 (m, 2H, H-2a, H-2b), 1.60 (s, 2H), 1.32 (s, 26H, lipid tail), 0.92 (t, $J = 6.8$ Hz, 3H, lipid terminal $-CH_3$). ^{13}C NMR (75 MHz, MeOD) δ 103.58, 103.27, 77.43, 76.41, 76.38, 72.11, 72.03, 70.19, 70.13, 69.47, 69.45, 57.17, 57.14, 48.04, 42.55, 42.47, 42.44, 31.61, 29.42, 29.31, 29.19, 25.77, 19.91, 23.67, 21.21, 11.80. HRMS: m/z $[M + Na]^+$ calc'd for $C_{31}H_{64}N_4O_9Na^+$: 659.4571, found: 659.2064. Elemental Analysis: calc'd: C, 58.46; H, 10.13; N, 8.80, found: C, 58.74; H, 10.22; N, 9.03.

3-Hexadecyloxy-2R-hydroxypropyl-1-para-toluenesulphonate (38)

The lipid diol **37** (2.0 g, 6.32 mmol) was dissolved in 20.0 ml DCM, cooled to 0 °C, then Et_3N (1.8 ml, 1.28 g), toluenesulphonylchloride (6.95 mmol, 1.33 g) and DMAP (0.04 g, 0.32 mmol) were added successively. The temperature was allowed to warm up to room temperature and the mixture stirred for 4 h. At the end of the reaction, mixture was diluted with ethylacetate (60.0 ml), washed with saturated aqueous ammonium chloride ($\times 3$), and brine ($\times 3$). The organic layer was dried over anhydrous sodium sulphate, concentrated, and purified using flash chromatography (hexanes/ethyl acetate, 4:1) to give **38** (1.8 g, 3.80 mmol) as a white flaky solid. Yield 60 %. 1H

NMR (300 MHz, CDCl₃) δ 7.78 (d, J = 8.2 Hz, 2H, aromatic protons), 7.33 (d, J = 8.1 Hz, 2H, aromatic protons), 4.11 – 4.00 (m, 2H, TsO-CH₂), 3.99 – 3.89 (m, 1H, HO-CH), 3.46 – 3.31 (m, 4H), 2.80 (d, J = 5.4 Hz, 1H, OH), 2.42 (s, 3H, Toluene -CH₃), 1.55 – 1.41 (m, 2H), 1.25 (s, 26H, lipid tail), 0.87 (t, J = 6.4 Hz, 3H, lipid terminal -CH₃). ¹³C NMR (75 MHz, CDCl₃) δ 144.90, 132.77, 129.88, 127.99, 71.73, 70.77, 70.56, 68.25, 31.93, 29.71, 29.68, 29.64, 29.61, 29.48, 29.37, 26.01, 22.68, 21.58, 14.11. ES-MS: m/z [M + Na]⁺ calc'd for C₂₆H₄₆NO₅Na⁺: 493.2964, found: 493.6788

3-Hexadecyloxy-2R-hydroxyl propyl-1-azide (39)

Compound **38** (1.3 g, 2.76 mmol) and sodium azide (10 equiv) were suspended in anhydrous DMF and was stirred at 90 °C for 18 h. Upon completion, the mixture was concentrated, diluted with ethyl acetate, and filtered to remove excess sodium azide. The filtrate was re-concentrated and purified with flash chromatography (hexanes/ethyl acetate, 9:1) to give **39** (0.85 g, 2.50 mmol) as a white wax-like solid. Yield 91 %. ¹H NMR (300 MHz, CDCl₃) δ 3.91 – 3.86 (m, 1H, HO-CH), 3.48 – 3.34 (m, 4H), 3.31 (dd, J = 5.5, 2.9 Hz, 2H, -CH₂N₃), 3.17 (s, 1H, OH), 1.55 – 1.41 (m, 2H), 1.25 (s, 26H, lipid tail), 0.85 (t, J = 6.6 Hz, 3H, terminal lipid -CH₃). ¹³C NMR (75 MHz, CDCl₃) δ 71.92, 71.71, 69.59, 53.54, 31.93, 29.71, 29.67, 29.61, 29.52, 29.47, 29.37, 26.05, 22.67, 14.03. ES-MS: m/z [M + Na]⁺ calc'd for C₁₉H₃₉N₃O₂Na⁺: 364.3, found: 364.5

1-O-Hexadecyloxy-2R-(3',4',6'-triacetyl-2-N-phthalimido-2'-deoxy- β -D-glucopyranosyl)-3-azido-sn-glycerol (40)

Compounds **23** (0.2 g, 0.38 mmol) and **39** (0.1 g, 0.31 mmol) were treated as describe in the general method for glycosylation reaction, to give **40** (0.12 g, 0.16 mmol) as a brownish white solid. Yield 53 %. ¹H NMR (300 MHz, CDCl₃) δ 7.97 – 7.63 (m, 4H, phthalimido aromatic protons), 5.80 (dd,

$J = 10.7, 9.1$ Hz, 1H, H-3), 5.53 (d, $J = 8.5$ Hz, 1H, H-1), 5.16 (dd, $J = 10.7$ Hz, 1H, H-4), 4.39 – 4.28 (m, 2H, H-2), 4.19 (dd, $J = 12.2, 2.5$ Hz, 1H), 3.96 – 3.73 (m, 2H, H-5), 3.60 (d, $J = 10.0, 4.8$ Hz, 1H), 3.48 – 3.30 (m, 4H), 3.27 – 3.16 (m, 1H), 2.12 (s, 3H, acetate $-CH_3$), 2.04 (s, 3H, acetate $-CH_3$), 1.88 (s, 3H, acetate $-CH_3$), 1.48 (m, 2H), 1.09 (s, 26H, lipid tail), 0.88 (t, $J = 6.6$ Hz, 3H, Lipid terminal $-CH_3$). ^{13}C NMR (75 MHz, $CDCl_3$) δ 170.58, 170.11, 169.47, 134.21, 131.56, 123.50, 98.61, 78.66, 71.96, 71.79, 70.74, 70.24, 69.03, 62.16, 54.64, 52.46, 31.93, 29.69, 29.66, 29.62, 29.58, 29.45, 29.36, 26.06, 22.69, 20.75, 20.63, 20.44, 14.11. ES-MS: m/z $[M + Na]^+$ calc'd for $C_{39}H_{58}N_4O_{11}Na^+$: 781.4, found: 781.4

1-O-Hexadecyloxy-2R-(2'-amino-2'-deoxy- β -D- glucopyranosyl)-3-azido-sn-glycerol (6)

Compound **40** (0.12 g, 0.16 mmol) was treated according to the general method for simultaneous removal of acetate and phthalimido to give **6** (0.04 g, 0.08 mmol) as an off white solid. Yield 49 %. 1H NMR (300 MHz, MeOD) δ 4.45 (d, $J = 8.0$ Hz, 1H, H-1), 4.12 – 3.95 (m, 1H), 3.74 – 3.65 (m, 3H), 3.63 – 3.54 (m, 2H), 3.51 – 3.38 (m, 4H), 3.32 – 3.27 (m, $J = 8.4$ Hz, 2H, H-3), 2.66 (dd, $J = 8.0, 6.8$, 1H, H-2), 1.64 – 1.49 (m, 2H), 1.32 (s, 26H), 0.93 (t, $J = 7.1$, Hz, 3H lipid terminal $-CH_3$). ^{13}C NMR (75 MHz, MeOD) δ 104.02, 78.30, 78.13, 77.23, 72.70, 71.78, 71.70, 62.78, 61.56, 58.30, 53.17, 33.15, 30.87, 30.83, 30.76, 30.70, 30.66, 30.55, 27.30, 23.81, 20.97, 14.57. HRMS: m/z $[M + Na]^+$ calc'd for $C_{25}H_{50}N_4O_6Na^+$: 525.3628, found: 525.3064. Elemental Analysis: calc'd: C, 59.73; H, 10.03; N, 11.15, found: C, 59.65; H, 10.13; N, 11.24

1-O-Hexadecyloxy-2R-(2'-amino-2'-deoxy- β -D- glucopyranosyl)-3-amino-sn- glycerol (7)

Compound **6** (0.03 g, 0.06 mmol) was treated according to the general method for azide reduction to give compound **7** (0.02 g, 0.04 mmol) as a white solid. Yield 65 %. 1H NMR (300 MHz, MeOD) δ 4.40 (d, $J = 8.1$ Hz, 1H, H-1), 3.93 – 3.82 (m, 1H, $-O-CH$), 3.75 – 3.67 (m, 3H), 3.60 – 3.41 (m,

4H), 3.36 – 3.22 (m, 2H, H-3), 2.97 – 2.71 (m, 2H, -CH₂NH₂), 2.63 (t, *J* = 8.4 Hz, 1H, H-2), 1.58 (m, 2H), 1.32 (s, 26H), 0.87 (t, *J* = 6.9 Hz, 3H).¹³C NMR (75 MHz, MeOD) δ 104.46, 80.02, 78.22, 77.78, 72.70, 72.67, 71.78, 62.81, 58.45, 43.77, 33.11, 30.80, 30.66, 30.51, 27.31, 23.77, 14.49. HRMS: *m/z* [M + Na]⁺ calc'd for C₂₅H₅₂N₂O₆Na⁺: 499.3723, found: 499.2997. Elemental Analysis: calc'd: C, 62.99; H, 11.00; N, 5.88, found: C, 63.05; H, 11.15; N, 6.01

2(R/S)-Azido-3-hexadecyloxy-1-propanol (44)

Compound **41** was synthesized as previously reported without any modification.²⁸ Diisopropylazodicarboxylate (DIAD; 3.2 ml, 15.00 mmol) was added to a solution of racemic mixture of 3-*O*-hexadecyl-*sn*-glycerol **34** (3.4 g, 13.00 mmol) in 180.0 ml of DCM at 0 °C. After the mixture was stirred for 3h under Nitrogen gas, Me₂SiN₃ was added. The mixture was stirred at the same temperature for additional 3 h, then at room temperature until glycerol **34** had completely reacted. The mixture was concentrated to give a yellow residue which was dissolved in a minimal amount of DCM and passed through a pad of silica gel in a sintered glass funnel. The pad was rinsed with hexane/EtOAc (50:1) until the excess yellow DIAD began to elute. After concentration of the eluted silyloxyazide, the residue was dissolved in 30.0 ml THF and treated with a solution of (nBu)₄NF (1.0 M, 25.0 ml) in THF. The mixture was stirred for 3 h at room temperature and diluted with 250.0 ml Et₂O, washed with water (×2), and brine (×2). The organic layer was separated, dried over anhydrous sodium sulphate and concentrated under vacuum. The crude product was purified by flash column chromatography (hexane/EtOAc, 4:1) to give compound **41** as a colorless gel. The NMR corresponds to previously reported data.²⁸ Yield was 50 %.

1-O-Hexadecyloxy-2S/R-azido,3-(-3',4',6'-triacetyl-2-N-phthalimido-2'-deoxy-β-D-glucopyranosyl)-glycerol (42)

The azido lipid **41** (0.28 g, 0.82 mmol) and the glycoside donor **23** (0.52 g, 0.99 mmol) were treated according to general method for glycosylation reaction to give the protected glycolipid **42** as an isomeric mixture (S:R, 1:1) (0.36 g, 0.48 mmol) of a white solid. Yield 58 %. ¹H NMR (300 MHz, CDCl₃) δ 7.85 – 7.69 (m, 4H, phthalimido aromatic protons), 5.79 (ddd, *J* = 10.7, 9.1, 4.7 Hz, 1H, H-3), 5.39 (dd, *J* = 10.9, 8.5 Hz, 1H, H-1), 5.16 (dd, *J* = 10.2, 9.1 Hz, 1H, H-4), 4.39 – 4.24 (m, 2H, H-2), 4.20 – 4.05 (m, 2H), 4.01 – 3.81 (m, 2H, H-5), 3.65 – 3.55 (m, 1H), 3.55 – 3.45 (m, 1H), 3.44 – 3.32 (m, 1H), 3.31 – 3.10 (m, 2H), 2.09 (s, 3H), 2.01 (s, 3H), 1.84 (s, 3H), 1.46 – 1.38 (m, 2H), 1.30 (s, 26H, lipid tail), 0.85 (t, *J* = 6.6 Hz, 3H, terminal lipid CH₃). ¹³C NMR (75 MHz, CDCl₃) δ 170.60, 170.06, 169.42, 134.27, 134.23, 131.47, 123.54, 98.56, 98.46, 71.96, 71.68, 71.61, 70.65, 70.59, 70.25, 69.94, 69.05, 68.91, 68.90, 61.93, 61.90, 60.54, 60.32, 59.90, 54.49, 31.90, 29.67, 29.63, 29.59, 29.55, 29.46, 29.39, 29.33, 25.90, 22.66, 20.98, 20.71, 20.58, 20.41, 14.18, 14.09. ES-MS: *m/z* [M + Na]⁺ calc'd for C₃₉H₅₈N₄O₁₁Na⁺: 781.4, found: 781.4

1-O-Hexadecyloxy-2S/R-amino-3-(-3',4',6'-triacetyl-2-N-phthalimido-2'-deoxy-β-D-glucopyranosyl)-glycerol (43)

Compound **42** (0.36 g, 0.48 mmol) was treated according to the general procedure for azide reduction to give **43** (0.25 g, 0.34 mmol) as a white solid. Yield 71 %. ¹H NMR (300 MHz, CDCl₃) δ 7.97 – 7.63 (m, 4H, phthalimido aromatic protons), 5.79 (t, *J* = 9.9 Hz, 1H, H-3), 5.35 (d, *J* = 8.4 Hz, 1H, H-1), 5.16 (t, *J* = 9.6 Hz, 1H, H-4), 4.37 – 4.29 (m, 1H, H-2), 4.22 – 4.08 (m, 1H), 3.92 – 3.77 (m, 2H, H-5), 3.75 – 3.59 (m, 1H), 3.48 (dd, *J* = 9.6, 5.3 Hz, 1H), 3.40 (dd, *J* = 9.6, 6.8 Hz, 1H), 3.26 – 3.06 (m, 3H), 3.06 – 2.94 (m, 1H, -CHNH₂), 2.25 (br. s, 2H, amino protons), 2.10 (s,

3H), 2.02 (s, 3H), 1.85 (s, 3H), 1.49 – 1.34 (m, 2H), 1.23 (s, 26H, lipid tail), 0.86 (t, $J = 6.4$ Hz, 3H, lipid terminal $-CH_3$). ^{13}C NMR (75 MHz, $CDCl_3$) δ 170.67, 170.12, 169.47, 134.34, 131.37, 123.62, 98.58, 98.37, 72.64, 72.48, 72.32, 71.88, 71.42, 70.71, 69.01, 62.02, 58.10, 54.65, 50.66, 50.61, 31.90, 29.68, 29.64, 29.58, 29.52, 29.45, 29.34, 26.05, 22.67, 20.74, 20.61, 20.43, 18.40, 14.10. ES-MS: m/z $[M + Na]^+$ calc'd for $C_{39}H_{60}N_2O_{11}Na^+$: 755.4, found: 755.4

1-O-Hexadecyloxy-2S/R-amino-3-(-2'-amino-2'-deoxy- β -D- glucopyranosyl)-glycerol (8)

Compound **43** (0.03 g, 0.04 mmol) was treated according to the general procedure for simultaneous removal acetate and phthalimido protecting group to give **8** (0.01 g, 0.023 mmol) as a white solid. Yield 57 % (S:R, 1:1). 1H NMR (300 MHz, MeOD) δ 4.70 (dd, $J = 8.3, 3.1$ Hz, 1H, H-1), 4.19 – 4.02 (m, 1H), 4.01 – 3.87 (m, 2H), 3.79 – 3.73 (m, 1H), 3.72 – 3.61 (m, 3H), 3.65 – 3.57 (m, 1H, H-3), 3.57 – 3.48 (m, 2H), 3.49 -3.32 (m, 2H, $-CHNH_2$), 2.96 (dd, $J = 10.3, 8.4$ Hz, 1H, H-2), 1.71 – 1.55 (m, 2H), 1.33 (s, 26H, lipid tail), 0.92 (t, $J = 6.4$ Hz, 3H, lipid terminal $-CH_3$). ^{13}C NMR (75 MHz, MeOD) δ 100.58, 100.18, 78.63, 73.85, 72.93, 71.74, 71.65, 68.58, 68.43, 62.15, 62.10, 52.72, 52.69, 33.09, 30.80, 30.77, 30.64, 30.53, 30.48, 27.13, 23.75. HRMS: m/z $[M + Na]^+$ calc'd for $C_{25}H_{52}N_2O_6Na^+$: 499.3723, found: 499.3450. Elemental Analysis: calc'd: C, 62.73; H, 11.00; N, 5.88, found: C, 62.99; H, 10.78; N, 5.55

1-O-Hexadecyloxy-2S/R-N-hexadecylacyl-3-(-3',4',6'-triacetyl-2-N-phthalimido-2'-deoxy- β -D- glucopyranosyl)-glycerol (45)

Compound **43** (0.13 g, 18.00 μ mol) was dissolved in 10.0 ml of anhydrous DMF. Palmitic acid **44** (0.054 g, 0.21 μ mol) and the coupling agent TBTU (0.08 g, 0.25 μ mol) were subsequently added under argon atmosphere, and stirred for 5 h at room temperature. After complete disappearance of **43**, the reaction mixture was concentrated and purified by flash chromatography

(hexanes/EtOAc, 4:1) to give **45** (0.1 g, 0.11 mmol) as a white compound which was characterized as deblocked analogue **9** Yield 60 %. ES-MS: m/z $[M + Na]^+$ calc'd for $C_{55}H_{90}N_2O_{12}Na^+$: 993.6, found: 993.4

1-O-Hexadecyloxy-2S/R-N-hexadecylacyl-3-(-2'-amino-2'-deoxy- β -D-glucoopyranosyl)-glycerol
(9)

Compound **45** (0.1 g, 0.11 mmol) was subjected to the treatment of the general method for simultaneous deprotection of acetate and phthalimido protecting group to give compound **9** (0.05 g, 0.06 mmol) as a white solid (S:R, 1:1). Yield was 58 %. 1H NMR (300 MHz, MeOD) δ 4.59 (dd, $J = 8.3, 6.3$ Hz, 1H, H-1 R/S), 4.42 – 4.20 (m, 1H, H-4 R/S), 3.92 (dd, $J = 12.1, 4.3$ Hz, 2H, H-6a R/S), 3.83 – 3.63 (m, 3H, H-6b R/S), 3.66 – 3.44 (m, 6H, H-3 R/S), 2.89 – 2.71 (m, 1H, H-2 R/S), 2.29 – 2.17 (m, 2H, -NHCO- CH_2), 1.71 - 1.51 (m, 4H), 1.33 (s, 50H, two lipid tails), 0.93 (t, $J = 6.2$ Hz, 6H, terminal - CH_3 of the two lipid tails). ^{13}C NMR (75 MHz, MeOD) δ 176.79, 100.75, 100.45, 78.56, 74.02, 72.49, 72.45, 71.81, 71.02, 70.71, 70.53, 62.32, 57.54, 55.16, 50.52, 50.39, 49.88, 37.29, 37.19, 33.11, 30.85, 30.81, 30.74, 30.59, 30.52, 30.30, 27.33, 27.13, 23.77, 14.48. HRMS: m/z $[M + Na]^+$ calc'd for $C_{41}H_{82}N_2O_7Na^+$: 737.6020, found: 737.3607. Elemental Analysis: calc'd: C, 68.86; H, 11.56; N, 3.92, found: C, 68.66; H, 11.73; N, 3.89

1-O-Hexadecyloxy-2S/R-N-methylcarbamoyl-3-(-3',4',6'-triacyl-2-N-phthalimido-2'-deoxy- β -D- glucoopyranosyl)-glycerol (**47**)

To a solution of compound **43** (0.12 g, 0.16 mmol) in DCM was added methylchloroformate **46** (0.03 g, 0.31 mmol) and Et_3N (0.04 g, 0.35 mmol) at 0 °C. The mixture was stirred overnight and concentrated under vacuum to give residue, which was purified by flash chromatography (hexanes/EtOAc, 3:2) to give the carbamate glycolipid **47** (0.1 g, 0.13 mmol) as a white solid (S:R,

1:1).¹⁵ Yield 80 %. ¹H NMR (300 MHz, CDCl₃) δ 7.92 – 7.68 (m, 4H, phthalimido aromatic protons), 5.79 (dd, *J* = 10.7, 9.1 Hz, 1H, H-3), 5.35 (d, *J* = 8.4 Hz, 1H, H-1), 4.83 (d, *J* = 7.4 Hz, 1H, carbamate -NH), 4.42 – 4.23 (m, 2H), 4.19 – 4.15 (m, 1H), 3.88 – 3.71 (m, 4H), 3.53 (s, 3H, carbamate -CH₃), 3.35 - 28 (m, 2H), 3.15 – 3.08 (m, 2H), 2.11 (s, 3H), 2.02 (s, 3H), 1.85 (s, 3H), 1.45 – 1.34 (m, 2H), 1.27 (s, 26H, lipid tail), 0.88 (t, *J* = 6.4 Hz, 3H, lipid terminal -CH₃). ¹³C NMR (75 MHz, CDCl₃) δ 170.69, 170.11, 169.47, 134.32, 134.28, 131.42, 123.62, 98.49, 98.39, 71.89, 71.39, 71.32, 70.67, 70.63, 68.95, 68.91, 68.76, 68.66, 61.98, 54.59, 31.91, 29.69, 29.64, 29.58, 29.45, 29.34, 26.00, 25.97, 22.67, 20.73, 20.61, 20.43, 14.11. ES-MS: *m/z* [M + Na]⁺ calc'd for C₄₁H₆₂N₂O₁₃Na⁺: 813.4, found: 813.3

1-O-Hexadecyloxy-2S/R-N-methylcarbamoyl-(2'-amino-2'-deoxy-β-D-glucopyranosyl)-glycerol
(10)

The protected carbamate glycolipid **47** (0.1 g, 0.13 mmol) was deprotected using the general method for simultaneous removal of acetate and phthalimido protecting group to give compound **10** (0.033 g, 0.06 mmol) as a white solid (S:R, 1:1). Yield 47 %. ¹H NMR (300 MHz, MeOD) δ 4.26 (dd, *J* = 8.1, 2.4 Hz, 1H, H-1), 4.00 – 3.89 (m, 2H), 3.87 (d, *J* = 1.5 Hz, 1H), 3.76 – 3.68 (m, 2H), 3.66 (s, 3H, carbamate -CH₃), 5.55 - 3.44 (m 4H, H-3), 3.38 – 3.22 (m, 3H), 2.65 – 2.58 (m, 1H, H-2) 1.60 – 1.55 (m, 2H), 1.31 (s, 26H, lipid tail), 0.92 (t, *J* = 6.8 Hz, 3H, lipid terminal -CH₃). ¹³C NMR (75 MHz, MeOD) δ 105.05, 104.71, 78.23, 77.57, 77.51, 72.44, 71.84, 71.74, 70.97, 70.60, 70.28, 62.80, 62.69, 58.36, 58.34, 52.56, 52.23, 33.11, 30.82, 30.79, 30.65, 30.59, 30.50, 27.27, 23.77, 14.49. HRMS: *m/z* [M + Na]⁺ calc'd for C₂₇H₅₄N₂O₈Na⁺: 557.3778, found: 557.3364. Elemental Analysis: calc'd: C, 60.65; H, 10.18; N, 5.24 found: C, 60.82; H, 10.31; N, 5.19.

5.6.3. Biological methods

5.6.3.1. Effect of GAELs on viability of epithelial cancer cell lines

The cell lines were cultured from frozen stocks originally obtained from ATCC. MDA-MB-231, JIMT-1, DU145 were grown in DMEM medium supplemented with 10% FBS. BT474 cells were grown in DMEM/F12 medium supplemented with 10% FBS. MiaPaCa2 was cultured in DMEM supplemented with 10% FBS and 2.5% horse serum. PC3 cells were cultured in F12K medium supplemented with 10% FBS. All the media contained penicillin/streptomycin.

The effects of the GAELs on the viability of the various epithelial cancer cell lines was determined as previously described.^{12,13,16} Briefly equal numbers of the cells were dispersed into 96-well plates. After 24 h, the cells were incubated with the compounds (0-30 μ M) for 48 h. At the end of the incubation, MTS reagent (20% vol/vol) was added and the plates were incubated for 1-4 h in a CO₂ incubator. The OD₄₉₀ was read with a plate reader (Molecular Devices). Wells with media but no cells were treated in similar fashion and the values utilized as blank. The results represent the mean \pm standard deviation of 6 independent determinations.

5.6.3.2. Isolation of breast cancer stem cells from BT-474 and prostate cancer stem cells from DU145 cell lines and determination of the effect of GAELs on the viability of the cancer stem cells.

A population enriched in BT474 breast cancer stem cells or DU145 prostate cancer stem cells was obtained by staining the cells for aldehyde dehydrogenase using the Aldefluor assay kit from Stem Cell Technologies (Vancouver, BC, Canada) according to the instruction of the manufacturer with the appropriate controls. The stained cells were sorted from the bulk population by flow cytometry on a 4 laser MoFloXPP high speed/pressure cell sorter. The cells were pelleted by centrifugation.

BT474 cells were resuspended into ultra-low adhesion plates in mammoCult medium (Stem cell Technologies). The DU145 stem cells were resuspended in their growth medium (DMEM/F12 medium supplemented with 20 ng/ml EGF, and 10 ng/ml basic FGF, 5 µg/ml insulin, 0.4% BSA, with 1% antibiotics).³⁶ The dishes were incubated at 37 °C in a CO₂ incubator for 4 days for spheroid formation.

The spheres are separated from single cells with a 40 µm nylon cell strainer. The spheres retained in the strainer were washed with PBS and trypsinised to obtain single cells. The cell numbers were counted with a Coulter ZM counter and the cells were dispersed into 48-well low adhesion plates (Grenier) in a volume of 500 µl. The cells were incubated for 4 days to allow for formation of spheroids. Subsequently, the stock GAELs in ethanol were diluted to twice the final concentration in the media and a volume of 500 µl was added to the wells. Wells with growth medium but no cells were treated as the wells with cells. After 5 days incubation, MTS reagent (2% vol/vol) was added to each well and the plates were incubated for 1-4 hrs for formation of colour. The OD₄₉₀ were read in a Molecular Device absorbance plate reader using the SpectroMax software.

5.6.3.3. Statistical analysis

The results represent the mean ± standard deviation of 6 independent determinations. Statistical significant difference test were carried using GraphPadInstat software. The data, that is, the mean values were subjected to one way analysis of variance (ANOVA) followed by Tukey-Kramer multiple comparison tests as post hoc test. Comparisons were carried out between the viability of controls and drug treated cells to determine if statistically significant differences existed between the two groups. The results of the effects of different concentrations of the compounds were also compared for statistically significant differences to determine if the cytotoxic activities of the drugs

are dose dependent. The anticancer activities of all the compounds **1-10** tested and the lead compound β -GLN were also compared using ANOVA followed by Tukey-Kramer multiple comparison tests at the following concentrations: 5, 7.5 and 10 μ M to determine if the difference in the potency of the drugs are statistically significant or not. A p value > 0.05 indicates no statistical differences while a p value <0.001 indicated statistical significant differences. The statistical analysis data are not included in this report.

5.7. Acknowledgements

This study was supported by research grants from the Canadian Breast Cancer Foundation Prairie/NWT to GA and Natural Science and Engineering Council of Canada (NSERC) grant to FS. Makanjuola Ogunsina is the recipient of a University of Manitoba and Manitoba provincial government graduate fellowships (UMGF and MGS).

5.8. References

- (1) World Cancer report 2014: UN News,
http://www.un.org/apps/news/story.asp/story.asp?NewsID=47067&Cr=cancer&Cr1=#.U1R-3WwU_IU (Viewed April 20, 2014).
- (2) Tan, D. S.; Gerlinger, M. B.; Swanton, C. Anti-cancer drug resistance: Understanding the mechanisms through the use of integrative genomics and functional RNA interference. *Eur. J. Cancer* **2010**, 46, 2166–2177.
- (3) Li, X.; Lewis, M. T.; Huang, J.; Gutierrez, C.; Osborne, C. K.; Wu, M. F. Intrinsic resistance of tumorigenic breast cancer cells to chemotherapy. *J. Natl. Cancer Inst.* **2008**, 100, 672–679.
- (4) Tanner, M.; Kapanen, A. I.; Junttila, T.; Raheem, O.; Grenman, S.; Elo, J.; Elenius, K.; Isola, J. Characterization of a novel cell line established from a patient with Herceptin-resistant breast cancer. *Mol. Cancer Ther.* **2004**, 3, 1585–1592.
- (5) Ajani, J. A.; Izzo, J. G.; Lee, J-S. Chemotherapy and Radiotherapy Resistance: Complexity, Reality, and Promise. *J. Clin. Oncol.* **2009**, 27, 162-163).
- (6) Garvalov, B. K.; Acker, T. Cancer stem cells: a new framework for the design of tumor therapies *J. Mol. Med.* **2011**, 89, 95–107.
- (7) Zabalova, R.; Stantic, M.; Stapelberg, M.; Prokopova, K.; Dong, J.; Truksa, J. et al, Drugs that Kill Cancer Stem-like Cells. In: Shostak S, editor. *Cancer Stem Cells Theories and Practice*, ISBN: 978-953-307-225-8, **2011**).
- (8) Naujokat, C.; Fuchs, D.; Opelz, G. Salinomycin in cancer: a new mission for an old agent. *Mol. Med. Rep.* **2010**, 3, 555-559.

- (9) Guzman, M.L.; Karnischky, L.; Peterson, D.R.; Howard, D.S.; Jordan C.T. The sesquiterpene lactone parthenolide induces apoptosis of human acute myelogenous leukemia and progenitor cells. *Blood* **2005**, 4163-4169.
- (10) Xiao, Z.; Sperl, B.; Ullrich, A.; Knyazev, P. Metformin and salinomycin as the best combination for the eradication of NSCLC monolayer cells and their alveospheres (cancer stem cells) irrespective of EGFR, KRAS, EML4/ALK and LKB1 status. *Oncotarget* **2014**, 5, 12877-12890
- (11) Fuchs, D.; Daniel, V.; Sadeghi, M.; Opelz, G.; Naujokat, C. Salinomycin overcomes ABC transporter mediated multidrug and apoptosis resistance in human leukemia stem cell-like KG-1a cells. *Biochem. Biophys. Res. Commun.* **2010**, 394, 1098-1104.
- (12) Fuchs, D.; Heinold, A.; Opelz, G.; Daniel, V.; Naujokat, C. Salinomycin induces apoptosis and overcome apoptosis resistance in human cancer cells. *Biochem. Biophys. Res. Commun.* **2009**, 390, 743-749.
- (13) Gong, C.; Yao, H.; Liu, Q.; Chen, J.; Shi, J.; Su, F.; Song, E. Marker of tumor initiating cells predict chemoresistance in breast cancer. *Plos ONE* **2010**, 5, Article ID e15630.
- (14) Kim, K.Y.; Yu, S.N.; Lee, S. Y.; Salinomycin –induced apoptosis of human prostate cancer cells due to accumulated reactive oxygen species and mitochondrial membrane depolarization. *Biochem. Biophys. Res. Commun.* **2011**, 413, 80-86.
- (15) Bardsley, M.R.; Horvth, V.J.; Azuzu, D.T. Kitlow stem cells cause resistance to kit/platelet-derived growth factor α inhibitors in murine gastrointestinal stromal tumors. *Gastroenterology* **2010**, 139, 942-952.

- (16) Zhang, G.N.; Liang, Y.; Zhou, J.; Chen, S.; Chen, G.; Zhanga, T.; Kang, T.; Zhao Y. Combination of salinomycin and gemcitabine eliminates pancreatic cancer cells. *Cancer let.* **2011**, 313, 137-144
- (17) Zhang, Y.; Zhang, H.; Wang, J.; Wang, X.; Zhang, Q. The eradication of breast cancer and cancer stem cells using octrotide modified paclitaxel active targeting micelles and salinomycin passive targeting micelles. *Biomaterials* **2012**, 33, 679-691
- (18) Erukulla, R. V.; Zhou, X.; Samadder, P.; Arthur, G.; Bittman, R. Synthesis and Evaluation of the Antiproliferative Effects of 1-O-Hexadecyl-2-Omethyl-3-O-(2-acetamido-2-deoxy- β -D-glucopyranosyl)-*sn*-glycerol and 1-O-Hexadecyl-2-O-methyl-3-O-(2-amino-2-deoxy- β -D-glucopyranosyl)-*sn*-glycerol on Epithelial Cancer Cell Growth. *J. Med. Chem.* **1996**, 39, 1545–1548
- (19) Samadder, P.; Bittman, R.; Byun, H. S.; Arthur, G. A glycosylated antitumor ether lipid kills cells via paraptosis-like cell death. *Biochem. Cell Biol.* **2009**, 87, 401–414
- (20) Samadder, P.; Byun, H.S.; Bittman, R.; Arthur, G. An active endocytosis pathway is required for the cytotoxic effects of glycosylated antitumor ether lipids. *Anticancer Res.* **2011**, 31, 3809–3818
- (21) Samadder, P.; Byun, H.; Bittman, R.; Arthur, G. Glycosylated antitumor ether lipids are more effective against oncogene-transformed fibroblasts than alkyllysophospholipids. *Anticancer Res.* **1998**, 18, 465–470
- (22) Samadder P.; Xu Y.; Schweizer F.; Arthur G. Cytotoxic properties of D-gluco-, D-galacto- and D-manno-configured 2-amino-2-deoxy-glycerolipids against epithelial

cancer cell lines and BT-474 breast cancer stem cells. *Eur. J. Med. Chem.* **2014**, 78,225-235

- (23) Xu, Y.; Ogunsina, M.; Samadder, P.; Arthur, G.; Schweizer, F. Structure-activity relationships of glucosamine-derived glycerolipids: the role of the anomeric linkage, the cationic charge and the glycerol moiety on the antitumor activity. *ChemMedChem* **2013**, 8, 511–520)
- (24) Ogunsina, M.; Pan H, Samadder, P.; Arthur, G.; Schweizer, F. Structure Activity Relationships of N-linked and Diglycosylated Glucosamine-Based Antitumor Glycerolipids. *Molecules*, **2013**, 18, 15288-15304.
- (25) Miyachi, H.; Azuma, A.; Ogasawara, A.; Uchimura, E.; Watanabe, N.; Kobayashi, Y.; Kato, F.; Kato, M.; Hashimoto, Y. Novel Biological Response Modifiers: Phthalimides with Tumor Necrosis Factor- α Production-Regulating Activity. *J. Med. Chem.* **1997**,40, 2858-2865.
- (26) Zahran, M. A. H.; Abdin, Y. G.; Osman, A. M. A.; Gamal-Eldeen, A. M.; Talaat, R. M.; Pedersen, E. B. Synthesis and Evaluation of Thalidomide and Phthalimide Esters as Antitumor Agents. *Arch. Pharm.*, 2014, 347, 642–649.
- (27) Schweizer F. Cationic amphiphilic peptides with cancer-selective toxicity. *Eur. J. Pharmacol.* **2009**, 625, 190-194
- (28) Byun, H-S.;Bittman, R.; Samadder, P.; Arthur, G. Synthesis and antitumor activity of ether glycerol-phospholipids bearing a carbamate moiety at the *sn*-2 position: selective sensitivity against prostate cancer cell lines. *ChemMedChem* **2010**, 5, 1045-1052)
- (29) Jahreiss, L.;Renna, M.; Bittman, R.; Arthur, G.; Rubinsztein, D. C. 1-O-hexadecyl-2-O-methyl-3-O-(2''acetamido-2''-deoxy- β -D-glucopyranosyl)-*sn*-glycerol

(GLN) induces cell death with more autophagosomes which is autophagy-independent.

Autophagy **2009**, 5,835–846).

- (30) Bera, S.; Dhondikubeer, R.; Findlay, B.; Zhanel, G.G.; Schweizer, F. Synthesis and antibacterial activities of Neomycin B-based lipids. *Molecules* **2012**, 17, 9129–9141
- (31) Antoszczak, M.; Huczyński, A. Anticancer Activity of Polyether Ionophore-Salinomycin *Anticancer Agents Med. Chem.* **2015**;15, 575-591
- (32) Arthur, G.; Bittman, R. Glycosylated antitumor ether lipids: activity and mechanism of action. *Anticancer Agents Med. Chem.* **2014**, 14, 592-596
- (33) Ning, X.; Shu, J.; Du, Y.; Ben, Q.; Li, Z. Therapeutic strategies targeting cancer stem cells. *Cancer Biol. Ther.* **2013**, 14, 295 - 303
- (34) Chen, K.; Huang, Y.; Chen, J. Understanding and targeting cancer stem cells: therapeutic implications and challenges. *Acta Pharmacol. Sin.* **2013**, 34, 732-740.
- (35) Oishi, N.; Wang, X. W. Novel therapeutic strategies for targeting liver cancer stem cells. *Int.J.Biol.Sci.* **2011**, 7, 517 – 535
- (36) Salvatori L.; Caporuscio F.; Verdina A.; Starace G.; Crispi S.; Nicotra M.R. et al. Cell-to-Cell Signaling Influences the Fate of Prostate Cancer Stem Cells and Their Potential to Generate More Aggressive Tumors. *PLoS ONE* **2012**, 7(2), e31467. doi:10.1371/journal.pone.0031467.

Chapter 6.

Replacing D-glucosamine with its L-enantiomer in glycosylated antitumor ether lipids (GAELs) retains cytotoxic effects against epithelial cancer cells and cancer stem cells

By Makanjuola Ogunsina, Pranati Samadder, Gilbert Arthur and Frank Schweizer.

To be revised for submission to J. Med. Chem.

6.1. Authorship considerations

Makanjuola Ogunsina was responsible for design, synthesis, purification and characterization of all glycolipids on the advice of Frank Schweizer. Biological studies were investigated by Makanjuola Ogunsina and Pranati Samadder on the advice of Gilbert Arthur. The preliminary draft of the paper was written by Makanjuola Ogunsina reviewed by Frank Schweizer and Gilbert Arthur, and then rendered into its final form by Makanjuola Ogunsina. Frank Schweizer and Gilbert Arthur are corresponding authors.

6.2. Abstract

Increasing evidence suggests that failure to cure cancer is due to the inability of current antitumor drugs to eradicate cancer stem cells (CSCs). We previously described D-glucosamine-based glycosylated antitumor ether lipids (D-GAELs) that were cytotoxic to CSCs. However, their susceptibility to metabolism makes them unsuitable for clinical development. Here, we describe metabolically inert L-glucosamine-based L-GAELs that retain the cytotoxic effects of the D-analogs including the ability to kill BT-474 breast CSCs. Adriamycin and cisplatin were unable to kill > 72% and > 30% of BT-474 CSCs respectively at (20 μ M) while the most potent L-GAELs achieved > 95% killing at 7.5 μ M. Moreover, the activity of L-GAELs was superior to

the anti CSC agent salinomycin. Mode of action studies indicate that L-GAELs like the D-GAELs kill cells via an apoptosis-independent mechanism that was not due to membranolytic effects. Therefore, replacing D-glucosamine with its L-sugar analogs had no effect on the activity and mechanism of action of GAELs. Thus the use of L-GAELs opens up new opportunities to develop metabolically inert L-sugar based antitumor agents.

6.3. Introduction

Glycosylated Antitumor Ether Lipids (GAELs) such as **1** are an emerging class of glycolipids with potent cytotoxicity against human epithelial cancer cell lines.¹⁻³ Unique features of GAELs include their apoptosis-independent mechanism of cell death, likely through methuosis^{4,5} and an ability to kill cancer stem cells (CSCs)³ a rare property not found in most clinical anticancer drugs. Increasing experimental data supports the notion that CSCs are responsible for tumor metastasis, relapse and resistance to both radio- and chemo-therapy.⁶ Therefore, effective anti-CSCs agents are required in the fight against cancer. In addition, induction of non-apoptotic cell death in cancer is an attractive approach that would avoid cross-resistance, a common challenge observed in cancer treatment with pro-apoptotic drugs. Although GAELs are active *in vitro*, lack of *in vivo* anticancer activity has impeded their development as clinically useful drugs.⁷ This inactivity has been ascribed to glycosidase-catalysed metabolic cleavage⁸ a problem bedeviling many carbohydrate-based lead structures.^[11] The sugar moieties employed to date in the development of GAELs are D-sugars of glucose, glucosamine, galactose, galactosamine, mannose and mannosamine^{3,4} that occur naturally in humans and are susceptible to degradation by human glycosidases. To prevent *in vivo* metabolic degradation of GAELs, a variety of strategies have been attempted including the synthesis of analogs with glycosidic thio-, triazole- and N-acylated-, as well as C-glycosidic linkages.^{2,4,7} However, with

the exception of C-glycosides, the resultant molecules showed significantly reduced antitumor activity. As the synthesis of D-glucosamine-based C-glycosides is lengthy, we explored the use of unnatural O-glycosidic L-gluco-configured GAELs (L-GAELs). L-Glucose, the enantiomer of D-glucose and its amino analog, L-glucosamine occur rarely in nature but can be produced by *Streptomyces griseus* in the form of N-methyl-L-glucosamine, a component of streptomycin. Metabolic studies, *in vitro* and *in vivo*, demonstrated that L-glucose is not metabolised in rats and yeast.^{9,10} This inability to metabolize L-glucose (and L-glycosides) is because enzymes involved in sugar metabolism in humans and animals are specific for D-glycosides.¹¹ We therefore hypothesized that metabolically inert L-GAELs may retain their potent antitumor properties. Here we present results confirming that L-glucosamine-based GAELs are active against human epithelial cancer cell lines derived from breast, prostate, and pancreatic tumors. We demonstrate that L-GAELs possess superior anti CSC properties when compared to salinomycin, a widely studied CSC cytotoxic agent and other clinically used anticancer drugs. We also provide insight into the mechanism of cell killing by L-glucosamine based GAELs.

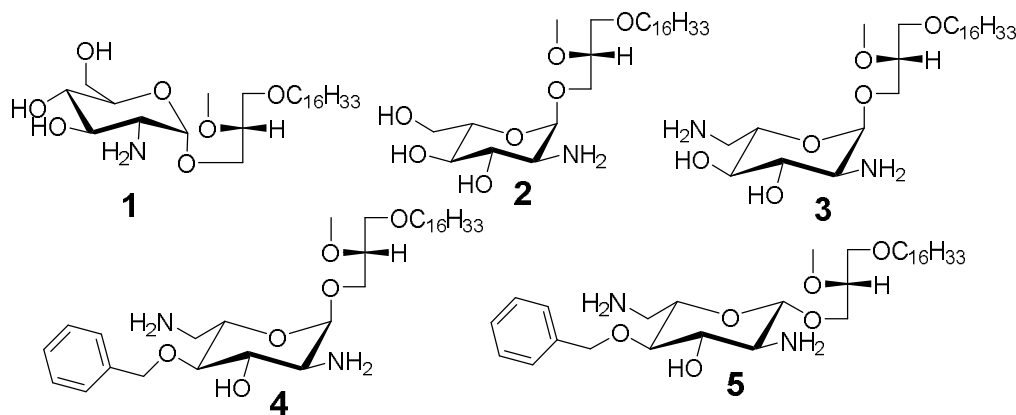
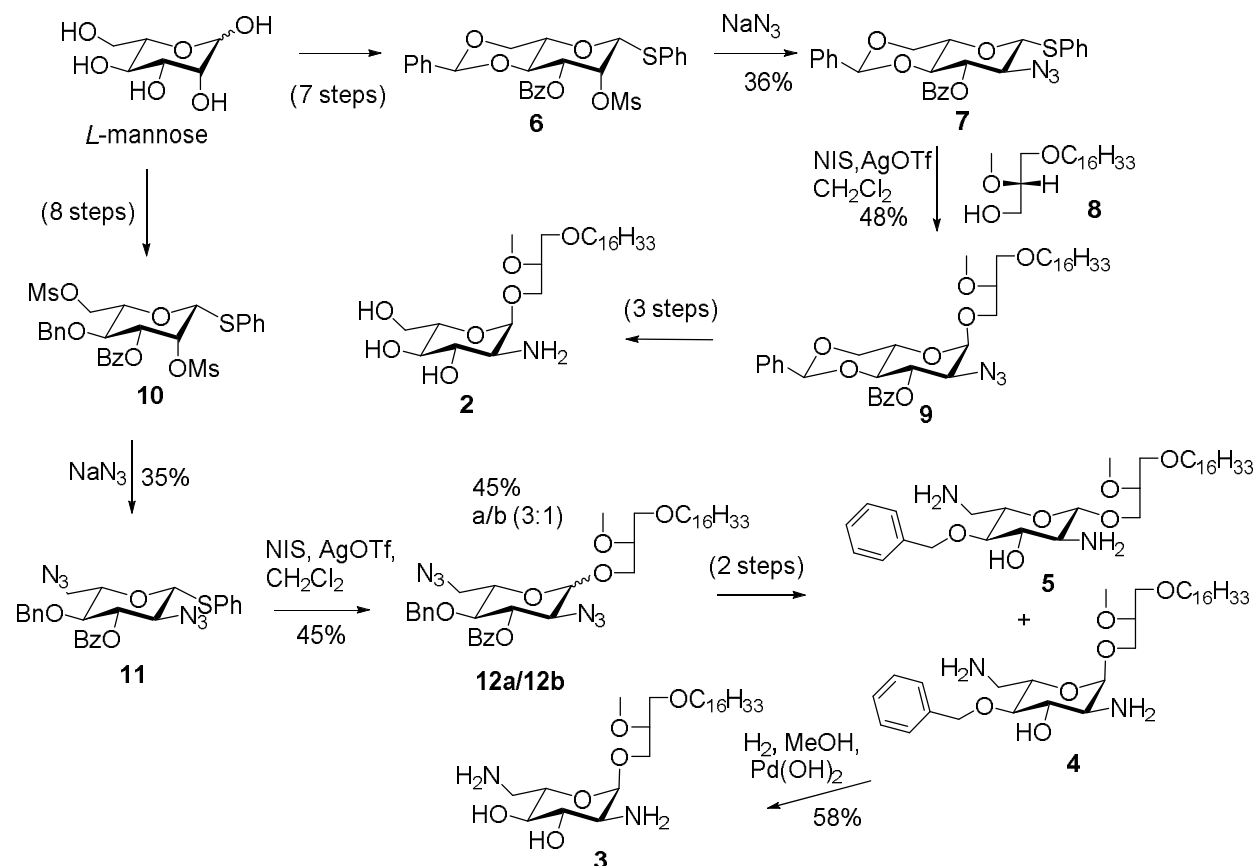


Figure 6.1. Structures of D- and L-glucosamine-based glycosylated antitumor ether lipids (GAELs) 1-5.

6.4. Result and Discussion

Previous SAR studies on D-GAELs have demonstrated that the antitumor properties of GAELs is affected by the nature of the sugar and the glycosidic linkage. These studies identified compound **1** as a potent GAEL (Figure 6.1).² A key feature of **1** is the presence of a primary amino function at the 2-position of D-glucose which is crucial for anticancer activity. Replacement of the primary amino function by hydroxyl-, azido, guanidino or benzyl-substituted amines-based resulted in a > 3-fold reduced cytotoxic activity.^{2,4,12} To study how substitution of the D-glucose moiety in **1** by L-glucose affects the antitumor properties we prepared *L-gluco*-based analog **2**. Moreover, we also prepared the diamino *L-gluco* based analog **3** to study how the presence of a second amino substituent at the 6-position of L-glucose affects the antitumor properties. In addition, compounds **4** and **5** were prepared to assess how decoration of the L-glucose scaffold and the nature of the L-glycosidic linkage affects the antitumor properties (Figure 6.1). The synthesis of L-GAELs **2-5** is outlined in Scheme 1. Because L-glucosamine is not commercially available, synthesis of **2** was initiated by conversion of commercially available L-mannose to activated thioglycoside **6** prepared in 7 steps. Displacement of the axial sulfonate ester with sodium azide afforded thioglycoside donor **7** which was coupled to commercially available lipid alcohol **8** to yield glycolipid **9**. Deblocking of the benzylidene- and benzoate-protecting groups and reduction of the azide function afforded desired L-glucosamine-based glycolipid **2**. The synthesis of the diamino-based L-GAELs **3-5** were prepared by double substitution of the bissulfonate ester **10** produced in 8 steps from L-mannose with sodiumazide to produce diazido-based thioglycoside donor **11**. Thioglycoside donor **11** was coupled to acceptor **8** to produce an anomeric mixture of glycolipids **12a** and **12b** ($\alpha:\beta$ ratio = 3:1). Hydrolysis of the benzoyl ester group in **12a** and **12b** followed by reduction of the azido function gave the desired

diamino L-GAELs **4** and **5**. Debenzylation of **4** using catalytic hydrogenation afforded diamino lipid **3** (Schemes 6.1 and S1).



Scheme 6.1. Synthetic strategy used to prepare L-glucosamine-based L-GAELs **2-5**.

The cytotoxicity of the L-GAELs **2-5** were investigated using six cell lines derived from human tumors: breast (BT-474, JIMT-1, MDA-MB-231), prostate (PC-3, DU-145) and pancreas (MiaPaCa-2). Compounds **2-5** were compared to the D-glucosamine-analog **1**, cisplatin and salinomycin, an experimental anti CSC agent (Figures 6.2, S1 and Table S1).¹⁴

L-GAEL **2** displayed cytotoxicity similar to that of the D-analog. The cytotoxic concentration that kill 50% of the cancer cells (CC_{50}) for compound **2**, 6.5 – 13.0 μM depending on the cell line, is similar to that of **1** 6.0 – 10.5 μM depending on the cell line. These results show that the

cytotoxic activity is retained when D-glucosamine is substituted with L-glucosamine in GAELs. In comparison to **2**, the diamino L-gluco analog **3** (CC₅₀ 4.0 – 11.0) shows improved antitumor properties across the panel of the epithelial cells. The benzylated analogs **4** and **5** were the most active in this series with very similar CC₅₀ values in the range of 2.0 - 6.0 μM across the panel of epithelial cells indicating that the anomeric configuration does not affect activity. This observation is in contrast to what was observed in our studies with the D-sugar GAEL series where we noticed that the α-anomer was slightly more active than the β-anomer.^{2,3}

Comparison of L-gluco derived GAELs with the cisplatin, revealed that all L-GAELs showed superior anticancer activity than cisplatin. Salinomycin was also less active than compounds **3-5** (Figure 6.2, Table S1). Adriamycin was more potent than GAELs **1-5** with respect to CC₅₀ concentrations, and possibly CC₉₀ values. Although adriamycin concentrations beyond 2 μM were not assessed in light of the fact that high concentrations are avoided *in vivo* due to its toxicity. However, in our studies, adriamycin did not achieve 90% cell death at concentrations between 2-25x the CC₅₀ value (Table S1, Figure S2). Unlike adriamycin, most of GAEL analogs exhibit > 90% cell death at less than two times the CC₅₀ concentration suggesting that L-GAELs may potentially eliminate tumor cells *in vivo* (Table S1, Figure S2). Moreover, the most potent L-GAELs **4** and **5** achieved > 95% cell death at 7.5 μM for all six tested epithelial cell lines (Figure 6.2 and S2).

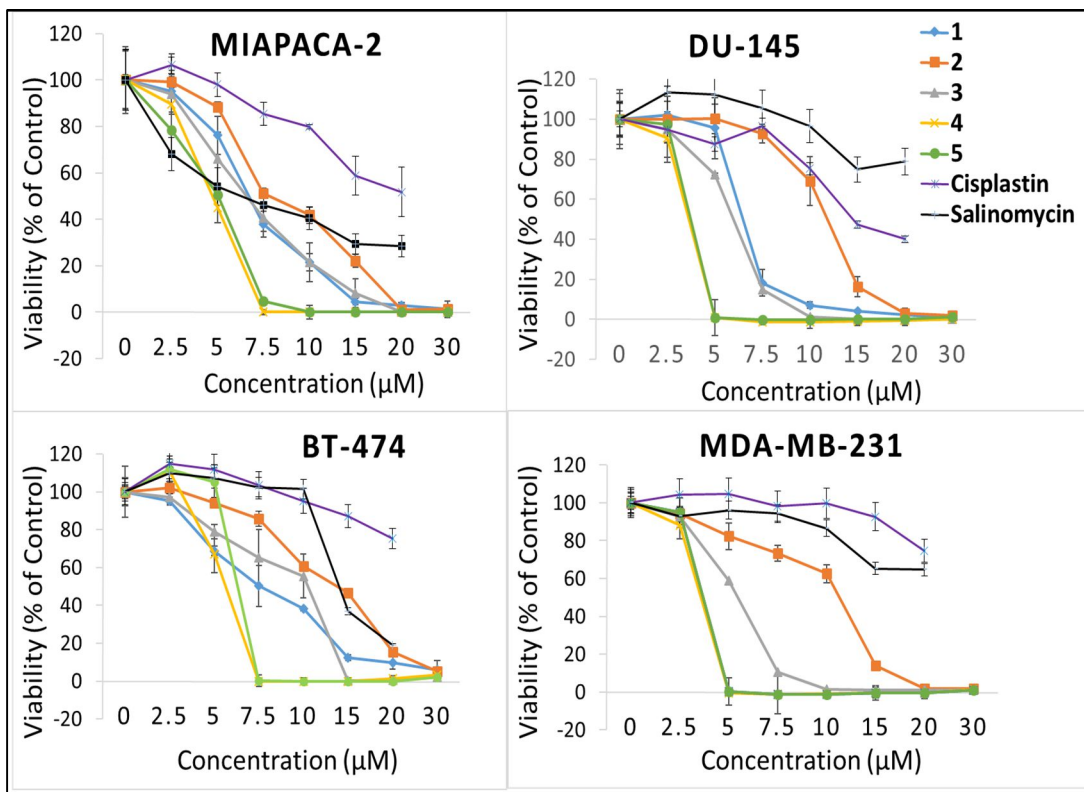


Figure 6.2. Effects of compounds 1-5, cisplatin and salinomycin on the viability of MiaPaCa-2, DU-145 BT-474 and MDA-MB-231 cell lines assessed by using the MTS assay. The results represent the mean \pm standard deviation of 6 independent determinations. Note: D-GAEL 1 was not tested against the MDA-MB-231 cell line.

After establishing that L-glucosamine based L-GAELs had comparable or better cytotoxicity than D-analog 1, we investigated whether like D-GAELs, L-glucosamine based L-GAELs could kill CSCs. The ability to impact CSC viability has assumed great importance in anti-cancer drug discovery since increasing experimental data support the hypothesis that CSCs are responsible for cancer homeostasis, progression, relapse and metastasis.¹³⁻¹⁵ Currently no single drug is clinically indicated for eradication of CSCs, though there are reports that some experimental compounds (eg metformin, salinomycin, lapatinib) can destroy CSCs.^{3,16-18} To

study the effects of L-GAELs **2-5** on CSCs, we isolated CSCs from BT-474 using aldehyde dehydrogenase (ALDH1) activity as a marker for stemness as described previously.^{1,3} The cells were grown in ultra-low adhesion wells for 4 days to form spheroids which were subsequently incubated with the test compounds for 3 days. The activity of compounds **2-5** were compared to salinomycin,¹⁹ cisplatin, adriamycin and myristylamine a classical amphiphile. The integrity of the spheroids was monitored microscopically and the viability of cells were determined with the MTS assay. All the L-GAELs, significantly disrupted the CSCs spheroids (Figure 6.3) at concentrations of 5 μ M and above (**4** and **5**) and 7.5 μ M and above (**2** and **3**). In contrast, the spheroids were intact in incubations with salinomycin (7.5 μ M), myristylamine (20 μ M), cisplatin (20 μ M) and adriamycin (20 μ M). With respect to viability, GAELs **4** and **5** were the most cytotoxic L-GAELs and induced > 95% CSCs death at 7.5 μ M (Figure 6.4). In comparison, salinomycin and adriamycin achieved 60% and 75% CSC death at equimolar concentration (7.5 μ M) and 87% and 72% CSC death respectively at highest concentration (20 μ M) tested. In contrast, myristylamine and cisplatin induced < 30% cell death at 20 μ M concentration. The results of our study on cancer cell lines and CSCs indicate that L-GAELs possess a greater potential to eliminate CSCs than the clinically used drugs adriamycin, cisplatin and the experimental anti-CSC agent salinomycin.

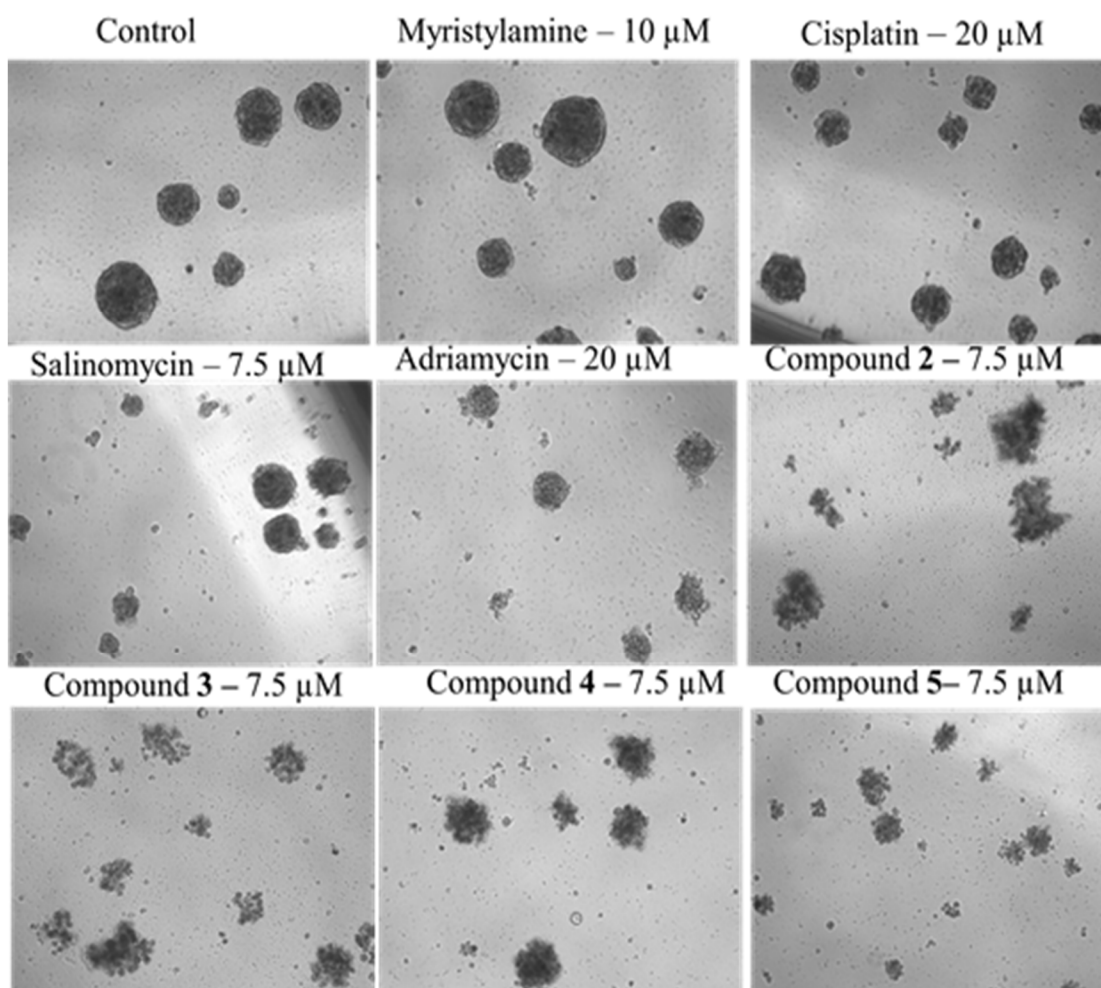


Figure 6.3. Effect of GAEL compounds 2-5, myristylamine, cisplatin and salinomycin, on the integrity of BT474 breast cancer stem cell spheroids. Equal numbers of BT-474 cancer stem cells were seeded into ultra-low adhesion 48-well plates and grown for 5 days to allow for spheroid formation. The spheroids were incubated with or without drugs for 3 days. The images were taken after 3 days of incubation with an Olympus IX70 microscope at a magnification of x10.

The molecular mechanism of cell death by GAELs is yet to be determined however, we previously reported that D-glucosamine-based GAELs killed cells via an apoptosis-independent mechanism.^{1,4,12} We therefore investigated whether the newly synthesized L-glucosamine based L-GAELs retain this mechanism. As the activation of caspases is essential to both extrinsic and

intrinsic apoptotic pathways,^{20,21} a reliable way to evaluate apoptotic-dependent cell death is to investigate the effect of caspase inhibitors on the ability of compounds to induce cell death.²² The effects of compounds **3** and **4** (0 – 8 μM) on the viability of DU-145 and JIMT-1 cell lines in the absence or presence of QVD-OPh (40 μM), a pan caspase inhibitor^{23,24} was investigated. No statistically significant differences were observed between the activity of the L-GAELs on the viability of the cells in the presence or absence of QVD-OPh (Figure 6.5). As a positive control similar studies with adriamycin, a pro-apoptotic anticancer agent showed a significant reduction in its activity in the presence of QVD-OPh, (Figure S4). The results of these studies indicate that activation of caspase is not required for the L-GAELs to kill the cells as previously reported for the D-glucosamine-derived D-GAELs.

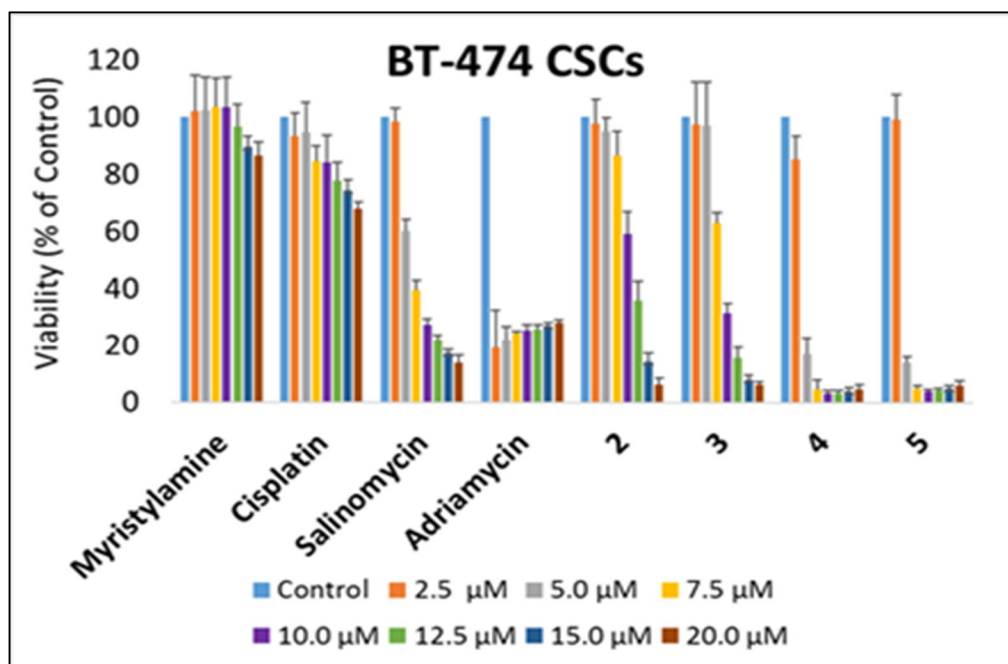


Figure 6.4. Effects of compounds **2-5**, myristylamine ($\text{C}_{14}\text{H}_{29}\text{NH}_2$), cisplatin, adriamycin and salinomycin (0-20 μM) on the viability of cancer stems cells isolated form BT-474 breast cancer

cell line, assessed by MTS assay. The results are the means \pm standard deviation for 6 independent determinations.

We next investigated if the cytotoxic effects of L-GAELs was due to potential membranolytic effects as many cationic amphiphiles can lyse cells. First, the haemolytic effects on ovine erythrocytes were studied. Our results showed that 30 μ M L-GAELs **2-5** induced $< 5\%$ hemolysis (Figure S3). Secondly, we investigated membrane lytic effects of the GAELs **4** and **5** on the DU145 cancer cell line using a cell impermeable DNA binding dye, ethidium homodimer-1 (EthD-1).²⁵ The results (Figure 6.6) showed that incubation with 6 μ M of compounds **4** and **5** for 6 h caused the cells to round up, a prelude to cell death, but EthD-1 staining was similar to controls. In contrast cells incubated with 0.01% Triton X-100 for 10 min stained bright red. Similar results were observed with JIMT-1 cells (Figure S5). Thus L-GAELs do not lyse the cell membranes at their cytotoxic concentration and cell death is not due to membranolytic effects.

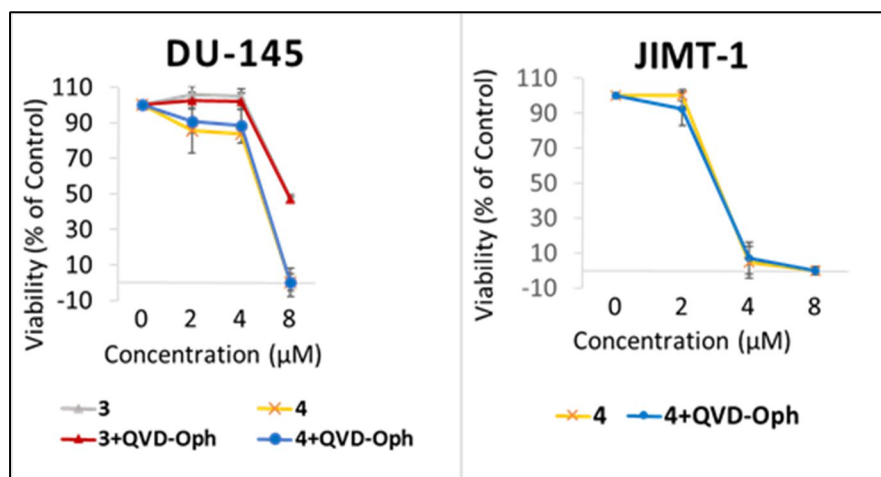


Figure 6.5. Evaluation of effect of pan-caspases inhibitor, QVD-Oph (40 μ m) on cytotoxicity of L-GAELs **3** and **4** against DU-145 and L-GAEL **4** against JIMT-1 cells. Cancer cell lines were treated with drugs in the presence or absence of QVD-Oph.

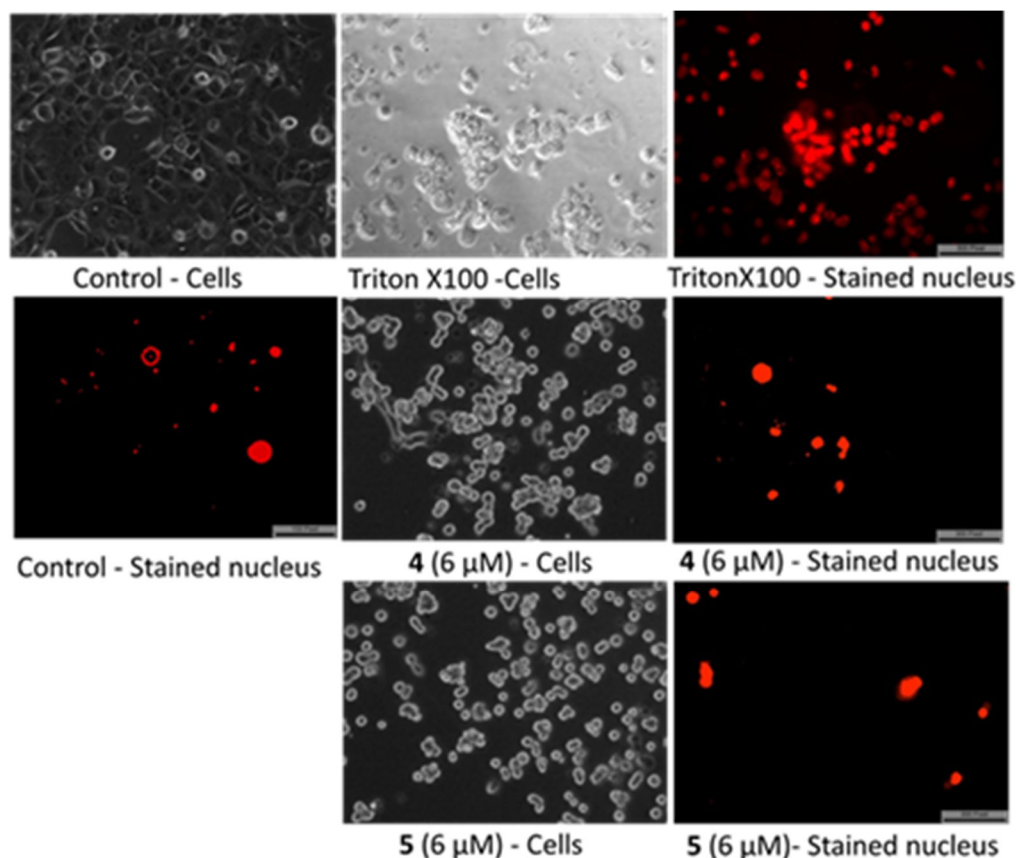


Figure 6.6. Evaluation of membrane effect of compounds **4** and **5** on DU-145 cell lines using cell impermeant ethidium homodimer-1 (EthD-1) dye that emits red fluorescence upon binding to DNA.^{25,26}

Further mode of action studies showed that L-GAELs produced clear large vacuoles in cells (Figure 6.7) similar to those produced by the D sugars which had been correlated with the ability to induce cell death.² Based on our previous report these vacuoles were formed by endocytic process, likely macropynocytosis because the size of the vacuoles $> 2 \mu\text{m}$ in diameter.^{12,27} The cytoplasmic vacuolization followed by cytolytic cell death due to lysosomal hydrolases is likely responsible for L-GAEL induced cell death.¹² The results of these studies show that both L- and D- GAELs' mechanism of cell death is likely to be by methuosis.^{25,28}

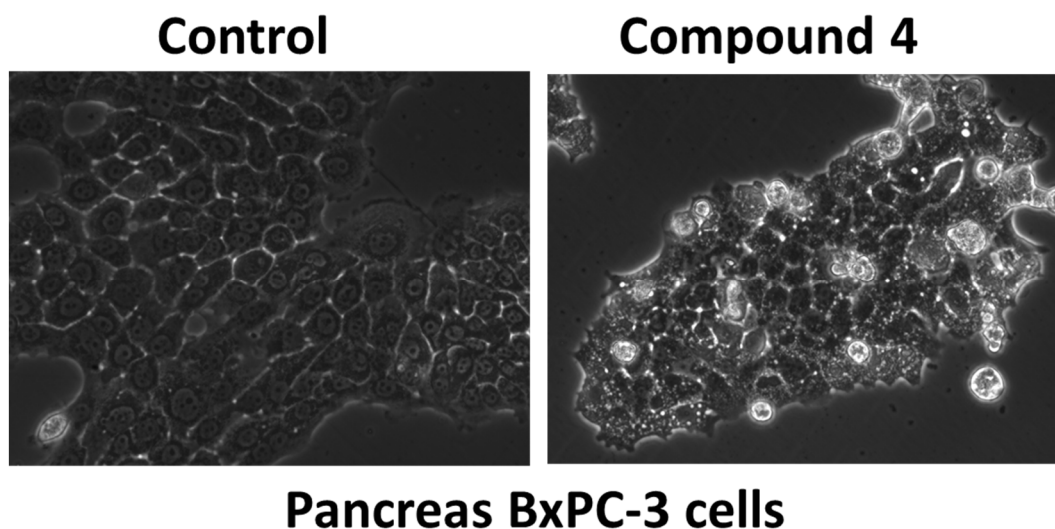


Figure 6.7. Formation of large vacuoles by 5 μM of **4** in BxPC-3 cells after 4 h of incubation observed on an Olympus IX70 microscope and the images recorded with an LCD camera.

To demonstrate that L-GAELs are metabolically stable, we investigated the stability of compound **2** in the presence of bovine liver glycosidases including α - and β - glucosidases, α - and β - N-acetylglucosaminidases, α - and β - galactosidases and α -mannosidases.^{29,30} The rationale for this investigation is because major pathway involved in metabolic cleavage of glycosides in human and animal is via glycosidases-catalyzed hydrolysis. Mass spectrometry, TLC and HPLC-MS analysis of compound **2** after incubation with the cocktail of bovine liver glycosidases showed no traces of hydrolytic products (chromatograms not provided, see SI for experimental details), whereas our control using p-Nitrophenol- α - glucosides were cleaved by these enzymes. This confirmed our hypothesis that glycosidases-catalysed hydrolysis of D-sugar derived GAEL can be prevented by substituting the D-sugar with unnatural L-sugar.

6.5. Conclusion

In conclusion, we have shown that replacement of D-glucosamine by its L-enantiomer in GAELs retains potent cytotoxic effects against human epithelial and CSCs. The most potent L-GAELs **4** and **5** kill ($\geq 95\%$) epithelial cancer cell lines and BT-474 CSCs at 7.5 μM by an apoptosis independent mechanism. Compounds **4** and **5** possess superior anti CSC activity compared to the clinically used anticancer drugs cisplatin and adriamycin and the investigational anti-CSC drug salinomycin. The increased metabolic stability of L-GAELs when combined with their potent anti CSC activity and apoptosis-independent mode of action opens up new opportunities to develop metabolically inert L-sugar-based antitumor agents.

6.6. Acknowledgements

This study was supported by research grants from the Canadian Breast Cancer Foundation Prairie/NWT to GA and Natural Science and Engineering Council of Canada (NSERC) grant to FS. Makanjuola Ogunsina is the recipient of a University of Manitoba and Manitoba provincial government graduate fellowships (UMGF and MGS).

6.7. Supplementary information

6.7.0. Content of Supplementary information

6.7.1. Results – Biology and chemistry

6.7.1.1. Table S1: CC₅₀ and CC₉₀ values of compounds 1 - 5, adriamycin, cisplatin and salinomycin against epithelial cells from human breast cancer (JIMT1, MDA-MB-231, BT-474), human prostate cancer (PC-3, DU-145) and human pancreas cancer (MiaPaCa-2)

6.7.1.2. Figure S1: Effects of compounds 1-5 on the viability of PC-3 and JIMT-1 cell lines assessed by using the MTS assay

6.7.1.3. Figure S2: Effects of adriamycin on the viability of MiaPaCa-2, MDA-MB-231, BT-474 and DU-145 cell lines

6.7.1.4. Figure S3: Hemolytic properties of GAELs 2 - 5 on ovine erythrocytes

6.7.1.5. Figure S4: Effect on cell viability of adriamycin in the absence or presence of pan-caspase inhibitor, QVD-OPh (40 μM) against DU-145 and JIMT-1 cells

6.7.1.6. Figure S5: Evaluation of membranolytic effect of GAELs 4 and 5 on JIMT-1 cells

6.7.1.7. Scheme S1. Synthesis of GAELs 2-5, reactions and conditions

6.7.2. Experimental section

6.7.2.1. Chemistry

6.7.2.1.1. General information

6.7.2.1.2. Synthesis of GAELs

6.7.2.2. Biological methods

6.7.2.2.1. Evaluation of GAELs' effect on viability of epithelial cancer cell lines

6.7.2.2.2. Demonstration of caspase-mediated-apoptosis independent mode of cell death

6.7.2.2.3. Determination of membranolytic effects of GAELs

6.7.2.2.4. Hemolytic assay

6.7.2.2.5. Isolation of breast cancer stem cells from BT-474 cell lines and determination of the effect of GAELs on the viability of the cancer stem cells

6.7.2.2.6. Evaluation of stability of L-glucosamine derived GAELs to cocktail of glycosidases in bovine liver extract, glycosidases fraction

6.7.2.3. Statistical analysis

6.7.2.4. Purity reports of compounds 3-5

6.7.1. Results – Biology and chemistry

Table S1. CC₅₀ and CC₉₀ values of **1 – 5**, adriamycin, cisplatin and salinomycin against epithelial cells from human breast cancer (JIMT1, MDAMB231, BT474), human prostate cancer (PC-3, DU-145) and human pancreas cancer (MiaPaCa2).^c

	JIMT1		MDAMB231		MiaPaCa2		PC3		BT474		DU-145	
	CC ₅₀ (μ M)	CC ₉₀ (μ M)	CC ₅₀ (μ M)	CC ₉₀ (μ M)	CC ₅₀ (μ M)	CC ₉₀ (μ M)	CC ₅₀ (μ M)	CC ₉₀ (μ M)	CC ₅₀ (μ M)	CC ₉₀ (μ M)	CC ₅₀ (μ M)	CC ₉₀ (μ M)
1	6.0	9.5	ND	ND	7.0	13.0	10.5	20.0	6.2	18.0	7.0	9.5
2^a	6.5	11.0	11.0	17.0	7.5	18.0	12.5	16.0	13.0	18.0	12.5	16.0
3	4.0	6.5	5.5	7.5	6.0	15.0	6.5	9.0	11.0	14.0	6.0	8.0
4	2.0	3.5	4.0	4.9	5.0	7.1	2.6	4.3	6.0	7.3	3.6	4.9
5	2.0	3.5	4.0	4.9	4.5	7.0	3.5	4.6	6.0	7.3	3.6	4.9
Adriamycin	ND	ND	0.08	>2.0	0.3	>2.0	ND	ND	0.6	>2.0	1.3	>2.0
Cisplatin	ND	ND	>20	>20	>20	>20	ND	ND	>20	>20	14.8	>20.0
Salinomycin	ND	ND	>20	>20	6.5	>20	ND	ND	14.0	>20	>20	>20.0

^cThe CC₅₀ value is defined as the concentration required to decrease cell viability by 50% relative to the untreated control, while the CC₉₀ value is defined as the concentration required to decrease cell viability by 90% relative to untreated control. The values were obtained by estimating the drug concentration at 50% and 10% viability on the y-axis using line plots. ND = Not determined. ^aCompound **2** contains <10% of the corresponding β -isomer.

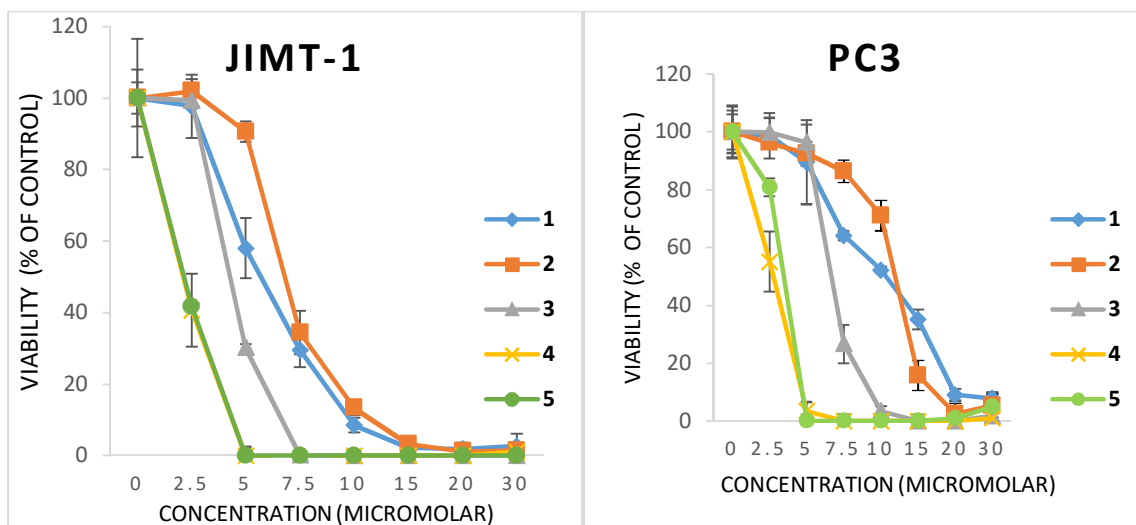


Figure S1: Effects of compounds 1-5, cisplatin and salinomycin on the viability of PC-3 and JIMT-1 cell lines assessed by using the MTS assay after 48 hours. The results represent the mean \pm standard deviation of 6 independent determinations.

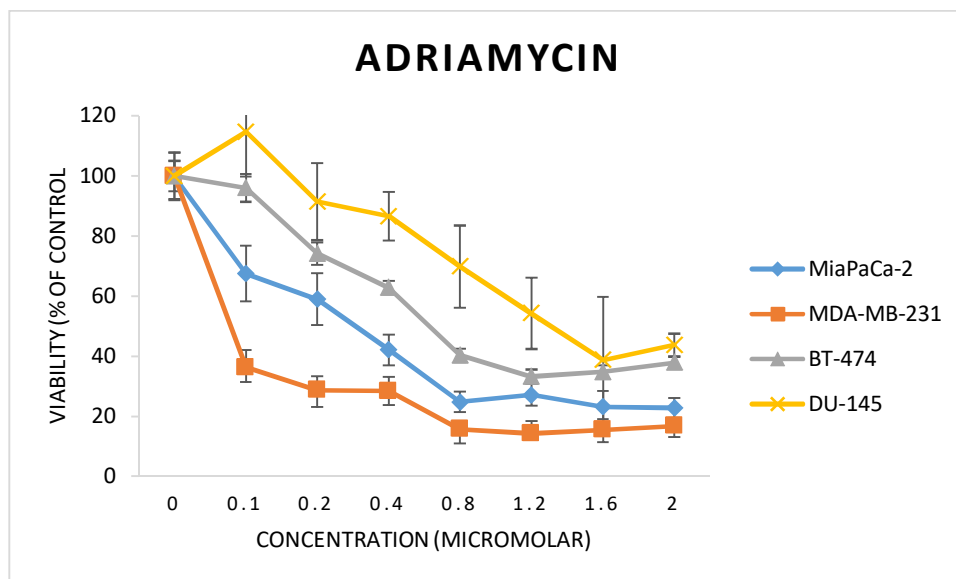


Figure S2: Effects of adriamycin on the viability of MiaPaCa-2, MDA-MB-231, BT-474 and DU-145 cell lines assessed by using the MTS assay after 48 hours. The results represent the mean \pm standard deviation of 6 independent determinations.

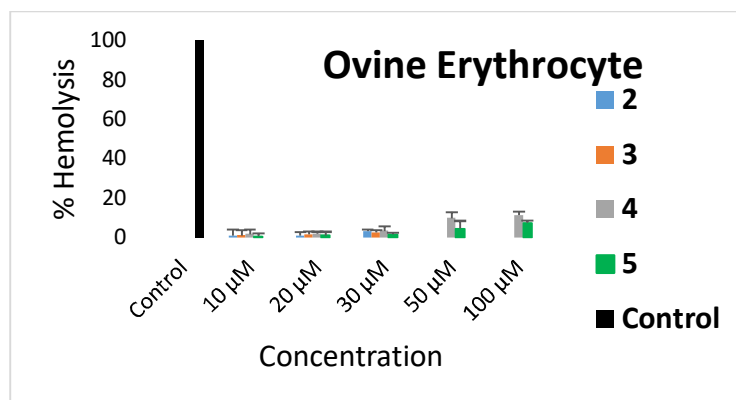


Figure S3: Hemolytic properties of GAELs 2 - 5 on ovine erythrocytes. The results represent the mean \pm standard deviation of 4 independent determinations. The hemolysis was percentage of control, 1% NH_4OH which achieved 100% hemolysis.

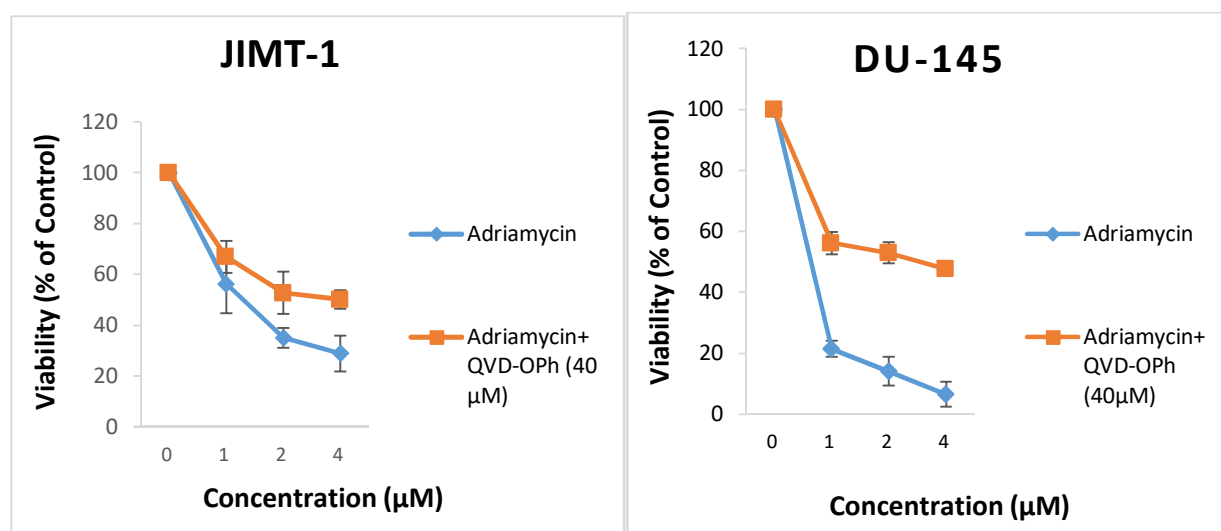


Figure S4: Evaluation of effect of pan-caspase inhibitor, QVD-OPh (40 μM) on cytotoxicity of adriamycin against DU-145 and JIMT-1 cancer cell lines. Cancer cell lines were treated with drugs in the presence or absence of QVD-OPh before viability was assessed with MTS assay. The results represent the mean \pm standard deviation of 6 independent determinations.

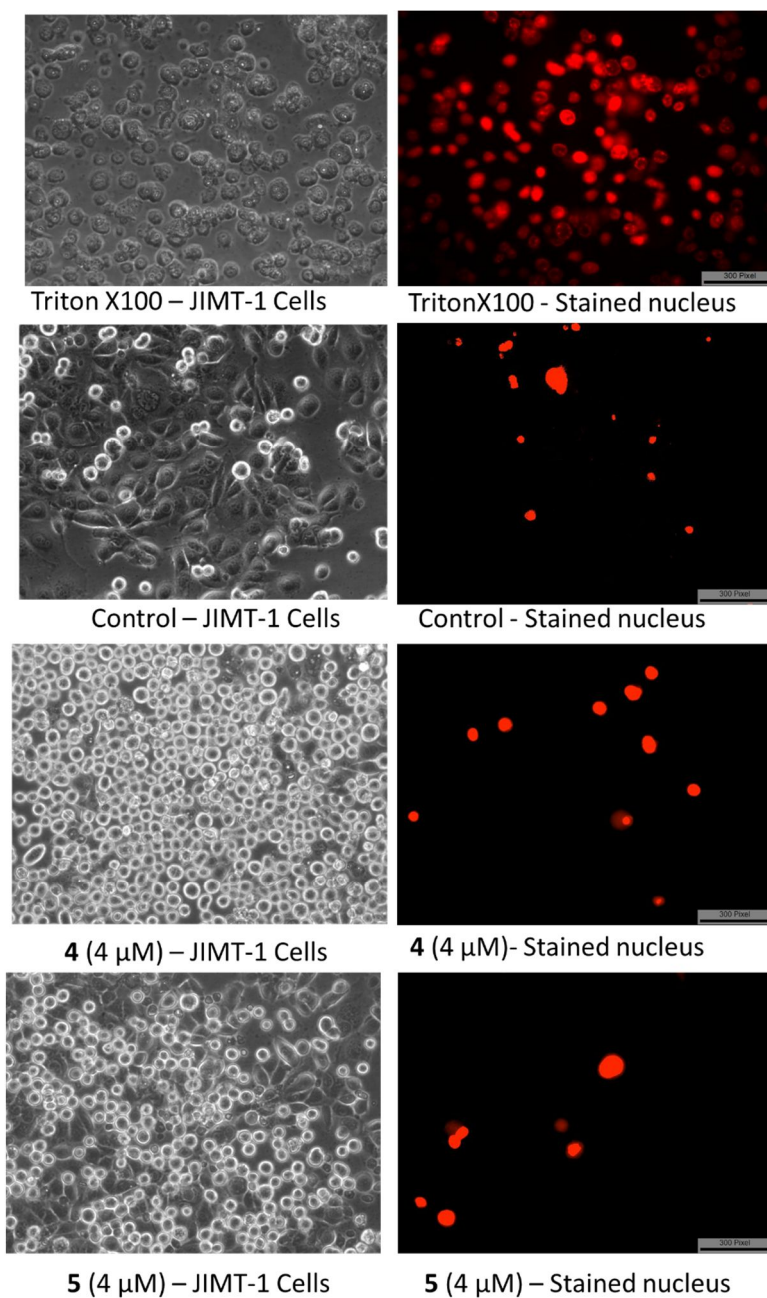
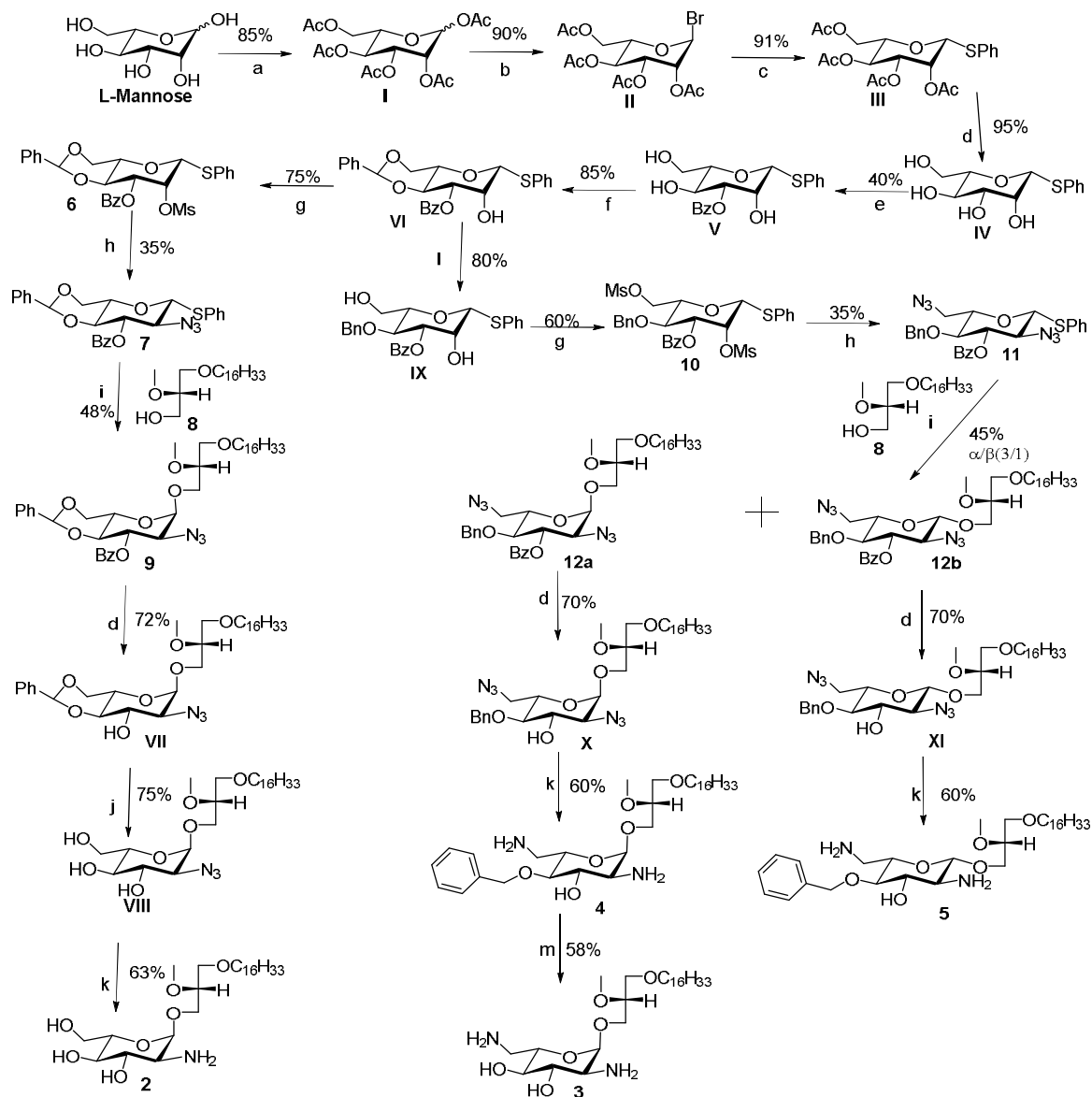


Figure S5: Evaluation of membranolytic effect of compounds **4** and **5** on JIMT-1 cell lines using cell impermeant ethidium homodimer-1 (EthD-1) dye that emits red fluorescence upon binding to DNA. The images were taken with an Olympus IX70 microscope at a magnification of x10.



Scheme S1. Synthesis of L-GAELs **2-5**. Reactions and Conditions; (a) Ac_2O , DMAP, Pyridine, 18 h, rt (b) HBr in AcOH (33%), DCM, 0°C , 2 h (c) PhSH, EtOAc, H_2O , Na_2CO_3 , TBAHS, rt, 6 h (d) MeONa, MeOH, 1h (e) Me_2SnCl_2 , BzCl, DIPEA, THF/ H_2O (19:1), rt, 16 h (f) $\text{PhCH}(\text{OMe})_2$, CSA, CH_3CN , rt, 4 h (g) MsCl, Pyridine, DMAP, rt, 18 h (h) DMF, NaN_3 , 120°C (i) AgOTf, NIS, DCM, 3 h, rt (j) AcOH, H_2O , 60°C , 5 h (k) $\text{P}(\text{CH}_3)_3$, THF, H_2O , 2 h, rt (l) $\text{BH}_3 \cdot \text{THF}$, TMSOTf, DCM, 4 h (m) H_2 , Pd, MeOH, 5 h

6.7.2. Experimental section

6.7.2.1. Chemistry

6.7.2.1.1. General information

Solvents were dried over CaH_2 . ^1H , ^{13}C NMR spectra were recorded on a Bruker Avance 500 NMR spectrometer, and chemical shifts reported (in ppm) relative to internal Me_4Si ($\delta = 0.0$) 500 or 300 MHz and at 126 or 75 MHz, respectively, and chemical shifts were reported in parts per million (ppm). Thin-layer chromatography (TLC) was carried out on aluminum or glass-backed silica gel GF plates (250 μm thickness) and plates were visualized by charring with 5% H_2SO_4 in MeOH and or short wavelength UV light. Compounds were purified by flash chromatography on silica gel 60 (230-400 ASTM mesh). ESI-MS analyses were performed on a Varian 500 MS Ion Trap Mass Spectrometer. MALDI-TOF-MS were performed on a Bruker Daltonics Ultraflex MALDI TOF/TOF Mass Spectrometer. Purity of compound **2** was assessed by elemental analysis of elements (C, H, N) and were within ± 0.5 % of the theoretical values. Purity of compounds **3-5** were assessed by HPLC-UV using a mobile phase gradient A: Water 0.1% TFA (Trifluoroacetic acid); B: Acetonitrile 0.1% TFA (Trifluoroacetic acid) Flow rate: 1 mL/min; Column: Kinetex 5 μm EVO RP C18 100 Å, 150 x 4.6 mm, Phenomenex Injection: 30 μL of 0.1 mg/mL; Equilibration time: at least 10 column volume of the initial gradient. The purity was $> 95\%$. L-mannose and other chemicals used were purchased from Sigma-Aldrich Canada.

6.7.2.1.2. Synthesis of GAELs

1, 2, 3, 4, 6 – Penta-O-acetyl α/β -L mannopyranoside (I)

L-mannose (2.00 g, 11.10 mmol), was dissolved in pyridine (40.0 ml), then acetic anhydride (11.00 ml, 111.00 mmol) was added followed by dimethyl amino pyridine (DMAP, 0.27 g 2.20mmol). The mixture was stirred vigorously for 18 h at room temperature and it was stopped by addition of methanol (10 ml) and then stirred for 15 minutes. The solvents were removed under high vac. The resulting residue was then dissolved in EtOAc (50.0 ml) and washed with 3% HCl solution (1 time), saturated sodium bicarbonate (2 times), distilled water (1 time) and brine (1 time). The resulting organic layer was dried over Na₂SO₄ and concentrated to dryness and purified by flash chromatography using EtOAc and hexane (1:1) to give **I** (3.7 g, 9.48 mmol) as $\alpha:\beta$ mixture (4:1). Yield was 85%. ES-MS: calcd: C₁₆H₂₂O₁₁Na⁺m/z: 414.1, found [M+Na]⁺ m/z: 414.5

2, 3, 4, 6-tetra-O-acetyl- α -L mannopyranosyl bromide (II)

Compound **I** (3.71 g, 9.48 mmol) was added at room temperature to 25.0 ml of HBr in AcOH (33% solution).³¹ The reaction was stirred for 2 h and then diluted with 25.0 ml of DCM. The solution was transferred to a separatory funnel containing ice cold water. The organic layer was washed with ice cold water until the pH is neutral. The organic layer was dried over anhydrous sodium sulphate and concentrated under vacuum to give α - anomer **II** (3.5 g, 8.5 mmol) as the desired product without further purification. 90% yield. Compound **II** was stored at -20°C until it was used. NMR data for compound **II** ¹H NMR (300 MHz, Chloroform-*d*) δ 6.31 (d, *J* = 1.7 Hz, 1H, H₁), 5.73 (dd, *J* = 2.7,10.1 Hz, 1H, H₃), 5.46 (dd, *J* = 2.7, 1.2 Hz, 1H, H₂), 5.38 (dd, *J* = 10.1, 3.5 Hz, 1H, H₄), 4.34 (dd, *J* = 12.4, 4.9 Hz, 1H, H_{6a}), 4.29 – 4.19 (m, 1H, H₅), 4.15 (dd, *J* = 12.4,

2.2 Hz, 1H, H_{6b}), 2.18 (s, 3H), 2.11 (s, 3H), 2.08 (s, 3H), 2.02 (s, 3H). ¹³C NMR (75 MHz, CDCl₃) δ 170.50, 169.68, 169.56, 169.53, 83.08, 72.87, 72.17, 67.95, 65.35, 61.47, 20.76, 20.68, 20.65, 20.57.³² ES-MS: calcd: C₁₄H₁₉O₉BrNa⁺ m/z: 433.0, found [M+Na]⁺ m/z: 432.9

Phenyl-2,3,4,6 tetra-O-acetyl-1-thio-β-L-mannopyranoside (III)

Compound **II** (1.01 g, 2.43 mmol) and thiophenol (0.36 ml, 3.6 mmol) were dissolved in 10.0 ml of EtOAc, followed by addition of 10.0 ml of 2M sodium carbonate. The solution was stirred vigorously and then TBAHS (0.82 g, 2.43 mmol) was added. The reaction mixture was stirred for 15 h at room temperature after which it was diluted with 40.0 ml of EtOAc and then washed with saturated sodium bicarbonate (2 times), distilled water (1 time) and brine (2 times). The organic layer was dried over anhydrous sodium sulphate and then concentrated under vacuum. The residue was purified by flash chromatography using EtOAc and hexane (4:6) to give **III** (0.97 g, 2.21 mmol) as off white solid. Yield 91%. Anomeric configuration was verified by J_{H1-C1} = 155.9 Hz.³³ NMR data for compound **III**: ¹H NMR (300 MHz, Methanol-*d*₄) δ 7.66 – 7.19 (m, 5H, aromatic protons), 5.64 (d, *J* = 1.2 Hz, 1H, H₁), 5.37 – 5.15 (m, 3H), 4.89 (s, 2H), 4.29 (dt, *J* = 13.2, 5.2 Hz, 1H), 4.18 – 4.07 (m, 1H), 3.90 (ddt, *J* = 8.7, 5.8, 2.5 Hz, 1H), 2.19 (s, Hz, 3H), 2.08 (s, 3H), 2.05 (d, 3H), 1.97 (s, 3H). ¹³C NMR (75 MHz, MeOD) δ 137.19, 132.50, 130.24, 85.77, 77.29, 73.16, 72.38, 67.12, 63.78, 20.82, 20.71, 20.60, 20.50. ES-MS: calcd: C₂₀H₂₄O₉SNa⁺ m/z: 463.1, found [M+Na]⁺ m/z: 463.4

Phenyl-1-thio-β-L-mannopyranoside (IV)

Compound **III** (0.97 g, 2.21 mmol) was suspended in 15.0 ml of methanol, followed by addition of catalytic amount of sodium methoxide (0.05 g). The solution was vigorously stirred for 1 h

after which the reaction was stopped using acidic ion exchange resin (0.10 g). The resin was filtered out and solvent removed under vac. The residue was purified by flash chromatography using 100% EtOAc to give **IV** (0.57 g, 2.10 mmol) as an off white solid. Yield 95%. NMR data for compound **IV**: ^1H NMR (300 MHz, Methanol- d_4) δ 7.57 – 7.18 (m, 5H, aromatic protons), 5.02 (d, J = 1.2 Hz, 1H, H-1), 4.08 (dd, J = 1.2, 3.3 Hz, 1H, H-2), 3.90 (dd, J = 12.0, 2.4 Hz, 1H, H-6a), 3.77 (dd, J = 12.1, 5.6 Hz, 1H, H-6b), 3.67 (dd, J_1 = 9.6 Hz, J_2 = 9.6 Hz 1H, H-4), 3.55 (dd, J = 9.5, 3.3 Hz, 1H, H-3), 3.39 – 3.25 (m, 1H). ^{13}C NMR (75 MHz, MeOD) δ 137.18, 131.02, 129.99, 127.79, 88.76, 82.38, 76.17, 74.26, 68.30, 62.87. ES-MS: calcd: $\text{C}_{12}\text{H}_{16}\text{O}_5\text{SNa}^+$ m/z: 295.1, found $[\text{M}+\text{Na}]^+$ m/z: 295.3.

Phenyl-3-benzoyl-1-thio- β -L-mannopyranoside (V)

Compound **IV** (0.50 g, 1.84 mmol) was dissolved in 12.0 ml of THF/water (19:1), then $(\text{CH}_3)_2\text{SnCl}_2$ (0.02g, 0.09 mmol) and DIPEA (0.74 ml, 3.68 mmol) were sequentially added. After 5 minutes of vigorous stirring, BzCl (0.28g, 2.02 mmol) was added and the solution was stirred for 6 h. After disappearance of starting material, the reaction was stopped with 3% HCl solution (20.0 ml) and extracted against EtOAc 40.0 ml, the separated aqueous layer was washed with EtOAc (2 times). The organic layers were combined and dried over anhydrous sodium sulphate and then concentrated under vacuum. The residue was then purified by flash chromatography using EtOAc hexane (6.5:3.5) to give **V** (0.27 g, 0.74 mmol) as a white foam. Yield was 40%. NMR data for compound **V**: ^1H NMR (300 MHz, Methanol- d_4) δ 8.27 – 7.15 (m, 10H, aromatic protons), 5.17 (d, J = 1.1 Hz, 1H, H₁), 5.08 (dd, J = 9.8, 3.3 Hz, 1H, H₃), 4.42 (dd, J = 3.4, 1.0 Hz, 1H, H₂), 4.11 (dd, J_1 = 9.8, 9.8 Hz 1H, H₄), 3.96 (dd, J = 12.0, 2.4 Hz, 1H, H_{6a}), 3.83 (dd, J = 12.0, 5.5 Hz, 1H, H_{6b}), 3.51 (ddd, J = 9.8, 5.5, 2.4 Hz, 1H, H₅). ^{13}C NMR (75

MHz, MeOD) δ 167.82, 136.86, 134.35, 131.51, 131.28, 130.91, 130.08, 129.52, 128.00, 88.66, 82.52, 79.06, 71.85, 65.71, 62.83. ES-MS: calcd: C₁₉H₂₀O₆SNa⁺m/z: 399.1, found [M+Na]⁺ m/z: 399.2

Phenyl-3-benzoyl-4,6-benzylidene-1-thio- β -L-mannopyranoside (VI)

Compound **V** (0.27 mg, 0.73 mmol) was dissolved in 10.0 ml of acetonitrile. To this solution, 10-camphorsulfonic acid (0.04 g, 0.18 mmol) and benzaldehyde dimethyl acetal (0.13 g, 0.88 mmol) were sequentially added under argon atmosphere and the mixture was vigorously stirred for 30 minutes. The reaction was then stopped with triethylamine. The mixture was concentrated under vacuum. The residue was purified by flash chromatography using EtOAc/ hexane (3:7) to give **VI** (0.29 g, 0.62 mmol) as a white solid in 85% yield. NMR data for compound **VI**: ¹H NMR (300 MHz, Chloroform-*d*) δ 8.17 - 7.23 (m, 15H, aromatic protons), 5.63 (s, 1H, benzylidene CH), 5.34 (dd, *J* = 10.2, 3.3 Hz, 1H, H₃), 5.10 (s, 1H, H₁), 4.61 (d, *J* = 3.3 Hz, 1H, H₂), 4.49 – 4.30 (m, 2H, H₄, H_{6a}), 3.98 (m, 1H, H_{6b}), 3.68 – 3.59 (m, 1H, H₅), 2.59 (broad s, 1H, C₂-OH). ¹³C NMR (75 MHz, CDCl₃) δ 165.83, 137.06, 133.47, 131.93, 129.92, 129.51, 129.22, 129.08, 128.51, 128.25, 128.05, 126.14, 101.83, 88.24, 75.41, 73.69, 71.79, 71.12, 68.49. ES-MS: calcd: C₂₆H₂₄O₆SNa⁺m/z: 487.1, found [M+Na]⁺ m/z: 486.7

Phenyl-3-benzoyl-4,6-benzylidene-2-methylsulphonyl-2-deoxy-1-thio- β -L-mannopyranoside (6)

To synthesize **6**, compound **VI** (0.93 g, 0.20 mmol) and methanesulphonyl chloride (0.069 g, 0.61 mmol) was dissolved in 10.0 ml of pyridine and reaction mixture was vigorously stirred for 18 h. The reaction was stopped by addition of 5.0 ml of methanol. The solvents were removed under vac and the residue was purified by flash chromatography using EtOAc/ hexane (2:8) to

give **6** (0.08 mg, 0.15 mmol) as a white solid. Yield was 75%. NMR data for compound **6**: ^1H NMR (300 MHz, Chloroform-*d*) δ 8.24 – 7.23 (m, 15H, aromatic protons), 5.65 (s, 1H, benzylidene CH), 5.56 (dd, $J = 3.2, 1.1$ Hz, 1H, H₂), 5.47 (dd, $J = 10.4, 3.1$ Hz, 1H, H₃), 5.15 (d, $J = 1.2$ Hz, 1H, H₁), 4.46 – 4.28 (m, 2H, H₄, H_{6a}), 3.93 – 4.01 (m, 1H, H_{6b}), 3.66 - 3.71 (m, 1H), 3.26 (s, 3H, mesylate CH₃). ^{13}C NMR (75 MHz, CDCl₃) δ 166.00, 136.81, 133.39, 132.42, 132.28, 130.23, 129.48, 129.29, 129.18, 128.76, 128.38, 128.28, 126.16, 101.91, 86.83, 80.18, 75.01, 72.14, 71.12, 68.27, 39.39. ES-MS: calcd: C₂₇H₂₆O₈S₂Na⁺m/z: 565.1, found [M+Na]⁺ m/z: 565.5.

Phenyl-2-azido-2-deoxy- 3-benzoyl-4,6-benzylidene -1-thio- β -L-glucopyranoside (7)

Compound **6** (0.67 g, 1.24 mmol) and sodium azide (0.81 g, 12.41 mmol) were dissolved in 10.0 ml of anhydrous N,N-dimethyl formamide under argon atmosphere and the reaction temperature was increased to 140°C. The reaction was vigorously stirred for 24 hours. At the end of the reaction the solvent was removed under vac and the residue was diluted with 20.0 ml EtOAc, then excess sodium azide was filtered. The EtOAc was removed under vac and then residue was purified by flash chromatography using EtOAc/dichloromethane/hexane mixture (2:1:8) to give **7** (0.21 g, 0.43 mmol) as a white precipitate. Yield was 36%. NMR data of **7**: ^1H NMR (300 MHz, Chloroform-*d*) δ 8.27 – 7.22 (m, 15H), 5.68 (dd, $J_1, J_2 = 9.5$ Hz, 1H, H₃), 5.57 (s, 1H, benzylidene CH), 4.81 (d, $J = 10.1$ Hz, 1H, H₁), 4.47 (dd, $J = 10.4, 4.8$ Hz, 1H, H_{6a}), 3.98 – 3.57 (m, 4H). ^{13}C NMR (75 MHz, CDCl₃) δ 165.48, 133.71, 130.01, 129.43, 128.91, 128.63, 128.33, 127.65, 127.37, 126.29, 101.45, 87.20, 78.55, 73.75, 70.81, 68.47, 64.15. ES-MS: calcd: C₂₆H₂₃N₃O₅SNa⁺m/z: 512.1, found [M+Na]⁺ m/z: 512.4.

1-O-Hexadecyl-2-O-methyl-3-O-(2'-azido-2'-deoxy-3'-benzoyl-4',6'-benzylidene- α -L-glucopyranosyl)-sn-glycerol (9)

The fully protected glycoside donor **7** (0.10 g, 0.20 mmol) and the glycoside acceptor **8** (0.09 g, 0.26 mmol) were dissolved in 15.0 ml of dichloromethane under argon atmosphere, then AgOTf (0.01 g, 0.04 mmol) and N-iodosuccinimide (0.07 g, 0.30 mmol) were simultaneously added. The reaction was vigorously stirred for 2 h after which it was stopped with saturated solution of sodium thiosulphate (5.0 ml) and then washed with 25.0 ml of saturated sodium thiosulphate solution (1 time), saturated sodium bicarbonate (3 times), water (1 time) and brine (1 time). The organic layer was then dried over anhydrous sodium sulphate and then concentrated under vac. The residue was purified by flash chromatography using EtOAc/dichloromethane/hexane mixture (1:1:8) to give α -anomer, **9** (0.07 g, 0.10 mmol) as a white solid in 48% yield. Compound **9** was slightly impured with < 10% of the corresponding β -anomer. NMR data of **9**: ^1H NMR (300 MHz, Chloroform-*d*) δ 8.22 – 7.14 (m, 10H, aromatic protons), 5.89 (dd, $J_1 = J_2 = 9.9$, Hz, 1H, H₃), 5.56 (s, 1H, benzylidene CH), 5.11 (d, $J = 3.6$ Hz, 1H, H₁), 4.37 (dd, $J = 10.3$, 4.8 Hz, 1H), 4.13 - 4.07 (m, 1H), 3.72-3.91 (m, 3H), 3.66 – 3.26 (m, 10H, H₂), 1.67 – 1.48 (m, 2H), 1.29 (broad s, 26H, lipid tail), 0.88 (t, $J = 7.6$ Hz, 3H). ^{13}C NMR (75 MHz, CDCl₃) δ 165.47, 136.90, 133.25, 129.94, 129.09, 128.40, 128.19, 127.56, 126.17, 101.67, 99.28, 79.67, 79.06, 71.88, 69.62, 69.50, 68.86, 68.11, 62.92, 61.90, 58.27, 31.96, 29.73, 29.52, 29.40, 26.14, 22.72, 14.15. ES-MS: calcd: C₄₀H₅₉N₃O₈Na⁺m/z: 732.4, found [M+Na]⁺ m/z: 732.6.

1-O-Hexadecyl-2-O-methyl-3-O-(2'-azido-2'-deoxy-4',6'-benzylidene- α -L-glucopyranosyl)-sn-glycerol (VII)

Compound **9** (0.68 g, 0.10 mmol) was dissolved in 10.0 ml of methanol, then excess sodium methoxide was added and the reaction was vigorously stirred for 3 h. The reaction was stopped by acidic ion exchange resin. The resin was filtered and the filtrate was concentrated under vacuum and the residue was purified by flash chromatography using EtOAc/dichloromethane/hexane mixture (3:1:7) to give **VII** (0.04 g, 0.07 mmol) as a white in 72% yield. NMR data of **VII**: ^1H NMR (300 MHz, Chloroform-*d*) δ 7.55 – 7.35 (m, 5H, aromatic protons), 5.56 (s, 1H, benzyldiene CH), 4.96 (d, J = 3.6 Hz, 1H, H_1), 4.29 – 4.19 (m, 2H), 3.92 (dd, J = 9.8, 4.8 Hz, 1H), 3.84 – 3.39 (m, 12H), 3.28 (dd, J = 10.0, 3.6 Hz, 1H, H_2), 1.62 – 1.53 (m, 2H), 1.32 (broad s, 26H, lipid tail), 0.90 (t, J = 6.6 Hz, 3H). ^{13}C NMR (75 MHz, CDCl_3) δ 149.67, 136.99, 129.36, 128.38, 126.30, 123.77, 102.11, 98.83, 81.93, 79.08, 71.87, 69.69, 68.86, 68.61, 67.91, 63.11, 62.50, 58.21, 31.95, 29.72, 29.64, 29.51, 29.38, 26.13, 22.71, 14.14. ES-MS: calcd: $\text{C}_{33}\text{H}_{55}\text{N}_3\text{O}_8\text{Na}^+$ m/z : 644.4, found $[\text{M}+\text{Na}]^+$ m/z : 644.5

1-O-Hexadecyl-2-O-methyl-3-O-(2'-azido-2'-deoxy- α -L-glucopyranosyl)-sn-glycerol (VIII)

Compound **VII** (0.04 g, 0.07 mmol) was dissolved in 10.0 ml acetic acid water mixture (4:1) and the reaction temperature was increased to 60°C. The reaction was vigorously stirred for 5 h, then it was concentrated and purified with EtOAc / hexane mixture (9:1) to give **VIII** (0.03 g, 0.05 mmol) as white solid. Yield was 75%. NMR data of **VIII**: ^1H NMR (300 MHz, Methanol- d_4) δ 4.92 (d, J = 3.5 Hz, 1H, H_1), 3.94 – 3.66 (m, 2H), 3.66 – 3.55 (m, 5H), 3.55 – 3.36 (m, 8H), 3.10 (dd, J = 10.5, 3.5 Hz, 1H, H_2), 1.71 – 1.51 (m, 2H), 1.32 (s, 26H, lipid tail), 0.88 (t, J = 6.6 Hz, 3H, terminal lipid CH_3). ^{13}C NMR (75 MHz, CD_3OD) δ 99.77, 80.55, 74.03, 72.69, 72.42, 72.07, 71.20, 68.17, 64.53, 62.45, 58.37, 33.12, 30.84, 30.80, 30.52, 27.29, 23.78, 14.51. ES-MS: calcd: $\text{C}_{26}\text{H}_{51}\text{N}_3\text{O}_7\text{Na}^+$ m/z : 540.4, found $[\text{M}+\text{Na}]^+$ m/z : 540.1.

1-O-Hexadecyl-2-O-methyl-3-O-(2'-amino-2'-deoxy- α -L-glucopyranosyl)-sn-glycerol (2)

To a solution of compound **VIII** (0.03 mg, 0.05 mmol) in THF (10.0 ml) was added 2.0 ml of water and 2.0 ml of 1 M trimethylphosphine in THF. The reaction was vigorously stirred for 2 h at room temperature after which it was concentrated under vac. The residue was purified by C-18 column using gradient elution with water/methanol to give **2** (0.02 g, 0.03 mmol) as a white solid in 63% yield. Compound **2** has traces of the β - anomer. NMR data for **2**: ^1H NMR (300 MHz, Methanol- d_4) δ 4.71 (d, $J = 3.6$ Hz, 1H, H₁), 3.76 – 3.66 (m, 1H), 3.62 (dd, $J = 11.8, 5.3$ Hz, 1H), 3.55 – 3.27 (m, 12H), 3.26 – 3.16 (m, 2H), 2.50 (dd, $J = 9.8, 3.5$ Hz, 1H, H₂), 1.43 – 1.53 (m, 2H), 1.22 (s, 26H, lipid tail), 0.83 (t, $J = 6.5$ Hz, 3H, terminal lipid CH₃). ^{13}C NMR (75 MHz, CD₃OD) δ 100.59, 80.50, 76.34, 74.22, 72.70, 71.88, 71.41, 67.92, 62.68, 58.26, 57.28, 33.11, 30.80, 30.65, 30.51, 27.29, 23.77, 14.49. MALDI-HRMS: calcd: C₂₆H₅₃NO₇Na⁺m/z: 514.3822, found [M+Na]⁺ m/z: 514.3819. Elemental Analysis: calcd: C, 63.51; H, 10.86; N, 2.85, found: C, 63.05; H, 11.01; N, 2.86.

Phenyl-3-benzoyl-4-benzyl-1-thio- β -L-mannopyranoside (IX)

To a solution of **VI** (0.47 mg, 1.00 mmol) in anhydrous dichloromethane (10.0 ml) were added 1M BH₃·THF (5.00 ml, 5.00 mmol) and TMSOTf (0.03 ml, 1.50 mmol), reaction was vigorously stirred at room temperature for 3 h. Then reaction was stopped by adding 1.0 ml of trimethylamine and stirred for another 15 minutes. The mixture was concentrated under vac and leftover solvent was co-removed by methanol (3 times). The residue was purified by flash chromatography using hexane/dichloromethane/ EtOAc mixture (5:1:4) to give **IX** (0.38 g, 0.80 mmol) as a white solid in 80% yield. NMR data for **IX**: ^1H NMR (300 MHz, Chloroform- d) δ

8.13 – 7.96 (m, 2H, aromatic protons), 7.71 – 7.09 (m, 13H, aromatic protons), 5.27 (dd, $J = 9.8$, 3.2 Hz, 1H, H₃), 5.04 (d, $J = 1.1$ Hz, 1H, H₁), 4.84 – 4.64 (m, 2H, benzyl CH₂), 4.50 (dd, $J = 1.1$, 3.2 Hz, 1H, H₂), 4.26 (dd, $J = 9.8$, 9.7 Hz, 1H, H₄), 3.98 (d, $J = 12.2$ Hz, 1H), 3.78 - 3.89 (m, 1H), 3.54 (ddd, $J = 9.7$, 4.2, 2.6 Hz, 1H, H₅), 2.73 (d, $J = 5.5$ Hz, 1H, C₂-OH), 2.42 (d, $J = 6.6$ Hz, 1H, C₆-OH). ¹³C NMR (75 MHz, CDCl₃) δ 165.74, 137.54, 133.61, 133.50, 131.57, 129.83, 129.53, 129.22, 128.60, 128.44, 128.07, 127.88, 87.20, 80.04, 77.29, 75.23, 72.17, 71.03, 61.96. ES-MS: calcd: C₂₆H₂₆O₆SNa⁺m/z: 489.1, found [M+Na]⁺ m/z: 488.8.

Phenyl-3-benzoyl-4-benzyl-2,6-dimethylsulphonyl-2,6-dideoxy-1-thio- β -L-mannopyranoside (10)

Compound **IX** (0.38 g, 0.80 mmol), methanesulphonyl chloride (0.28 mg, 2.45 mmol) and catalytic amount of dimethyl amino pyridine (0.0g) were dissolved in pyridine (10.0 ml) under argon atmosphere. The reaction was stirred for 24 hours after which it was stopped with 5.0 ml of methanol. The solvents were removed under vac and the residue was dissolved in dichloromethane and washed with 3% HCl solution (2 times), saturated sodium bicarbonate solution (2 times) and water (1 time). The organic layer was dried over anhydrous sodium sulphate. The organic layer was concentrated under vac and the residue was purified by flash chromatography using hexane/dichloromethane/ EtOAc mixture (5:2:3) to give **10** (0.40 g, 0.64 mmol) as an off white solid. Yield was 80%. NMR data of **10**: ¹H NMR (300 MHz, Chloroform-*d*) δ 8.22 – 8.08 (m, 2H aromatic protons), 7.74 – 7.05 (m, 13H, aromatic protons), 5.39 – 5.47 (m, 2H, H₂, H₃), 5.11 (dd, $J = 1.1$ Hz 1H, H₁), 4.79 – 4.60 (m, 2H, benzyl CH₂), 4.49 (dd, $J = 11.8$, 1.9 Hz, 1H, H_{6a}), 4.39 (dd, $J = 11.7$, 4.6 Hz, 1H, H_{6b}), 4.13 (dd, $J = 10.5$, 8.5 Hz, 1H), 3.75 – 3.66 (m, 1H, H₅), 3.18 (s, 3H, mesylate CH₃), 3.07 (s, 3H, mesylate CH₃). ¹³C NMR (75 MHz,

CDCl₃) δ 165.70, 149.88, 136.94, 135.99, 133.69, 132.34, 131.98, 130.12, 129.47, 129.11, 128.65, 128.57, 128.23, 123.79, 85.27, 79.72, 77.47, 75.50, 74.36, 71.78, 68.44, 39.31, 37.96. ES-MS: calcd: C₂₈H₃₀O₁₀S₃Na⁺ m/z: 645.1, found [M+Na]⁺ m/z: 645.3.

Phenyl-3-benzoyl-4-benzyl-2,6-diazido-2,6-dideoxy-1-thio- β -L-glucoopyranoside (11)

To a solution of compound **10** (0.40 g, 0.64 mmol) in 10.0 ml of N,N-dimethylformamide was added sodium azide (0.86 g, 13.2 mmol) under argon atmosphere. The reaction temperature was increased to 140°C and it was vigorously stirred for 24 h. At the end of the reaction the solvent was removed under vac and the residue was diluted with 20.0 ml EtOAc, then excess sodium azide was filtered out. The EtOAc was removed under vac and the residue was purified by flash chromatography using EtOAc /dichloromethane/hexane mixture (1:1:8) to give the fully protected glycoside donor **11** (0.13 g, 0.26 mmol) as a white solid. Yield was 41%. NMR data of compound **11**: ¹H NMR (300 MHz, Chloroform-*d*) δ 8.14 – 8.06 (m, 2H, aromatic protons), 7.76 – 7.67 (m, 2H, aromatic protons), 7.67 – 7.46 (m, 5H), 7.47 – 7.11 (m, 6H, aromatic protons), 5.50 (dd, *J* = 9.4 Hz, 1H, H₃), 4.64 (d, *J* = 10.1 Hz, 1H, H₁), 4.61 – 4.50 (m, 2H, Benzyl CH₂), 3.75 (dd, *J*₁ = *J*₂ = 9.3 Hz, 1H, H₄), 3.70 – 3.59 (m, 2H, H₅, H_{6a}), 3.51 (dd *J* = 10.1, 9.4 Hz, 1H, H₂), 3.44 (dd, *J* = 13.4, 4.5 Hz, 1H, H_{6b}). ¹³C NMR (75 MHz, CDCl₃) δ 165.42, 136.93, 134.60, 133.62, 130.27, 129.91, 129.30, 129.25, 129.15, 129.01, 128.65, 128.49, 128.20, 128.16, 127.60, 127.24, 86.15, 78.35, 76.53, 75.97, 75.02, 63.47, 51.14. ES-MS: calcd: C₂₆H₂₄N₆SNa⁺ m/z: 539.2, found [M+Na]⁺ m/z: 539.1.

Synthesis of Compounds 12a/b

The fully protected glycoside donor **11** (0.14 g, 0.26 mmol) and the glycoside acceptor **8** (0.13 g, 0.40 mmol) were dissolved in 15.0 ml of dichloromethane under argon atmosphere, then AgOTf (0.01 g, 0.05 mmol) and N-iodosuccinimide (0.12 g, 0.52 mmol) were simultaneously added. The reaction was vigorously stirred for 2 h after which it was stopped with saturated solution of sodium thiosulphate (5.0 ml) and then washed with 25.0 ml of saturated sodium thiosulphate solution (1 time), saturated sodium bicarbonate (3 times), water (1 time) and brine (1 time). The organic layer was then dried over anhydrous sodium sulphate and then concentrated under vac. The residue, anomeric mixture, was purified by flash chromatography using EtOAc /dichloromethane/hexane mixture (1:1:8) to give α - and β - anomers, **12a** (0.07 g, 0.09 mmol) and **12b** (0.02 g, 0.03 mmol) respectively in pure form. Reaction yield was 45%. NMR data of compounds **12a/b** are below

1-O-Hexadecyl-2-O-methyl-3-O-(3'-benzoyl-4'-benzyl-2',6'-diazido-2',6'-dideoxy- α -L-glucopyranosyl)-sn-glycerol (12a)

^1H NMR (300 MHz, Chloroform-*d*) δ 8.10 (d, $J = 7.2$ Hz, 2H, benzoyl *o*- protons) 7.67 – 7.56 (m, 1H, benzoyl *p*- proton), 7.49 (t, $J = 7.6$ Hz, 2H, benzoyl *m*- protons), 7.34 – 7.10 (m, 5H, benzyl aromatic protons), 5.85 (dd, $J = 10.7, 8.9$ Hz, 1H, H₃), 5.09 (d, $J = 3.5$ Hz, 1H, α -H₁), 4.61 - 4.55 (m, 2H, benzyl CH₂), 4.15 – 4.02 (m, 1H, H₅), 3.91 – 3.77 (m, 2H), 3.71 (dd, $J = 10.3, 3.9$ Hz, 1H), 3.67 – 3.39 (m, 10H), 3.31 (dd, $J = 10.7, 3.5$ Hz, 1H, H₂), 1.55 - 1.66 (m, 2H), 1.28 (broad s, 26H, lipid tail), 0.91 (t, $J = 7.5$ Hz, 3H, terminal lipid CH₃). ^{13}C NMR (75 MHz, CDCl₃) δ 165.44, 137.10, 133.42, 129.88, 129.51, 128.54, 128.43, 128.07, 98.39, 79.08, 76.76, 74.97, 72.57, 71.87, 70.22, 69.69, 68.14, 61.46, 58.33, 51.04, 31.95, 29.73, 29.69, 29.64, 29.52,

29.39, 26.13, 22.72, 14.15. ES-MS: calcd: C₄₀H₆₀N₆O₇Na⁺m/z: 759.5, found [M+Na]⁺ m/z: 759.4.

1-O-Hexadecyl-2-O-methyl-3-O-(3'-benzoyl-4'-benzyl-2',6'-diazido-2',6'-dideoxy-β-L-glucopyranosyl)-sn-glycerol (12b)

¹H NMR (300 MHz, Chloroform-*d*) δ 8.10 (d, *J* = 7.2 Hz, 2H, benzoyl *o*- protons) 7.65 – 7.56 (m, 1H, benzoyl *p*- proton), 7.50 (t, *J* = 7.6 Hz, 2H, benzoyl *m*- protons) 7.32 – 7.06 (m, 5H, benzyl aromatic protons), 5.34 (dd, *J* = 10.4, 8.8 Hz, 1H, H₃), 4.59 (d, *J* = 7.6 Hz, 1H, β-H₁), 4.57 – 4.45 (m, 2H, benzyl CH₂), 4.08 (dd, *J* = 10.7, 3.2 Hz, 1H), 3.78 – 3.67 (m, 2H), 3.67 – 3.28 (m, 12H), 1.57 – 1.62 (m, 2H), 1.31 (broad s, 26H, lipid tail), 0.90 (t, *J* = 7.5 Hz, 3H). ¹³C NMR (75 MHz, CDCl₃) δ 165.35, 136.82, 133.51, 129.89, 129.40, 129.06, 128.58, 128.47, 128.20, 128.16, 102.27, 79.36, 76.47, 74.93, 74.65, 74.52, 71.83, 69.77, 69.69, 64.48, 58.00, 51.03, 31.95, 29.72, 29.68, 29.63, 29.57, 29.52, 29.49, 29.38, 26.11, 26.07, 22.71, 14.14. ES-MS: calcd: C₄₀H₆₀N₆O₇Na⁺m/z: 759.5, found [M+Na]⁺ m/z: 759.3.

1-O-Hexadecyl-2-O-methyl-3-O-(4'-benzyl-2',6'-diazido-2',6'-dideoxy-α-L-glucopyranosyl)-sn-glycerol (X)

Compound **12a** (0.07 g, 0.09 mmol) was dissolved in 10.0 ml of methanol, then excess sodium methoxide was added and the reaction was vigorously stirred for 3 h. The reaction was stopped by adding ion exchange resin. The resin was filtered and the filtrate was concentrated under vacuum, then the residue was purified by flash chromatography using EtOAc /dichloromethane/hexane mixture (2:1:7) to give **X** (0.04 g, 0.06 mmol) as a white solid. Yield

was 70%. NMR data of **X**: ^1H NMR (300 MHz, Chloroform-*d*) δ 7.48 – 7.25 (m, 5H, aromatic proton), 4.95 (d, $J = 3.6$ Hz, 1H, $\alpha\text{-H}_1$), 4.80 (dd, $J = 11.4$ Hz, 2H, benzyl CH_2), 4.12 (dd, $J = 10.3, 8.5$, Hz, 1H, H_3), 3.98 – 3.85 (m, 1H, -CH-O-CH_3), 3.78 (dd, $J = 9.1, 3.8$ Hz, 1H), 3.69 – 3.35 (m, 12H), 3.21 (dd, $J = 10.3, 3.6$ Hz, 1H, H_2), 2.47 (d, $J = 3.4$ Hz, 1H, $\text{C}_3\text{-OH}$), 1.50 – 1.62 (m, 2H), 1.35 (s, 26H, lipid tail), 0.91 (t, $J = 7.6$ Hz, 3H, terminal lipid CH_3). ^{13}C NMR (75 MHz, CDCl_3) δ 137.80, 128.74, 128.26, 128.01, 97.88, 79.07, 78.92, 75.14, 71.86, 71.79, 70.21, 69.78, 67.81, 63.06, 58.21, 51.20, 31.95, 29.72, 29.68, 29.63, 29.51, 29.38, 26.12, 22.71, 14.14. ES-MS: calcd: $\text{C}_{33}\text{H}_{56}\text{N}_6\text{O}_6\text{Na}^+$ m/z : 655.4, found $[\text{M}+\text{Na}]^+$ m/z : 655.6.

1-O-Hexadecyl-2-O-methyl-3-O-(4'-benzyl-2',6'-diazido-2',6'-dideoxy- β -L-glucopyranosyl)-sn-glycerol (XI)

Compound **12b** (0.02 g, 0.03 mmol) was dissolved in 10.0 ml of methanol, then excess sodium methoxide was added and the reaction was vigorously stirred for 3 h. The reaction was stopped by acidic ion exchange resin. The resin was filtered and the filtrate was concentrated under vacuum and the residue was purified by flash chromatography using EtOAc /dichloromethane/hexane mixture (2:1:7) to give **XI** (0.01 g, 0.02 mmol) as a white solid. Yield was 70%. NMR data of **XI**: ^1H NMR (300 MHz, Chloroform-*d*) δ 7.48 – 7.24 (m, 5H, aromatic protons), 4.78 (m, 2H, benzyl CH_2) 4.42 (d, $J = 7.9$ Hz, 1H, $\beta\text{-H}_1$), 4.06 (dd, $J = 10.5, 3.0$ Hz, 1H), 3.68 (dd, $J = 10.6, 5.4$ Hz, 1H), 3.62 – 3.31 (m, 14H), 2.51 (broad s, 1H, $\text{C}_3\text{-OH}$), 1.52 – 1.61 (m, 2H), 1.34 (broad s, 26H), 0.89 (t, $J = 7.6$ Hz, 3H). ^{13}C NMR (75 MHz, CDCl_3) δ 137.67, 128.67, 128.23, 128.16, 102.14, 79.33, 77.87, 75.26, 74.96, 74.74, 71.81, 69.85, 69.67,

66.40, 58.02, 51.27, 31.95, 29.72, 29.64, 29.51, 29.38, 26.11, 22.71. ES-MS: calcd: $C_{33}H_{56}N_6O_6Na^+$ m/z: 655.4, found $[M+Na]^+$ m/z: 655.8.

1-O-Hexadecyl-2-O-methyl-3-O-(4'-benzyl-2',6'-diamino-2',6'-dideoxy- α -L-glucopyranosyl)-sn-glycerol (4)

To a solution of compound **X** (0.04 g, 0.06 mmol) in THF (10.0 ml) was added 2.0 ml of water and 2.0 ml of 1M trimethylphosphine in THF. The reaction was vigorously stirred for 2 h at room temperature after which it was concentrated under vac. The residue was purified by C-18 column using gradient elution with water/methanol to give **4** (0.03 g, 0.04 mmol) as a white solid. Yield was 60%. NMR data for **4**: 1H NMR (300 MHz, Methanol- d_4) δ 7.41 – 7.07 (m, 5H, aromatic proton), 4.85 (d, $J = 11.3$, 1H, benzyl CH_2), 4.68 (d, $J = 3.6$, 1H, α - H_1), 4.55 (dd, $J = 11.3$, 1H, benzyl CH_2), 3.72 – 3.60 (m, 1H, $-CH-O-CH_3$), 3.58 – 3.28 (m, 12H), 3.07 (dd, $J = 10.0$, 1.5 Hz, 1H, H_{6b}), 2.59 – 2.46 (m, 2H, H_2 , H_{6a}), 1.55 – 1.36 (m, 2H, $-OCH_2CH_2$), 1.19 (broad s, 26H), 0.80 (t, $J = 6.7$, 3H, terminal lipid CH_3). ^{13}C NMR (75 MHz, MeOD) δ 139.99, 129.31, 128.82, 100.36, 80.83, 80.40, 76.80, 75.66, 73.08, 72.71, 71.14, 67.78, 58.27, 57.68, 43.72, 33.12, 30.83, 30.63, 30.52, 27.29, 23.78, 14.51. MALDI-HRMS: calcd: $C_{33}H_{60}N_2O_6Na^+$ m/z: 603.4451, found $[M+Na]^+$ m/z: 603.4260

1-O-Hexadecyl-2-O-methyl-3-O-(2',6'-diamino-2',6'-dideoxy- α -L-glucopyranosyl)-sn-glycerol (3)

To a solution of compound **4** (0.02 g, 0.03 mmol) in methanol was added palladium hydroxide on carbon (20 mg) and the reaction was stirred vigorously under hydrogen atmosphere for 15 h.

Then the catalyst was filtered and the solvent removed under vac. The residue was purified by C-18 column using gradient elution with water/methanol to give **3** (0.01 g, 0.02 mmol) as a white solid. NMR data of **3**: ^1H NMR (500 MHz, Methanol- d_4) δ 4.77 (d, $J = 3.7$ Hz, 1H, $\alpha\text{-H}_1$), 3.83 – 3.73 (m, 1H, -CH-O-CH_3), 3.61 – 3.39 (m, 11H), 3.14 (dd, $J = 9.8, 8.8$ Hz, 1H, H_3), 2.97 (dd, $J = 13.4, 3.1$ Hz, 1H, H_{6a}), 2.71 (dd, $J = 13.4, 7.1$ Hz, 1H, H_{6b}), 2.56 (dd, $J = 9.9, 3.7$ Hz, 1H, H_2), 1.63 – 1.49 (m, 2H, $\text{-OCH}_2\text{CH}_2\text{-}$), 1.29 (broad s, 26H, lipid tail), 0.89 (t, $J = 6.9$ Hz, 3H, terminal lipid CH_3). ^{13}C NMR (126 MHz, CD_3OD) δ 99.09, 79.03, 74.76, 72.54, 72.06, 71.22, 69.85, 66.54, 56.82, 55.91, 42.38, 31.64, 29.34, 29.32, 29.03, 25.83, 22.30, 12.99. MALDI-HRMS: calcd: $\text{C}_{26}\text{H}_{54}\text{N}_2\text{O}_6\text{Na}^+$ m/z: 513.3982, found $[\text{M}+\text{Na}]^+$ m/z: 513.4010.

1-O-Hexadecyl-2-O-methyl-3-O-(4'-benzyl-2',6'-diamino-2',6'-dideoxy- β -L-glucopyranosyl)-sn-glycerol (5)

To a solution compound **XI** (0.01 g, 0.02 mmol) in THF (10.0 ml) was added 2.0 ml of water and 2.0 ml of 1M trimethylphosphine in THF. The reaction was vigorously stirred for 2 h at room temperature after which it was concentrated under vac. The residue was purified by C-18 column using gradient elution with water/methanol to give **5** (0.01 g, 0.01 mmol) as a white solid. Yield was 60%. NMR data for **5**: ^1H NMR (500 MHz, Methanol- d_4) δ 7.43 – 7.20 (m, 5H, aromatic proton), 4.78 (dd, $J = 11.2$ Hz, 2H, benzyl CH_2), 4.23 (d, $J = 7.9$ Hz, 1H, $\beta\text{-H}_1$), 3.93 – 3.98 (m, 1H, -CH-O-CH_3), 3.67 – 3.45 (m, 10H, -OCH_3 , H_5), 3.36 – 3.11 (m, 2H), 2.95 (dd, $J = 13.4, 2.8$ Hz, 1H, H_{6b}), 2.72 – 2.55 (m, 2H, $\text{H}_2, \text{H}_{6a}$), 1.58 – 1.54 (m, 2H, $\text{-OCH}_2\text{CH}_2\text{-}$), 1.28 (broad s, 26H, lipid tail), 0.89 (t, $J = 6.8$ Hz, 3H, terminal lipid CH_3). ^{13}C NMR (126 MHz, MeOD) δ 138.43, 127.95, 127.38, 103.65, 79.45, 79.33, 76.61, 75.73, 74.24, 71.24, 69.66, 68.81, 57.37, 56.69,

42.42, 31.65, 29.36, 29.33, 29.15, 29.05, 25.80, 22.31, 13.01. MALDI-HRMS: calcd: $C_{33}H_{60}N_2O_6Na^+$ m/z: 603.4451, found $[M+Na]^+$ m/z: 603.3758

6.7.2.2. Biological methods

6.7.2.2.1. Evaluation of GAELs' Effect on viability of epithelial cancer cell lines

The cell lines were cultured from frozen stocks originally obtained from ATCC. MDA-MB-231, JIMT-1, DU145 were grown in DMEM medium supplemented with 10% FBS. BT474 cells were grown in DMEM/F12 medium supplemented with 10% FBS. MiaPaCa2 was cultured in DMEM supplemented with 10% FBS and 2.5% horse serum. PC3 cells were cultured in F12K medium supplemented with 10% FBS. All the media contained penicillin/streptomycin. The effects of the GAELs on the viability of the various epithelial cancer cell lines was determined as previously described.^{2,3,7,34} Briefly equal numbers of the cells were dispersed into 96-well plates. After 24 h, the cells were incubated with the compounds (0-30 μ M) for 48 h. At the end of the incubation, MTS reagent (20% vol/vol) was added and the plates were incubated for 1-4 h in a CO₂ incubator. The OD₄₉₀ was read with a plate reader (Molecular Devices). Wells with media but no cells were treated in similar fashion and the values utilized as blank. The results represent the mean \pm standard deviation of 6 independent determinations.

6.7.2.2.2. Demonstration of Caspase- independent mode of cell death

JIMT-1 and DU145 were grown in DMEM medium containing penicillin/streptomycin and supplemented with 10% FBS. Equal numbers of the cells were dispersed into 96-well plates, after 4 h, the cells were treated with pan-caspase inhibitor QVD-OPh (40 μ M). After 20 h, the cell were incubated with the varying concentration of the compounds (0 – 9 μ M) for 48 h. At the

end of the incubation, MTS reagent (20% vol/vol) was added and the plates were incubated for 1-4 h in a CO₂ incubator. The OD₄₉₀ was read with a plate reader (Molecular Devices). Wells with media but no cells were treated in similar fashion and the values utilized as blank. The results represent the mean ± standard deviation of 6 independent determinations.

6.7.2.2.3. Determination of membranolytic effects of GAELs

JIMT-1 and DU145 were grown in DMEM medium supplemented with 10% FBS and antibiotics, penicillin/streptomycin. Equal numbers of the cells were dispersed into 96-well plates. After 24 h, the cells were incubated with varying concentration of the compounds **4** and **5** (4 - 6 µM) for 5 - 6 h. Subsequently, the cell membrane impermeant DNA staining dye, ethidium homodimer-1 (EthD-1, Molecular Probes) at a final concentration of 2 µM was added and the cells analysed by fluorescence microscopy.²⁵ EthD-1 staining was compared to negative controls with no treatment and positive control treated with 0.01% Triton X-100 for 10 min.

6.7.2.2.4. Hemolytic assay

The hemolytic activity of the GAEL analogs was evaluated using ovine erythrocyte. Sheep whole blood was collected from a slaughter house into a container containing disodium EDTA in a buffered saline (10mM Tris, 150 mM NaCl, pH 7.4). The erythrocytes were prepared and wash with buffered saline as previously reported.^{35,36} For the assay, the erythrocyte suspension, varying amounts of the GAEL drugs, the saline buffer and the appropriate amount of the vehicle used for dissolving the compounds were pipetted to an Eppendorf tubes to give a final volume of 1500 µL and cell density of 2.5×10^8 cells/ml. The suspensions were incubated with gentle shaking in Eppendorf thermomixer for 30 minutes. The eppendorf tubes were cooled in ice water

and centrifuged at 2000g and 4°C for 5 minutes. 200 µL of the supernatant was dissolved in 1800 µL of 0.5% NH₄OH and the optical density (OD) was recorded using 1mL cuvette at 540 nm in a spectrophotometer. For the 0% hemolysis, buffer and vehicle used to dissolve the drug were added instead of the drug and for the 100% hemolysis 1% NH₄OH was used. % hemolysis was calculated using the optical density (OD) values as shown below:

$$\% \text{ hemolysis} = (X - 0\%) / (100\% - 0\%)$$

X is OD values of the drugs at varying concentration.

6.7.2.2.5. Isolation of cancer stem cells from BT-474 cell lines and determination of the effect of GAELs on the viability of the cancer stem cells.

A population enriched in BT474 breast cancer stem cells was obtained by staining the cells for aldehyde dehydrogenase using the Aldefluor assay kit from Stem Cell Technologies (Vancouver, BC, Canada) according to the instruction of the manufacturer with the appropriate controls. The stained cells were sorted from the bulk population by flow cytometry on a 4 laserMoFloXPP high speed/pressure cell sorter. The cells were pelleted by centrifugation and resuspended into ultra-low adhesion plates in mammocult medium (Stem Cell Technologies). The dishes were incubated at 37°C in a CO₂ incubator for 5 days for spheroid formation.

The spheres are separated from single cells with a 40 µm nylon cell strainer. The spheres retained in the strainer were washed with PBS and trypsinised to obtain single cells. The cell numbers were counted with a Coulter ZM counter and the cells were dispersed into 96-well ultra-low adhesion plates in a volume of 100 µl. The cells were incubated for 3 days to allow for formation of spheroids. Subsequently, the stock GAELs in ethanol were diluted to twice the final concentration in the media and a volume of 100 µl was added to each wells. Wells with

growth medium but no cells were treated as the wells with cells. After 3-day incubation, MTS reagent (20% vol/vol) was added to each well and the plates were incubated for 1-4 h for formation of color. The OD₄₉₀ were read in a Molecular Device absorbance plate reader using the SpectroMax software.

6.7.2.2.6. Evaluation of stability of L-glucosamine derived GAELs to cocktail α - and β -glycosidases

Bovine liver extract, containing glucosidases, mannosidases, galactosidases and glucosaminidases, was prepared from beef liver as previously reported^{30,37} Fresh whole beef liver was obtained from a slaughter house (Robert Farm, Winnipeg). The connective tissue covering the liver was removed, and 100 g of the tissue was cut into small pieces and homogenized in 1 L of cold water (4°C) in a blender for a minute. The pH was adjusted to 4.8 using 1 M citric acid. The mixture was centrifuged and the 0.20 M to 0.60 M saturated ammonium sulfate fraction precipitate was obtained. The fraction was dissolved in distilled water and dialyzed at 4°C against water for 24 h, and against 0.05 M sodium citrate buffer, pH 5.0, for a further 24 h.³⁷ Undissolved precipitates were discarded and the supernatant was stored at -20°C. At this temperature the glycosidases can be stable for many months.³⁷ The protein content of the fraction was 7.5mg/ml based on protein assay using Cytoskeleton precision red advanced protein assay reagent as stipulated by manufacturer.

The glycosidases activity of the fraction was assessed as previously described^[10]. Briefly, the assay mixture (2 ml) consisted of 0.5 ml of 0.2 M citric acid-NaOH buffer, pH 4.4, 0.4 ml of 25 mM of p-Nitrophenyl α -glucoside, 25 μ L of enzyme solution, 0.225 ml of buffer solution used as vehicle for the enzyme and 0.85 ml of distilled water. The final concentration of the substrate in

the incubated mixture was 10 mM. After incubation for 1 h at 38°C, 2 ml of 0.4 M glycine-NaOH buffer, pH 10.5 was added. The solution was centrifuged and the liberated p-Nitrophenol was measured by spectrophotometer at 410 nm. The activity of enzyme was calculated to be 19.26 µg/mg/hr.³⁸

To assess the stability of L-glucosamine GAEL **2** to the liver glycosidases fraction, the reaction mixture (50 µL) contained 7.5 µL of 0.2 M sodium citrate buffer, pH 4.4, 12.5 µL of 30 mM of the substrate i.e. compound **2**, 25 µL of the glycosidase fraction in 0.05 M sodium citrate buffer, pH 5.0 and 5 µL of 10% Triton X100 for solubilization of the substrate in the mixture. For the control without enzyme 25 µL of 0.05 M sodium citrate buffer, pH 5.0 were used. Triton X100 was established to have no effect on enzyme activity. After 1 h incubation, 25 µL of methanol was added to inactivate the enzyme and the supernatant was analyzed using both mass spectrometry and LC-MS to determine the presence of enzymatic degradation product. Three repeats of the experiment were carried out. The result showed that compound **2** was resistant to animal glycosidases catalyzed hydrolysis. This outcome is a confirmation of our hypothesis that unnatural L-sugar based GAELs will be resistant to metabolic degradation especially glycosidases-catalyzed hydrolysis.

6.7.2.3. Statistical analysis

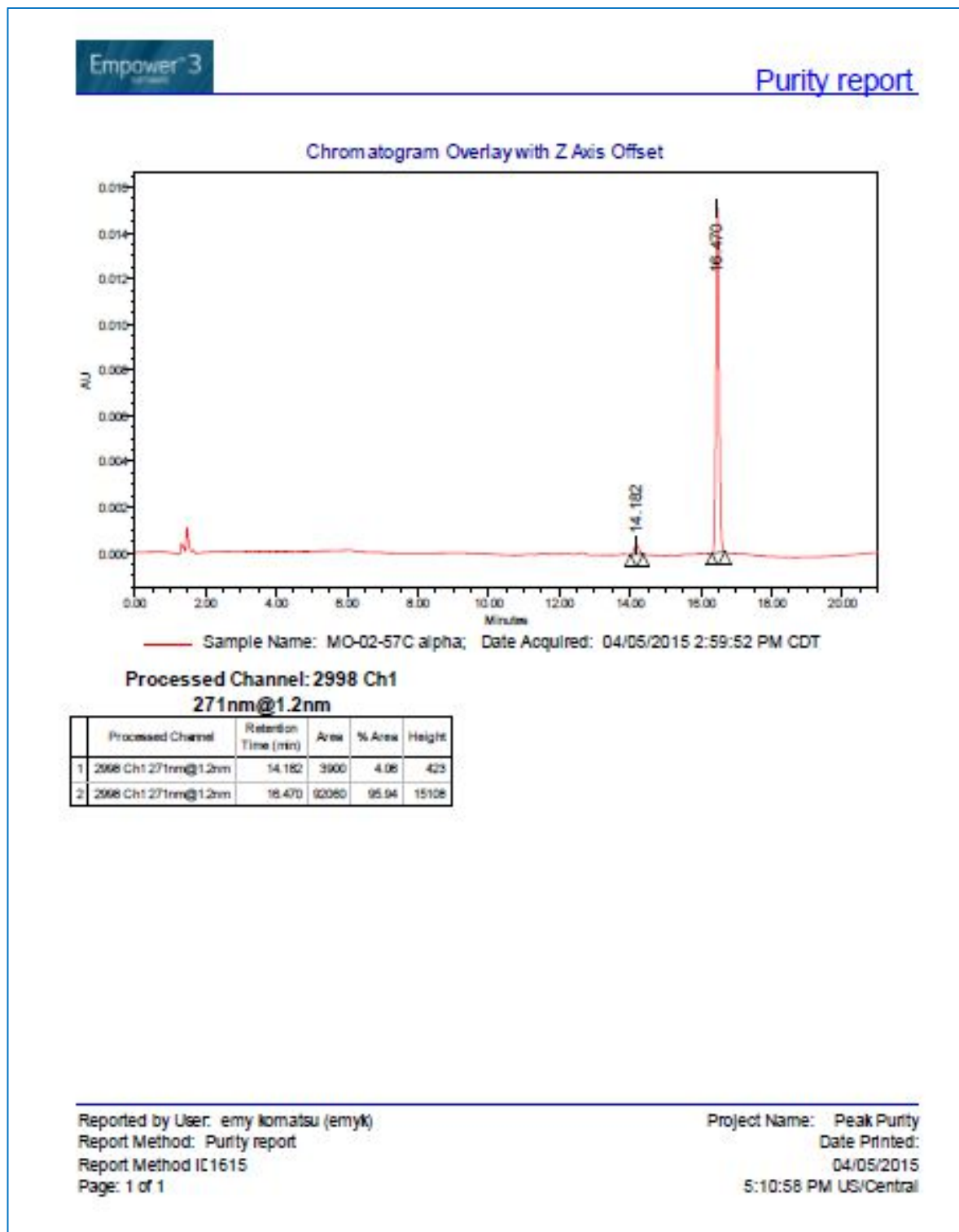
The results represent the mean ± standard deviation of 6 independent determinations. Statistical significant difference tests were carried using GraphPadInstat software. The data, that is, the mean values were subjected to one-way analysis of variance (ANOVA) followed by Tukey-Kramer multiple comparison tests as post hoc test. Comparisons were carried out between the viability of controls and drug treated cells to determine if statistically significant differences existed between the two groups. The results of the effects of different concentrations of the

compounds were also compared for statistically significant differences to determine if the cytotoxic activities of the drugs are dose dependent. The anticancer activities of the compounds **1 – 5**, salinomycin, cisplatin and myristylamine tested were also compared using ANOVA followed by Tukey-Kramer multiple comparison tests at the following concentrations: 5, 7.5 and 10 μM to determine if the difference in the potency of the drugs are statistically significant or not. A p value > 0.05 indicates no statistical differences while a p value <0.001 indicated statistical significant differences.

6.7.2.4. Purity report of compounds 3-5

Compound 3 purity report -

HPLC-UV chromatogram

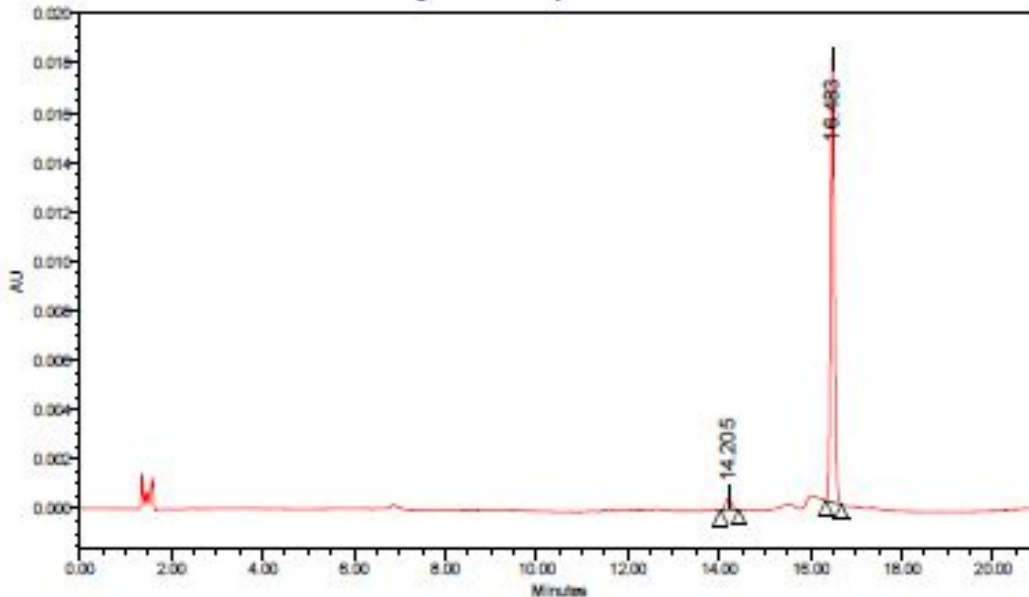


Compound 4 purity report - HPLC-UV chromatogram



Purity report

Chromatogram Overlay with Z Axis Offset



— Sample Name: MO-02-57B alpha; Date Acquired: 04/05/2015 3:42:46 PM CDT

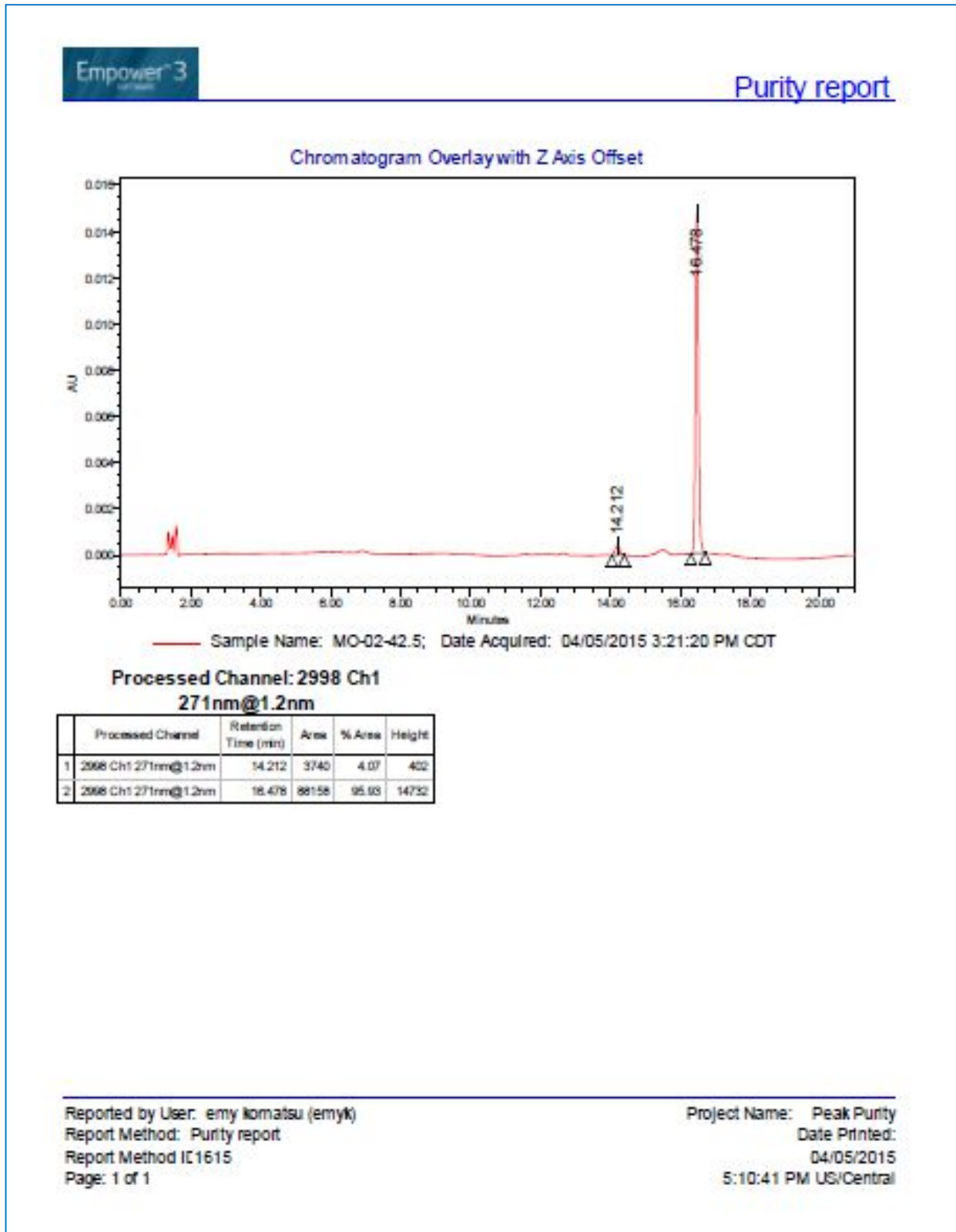
Processed Channel: 2998 Ch1
271nm@1.2nm

	Processed Channel	Retention Time (min)	Area	% Area	Height
1	2998 Ch1 271nm@1.2nm	14.205	4580	4.20	505
2	2998 Ch1 271nm@1.2nm	16.483	104102	95.80	17951

Reported by User: emy komatsu (emyk)
Report Method: Purity report
Report Method IC1615
Page: 1 of 1

Project Name: Peak Purity
Date Printed:
04/05/2015
5:10:23 PM US/Central

Compound 5 purity report - HPLC-UV chromatogram



6.8. References

- (1) Arthur, G.; Schweizer, F.; Ogunsina, M. Carbohydrates in Drug Design and Discovery; Jimenez-Barbero, J., Canada, F. J., Martin-Santamaria, S., Eds.; RSC Drug Discovery; Royal Society of Chemistry: Cambridge, 2015.
- (2) Xu, Y.; Ogunsina, M.; Samadder, P.; Arthur, G.; Schweizer, F. Structure-Activity Relationships of Glucosamine-Derived Glycerolipids: The Role of the Anomeric Linkage, the Cationic Charge and the Glycero Moiety on the Antitumor Activity. *ChemMedChem* **2013**, *8* (3), 511–520.
- (3) Samadder, P.; Xu, Y.; Schweizer, F.; Arthur, G. Cytotoxic Properties of D-Gluco-, D-Galacto- and D-Manno-Configured 2-Amino-2-Deoxy-Glycerolipids against Epithelial Cancer Cell Lines and BT-474 Breast Cancer Stem Cells. *Eur. J. Med. Chem.* **2014**, *78* (78), 225–235.
- (4) Arthur, G.; Bittman, R. Glycosylated Antitumor Ether Lipids: Activity and Mechanism of Action. *Anticancer. Agents Med. Chem.* **2014**, *14* (4), 592–606.
- (5) Maltese, W. A.; Overmeyer, J. H. Non-Apoptotic Cell Death Associated with Perturbations of Macropinocytosis. *Front. Physiol.* **2015**, *6* (FEB), 1–10.
- (6) Dean, M.; Fojo, T.; Bates, S. Tumour Stem Cells and Drug Resistance. *Nat. Rev. Cancer* **2005**, *5* (4), 275–284.
- (7) Ogunsina, M.; Pan, H.; Samadder, P.; Arthur, G.; Schweizer, F. Structure Activity Relationships of N-Linked and Diglycosylated Glucosamine-Based Antitumor

- Glycerolipids. *Molecules* **2013**, *18* (12), 15288–15304.
- (8) García-Álvarez, I.; Groult, H.; Casas, J.; Barreda-Manso, M. A.; Yanguas-Casás, N.; Nieto-Sampedro, M.; Romero-Ramírez, L.; Fernández-Mayoralas, A. Synthesis of Antimitotic Thioglycosides: In Vitro and in Vivo Evaluation of Their Anticancer Activity. *J. Med. Chem.* **2011**, *54* (19), 6949–6955.
- (9) Livesey, G.; Brown, J. C. Whole Body Metabolism Is Not Restricted to D-Sugars Because Energy Metabolism of L-Sugars Fits a Computational Model in Rats. *J. Nutr.* **1995**, *125* (12), 3020–3029.
- (10) Rudney, H. The Utilization of L-Glucose by Mammalian Tissues and Bacteria. *Science* **1940**, *92* (2379), 112–113.
- (11) Thibodeaux, C. J.; Melançon, C. E.; Liu, H. Natural-Product Sugar Biosynthesis and Enzymatic Glycodiversification. *Angew. Chem. Int. Ed. Engl.* **2008**, *47* (51), 9814–9859.
- (12) Samadder, P.; Byun, H.-S.; Bittman, R.; Arthur, G. An Active Endocytosis Pathway Is Required for the Cytotoxic Effects of Glycosylated Antitumor Ether Lipids. *Anticancer Res* **2011**, *31* (11), 3809–3818.
- (13) Zhang, Y.; Wu, M.; Han, X.; Wang, P.; Qin, L. High-Throughput, Label-Free Isolation of Cancer Stem Cells on the Basis of Cell Adhesion Capacity. *Angew. Chem. Int. Ed. Engl.* **2015**, *54* (37), 10838–10842.
- (14) Zhao, J. Cancer Stem Cells and Chemoresistance: The Smartest Survives the Raid. *Pharmacol. Ther.* **2016**.
- (15) Skvortsova, I.; Debbage, P.; Kumar, V.; Skvortsov, S. Radiation Resistance: Cancer Stem

- Cells (CSCs) and Their Enigmatic pro-Survival Signaling. *Semin. Cancer Biol.* **2015**, *35*, 39–44.
- (16) Gupta, P. B.; Onder, T. T.; Jiang, G.; Tao, K.; Kuperwasser, C.; Weinberg, R. A.; Lander, E. S. Identification of Selective Inhibitors of Cancer Stem Cells by High-Throughput Screening. *Cell* **2009**, *138* (4), 645–659.
- (17) Vazquez-Martin, A.; Oliveras-Ferreros, C.; Del Barco, S.; Martin-Castillo, B.; Menendez, J. A. The Anti-Diabetic Drug Metformin Suppresses Self-Renewal and Proliferation of Trastuzumab-Resistant Tumor-Initiating Breast Cancer Stem Cells. *Breast Cancer Res. Treat.* **2011**, *126* (2), 355–364.
- (18) Zobalova, R. .; Stantic, M. .; Stapelberg, M. .; Prokopova, K. .; Dong, J. .; Truksa, J. et al. Drugs That Kill Cancer Stem-like Cells. In *Cancer Stem Cells Theories and Practice*; Shosta, S., Ed.; InTech, 2011; pp 361–378.
- (19) Naujokat, C.; Steinhart, R. Salinomycin as a Drug for Targeting Human Cancer Stem Cells. *J. Biomed. Biotechnol.* **2012**, *2012*, 1–17.
- (20) Fuentes-Prior, P.; Salvesen, G. S. The Protein Structures That Shape Caspase Activity, Specificity, Activation and Inhibition. *Biochem. J.* **2004**, *384* (Pt 2), 201–232.
- (21) Debatin, K.-M.; Krammer, P. H. Death Receptors in Chemotherapy and Cancer. *Oncogene* **2004**, *23* (16), 2950–2966.
- (22) Almeida, S.; Brett, A. C.; Góis, I. N.; Oliveira, C. R.; Rego, A. C. Caspase-Dependent and -Independent Cell Death Induced by 3-Nitropropionic Acid in Rat Cortical Neurons. *J. Cell. Biochem.* **2006**, *98* (1), 93–101.

- (23) Keoni, C. L.; Brown, T. L. Inhibition of Apoptosis and Efficacy of Pan Caspase Inhibitor, Q-VD-OPh, in Models of Human Disease. *J. Cell Death* **2015**, *8*, 1–7.
- (24) Caserta, T. M.; Smith, A. N.; Gultice, A. D.; Reedy, M. A.; Brown, T. L. Q-VD-OPh, a Broad Spectrum Caspase Inhibitor with Potent Antiapoptotic Properties. *Apoptosis* **2003**, *8* (4), 345–352.
- (25) Krämer, S. D.; Wunderli-Allenspach, H. No Entry for TAT(44–57) into Liposomes and Intact MDCK Cells: Novel Approach to Study Membrane Permeation of Cell-Penetrating Peptides. *Biochim. Biophys. Acta - Biomembr.* **2003**, *1609* (2), 161–169.
- (26) Markovits, J.; Roques, B. P.; Le Pecq, J. B. Ethidium Dimer: A New Reagent for the Fluorimetric Determination of Nucleic Acids. *Anal. Biochem.* **1979**, *94* (2), 259–264.
- (27) Lim, J. P.; Gleeson, P. A. Macropinocytosis: An Endocytic Pathway for Internalising Large Gulps. *Immunol. Cell Biol.* **2011**, *89* (8), 836–843.
- (28) Maltese, W. A.; Overmeyer, J. H. Methuosis: Nonapoptotic Cell Death Associated with Vacuolization of Macropinosome and Endosome Compartments. *Am. J. Pathol.* **2014**, *184* (6), 1630–1642.
- (29) Langley, T. J.; Jevons, F. R. Characterization of Beef-Liver Glycosidases Possibly Involved in Glycoprotein Degradation. *Arch. Biochem. Biophys.* **1968**, *128* (2), 312–318.
- (30) Weissmann, B.; Hadjiioannou, S.; Tornheim, J. Oligosaccharase Activity of P-IV-Acetyl-D-Glucosaminidase of Beef Liver *. *J. Biol. Chem.* **1964**, *239* (1), 59–63.
- (31) Czechura, P.; Tam, R. Y.; Dimitrijevic, E.; Murphy, A. V; Ben, R. N. The Importance of Hydration for Inhibiting Ice Recrystallization with C-Linked Antifreeze Glycoproteins. *J.*

- Am. Chem. Soc.* **2008**, *130* (10), 2928–2929.
- (32) Emmadi, M.; Kulkarni, S. S. Rapid Transformation of D-Mannose into Orthogonally Protected D-Glucosamine and D-Galactosamine Thioglycosides. *J. Org. Chem.* **2011**, *76* (11), 4703–4709.
- (33) Pedretti, V.; Veyrières, A.; Sinaÿ, P. A Novel 13 O→C Silyl Rearrangement in Carbohydrate Chemistry: Synthesis of α -D-Glycopyranosyltrimethylsilanes. *Tetrahedron* **1990**, *46* (1), 77–88.
- (34) Erukulla, R. K.; Zhou, X.; Samadder, P.; Arthur, G.; Bittman, R. Synthesis and Evaluation of the Antiproliferative Effects of 1-O-Hexadecyl-2-O-Methyl-3-O-(2'-acetamido-2'-deoxy-Beta-D- Glucopyranosyl)-Sn-Glycerol and 1-O-Hexadecyl-2-O-Methyl-3-O-(2'-amino-2'-deoxy-Beta-D-Glucopyranosyl)-Sn-Glycerol on Epithelial Canc. *J. Med. Chem.* **1996**, *39* (7), 1545–1548.
- (35) Hanson, M. S.; Stephenson, A. H.; Bowles, E. A.; Sridharan, M.; Adderley, S.; Sprague, R. S. Phosphodiesterase 3 Is Present in Rabbit and Human Erythrocytes and Its Inhibition Potentiates Iloprost-Induced Increases in cAMP. *Am. J. Physiol. Heart Circ. Physiol.* **2008**, *295* (2), H786–H793.
- (36) Evans, B. C.; Nelson, C. E.; Yu, S. S.; Beavers, K. R.; Kim, A. J.; Li, H.; Nelson, H. M.; Giorgio, T. D.; Duvall, C. L. Ex Vivo Red Blood Cell Hemolysis Assay for the Evaluation of pH-Responsive Endosomolytic Agents for Cytosolic Delivery of Biomacromolecular Drugs. *J. Vis. Exp.* **2013**, No. 73, e50166.
- (37) Langley, T. J.; Jevons, F. R. Characterization of Beef-Liver Glycosidases Possibly Involved in Glycoprotein Degradation. *Arch. Biochem. Biophys.* **1968**, *128* (2), 312–318.

- (38) Findlay, J.; Levvy, G. A.; Marsh, C. A. Inhibition of Glycosidases by Aldonolactones of Corresponding Configuration. 2. Inhibitors of Beta-N-Acetylglucosaminidase. *Biochem. J.* **1958**, *69* (3), 467–476.

Chapter 7

Cytotoxic Properties of L-Sugar Linked Amino Lipids in Cancer Cells and Stem Cells

By Makanjuola Ogunsina¹, Pranati Samadder², Gilbert Arthur² and Frank Schweizer¹

7.1. Authorship considerations

Makanjuola Ogunsina was responsible for design, synthesis, purification and characterization of all glycolipids on the advice of Frank Schweizer. Biological studies were investigated by Makanjuola Ogunsina and Pranati Samadder on the advice of Gilbert Arthur. The preliminary draft of the paper was written by Makanjuola Ogunsina reviewed by Frank Schweizer and Gilbert Arthur, and then rendered into its final form by Makanjuola Ogunsina. Frank Schweizer and Gilbert Arthur are corresponding authors.

7.2. Abstract

A major impediment to successfully treating cancer is the inability of clinically available drugs to kill cancer stem cells (CSCs), a subset of tumor cells that mediate progression, resistance and relapse of the cancer. We recently identified metabolically stable L-glucosamine-based glycosylated antitumor ether lipids (GAELs) that were cytotoxic to both cancer cells and cancer stem cells. In the absence of commercially available L-glucosamine, many synthetic steps were needed and the overall yield was poor. To overcome this setback and to expand on our working hypothesis, that replacement of a D-sugar with L-sugar unnatural to mammals in GAELs will enhance stability to glycosidases while retaining antitumor activity, we explored the effect of replacing L-glucosamine in GAELs with other commercially available L-sugars including L-rhamnose, L-glucose and L-mannose on the anticancer activity of the compounds. The most potent analog synthesised, 3-amino-1-*O*-hexadecyloxy-2R-(*O*- α -L-rhamnopyranosyl)-

sn-glycerol **4**, demonstrated a potent antitumor effect against twelve human cancer cell lines derived from breast, prostate, pancreas and brain tumor. The activity observed was superior to that observed with cisplatin and chlorambucil, two clinically used anticancer agents. Compound **4** also displayed impressive cytotoxicity against CSCs originating from breast, prostate and pancreas cancer similar to or better than that of salinomycin, a well studied anti-CSCs agents. Moreover, this compound induced cell death by a non-membranolytic caspase-independent pathway. *In vivo* tolerability study showed that 3-amino-1-*O*-hexadecyloxy-2R-(*O*- α -L-rhamnopyranosyl)-*sn*-glycerol is safe and well tolerated in mice up to 300 mg/kg orally or 50 mg/kg intravenously without any identified damage to vital organs.

7.3 Introduction

Diseases have plagued humans for millennia. With advancement in medical and biomedical sciences and technology, some of these maladies have been eradicated although others, including cancer, still threaten life. Cancer has a tremendous burden on society costs in the US (medical and lost productivity) in 2010 were estimated to be \$263.8 billion.¹ Despite increasing investment in cancer research and treatment, the number of new cases and cancer deaths are increasing in both the developed and the developing world, affecting both males and females in nearly the same proportion.²⁻⁴

Tumor relapse which can materialize within months to decades after initial treatment^{5,6} is a major obstacle to the successful treatment of cancer by surgery, chemo- radio- therapy or other forms of therapy. Prognosis of refractory tumors is very poor as a consequence of resistance to previously used drugs and possibly intrinsic resistance to other drugs.⁷ Relapsed cancers are usually more virulent and highly metastasizing.^{8,9} The major cause of cancer recurrence has

been associated with cancer stem cells (CSCs).^{10,11} CSCs have been identified and isolated from virtually all solid and hematological tumors.¹¹⁻¹⁵ They are small subpopulation of cells within tumor that maintains tumor homeostasis, progression, resistance to drug and metastasis.¹⁶⁻²³ As a result of the resistance of CSCs to most anticancer agents, when the tumor is treated, the bulk of the tumor cells will die leaving behind a small population of CSCs which are able to self-renew and to differentiate into cells that reconstitute the tumors.²⁴⁻²⁶ Resistance of CSCs to anticancer drugs is linked to their ability to escape various death pathways including apoptosis.²⁷⁻³⁰ Because of the central role of CSCs in tumor development, progression, and relapse, any effective anticancer drug must be able to kill CSCs.³¹⁻³³ Only few compounds have been reported to kill CSCs which include temozolomide, parthenolide, salinomycin, metformin, and lapatinib.³⁴⁻³⁸ But the toxicity of these drugs at the concentrations at which they kill CSCs may prevent them from clinical use.³⁹

Glycosylated antitumor ether lipids (GAELs) a subclass of antitumor ether lipids (AELs) were recently discovered to be cytotoxic to CSCs.⁴⁰ AELs are synthetic ether lipids that possess anticancer activity and comprise three subclasses; the alkyllysophospholipid (ALP), alkylphosphocholine (APC) and the non-phosphorylated GAELs. The cytotoxic properties of GAELs, prototypified by **β -GLN 9** and **α -GLN 10** (Figure 7.1) have been established to be superior to the most studied AEL, edelfosine.^{41,42} Unlike ALPs and APCs, which kill cells by apoptosis, GAELs kill cells by an apoptosis independent mechanism, likely methuosis.^{40,43-45} This mode of cell death appears to involve the disturbance of the endocytosis pathway to generate macropinosome-derived vacuoles that promote events which ultimately cause cell death.⁴³⁻⁴⁵ CSC appear to be susceptible to this mode of cell death since a number of D-GAELs including **9** and **10** were cytotoxic to CSCs isolated from BT-474 cell line.⁴⁰ The clinical

development of the D-GAELs is hampered by their poor metabolic stability in *in vivo* experiments.^{41,46}

Recently, a metabolically stable L-glucosamine-derived GAELs such as **8** (Figure 7.1) that are cytotoxic to both cancer cells and cancer stem cells were identified.⁴⁷ These analogs unlike D-glucosamine based GAELs such as **β -GLN 9** and **α -GLN 10** are resistant to metabolic degradation especially by glycosidases which are ubiquitous in human and overexpressed in many types of cancers.^{48,49} The major challenge to further development of L-glucosamine analogs is its cumbersome synthetic procedures and overall poor yield. The reason for this being commercial unavailability of L-glucosamine. To address this problem and to expand on our working hypothesis, that replacement of D-sugars with L-sugars unnatural to mammals in GAELs will enhance stability to glycosidases, without affecting the cytotoxic activity, we have employed commercially available L-sugars: L-mannose, L-glucose and L-rhamnose to synthesize new analogs **3 - 7**.

Herein we report on the cytotoxicity of the synthesized L-GAELs with sugars unnatural to human and other mammals and reference compounds against epithelial cancer cell lines derived from a variety of human cancers. The effect of the compounds on the viability of CSCs derived from breast, prostate and pancreatic cancer cell lines was also investigated. We also determined if compound **4** retains the apoptosis independent mechanism of cell death observed in cytotoxic GAELs and its effect on integrity of cell membrane using ovine erythrocytes, DU-145 and JIMT-1 cell lines. Additionally, we confirmed the stability of compound **4** to glycosidases to prove our hypothesis. We also provide insight into mode of action of compound **4** and its safety profile in an animal model.

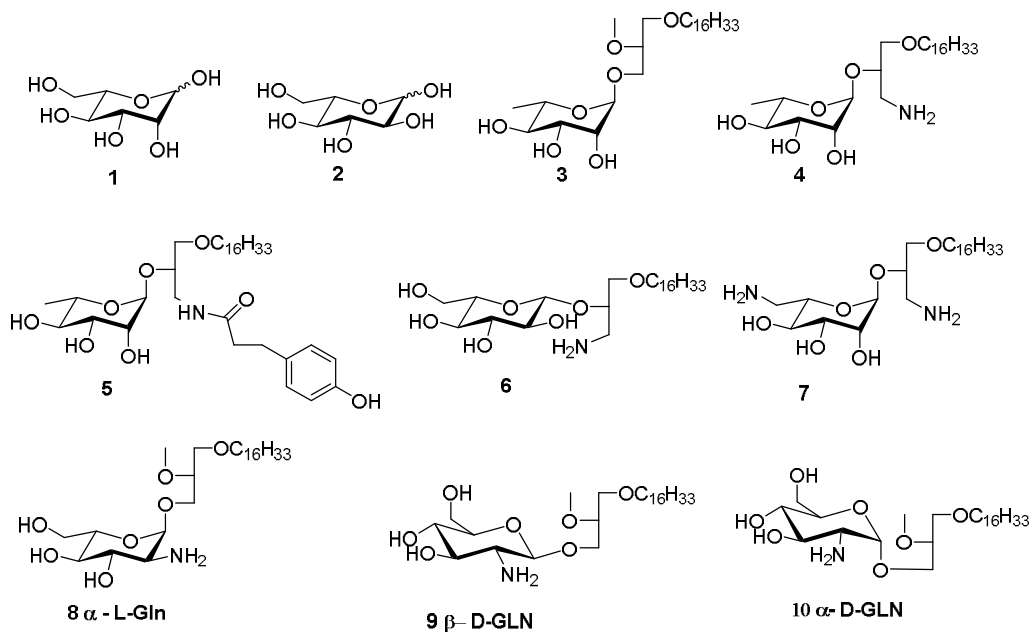


Figure 7.1. List of compounds tested in this study. L- mannose **1** and L-glucose **2** were included to determine if they are independently cytotoxic. Compound **3-7** are the new L-sugar derived GAELs investigated in this report, while L-glucosamine **8**, D- Glucosamine analogs **9** and **10** are reference GAELs.

7.4. Results

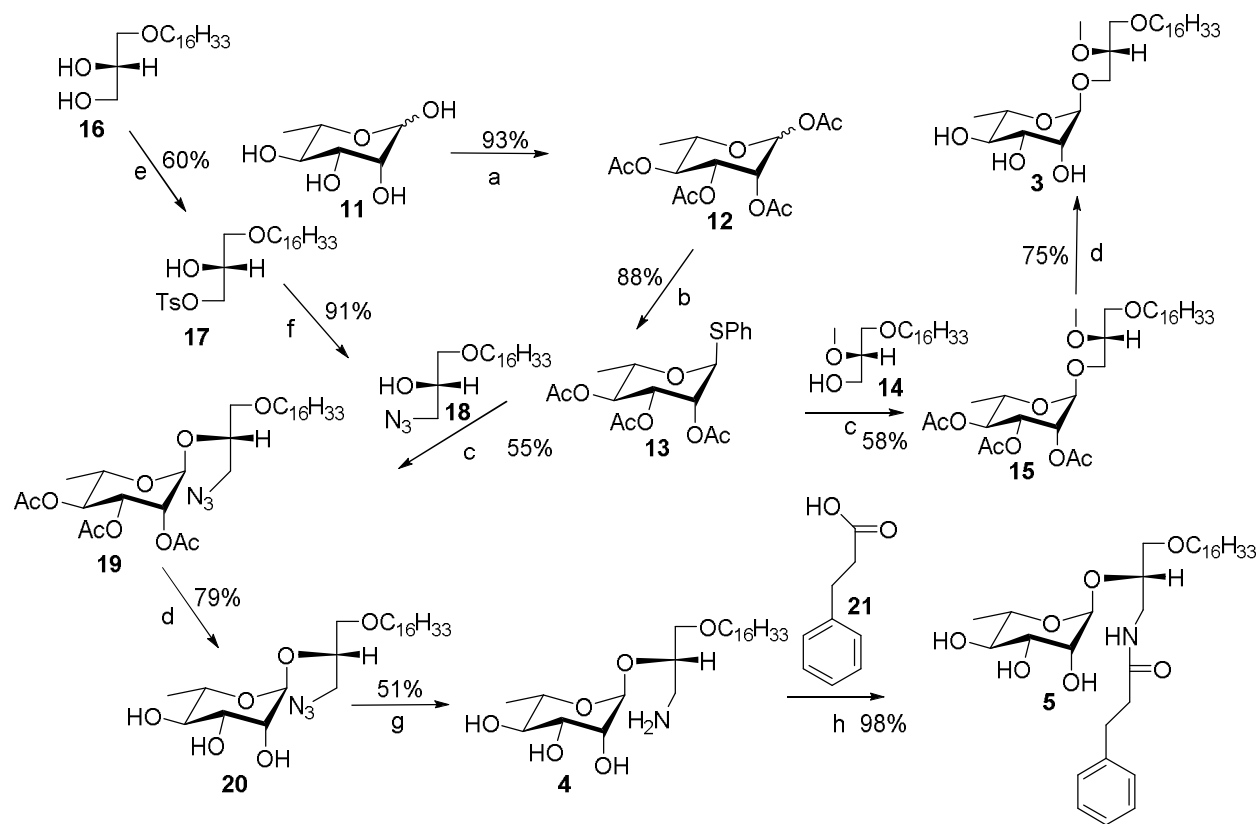
Several novel L- GAELs analogues, compounds **3-8**, were synthesized and assessed for their cytotoxic activity in order to provide insight on structural features required for activity. The neutral glycerolipid **3** was synthesized to evaluate the effect of replacing L-glucosamine of compound **8** and D- glucosamine of **9** and **10** with a neutral sugar L-rhamnose. Compound **4** was synthesized to evaluate the effect of introducing a cationic moiety into L- rhamnose based glycerolipid. The primary position of the amine was selected for ease of synthesis. Compound **5** was synthesised to evaluate the effect of amide linkage with p-hydroxyphenyl propionic acid. The L-glucose based cationic **6** was synthesized to evaluate the effect of different

types of sugars when compared to **4**. The biscationic **7** was selected to evaluate the effect of the two amino moieties, because previous experience with L-glucosamine analogs showed that additional amino substituent at C-6 position of the sugar enhanced potency and to evaluate the effect of L- manno-configured sugar on cytotoxicity of GAELs.

7.4.1. Synthesis of L-Sugar Derived Glycolipids **3 -7**

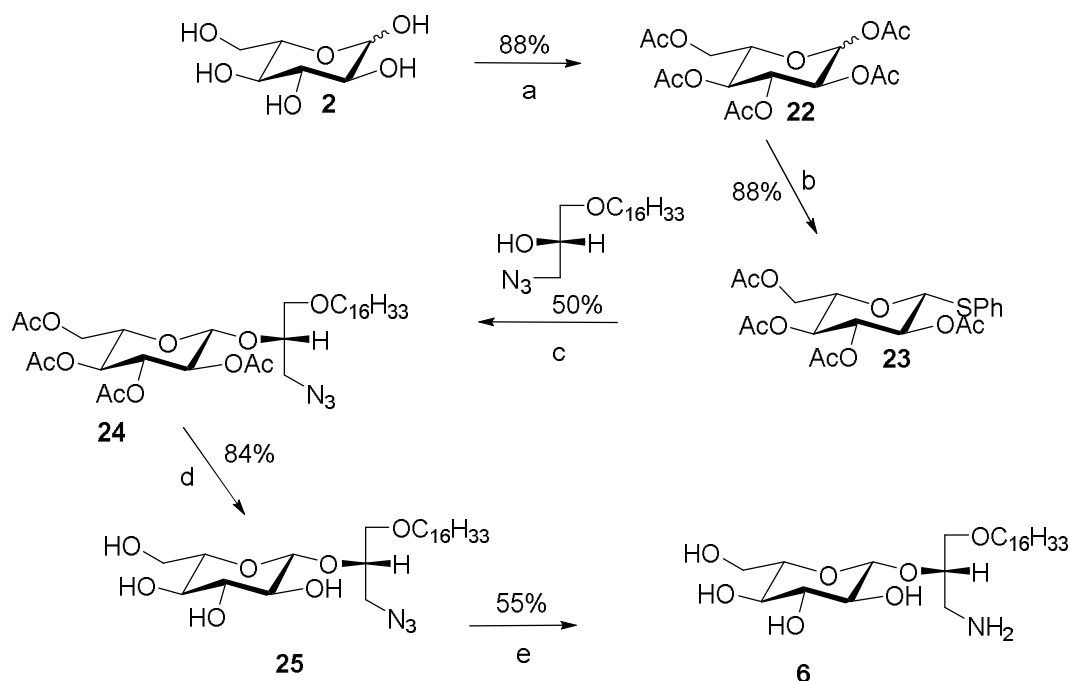
The hydroxyl groups of L-rhamnose **11** was protected with acetyl groups using acetic anhydride in pyridine and dimethyl aminopyridine as catalyst to give the tetraacetate **12** as indicated in Scheme 7.1. The phenyl thioglycoside **13** was synthesized from **12** by $\text{BF}_3 \cdot \text{OEt}_2$ promoted glycosylation with thiophenol. Silver triflate promoted glycosylation of **13** to the commercially available glycerolipid alcohol **14** to yield the fully protected glycolipid **15**. Sodium methoxide-catalysed deblocking of **15** in methanol gave the desired glycolipid **3** (Scheme 7.1).

Synthesis of compound **4** was achieved by glycosylation of the glycoside donor **13** with the acceptor, azido lipid **18** as described above to give the fully protected azidoglycolipid **19**. The azido glycerolipid **18** was made from the commercially available glycerol-analogue **17** as previously described.⁵⁰ Compound **19** was deacetylated to give the azide **20**. Reduction of the azido substituent of **20** was accomplished by using trimethyl phosphine in THF/ water mixture to give monocationic compound **4** (Scheme 7.1). Attempts to use catalytic hydrogenation for this step was not successful because of many degradation products. The amide **5** was synthesized by coupling **4** to p-hydroxyphenylproprionic acid **21** using TBTU⁵⁰ (Scheme 7.1).



Scheme 7.1. Synthesis of compounds **3-5**. *Reagents and conditions:* (a) Ac_2O , DMAP, Pyridine, 18 h, rt (b) PhSH , $\text{BF}_3 \cdot \text{Et}_2\text{O}$, DCM, 18 h, rt (c) AgOTf , NIS, DCM, 3 h, rt (d) MeONa , MeOH, 1h (e) TsCl , Pyridine, DMAP, 0°C - rt, 18 h (f) DMF, NaN_3 , 70°C (g) $\text{P}(\text{CH}_3)_3$, THF, H_2O , 2 h, rt (h) TBTU , DMF, argon, 5h. Abbreviations: 4-Dimethyl amino pyridine (DMAP), Dichloromethane (DCM), *N,N*-dimethylformamide (DMF), room temperature (rt), *N*-iodosuccinimide (NIS).

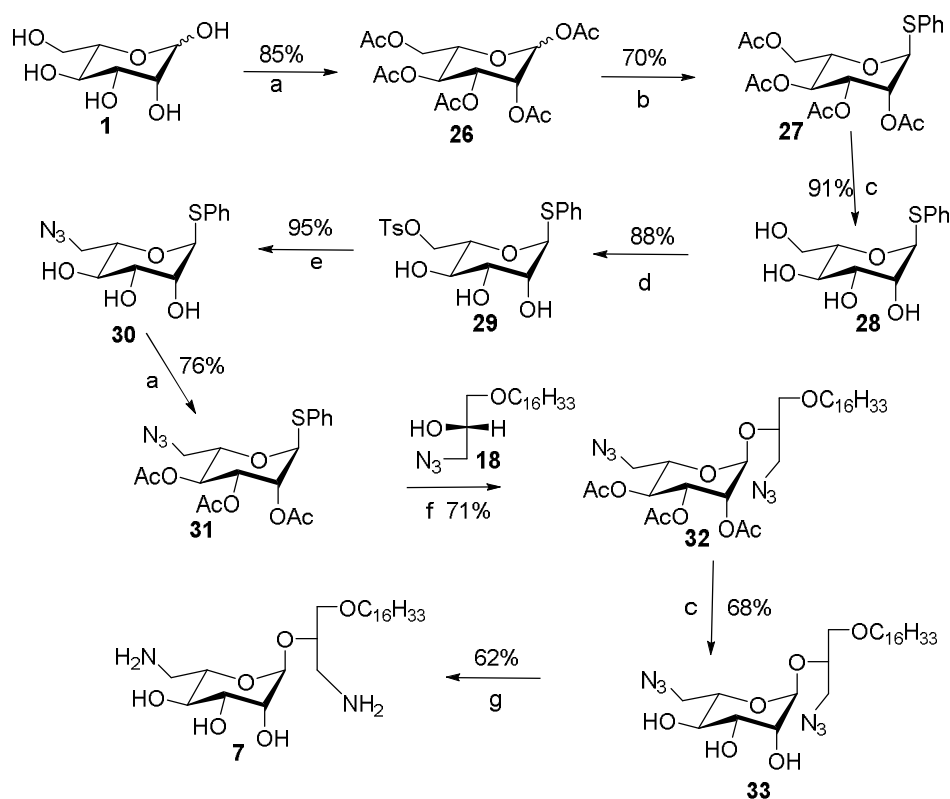
The cationic L-glucose based Compound **6** was synthesized from L-glucose **2** following the same procedure described above for the synthesis of compound **4** (Scheme 7.2).



Scheme 7.2. Synthesis of compound 6. *Reagents and conditions:* (a) Ac₂O, DMAP, Pyridine, 18 h, rt (b) PhSH, BF₃·Et₂O, DCM, 18 h, rt (c) AgOTf, NIS, DCM, 3 h, rt (d) MeONa, MeOH, 1h (e) P(CH₃)₃, THF, H₂O, 2 h, rt (h)TBTU, DMF, argon, 5h. Abbreviations: 4-Dimethyl amino pyridine (DMAP), Dichloromethane (DCM), N,N-dimethylformamide (DMF), room temperature (rt), *N*-iodosuccinimide (NIS)

Compound 7 was synthesized by coupling of glycoside donor 31 to lipid alcohol 18 to afford α -glycolipid 32 (Scheme 7.3). The glycoside donor 31 was synthesized from L-mannose 1 in six steps. At first, the hydroxyl functions of L-mannose 1 were acylated to afford pentaacetate 26 as described above. Compound 26 was converted into thiophenyl glycoside 27 by BF₃·Et₂O promoted glycosylation with thiophenol. Deacetylation of 27 gave compound 28. The azido function at the C-6-position was installed by selective activation of the C-6 hydroxyl group in 28 as sulphonate ester to give 29, followed by nucleophilic displacement of the sulphonate group by sodium azide in DMF to afford the 6-azido analog 30. Protection of the remaining hydroxyl

groups using acetic anhydride in pyridine produced the glycoside donor **31**. Donor **31** was used in glycosylation reaction with azido lipid alcohol **18** to produce glycolipid **32**. The ester groups were deprotected to afford the diazido compound **33** which was subsequently subjected to azide reduction using trimethyl-phosphine in THF/water to produce the desired α -anomeric glycolipid **7** (Scheme 7.3).



Scheme 7.3. Synthesis of compounds **7**. *Reagents and condition:* (a) Ac₂O, DMAP, Pyridine, 18 h, rt (b) PhSH, BF₃·Et₂O, DCM, 18, h, rt (c) MeONa, MeOH, 1h (d) TsCl, Pyridine, DMAP, 0°C - rt, 18 h (e) DMF, NaN₃, 70°C (f) AgOTf, NIS, DCM, 3 h, rt (g) P(CH₃)₃, THF, H₂O, 2 h, rt. Abbreviations: 4-Dimethyl amino pyridine (DMAP), Dichloromethane (DCM), *N,N*-dimethylformamide (DMF), room temperature (rt), *N*-iodosuccinimide (NIS)

7.4.2. Biological and biochemical studies

7.4.2.1. In Vitro Screening of L-Sugar Derived Glycolipids' Cytotoxic Activity Against Human Epithelial Cancer Cell Lines: BT-474, JIMT-1, MDA-MB-231 (breast), DU-145, PC-3 (prostate) and MiaPaCa2 (pancreas)

The cytotoxic properties of compounds **3-7** were initially determined against exponentially growing human epithelial cancer cell lines including BT-474, JIMT-1, MDA-MB-231 (breast), DU-145, PC-3 (prostate) and MiaPaCa2 (pancreas). The effects of L-mannose **1** and L-glucose **2** were also tested to determine if these L-sugars displayed any cytotoxicity against the cancer cells as sugars like L-rhamnose and D-glucosamine have been previously reported to possess some cytotoxic activity.⁵¹⁻⁵³ Experiments were also conducted with α -L-glucosamine based **8**, β -D-glucosamine based **9** which were used as Reference compounds. The cells were incubated with differing concentrations of **1-9** (0-30 μ M) for 48 h followed by assessment of cell viability using MTS assay. As shown in Figure 7.2 and Table 7.1, the most potent of the newly synthesized compounds was the L-rhamno configured glycolipid **4** with CC₅₀ values of 4.8 - 14 μ M while greater than 90% loss of cell viability was observed at a concentration range of 7.5 – 15.0 μ M for all the cell lines with the exception of BT-474 cell lines where 90% cell death was achieved at 20 μ M. This compound carries a primary amino group at the *sn*-3 position of the glycerolipid and L-rhamno sugar at the *sn*-2 position via an α -rhamnosidic linkage. Out of these six cell lines, MDA-MB- 231 a cisplatin resistant and triple negative breast cancer cell line was most sensitive to compound **4**. The second most potent compound was the L-manno configured bisamine **7** which in contrast to **4** bears a primary amino substituent at the position C-6 of the sugar. This compound was typically 2- to 4-times less active than glycolipid **4** with CC₅₀ values in the range of 12.5 - 25 μ M (Table 7.1). This is in contrast to previous observation with L-

glucosamine derived GAELs where a primary amino substituent at the C-6 of the L-glucose scaffold enhanced activity. But it is noteworthy that in the D-sugar GAEL series, there was significant loss of activity with mannose analogs, CC_{50} was not reached at 30 μ M.

The sugars, L-mannose **1** and L-glucose **2** were not cytotoxic at the highest dose (>30 μ M) tested. The L-rhamnose based analog **3** which is devoid of any amino group and amide **5** were significantly less active than **4**, **7** and **8** with CC_{50} values ≥ 21.5 μ M across all the six cell lines. Furthermore, compound **6**, an analog of **4** where the L-rhamnose is replaced with L-glucose is significantly less active. We were unable to achieve CC_{50} at the highest concentration tested (30 μ M). The reduced cytotoxicity of compounds **3** and **5** when compared to that of compound **4** demonstrated that the free amine is an important structural feature required for cytotoxicity of L-sugar-derived GAELs. This is consistent with earlier results on D-glucose-derived GAEL series.⁴¹

Comparison of the cytotoxicity of L-rhamnose linked glycerolipid **4** with L- and D-glucosamine based analogs **8** and **9** respectively showed that **4** is more active (CC_{50} 4.8 -11.0 μ M vs 6.5 -12 μ M and 8.0 – 13.5) across all the cell lines but BT-474 (Figure 7.2, Table 7.1).

The activities of compounds **3** – **5** and **7** against the cancer cell lines were compared with those of clinically-used anticancer agents: chlorambucil, cisplatin and the experimental anticancer agent salinomycin. As shown in Table 1, compounds **3** – **5** and **7** were more potent across the six cell lines than chlorambucil. A CC_{50} concentration for the latter was not attained even at a concentration as high as 150 μ M. Compounds **4** and **7** also displayed superior cytotoxicity than cisplatin against all the cell lines. Cisplatin did not achieve 50% cell death at 20 μ M against BT-474, MDA-MB-231 and MiaPaCa-2 cell lines. Salinomycin was also less

active than compound **4** (Compare Figure 7.2H). Salinomycin had little effect on DU145 and MDA-MB-231 cells. A low CC_{50} concentration, 6.5 μ M, for salinomycin against MiaPaCa-2 cell lines was obtained, however at the highest dose tested (20 μ M), about 28% of the cells were viable compared to < 1% for compound **4**.

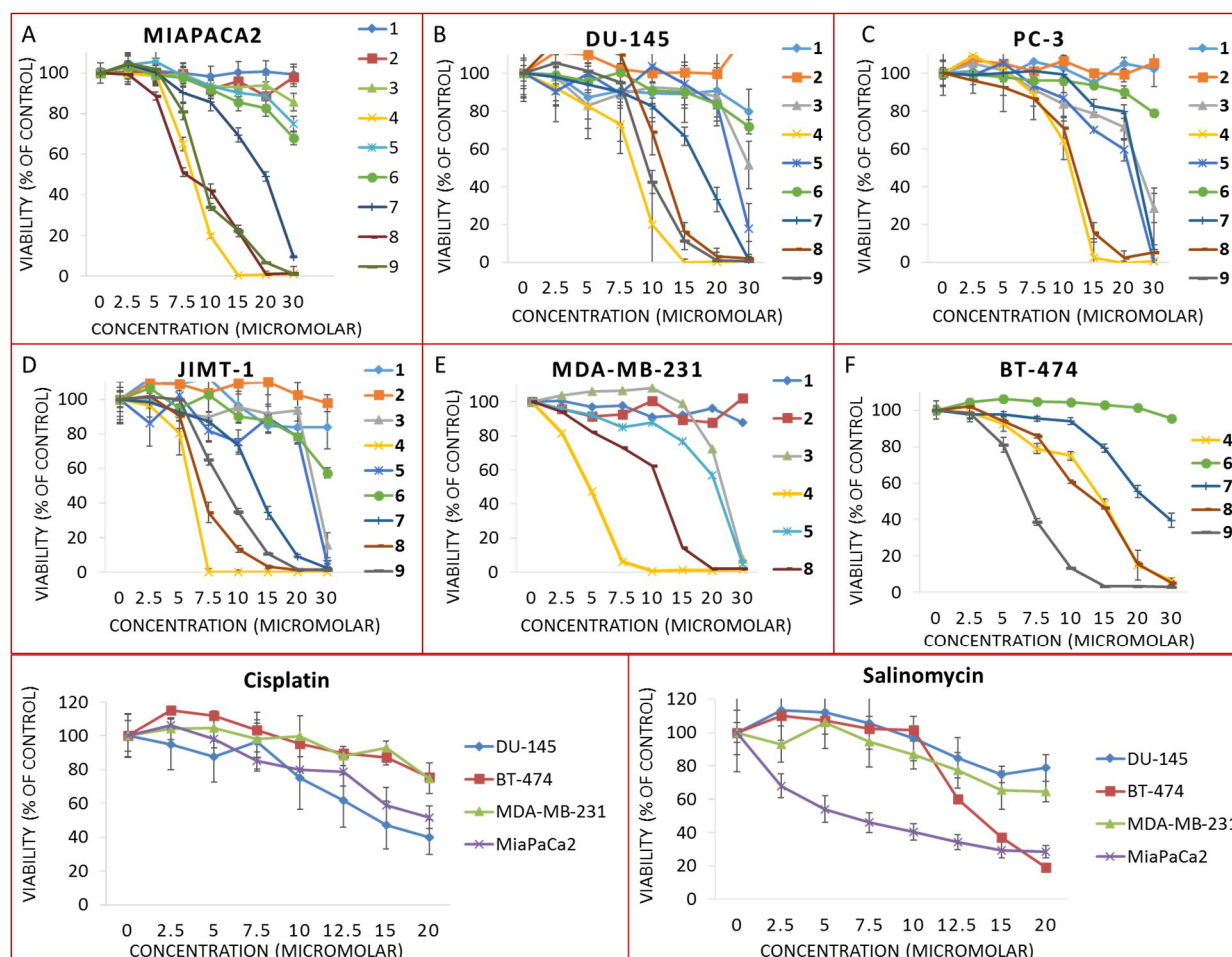


Figure 7.2. Effects of compounds **1** – **9** on the viability of MiaPaCa-2 (**A**) DU-145 (**B**), PC3 (**C**), JIMT-1 (**D**), MDA-MB-231 (**E**) and BT-474 (**F**) cell lines. Effect of cisplatin (**G**) and salinomycin (**H**) on DU-145, MDA-MB-231, BT-474 and MiaPaCa2 cells lines. DU-145, MDA-MB-231, and JIMT-1 cells were cultured in DMEM medium supplemented with 10% FBS, MiaPaCa2 cells were cultured in DMEM medium supplemented with 2.5% horse serum and 10%

FBS, BT-474 cells were cultured in DMEM/F12 medium supplemented with 10% FBS, and PC3 cells were cultured in F12K medium supplemented with 10% FBS. Equal numbers were dispersed into 96-well plates. After 24 h, the cells were incubated with compounds **1-9** (0-30 μ M) for 48 h. At the end of the incubation, MTS reagent (20% vol/vol) was added and the plates were incubated for 1- 4 h. The OD490 was read with a plate reader. Wells with media but no cells were treated in similar fashion and the values utilized as blank. The results represent the mean \pm standard deviation of 6 independent determinations.

	MDA-MB-231	JIMT1	BT-474	MiaPaCa2	DU-145	PC-3
Chlorambucil	>150	>150	>150	>150	>150	>150
Cisplatin	>20	NT	>20	>20	9.2	NT
Salinomycin	>20	NT	14.5	6.5	>20	NT
1	>30	>30	NT	>30	>30	>30
2	>30	>30	NT	>30	>30	>30
3	26	28	NT	>30	25	25.0
4	4.8	5.5	14	8.5	8.2	11.0
5	23	25	NT	>30	30	21.5
6	NT	>30	>30	>30	>30	>30
7	NT	12.5	21	19	17.5	25
8	11.0	6.5	13	7.5	12.5	12.5
9	NT	9.0	8	9.0	9.0	13.5

Table 7.1. CC₅₀ values of compounds **1 - 10**, Chlorambucil, salinomycin, and cisplatin on a panel of human epithelial cancer cell lines: breast (BT474, JIMT1, MDA-MB-231), pancreas

(MiaPaCa2) and prostrate (DU145, PC3). The CC_{50} value is defined as the concentration required to decrease cell viability by 50% relative to the untreated control.

7.4.2.2. Evaluation of Cytotoxicity of Compound 4 On A Panel of Triple Negative Breast Cancer (TNBC) Cell Lines

As mentioned above, compound **4** was more potent against the MDA-MB-231 cell line, a TNBC (estrogen receptor, progesterone receptor and HER2 negative) cell line, with CC_{50} value less than $5\mu\text{M}$, compared to other cell lines (Table 7.1). Thus we tested glycolipid **4** against a panel of TNBC cell lines including BT549, MDA-MB-453, MDA-MB-468, Hs578t and MDA-MB-231. These cells were chosen on the basis of differences in their origin, genotype and phenotype. For instance, MDA-MB-231, BT549 and Hs578t are very invasive in vitro and have been described as ‘mesenchymal or stromal like’ because of their high expression of vimentin while MDA-MB-453 and MDA-MB-468 are less invasive in vitro and are ‘weakly luminal epithelial like’.⁵⁴

The results of the studies with the TNBC cells (Figure 7.3, Table 7.2) showed that compound **4** was most active against the Hs578t cell line, derived from primary a carcinosarcoma, a very rare form of breast cancer,^{54,55} with > 95% cell death at $6\mu\text{M}$ (Figure 7.3, table 7.2). The next sensitive cell line is MDA-MB-231, derived from pleural metastasis of invasive ductal carcinoma.⁵⁶ 100% cell death of MDA-MB-231 was accomplished at $9\mu\text{M}$ of compound **4**. MDA-MB-468 cell line with amplified epidermal growth factor receptor gene, originally isolated from pleural metastasis of breast adenocarcinoma,⁵⁷ and BT549 isolated from primary papillary invasive ductal carcinoma⁵⁴ were less sensitive to compound **4** than MDA-MB-231 with > 90% cell death accomplished at $12\mu\text{M}$. The androgen positive MDA-MB-453

cell line with amplified ERBB2 gene, originally derived from the pleural metastasis of adenocarcinoma of the breast was the least sensitive,⁵⁶ just 60% cell death was attained at the highest concentration tested, 15 μ M.

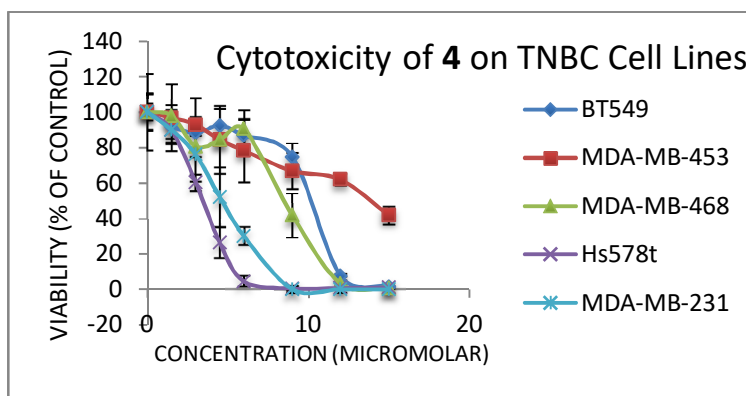


Figure 7.3. Cytotoxic Effect of compound 4 on triple negative breast cancer cell lines: BT549, MDA-MB-453, MDA-MB-468, Hs578t and MDA-MB-231.

	MDA-MB-231		BT549		MDA-MB-453		MDA-MB-468		Hs578t	
	CC ₅₀	CC ₉₀								
4	4.6	7.8	10.2	11.8	13.8	>15	8.4	11.2	3.4	5.4

Table 7.2. CC₅₀ and CC₉₀ values of compounds 4 on a panel of human triple negative breast cancer cell lines: MDA-MB-231, BT549, MDA-MB-453, MDA-MB-468 and Hs578t. The CC₅₀ value is defined as the concentration required to decrease cell viability by 50% relative to the untreated control, while the CC₉₀ value is defined as the concentration required to decrease cell viability by 90% relative to untreated control. The values were obtained by estimating the drug concentration at 50% and 10% viability on the y-axis using line plots.

7.4.2.3. Assessment of Cytotoxicity of Compound 4 on Glioblastoma Cell Lines

Glioblastomas are highly malignant brain tumors that are difficult to treat with current therapy. The effect of compound 4 on two glioblastoma cell lines was investigated. The U-87 cell line was initially established from a woman with glioblastoma multiforme while U-251 cell line was originally established from a 75 year old man.^{58,59} Both cell lines showed up-regulation of the PI3K/Akt pathway as a result of over expression of Akt which may be responsible for their resistance to apoptosis.^{58,59} Studies on the effect of compound 4 on the viability of the cells showed that 95% of U-87 cells were killed at a concentration of 6 μM while the U-251 cell required 12.5 μM to achieve a similar level of cell death (Figure 7.4, Table 7.3). Activities of the reference compound 9, the D-glucosamine based GAEL were 12 and 20 μM to achieve > 95% cell death for U-87 and U-251 cell lines respectively (Figure 4). The difference between the potency of compound 4 and 9 is statistically significant, this shows that the L-rhamnose derived compound 4 is more potent than our reference D-glucosamine analog 9 with respect to killing glioblastoma cells.

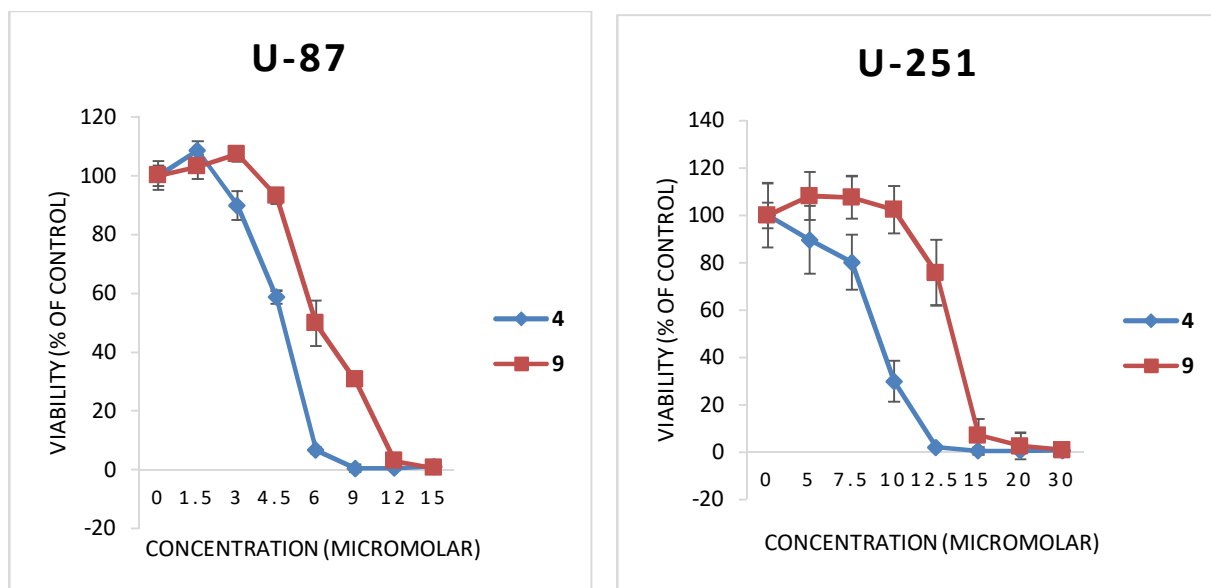


Figure 7.4. Cytotoxic Effect of compound 4 on glioblastoma cell lines - U-87 and U-251.

	U-87		U-251	
	CC ₅₀	CC ₉₀	CC ₅₀	CC ₉₀
4	4.8	5.8	8.5	11
9	6.0	11.5	13	14

Table 7.3. CC₅₀ and CC₉₀ values of compounds 4 on glioblastoma U-87 and U-251 cell lines. The CC₅₀ value is defined as the concentration required to decrease cell viability by 50% relative to the untreated control, while the CC₉₀ value is defined as the concentration required to decrease cell viability by 90% relative to untreated control. The values were obtained by estimating the drug concentration at 50% and 10% viability on the y-axis using line plots.

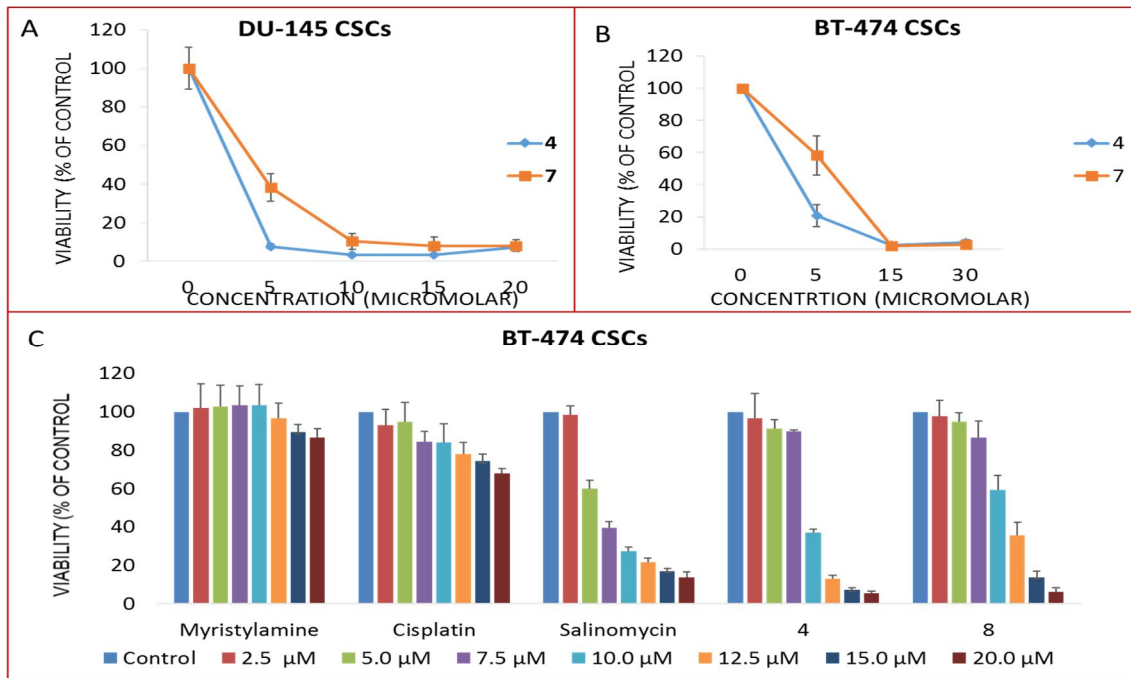
7.4.2.4. Effect of monoamino L-Rhamnose 4 and Diamino L-Mannose 7 Based GAELS on the Integrity and Viability of Breast and Prostate Cancer Stem Cells Isolated from BT-474, and DU-145

Determination of the anti-CSC properties of the L-sugar based GAELS, **4** and **7** were carried out using CSC enriched fractions from BT-474 and DU-145 cells. Strong expression of ALDH by cells was used as the sorting criterion for BT-474 and DU-145 cell lines.⁴⁰ The sorted cells were cultured in low-adhesion culture plates in stem cell growth media. The CSC spheroids were isolated by cell sieving, trypsinised and counted. Equal numbers were dispersed in ultra-low adhesion wells and allowed to form spheroids. The L-sugar GAELS **4**, **7** or **8** and the reference compounds, salinomycin, myristylamine or cisplatin were added to the spheroids.

Figure 7.5A shows the results of the effects of GAELS **4** and **7** on the viability of prostate DU-145 CSC spheroids after 6-day incubation. Compound **4** which killed > 90% of the spheroids at 5 μM is more potent than **7** which only attained the same level of cell death at 15 μM . Figure 7.5B shows the outcome of 6-day incubation of breast BT-474 CSC mammospheres with compound **4** and **7**. Compound **4** as previously observed was more potent than **7**, this can be discerned based on CSC mammosphere viability at 5 μM , 20% vs 58%, although both compounds reached nearly 100% CSCs death at 15 μM .

To determine that the ability of the L-rhamnose based compounds **4** and the glucosamine based compound **8** to kill CSCs spheroid is not just an amphiphilic effect, the activities of the GAELS against BT-474 CSC mammospheres were compared with myristylamine, a classical amphiphile. Experiments with the clinical anticancer drugs, cisplatin and salinomycin were also conducted. (Figure 7.5C). Incubation of the compounds with the spheroids was for 3 days to

enable differences to be readily discerned. The results of the effects on the viability and spheroid integrity are shown in Figure 7.5C and 7.5D respectively. The result showed that cisplatin can neither kill nor disintegrate CSC mammospheres. At the highest dose tested, 20 μ M, about 70% of the cells were viable and the large and compact spheroids remained. Myristylamine also did not show any significant effect on viability and integrity of the mammospheres. Thus the effect of GAELs to kill or disintegrate CSCs spheroid is not simply a function of its amphiphilic properties. The GAELs and salinomycin were able to kill the cells. Salinomycin at concentrations $\leq 10 \mu$ M appeared to be more active than the GAELs **4** and **8** but we observed that at the highest concentration tested, 20 μ M, 87% CSCs death was attained with salinomycin while at the same concentration the GAELs **4** and **8** accomplished about 95% cancer stem cells death. Though this difference is small it is statistically significant. At 7.5 μ M the GAELs were able to disintegrate the CSCs spheroid better than Salinomycin. Summing up we can infer from the above results that compound **4** may be a better agent in eradication and disintegration of CSCs spheroids than Salinomycin, the most studied anti-CSCs agent.



D

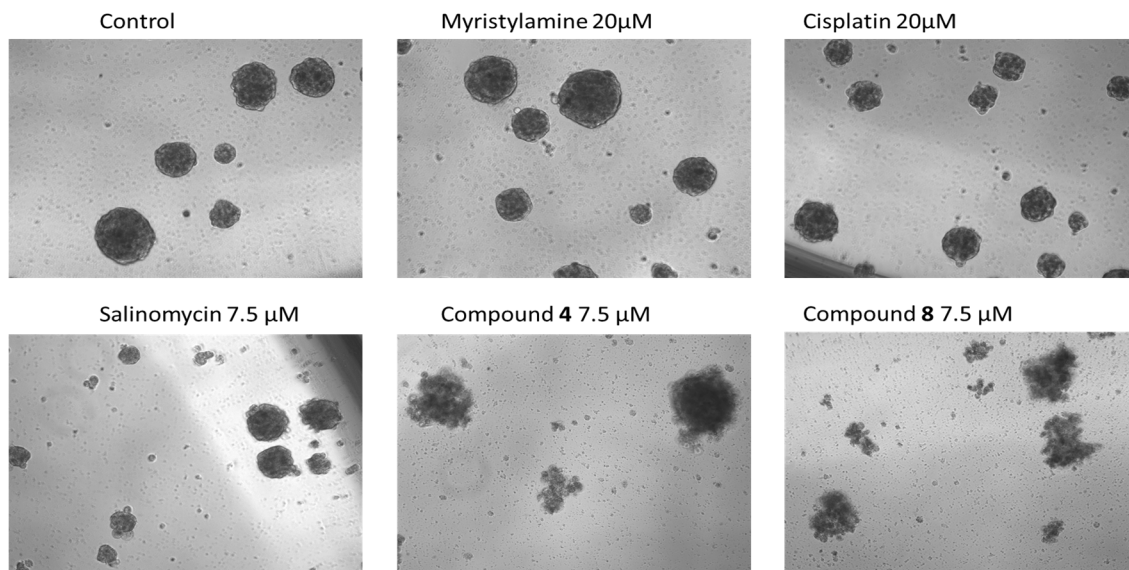


Figure 7.5. Effect of compound 4, 8, Salinomycin, Cisplatin and Myristylamine on viability and integrity of DU-145 and BT474 breast cancer stem cell spheroids. Equal numbers of DU-145 or BT-474 CSCs with high expression of aldehyde dehydrogenase 1 (ALDH1) were seeded into

ultra-low adhesion 48-well plates and grown for 5 days to allow for spheroid formation. The spheroids were incubated with or without drugs for 6 days (A and B) or 3 days (C) after which their viability were assessed with MTS assay. To assess the effect of the drugs on the integrity of BT-474 mammosphere (D), the images were taken after 3 days of incubation with an Olympus IX70 microscope at a magnification of x10.

7.4.2.5. Determination of the Effect of Pan-Caspases Inhibition on Cytotoxicity of Compound 4 in JIMT-1 And DU-145 Cell Lines

One of the hallmark features of cytotoxic GAELs is their ability to kill cancer cells via an apoptosis-independent mechanism. This is the major reason for testing them against CSCs which are known to be resistant to apoptosis. One of the molecular bases for CSCs' resistance to apoptosis may be due to their overexpression of apoptosis inhibitor proteins including caspase inhibitors.⁶⁰ The majority of the biological activity described as apoptosis is mediated by cysteine proteases called caspases. So to evaluate if the cell death induced by **4** and **8** is apoptosis independent we tested their ability to kill JIMT-1 and DU-145 cell lines in the presence or absence of QVD-OPh, one of the most effective pan-caspases inhibitors.⁶¹ Reduced cytotoxicity in the presence of the caspases inhibitor is an indication of caspase mediated apoptosis, while a lack of statistically significant differences shows that the cytotoxicity of the compound is apoptosis-independent.

The results of the experiments (Figure 7.6) showed that there was no statistically significant difference between cell death observed with GAEL treatment in the presence or absence of the pan-caspase inhibitor (40 μ M). To verify this result we used Adriamycin a clinical anticancer agent that kill cells via apoptosis as a control. Our result showed the pan-caspase

inhibitor significantly reduced cytotoxicity of Adriamycin in JIMT-1 and DU-145 cell lines at all concentration tested. The results of the studies show that GAELs **4** and **8** kill cancer cells via a caspase-independent pathway(s).

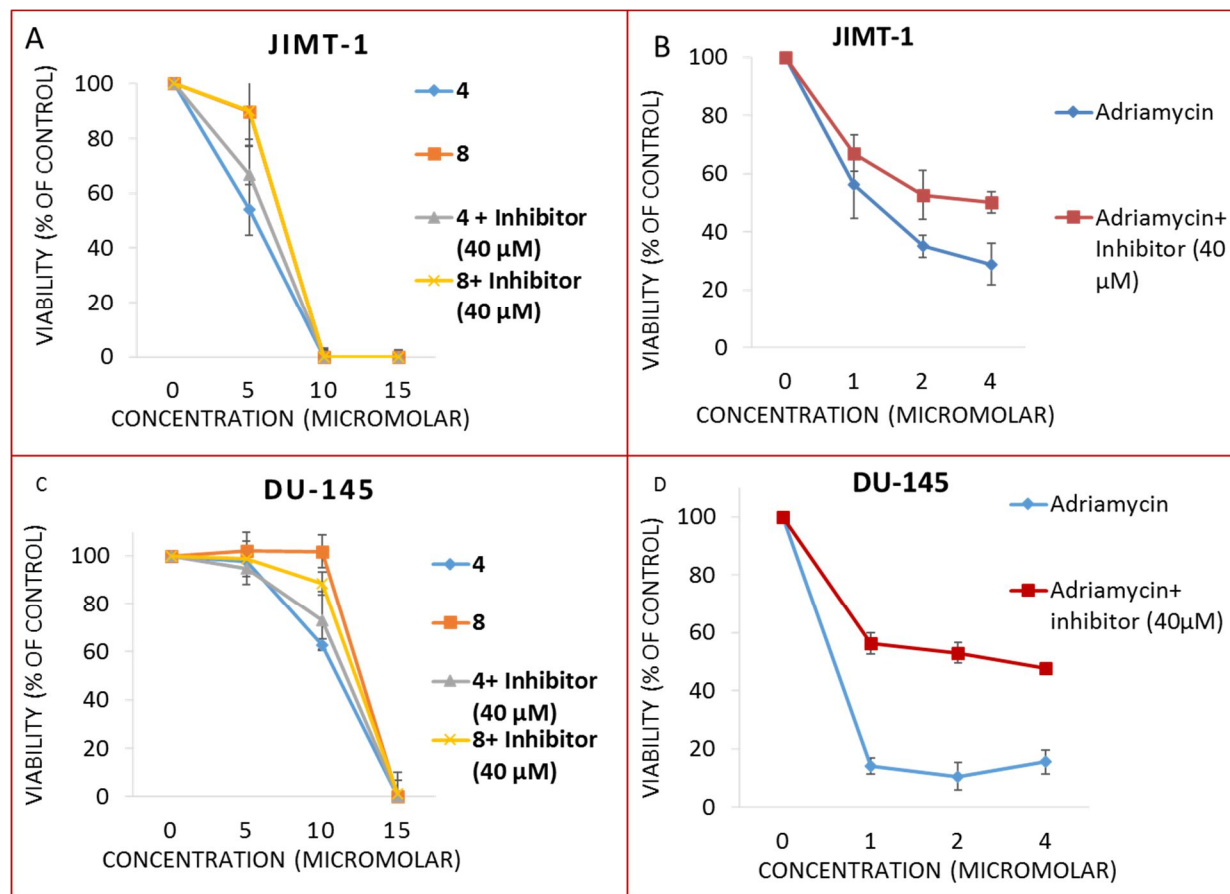


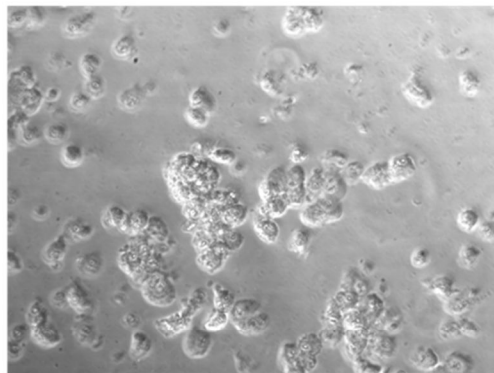
Figure 7.6. Demonstration of caspase/apoptosis independent cell death. Cancer cell lines were treated with various concentration of GAELs in the presence or absence of the pan-caspase inhibitor. JMT-1 cell lines treated with varying concentration of GAELs **4** and **8** (A) Adriamycin (B), DU-145 cell lines treated with varying concentration of GAELs **4** and **8** (C) Adriamycin (D) JIMT-1 and DU-145 cells were cultured in DMEM medium supplemented with 10% FBS. Equal numbers were dispersed into 96-well plates, after 4 h they were treated with pan-caspase inhibitor QVD-OPh (40 μm). After 20 h, the cells were incubated with varying concentration of

tested drugs (0 – 6 μ M) for 48 h. At the end of the incubation, MTS reagent (20% vol/vol) was added and the plates were incubated for 1-4 h. The OD490 was read with a plate reader. Wells with media but no cells were treated in similar fashion and the values utilized as blank. The results represent the mean \pm standard deviation of 6 independent determinations.

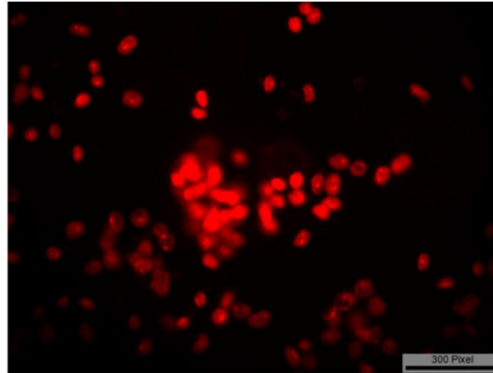
7.4.2.6. Evaluation of Effect of L-Rhamnose based GAEL 4 on Integrity of DU145 or JIMT-1 Cell Membranes

After determining that the mechanism of cell death of compound **4** is independent of caspases-mediated apoptosis, we evaluated if cell death was due to membrane disruption or lysis using the cell impermeant ethidium homodimer-1 (EthD-1) dye that emits red fluorescence upon binding to DNA.²⁶ JIMT-1 and DU-145 were treated with compound **4** at 10 and 15 μ M respectively. After 4 - 6 h, the cells were treated with ethidium homodimer-1 (EthD-1) dye and monitored under fluorescence microscopy. Comparison of cells treated with compound **4** and untreated control in both JIMT-1 and DU-145 cell lines demonstrated that there was no significant cell membrane lysis. In contrast cells incubated with 0.01% Triton X-100 for 10 min stained bright red (Figure 7.7).

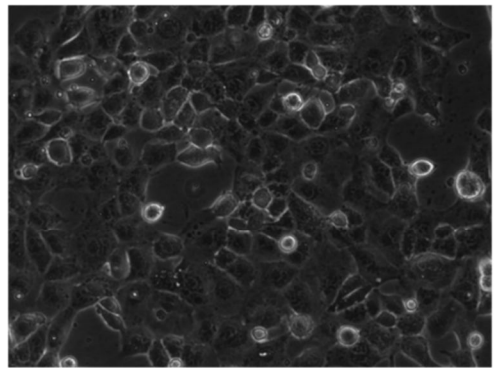
A



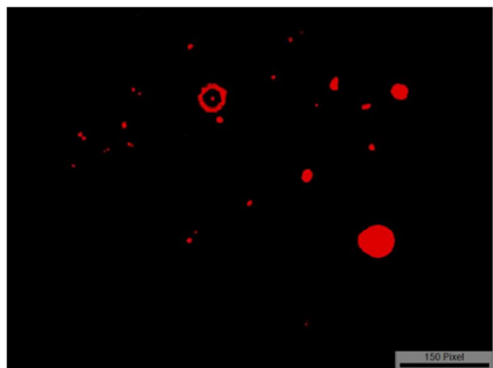
Triton X100 – DU-145 Cells



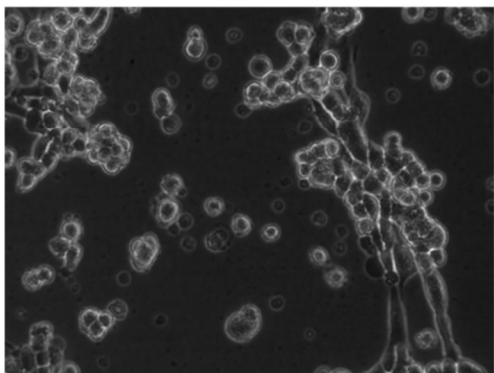
TritonX100 - Stained nucleus



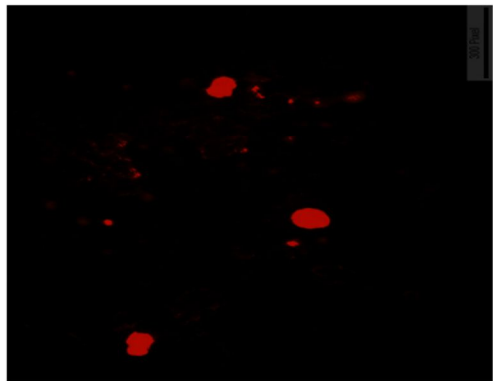
Control – DU-145 Cells



Control - Stained nucleus



4 (15 μM) – DU-145 Cells



4 (15μM)- Stained nucleus

B

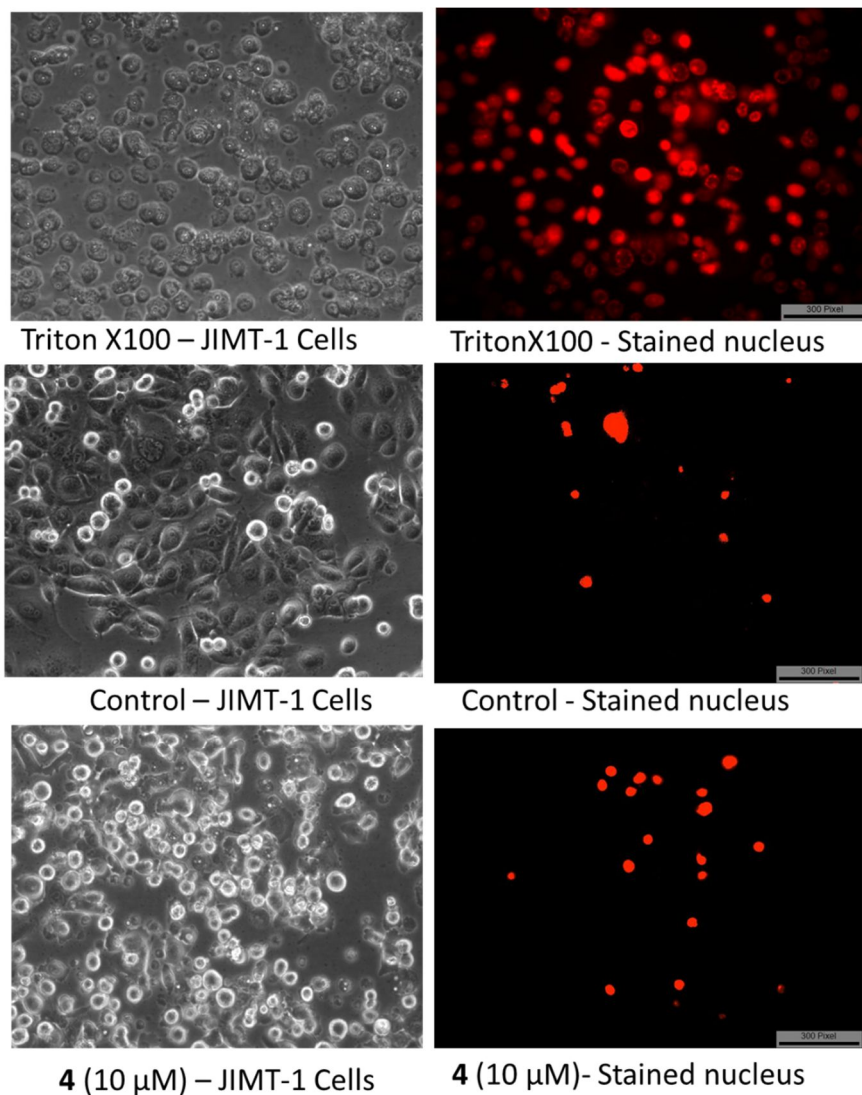


Figure 7.7. Evaluation of effect of compound **4** on cell membrane of DU-145 and JIMT-1 cell lines using cell impermeant ethidium homodimer-1 (EthD-1) dye that emits red fluorescence upon binding to DNA.²⁶

7.4.2.7. Hemolytic Properties of L-Rhamno Configured GAEL 4

To further evaluate the membrane lytic properties of compound 4 and its compatibility with intravenous administration, we investigated its capacity to lyse ovine erythrocyte using a previously reported protocol.⁶⁴ Our result (Figure 7.8) demonstrated that compound 4 is not hemolytic up to a concentration of 100 μ M which is 10 X higher than the concentration that kills > 95% of cancer cells and CSCs. The highest hemolysis observed was about 6.6% at 100 μ M. These results indicated that, L-Rhamnose derived GAEL 4 maybe compatible with intravenous administration without concern for hemolytic anemia.

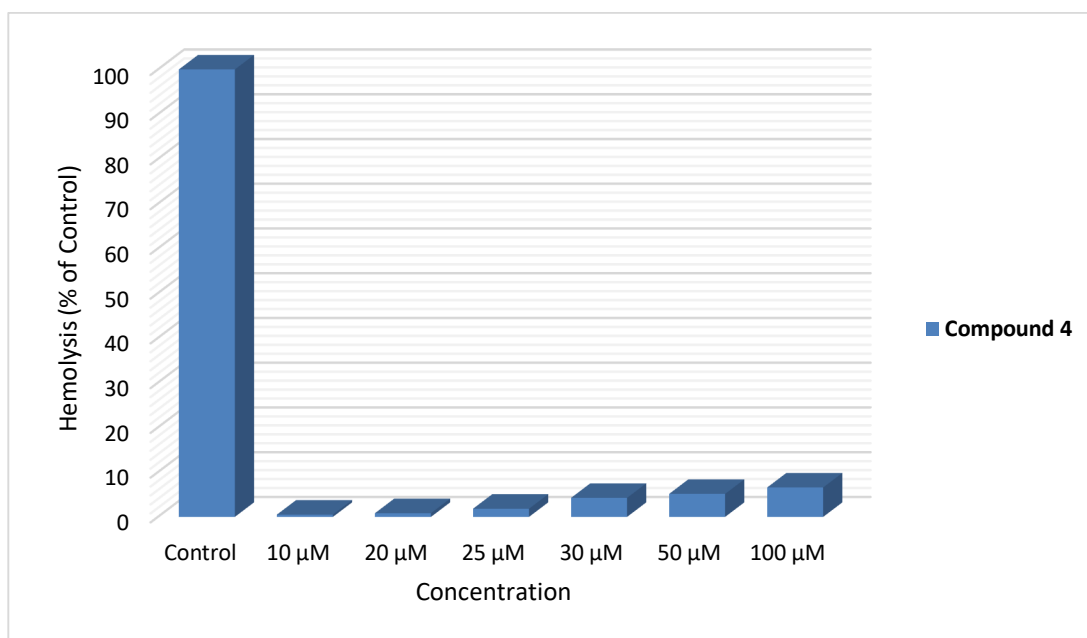


Figure 7.8. Hemolytic properties of GAEL 4 using freshly isolated ovine erythrocytes. 1% ammonium hydroxide was used for 100% hemolysis, the control. The values were determined as % of control.

7.4.2.8. Demonstration of Stability of L-Rhamno Configured GAEL 4 To Glycosidases

To confirm our hypothesis, that L-sugar derived GAELs are stable to animal or human glycosidases, we investigated the stability of compound **4** in the presence of bovine liver glycosidases extract which has been reported to contain a cocktail of different glycosidases including: α - and β - glucosidases, N-acetyl α - and β - glucosaminidases, α - and β - galactosidases and α -mannosidases.⁶⁵ Mass spectrometry, TLC and HPLC-MS analysis of compound **4** after treatment with the glycosidase extract showed no traces of products of enzymatic hydrolysis, where its D-glucose analog were cleaved. Also we used a randomly radioactive ³H labelled analog of **4** to investigate stability of **4** to these hydrolases. Degree of hydrolysis was measured by monitoring distribution of radioactivity using a high performance TLC plate (chromatogram not provided). Analysis of the radioactive distribution on the chromatogram showed that there was no enzyme-catalysed hydrolysis after 1 h of incubation with the glycosidases. The radioactive distribution of the enzyme treated sample is very similar (>95%) similar to that of sample that was not treated with the enzymes. This outcome confirmed our hypothesis that glycosidases-catalysed hydrolysis of D-sugar GAEL can be prevented by substituting the D-sugar with L-sugar unnatural to human.

7.4.2.9. Evaluation of Toxicity/Tolerability of Compound 4 Administered Orally and Intravenously in Rag2M mice.

The results of studies presented above have identified L-rhamnose linked amino lipid **4** as the most potent compound and a suitable lead representative of GAELs with L-sugars. The tolerability and toxicity of the compound in Rag2M mice was investigated to determine the maximum tolerated dose (MTD) that could potentially be used for efficacy studies with cancer xenografts. We chose this method instead of using normal cells like fibroblasts or normal epithelial cells because results from such experiments are not always translatable to animals or

humans. Two routes of administration, oral and intravenous were used. The results of the study are presented in Figure 7.9. For oral administration, the MTD was determined to be 300 mg/kg while for intravenous administration, the MTD was 50 mg/kg. At these doses, necropsy revealed no damage to vital organs and no weight loss was determined within two weeks of administration of the drug. The only observable effect was gas in the intestines.

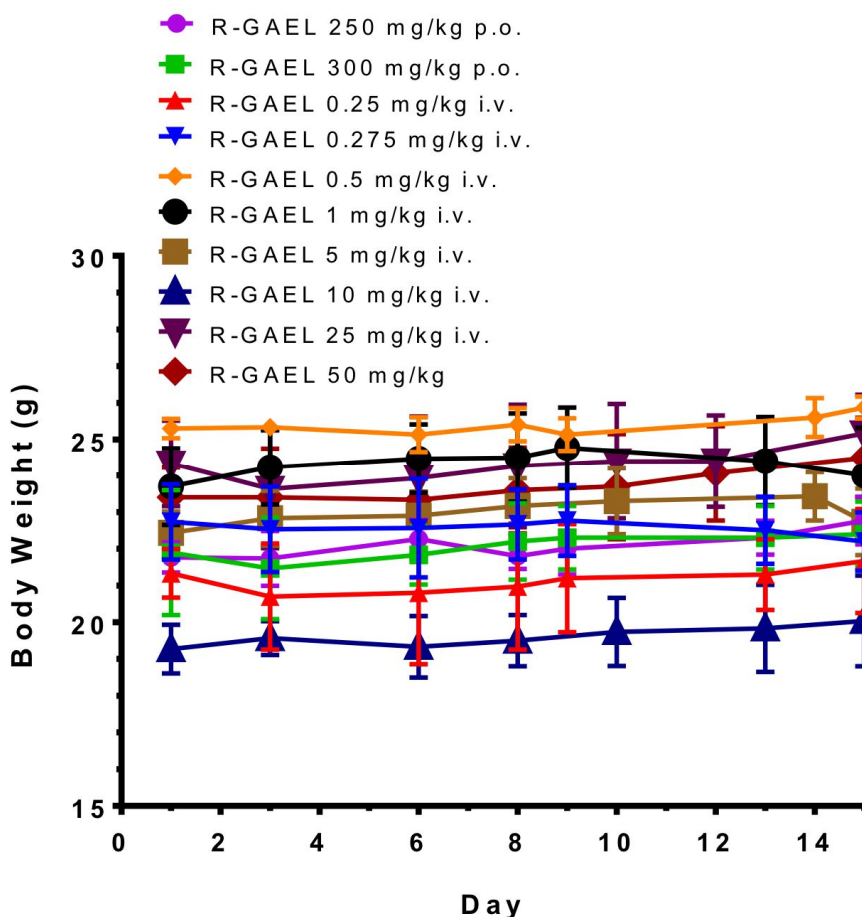


Figure 7.9. Tolerability study, effect of compound 4 on weight of animal

7.5. Discussion and Conclusion

GAELs are a promising class of investigational anticancer agents with potent antitumor activity against a range of cancer cell lines and CSCs. The most potent analog we reported here,

the L-rhamnose configured analog **4**, showed CC₅₀ values in the range of 3.4 to 13.8 μ M across 12 phenotypically and genotypically different human cancer cell lines including, pancreas, breast, prostate and glioblastoma. This analog has a primary amino substituent and L-rhamnose at position *sn*-3 and *sn*-2 of the glycerolipid respectively. The L- rhamnose based analog **3** and the amide **5** were significantly less potent than **4**. This observation shows that the primary amino substituent is very central to cytotoxicity of this series of GAELs. This is akin to our experience with D-sugar based GAELs. Compound **6** an analog in which the L-rhamnose of **4** was replaced with L-glucose showed very minimal cytotoxicity, in fact CC₅₀ values were not attained across all the cell lines at the highest tested concentration. This is a convincing evidence that the nature and type of sugar moiety in GAELs play a crucial role in their cytotoxicity. Compound **7** an analog with -CH₂NH₂ in place of -CH₃ of compound **4** at C-5 position of the sugar was consistently less active than **4** but more active than compounds **3**, **5** and **6**. This was surprising, because previous studies with D-sugar GAELs and L-glucosamine GAELs series revealed that cytotoxicity was enhanced by introducing an additional amino substituent at position C-6 of the sugar. This reduced effect could be due to the change in configuration of the sugar from L-rhamnose to L-mannose. D-manno configured GAELs were not active at a concentration of 30 μ M.⁴⁰ Thus, the antitumor activity of GAELs is significantly dependent on sugar configuration. The cytotoxicity of **4** was demonstrated to be significantly better than that of anticancer drugs like chlorambucil, cisplatin and the experimental anti-CSC agent, salinomycin. Also, the activity of **4** is better than that of L-glucosamine derived **8** and D-glucosamine based **9** against most of the cell lines except BT-474.

The expanded studies on the effect of the compounds on TNBC cell lines were conducted based on observation that the TNBC cell line, MDA-MB-231 was more sensitive than the non –

TNBC cell line BT474, suggesting that TNBC cells could be more susceptible to **4**. The results we obtained clearly showed that the presence or absence of HER/2, ER, and PR was not a determinant in the susceptibility of the cells to compound **4**. For example, the hormone receptor positive (HER/2, ER, PR) BT-474 and the hormone receptor negative (HER/2, ER, PR) MDA-MB-453 had similar CC_{50} 's of 14 μ M vs 13.8 μ M. Also, JIMT-1 cell line (non TNBC) was more sensitive to compound **4** than some TNBC cell lines. Thus the presence or absence of the 3 hormone receptors is not the determining factor for susceptibility of cancer cells to the new compounds. Other phenotypical or genotypical features may be responsible for these differences in susceptibility, but it is really fascinating to see here that compound **4** can kill cancer cells of different phenotype and genotype.

The study also demonstrated that compound **4** can kill glioblastoma cell lines, this is interesting because available drugs for treatment of glioblastoma are very ineffective. The recurring rate in this brain cancer after treatment is approximately 100%. Therefore, the L-rhamnose derived GAEL **4** is a potential new compound for treatment of brain tumor, glioblastoma, though further extensive study is required.

Targeting CSCs is now one of the major areas in cancer drug discovery because of their central role in cancer pathogenesis and recurrence.^{66,67} Currently no drug is clinically indicated for eradication of CSCs in cancer patients, although metformin is currently in phase III clinical trials for this purpose. We have demonstrated herein that the L-sugar derived GAELs displayed significant anti-CSC properties. The new GAELs **4**, **7** and **8** showed significant potent cytotoxicity against breast and prostate CSCs isolated from BT-474, DU-145 and MiaPaCa2 cell lines respectively. One noticeable feature of these GAELs is their ability to disintegrate the tumorsphere and kill virtually all the CSCs. Salinomycin, an investigational anti-CSCs agent

demonstrated similar or less cytotoxicity compared to GAELs **4** and **8** but was significantly less effective in disintegrating CSC spheroids. Drugs like cisplatin and myristylamine are ineffective in killing CSCs. The lack of effect of myristylamine, a classical amphiphile, on cytotoxicity and disintegration of CSCs is a proof that activity of GAELs against CSCs is not just a detergent/amphiphilic effect. Based on the ability of these GAELs to disrupt spheroid integrity and kill CSCs from different tumor types, we postulated that the anti-CSC effect may be an inherent characteristic of cytotoxic GAELs.

Studies conducted to provide insight on the mode of cell death induced by **4** revealed that death occurs via an apoptosis-independent pathway. Thus, the mechanism of action of **4** may be similar to that described for the D-glucosamine based GAEL **9**.⁴⁰ This non-apoptotic mechanism of cell death may explain why this compound and other cytotoxic GAELs can kill CSCs. CSCs are known for their resistance to apoptosis and escaping cell death through many mechanisms including over expression of proteins that inhibit caspases and apoptosis.^{16,27,30,68-72} Also the result of membrane disruption experiment using a cell impermeant ethidium homodimer-1 (EthD-1) dye demonstrated that GAEL **4** do not kill cells by membrane disruption or necrosis. The fact that the cells were rounding up as they were dying may imply possible interference with the cell cytoskeleton. Our hemolysis assay on ovine erythrocytes further confirmed that L-sugar GAELs induced cell death is not due to interference with cell membrane integrity. The results also indicate that L-rhamnose derived GAEL **4** may be safely delivered by intravenous administration.

Stability, toxicity and tolerability are major issues in drug development especially GAELs. The outcome of investigation on stability of the L-rhamnose based GAEL **4** to a cocktail of glycosidases extracted from beef liver confirmed our hypothesis that replacing D-sugar with

L- sugar can prevent glycosidase-catalysed hydrolysis. The fact that a maximum tolerable doses was attained when **4** was either orally or intravenously administered in mice provides evidence that in mice L-rhamnose **4** was not inactivated by metabolic degradation. The tolerability study also demonstrated that compound **4** is compatible with both oral and intravenous administration.

In conclusion, this study identified a new GAEL compound, an L-rhamnose derived GAEL **4** with potent cytotoxicity against a spectrum of cancer cell lines and CSCs isolated from human cancers. This glycolipid is resistant to glycosidases-catalysed cleavage and metabolic degradation in animal. Also this compound is well tolerated in animal up to 300mg/kg orally and 50 mg/kg intravenously without any identified damage to vital organs.

7.6. Experimental data

7.6.1. Chemistry

7.6.1.1. Materials and methods: Synthesis of GAELs

Solvents were dried over CaH₂. ¹H, ¹³C NMR spectra were recorded on a Bruker Avance 500 NMR spectrometer, and chemical shifts reported (in ppm) relative to internal Me₄Si ($\delta = 0.0$) 500 or 300 MHz and at 126 or 75 MHz, respectively, and chemical shifts were reported in parts per million (ppm). Thin-layer chromatography (TLC) was carried out on aluminum or glass-backed silica gel GF plates (250 μ m thickness) and plates were visualized by charring with 5% H₂SO₄ in MeOH and or short wavelength UV light. Compounds were purified by flash chromatography on silica gel 60 (230-400 ASTM mesh). ESI-MS analyses were performed on a Varian 500 MS Ion Trap Mass Spectrometer. MALDI-TOF-MS were performed on a Bruker Daltonics Ultraflex MALDI TOF/TOF Mass Spectrometer. Purity of compound **3-7** was assessed by elemental analysis of elements (C, H, N) and were within ± 0.5 % of the theoretical values.

7.6.1.2. Synthesis

1,2,3,4 L-rhamnopyranosyl tetraacetate (12)

L-rhamnose **11** (0.99 g, 5.49 mmol) was dissolved in 20.0 ml pyridine at room temperature, then acetic anhydride (5.20 ml, 54.90 mmol) and dimethyl amino pyridine (0.10 g) were sequentially added and the reaction was vigorously stirred for 18 h after which it was stopped by addition of methanol (10.0 ml) and then stirred for 15 minutes. The solvents were removed under high vac. The resulting residue was then dissolved in ethyl acetate (50.0 ml) and washed with 3% HCl solution (1 time), saturated sodium bicarbonate (2 times), distilled water (1 time) and brine (1 time). The resulting organic layer was dried over Na₂SO₄ and concentrated to dryness and purified by flash chromatography using ethyl acetate and hexane (1:1) to give **12** (1.71 g, 5.12 mmol) as α , β mixture (9:1). Yield was 93%. NMR data for α - anomer of compound **12**: ¹H NMR (300 MHz, Chloroform-*d*) δ 6.01 (d, *J* = 1.8 Hz, 1H, H-1), 5.31 (dd, *J* = 10.1, 3.5 Hz, 1H, H-3), 5.25 (dd, *J* = 3.5, 1.8 Hz, 1H, H-2), 5.12 (dd, *J* = 10.1, 9.9 Hz, 1H, H-4), 3.93 (m, 1H), 2.17 (s, 3H), 2.16 (s, 3H), 2.06 (s, 3H), 2.00 (s, 3H), 1.24 (d, *J* = 6.2 Hz, 3H, H-6). ¹³C NMR (75 MHz, CDCl₃) δ 170.05, 169.81, 169.79, 168.35, 90.65, 70.48, 68.77, 68.72, 68.65, 20.89, 20.77, 20.74, 20.67, 17.44. ES-MS: calcd: C₁₄H₂₀O₉Na⁺ m/z: 355.1, found [M+Na]⁺ m/z: 355.5.

Phenyl-2,3,4-triacetyl-1-thio- α -L-rhamnopyranoside (13)

The tetraacetate **12** (1.71 g, 5.12 mmol) was dissolved in 20.0 ml DCM, then thiophenol (0.68 g, 6.14 mmol) and BF₃·Et₂O (0.87 g, 6.14 mmol) were sequentially added. The reaction was stirred vigorously for 18 h after which it was stopped with 20 ml saturated sodium bicarbonate at 0°C. The organic layer was separated using separatory funnel and subsequently washed with saturated 20.0 ml of sodium bicarbonate (2 times), 20.0 ml of water (1 time) and 20.0 ml of brine

(1 time). The organic layer was dried over anhydrous sodium bicarbonate and then concentrated under vacuum. The residue was then purified by flash chromatography using ethyl acetate and hexane (4:6) to give mainly α -anomer of **13** (1.72 g, 4.5 mmol). Yield was 88%. NMR data for anomer of compound **13**: ^1H NMR (300 MHz, Chloroform-*d*) δ 7.59 – 7.22 (m, 5H, aromatic protons), 5.51 (dd, $J = 3.4, 1.1$ Hz, 1H, H-2), 5.42 (d, $J = 1.1$ Hz, 1H, H-1), 5.30 (dd, $J = 10.0, 3.4$ Hz 1H, H-3), 5.19 (dd, $J = 9.6, 10.0$ Hz, 1H, H-4), 4.42 - 4.34 (m, 1H, H-5), 2.15 (s, 3H), 2.09 (s, 3H), 2.05 (s, 3H), 1.26 (d, $J = 6.2$ Hz, 3H, H-6). ^{13}C NMR (75 MHz, CDCl_3) δ 169.99, 169.98, 169.91, 132.08, 131.85, 129.19, 127.89, 85.71, 71.34, 71.17, 69.40, 67.79, 20.91, 20.82, 20.69, 17.35. ES-MS: calcd: $\text{C}_{18}\text{H}_{22}\text{O}_7\text{SNa}^+$ m/z: 405.1, found $[\text{M}+\text{Na}]^+$ m/z: 405.3.

1-Hexadecyloxyl-2R-methoxyl-3-(2'3'4'-triacetyl- α -L-rhamnopyranosyl)-sn-glycerol (15)

The fully protected glycoside donor **13** (153 mg, 0.4 mmol) and the glycoside acceptor **14** (140 mg, 0.4 mmol) were dissolved in 15 ml of DCM under argon atmosphere, then AgOTf (0.02 g, 0.08 mmol) and N-iodosuccinimide (0.14 g, 0.60 mmol) were simultaneously added. The reaction was vigorously stirred for 2 h after which it was stopped with saturated solution of sodium thiosulphate (5.0 ml) and then washed with 25.0 ml of saturated sodium thiosulphate solution (1 time), saturated sodium bicarbonate (3 times), water (1 time) and brine (1 time). The organic layer was then dried over anhydrous sodium sulphate and then concentrated under vac. The residue, was purified by flash chromatography using ethyl acetate/hexane mixture (4:6) to give α -anomer, **15** (0.19 g, 0.31 mmol) as a white solid. Yield was 58%. NMR data of **15**: ^1H NMR (300 MHz, Chloroform-*d*) δ 5.36 – 5.19 (m, 2H, H-2, H-3), 5.04 (dd, $J = 9.7, 9.7$ Hz, 1H, H-4), 4.73 (d, $J = 1.5$ Hz, 1H, H-1), 3.93 – 3.84 (m, 1H, H-5), 3.79 – 3.63 (m, 1H), 3.61 – 3.34 (m, 9H), 2.12 (s, 3H), 2.02 (s, 3H), 1.96 (s, 3H), 1.50 – 1.48 (m, 2H), 1.23 (broad s, 26H, lipid

tail), 1.20 (d, $J = 6.2$ Hz, 3H, H-6), 0.85 (t, $J = 6.6$ Hz, 3H, terminal lipid CH₃). ¹³C NMR (75 MHz, CDCl₃) δ 170.01, 169.92, 169.87, 97.58, 78.94, 71.78, 71.12, 69.80, 69.67, 69.12, 67.35, 66.34, 58.20, 31.89, 29.66, 29.62, 29.47, 29.33, 26.09, 22.65, 20.85, 20.74, 20.67, 17.39, 14.08. ES-MS: calcd: C₃₂H₅₈O₁₀Na⁺ m/z: 625.4, found [M+Na]⁺ m/z: 624.8.

1-Hexadecyl-2R-methoxyl-3-O- α -L-rhamnopyranosyl-sn-glycerol (3)

Compound **15** (0.19 g, 0.31 mmol) was dissolved in 15.0 ml of methanol, then catalytic amount of sodium methoxide was added and the reaction was vigorously stirred for 3 h. The reaction was stopped by acidic ion exchange resin. The resin was filtered and the filtrate was concentrated under vacuum and the residue was purified by flash chromatography using ethyl acetate/hexane mixture (9:1) to give **3** (0.11 g, 0.23 mmol) as a white solid. Yield was 75%. NMR data of **3**: ¹H NMR (300 MHz, Chloroform-*d*) δ 4.78 (d, $J = 1.1$, 1H, H-1), 4.12 (s, 3H, OH, rhamnose -OH), 3.97 (dd, $J = 1.1, 3.3$ Hz, 1H, H-2), 3.83 – 3.63 (m, 3H), 3.63 – 3.53 (m, 1H), 3.53 – 3.36 (m, 9H), 1.56 (m, 2H), 1.31 (d, $J = 6.0$ Hz, 3H, H-6), 1.28 (broad s, 26H, lipid tail), 0.89 (t, $J = 6.5$ Hz, 3H, terminal lipid CH₃). ¹³C NMR (75 MHz, CDCl₃) δ 99.92, 79.03, 72.80, 71.84, 71.68, 70.89, 69.99, 68.24, 66.71, 58.04, 31.94, 29.72, 29.69, 29.37, 26.13, 22.70, 17.55, 14.12. MALDI-HRMS: calcd: C₂₆H₅₂O₇Na⁺ m/z: 499.3611, found [M+Na]⁺ m/z: 499.3615.

p-Toluenyl, 3-hexadecyloxy-2R-hydroxyl propyl-1-sulphonate (17)

The lipid diol **16** (2.00 g, 6.32 mmol) was dissolved in dissolved in 20 ml DCM, cooled to 0°C, then Et₃N (1.28 g, 1.80 ml,) was added followed by 4- toluenesulphonyl chloride (1.33 g, 6.95 mmol) and DMAP (0.04 g, 0.32 mmol). The temperature was allowed to increase to room temperature (23°C) and the mixture was stirred for 4 h. At the end of reaction, the mixture was diluted with ethyl (60.0 ml) acetate, washed with saturated aqueous ammonium chloride (3

times), brine (3 times). The organic layer was then dried over sodium sulphate, concentrated under vacuum and the residue was purified using flash chromatography using hexane/ethyl acetate (8:2) to give **17** (1.80 g, 3.80 mmol) as a white flaky solid. Yield was 60%. NMR data of **17**: ^1H NMR (300 MHz, Chloroform-*d*) δ 7.78 (d, J = 8.2 Hz, 2H, aromatic protons), 7.33 (d, J = 8.1 Hz, 2H, aromatic protons), 4.11 – 4.00 (m, 2H, TsO-CH₂), 3.99 – 3.89 (m, 1H, HO-CH), 3.46 – 3.31 (m, 4H), 2.80 (d, J = 5.4 Hz, 1H, OH), 2.42 (s, 3H, toluene -CH₃), 1.55 – 1.41 (m, 2H), 1.25 (s, 26H, Lipid tail), 0.87 (t, J = 6.4 Hz, 3H, lipid terminal -CH₃). ^{13}C NMR (75 MHz, CDCl₃) δ 144.90, 132.77, 129.88, 127.99, 71.73, 70.77, 70.56, 68.25, 31.93, 29.71, 29.68, 29.64, 29.61, 29.48, 29.37, 26.01, 22.68, 21.58, 14.11. ES-MS: calcd: C₂₆H₄₆NO₅Na⁺m/z: 493.3, found [M+Na]⁺ m/z: 493.7

3-Hexadecyloxy-2R-hydroxyl propyl-1-azide (18)

Compound **17** (1.30 g, 2.76 mmol) and sodium azide (1.81 g, 27.60 mmol) were suspended in anhydrous DMF and the mixture was stirred at 90°C for 18 h. at the end of the reaction the mixture was concentrated then diluted with ethyl acetate and filtered to remove excess sodium azide. The filtrate was then concentrated and purified with flash chromatography using hexane/ethyl acetate (9:1) to give **18** (0.85 g, 2.50 mmol) as a white wax like solid. Yield was 91%. ^1H NMR (300 MHz, Chloroform-*d*) δ 3.92 – 3.86 (m, 1H, HO-CH), 3.48 – 3.34 (m, 4H), 3.31 (dd, J = 5.5, 2.9 Hz, 2H, -CH₂N₃), 3.17 (s, 1H, OH), 1.55 – 1.41 (m, 2H), 1.25 (s, 26H, Lipid tail), 0.85 (t, J = 6.6 Hz, 3H, terminal lipid -CH₃). ^{13}C NMR (75 MHz, CDCl₃) δ 71.92, 71.71, 69.59, 53.54, 31.93, 29.71, 29.67, 29.61, 29.52, 29.47, 29.37, 26.05, 22.67, 14.03. ES-MS: calcd: C₁₉H₃₉N₃O₂Na⁺m/z: 364.3, found [M+Na]⁺m/z: 364.5

3-Azido-1-hexadecyloxy-2R-(2'3'4'-tri-O-acetyl-O- α -L-rhamnopyranosyl)-sn-glycerol (19)

The fully protected glycoside donor **13** (0.15 g, 0.41 mmol) and the glycoside acceptor **18** (0.12 g, 0.36 mmol) were dissolved in 15.0 ml of DCM under argon atmosphere, then AgOTf (0.02 g, 0.08 mmol) and N-iodosuccinimide (0.14 g, 0.60 mmol) were simultaneously added. The reaction was vigorously stirred for 2 h after which it was stopped with saturated solution of sodium thiosulphate (5.0 ml) and then washed with 25.0 ml of saturated sodium thiosulphate solution (1 time), saturated sodium bicarbonate (3 times), water (1 time) and brine (1 time). The organic layer was then dried over anhydrous sodium sulphate and then concentrated under vac. The residue, was purified by flash chromatography using ethyl acetate/hexane mixture (4:6) to give α -anomers, **19** (0.12 g, 0.20 mmol) as a white solid. Yield was 55%. NMR data of **19**: ^1H NMR (300 MHz, Chloroform-*d*) δ 5.30 (dd, $J = 10.0, 3.6$ Hz, 1H, H-3), 5.25 (dd, $J = 3.6, 1.7$ Hz, 1H, H-2), 5.06 (dd, $J = 9.8, 9.9$ Hz, 1H, H-4), 4.93 (d, $J = 1.7$ Hz, 1H, H-1), 4.18 – 3.99 (m, 1H, H-5), 3.95 – 3.83 (m, 1H), 3.58 – 3.29 (m, 6H), 2.14 (s, 3H), 2.03 (s, 3H), 1.98 (s, 3H), 1.57 – 1.52 (m, 2H), 1.25 (broad s, 26H, lipid tail), 1.20 (d, $J = 6.3$ Hz, 3H, H-6), 0.87 (t, $J = 6.6$ Hz, 3H). ^{13}C NMR (75 MHz, CDCl_3) δ 170.01, 169.95, 169.84, 97.22, 76.46, 71.77, 71.09, 70.48, 70.01, 68.92, 66.68, 51.68, 31.91, 29.68, 29.49, 29.34, 26.13, 20.87, 20.75, 20.67, 17.34, 14.09. ES-MS: calcd: $\text{C}_{31}\text{H}_{55}\text{N}_3\text{O}_9\text{Na}^+$ m/z : 636.4, found $[\text{M}+\text{Na}]^+$ m/z : 636.5.

3-Azido-1-hexadecyloxy-2R-O- α -L-rhamnopyranosyl)-sn-glycerol (20)

Compound **19** (0.12 g, 0.20 mmol) was dissolved in 15.0 ml of methanol, then catalytic amount of sodium methoxide was added and the reaction was vigorously stirred for 3 h. The reaction was stopped by acidic ion exchange resin. The resin was filtered and the filtrate was concentrated under vacuum and the residue was purified by flash chromatography using ethyl acetate/hexane

mixture (9:1) to give **20** (0.08 g, 0.16 mmol) as a white solid. Yield was 79%. NMR data of **20**: ¹H NMR (300 MHz, Chloroform-*d*) δ 4.95 (d, *J* = 1.1, 1H, H-1), 4.19 – 3.95 (m, 1H, H-5), 4.03 – 3.85 (m, 2H), 3.77 (d, *J* = 8.3, 3.5 Hz, 1H, H-3), 3.62 – 3.27 (m, 10H), 1.58 – 1.54 (m, 2H), 1.32 (d, *J* = 6.4 Hz, 3H, H-6), 1.27 (broad s, 26H), 0.88 (d, *J* = 7.1 Hz, 3H). ¹³C NMR (75 MHz, CDCl₃) δ 100.04, 76.26, 72.70, 71.83, 71.60, 71.09, 70.33, 68.67, 51.71, 31.94, 29.73, 29.52, 29.38, 26.11, 22.70, 17.48, 14.12. ES-MS: calcd: C₂₅H₄₉N₃O₆Na⁺m/z: 500.4, found [M+Na]⁺ m/z: 500.4.

3-Amino-1-O-hexadecyloxy-2R-(O-α-L-rhamnopyranosyl)-sn-glycerol (4)

To a solution compound **20** (0.10 g, 0.21 mmol) in THF (7.0 ml) was added 1.5 ml of water and 2.6 ml of 1M trimethylphosphine in THF. The reaction was vigorously stirred for 2 h at room temperature after which it was concentrated under vac. The residue was purified by C-18 column using gradient elution with water/methanol to give **4** (0.06 g, 0.13 mmol) as a white solid. Yield was 61%. NMR data for **4**: ¹H NMR (300 MHz, Methanol-*d*₄) δ 4.65 (d, *J* = 1.3 1H, H-1) 3.65 (dd, *J* = 1.3,3.4 Hz, 1H, H-2), 3.48 – 3.56 (m, 2H), 3.45 (dd, *J* = 9.5, 3.4 Hz, 1H, H-3), 3.37 – 3.29 (m, 1H, H-5), 3.29 – 3.11 (m, 4H), 2.59 – 2.42 (m, 2H), 1.40 -1.34 (m, 2H), 1.08 (broad s, 29H, H-6, lipid tail), 0.69 (t, *J* = 6.4 Hz, 3H, lipid terminal –CH₃). ¹³C NMR (75 MHz, MeOD) δ 101.91, 79.55, 73.98, 72.69, 72.66, 72.45, 72.39, 70.10, 43.50, 33.10, 30.81, 30.78, 30.66, 30.50, 27.33, 23.76, 18.08, 14.47. MALDI-HRMS: calcd: C₂₅H₅₁NO₆Na⁺ m/z: 484.3614, found [M+Na]⁺ m/z: 484.3611.

3-(3-(p-hydroxy-phenyl-propyl)-amido-1-O-Hexadecyloxy-2R-(O-α-L-rhamnopyranosyl)-sn-glycerol (5)

To a solution of p-hydroxyphenyl propionic acid **21** (0.02 g, 0.11 mmol), TBTU (0.05 g, 0.14 mmol) and diisopropyl ethyl amine (0.02 g, 0.14 mmol) in 5.0 ml of DMF which has been stirring for 20 minutes was added **4** (0.05g, 0.11 mmol). The reaction was vigorously stirred for 8 h after which it was diluted with methanol. The solvents were removed in vacuo and the residue was purified by flash chromatography using ethylacetate to give **5** (0.07 g, 0.11 mmol) as an off white solid. Yield was 98%. NMR data of **5**: ^1H NMR (300 MHz, Methanol- d_4) δ 6.94 (d, $J = 8.3$ Hz, 2H, aromatic proton), 6.62 (d, $J = 8.3$ Hz, 2H, aromatic proton), 4.72 (d, $J = 1.9$ Hz, 1H, H-1), 3.80 – 3.62 (m, 2H), 3.55 (dd, $J = 9.8, 5.7$ Hz, 1H), 3.41 – 3.21 (m, 7H), 3.16 (dd, $J = 13.8, 5.6$ Hz, 1H), 2.73 (t, $J = 7.5$ Hz, 2H, propinamide CH_2), 2.36 (t, $J = 7.7$ Hz, 2H, propinamide CH_2), 1.49 – 1.41 (m, 2H), 1.21 (broad s, 26H, lipid tail), 1.16 (d, $J = 6.2$ Hz, 3H, H-6), 0.82 (t, $J = 6.4$ Hz, 3H, lipid terminal CH_3). ^{13}C NMR (75 MHz, MeOD) δ 175.67, 156.96, 132.79, 130.30, 116.30, 101.26, 76.32, 74.02, 72.67, 72.53, 72.34, 70.00, 49.89, 48.18, 40.92, 39.32, 33.10, 32.20, 30.82, 30.70, 30.50, 27.32, 23.76, 18.09, 14.48. MALDI-HRMS: calcd: $\text{C}_{34}\text{H}_{59}\text{NO}_7\text{Na}^+$ m/z: 632.4138, found $[\text{M}+\text{Na}]^+$ m/z: 632.4590.

*α/β -L-glucopyranosyl-1,2,3,4,5-pentaacetate (**22**)*

L-glucose **2** (0.90 g, 5.00 mmol) was dissolved in 20.0 ml pyridine at room temperature, then acetic anhydride (5.20 ml, 54.90 mmol) and dimethyl amino pyridine (0.10 g,) were sequentially added and the reaction was vigorously stirred for 18 h after which it was stopped by addition of methanol (10.0 ml) and then stirred for 15 minutes. The solvents were removed under high vac. The resulting residue was then dissolved in ethyl acetate (50.0 ml) and washed with 3% HCl solution (1 time), saturated sodium bicarbonate (2 times), distilled water (1 time) and brine (1 time). The resulting organic layer was dried over Na_2SO_4 and concentrated to dryness and purified by flash chromatography using ethyl acetate and hexane (1:1) to give **22** (1.70 g, 4.40

mmol) as α , β mixture (3:2). Yield was 88%. Characteristic proton NMR data for **22**: ^1H NMR (300 MHz, Chloroform-*d*) δ 6.35 (d, $J = 3.7$ Hz, 3H, α -H-1), 5.73 (d, $J = 8.2$ Hz, 2H, β -H-1). ES-MS: calcd: $\text{C}_{16}\text{H}_{22}\text{O}_{11}\text{Na}^+$ m/z: 413.1, found $[\text{M}+\text{Na}]^+$ m/z: 413.4.

Phenyl-2,3,4,6-tetra-O-acetyl-1-thio- β -L-glucopyranoside (23)

The pentaacetate **22** (1.70 g, 4.40 mmol) was dissolved in 20.0 ml DCM, then thiophenol (0.68 g, 6.14 mmol) and $\text{BF}_3 \cdot \text{Et}_2\text{O}$ (0.87 g, 6.14 mmol) were sequentially added. The reaction was stirred vigorously for 18 h after which it was stopped with 20.0 ml saturated sodium bicarbonate at 0°C . The organic layer was separated using separatory funnel and subsequently washed with saturated 20.0 ml of sodium bicarbonate (2 times), 20.0 ml of water (1 time) and 20.0 ml of brine (1 time). The organic layer was dried over anhydrous sodium bicarbonate and then concentrated *in vacuo*. The residue was then partially purified by flash chromatography using ethyl acetate and hexane (4:6) to give mainly β -anomer of **23** (1.72 g, 4.50 mmol). Yield was 88%. Compound **23** was not characterised.

3-Azido-1-hexadecyloxy-2R-(2'3'4'6'-tetra-O-acetyl-O- β -L-glucopyranosyl)-sn-glycerol (24)

The fully protected glycoside donor **23** (0.18 g, 0.40 mmol) and the glycoside acceptor **18** (0.15 g, 0.44 mmol) were dissolved in 15.0 ml of DCM under argon atmosphere, then AgOTf (0.02 g, 0.08 mmol) and N-iodosuccinimide (0.18 g, 0.80 mmol) were simultaneously added. The reaction was vigorously stirred for 2 h after which it was stopped with saturated solution of sodium thiosulphate (5.0 ml) and then washed with 25.0 ml of saturated sodium thiosulphate solution (1 time), saturated sodium bicarbonate (3 times), water (1 time) and brine (1 time). The organic layer was then dried over anhydrous sodium sulphate and then concentrated under *vac.*

The residue, was purified by flash chromatography using ethyl acetate/hexane mixture (4:6) to give **24** (0.13g, 0.20 mmol) as a white solid. Yield was 50%

^1H NMR (300 MHz, Chloroform-*d*) δ 5.22 (dd, $J = 9.4, 9.4$ Hz, 1H, H-4), 5.10 (dd, $J = 9.6, 9.6$ Hz, 1H, H-3), 4.97 (dd, $J = 9.6, 7.9$ Hz 1H, H-2), 4.75 (d, $J = 7.9$ Hz, 1H, H-1), 4.25 – 4.18 (m, 2H), 4.02 – 3.90 (m, 1H), 3.78 – 3.69 (m, 1H), 3.53 – 3.23 (m, 6H), 2.10 (s, 3H), 2.05 (s, 3H), 2.04 (s, 3H), 2.02 (s, 3H), 1.59 – 1.52 (m, 2H), 1.27 (broad singlet, 26H, Lipid tail), 0.89 (h, $J = 6.1$ Hz, 3H, Lipid terminal -CH₃). ^{13}C NMR (75 MHz, CDCl₃) δ 170.65, 170.29, 169.37, 169.17, 100.44, 77.64, 72.83, 71.93, 71.85, 71.47, 70.58, 68.47, 61.90, 52.06, 31.93, 29.70, 29.66, 29.61, 29.49, 29.36, 26.12, 22.70, 20.72, 20.62, 14.12. ES-MS: calcd: C₃₃H₅₇N₃O₁₁Na⁺m/z: 694.4, found [M+Na]⁺ m/z: 694.8.

3-Azido-1-hexadecyloxy-2R-O-β-L-glucopyranosyl-sn-glycerol (25)

Compound **24** (0.13 g, 0.20 mmol) was dissolved in 15.0 ml of methanol, then catalytic amount of sodium methoxide was added and the reaction was vigorously stirred for 3 h. The reaction was stopped by acidic ion exchange resin. The resin was filtered and the filtrate was concentrated under vacuum and the residue was dissolved in ethyl acetate and filtered through a pad of silica gel to give **25** (0.09 g, 0.17 mmol) as a white solid. Yield was 84%. Compound **25** was not characterised. ES-MS: calcd: C₂₅H₄₉N₃O₇Na⁺m/z: 526.4, found [M+Na]⁺ m/z: 526.5.

3-Amino-1-hexadecyloxy-2R-O-β-L-glucopyranosyl-sn-glycerol (6)

To a solution of compound **25** (0.09 g, 0.17 mmol) in THF (7.0 ml) was added 1.5.0 ml of water and 2.6 ml of 1M trimethylphosphine in THF. The reaction was vigorously stirred for 2 h at room temperature after which it was concentrated under vac. The residue was purified by C-18 column using gradient elution with water/methanol to give **6** (0.06 g, 0.09 mmol) as a white

solid. Yield was 55%. NMR data for **6**: ^1H NMR (300 MHz, Methanol- d_4) δ 4.35 (d, $J = 7.7$, Hz, 1H, H-1), 3.81 (dd, $J = 13.7$, 3.6 Hz, 2H, -CH-CH₂O-), 3.69 – 3.36 (m, 6H), 3.34 – 3.07 (m, 4H), 1.59 – 1.38 (m, 3H), 1.22 (broad s, 26H, Lipid tail), 0.85 (t, $J = 7.3$, 3H, Lipid terminal -CH₃). ^{13}C NMR (75 MHz, MeOD) δ 103.87, 79.65, 78.17, 77.96, 75.13, 72.76, 72.35, 71.66, 62.80, 43.87, 33.09, 30.81, 30.78, 30.49, 27.26, 23.75, 14.46. MALDI-HRMS: calcd: C₂₅H₅₁NO₇Na⁺ m/z: 500.3563, found [M+Na]⁺ m/z: 500.3740.

1, 2, 3, 4, 6 - Pentaacetyl α/β -L mannopyranoside (26)

L-mannose **1** (2.00 g, 11.10 mmol), was dissolved in pyridine (40.0 ml), then acetic anhydride (11.00 ml, 111.00 mmol) was added followed by dimethyl amino pyridine (DMAP, 0.27 g 2.20 mmol). The mixture was stirred vigorously for 18 h at room temperature and it was stopped by addition of methanol (10.0 ml) and then stirred for 15 minutes. The solvents were removed under high vac. The resulting residue was then dissolved in ethyl acetate (50.0 ml) and washed with 3% HCl solution (1 time), saturated sodium bicarbonate (2 times), distilled water (1 time) and brine (1 time). The resulting organic layer was dried over Na₂SO₄ and concentrated to dryness and purified by flash chromatography using ethyl acetate and hexane (1:1) to give **26** (3.70 g, 9.48 mmol) as α , β mixture (4:1). Yield was 85%. NMR data for α - anomer of compound **26**: ^1H NMR (300 MHz, Chloroform- d) δ 5.94 (d, $J = 1.9$ Hz, 1H, H-1), 5.24 – 5.06 (m, 3H, H-2), 4.14 (dd, $J = 12.7$, 4.9 Hz, 1H, H-6_a), 4.05 – 3.85 (m, 2H, H-5, H-6_b), 2.09 (s, 3H), 2.01 (s, 3H), 1.96 (s, 3H), 1.92 (s, 3H), 1.82 (s, 3H). ^{13}C NMR (75 MHz, CDCl₃) δ 170.34, 169.73, 169.50, 169.34, 167.88, 90.44, 70.45, 68.63, 68.20, 65.39, 61.94, 20.62, 20.53, 20.48, 20.44, 20.41. ES-MS: calcd: C₁₆H₂₂O₁₁Na⁺ m/z: 414.1, found [M+Na]⁺ m/z: 414.5

Phenyl-2,3,4,6-tetra-O-acetyl-1-thio- α -L-mannopyranoside (27)

The pentaacetate **26** (1.50 g, 3.35 mmol) was dissolved in 30.0 ml DCM, then thiophenol (1.30 g, 11.50 mmol) and $\text{BF}_3 \cdot \text{Et}_2\text{O}$ (1.60 g, 11.50 mmol) were sequentially added. The reaction was stirred vigorously for 18 h after which it was stopped with 30 ml saturated sodium bicarbonate at 0°C . The organic layer was separated using separatory funnel and subsequently washed with saturated 35.0 ml of sodium bicarbonate (2 times), 30.0 ml of water (1 time) and 30.0 ml of brine (1 time). The organic layer was dried over anhydrous sodium bicarbonate and then concentrated *in vacuo*. The residue was then purified by flash chromatography using ethyl acetate and hexane (4:6) to give mainly α -anomer of **27** (0.99 g, 2.35 mmol). Yield was 70%. NMR data of compound **27** is similar to previously reported data.^{73,74} ES-MS: calcd: $\text{C}_{20}\text{H}_{24}\text{O}_9\text{Na}^+$ m/z: 463.1, found $[\text{M}+\text{Na}]^+$ m/z: 462.9

Phenyl-1-thio- α -L-mannopyranoside (28)

Compound **27** (1.00 g, 2.35 mmol) was dissolved in 15.0 ml of methanol, then catalytic amount of sodium methoxide was added and the reaction was vigorously stirred for 3 h. The reaction was stopped by acidic ion exchange resin. The resin was filtered and the filtrate was concentrated under vacuum and the residue was dissolved in ethyl acetate and filtered again through a pad of silica gel to give **28** (0.58 g, 2.14 mmol) as a white solid. Yield was 91%. This compound was used without further purification and characterization for the next step.

Phenyl-6-tosyl-1-thio- α -L-mannopyranoside (29)

Compound **28** (1.31 g, 4.80 mmol) was dissolved in 20.0 ml pyridine, cooled to 0°C , then toluenesulphonylchloride (1.06 g, 5.54 mmol) and DMAP (0.05 g, 0.41 mmol) were added. The temperature was allowed to increase to room temperature and the mixture was stirred

for 18 h. At the end of reaction, the mixture was diluted with methanol after which the solvents were removed in vacuo. The residue was diluted with 40.0 ml ethyl acetate and the washed sodium bicarbonate solution (3 times), brine (3 times). The organic layer was then dried over sodium sulphate and then concentrated under vacuum and the residue was partially purified by flash chromatography using ethyl acetate (100%) to give **29** (1.81 g, 4.24 mmol) as a white solid. Yield was 88%. **29** was not characterized using NMR. ES-MS: calcd: C₁₉H₂₂O₇S₂Na⁺m/z: 449.1, found [M+Na]⁺m/z: 449.5.

Phenyl-6-azido-1-thio- α -L-mannopyranoside (30)

Compound **29** (1.81 g, 4.24 mmol) and sodium azide (1.80 g, 27.60 mmol) were suspended in anhydrous DMF and the mixture was stirred at 90°C for 18 h. at the end of the reaction the mixture was concentrated then diluted with ethyl acetate and filtered to remove excess sodium azide. The filtrate was then concentrated and partially purified with flash chromatography using hexane/ ethyl acetate (1:9) to give **30** (1.20 g, 4.04 mmol) as a white solid. Yield was 95%. ES-MS: calcd: C₁₂H₁₅N₃O₄SNa⁺m/z: 320.1, found [M+Na]⁺m/z: 320.3

Phenyl-2,3,4-tri-O-acetyl-6-azido-1-thio- α -L-mannopyranoside (31)

Compound **30** (1.20 g, 4.04 mmol) was dissolved in pyridine (50.0 ml), then acetic anhydride (2.00 ml, 20.00 mmol) was added followed by dimethyl amino pyridine (DMAP, 0.05g, 0.41 mmol). The mixture was stirred vigorously for 18 h at room temperature and it was stopped by addition of methanol (10.0 ml) and then stirred for 15 minutes. The solvents were removed under high vac. The resulting residue was then dissolved in ethyl acetate (50.0 ml) and washed with 3% HCl solution (1 time), saturated sodium bicarbonate (2 times), distilled water (1 time) and brine

(1 time). The resulting organic layer was dried over Na₂SO₄ and concentrated to dryness and purified by flash chromatography using ethyl acetate and hexane (1:1) to give **31** (1.31 g, 3.10 mmol) white solid. Yield was 76 %. NMR data of compound **31**: ¹H NMR (300 MHz, Chloroform-*d*) δ 7.54 – 7.10 (m, H, aromatic protons), 5.54 – 5.37 (m, 2H, H-1, H-3), 5.32 – 5.19 (m, 2H, H-2, H-4), 4.43 – 4.38 (m, 1H, H-5), 3.41 – 3.17 (m, 2H, H-6), 2.07 (s, 3H), 2.03 (s, 3H), 1.90 (s, 3H). ¹³C NMR (75 MHz, CDCl₃) δ 169.72, 169.64, 132.49, 132.01, 129.27, 128.12, 85.64, 71.01, 70.81, 69.18, 67.14, 50.98, 20.69, 20.58, 20.50. ES-MS: calcd: C₁₈H₂₁N₃O₇SNa⁺ m/z: 446.1, found [M+Na]⁺ m/z: 446.4

3-Azido-1-hexadecyloxy-2R-(6'-azido-2'3'4'-tri-O-acetyl-O-α-L-mannopyranosyl)-sn-glycerol
32

The fully protected glycoside donor **31** (0.20 g, 0.47 mmol) and the glycoside acceptor **18** (0.18 g, 0.52 mmol) were dissolved in 15.0 ml of DCM under argon atmosphere, then AgOTf (0.02 g, 0.09 mmol) and N-iodosuccinimide (0.16g, 0.71 mmol) were simultaneously added. The reaction was vigorously stirred for 2 h after which it was stopped with saturated solution of sodium thiosulphate (5.0 ml) and then washed with 25.0 ml of saturated sodium thiosulphate solution (1 time), saturated sodium bicarbonate (3 times), water (1 time) and brine (1 time). The organic layer was then dried over anhydrous sodium sulphate and then concentrated under vac. The residue, was purified by flash chromatography using ethyl acetate/hexane mixture (4:6) to give **32** (0.220 g, 0.34 mmol) as a white solid. Yield was 71%. NMR data of **32**: ¹H NMR (300 MHz, Chloroform-*d*) δ 5.38 (dd, *J* = 9.9, 3.3 Hz, 1H, H-3), 5.32 – 5.20 (m, 2H, H-2, H-4), 5.06 (d, *J* = 1.8 Hz, 1H, H-1), 4.20 (ddd, *J* = 9.5, 5.6, 3.4 Hz, 1H, H-5), 4.07 – 3.89 (m, 1H), 3.64 – 3.23 (m, 8H, H-6), 2.18 (s, 3H), 2.06 (s, 3H), 2.01 (s, 3H), 1.61 – 1.54 (m, 2H), 1.27 (broad s, 26H, lipid tail), 0.89 (t, *J* = 6.5 Hz, 3H, lipid terminal -CH₃). ¹³C NMR (75 MHz, CDCl₃) δ 170.01, 169.81,

97.13, 76.84, 71.80, 70.35, 70.23, 69.69, 68.66, 67.20, 51.76, 51.18, 31.93, 29.70, 29.64, 29.52, 29.37, 26.15, 22.70, 20.88, 20.72, 14.12. ES-MS: calcd: C₃₁H₅₄N₆O₉Na⁺m/z: 677.4, found [M+Na]⁺m/z: 677.8

3-Azido-1-hexadecyloxy-2R-(6'-azido-O- α -L-mannopyranosyl)-sn-glycerol (33)

Compound **32** (0.22 g, 0.34 mmol) was dissolved in 15.0 ml of methanol, then catalytic amount of sodium methoxide (0.05 g) was added and the reaction was vigorously stirred for 3 h. The reaction was stopped by acidic ion exchange resin. The resin was filtered and the filtrate was concentrated under vacuum and the residue was purified by flash chromatography using ethyl acetate/hexane mixture (9:1) to give **33** (0.120 g, 0.23 mmol) as a white solid. Yield was 68%. NMR data of **33**: ¹H NMR (300 MHz, Methanol-*d*₄) δ 5.02 (d, *J* = 1.9 Hz, 1H, H-1), 4.10 - 3.89 (m, 2H, H-3), 3.96 - 3.81 (m, 2H, H-2), 3.78 - 3.57 (m, 3H), 3.56 - 3.28 (m, 6H), 1.62 - 1.58 (m, 2H), 1.33 (broad s, 26H, lipid tail), 0.91 (t, *J* = 6.6 Hz, 3H, lipid terminal -CH₃). ¹³C NMR (75 MHz, MeOD) δ 101.93, 77.92, 74.29, 72.72, 72.18, 72.15, 71.65, 69.45, 53.23, 52.92, 33.16, 30.89, 30.79, 30.57, 27.33, 23.82, 14.59. ES-MS: calcd: C₂₅H₄₈N₆O₆Na⁺m/z: 528.4, found [M+Na]⁺m/z: 528.7

3-Amino-1-hexadecyloxy-2R-(6'-amino-6'-deoxy-O- α -L-mannopyranosyl)-sn-glycerol (7)

To a solution of compound **33** (0.12 g, 0.23 mmol) in THF (7.0 ml) was added 1.5 ml of water and 2.6 ml of 1M trimethylphosphine in THF. The reaction was vigorously stirred for 2 h at room temperature after which it was concentrated under vac. The residue was purified by C-18 column using gradient elution with water/methanol to give **7** (0.07 g, 0.14 mmol) as a white solid. Yield was 62%. NMR data for **7**: ¹H NMR (300 MHz, Methanol-*d*₄) δ 4.83 (d, *J* = 2.0 Hz, 1H, H-1), 3.79 (dd, *J* = 5.0, 2.0 Hz, 1H, H-2), 3.71 - 3.62 (m, 2H), 3.58 - 3.43 (m, 3H, H-5),

3.38– 3.17 (m, 4H), 2.94 – 2.82 (m, 1H), 2.83 – 2.60 (m, 2H, H-6), 1.59 – 1.38 (m, 2H), 1.21 (broad s, 26H, lipid tail), 0.83 (t, $J = 6.6$ Hz, 3H, lipid terminal $-CH_3$). ^{13}C NMR (75 MHz, MeOD) δ 101.52, 79.00, 74.36, 72.75, 72.70, 72.44, 72.34, 69.51, 43.45, 43.26, 33.12, 30.84, 30.70, 30.52, 27.37, 23.78, 14.51. MALDI-HRMS: calcd: $C_{25}H_{52}N_2O_6Na^+$ m/z: 499.3723, found $[M+Na]^+$ m/z: 499.3409.

7.6.2. Biological Methods

7.6.2.1. Determination of Cytotoxicity of GAELs on cancer cell lines

The cell lines were cultured from frozen stocks originally obtained from ATCC. MDA-MB-231, JIMT-1, DU145, MDA-MB-468, Hs578t and MDA-MB-453 were grown in DMEM medium supplemented with 10% FBS. BT474 cells were grown in DMEM/F12 medium supplemented with 10% FBS. MiaPaCa2 was cultured in DMEM supplemented with 10% FBS and 2.5% horse serum. PC3 cells were cultured in F12K medium supplemented with 10% FBS. All the media contained penicillin/streptomycin. U-251 and U-87 in Eagle MEM supplemented by 10% FBS, 1% Non essential amino acids, 1 mM sodium pyruvate and 2mM glutamine. BT-549 was cultured in RPMI 1640 medium supplemented with 10% FBS.

The effects of the GAELs on the viability of the various epithelial cancer cell lines was determined as previously described.^{12,13,16} Briefly equal numbers of the cells were dispersed into 96-well plates. After 24 h, the cells were incubated with the compounds (0-30 μ M) for 48 h. At the end of the incubation, MTS reagent (20% vol/vol) was added and the plates were incubated for 1-4 h in a CO₂ incubator. The OD₄₉₀ was read with a plate reader (Molecular Devices). Wells with media but no cells were treated in similar fashion and the values utilized as blank. The results represent the mean \pm standard deviation of 6 independent determinations.

7.6.2.2. Isolation of breast cancer stem cells from breast BT-474 and prostate DU-145 cancer stem cells from DU145 cell lines and determination of the effect of GAELs on the viability of the cancer stem cells.

A population enriched in BT474 breast cancer stem cells or DU145 prostate cancer stem cells was obtained by staining the cells for aldehyde dehydrogenase using the Aldefluor assay kit from Stem Cell Technologies (Vancouver, BC, Canada) according to the instruction of the manufacturer with the appropriate controls. The stained cells were sorted from the bulk population by flow cytometry on a 4 laser MoFloXPP high speed/pressure cell sorter. The cells were pelleted by centrifugation. BT474 cells were resuspended into ultra-low adhesion plates in mammoCult medium (Stem cell Technologies). The DU145 stem cells were resuspended in their growth medium (DMEM/F12 medium supplemented with 20 ng/ml EGF, and 10 ng/ml basic FGF, 5 µg/ml insulin, 0.4% BSA, with 1% antibiotics.³⁵ The dishes were incubated at 37°C in a CO₂ incubator for 4 days for spheroid formation.

The spheres were separated from single cells with a 40 µm nylon cell strainer. The spheres retained in the strainer were washed with PBS and trypsinised to obtain single cells. The cell numbers were counted with a Coulter ZM counter and the cells were dispersed into 48-well low adhesion plates (Grenier) in a volume of 500 µl. The cells were incubated for 4 days to allow for formation of spheroids. Subsequently, the stock GAELs in ethanol were diluted to twice the final concentration in the media and a volume of 500 µl was added to the wells. Wells

with growth medium but no cells were treated as the wells with cells. After 5 days incubation, MTS reagent (2% vol/vol) was added to each well and the plates were incubated for 1-4 h for formation of colour. The OD₄₉₀ were read in a Molecular Device absorbance plate reader using the SpectroMax software.

7.6.2.3. Preparation of bovine liver glycosidases fraction

The glycosidases fraction were prepared from beef liver as previously reported.^{65,75} Fresh whole beef liver was obtained from a slaughter house in Winnipeg (Robert farm). The connective tissue covering the liver was peeled off. 100 g was cut into small pieces before they were homogenized using a liter of cold water (4°C) in a blender for about 1 minute. The pH was adjusted to 4.8 using 1 M citric acid. Then the homogenized mixture was centrifuged and 0.20 to 0.60 saturated ammonium sulfate precipitate obtained from the supernatant solution was dialyzed at 4°C against water for 24 h, and against 0.05 M sodium citrate buffer, pH 5.0, for a further 24 h. The undissolved left over was discarded and the supernatant was stored at -20°C. At this temperature the glycosidases can be stable for many months.⁶⁵ The protein content of the fraction was 7.5mg/ml based on protein assay using Cytoskeleton precision red advanced protein assay reagent as stipulated by manufacturer. We determined the glycosidases activity using a previously reported assay where p-Nitrophenol- α -glucopyranoside was used as substrate at 410 nm.⁷⁶

7.6.2.4. Demonstration of activity of bovine liver glycosidase fraction

The glycosidases activity of the bovine liver glycosidases was determined using liberation of p-nitrophenol form using p-nitrophenyl α -glucoside. The incubated mixture (2ml) contained 0.5 ml

of 0.2 M citric acid-NaOH buffer, pH 4.4, 0.4 ml of 25 mM of p-nitrophenyl α -glucoside, 25 μ L of enzyme solution, 0.225 ml of buffer solution used as vehicle for the enzyme and 0.85 ml of distilled water. The final concentration of the substrate in the incubated mixture was 10 mM. After incubation for 1 h at 38°C, 2 ml of 0.4 M glycine-NaOH buffer, pH 10.5 was added. The solution was centrifuged and the liberated p-Nitrophenol was measured by spectrophotometer at 410 nm. The activity of enzyme was calculated to be 19.26 μ g/mg/h.⁷⁶

7.6.2.5. Demonstration of stability of glycolipid 4 to bovine liver glycosidases fraction

To assess the stability of glycolipid 4 to cocktail of glycosidases in the bovine liver fraction two techniques were used. First was mass spectrometer analysis of the substrate after incubation with the glycosidases while the second technique was radioactivity tracing on high performance TLC plate using a ³H labelled analog of compound 4 after incubation with the glycosidases. For the first method the incubated mixture (50 μ L) contained 7.5 μ L of 0.2 M sodium citrate buffer, pH 4.4, 12.5 μ L of 30 mM of the substrate i.e. compound 4, 25 μ L of the glycosidase fraction in 0.05 M sodium citrate buffer, pH 5.0 and 5 μ L of 10% triton X100 for solubilization of the substrate in the mixture. For the control without enzyme 25 μ L of 0.05 M sodium citrate buffer, pH 5.0 were used. It is noteworthy that triton X100 has no effect on enzyme activity. After 1 h incubation, 25 μ L of methanol was added to inactivate the enzyme and the supernatant was analyzed using both mass spectrometry and LC-MS to investigate the presence of enzymatic degradation product. Three repeats of the experiment were carried out.

For the radiotracing experiment 15 μ L of the radio ³H labelled compound 4 was bulked up with unlabeled analog 4 to achieve a concentration of 30 mM in water and then treated as described above. At the end of incubation period 5 μ L of the supernatant was co-spotted with both

rhamnose and unlabeled analog on high performance TLC plate, and developed using chloroform, methanol and acetic acid mixture (6.5:2.5:1). Iodine tank was used for visualization. Then each band of spot was scraped from the TLC plate, dissolved in 1 ml of water after which 10 ml of scintillation solution was added. The mixture was then left in darkness overnight before counting the radioactivity using a scintillation counter. The distribution of radioactivity in enzyme treated test was compared with that of control for determination of hydrolysis by the glycosidases.

7.6.2.6. Determination of membranolytic effects of GAELs

JIMT-1 and DU145 were grown in DMEM medium supplemented with 10% FBS and antibiotics, penicillin/streptomycin. Equal numbers of the cells were dispersed into 96-well plates. After 24 h, the cells were incubated with varying concentration of the compounds **4** and **5** (4 - 6 μ M) for 5 - 6 h. Subsequently, 2 μ M of the cell membrane impermeant dye, ethidium homodimer-1 (EthD-1, Molecular Probes) that emits red fluorescence upon binding to DNA was added and the cells analysed by fluorescence microscopy. EthD-1 staining was compared to negative controls with no treatment and positive control treated with 0.01% Triton X-100 for 10 min.

7.6.2.7. Demonstration of Caspase-mediated-apoptosis independent mode of cell death

JIMT-1, DU145 were grown in DMEM medium containing penicillin/streptomycin and supplemented with 10% FBS. Equal numbers of the cells were dispersed into 96-well plates, after 4h, the cells were treated with pan-caspase inhibitor QVD-OPh (40 μ M). After 20 h, the cell were incubated with the varying concentration of the compounds (0 – 9 μ M) for 48 h. At the

end of the incubation, MTS reagent (20% vol/vol) was added and the plates were incubated for 1-4 h in a CO₂ incubator. The OD₄₉₀ was read with a plate reader (Molecular Devices). Wells with media but no cells were treated in similar fashion and the values utilized as blank. The results represent the mean ± standard deviation of 6 independent determinations.

7.6.2.8. Hemolytic assay

The hemolytic activity of the GAEL analogs was evaluated using ovine erythrocyte. Sheep whole blood was collected from a slaughter house into a vessel containing disodium EDTA (1.2 g/ml) in a buffered saline (10mM Tris, 150 mM NaCl, pH 7.4). The erythrocytes were prepared and wash with buffered saline as previously reported.^{77,78} For the assay, the erythrocyte suspension, varying amounts of the GAEL drugs, the saline buffer and the appropriate amount of the vehicle used for dissolving the compounds were pipetted to an Eppendorf tubes to give a final volume of 1500 µL and cell density of 2.5×10^8 cells/ml. The suspensions were incubated with gentle shaking in Eppendorf thermomixer for 30 minutes. The eppendorf tubes were cooled in ice water and centrifuged at 2000g and 4°C for 5 minutes. 200 µL of the supernatant was dissolved in 1800 µL of 0.5% NH₄OH and the optical density (OD) was recorded using 1mL cuvette at 540 nm in a spectrophotometer. For the 0% hemolysis, buffer and vehicle used to dissolve the drug were added instead of the drug and for the 100% hemolysis 1% NH₄OH was used. % hemolysis was calculated using the optical density (OD) values as shown below:

$$\% \text{ hemolysis} = (X - 0\%) / (100\% - 0\%)$$

X is OD values of the drugs at varying concentration.

7.6.2.9. Statistical analysis

The results represent the mean \pm standard deviation of 6 independent determinations. Statistical significant difference test was carried using GraphPadInstat software. The data, that is, the mean values were subjected to one-way analysis of variance (ANOVA) followed by Tukey-Kramer multiple comparison tests as post hoc test. Comparisons were carried out between the viability of controls and drug treated cells to determine if statistically significant differences existed between the two groups. The results of the effects of different concentrations of the compounds were also compared for statistically significant differences to determine if the cytotoxic activities of the drugs are dose dependent. The anticancer activities of all the compounds **1-7** tested and the lead compound **8-10** were also compared using ANOVA followed by Tukey-Kramer multiple comparison tests at the following concentrations: 5, 7.5 and 10 μ M to determine if the difference in the potency of the drugs are statistically significant or not. A p value > 0.05 indicates no statistical differences while a p value <0.001 indicated statistical significant differences. The statistical analysis data are not included in this report.

7.7. Acknowledgements

This study was supported by research grants from the Canadian Breast Cancer Foundation Prairie/NWT to GA and Natural Science and Engineering Council of Canada (NSERC) grant to FS. Makanjuola Ogunsina is the recipient of a University of Manitoba and Manitoba provincial government graduate fellowships (UMGF and MGS). We are grateful to BC cancer institute who helped us with animal study on contractual basis.

References

- (1) Cancer | At A Glance Reports | Publications | Chronic Disease Prevention and Health Promotion | CDC <http://www.cdc.gov/chronicdisease/resources/publications/aag/dcpc.htm> (accessed Aug 13, 2015).
- (2) CDC - The Global Burden of Cancer <http://www.cdc.gov/cancer/international/burden.htm> (accessed Aug 13, 2015).
- (3) The Global Burden of Cancer 2013 | Institute for Health Metrics and Evaluation <http://www.healthdata.org/research-article/global-burden-cancer-2013> (accessed Aug 13, 2015).
- (4) Global Cancer Burden to Nearly Double by 2030 <http://www.cancer.org/myacs/newengland/global-cancer-burden-to-double-by-2030> (accessed Aug 13, 2015).
- (5) McGowan, P. M.; Kirstein, J. M.; Chambers, A. F. Micrometastatic Disease and Metastatic Outgrowth: Clinical Issues and Experimental Approaches. *Future Oncol.* **2009**, *5* (7), 1083–1098.
- (6) Chao, M. P. Treatment Challenges in the Management of Relapsed or Refractory Non-Hodgkin's Lymphoma - Novel and Emerging Therapies. *Cancer Manag. Res.* **2013**, *5*, 251–269.
- (7) Wikman, H.; Vessella, R.; Pantel, K. Cancer Micrometastasis and Tumour Dormancy. *APMIS* *116* (7–8), 754–770.
- (8) Pantel, K.; Alix-Panabières, C.; Riethdorf, S. Cancer Micrometastases. *Nat. Rev. Clin.*

- Oncol.* **2009**, *6* (6), 339–351.
- (9) Pantel, K.; Alix-Panabières, C. Circulating Tumour Cells in Cancer Patients: Challenges and Perspectives. *Trends Mol. Med.* **2010**, *16* (9), 398–406.
- (10) Lobo, N. A.; Shimono, Y.; Qian, D.; Clarke, M. F. The Biology of Cancer Stem Cells. *Annu. Rev. Cell Dev. Biol.* **2007**, *23*, 675–699.
- (11) Kreso, A.; Dick, J. E. Evolution of the Cancer Stem Cell Model. *Cell Stem Cell* **2014**, *14* (3), 275–291.
- (12) Collins, A. T.; Berry, P. A.; Hyde, C.; Stower, M. J.; Maitland, N. J. Prospective Identification of Tumorigenic Prostate Cancer Stem Cells. *Cancer Res.* **2005**, *65* (23), 10946–10951.
- (13) Li, C.; Heidt, D. G.; Dalerba, P.; Burant, C. F.; Zhang, L.; Adsay, V.; Wicha, M.; Clarke, M. F.; Simeone, D. M. Identification of Pancreatic Cancer Stem Cells. *Cancer Res.* **2007**, *67* (3), 1030–1037.
- (14) Clarke, M. F.; Dick, J. E.; Dirks, P. B.; Eaves, C. J.; Jamieson, C. H. M.; Jones, D. L.; Visvader, J.; Weissman, I. L.; Wahl, G. M. Cancer Stem Cells--Perspectives on Current Status and Future Directions: AACR Workshop on Cancer Stem Cells. *Cancer Res.* **2006**, *66* (19), 9339–9344.
- (15) Visvader, J. E.; Lindeman, G. J. Cancer Stem Cells in Solid Tumours: Accumulating Evidence and Unresolved Questions. *Nat. Rev. Cancer* **2008**, *8* (10), 755–768.
- (16) Sampieri, K.; Fodde, R. Cancer Stem Cells and Metastasis. *Semin. Cancer Biol.* **2012**, *22* (3), 187–193.

- (17) Kucia, M.; Reza, R.; Miekus, K.; Wanzeck, J.; Wojakowski, W.; Janowska-Wieczorek, A.; Ratajczak, J.; Ratajczak, M. Z. Trafficking of Normal Stem Cells and Metastasis of Cancer Stem Cells Involve Similar Mechanisms: Pivotal Role of the SDF-1-CXCR4 Axis. *Stem Cells* **2005**, *23* (7), 879–894.
- (18) Li, F.; Tiede, B.; Massagué, J.; Kang, Y. Beyond Tumorigenesis: Cancer Stem Cells in Metastasis. *Cell Res.* **2007**, *17* (1), 3–14.
- (19) Charafe-Jauffret, E.; Ginestier, C.; Iovino, F.; Tarpin, C.; Diebel, M.; Esterni, B.; Houvenaeghel, G.; Extra, J.-M.; Bertucci, F.; Jacquemier, J.; Xerri, L.; Dontu, G.; Stassi, G.; Xiao, Y.; Barsky, S. H.; Birnbaum, D.; Viens, P.; Wicha, M. S. Aldehyde Dehydrogenase 1-Positive Cancer Stem Cells Mediate Metastasis and Poor Clinical Outcome in Inflammatory Breast Cancer. *Clin. Cancer Res.* **2010**, *16* (1), 45–55.
- (20) Karnoub, A. E.; Dash, A. B.; Vo, A. P.; Sullivan, A.; Brooks, M. W.; Bell, G. W.; Richardson, A. L.; Polyak, K.; Tubo, R.; Weinberg, R. A. Mesenchymal Stem Cells within Tumour Stroma Promote Breast Cancer Metastasis. *Nature* **2007**, *449* (7162), 557–563.
- (21) Charafe-Jauffret, E.; Ginestier, C.; Iovino, F.; Wicinski, J.; Cervera, N.; Finetti, P.; Hur, M.-H.; Diebel, M. E.; Monville, F.; Dutcher, J.; Brown, M.; Viens, P.; Xerri, L.; Bertucci, F.; Stassi, G.; Dontu, G.; Birnbaum, D.; Wicha, M. S. Breast Cancer Cell Lines Contain Functional Cancer Stem Cells with Metastatic Capacity and a Distinct Molecular Signature. *Cancer Res.* **2009**, *69* (4), 1302–1313.
- (22) Hermann, P. C.; Huber, S. L.; Herrler, T.; Aicher, A.; Ellwart, J. W.; Guba, M.; Bruns, C. J.; Heeschen, C. Distinct Populations of Cancer Stem Cells Determine Tumor Growth and

- Metastatic Activity in Human Pancreatic Cancer. *Cell Stem Cell* **2007**, *1* (3), 313–323.
- (23) Wicha, M. S. Cancer Stem Cells and Metastasis: Lethal Seeds. *Clin. Cancer Res.* **2006**, *12* (19), 5606–5607.
- (24) Yu, Z.; Pestell, T. G.; Lisanti, M. P.; Pestell, R. G. Cancer Stem Cells. *Int. J. Biochem. Cell Biol.* **2012**, *44* (12), 2144–2151.
- (25) Reya, T.; Morrison, S. J.; Clarke, M. F.; Weissman, I. L. Stem Cells, Cancer, and Cancer Stem Cells. *Nature* **2001**, *414* (6859), 105–111.
- (26) Guo, W.; Lasky, J. L.; Wu, H. Cancer Stem Cells. *Pediatr. Res.* **2006**, *59* (4 Pt 2), 59R–64R.
- (27) Fulda, S. Regulation of Apoptosis Pathways in Cancer Stem Cells. *Cancer Lett.* **2013**, *338* (1), 168–173.
- (28) Liu, G.; Yuan, X.; Zeng, Z.; Tunici, P.; Ng, H.; Abdulkadir, I. R.; Lu, L.; Irvin, D.; Black, K. L.; Yu, J. S. Analysis of Gene Expression and Chemoresistance of CD133+ Cancer Stem Cells in Glioblastoma. *Mol. Cancer* **2006**, *5* (1), 67.
- (29) Tagscherer, K. E.; Fassl, A.; Campos, B.; Farhadi, M.; Kraemer, A.; Böck, B. C.; Macher-Goeppinger, S.; Radlwimmer, B.; Wiestler, O. D.; Herold-Mende, C.; Roth, W. Apoptosis-Based Treatment of Glioblastomas with ABT-737, a Novel Small Molecule Inhibitor of Bcl-2 Family Proteins. *Oncogene* **2008**, *27* (52), 6646–6656.
- (30) Fulda, S.; Vucic, D. Targeting IAP Proteins for Therapeutic Intervention in Cancer. *Nat. Rev. Drug Discov.* **2012**, *11* (2), 109–124.

- (31) Boman, B. M.; Wicha, M. S. Cancer Stem Cells: A Step toward the Cure. *J. Clin. Oncol.* **2008**, *26* (17), 2795–2799.
- (32) Dingli, D.; Michor, F. Successful Therapy Must Eradicate Cancer Stem Cells. *Stem Cells* **2006**, *24* (12), 2603–2610.
- (33) Al-Hajj, M.; Becker, M. W.; Wicha, M.; Weissman, I.; Clarke, M. F. Therapeutic Implications of Cancer Stem Cells. *Curr. Opin. Genet. Dev.* **2004**, *14* (1), 43–47.
- (34) Beier, D.; Röhrli, S.; Pillai, D. R.; Schwarz, S.; Kunz-Schughart, L. A.; Leukel, P.; Proescholdt, M.; Brawanski, A.; Bogdahn, U.; Trampe-Kieslich, A.; Giebel, B.; Wischhusen, J.; Reifenberger, G.; Hau, P.; Beier, C. P. Temozolomide Preferentially Depletes Cancer Stem Cells in Glioblastoma. *Cancer Res.* **2008**, *68* (14), 5706–5715.
- (35) Zobalova, R. .; Stantic, M. .; Stapelberg, M. .; Prokopova, K. .; Dong, J. .; Truksa, J. et al. Drugs That Kill Cancer Stem-like Cells. In *Cancer Stem Cells Theories and Practice*; Shosta, S., Ed.; InTech, 2011; pp 361–378.
- (36) Vazquez-Martin, A.; Oliveras-Ferraros, C.; Del Barco, S.; Martin-Castillo, B.; Menendez, J. A. The Anti-Diabetic Drug Metformin Suppresses Self-Renewal and Proliferation of Trastuzumab-Resistant Tumor-Initiating Breast Cancer Stem Cells. *Breast Cancer Res. Treat.* **2011**, *126* (2), 355–364.
- (37) Beier, D.; Rohrl, S.; Pillai, D. R.; Schwarz, S.; Kunz-Schughart, L. A.; Leukel, P.; Proescholdt, M.; Brawanski, A.; Bogdahn, U.; Trampe-Kieslich, A.; Giebel, B.; Wischhusen, J.; Reifenberger, G.; Hau, P.; Beier, C. P. Temozolomide Preferentially Depletes Cancer Stem Cells in Glioblastoma. *Cancer Res.* **2008**, *68* (14), 5706–5715.

- (38) Gupta, P. B.; Onder, T. T.; Jiang, G.; Tao, K.; Kuperwasser, C.; Weinberg, R. A.; Lander, E. S. Identification of Selective Inhibitors of Cancer Stem Cells by High-Throughput Screening. *Cell* **2009**, *138* (4), 645–659.
- (39) Boehmerle, W.; Endres, M. Salinomycin Induces Calpain and Cytochrome c-Mediated Neuronal Cell Death. *Cell Death Dis.* **2011**, *2*, e168.
- (40) Samadder, P.; Xu, Y.; Schweizer, F.; Arthur, G. Cytotoxic Properties of D-Gluco-, D-Galacto- and D-Manno-Configured 2-Amino-2-Deoxy-Glycerolipids against Epithelial Cancer Cell Lines and BT-474 Breast Cancer Stem Cells. *Eur. J. Med. Chem.* **2014**, *78* (78), 225–235.
- (41) Arthur, G.; Schweizer, F.; Ogunsina, M. Carbohydrates in Drug Design and Discovery; Jimenez-Barbero, J., Canada, F. J., Martin-Santamaria, S., Eds.; RSC Drug Discovery; Royal Society of Chemistry: Cambridge, 2015.
- (42) Arthur, G.; Bittman, R. Glycosylated Antitumor Ether Lipids: Activity and Mechanism of Action. *Anticancer. Agents Med. Chem.* **2014**, *14* (4), 592–606.
- (43) Samadder, P.; Byun, H. S.; Bittman, R.; Arthur, G. Glycosylated Antitumor Ether Lipids Are More Effective against Oncogene-Transformed Fibroblasts than Alkyllysophospholipids. *Anticancer Res.* **1998**, *18* (1A), 465–470.
- (44) Samadder, P.; Byun, H.-S.; Bittman, R.; Arthur, G. An Active Endocytosis Pathway Is Required for the Cytotoxic Effects of Glycosylated Antitumor Ether Lipids. *Anticancer Res* **2011**, *31* (11), 3809–3818.
- (45) Samadder, P.; Bittman, R.; Byun, H.-S.-S.; Arthur, G. A Glycosylated Antitumor Ether

- Lipid Kills Cells via Paraptosis-like Cell Death. *Biochem. Cell Biol.* **2009**.
- (46) Ogunsina, M.; Pan, H.; Samadder, P.; Arthur, G.; Schweizer, F. Structure Activity Relationships of N-Linked and Diglycosylated Glucosamine-Based Antitumor Glycerolipids. *Molecules* **2013**, *18* (12), 15288–15304.
- (47) Ogunsina, M.; Samadder, P.; Arthur, G.; Schweizer, F. *Replacing D-Glucosamine with Its L-Enantiomer in Glycosylated Antitumor Ether Lipids (GAELs) Retains Cytotoxic Effects against Epithelial Cancer Cells and Cancer Stem Cells*; Winnipeg, 2016 (Manuscript under preparation).
- (48) Gerber-Lemaire, S.; Juillerat-Jeanneret, L. Glycosylation Pathways as Drug Targets for Cancer: Glycosidase Inhibitors. *Mini-Reviews Med. Chem.* **2006**, *6* (9), 1043–1052.
- (49) Dube, D. H.; Bertozzi, C. R. Glycans in Cancer and Inflammation--Potential for Therapeutics and Diagnostics. *Nat. Rev. Drug Discov.* **2005**, *4* (6), 477–488.
- (50) Ogunsina, M.; Samadder, P.; Idowu, T.; Arthur, G.; Schweizer, F. Design, Synthesis and Evaluation of Cytotoxic Properties of Bisamino Glucosylated Antitumor Ether Lipids against Cancer Cells and Cancer Stem Cells. *Med. Chem. Commun.* **2016**.
- (51) Tomsik, P.; Soukup, T.; Cermakova, E.; Micuda, S.; Niang, M.; Sucha, L.; Rezacova, M. L-Rhamnose and L-Fucose Suppress Cancer Growth in Mice. *Cent. Eur. J. Biol.* **2011**, *6* (1), 1–9.
- (52) Malm, S. W.; Hanke, N. T.; Gill, A.; Carbajal, L.; Baker, A. F. The Anti-Tumor Efficacy of 2-Deoxyglucose and D-Allose Are Enhanced with p38 Inhibition in Pancreatic and Ovarian Cell Lines. *J. Exp. Clin. Cancer Res.* **2015**, *34*, 31.

- (53) Fjelde, A.; Sorkin, E.; Rhodes, J. M. The Effect of Glucosamine on Human Epidermoid Carcinoma Cells in Tissue Culture. *Exp. Cell Res.* **1956**, *10* (1), 88–98.
- (54) Lacroix, M.; Leclercq, G. Relevance of Breast Cancer Cell Lines as Models for Breast Tumours: An Update. *Breast Cancer Res. Treat.* **2004**, *83* (3), 249–289.
- (55) Hackett, A. J.; Smith, H. S.; Springer, E. L.; Owens, R. B.; Nelson-Rees, W. A.; Riggs, J. L.; Gardner, M. B. Two Syngeneic Cell Lines from Human Breast Tissue: The Aneuploid Mammary Epithelial (Hs578T) and the Diploid Myoepithelial (Hs578Bst) Cell Lines. *J Natl Cancer Inst* **1977**, *58* (6), 1795–1806.
- (56) Cailleau, R.; Young, R.; Olive, M.; Reeves, W. J. . J. Breast Tumor Cell Lines From Pleural Effusions. *J Natl Cancer Inst* **1974**, *53* (3), 661–674.
- (57) Cailleau, R.; Olivé, M.; Cruciger, Q. V. J. Long-Term Human Breast Carcinoma Cell Lines of Metastatic Origin: Preliminary Characterization. *In Vitro* **1978**, *14* (11), 911–915.
- (58) Koul, D.; Shen, R.; Bergh, S.; Sheng, X.; Shishodia, S.; Lafortune, T. A.; Lu, Y.; de Groot, J. F.; Mills, G. B.; Yung, W. K. A. Inhibition of Akt Survival Pathway by a Small-Molecule Inhibitor in Human Glioblastoma. *Mol. Cancer Ther.* **2006**, *5* (3), 637–644.
- (59) Jacobs, V. L.; Valdes, P. A.; Hickey, W. F.; De Leo, J. A. Current Review of in Vivo GBM Rodent Models: Emphasis on the CNS-1 Tumour Model. *ASN Neuro* **2011**, *3* (3), e00063.
- (60) He, Y.-C.; Zhou, F.-L.; Shen, Y.; Liao, D.-F.; Cao, D. Apoptotic Death of Cancer Stem Cells for Cancer Therapy. *Int. J. Mol. Sci.* **2014**, *15* (5), 8335–8351.
- (61) Keoni, C. L.; Brown, T. L. Inhibition of Apoptosis and Efficacy of Pan Caspase Inhibitor,

- Q-VD-Oph, in Models of Human Disease. *J. Cell Death* **2015**, *8*, 1–7.
- (62) Markovits, J.; Roques, B. P.; Le Pecq, J. B. Ethidium Dimer: A New Reagent for the Fluorimetric Determination of Nucleic Acids. *Anal. Biochem.* **1979**, *94* (2), 259–264.
- (63) Krämer, S. D.; Wunderli-Allenspach, H. No Entry for TAT(44–57) into Liposomes and Intact MDCK Cells: Novel Approach to Study Membrane Permeation of Cell-Penetrating Peptides. *Biochim. Biophys. Acta - Biomembr.* **2003**, *1609* (2), 161–169.
- (64) Datrie, M.; Schumann, M.; Wieprecht, T.; Winkler, A.; Beyermann, M.; Krause, E.; Matsuzaki, K.; Murase, O.; Bienert, M. Peptide Helicity and Membrane Surface Charge Modulate the Balance of Electrostatic and Hydrophobic Interactions with Lipid Bilayers and Biological Membranes. *Biochemistry* **1996**, *35* (96), 12612–12622.
- (65) Langley, T. J.; Jevons, F. R. Characterization of Beef-Liver Glycosidases Possibly Involved in Glycoprotein Degradation. *Arch. Biochem. Biophys.* **1968**, *128* (2), 312–318.
- (66) Yuan, S.; Wang, F.; Chen, G.; Zhang, H.; Feng, L.; Wang, L.; Colman, H.; Keating, M. J.; Li, X.; Xu, R.-H.; Wang, J.; Huang, P. Effective Elimination of Cancer Stem Cells by a Novel Drug Combination Strategy. *Stem Cells* **2013**, *31* (1), 23–34.
- (67) Hu, Y.; Fu, L. Targeting Cancer Stem Cells: A New Therapy to Cure Cancer Patients. *Am. J. Cancer Res.* **2012**, *2* (3), 340–356.
- (68) Fulda, S.; Pervaiz, S. Apoptosis Signaling in Cancer Stem Cells. *Int. J. Biochem. Cell Biol.* **2010**, *42* (1), 31–38.
- (69) Fulda, S. Regulation of Apoptosis Pathways in Cancer Stem Cells. *Cancer Lett.* **2013**, *338* (1), 168–173.

- (70) *Apoptosis: Involvement of Oxidative Stress and Intracellular Ca²⁺ Homeostasis*; Springer Science & Business Media, 2009.
- (71) Dai, Y.; Lawrence, T. S.; Xu, L. Overcoming Cancer Therapy Resistance by Targeting Inhibitors of Apoptosis Proteins and Nuclear Factor-Kappa B. *Am. J. Transl. Res.* **2009**, *1* (1), 1–15.
- (72) Deming, P. B.; Schafer, Z. T.; Tashker, J. S.; Potts, M. B.; Deshmukh, M.; Kornbluth, S. Bcr-Abl-Mediated Protection from Apoptosis Downstream of Mitochondrial Cytochrome c Release. *Mol. Cell. Biol.* **2004**, *24* (23), 10289–10299.
- (73) Ziegler, T.; Lemanski, G. Double Asymmetric Induction During Intramolecular Glycosylation. *European J. Org. Chem.* **1998**, *1998* (1), 163–170.
- (74) Silva, D. J.; Sofia, M. J. Novel Carbohydrate Scaffolds. Assembly of a Uridine–mannose Scaffold Based on Tunicamycin. *Tetrahedron Lett.* **2000**, *41* (6), 855–858.
- (75) Weissmann, B.; Hadjiioannou, S.; Tornheim, J. Oligosaccharase Activity of P-IV-Acetyl-D-Glucosaminidase of Beef Liver *. *J. Biol. Chem.* **1964**, *239* (1), 59–63.
- (76) Findlay, J.; Levvy, G. A.; Marsh, C. A. Inhibition of Glycosidases by Aldonolactones of Corresponding Configuration. 2. Inhibitors of Beta-N-Acetylglucosaminidase. *Biochem. J.* **1958**, *69* (3), 467–476.
- (77) Hanson, M. S.; Stephenson, A. H.; Bowles, E. A.; Sridharan, M.; Adderley, S.; Sprague, R. S. Phosphodiesterase 3 Is Present in Rabbit and Human Erythrocytes and Its Inhibition Potentiates Iloprost-Induced Increases in cAMP. *Am. J. Physiol. Heart Circ. Physiol.* **2008**, *295* (2), H786-93.

- (78) Evans, B. C.; Nelson, C. E.; Yu, S. S.; Beavers, K. R.; Kim, A. J.; Li, H.; Nelson, H. M.; Giorgio, T. D.; Duvall, C. L. Ex Vivo Red Blood Cell Hemolysis Assay for the Evaluation of pH-Responsive Endosomolytic Agents for Cytosolic Delivery of Biomacromolecular Drugs. *J. Vis. Exp.* **2013**, No. 73, e50166.

Chapter 8

Summary and Future Work

8.1. Summary

As discussed in Chapter 1, the development of glycosylated antitumor ether lipids (GAELs) spans the last 30 years. Reviews on synthesis, cytotoxicity evaluation and mechanistic studies of various GAEL analogs that were investigated have been published either as a review article¹ or a book Chapter.² Here I will only summarise my contribution to the development of GAELs as anticancer agents. This contribution will be based on proposed structural modifications presented in Chapter 2 which covers studies on both D-sugar and L-sugar derived GAELs (see Figure 8.1) as well as investigation into their mechanisms of action.

The lead molecule for this investigation is 1-O-hexadecyl-2-O-methyl-3-O-(2'-amino-2'-deoxy- β -D-glucopyranosyl)-*sn*-glycerol **1**, simply described as **GLN**. This compound is the most studied analog of GAELs.¹⁻¹¹ It was the discovery of the potency of this compound compared to edelfosine and its apoptosis-independent mode of cell death that renewed the interest in the current development of GAELs as possible clinical anticancer agents. My foray into structural modifications of GAELs started with investigating the effect of removing the 2-O-methyl-glycero moiety of **GLN**, where the palmitoyl alcohol was directly glycosylated to the glucosamine **2**. This analog was slightly less active than **GLN**, an indication that the glycerol moiety may not be pivotal to cytotoxicity.³ Another modification made to the glycerol moiety was removal of the short ether linkage **3**. The activity was similar to that of **GLN**. This indicated that the glycerol backbone probably contributed to the length of the alkyl chain which in turn

increases lipophilicity and subsequent absorption into the cell and corresponding increased activity.

Another modification made to the glycerol backbone was the replacement of the methoxy group with another glucosamine moiety to see if additional amino sugar will enhance activity **4**. There were two reasons for this modification; first, to investigate the effect of the additional amino moiety from the second sugar and secondly to see the effect of the sugar moiety. Based on literature glucosamine demonstrated cytotoxicity against cancer cell lines^{12,13} and GAELs devoid of amino substituent were less active.^{1,14} The diglycosylated analog **4** was significantly less active than **GLN 1**. This may be attributed to increased hydrophilicity as a result of the additional sugar, thus reducing its absorption into the cells. To evaluate the importance of the stereochemistry at *sn*-2 position of the glycerol moiety, we synthesized the diastereomer mixture **5** of the diglycosylated analog discussed above based on the stereochemistry at the *sn*-2 position of the glycerol moiety. We observed that stereochemistry at that position has no effect on activity.³

Another modification made on the glycerol backbone of **GLN**, is the replacement of the methoxy group with longer hexadecyl lipid tail but via an amide linkage **6**. Our rationale behind this was that two lipid moieties will increase lipophilicity and potentially enhance absorption to increase activity. Our result demonstrated otherwise, the analog was significantly less potent than **GLN**. The cause of this observation may be due to high lipophilicity and the compound was unable to penetrate the cell membrane which requires a balance between lipophilicity and hydrophilicity of a compound.

One more modification made on the glycerol moiety was introduction of carbamoyl moiety into the *sn*-2 position of the glycerol backbone **7**. The reason for this modification was to

achieve selectivity to prostate cancer cell lines. Such a modification on edelfosine enhanced its selectivity against prostate cancer cell lines.¹⁵ Our result showed otherwise. Modifications in compounds **2-7** did not result in improved activity.

Before the discovery of **GLN**, all studied GAELs were significantly less potent than edelfosine.^{1,16} These analogs lacked the amino substituent. So the enhanced activity of **GLN** compared to its glucose analog was attributed to the amino substituent at C-2 position of the sugar.¹⁷ In order to increase the antitumor properties of **GLN**, a second amino substituent was introduced via bioisosteric replacement of the hydroxyl group at the C-6 position of the sugar to give **8**. Interestingly this modification doubled the potency. When we observed that this modification enhanced activity, an analog with α -anomeric configuration **9** was synthesized. The rationale for this was because previous studies on **GLN** and its galactosamine analog indicated that α - anomeric configuration can significantly enhance cytotoxicity relative to β - anomer.^{3,10} The α - anomer of **GLN** analog **9** with two amino substituents on C-2 and C-6 positions of the sugar is one of the most potent GAELs synthesised to date. Another analog of **GLN** containing two amino substituents on C-2 and C-6 position but without the methoxy group **10** was synthesized. It was slightly more active than the derivative with methoxy group **8**. This observation confirms the fact that a methoxy group at *sn*-2 position of the glycerol is not critical for activity. After discovery that the presence of a second amino substituent enhances antitumor activity, we decided to systematically explore the SAR on diamino-based glycolipids.

To determine what effect the positioning of the second amino substituent in the molecule had on activity, an analog of **GLN** **11** was synthesized where the methoxy group was replaced with an amine. The activity of this analog was significantly better than that of **GLN** but not as great as that of analog with the two amines on the sugar, **8**. To further determine the effect of the

position of second amino group on GAELs, another **GLN** analog was synthesized where the glucosamine was moved to the *sn*-2 position of glycerol backbone and the second amine was introduced to the *sn*-3 position of the glycerol moiety **12**. This analog was significantly less potent than **GLN**. This could be attributed to the possible interaction between the two amines which probably acquired cationic charge in physiologic solution, because their pK_a values are greater than >11. The interaction between these charged moieties may affect the active conformation of the molecule. To support this, another analog with a neutral azido moiety at the *sn*-3 position of the glycerol backbone **13** was synthesized; this analog had comparable cytotoxicity as **GLN**. The inferences from these analogs with bisamine are: additional amino moiety enhanced activity and the activity is the best when the two amino moieties are based on the sugar. Also the *sn*-3 position of the glycerol is the favourable position for the glucosamine moiety.

Previous studies demonstrated that modifications made to the amino substituent of glucosamine in GAELs significantly reduced activity.^{1,3,4,8,9,11} Such modifications include acetamido, various benzylamino, azido or guanidyl substituents at C-2 position glucosamine portion of **GLN**. The reduced cytotoxicity as a result these chemical changes suggests that the presence of a primary amino group is critical to cytotoxic effects of GAELs. We investigated whether a lack of a primary amino function at the C-2 position in diamino-based GAELs affects the antitumor properties. Therefore, an analog of **GLN** was synthesized with free amine on position C-6 of the sugar and a phthalimido substituent at the C-2 position **14**. We observed significant reduction in activity. This was unexpected taking into consideration that many compounds bearing phthalimido moiety are cytotoxic agents¹⁸⁻²⁰ and also there is a free amino substituent in this compound. This observation supports the notion that a primary amino group at

the C-2 position is important for activity or bulky substituent at that position may reduce activity. However, until analogs with amino function in different positions and small substituents at C-2 of the sugar are prepared we can not conclude that modification at C-2 of the sugar should be avoided.

Stability, especially to glycosidases, has been a major concern in the development of GAELs. *In vivo* tolerability and efficacy studies of **GLN** in mice yielded no positive result despite impressive *in vitro* effect. This lack of stability was thought to be due to glycosidase-assisted cleavage. Various efforts to improve stability of GAELs to glycosidases including synthesis of glycosidases-resistant thio and amido linkages led to loss of activity. To address this challenge, an analog where the glycerol moiety of the lipid was substituted with triazole via a N-glycosidic linkage **15** was synthesized but it was not as active as **GLN**. At this juncture we hypothesised that the *O*-glycosidic linkages maybe very important to activity of GAELs.

To retain the crucial *O*-glycosidic linkage, we initially employed L-glucosamine, an enantiomer of D-glucosamine in **GLN**. Our rationale for this strategy was because humans and other mammals lack metabolic enzyme including L-glycosidases that can degrade L-glucosamine based GAEL. Our hypothesis was validated because L-glucosamine analog of **GLN 16** demonstrated comparable activity. Further structural optimization of this compound which include introduction of amino substituent to position C-6, **17** and benzyl ether at C-4 of the sugar **18, 19** significantly enhanced activity. Further studies using other L-sugars including L-rhamnose **20 – 22**, L- glucose **23**, L- mannose **24** and showed that the configuration of the sugar and presence of amino group have immense effect on cytotoxicity. For instance, a **GLN** analog where the D-glucosamine was replaced with a L- rhamnose **20** was significantly less potent. But when an amino substituent was introduced into *sn*-3 and the rhamnose at *sn*-2 position of the

glycerolipid **21**, there was significant activity. Conversion of amine in **21** to amide **22** significantly reduced activity. When the L-rhamnose in the very active **21** was replaced with L-glucose **23** or L-mannose **24** there was significant loss of activity.

Overall, compounds **9,10,18,19** and **21** are candidates for advanced preclinical and clinical studies because of their impressive cytotoxicity against cancer cells and CSCs from variety of human cancers. Preliminary investigation into the mechanism of action showed that these compounds induced cell death via apoptosis independent mechanism which is devoid of membrane disruption or lysis. Further mode of action investigation revealed that these compounds promote extreme vacuolization of cells via perturbation of an endocytic pathway likely macropinocytosis. This type of vacuolization is usually characteristic of methuosis, a type of an apoptosis-independent mechanism of cell death.

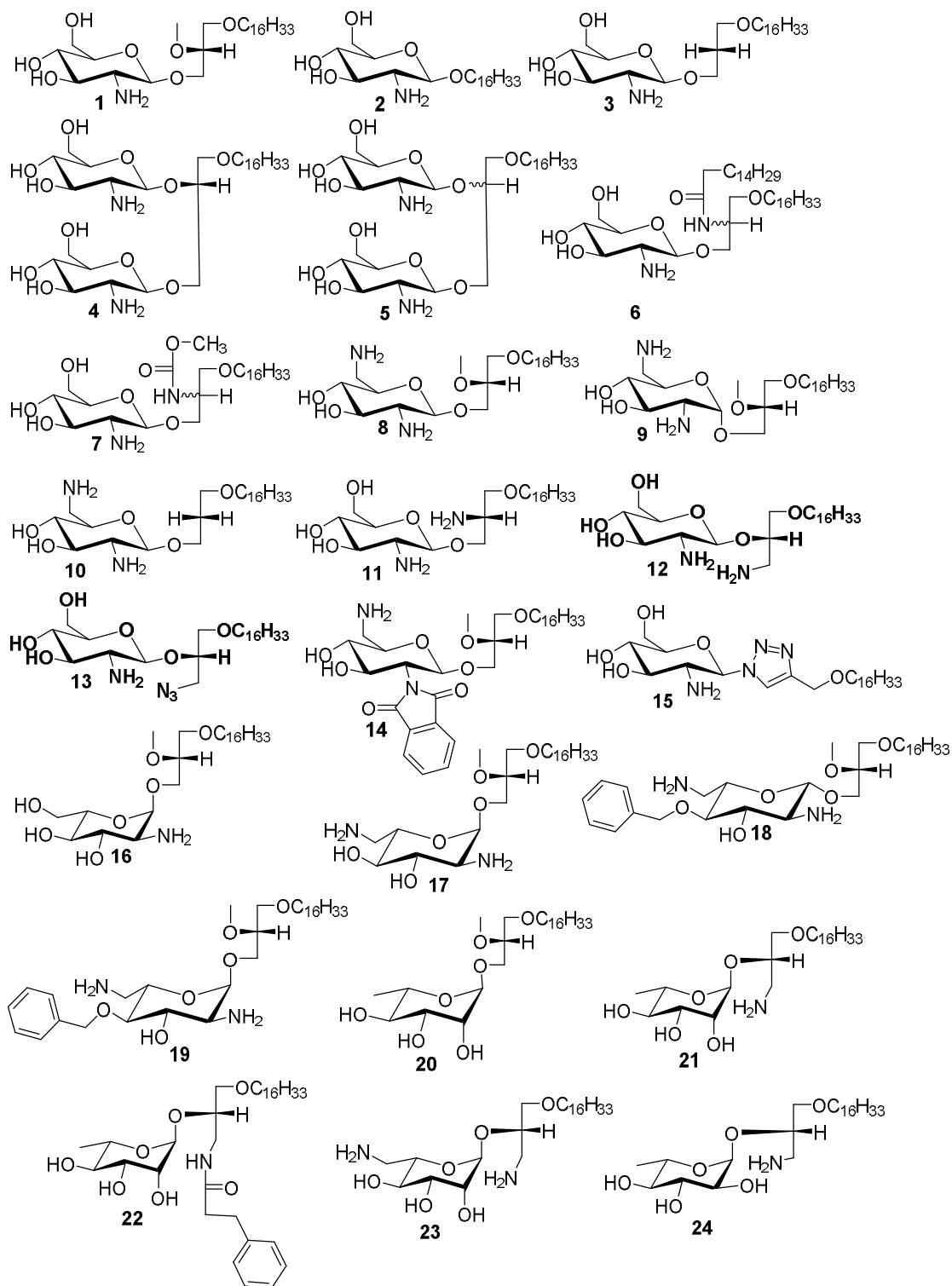


Figure 8.1. List of some important GAELs synthesised and evaluated for anticancer activity in this thesis

8.2. Future work

As mentioned in Chapter 1, the systematic development of GAELs, especially structural activity relationship studies, gained momentum in the recent time. With this work, insights were provided into various structural features that can affect activity but lot needs to be done. The discovery of L-sugar derived GAELs which are glycosidase resistant have opened a new dimension in the discovery of metabolically stable GAELs. The L-glucosamine based GAELs have been optimised to a significant extent, there are still opportunities for further optimization. These include variation in substituent at C-4 of the sugar, evaluation of importance of C-3 hydroxyl group and introducing various substituents into this group to evaluate their effect on cytotoxicity.

Studies on α -D galactosamine analog of **GLN** demonstrated that it was significantly more potent,¹⁰ but further optimization of this promising compound has not been explored either in the D-sugar or L-sugar series. Therefore, in the future, it will be a great idea to explore structural modifications that enhanced activity in both D- and L- glucosamine series on D- or L- galactosamine based GAELs.

Additionally, using other rare D-sugars like allose, altriose and their amino derivatives similar to sugar moiety in GAELs may also enhance stability. Glycosidases that hydrolyse glycosides of these sugars have not been identified in human and animal, therefore their GAELs analogs maybe very stable in *in vivo* studies. Allose in particular has been reported for its anticancer activity in cell based studies.²¹⁻²³ Therefore its logical to incorporate this molecule or its amino analog into GAEL and this may lead to synthesis of potentially useful compounds

Investigation into mode of cell death of GAELs, especially new analogs discovered in this study, is still in its infancy, therefore extensive and rigorous mechanistic studies are required to elucidate the death pathway explored by these compounds to kill cancer cells and cancer stem cells. One important mode of action to investigate is methuosis. The formation of large vacuoles by many active GAELs pointed significantly that the likely mechanism of action of GAELs is methuosis,^{2,3,9,24,25} but this has not been confirmed. This information maybe a useful tool in the discovery of new compounds that maybe targeting same pathway and also optimization of structures of available GAELs. Moreover, synthesis of GAEL analogs that may be useful in further elaboration of pharmacokinetic and pharmacodynamics properties especially in *in vivo* studies is another direction to go.

Currently, we have limited information on anticancer activity of GAELs in animal studies. There is a need for optimization of synthetic procedures involved in making the potent analogs in Figure 8.1 in order to make substantial amount for extensive animal studies. Its this type of study that can really validate the usefulness of GAELs as potential anticancer drugs.

8.3. References

- (1) Arthur, G.; Bittman, R. Glycosylated Antitumor Ether Lipids: Activity and Mechanism of Action. *Anticancer. Agents Med. Chem.* **2014**, *14* (4), 592–606.
- (2) Arthur, G.; Schweizer, F.; Ogunsina, M. Carbohydrates in Drug Design and Discovery; Jimenez-Barbero, J., Canada, F. J., Martin-Santamaria, S., Eds.; RSC Drug Discovery; Royal Society of Chemistry: Cambridge, 2015.
- (3) Xu, Y.; Ogunsina, M.; Samadder, P.; Arthur, G.; Schweizer, F. Structure-Activity Relationships of Glucosamine-Derived Glycerolipids: The Role of the Anomeric Linkage, the Cationic Charge and the Glycerol Moiety on the Antitumor Activity. *ChemMedChem* **2013**, *8* (3), 511–520.
- (4) Jahreiss, L.; Renna, M.; Bittman, R.; Arthur, G.; Rubinsztein, D. C. 1-O-Hexadecyl-2-O-Methyl-3-O-(2'-acetamido-2'-deoxy-Beta-D-Glucopyranosyl)-Sn-Glycerol (Gln) Induces Cell Death with More Autophagosomes Which Is Autophagy-Independent. *Autophagy* **2009**, *5* (6), 835–846.
- (5) Arthur, Gilbert; Samadder, P. *Tolerability of Rag2M Mice to 1-O-Hexadecyl-2-O-Methyl-3-O-(2'-amino-2'-deoxy-β-D-Glucopyranosyl)-Sn-Glycerol (Unpublished)*; Winnipeg, 2012.
- (6) Yang, G.; Franck, R. W.; Bittman, R.; Samadder, P.; Arthur, G. Synthesis and Growth Inhibitory Properties of Glucosamine-Derived Glycerolipids. *Org. Lett.* **2001**, *3* (2), 197–200.
- (7) Samadder, P.; Bittman, R.; Byun, H.-S.; Arthur, G. A Glycosylated Antitumor Ether Lipid

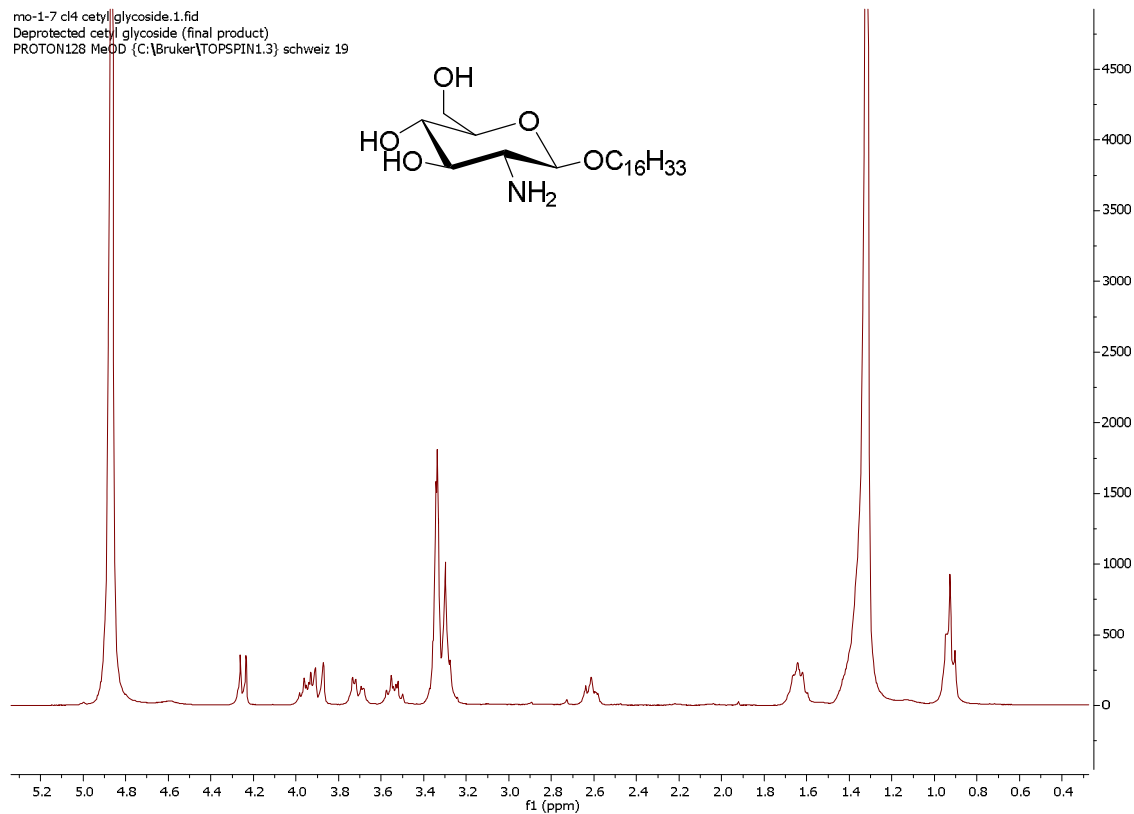
- Kills Cells via Paraptosis-like Cell Death. *Biochem. Cell Biol.* **2009**, *87* (2), 401–414.
- (8) Jahreiss, L.; Renna, M.; Bittman, R.; Arthur, G.; Rubinsztein, D. C. 1- O -Hexadecyl-2- O -Methyl-3- O -(2'-acetamido-2'-deoxy- β -D-Glucopyranosyl)- Sn -Glycerol (Gln) Induces Cell Death with More Autophagosomes Which Is Autophagy-Independent. *Autophagy* **2009**, *5* (6), 835–846.
- (9) Samadder, P.; Byun, H.-S.; Bittman, R.; Arthur, G. An Active Endocytosis Pathway Is Required for the Cytotoxic Effects of Glycosylated Antitumor Ether Lipids. *Anticancer Res* **2011**, *31* (11), 3809–3818.
- (10) Samadder, P.; Xu, Y.; Schweizer, F.; Arthur, G. Cytotoxic Properties of D-Gluco-, D-Galacto- and D-Manno-Configured 2-Amino-2-Deoxy-Glycerolipids against Epithelial Cancer Cell Lines and BT-474 Breast Cancer Stem Cells. *Eur. J. Med. Chem.* **2014**, *78* (78), 225–235.
- (11) Samadder, P.; Byun, H.-S.; Bittman, R.; Arthur, G. An Active Endocytosis Pathway Is Required for the Cytotoxic Effects of Glycosylated Antitumor Ether Lipids.
- (12) Fjelde, A.; Sorkin, E.; Rhodes, J. M. The Effect of Glucosamine on Human Epidermoid Carcinoma Cells in Tissue Culture. *Exp. Cell Res.* **1956**, *10* (1), 88–98.
- (13) Jung, C.-W.; Jo, J.-R.; Lee, S.-H.; Park, Y.-K.; Jung, N.-K.; Song, D.-K.; Bae, J.; Nam, K.-Y.; Ha, J.-S.; Park, I.-S.; Park, G.-Y.; Jang, B.-C.; Park, J.-W. Anti-Cancer Properties of Glucosamine-Hydrochloride in YD-8 Human Oral Cancer Cells: Induction of the Caspase-Dependent Apoptosis and down-Regulation of HIF-1 α . *Toxicol. In Vitro* **2012**, *26* (1), 42–50.

- (14) Erukulla, R. K.; Zhou, X.; Samadder, P.; Arthur, G.; Bittman, R. Synthesis and Evaluation of the Antiproliferative Effects of 1-O-Hexadecyl-2-O-Methyl-3-O-(2'-acetamido-2'-deoxy-Beta-D- Glucopyranosyl)-Sn-Glycerol and 1-O-Hexadecyl-2-O-Methyl-3-O- (2'-amino-2'-deoxy-Beta-D-Glucopyranosyl)-Sn-Glycerol on Epithelial Canc. *J. Med. Chem.* **1996**, *39* (7), 1545–1548.
- (15) Byun, H.-S.; Bittman, R.; Samadder, P.; Arthur, G. Synthesis and Antitumor Activity of Ether Glycerophospholipids Bearing a Carbamate Moiety at the Sn-2 Position: Selective Sensitivity against Prostate Cancer Cell Lines. *ChemMedChem* **2010**, *5* (7), 1045–1052.
- (16) Samadder, P.; Byun, H. S.; Bittman, R.; Arthur, G. Glycosylated Antitumor Ether Lipids Are More Effective against Oncogene-Transformed Fibroblasts than Alkyllysophospholipids. *Anticancer Res.* *18* (1A), 465–470.
- (17) Erukulla, R. K.; Zhou, X.; Samadder, P.; Arthur, G.; Bittman, R. Synthesis and Evaluation of the Antiproliferative Effects of 1-O-Hexadecyl-2-O-Methyl-3-O-(2'-acetamido-2'-deoxy-Beta-D- Glucopyranosyl)-Sn-Glycerol and 1-O-Hexadecyl-2-O-Methyl-3-O- (2'-amino-2'-deoxy-Beta-D-Glucopyranosyl)-Sn-Glycerol on Epithelial Canc. *J. Med. Chem.* **1996**, *39* (7), 1545–1548.
- (18) Yang, Y. J.; Yang, Y. N.; Jiang, J. S.; Feng, Z. M.; Liu, H. Y.; Pan, X. D.; Zhang, P. C. Synthesis and Cytotoxic Activity of Heterocycle-Substituted Phthalimide Derivatives. *Chinese Chem. Lett.* **2010**, *21* (8), 902–904.
- (19) Aliabadi, A.; Mohammadi-Farani, A.; Hosseinzadeh, Z.; Nadri, H.; Moradi, A.; Ahmadi, F. Phthalimide Analogs as Probable 15-Lipoxygenase-1 Inhibitors: Synthesis, Biological Evaluation and Docking Studies. *DARU J. Pharm. Sci.* **2015**, *23* (1), 36.

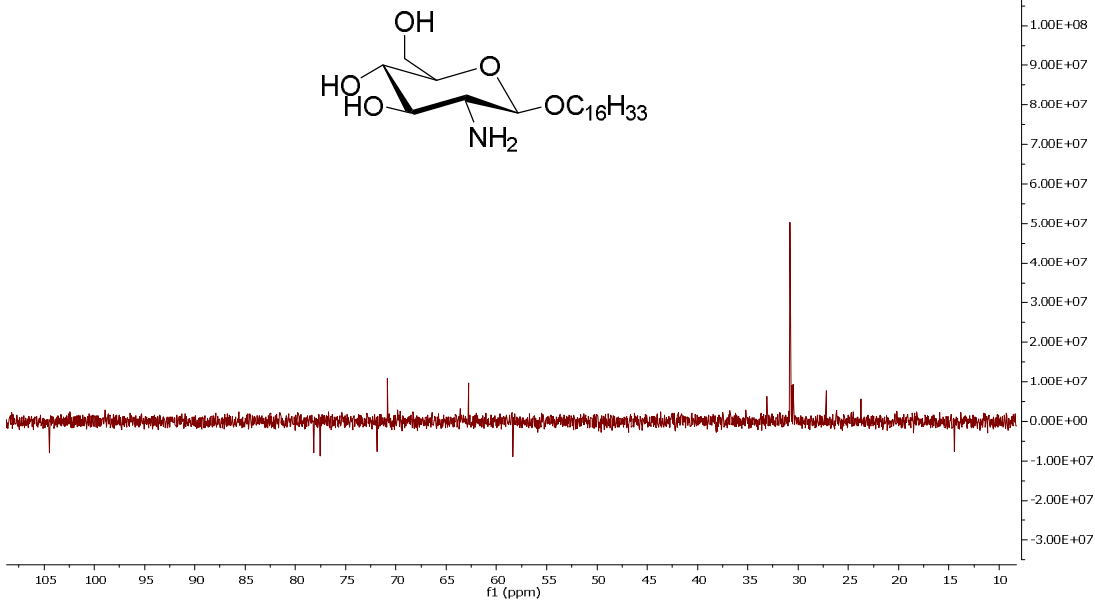
- (20) Ferreira, P. M. P.; Costa, P. M. Da; Costa, A. D. M.; Lima, D. J. B.; Drumond, R. R.; Silva, J. D. N.; Moreira, D. R. D. M.; Oliveira Filho, G. B. De; Ferreira, J. M.; Queiroz, M. G. R. De; Leite, A. C. L.; Pessoa, C. Cytotoxic and Toxicological Effects of Phthalimide Derivatives on Tumor and Normal Murine Cells. *An. Acad. Bras. Cienc.* **2015**, *87* (1), 313–330.
- (21) Sui, L.; Dong, Y.; Watanabe, Y.; Yamaguchi, F.; Hatano, N.; Izumori, K.; Tokuda, M. Growth Inhibitory Effect of D-Allose on Human Ovarian Carcinoma Cells in Vitro. *Anticancer Res.* *25* (4), 2639–2644.
- (22) Malm, S. W.; Hanke, N. T.; Gill, A.; Carbajal, L.; Baker, A. F. The Anti-Tumor Efficacy of 2-Deoxyglucose and D-Allose Are Enhanced with p38 Inhibition in Pancreatic and Ovarian Cell Lines. *J. Exp. Clin. Cancer Res.* **2015**, *34*, 31.
- (23) Yamaguchi, F.; Takata, M.; Kamitori, K.; Nonaka, M.; Dong, Y.; Sui, L.; Tokuda, M. Rare Sugar D-Allose Induces Specific up-Regulation of TXNIP and Subsequent G1 Cell Cycle Arrest in Hepatocellular Carcinoma Cells by Stabilization of p27kip1. *Int. J. Oncol.* **2008**, *32* (2), 377–385.
- (24) Maltese, W. A.; Overmeyer, J. H. Non-Apoptotic Cell Death Associated with Perturbations of Macropinocytosis. *Front. Physiol.* **2015**, *6* (FEB), 1–10.
- (25) Maltese, W. A.; Overmeyer, J. H. Methuosis: Nonapoptotic Cell Death Associated with Vacuolization of Macropinosome and Endosome Compartments. *Am. J. Pathol.* **2014**, *184* (6), 1630–1642.

Appendix

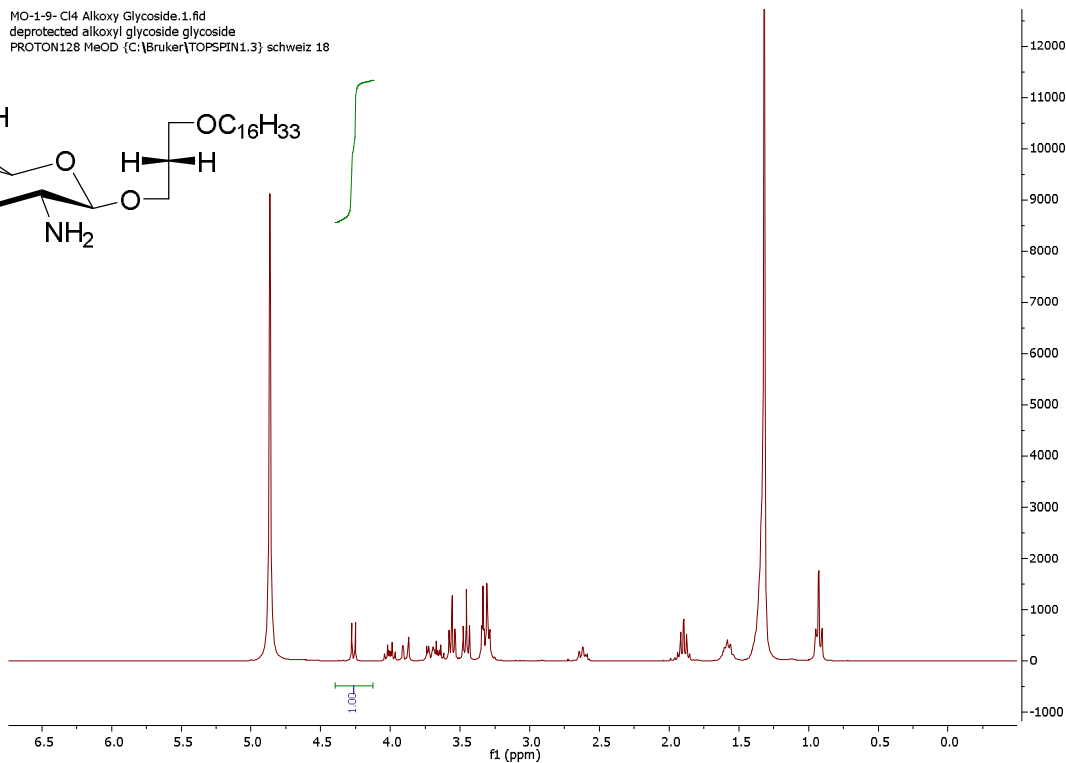
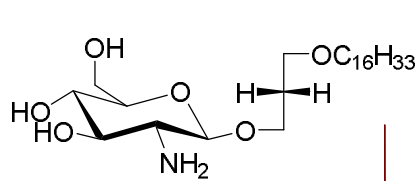
NMR Spectra of Some Important Compounds Presented in this thesis



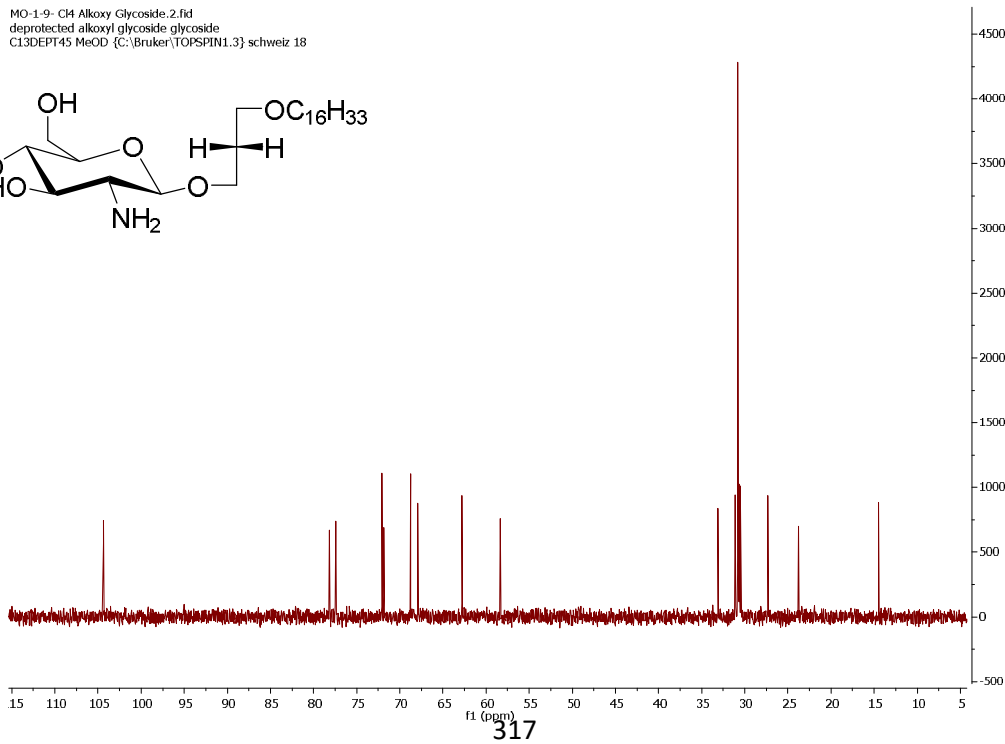
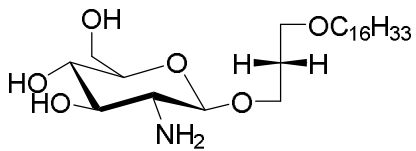
mo-1-7 c14 cetyl glycoside.2.1.1r
Deprotected cetyl glycoside (final product)
C13DEPT135 MeOD {C:\Bruker\TOPSPIN1.3} schweiz 19



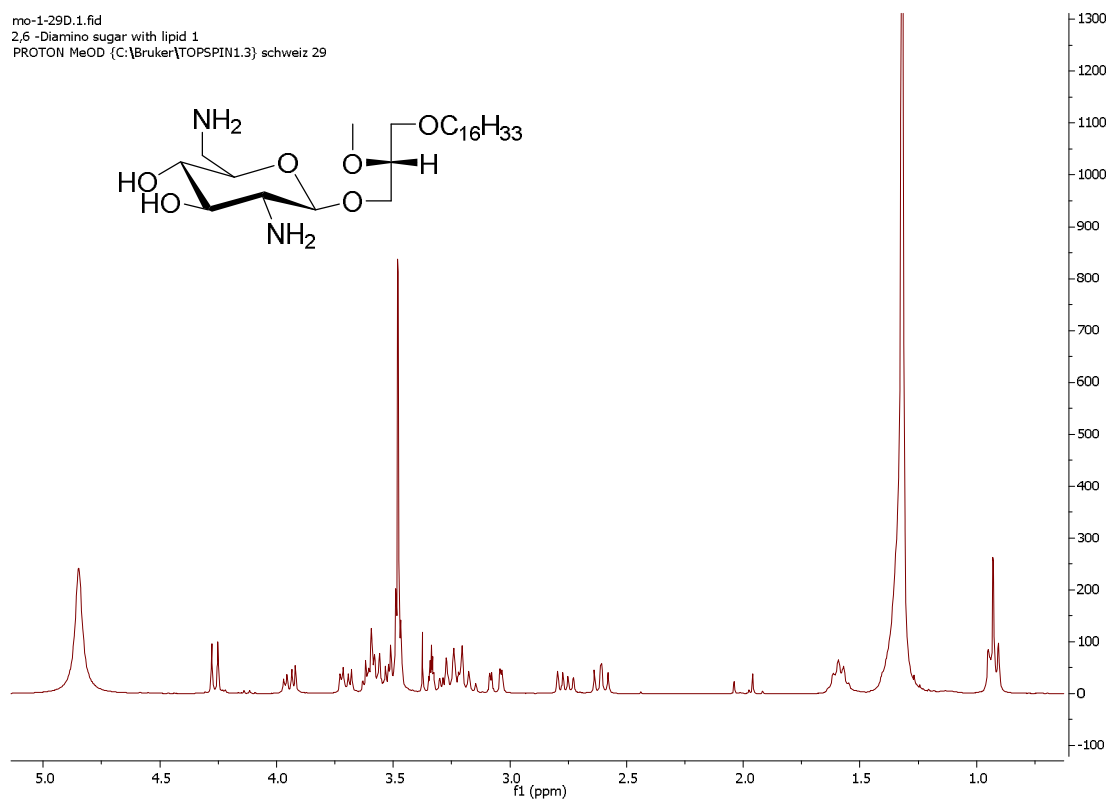
MO-1-9- C14 Alkoxy Glycoside.1.fid
deprotected alkoxy glycoside glycoside
PROTON128 MeOD (C:\Bruker\TOPSPIN1.3) schweiz 18



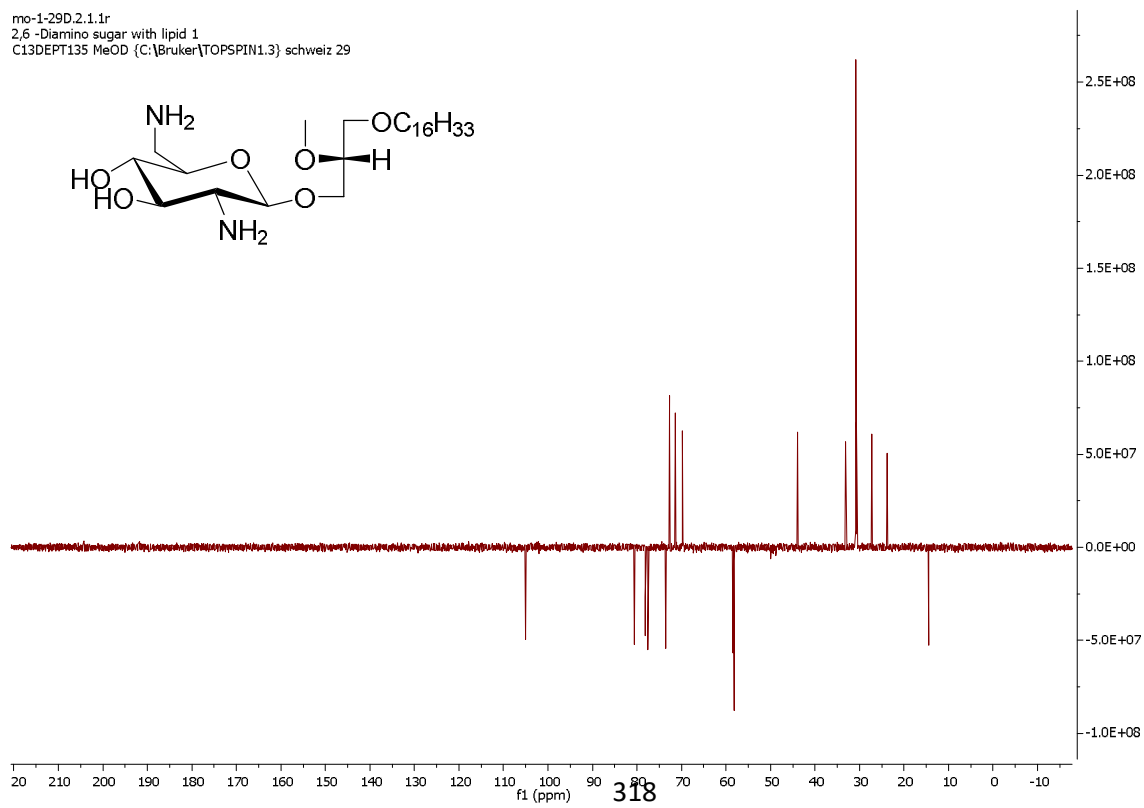
MO-1-9- C14 Alkoxy Glycoside.2.fid
deprotected alkoxy glycoside glycoside
C13DEPT45 MeOD (C:\Bruker\TOPSPIN1.3) schweiz 18



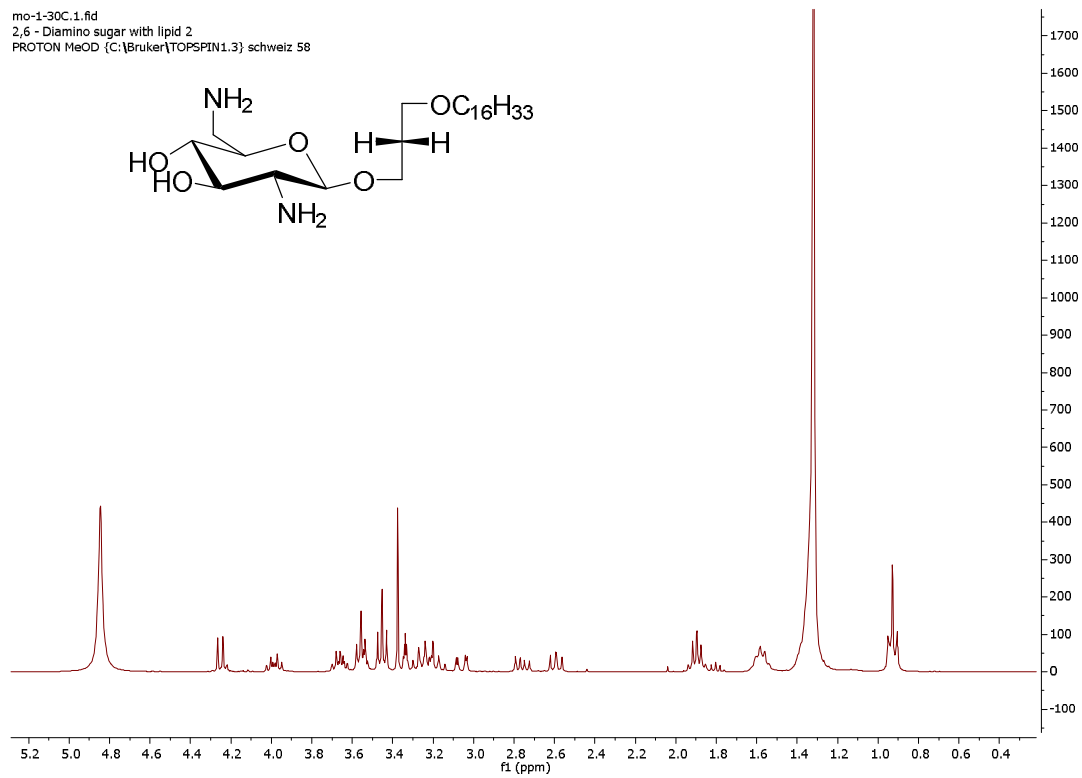
mo-1-29D.1.fid
2,6 -Diamino sugar with lipid 1
PROTON MeOD (C:\Bruker\TOPSPIN1.3) schweiz 29



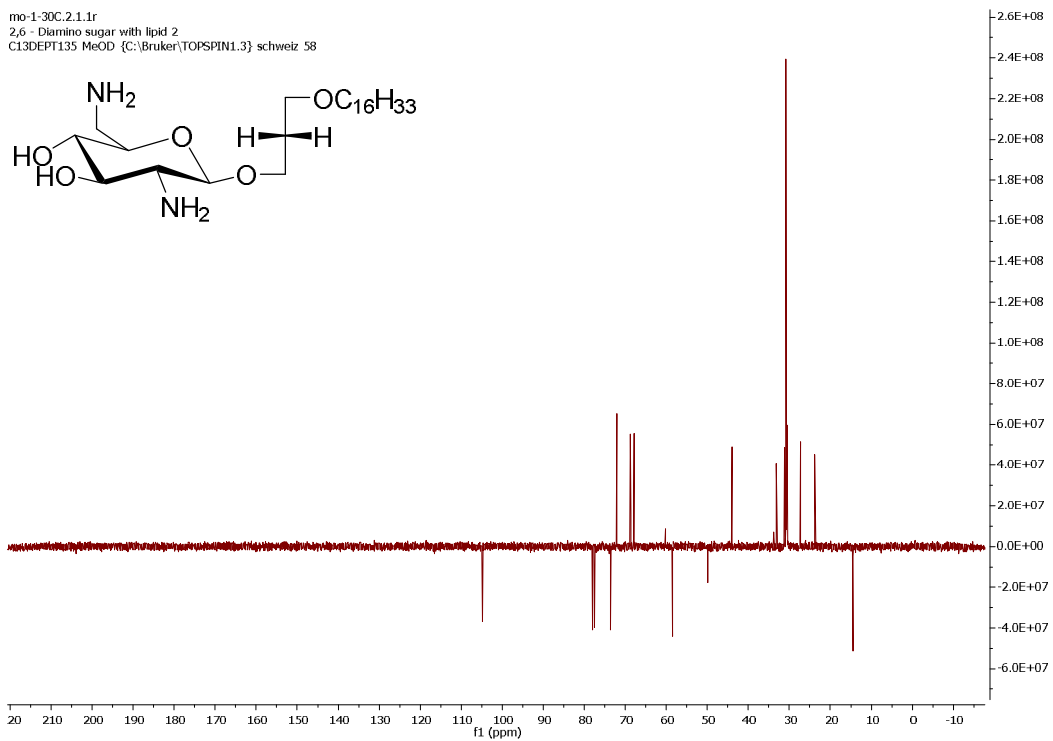
mo-1-29D.2.1.1r
2,6 -Diamino sugar with lipid 1
C13DEPT135 MeOD (C:\Bruker\TOPSPIN1.3) schweiz 29



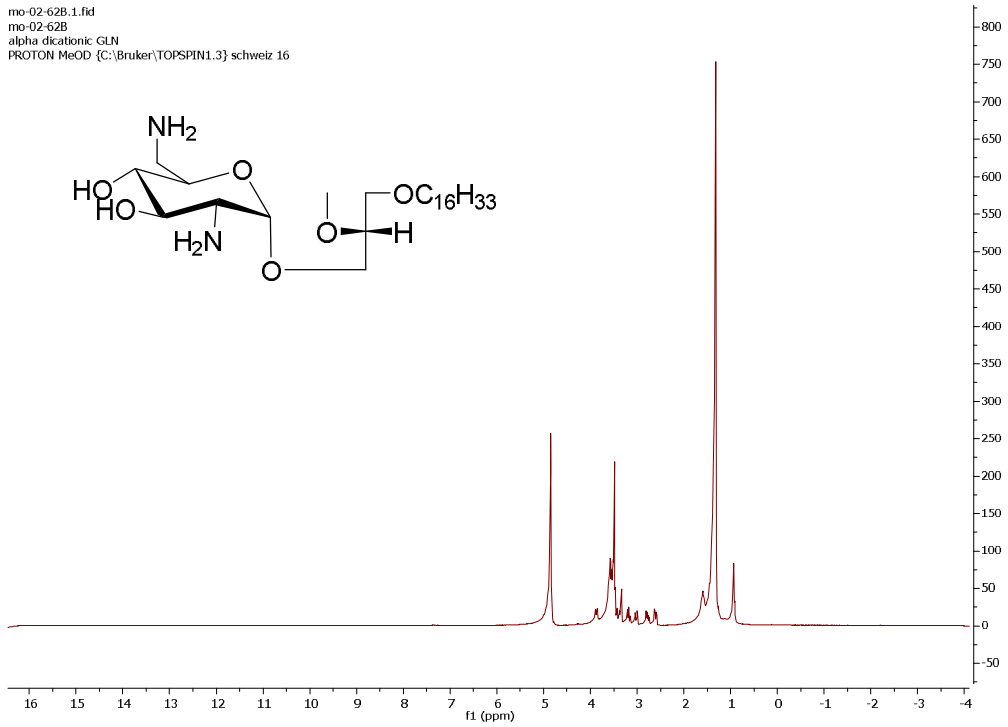
mo-1-30C.1.fid
2,6 - Diamino sugar with lipid 2
PROTON MeOD {C:\Bruker\TOPSPIN1.3} schweiz 58



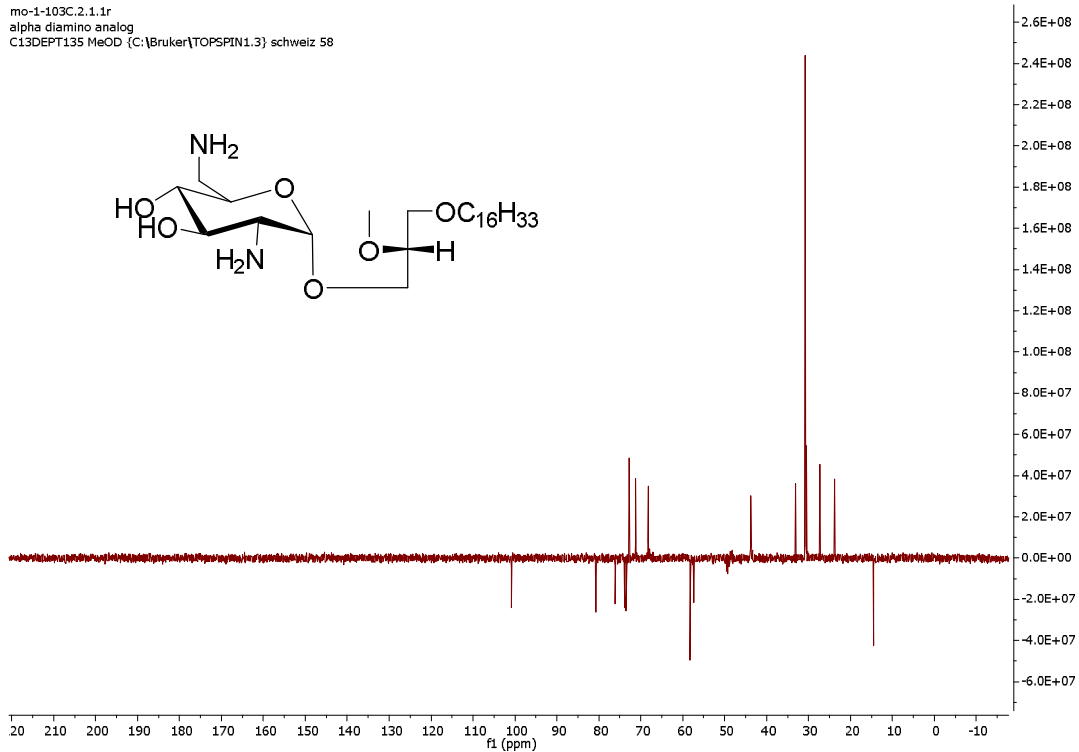
mo-1-30C.2.1.1r
2,6 - Diamino sugar with lipid 2
C13DEPT135 MeOD {C:\Bruker\TOPSPIN1.3} schweiz 58



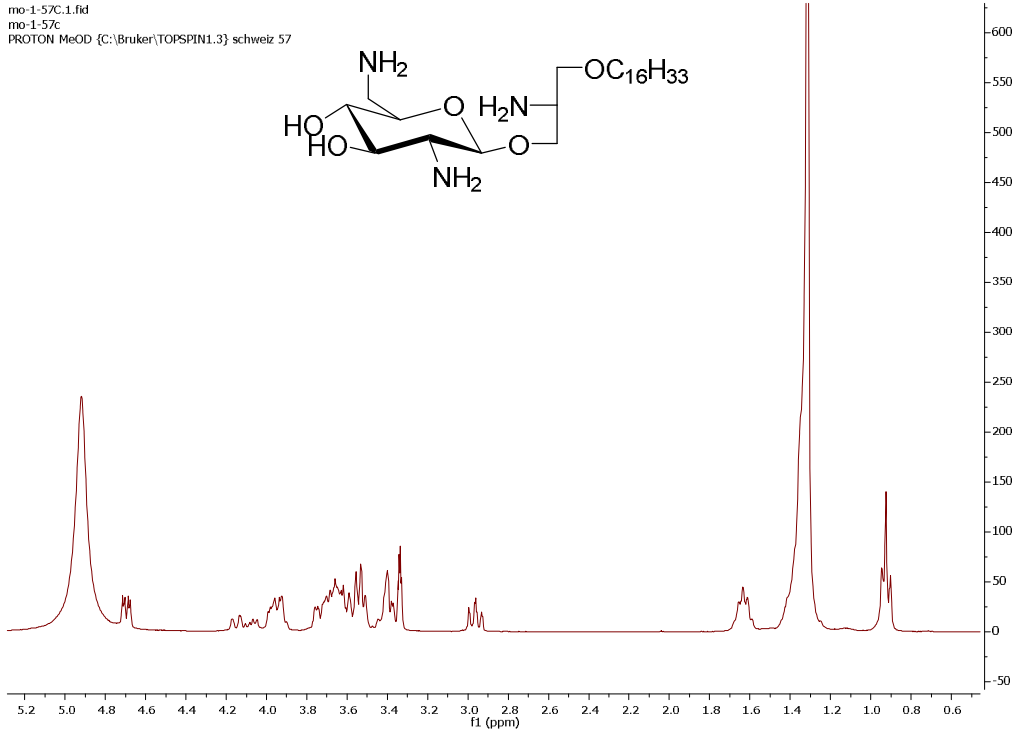
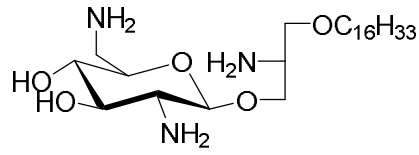
mo-02-62B.1.fid
mo-02-62B
alpha dicationic GLN
PROTON MeOD {C:\Bruker\TOPSPIN1.3} schweiz 16



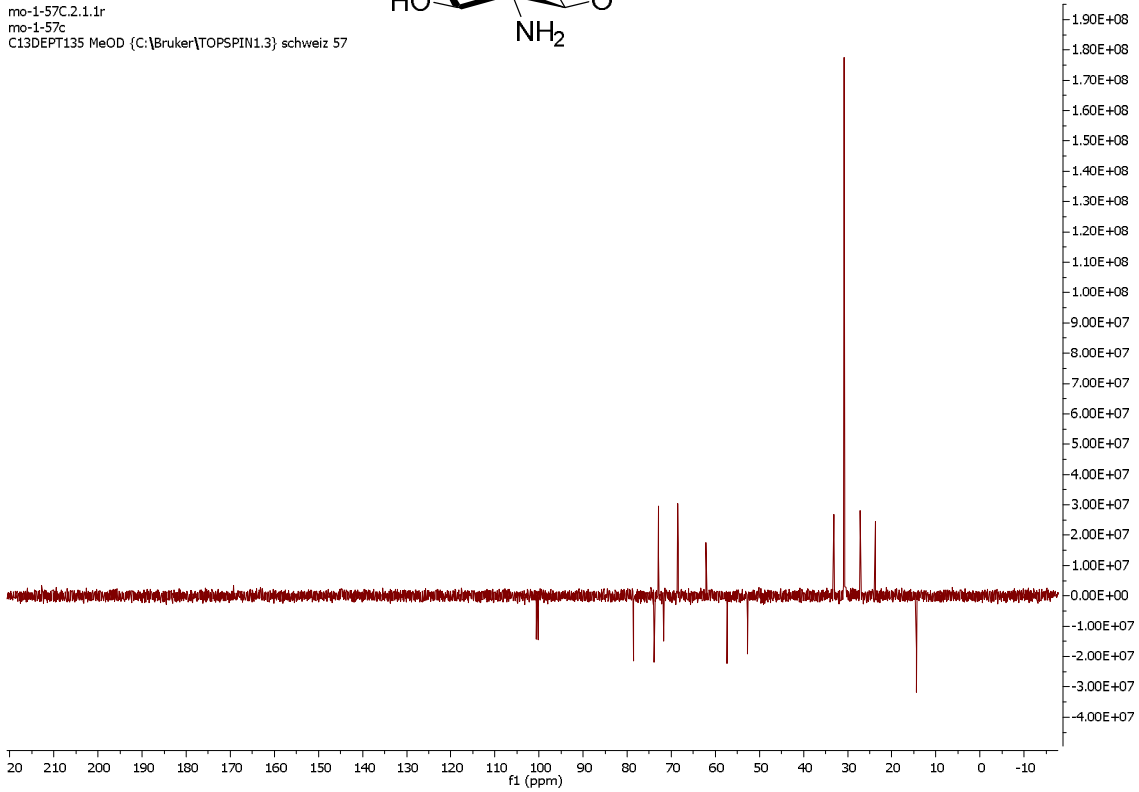
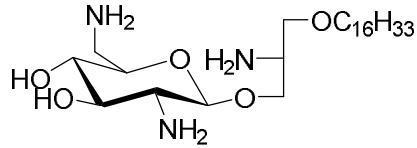
mo-1-103C.2.1.1r
alpha diamino analog
C13DEPT135 MeOD {C:\Bruker\TOPSPIN1.3} schweiz 58



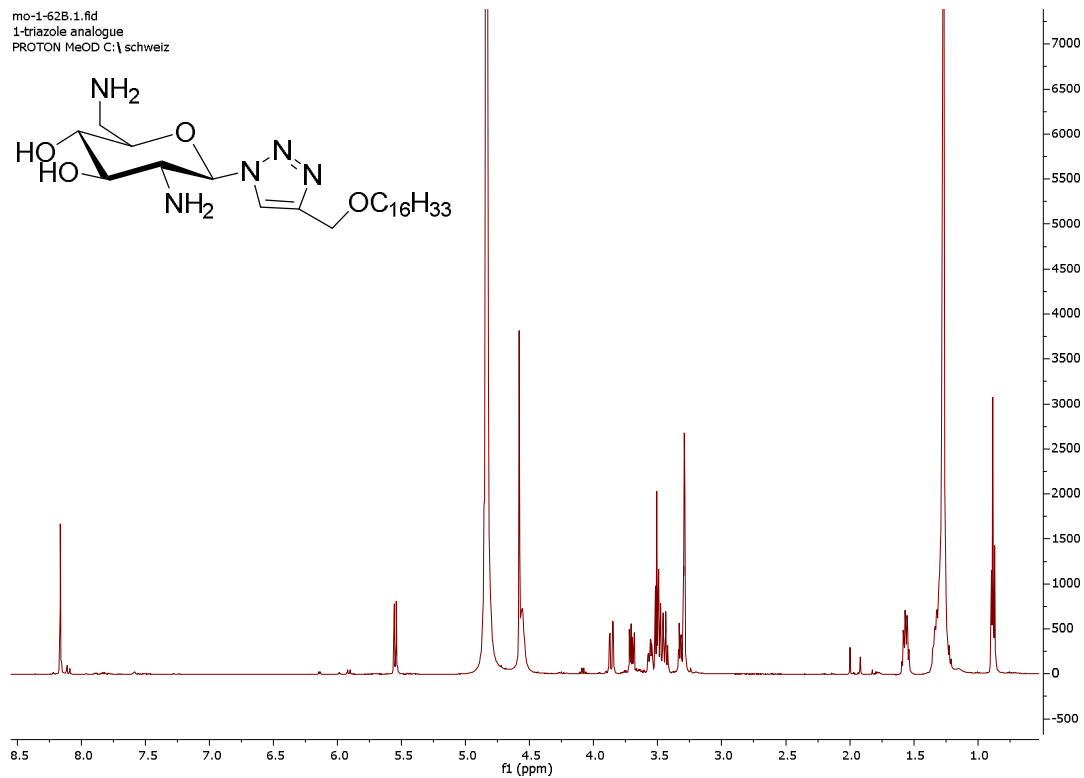
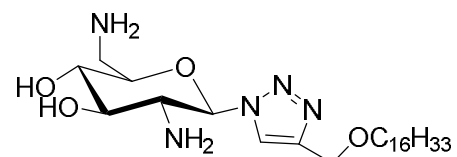
mo-1-57C.1.fid
mo-1-57c
PROTON MeOD (C:\Bruker\TOPSPIN1.3) schweiz 57



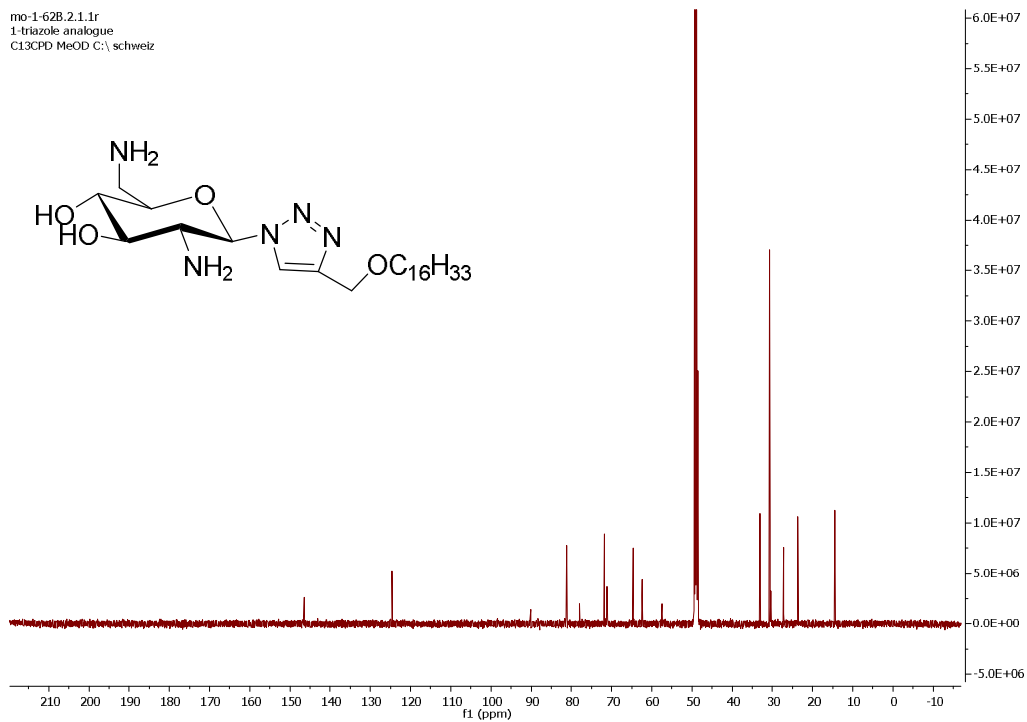
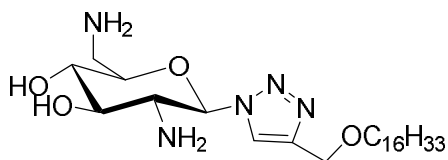
mo-1-57C.2.1.1r
mo-1-57c
C13DEPT135 MeOD (C:\Bruker\TOPSPIN1.3) schweiz 57



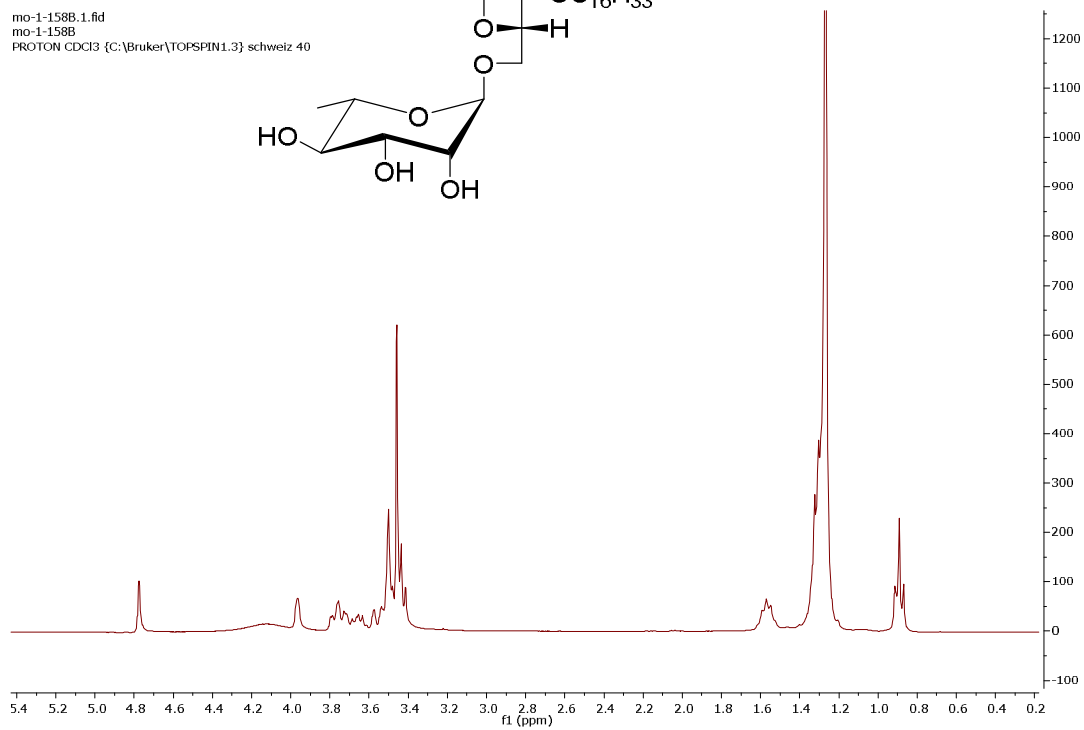
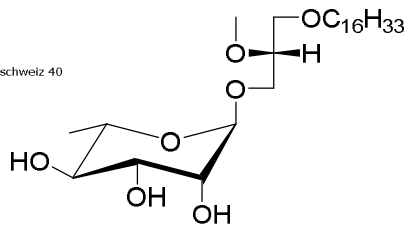
mo-1-62B.1.fid
1-triazole analogue
PROTON MeOD C:\schweiz



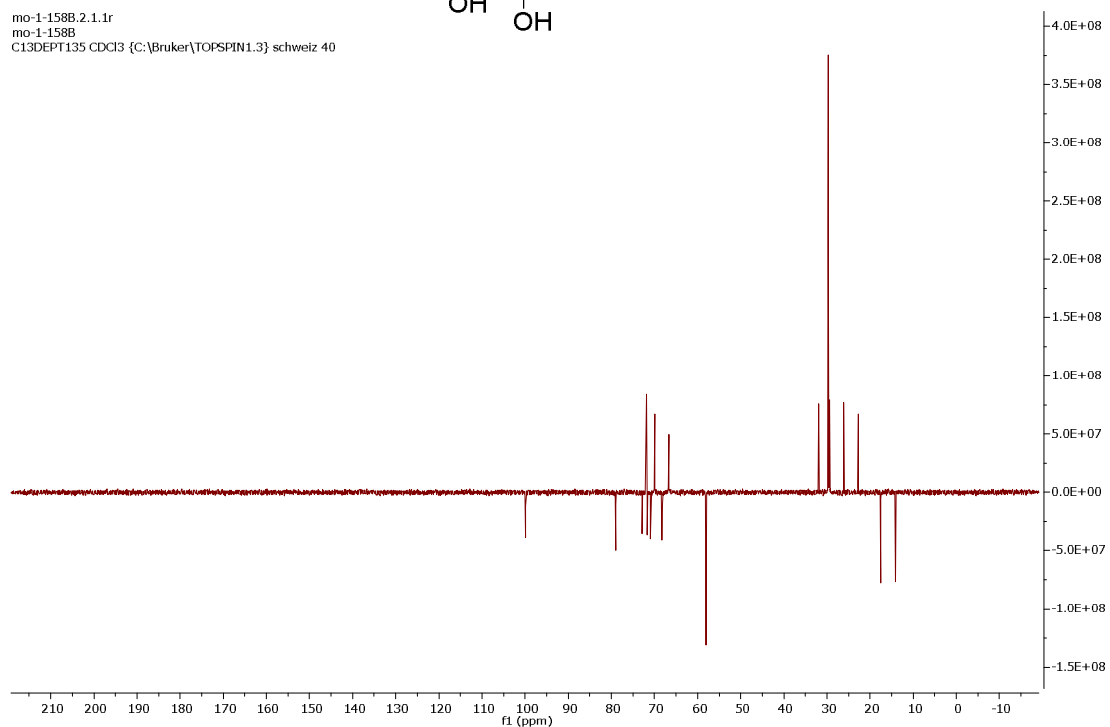
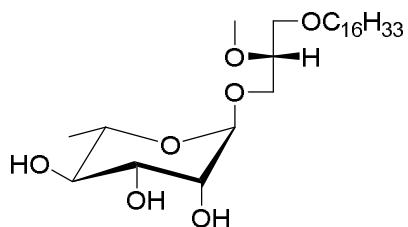
mo-1-62B.2.1.1r
1-triazole analogue
Cl3CPD MeOD C:\schweiz



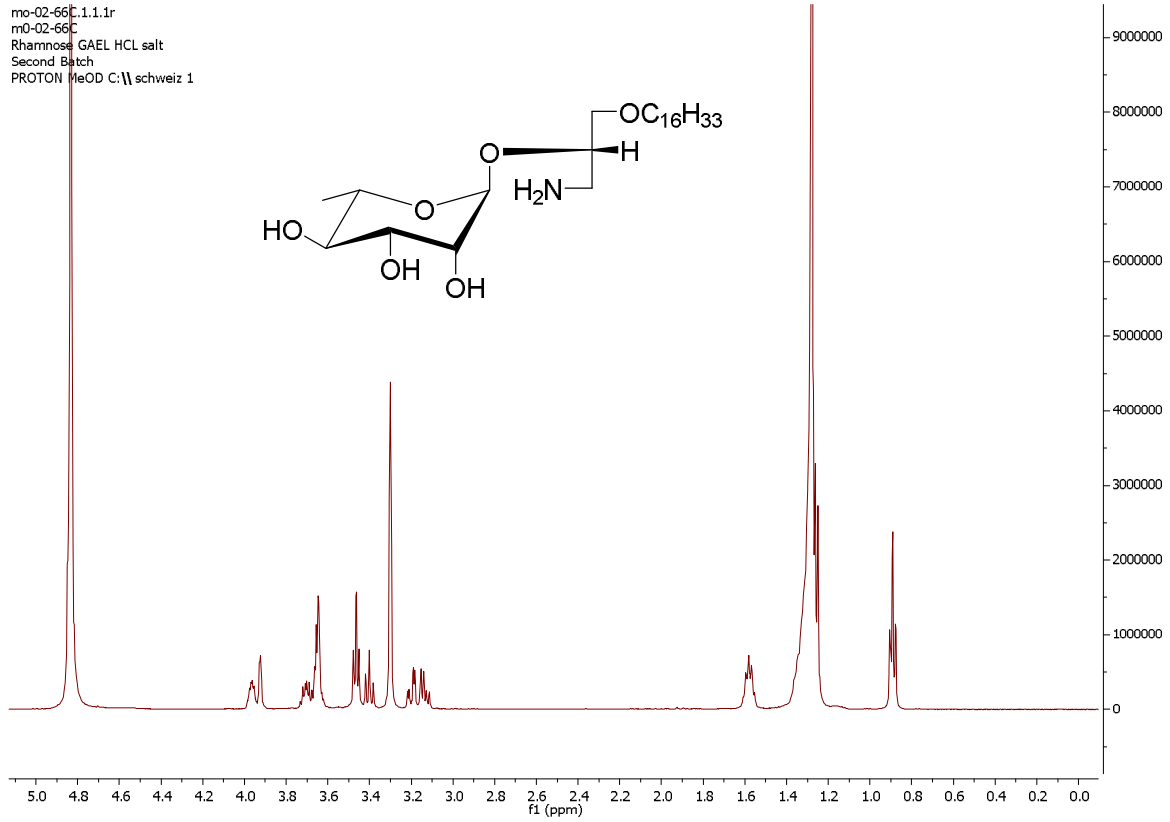
mo-1-158B.1.fid
mo-1-158B
PROTON CDCl3 {C:\Bruker\TOPSPIN1.3} schweiz 40



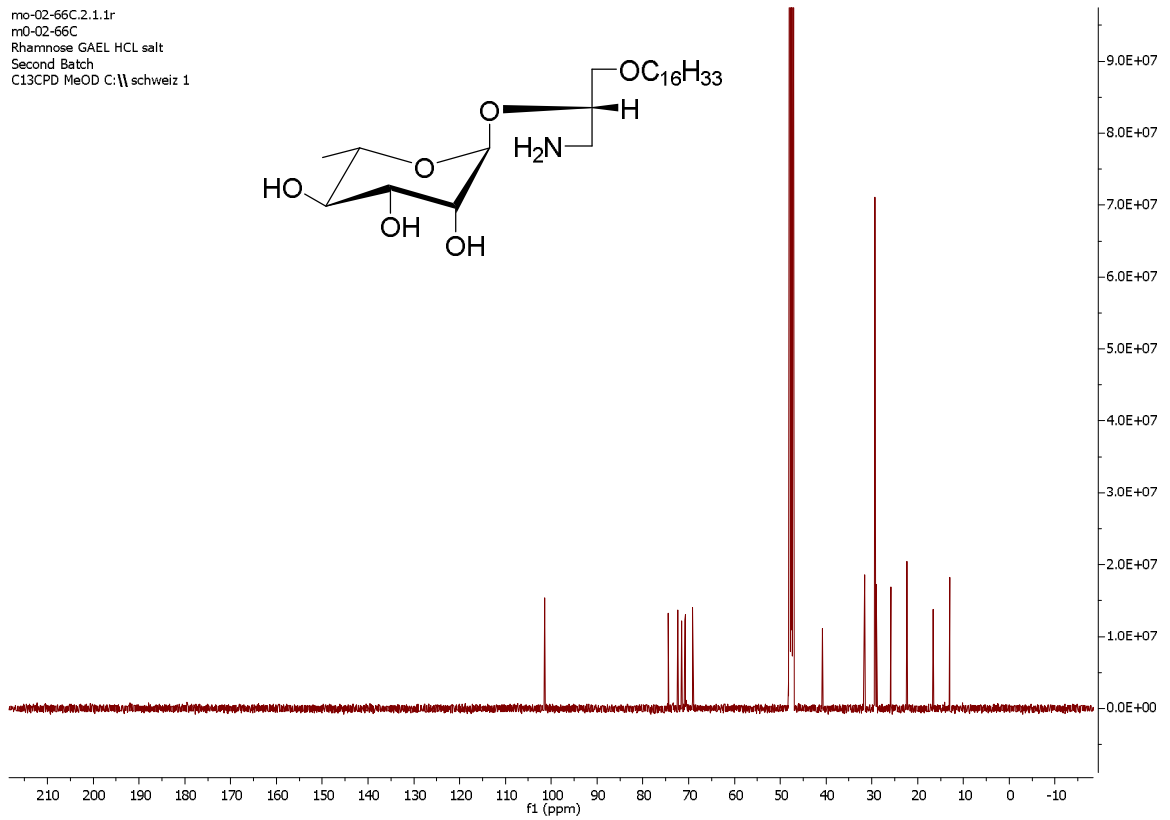
mo-1-158B.2.1.1r
mo-1-158B
C13DEPT135 CDCl3 {C:\Bruker\TOPSPIN1.3} schweiz 40



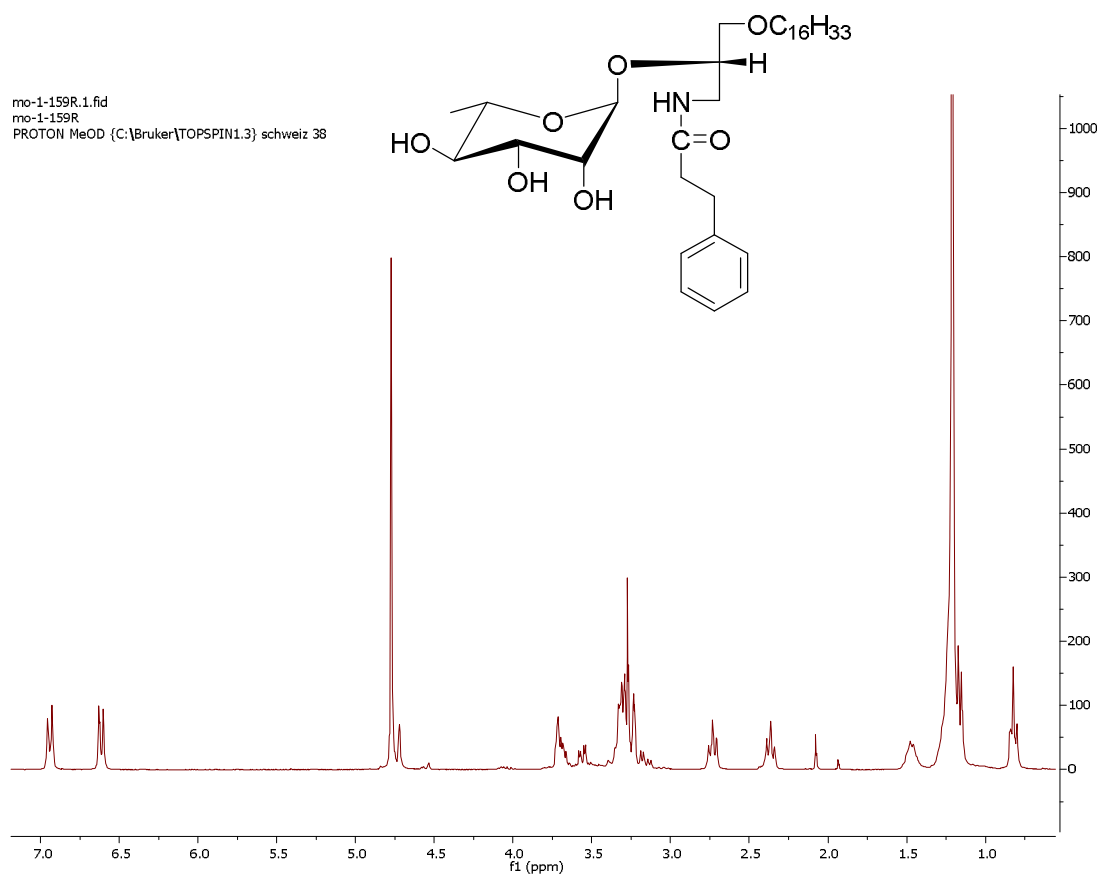
mo-02-66C.1.1.1r
m0-02-66C
Rhamnose GAEL HCL salt
Second Batch
PROTON MeOD C:\\schweiz 1



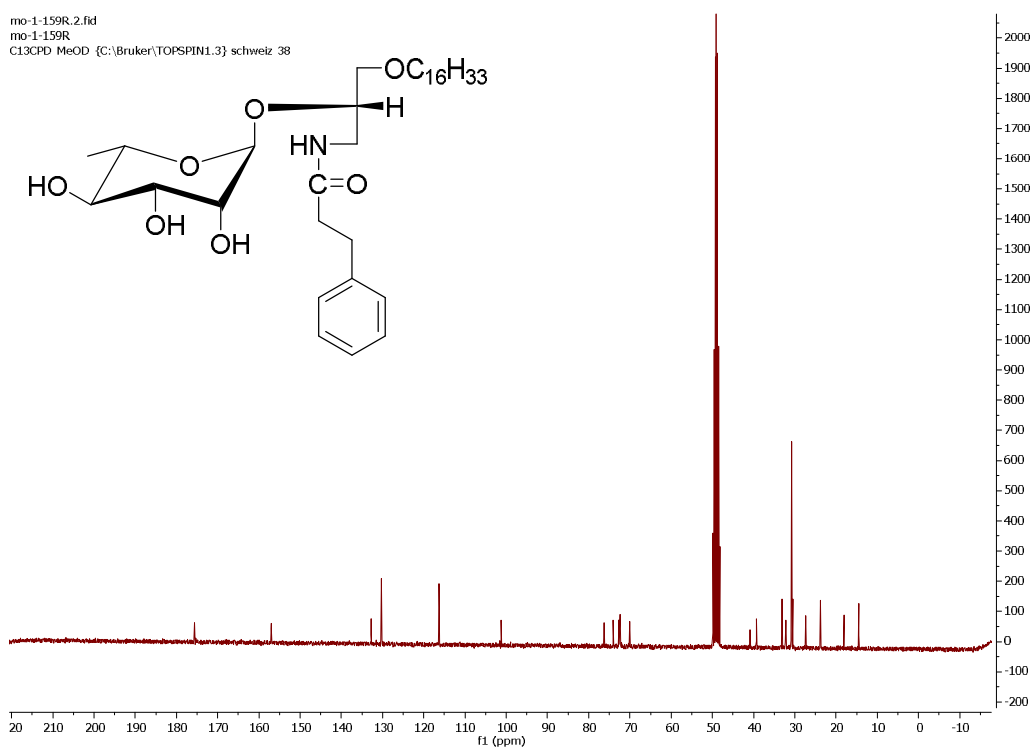
mo-02-66C.2.1.1r
m0-02-66C
Rhamnose GAEL HCL salt
Second Batch
C13CPD MeOD C:\\schweiz 1



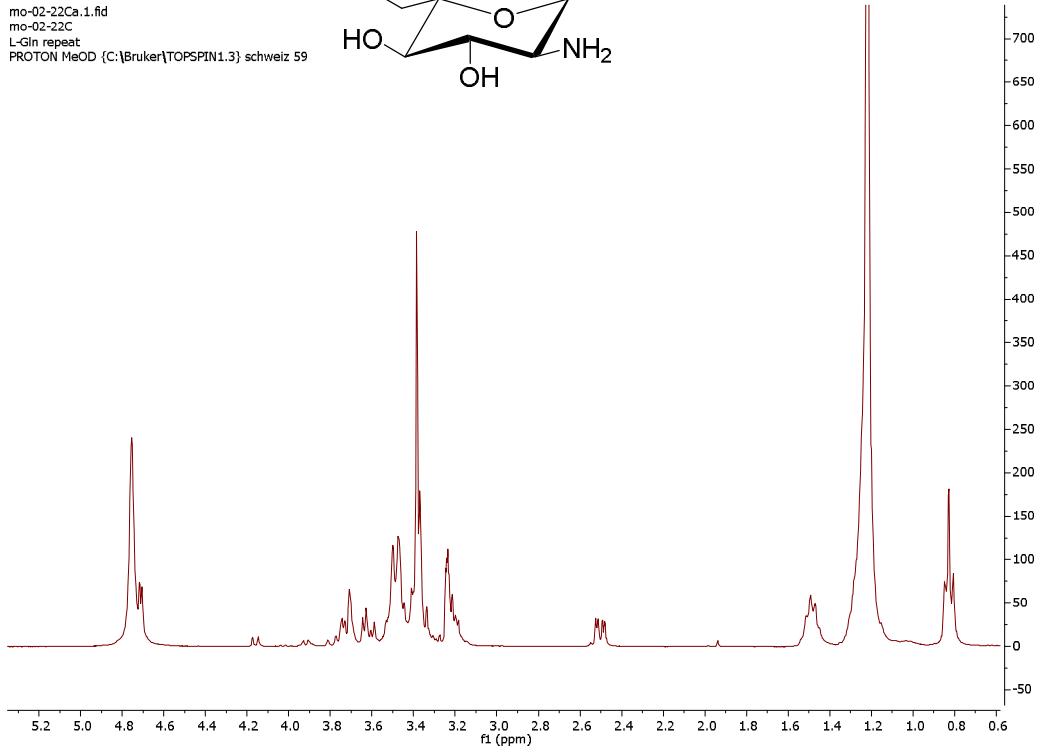
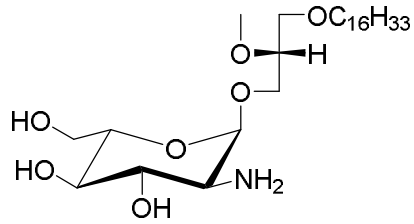
mo-1-159R.1.fid
mo-1-159R
PROTON MeOD {C:\Bruker\TOPSPIN1.3} schweiz 38



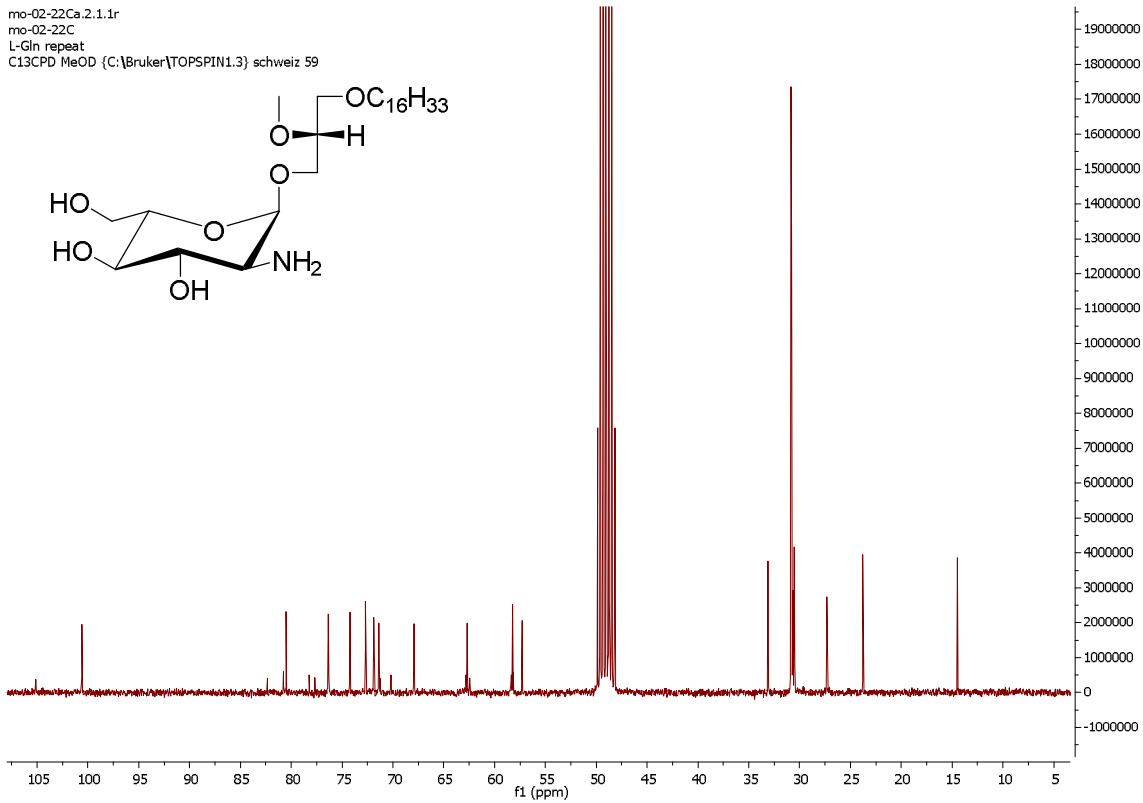
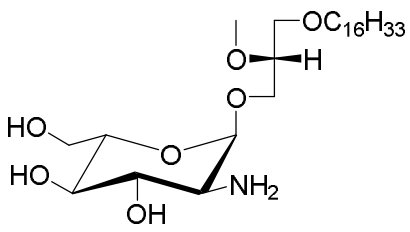
mo-1-159R.2.fid
mo-1-159R
C13CPD MeOD {C:\Bruker\TOPSPIN1.3} schweiz 38



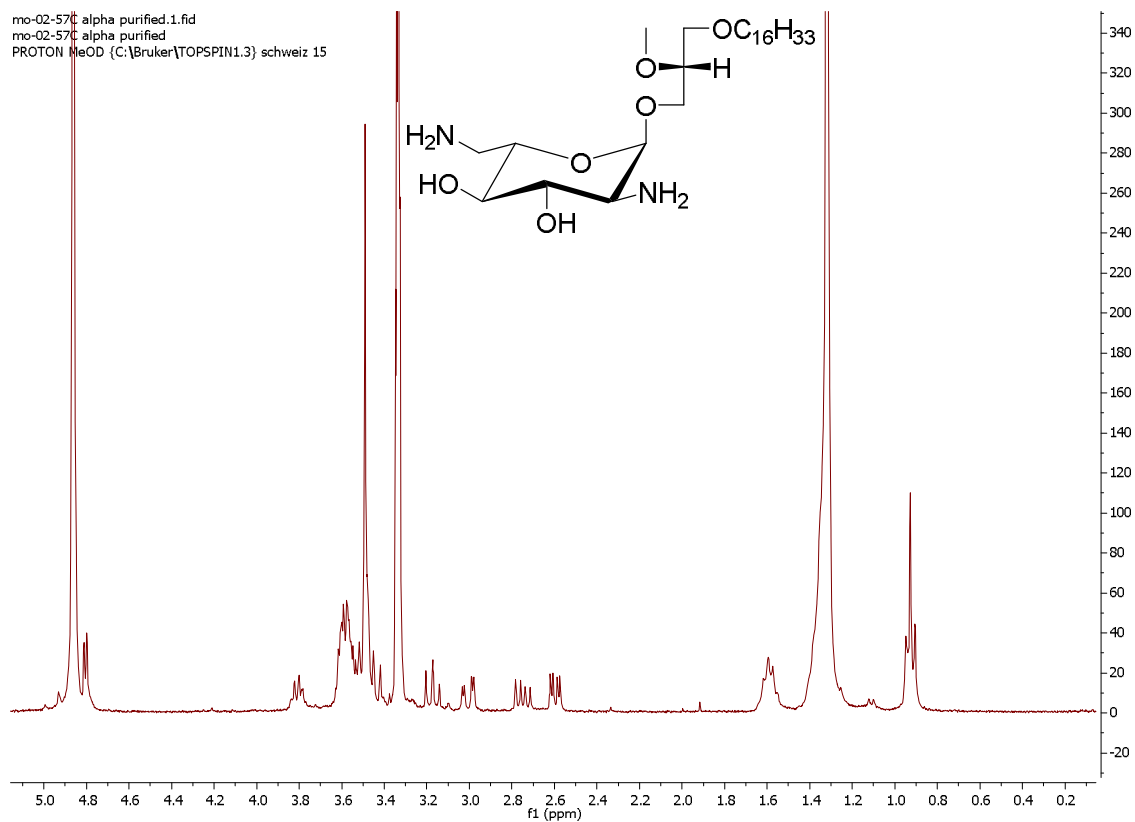
mo-02-22Ca.1.fid
mo-02-22C
L-Gln repeat
PROTON MeOD {C:\Bruker\TOPSPIN1.3} schweiz 59



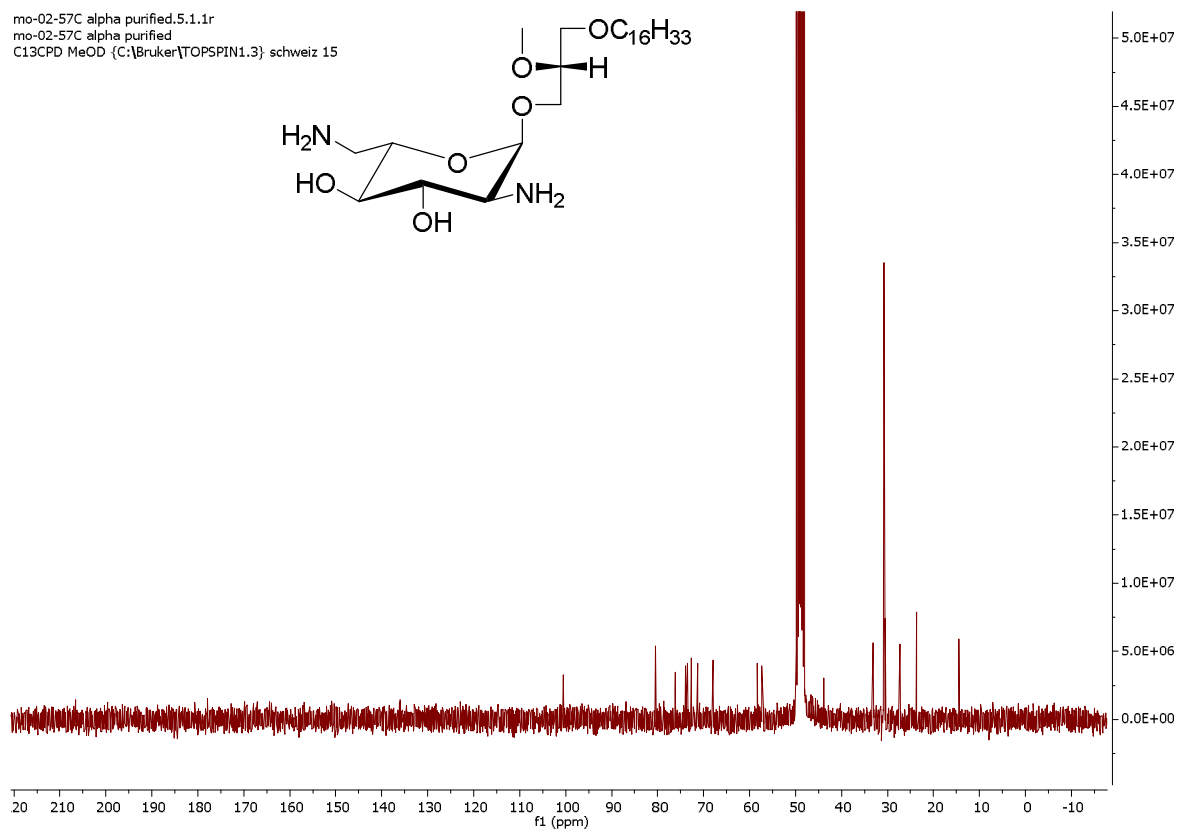
mo-02-22Ca.2.1.1r
mo-02-22C
L-Gln repeat
C13CPD MeOD {C:\Bruker\TOPSPIN1.3} schweiz 59



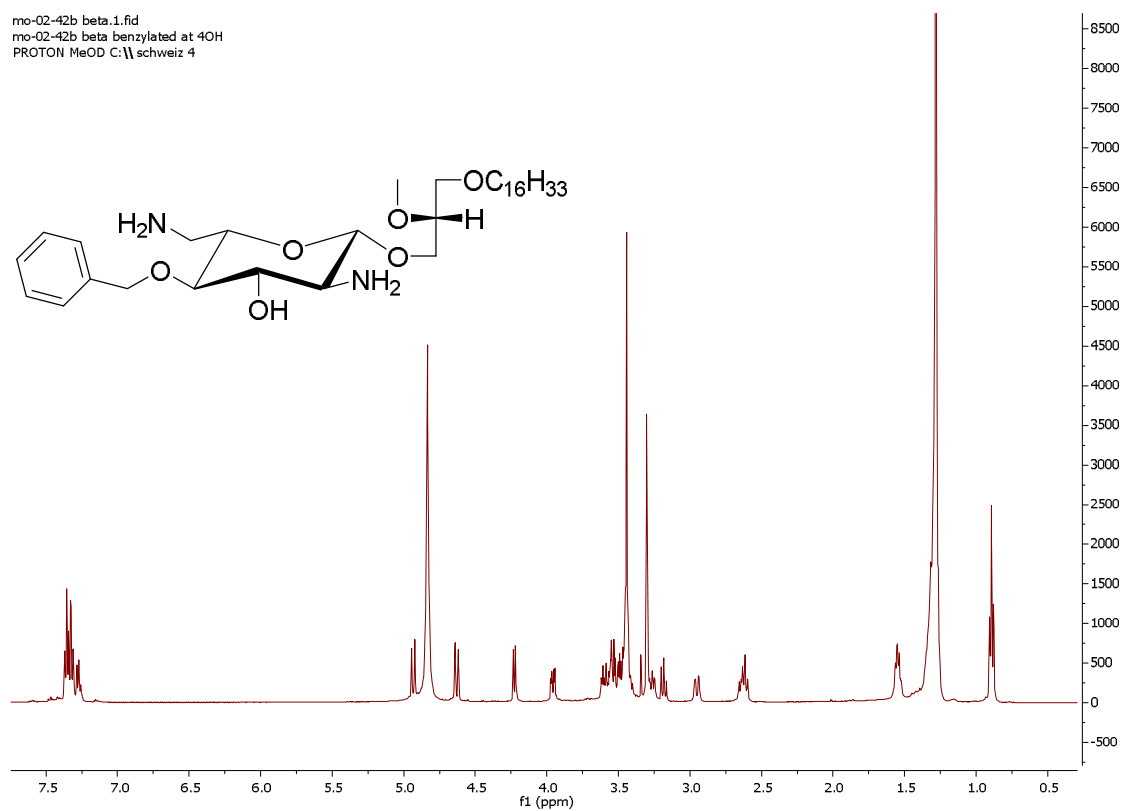
mo-02-57C alpha purified.1.fid
mo-02-57C alpha purified
PROTON MeOD (C:\Bruker\TOPSPIN1.3) schweiz 15



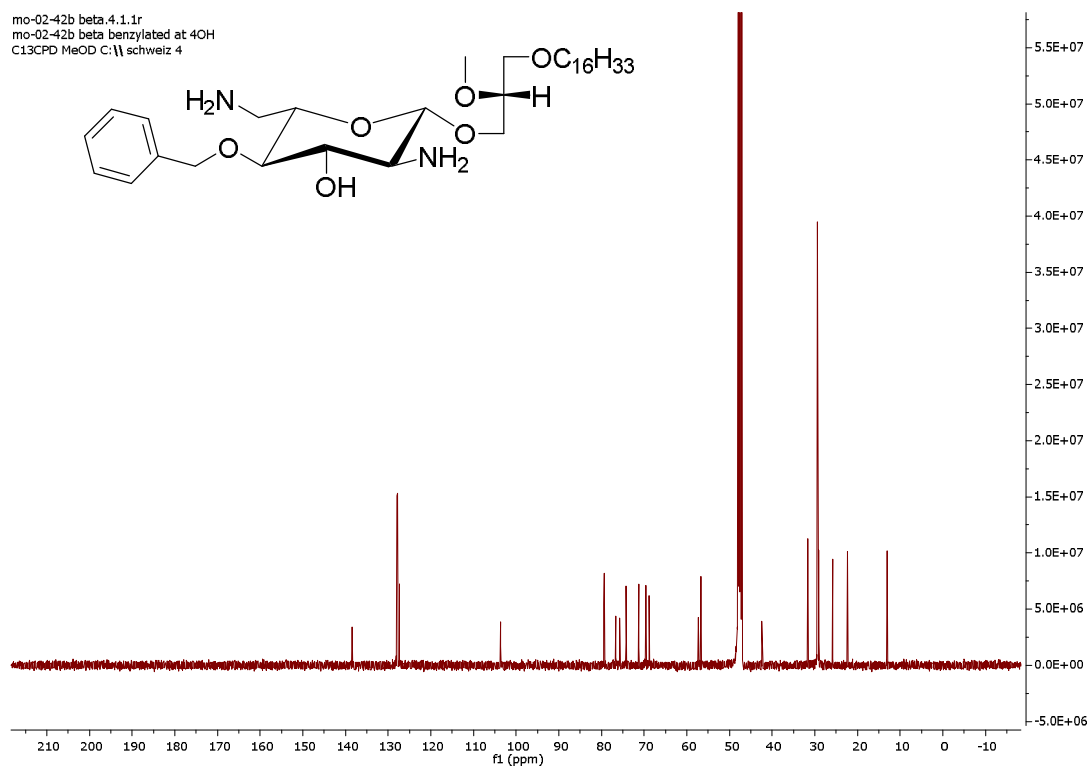
mo-02-57C alpha purified.5.1.1r
mo-02-57C alpha purified
C13CPD MeOD (C:\Bruker\TOPSPIN1.3) schweiz 15



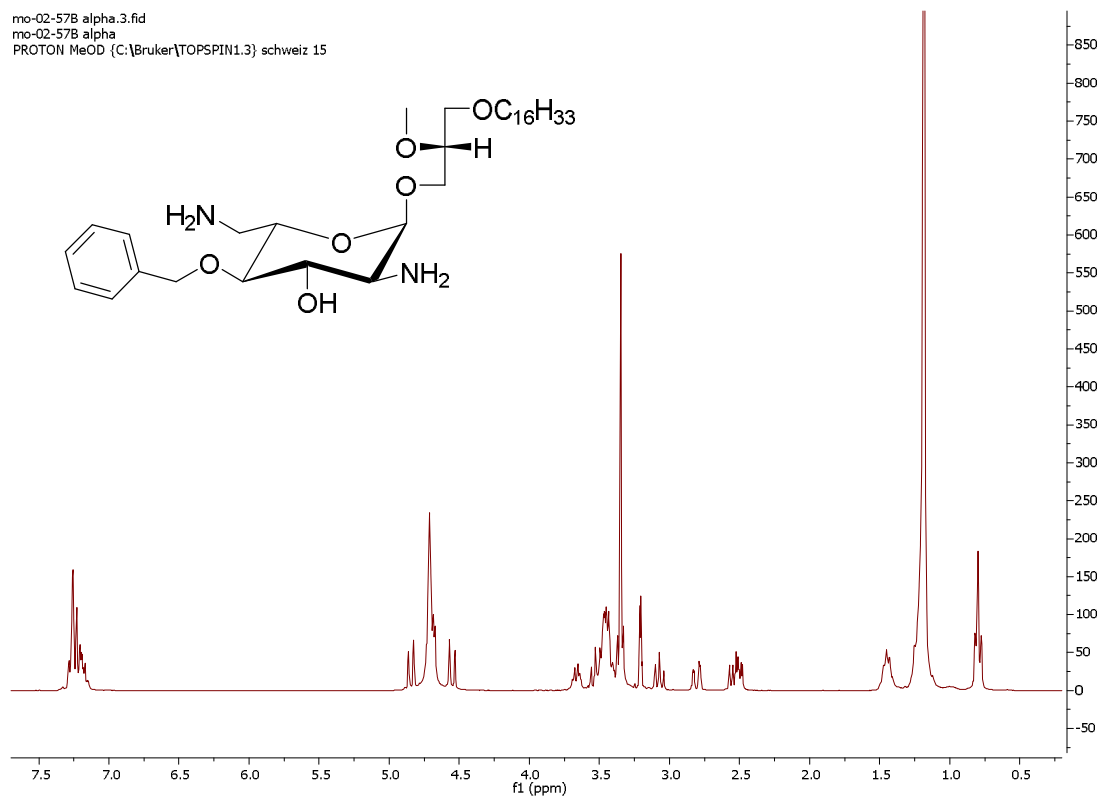
mo-02-42b beta.1.fid
mo-02-42b beta benzylated at 4OH
PROTON MeOD C:\schweiz 4



mo-02-42b beta.4.1.1r
mo-02-42b beta benzylated at 4OH
C13CPD MeOD C:\schweiz 4



mo-02-57B alpha.3.fid
mo-02-57B alpha
PROTON MeOD {C:\Bruker\TOPSPIN1.3} schweiz 15



mo-02-57B alpha.7.fid
mo-02-57B alpha
C13CPD MeOD {C:\Bruker\TOPSPIN1.3} schweiz 15

